

January, 2022



NI 43-101 TECHNICAL REPORT

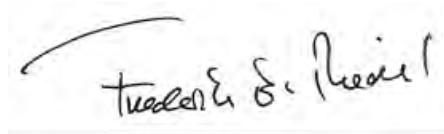
DEFINITIVE FEASIBILITY STUDY UPDATE
MINERA SALAR BLANCO - LITHIUM PROJECT
STAGE ONE
III REGIÓN, CHILE



DATE AND SIGNATURE PAGE

This report titled "NI 43-101 Technical Report: Definitive Feasibility Study Update, Minera Salar Blanco- Lithium Project, Stage One, III Region Chile - dated January 07, 2022, was prepared and signed by the following author:

(Signed & Sealed) "*Frederik Reidel*"



Dated at Santiago, Chile

Frederik Reidel, CPG

Effective and signed January 7, 2022

(Signed & Sealed) "*Peter Ehren*"



Dated at Santiago, Chile

Peter Ehren, MSc, AusIMM CP

Effective and signed January 7, 2022

(Signed & Sealed) "*Marek Dworzanowski*"



Dated at Santiago, Chile

Marek Dworzanowski, Pr. Eng, BSc (Hons)

Effective and signed January 7, 2022

TABLE OF CONTENTS

1. SUMMARY	21
1.1 Terms of Reference.....	21
1.2 Property Description and Ownership	21
1.3 Physiography, Climate, and Access.....	22
1.4 Exploration and Drilling.....	23
1.4.1 Geophysics:	23
1.4.2 Exploration drilling:	23
1.4.3 Test Production and well installations	24
1.4.4 Pumping tests:.....	25
1.4.5 Laboratory brine and drainable porosity analysis:.....	25
1.5 Geology and Mineralization.....	26
1.5.1 Geology	26
1.5.2 Mineralization	26
1.6 Status of Exploration, Development and Operations	27
1.7 Brine Resource Estimates	27
1.8 Brine Reserve Estimate.....	30
1.9 Exploration Potential	31
1.10 Lithium Recovery Process	31
1.11 Project infrastructure.....	33
1.12 Market Studies and Contracts.....	36
1.12.1 Consumption	36
1.12.2 Processing and Production.....	38
1.12.3 Prices	39
1.12.4 Cost.....	41
1.13 Environmental Studies, Permitting and Social or Community Impact.....	42
1.14 Capital and Operating Cost	43
1.14.1 Capital Expenditures – CAPEX	43
1.14.2 Operating Cost Estimate	43
1.15 Economic Analysis	45
1.16 Conclusions and Recommendations	47
1.16.1 Conclusions.....	47
1.16.2 Recommendations	49
2. INTRODUCTION	50
2.1 Terms of Reference.....	50
2.2 Sources of Information	50
2.3 Units	52

3. RELIANCE ON OTHER EXPERTS.....	53
4. PROPERTY DESCRIPTION AND LOCATION	54
4.1 Property location	54
4.2 Tenure	55
4.3 History of ownership.....	58
4.4 Royalties.....	59
4.5 Environmental Liabilities.....	59
4.6 Other Significant Factors and Risks.....	59
5. ACCESSIBILITY, CLIMATE, LOCAL RESOURCES, INFRASTRUCTURE AND PHYSIOGRAPHY	60
5.1 Physiography.....	60
5.2 Accessibility.....	60
5.3 Climate	60
5.3.1 Temperature	60
5.3.2 Precipitation	61
5.3.3 Solar Radiation	67
5.3.4 Evaporation	69
5.4 Local Resources.....	74
5.5 Infrastructure	74
6. HISTORY.....	75
6.1 CORFO (1980's)	75
6.2 Prior Ownership and Ownership Changes	75
6.3 Brine Exploration Work by Previous Owners.....	76
6.3.1 Litio 1-6 (2007)	76
6.3.2 MLE / Li3 - Resource Evaluation Program (2011/2)	76
6.3.3 BBL - AMT Geophysics and Pumping tests (2015).....	78
6.3.4 MSB - Resource and Reserve Evaluation Program (2016/8).....	78
6.3.5 Previous Water Exploration in Salar de Maricunga	80
7. GEOLOGICAL SETTING AND MINERALIZATION	85
7.1 Regional Geology	85
7.2 Local Geology	91
7.3 Mineralization	106
8. DEPOSIT TYPE.....	109
8.1 General.....	109
8.2 Hydrogeology.....	110
8.3 Water Balance.....	114
8.4 Drainable Porosity.....	115
8.5 Permeability	115

9. EXPLORATION.....	117
9.1 Overview	117
9.2 Geophysical Surveys	117
9.2.1 Seismic refraction tomography (2011).....	117
9.2.2 AMT / TEM (2015)	118
9.2.3 Gravimetry	119
9.3 Test Trenching (2011)	122
10.DRILLING.....	126
10.1 Overview	126
10.2 Exploration drilling	127
10.2.1 Sonic Drilling.....	127
10.2.2 Rotary tricone/HWT drilling	131
10.2.3 Diamond core drilling	131
10.3 Monitoring - and Production Well Drilling.....	131
10.3.1 Reverse circulation (RC) drilling and piezometer installations (2011)	131
10.3.2 Production well drilling	132
10.3.3 Piezometer installations - 2016.....	132
10.4 Pumping Tests (2015 and 2017)	132
11.SAMPLE PREPARATION, ANALYSIS, AND SECURITY	151
11.1 Sampling Methods	151
11.1.1 Sampling procedures – sonic and diamond core drilling	151
11.1.2 Sampling procedures – RC drilling.....	153
11.1.3 Sampling procedures - rotary / HWT drilling (2017)	154
11.2 BRINE ANALYSIS AND QUALITY CONTROL RESULTS.....	156
11.2.1 Analytical methods.....	156
11.2.2 Analytical Quality Assurance and Quality Control (“QA/QC”) 2011 Program.....	157
11.2.3 Analytical accuracy 2011 Program	158
11.2.4 Analytical Quality Assurance and Quality Control (“QA/QC”) 2016-2018 Program.....	164
11.2.5 Analytical accuracy 2016-2018 Program.....	165
11.2.6 Additional QA/QC analysis 2016-2018 Program	169
11.2.7 Analytical Quality Assurance and Quality Control (“QA/QC”) 2021 Program.....	171
11.2.8 Analytical accuracy 2021 Program	171
11.3 DRAINABLE POROSITY ANALYSIS AND QUALITY CONTROL RESULTS.....	175
11.3.1 DBSA 2011	175
11.3.2 GSA 2016-2018.....	180
11.3.3 Quality Control – GSA and Core Laboratory Determinations of Sy and Pt	190
11.3.4 GSA 2021	192
12.DATA VERIFICATION	196

13. MINERAL PROCESSING AND METALLURGICAL TESTING	197
13.1 Background – Li3 / MLE 2011 Exploration Program.....	197
13.2 Experimental Procedure.....	197
13.3 Results of the Evaporation Tests.....	199
13.4 POSCO Process Tests – 2012/13	204
13.5 2016 and 2018 Evaporation Pond Tests.....	204
13.6 2017 and 2018 Salt Removal and Lithium Carbonate Tests.....	208
13.6.1 Results of Salt removal Plant.....	209
13.6.2 Results of Lithium Carbonate Testing	210
13.7 2019, 2020 and 2021 Salt Removal and Lithium Carbonate Tests.....	211
14. BRINE RESOURCE ESTIMATES	214
14.1 Overview	214
14.2 Resource Model Domain and Aquifer Geometry.....	214
14.3 Specific Yield.....	215
14.4 Brine Concentrations.....	215
14.5 Resource Category	216
14.6 Resource Model Methodology and Construction	217
14.6.1 Univariate statistical description.....	218
14.6.2 Variography	222
14.7 Grade Estimate.....	243
14.8 Resource Estimate.....	249
15. MINERAL RESERVE ESTIMATES	251
15.1 Model Domain.....	251
15.2 Meshing and Layering	251
15.3 Flow Boundary Conditions	254
15.3.1 Direct Recharge	255
15.3.2 Catchment Inflows	255
15.3.3 Evapotranspiration and diffuse groundwater discharge.....	257
15.3.4 Pumping wells	259
15.4 Hydrogeological Units and Parameters.....	261
15.4.1 Main Hydrogeological Units	261
15.4.2 Unsaturated Parameters.....	265
15.4.3 Lithium Transport Parameters	267
15.5 Density considerations.....	269
15.6 Solver and Convergence Criteria.....	269
15.7 Calibration Methodology	269
15.7.1 Steady State Calibration	269
15.7.2 Transient Calibration	274

15.8	Calibration Results.....	276
15.8.1	Steady State calibration	276
15.8.2	Pumping Test Calibration	288
15.9	Brine Reserve Analysis	293
15.9.1	Approach	293
15.9.2	Wellfield Layout	293
15.9.3	LCE Production Simulations.....	297
15.9.4	Water Table Predictions	299
15.9.5	Reserve Estimate	301
16.	MINING METHODS.....	302
16.1	General Description.....	302
16.2	Wellfield Layout	302
17.	RECOVERY METHODS.....	303
17.1	Overview	303
17.2	Operation of the Solar Evaporation Ponds	307
17.3	Salt Removal Plant – Phase 1	309
17.4	Lithium Carbonate Plant	313
17.5	Reagents for the process.....	317
17.5.1	Preparation of Soda Ash solution.....	317
17.5.2	Preparation of calcium hydroxide	318
17.6	Water purification	318
17.7	Lithium Carbonate Plant Solid waste management.....	318
18.	PROJECT INFRASTRUCTURE	319
18.1	Objective	319
18.2	Project Access.....	322
18.3	Temporary Installations	325
18.3.1	Contractors Installations	325
18.4	Permanent Installations	325
18.4.1	Brine production wellfield.....	325
18.4.2	Transfer Ponds and pumping station.	326
18.4.3	Auxiliary Pond.....	326
18.4.4	Evaporation Ponds	326
18.4.5	Process Plants.....	327
18.4.6	Auxiliary Installations	331
18.5	Mining Camp	332
18.5.1	Dorms	332
18.5.2	Dining Room	333
18.5.3	Recreation Areas	333

18.5.4	Polyclinic.....	333
18.6	Services.....	333
18.6.1	Electrical Energy	333
18.6.2	Water.....	334
18.7	Engineering Deliverables	336
19.	MARKET STUDIES AND CONTRACTS	338
19.1	Consumption	338
19.1.1	Lithium-ion battery market	340
19.2	Resources, processing and production	342
19.3	Prices	345
19.4	Costs	348
20.	ENVIROMENTAL STUDIES, PERMITTING AND SOCIAL OR COMMUNITY IMPACT.....	350
20.1	Environmental Studies and permitting	350
20.2	Environmental Baseline Study	351
20.2.1	Climate and Meteorology.....	351
20.2.2	Air Quality.....	351
20.2.3	Noise.....	352
20.2.4	Vibrations	353
20.2.5	Geology, Geomorphological and Geological Risks	354
20.2.6	Soils	355
20.2.7	Hydrogeology and Water Balance.....	355
20.2.8	Archaeological Heritage and Palaeontology	355
20.2.9	Landscape.....	355
20.2.10	Biodiversity and Natural Scenery	356
20.2.11	Territorial Use and Planning	357
20.2.12	Flora, Vegetation and Fauna	357
20.2.13	Aquatic Continental Ecosystems	359
20.2.14	Social and Community.....	359
20.3	Waste and tailing management	359
21.	CAPITAL AND OPERATING COSTS.....	361
21.1	Capital Cost Estimate	361
21.1.1	Capital Expenditures – CAPEX	361
21.1.2	Brine production wellfield and pipeline delivery system.....	362
21.1.3	Evaporation Ponds	363
21.1.4	Salt Removal Plant.....	364
21.1.5	Lithium Carbonate Plant.....	365
21.1.6	General Services.....	365
21.1.7	Infrastructure and Equipment.....	366

21.1.8	Indirect Cost	367
21.1.9	Exclusions	367
21.1.10	Currency	367
21.2	Operating Cost Estimate	368
21.2.1	Operating Expenses Summary – OPEX	368
21.2.2	Reagents Costs	369
21.2.3	Energy Cost.....	369
21.2.4	Maintenance Cost	370
21.2.5	Salt Harvest and Transport.....	371
21.2.6	Manpower, Catering and Camp Services Cost	371
21.2.7	Product Transportation Costs	372
21.2.8	Indirect Costs.....	373
22.	ECONOMIC ANALYSIS.....	374
22.1	Evaluation Criteria	374
22.2	Income Tax and Royalties.....	375
22.2.1	Income Taxes.....	375
22.2.2	Value Added Tax (19 % flat on all items).....	375
22.2.3	Government Royalties.....	375
22.2.4	Other Payments.....	376
22.3	Capital Expenditures	376
22.4	Lithium Carbonate Production and Ramp Up	377
22.5	Operating Costs.....	378
22.6	Production Revenues	379
22.7	Cash Flow Projection	379
22.8	Economic Evaluation Results.....	381
22.8.1	Project Life.....	382
22.8.2	Sensitivity Analysis	382
23.	ADJACENT PROPERTIES	387
24.	OTHER RELEVANT INFORMATION.....	388
24.1	Exploration Potential.....	388
24.2	Future Expansion.....	390
24.3	Project Schedule.....	390
25.	INTERPRETATION AND CONCLUSIONS.....	392
25.1	Hydrology, Resources and Reserve Estimate	392
25.2	Permits	395
25.2.1	Chilean Nuclear Energy Commission (CChEN)	395
25.2.2	Environmental Impact Assessment	395
25.2.3	Water Rights.....	396



25.3	Economics	396
26.	RECOMMENDATIONS.....	398
26.1	ENERGY EXPENSES AND COGENERATION	399
27.	REFERENCES	400
APPENDIX 1	408

LIST OF TABLES

Table 1-1 Maximum, average and minimum elemental concentrations of the Maricunga brine....	26
Table 1-2 Drainable porosity values applied in the resource model	28
Table 1-3 Lithium and Potassium Measured and Indicated Resources of the Stage One Project – ‘Old Code’ Concessions - dated September 20, 2021.....	29
Table 1-4 OCC resources expressed LCE and potash	29
Table 1-5. Stage One Brine Mining Reserve for pumping to ponds.....	30
Table 1-6. Stage One Brine Production Reserve for Lithium Carbonate production (assuming 65% lithium process recovery efficiency)	30
Table 1-7 Total Capital Expenditures	43
Table 1-8 Average Operating Costs.....	44
Table 1-9 Base Case Economic Results (full equity project funding)	45
Table 1-10 Economic Results (50/50 debt / equity project funding)	45
Table 1-11 Project Summary Cash Flow Projection	46
Table 4-1 MSB mining concessions	55
Table 5-1 Average monthly temperature at the Lobo Marte Project (°C)	61
Table 5-2 DGA Meteorological stations with long-term precipitation records	61
Table 5-3 Selected PUC-DGA weather stations with partial precipitation records	62
Table 5-4 Monthly solar radiation data (W/M2) for the Marte and Lobo Stations.....	68
Table 5-5 Evaporation rates used for the Maricunga Basin water balance	72
Table 6-1 Estimated mineral resources for the Litio 1-6 claims – April 9, 2012	77
Table 6-2 Measured, Indicated and Inferred Lithium and Potassium Resources for the Blanco Project, December 24, 2018	79
Table 6-3 Blanco Project Lithium Reserve Estimate (assuming 58% lithium process recovery efficiency), January 15, 2019.....	79
Table 7-1 Maximum, average and minimum elemental concentrations of the Maricunga brine..	106
Table 7-2 Average values (g/L) of key components and ratios for the Maricunga brine.....	106
Table 7-3 Comparative chemical composition of various salars (weight %).	108
Table 8-1 Water Balance for the Salar de Maricunga Basin.....	114
Table 8-2 Results of drainable porosity analyses (2011-2021)	115
Table 8-3 Summary of permeability values.....	116
Table 9-1 Results of Trench pumping tests	123
Table 10-1 Summary of 2011 – 2021 boreholes	129
Table 10-2 Wells P1, P2 and P4 pumping test layout	135
Table 10-3 P-1 pumping test results	140
Table 10-4 P-2 pumping test results	144
Table 10-5 P-2 pumping test results (2017)	145
Table 10-6 P-4 pumping test results (2017)	150

Table 11-1 List of analyses requested from the University of Antofagasta and Alex Stewart Argentina SA Laboratories	157
Table 11-2 Standards analysis results from U. Antofagasta (2011)	161
Table 11-3 Check assays (U. Antofagasta vs. Alex Stewart): RMA regression statistics	162
Table 11-4 Check assays between the University of Antofagasta and Alex Stewart	163
Table 11-5 Duplicate analyses from the University of Antofagasta.....	163
Table 11-6 Standards analysis results from U. Antofagasta (2016-2018).....	167
Table 11-7 Check assays between the University of Antofagasta and Alex Stewart	168
Table 11-8 Duplicate analyses from the University of Antofagasta.....	169
Table 11-9 Comparison of lithium concentrations in centrifuge and bailed brine samples.....	170
Table 11-10 Standards analysis results from AAA (2021)	173
Table 11-11 Check assays between AAA and UoA.....	174
Table 11-12 Duplicate analyses at AAA laboratory	175
Table 11-13 Results of laboratory specific yield (Sy) analyses	178
Table 11-14 GSA laboratory tests performed	181
Table 11-15 Sample lithology and GSA classification.....	182
Table 11-16 Summary of total porosity and specific yield by lithological group and laboratory ...	189
Table 11-17 Comparison of Sy values between GSA and Corelabs.....	191
Table 11-18 Comparison of Total Porosity between GSA and Corelabs	191
Table 11-19 Summary of samples analysed for Porosity and Sy in GSA Laboratory (2021)	193
Table 11-20 Summary of GSA drainable porosity analyses by lithology (2021 samples)	194
Table 13-1 Chemical composition (% weight) of brines used in the test work.....	198
Table 13-2 Brine compositions during evaporation of the untreated brine.....	199
Table 13-3 Salts compositions during evaporation of the untreated brine	200
Table 13-4 Crystallized Salts in the harvest.....	201
Table 13-5 Brine composition during evaporation of the treated brine	203
Table 13-6 Wet salt compositions during evaporation of the treated brine	203
Table 14-1 Drainable porosity values applied in the resource model	215
Table 14-2 Summary of brine chemistry composition	215
Table 14-3 Summary of univariate statistics of potassium lithium and potassium	219
Table 14-4 Parameters for the calculation of the experimental variograms.....	222
Table 14-5 Lithium and Potassium Measured and Indicated Resources of the Stage One Project – ‘Old Code’ Concessions - dated September 20, 2021	249
Table 14-6 Stage One (OCC) mineral resources expressed as LCE and KCL.....	249
Table 15-1 Layer distribution	252
Table 15-2. Saturated hydraulic parameter values	264
Table 15-3. Unsaturated parameter values	266
Table 15-4. Effective porosity for transport simulations	267
Table 15-5. Observation wells for steady state calibration	270

Table 15-6. Flux targets for the steady state calibration	274
Table 15-7. Observation wells for pumping tests	276
Table 15-8. Calibrated hydraulic conductivities.....	277
Table 15-9. Calibrated transfer rate coefficients	278
Table 15-10. Observed and simulated water levels.....	286
Table 15-11. Simulated water balance.....	288
Table 15-12. Calibrated specific storage	288
Table 15-13. P-1 Test maximum simulated and observed drawdown values	289
Table 15-14. P-2 Test maximum simulated and observed drawdown values	290
Table 15-15. P-4 Test maximum simulated and observed drawdown values	291
Table 15-16. Summary of production well construction details.....	295
Table 15-17 Simulated Stage One brine pumping schedule	296
Table 15-18. Stage One Brine Mining Reserve for pumping to ponds.....	301
Table 15-19. Stage One Brine Production Reserve for Lithium Carbonate production (assuming 65% lithium process recovery efficiency)	301
Table 17-1 Annual generation of salts from evaporation ponds	309
Table 17-2 Annual generation of discard salts from Phase 1.....	310
Table 17-3 Annual generation of discard salts from Phase 2.....	314
Table 17-4 Reagents used in the process.....	317
Table 18-1 Worley Engineering Deliverables	336
Table 18-2 GEA Engineering Deliverables	337
Table 19-1 Average annual price forecast trend for technical-grade lithium carbonate, (US\$/t), 2021 to 2036	347
Table 21-1 Total Capital Expenditures	362
Table 21-2 Brine Production Wellfield Cost Estimate	363
Table 21-3 Evaporation Ponds Cost Estimate	364
Table 21-4 Salt Removal Plant Cost Estimate.....	364
Table 21-5 Lithium Carbonate Plant Cost Estimate	365
Table 21-6 General Services Cost Estimate.....	366
Table 21-7 Infrastructure and Equipment Cost Estimate.....	366
Table 21-8 Indirect Costs.....	367
Table 21-9 Average Operating Costs.....	368
Table 21-10 Reagents Costs	369
Table 21-11 Energy Cost.....	370
Table 21-12 Maintenance Cost	370
Table 21-13 Salt Harvest and Transport Cost.....	371
Table 21-14 Manpower, Catering and Camp Services Cost	372
Table 21-15 Soda Ash and Lithium Carbonate Transportation Costs	373
Table 21-16 General & Administration	373

Table 22-1 Capex Schedule	377
Table 22-2 Production Ramp Up (%)	377
Table 22-3 Li ₂ CO ₃ Production	378
Table 22-4 Operating Costs	379
Table 22-5 Production Revenues (Selected Years).....	379
Table 22-6 Project Summary Cash Flow Projection	380
Table 22-7 Base Case Economic Results (full equity project funding)	381
Table 22-8 Loan Disbursement and Repayment	383
Table 22-9 Economic Results (50/50 debt / equity project funding)	383
Table 22-10 Project After Taxes – NPV 8% Sensitivity	384
Table 22-11 Project After Taxes – IRR Sensitivity.....	385
Table 22-12 Sensitivity to Royalty Rate.....	386
Table 24-1 Project exploration target estimate	389
Table 25-1 Summary of the average brine composition (g/l) and ratios	392
Table 25-2 Measured and Indicated Lithium and Potassium Resources of the Stage One Project – ‘Old Code’ Concessions – Dated September 20, 2021	393
Table 25-3 OCC resources expressed LCE and potash	393
Table 25-4. Stage One Brine Mining Reserve for pumping to ponds.....	394
Table 25-5. Stage One Brine Production Reserve for Lithium Carbonate production (assuming 65% lithium process recovery efficiency)	394

LIST OF FIGURES

Figure 1-1 General Process Diagram	32
Figure 1-2 Project location presenting all main installations.....	34
Figure 1-3 World: Consumption of lithium by first use, 2011 and 2021e (t LCE)	37
Figure 1-4 World: Forecast consumption of lithium by first use, 2020-2036 (000t LCE).....	37
Figure 1-5 World: Forecast consumption of lithium by product, 2020-2036 (kt LCE)	38
Figure 1-6 Lithium chemical balance, 2021-2036 (kt LCE)	39
Figure 1-7: Average annual contract and spot price forecast for battery-grade lithium carbonate, 2019-2036 (US\$/t).....	40
Figure 1-8: Lithium carbonate cash cost curve, 2031 (US\$/t LCE)	41
Figure 4-1 Location map of the Project.....	54
Figure 4-2 Location map of MSB mining concessions	57
Figure 5-1 Isotherm map for Salar de Maricunga	63
Figure 5-2a Precipitation data for the Maricunga weather station (PUC-DGA) 2007/2008.....	64
Figure 5-3 Precipitation data from the Marte and Lobo stations 2009/2010	65
Figure 5-4 Isohyet map for Salar de Maricunga.....	66
Figure 5-5 MSB weather station in the plant site area	67
Figure 5-6 Solar radiation distribution in Chile	68
Figure 5-7 Average hourly solar radiation intensity at the Marte and Lobo stations 2009/2010	69
Figure 5-8 Elevation versus average annual pan evaporation	70
Figure 5-9 Monthly distribution of average annual Pan Evaporation.....	71
Figure 5-10 Temperature - Blanco station (2016 –2020).....	72
Figure 5-11 Precipitation - Blanco station (2016-2020)	73
Figure 5-12 Fresh water Class A Pan Evaporation - Blanco Station 2016-2020	73
Figure 5-13 Diluted Brine Class A Pan Evaporation – Blanco Station (2016-2020).....	74
Figure 6-1 Location map of wells installed by Compania Mantos de Oro and Chevron 1988/1990	82
Figure 6-2 Lithological logs of Compania Mantos de Oro wells SP-2, SR-3 and SR-6.....	83
Figure 6-3 Lithological logs of Compania Mantos de Oro wells SR-1, SR-2, SR-4, SP-4 and Chevron well CAN-6.....	84
Figure 7-1 Morphotectonic units of the Andean Cordillera in northern Chile.....	85
Figure 7-2 Regional Geology of the Maricunga Basin	87
Figure 7-3 General N-S and W-E Sections through the Maricunga geological model	93
Figure 7-4 Details of the Upper Halite unit	97
Figure 7-5 Details of the Lacustrine unit.....	98
Figure 7-6 Details of the Deep Halite unit.....	99
Figure 7-7 Details of the Alluvium Deposits.....	100
Figure 7-8 Details on the Volcanoclastic unit.....	101
Figure 7-9 Details of the Lower Sand unit.....	102
Figure 7-10 Details of the Lower Volcanoclastics unit	103

Figure 7-11 Details of the Volcanic Breccia Unit	104
Figure 7-12 Modelled depth to bedrock for Salar de Maricunga	105
Figure 7-13 Comparison of brines from various salars in Janecke Projection	107
Figure 8-1 Conceptual model for mature and immature salars showing the distribution of the facies and the main hydrogeological components. (Houston, <i>et al.</i> , 2011.)	109
Figure 8-2 W-E Hydrogeological cross section	112
Figure 8-3 Salar de Maricunga hydrographic basin.....	113
Figure 9-1 Location map of seismic refraction tomography, AMT and gravity profiles	120
Figure 9-2 Seismic Tomography Line 1.....	121
Figure 9-3 Test Trench T6 in the Upper Halite	122
Figure 9-4a – 9.4e Pumping test analyses for Trench pumping tests T1, T2, T3, T5 and T6.....	124
Figure 10-1 Location map of the boreholes (2011 - 2021 programs)	128
Figure 10-2 Collecting RC Airlift Flow Measurements (2011)	133
Figure 10-3 Installation of surface casing in well P-1 (2011)	134
Figure 10-4 Layout of pumping test P-1 and P-2.....	137
Figure 10-5 Pumping test P-1 layout.....	138
Figure 10-6 V-notch tank during P-1 constant rate test	138
Figure 10-7 Water level responses P-1 constant rate test.....	139
Figure 10-8 P-1 pumping test interpretation	140
Figure 10-9 Pumping test P-2 layout.....	142
Figure 10-10 Water level responses P-2 constant rate test.....	142
Figure 10-11 P-2 pumping test interpretation	143
Figure 10-12 Li and K concentrations during the P-1 and P-2 pumping tests.....	144
Figure 10-13 Water level responses P-2 constant rate test (2017)	145
Figure 10-14 Pumping test P-4 layout.....	147
Figure 10-15 Water level responses P-4 constant rate test (2017)	148
Figure 10-16 P-4 pumping test interpretation	149
Figure 11-1 Collection of field parameters of the brine samples at the wellhead	152
Figure 11-2 Porosity and brine samples.....	153
Figure 11-3 RC drill chip samples	154
Figure 11-4 Fluorescein tracer dye in the rotary drilling fluid	155
Figure 11-5 Comparison of lithium concentrations in centrifuge and bailed brine samples.....	170
Figure 11-6 DBSA laboratory specific yield (Sy) analyses against total porosity.....	178
Figure 11-7 Comparison of BGS and DBSA specific yield (Sy) analyses.....	179
Figure 11-8 Comparison of BGS and DBSA total porosity (Pt) analyses.....	180
Figure 11-9 Rejected core samples	183
Figure 11-10 Relative Solution Release Capacity (RSRC) HQ core sample testing.....	185
Figure 11-11 GSA specific yield vs GSA total porosity.....	187
Figure 11-12 Lithologically classified Pt and Sy distributions and statistics.....	188

Figure 11-13 Comparison of total porosity estimated by GSA using RSRC method and Core laboratory using the Centrifuge method	189
Figure 11-14 Comparison of specific yield estimated by GSA using RSRC method and Core laboratory using the Centrifuge method	190
Figure 11-15 Comparison of Sy values between GSA and Corelabs	191
Figure 11-16 Comparison of Total Porosity between GSA and Corelabs.....	192
Figure 11-17 Comparison of total and drainable porosities between GSA and DBSA.....	195
Figure 13-1 General view of evaporation chambers.....	198
Figure 13-2 Evaporation curves plotted versus % Li in the brine.....	202
Figure 13-3 MSB evaporation ponds.....	205
Figure 13-4 MSB harvesting of salts.....	206
Figure 13-5 Evaporation curves plotted versus % Li of pilot ponds compared with test work realized in University of Antofagasta 2011 (UA).....	207
Figure 13-6 Evaporation curves plotted versus % Li of pilot ponds compared with testwork realized at University of Antofagasta 2011 (UA)	208
Figure 13-7 Evaporation and cooling curves plotted in a Janecke projection of testwork realized at University of Antofagasta 2011 (UA)	211
Figure 13-8 Extraction stages E1-E5 at 26 h after start-up	213
Figure 14-1 Lithium and potassium distribution.....	220
Figure 14-2 Histogram of potassium and lithium concentrations	221
Figure 14-3 Scatter plot of lithium versus potassium concentrations	222
Figure 14-4 Horizontal experimental variogram and variogram model for lithium within the alluvial deposits and lower sand	225
Figure 14-5 Horizontal experimental variogram and variogram model for lithium within the Lacustrine region.....	226
Figure 14-6 Horizontal experimental variogram and variogram model for lithium within the halite and deep halite region	227
Figure 14-7 Horizontal experimental variogram and variogram model for lithium within the volcanoclastic, lower volcanoclastic and volcanic breccia	228
Figure 14-8 Vertical experimental variogram and variogram model for lithium within the alluvial deposits and lower sand	229
Figure 14-9 Vertical experimental variogram and variogram model for lithium within the Lacustrine region	230
Figure 14-10 Vertical experimental variogram and variogram model for lithium within the halite and deep halite region	231
Figure 14-11 Vertical experimental variogram and variogram model for lithium within the volcanoclastic, lower volcanoclastic and volcanic breccia	232
Figure 14-12 Horizontal experimental variogram and variogram model for potassium within the alluvial deposits and lower sand	233

Figure 14-13 Horizontal experimental variogram and variogram model for potassium within the Lacustrine region.....	234
Figure 14-14 Horizontal experimental variogram and variogram model for potassium within the halite and deep halite region	235
Figure 14-15 Horizontal experimental variogram and variogram model for potassium within the volcanoclastic, lower volcanoclastic and volcanic breccia	236
Figure 14-16 Vertical experimental variogram and variogram model for potassium within the alluvial deposits and lower sand region	237
Figure 14-17 Vertical experimental variogram and variogram model for potassium within the Lacustrine region 11	238
Figure 14-18 Vertical experimental variogram and variogram model for potassium within the halite and deep halite region	239
Figure 14-19 Vertical experimental variogram and variogram model for potassium within the volcanoclastic, lower volcanoclastic and volcanic breccia	240
Figure 14-20 Lithium concentration distribution	241
Figure 14-21 Potassium concentration distribution	242
Figure 14-22 3D lithium grade distribution in comparison to the geological model	244
Figure 14-23 N-S section through the resource model showing the lithium grade distribution....	245
Figure 14-24 W-E section through the resource model showing the lithium grade distribution...	246
Figure 14-25 SW-NE section through the resource model showing the lithium grade distribution	247
Figure 14-26 Distribution of resource classification areas	248
Figure 15-1 Model domain and mesh element size	253
Figure 15-2 Mesh vertical extension	254
Figure 15-3 Model boundary conditions (WorleyParsons, 2019)	255
Figure 15-4 Indirect, lateral recharge to Salar de Maricunga from the surrounding catchments..	256
Figure 15-5. Evapotranspiration and diffuse groundwater discharge zones	258
Figure 15-6 Pumping wells in the model domains	260
Figure 15-7. Surface hydrogeological units	262
Figure 15-8 Geological units in cross section	263
Figure 15-9. Initial distribution of lithium concentration	268
Figure 15-10. Location of head observation wells for steady state calibration	273
Figure 15-11. Pumping test locations	275
Figure 15-12. Calibrated evapotranspiration rates	279
Figure 15-13 Calibrated diffuse seepage rates	280
Figure 15-14. Simulated steady state water table	282
Figure 15-15 Calibration residual map	283
Figure 15-16. Observed vs. simulated water levels – entire model domain	284
Figure 15-17. Observed vs. simulated water levels – reserve area	285

Figure 15-18. P-1 Test simulated and observed drawdowns.....	289
Figure 15-19. P-2 Test simulated and observed drawdowns.....	291
Figure 15-20. P-4 Test simulated and observed drawdowns.....	292
Figure 15-21 Layout of the Stage One brine production wellfield.....	294
Figure 15-22. Stage One annual brine production rates.....	297
Figure 15-23 Stage One LCE contained in the pumped brine	298
Figure 15-24. Average lithium concentration of wellfield production.....	298
Figure 15-25. Predicted drawdown after Year 20	300
Figure 17-1 Water Activity versus % Li in the tested brine	304
Figure 17-2 General Process Diagram	305
Figure 17-3 Process Block Diagram	306
Figure 17-4 Evaporation Ponds Diagram.....	308
Figure 17-5 Simplified Salt Removal Plant Process Diagram (1/2).....	311
Figure 17-6 Simplified Salt Removal Plant Process Diagram (2/2).....	312
Figure 17-7 Simplified Lithium Carbonate Plant Process Diagram (1/2).....	315
Figure 17-8 Simplified Lithium Carbonate Plant Process Diagram (2/2).....	316
Figure 18-1 Location of Salar de Maricunga	319
Figure 18-2 Project location presenting all main installations.....	321
Figure 18-3 Project Access from Route 5	322
Figure 18-4 Project Access from Copiapó-Paipote.....	323
Figure 18-5 Project Access from Antofagasta	324
Figure 18-6 Project Plants Installations.....	327
Figure 18-7 Basic Engineering 3D Salt Removal Plant.....	328
Figure 18-8 Metso Outotec Solvent Extraction.....	328
Figure 18-9 Basic Engineering 3D Lithium Carbonate Plant.....	329
Figure 18-10 Eurodia Ionic Exchange	329
Figure 18-11 Soda Ash storage (solid and liquid), preparation and distribution	330
Figure 18-12 Transmission Line Route	334
Figure 19-1 World: Consumption of lithium by first use, 2011 and 2021e (t LCE)	338
Figure 19-2 World: Forecast consumption of lithium by first use, 2020-2036 (000t LCE).....	339
Figure 19-3 World: Forecast consumption of lithium by product, 2020-2036 (kt LCE)	339
Figure 19-4: Global penetration rate of electric passenger vehicles, 2020-2036 (% of sales).....	341
Figure 19-5: World Li-ion battery use by market, 2020-2036 (GWh)	341
Figure 19-6 Global lithium resources and reserves by country, 2021	342
Figure 19-7: Simplified overview of mine-to-product flow.....	343
Figure 19-8 World: Forecast refined supply for lithium, 2020-2036 (kt LCE)	344
Figure 19-9 Lithium chemical balance, 2021-2036 (kt LCE)	344
Figure 19-10: Average annual contract and spot price forecast for battery-grade lithium carbonate, 2019-2036 (US\$/t).....	346

Figure 19-11: Lithium carbonate cash cost curve, 2031 (US\$/t LCE)	348
Figure 19-12: Lithium carbonate production costs in Chile, including royalties, 2031 (US\$/t LCE) 349	
Figure 20-1 Weather and Air Quality Monitoring Station – MSB	352
Figure 20-2 Measurement Locations for Noise and Vibration for Humans	353
Figure 20-3 Measurement Locations for Noise and Vibration for Fauna	354
Figure 20-4 Landscape Units UP1 and UP2	356
Figure 20-5 Endemic Vegetation on Shore of Salar de Maricunga	358
Figure 20-6 Vulnerable Reptiles and Endangered Mammals.....	358
Figure 22-1 Li ₂ CO ₃ Production	378
Figure 22-2 Yearly Cash Flow	381
Figure 22-3 Cumulative Cash Flow	382
Figure 22-4 Project After Taxes NPV 8% Sensitivity	384
Figure 22-5 Project After Taxes IRR Sensitivity	385
Figure 24-1 Schematic of the lithium exploration target.....	388
Figure 24-2 Project Execution Schedule.....	391

1. SUMMARY

1.1 TERMS OF REFERENCE

The Stage One Project (herein the “Project”) is owned and operated by Minera Salar Blanco S.A. (“Minera Salar Blanco or MSB”). MSB is in turn owned by Lithium Power International (ASX:LPI) 51.55%; Minera Salar Blanco SpA (previously BBL) 31.31%; and Bearing Lithium Corp. (TSXV: BRZ) 17.14%. This report was prepared by Worley and Atacama Water for MSB to provide a National Instrument 43-101 (“NI 43-101”) compliant Definitive Feasibility Study (“DFS”) of its “Stage One Project” located in Salar de Maricunga in the Atacama Region of northern Chile. This report provides an independent updated Mineral Reserve estimate and a technical appraisal of the economic viability of the production of an average of 15,200 TPY of battery grade lithium carbonate over a 20-year mine-life from the lithium contained on the ‘Old Code’ mining concessions (OCC) owned by MSB, based on additional exploration work carried out to 400 m depth during 2021. The OCC are constituted under the 1932 Chilean Mining Code and do not require a special license from the Chilean Government (Contrato Especial de Operación del Litio – CEOL) for the production and sale of lithium products. Resource estimates are for lithium and potassium contained in brine. The report was prepared under the guidelines of NI 43-101 and in conformity with its standards.

All items related to geology, hydrogeology, mineral resources and reserves were prepared by Atacama Water. Peter Ehren was responsible for preparing all technical items related to brine chemistry and mineral processing. Capital and Operating expenditures mentioned in this report were estimated by Worley, relying on quotations requested from equipment, chemicals and other suppliers, as well as from its project data base. Worley relied extensively on Minera Salar Blanco and its consultants, as cited in the text of the study and the references, for information on future prices of lithium carbonate, legislation and tax in Chile, as well as for general project data and information.

This report was reviewed by Mr. Marek Dworzanowski, CEng., BSc (Hons), HonFSAIMM, FIMMM of Worley, Mr. Peter Ehren, MSc, MAusIMM and Mr. Frits Reidel, CPG. Mr. Marek Dworzanowski, Mr. Peter Ehren and Mr. Frits Reidel are “qualified persons” (QP) and are independent of MSB as such terms are defined by NI 43-101.

1.2 PROPERTY DESCRIPTION AND OWNERSHIP

The Project is located 170 km northeast of Copiapó in the III Region of northern Chile at an elevation of 3,750 masl. The property is centred at approximately 492,000 mE, 7,025,000 mN (WGS 84 datum UTM Zone 19). The Project covers 1,125 ha of mineralized ground in Salar de Maricunga; 100 ha just

to the northeast of the Salar for camp and evaporation test facilities, and an additional 1,800 ha eight km north of the Salar for the construction of evaporation ponds, process and plant facilities.

The mineralized area of the Stage One Project is comprised of the following mining concessions: *Cocina 19-27* (450 ha), *Salamina*, *Despreciada*, and *San Francisco* (675 ha). These concessions, known as ‘Old Code’ mining concessions (OCC), were constituted under the 1932 Chilean mining law and have “grand-fathered” rights for the production and sale of lithium products. The OCC does not require any special license from the Chilean Government (Contrato Especial de Operacion del Litio – CEOL) for the production and sale of lithium products. MSB also own 100% of the *Litio 1-6* concessions comprising 1,438 ha, known as ‘New Code’ concessions, where a future expansion is under evaluation. The *Litio 1-6* concessions do require a special license or CEOL for their exploitation.

1.3 PHYSIOGRAPHY, CLIMATE, AND ACCESS

The hydrographic basin of Salar de Maricunga covers 2,195 km² in the Altiplano of the III Region. The average elevation of the basin is 4,295 masl while the maximum and minimum elevations are 6,749 masl and 3,738 masl respectively. The Salar is located in the northern extent of the hydrographic basin and covers 142.2 km² (DGA 2009). The salar nucleus sits at an elevation of approximately 3,750 masl.

The principal surface water inflow into the lower part of basin occurs from Rio Lamas which originates in Macizo de Tres Cruces. Average flow in Rio Lamas (at El Salto) is measured at 240 l/s. All flows from the Rio Lamas infiltrate into the Llano de Cienaga Redonda (DGA 2009). The second largest surface water inflow to the lower part of the basin occurs from Quebrada Cienaga Redonda. Average flow (at La Barrera) is measured at 20 l/s; all flow infiltrates also into the Llano de Cienaga Redonda (DGA 2009).

Laguna Santa Rosa is located at the southwest extent of the basin valley floor and is fed mainly locally by discharge of groundwater. Laguna Santa Rosa drains north via a narrow natural channel into the Salar itself. Additional groundwater discharge occurs along the path of this channel and surface water flow north towards the Salar has been recorded at a range of 200-300 l/s (DGA 2009). Tres Cruces National Park is located in the southern part of the Maricunga watershed and includes Laguna Santa Rosa.

The Project is accessed from the city of Copiapó via National Highway 31. Highway 31 is paved for approximately two-third of the distance and is a well-maintained gravel surface road thereafter. National Highway 31 extends through to Argentina via the Paso San Francisco. Access to Maricunga from the city of El Salvador is via a well-maintained gravel surface highway. Occasional high snowfalls in the mountains may close the highways for brief periods during the winter.

The climate at the property is that of a dry, cold, high-altitude desert, which receives irregular rainfall from storms between December and March and snowfall during the winter months of late May to September. The average annual temperature in Salar de Maricunga is estimated at 5 to 6°C. Average annual precipitation is estimated at 150 mm and average annual potential evaporation is estimated between 2,100 mm and 2,400 mm.

1.4 EXPLORATION AND DRILLING

The following exploration, drilling and testing programs carried out on the MSB concessions between 2011 and 2021:

1.4.1 GEOPHYSICS:

- A seismic tomography survey was carried out by GEC along six profiles (S1 through S6) for a total of 23-line km to help define basin lithology and geometry.
- An AMT / TEM geophysical survey was completed by Wellfield Services along 6 profiles across the Salar covering a total of 75-line km. 383 AMT soundings were collected at a 200 m to 250 m station spacing; 15 TDEM soundings were carried out at the end and centre of each AMT profile. The purpose of the AMT survey was to help map the basin geometry and the fresh water / brine interface.
- A regional gravity survey was carried out along six profiles (parallel to the AMT survey) for a total of 75-line km across the Salar. The station spacing along the profiles varied between 250 m and 500 m. The objective of the gravity survey was to help define the geometry of the bedrock contact in the Salar.

1.4.2 EXPLORATION DRILLING:

- Twelve sonic boreholes were drilled between 2011 and 2018 as follows: C-1 through C-6 to 150 m depth; S-1A, S-2, S-18, S-23, and S-24 to 200 m depths and S-20 to 40 m depth. Undisturbed samples were collected from the sonic core at 3 m to 6 m intervals for drainable porosity analyses and other physical parameters. Brine samples were collected during the sonic drilling at 3 m to 6 m intervals for chemistry analyses. All sonic boreholes were completed as observation wells on completion of drilling.
- A total of 915 m of exploration RC drilling was carried out for the collection of chip samples for geologic logging, brine samples for chemistry analyses and airlift data to assess relative aquifer permeability. The RC boreholes were completed as observation wells for use during future pumping tests.

- Eight exploration boreholes (S-3, S-3A, S-5, S-6, S-10, S-11, S-13, and S-19) for a total of 1,709 m were drilled using the tricone rotary method at 3-7/8 and 5-1/2 inch diameter; HWT casing was installed in each borehole to selected depths as required to provide adequate borehole stability. Drill cuttings were collected at 2 m intervals. Brine samples were collected at a 6 m interval. Six of the nine exploration holes were completed as piezometers through the installation of 2-inch diameter blank and screened PVC casing.
- Six boreholes (S-8, S-12, S-15, S-16, S-17, and S-21) for a total of 205 m were drilled as monitoring wells using the rotary method at 5-1/2 inch diameter. Drill cuttings were collected at 2 m intervals; brine sampling took place at selected depth intervals. All six holes were completed with 2-inch diameter blank and screened PVC casing.
- Five (5) tricone / HQ /HWT core holes (S-25 through S-29) were drilled on the OCC by Major Drilling with tricone from ground surface to 200 m depth and cored at HQ diameter from 200 m to 400 m depth. HWT casing was installed during the drilling to provide hole stability and facilitate depth-representative brine sampling. Continuous HQ core was collected for geological logging and the preparation of 'undisturbed' sub-samples (66) at 12 m intervals between 200 m and 400 m depth.
- The five boreholes were completed as monitoring wells with blank and slotted 3-inch diameter PVC casing to facilitate BMR logging and future water level and brine chemistry monitoring.
- BMR and LithSight downhole logging was carried out in boreholes S-25 through S-29 by geophysical contractor Zelandez.

1.4.3 TEST PRODUCTION AND WELL INSTALLATIONS

- Two test production wells (P-1 and P-2) were drilled at 17-1/2 inch diameter to a total depth of 150 m using the flooded reverse method. The wells were completed with 12 inch diameter blank and screened PVC casing in the Upper Halite brine unit and lower semi-confined brine aquifer.
- One production well (P-4) was drilled at 17-1/2 inch diameter to a depth of 180 m using the flooded reverse method. The well was completed with 12 inch diameter PVC blank and screened production casing. The screened interval of the well was completed in the lower semi-confined to confined aquifer, below and isolated from the Upper Halite unit.
- One production well (P-5) was drilled at 17-1/2 inch diameter to a depth of 400 m using the flooded reverse method. The well was completed with 12-inch diameter SS blank and screened production casing. The screened interval of the well was completed in the deep brine aquifer.

1.4.4 PUMPING TESTS:

- Two long-term pumping tests were carried out on production wells P-1 (14 days) and P-2 (30 days) at 37 L/s and 38 L/s, respectively. Water level responses were measured in four monitoring wells adjacent to each production well.
- One 30-day pumping test was carried on production well P-4 at a pumping rate of 25 l/s. Water level measurements were made in adjacent monitoring wells P4-1 (lower aquifer completion), P4-2 (upper halite), P4-3 (upper halite) and P4-4 (upper halite).
- One 7-day pumping test was carried out on the previously drilled production well P-2 at a flow rate of 45 l/s. A packer was installed in the well at 40 m depth so that brine inflow during the pumping test was limited to the upper halite aquifer. Water level measurements were made in four adjacent monitoring wells during the 7-day pumping test.
- Six test trenches adjacent to sonic boreholes C1 through C6 were completed to a depth of 3 m and 24-hour pumping tests were carried out in each trench.
- One 30-day pumping test is being carried out on production well P-5 at a pumping rate of 35 l/s. Water level measurements are being made in adjacent exploration well S-25.

1.4.5 LABORATORY BRINE AND DRAINABLE POROSITY ANALYSIS:

- 718 primary brine samples (not including QA/QC samples) analysed by the University of Antofagasta, Alex Steward Assayers, or Andes Analytical Assays were used in the mineral resource estimation.
- 561 undisturbed samples from the sonic and HQ core were analysed by Daniel B Stephens and Associates (DBSA), Geo Systems Analysis (GSA) or Corelabs for drainable porosity and other physical parameters.

1.5 GEOLOGY AND MINERALIZATION

1.5.1 GEOLOGY

Based on the drilling campaigns carried out in the Salar between 2011 and 2021, eight major geological units were identified and correlated from the logging of drill cuttings and undisturbed core to a general depth of up to 400 m. Only borehole S-29 on the western edge of the Salar encountered bedrock at 219 m depth. Salar de Maricunga is a mixed style salar. An upper halite unit occurs (up to 34 m in thickness) in the central northern part of the Salar and hosts the upper brine aquifer. The halite unit is underlain by low permeability lacustrine sediments. The Salar is surrounded by relative coarse grained alluvial and fluvial sediments. These fans demark the perimeter of the actual salar and at depth grade towards the centre of the Salar where they form the distal facies with an increase in sand and silt. At depth two unconsolidated volcanoclastic units have been identified that appear quite similar. These two volcanoclastic units are separated by a relatively thin and continuous sand unit which may be reworked material of the lower volcanoclastic unit. A volcanic breccia was identified on the northern and western parts of the OCC that locally interfingers with the lower volcanoclastic unit. A lower brine aquifer is hosted in the lower alluvial, volcanoclastic, and volcanic breccia units (below the lacustrine sediments).

1.5.2 MINERALIZATION

The brines from Maricunga are solutions nearly saturated in sodium chloride with an average concentration of total dissolved solids (TDS) of 311 g/L. The average density is 1.20 g/cm³. Other components present in the Maricunga brine are: K, Li, Mg, Ca, SO₄, HCO₃ and B. Elevated values of strontium (mean of 359 mg/L) also have been detected. Table 1-1 shows a breakdown of the principal chemical constituents in the Maricunga brine including maximum, average, and minimum values, based on the 718 brine samples that were collected from the exploration boreholes during the 2011 - 2021 drilling programs (all concessions).

Table 1-1 Maximum, average and minimum elemental concentrations of the Maricunga brine

	B	Ca	Cl	Li	Mg	K	Na	SO ₄	Density
Units	mg/L	mg/L	mg/L	mg/L	mg/L	mg/L	mg/L	mg/L	g/cm ³
Maximum	1,993	36,950	233,800	3,375	21,800	20,640	105,851	2,960	1.31
Average	572	12,847	192,723	1,122	7,327	8,142	87,106	711	1.20
Minimum	234	4,000	89,441	460	2,763	2,940	37,750	259	1.10

1.6 STATUS OF EXPLORATION, DEVELOPMENT AND OPERATIONS

MSB completed a first positive DFS for the original Blanco Project in 2019 based on brine production from all concessions (OCC and Litio 1-6) to 200 m depth and a 20 Ktpy LCE production capacity.

MSB received all environmental approvals (RCA) from the Chilean authorities in February 2020 for the construction and operation of mining and processing facilities to produce 20 Ktpy of LCE over a 20-year mine-life. MSB received in 2018 a license from the Chilean Nuclear Energy Commission (CCHEN) for the production and sale of 35,554 tons of Lithium Metal Equivalent (LME) from the OCC.

This NI 43-101 technical report presents the results of the DFS for the Stage One project based on brine production only from the OCC to support an average of 15.2 Ktpy of LCE mining and processing facilities over a 20-year mine-life. The currently approved environmental permits will support this Stage One Project development.

It is expected that the financing structuring for the Stage One project will be successfully completed during 2022 and that a Project construction decision can be made immediately thereafter by the end of the year.

1.7 BRINE RESOURCE ESTIMATES

The brine resource estimate was determined by defining the aquifer geometry, the drainable porosity or specific yield (Sy) of the hydrogeological units in the Salar, and the concentration of the elements of economic interest, mainly lithium and potassium. Brine resources were defined as the product of the first three parameters.

The model resource estimate is limited to the OCC mining concessions in Salar de Maricunga that cover an area of 1,125 ha.

The resource model domain is constrained by the following factors:

- The top of the model coincides with the brine level in the Salar that was measured in the monitoring wells installed in the Salar.
- The lateral boundaries of the model domain are limited to the area of the OCC mining concessions.
- The bottom of the model domain coincides with the bedrock contact or 400 m depth.

The specific yield values used to develop the resources are based on results of the logging and hydrogeological interpretation of chip samples and recovered core of 8 rotary boreholes and 17

sonic and HQ core holes, results of drainable porosity analyses carried out on 561 undisturbed samples from sonic- and HQ core by GeoSystems Analysis, Daniel B Stephens and Associates, Corelabs, and four pumping tests. Boreholes within the measured and indicated resource areas are appropriately spaced at a borehole density of one bore per 1.5 km². Table 1-2 shows the drainable porosity values assigned to the different geological units for the resource model.

The distributions of lithium and potassium concentrations in the model domain are based on a total of 718 brine analyses (not including QA/QC analyses) mentioned in Section 1.3 above.

Table 1-2 Drainable porosity values applied in the resource model

Unit	Count	Sy Average
Halite	6	0.06
Lacustrine	323	0.02
Deep Halite	8	0.06
Alluvial Deposits	31	0.14
Lower Sand	20	0.06
Volcanoclastics	72	0.12
Lower Volcanoclastics	7	0.08
Volcanic Breccia	52	0.13

The resource estimation for the Project was developed using the Stanford Geostatistical Modelling Software (SGeMS) and the geological model as a reliable representation of the local lithology. The principal author was closely involved with the block model development; all results have been reviewed and checked at various stages and are believed to be valid and appropriate for these resource estimates. Table 1-3 shows the Measured and Indicated Resource for lithium and potassium for the OCC.

Table 1-3 Lithium and Potassium Measured and Indicated Resources of the Stage One Project – ‘Old Code’ Concessions - dated September 20, 2021

	Measured (M)		Indicated (I)		M+I	
	Li	K	Li	K	Li	K
Area (Km ²)	4.5		6.76		11.25	
Aquifer volume (km ³)	1.8		1.8		3.6	
Mean specific yield (Sy)	0.09		0.12		0.1	
Brine volume (km ³)	0.162		0.216		0.378	
Mean grade (g/m ³)	87	641	111	794	99	708
Concentration (mg/l)	968	7,125	939	6,746	953	6,933
Resource (tonnes)	154,500	1,140,000	203,500	1,460,000	358,000	2,600,000

Notes to the resource estimate:

1. CIM definitions (2014) were followed for Mineral Resources.
2. The Qualified Person for this Mineral Resource estimate is Frits Reidel, CPG.
3. No cut-off values have been applied to the resource estimate.
4. Numbers may not add due to rounding.
5. The effective date is September 20, 2021.

Table 1-4 shows the total resources of the OCC expressed as lithium carbonate equivalent (LCE) and potash (KCl).

Table 1-4 OCC resources expressed LCE and potash

	M+I Resources	
	LCE	KCL
Tonnes	1,905,000	4,950,000

1. Lithium is converted to lithium carbonate (Li₂CO₃) with a conversion factor of 5.32.
2. Potassium is converted to potash with a conversion factor of 1.9
3. Numbers may not add due to rounding

It should be noted that the OCC M+I Resources described in Table 1-3 and 1-4 are in addition to the M+I Resources (2018) of 184 Kt Lithium (979 Kt LCE) in the Litio 1-6 concessions to a depth of 200m.

1.8 BRINE RESERVE ESTIMATE.

A three-dimensional finite element groundwater flow and transport model (FEFLOW code) was constructed and successfully calibrated to steady state pre-mining conditions and to transient pumping test responses. The calibrated model was used to simulate brine production scenarios from the Stage One concessions over a 20-year project life. These simulations form the basis for the Stage One Lithium Mineral Reserve Estimate.

The reserve estimate for the Stage One Project was prepared in accordance with the guidelines of National Instrument 43-101 and uses the best practices methods specific to brine resources. The lithium reserves are summarized in Table 1-5 and Table 1-6

Table 1-5. Stage One Brine Mining Reserve for pumping to ponds

Category	Year	Brine Vol (Mm3)	Ave Li conc (mg/l)	Li metal (tonnes)	LCE (tonnes)
Proven	1-7	19	1,024	14,000	75,000
Probable	1-7	13		19,000	102,000
Probable	8-20	60	950	57,000	302,000
All	1-20	92	976	90,000	479,000

Table 1-6. Stage One Brine Production Reserve for Lithium Carbonate production (assuming 65% lithium process recovery efficiency)

Category	Year	Brine Vol (Mm3)	Ave Li conc (mg/l)	Li metal (tonnes)	LCE (tonnes)
Proven	1-7	19	1,024	9,000	49,000
Probable	1-7	13		12,000	66,000
Probable	8-20	60	950	37,000	196,000
All	1-20	92	976	58,000	311,000

Notes to the Reserve Estimate:

1. The Stage One Reserve Estimate includes an optimized wellfield configuration and pumping schedule to comply with environmental constraints and water level decline restrictions as part of the environmental approval document (RCA) issued by the Chilean Environmental Agency.
2. Lithium is converted to lithium carbonate (Li_2CO_3) with a conversion factor of 5.32
3. The qualified Person for the Mineral Reserve estimate Frits Reidel, CPG
4. The effective date for the Reserve Estimate is December 22, 2021.

5. Numbers may not add due to rounding effects.
6. Approximately 25 percent of the Measured and Indicated Resources are converted to Proven and Probable Reserves as brine feed from the production wellfield to the evaporation ponds without accounting for the lithium process recovery efficiency. The overall conversion from M+I Resources to Total Reserves including lithium process recovery efficiency of 65% is approximately 16 percent.

1.9 EXPLORATION POTENTIAL

Measured and Indicated Resources have been defined to 400 m depth in the OCC (1.9 Mt LCE) and to 200 m depth in the Litio 1-6 concessions (1.0 Mt LCE). The geological model for the Project suggests that the same geological units that host the lower brine aquifer below the OCC between 200 and 400 m depth continue below the Litio 1-6 concessions. Geophysical data suggest that the lower aquifer hosted in the Volcanoclastic units and Volcanic breccia continues to the bedrock contact at a variable depth of up to 550 m. An exploration target has been identified below the base of the current M+I Resources in the OCC and Litio 1-6 concessions to the bedrock contact with an estimated 1,2 Mt – 2,1 Mt LCE providing a significant potential for resource expansion.

1.10 LITHIUM RECOVERY PROCESS

The facilities have been designed to produce an average of 15,200 TPY of lithium carbonate (Li_2CO_3) battery grade over a 20-year mine-life.

The brine obtained from the production wells in the Salar is pumped to evaporation ponds, where it is concentrated through evaporation causing the saturation of the salts crystallizing mainly halite, sylvinite and carnallite. All crystalized salts are periodically harvested from the ponds and stored in stockpiles defined for such purpose.

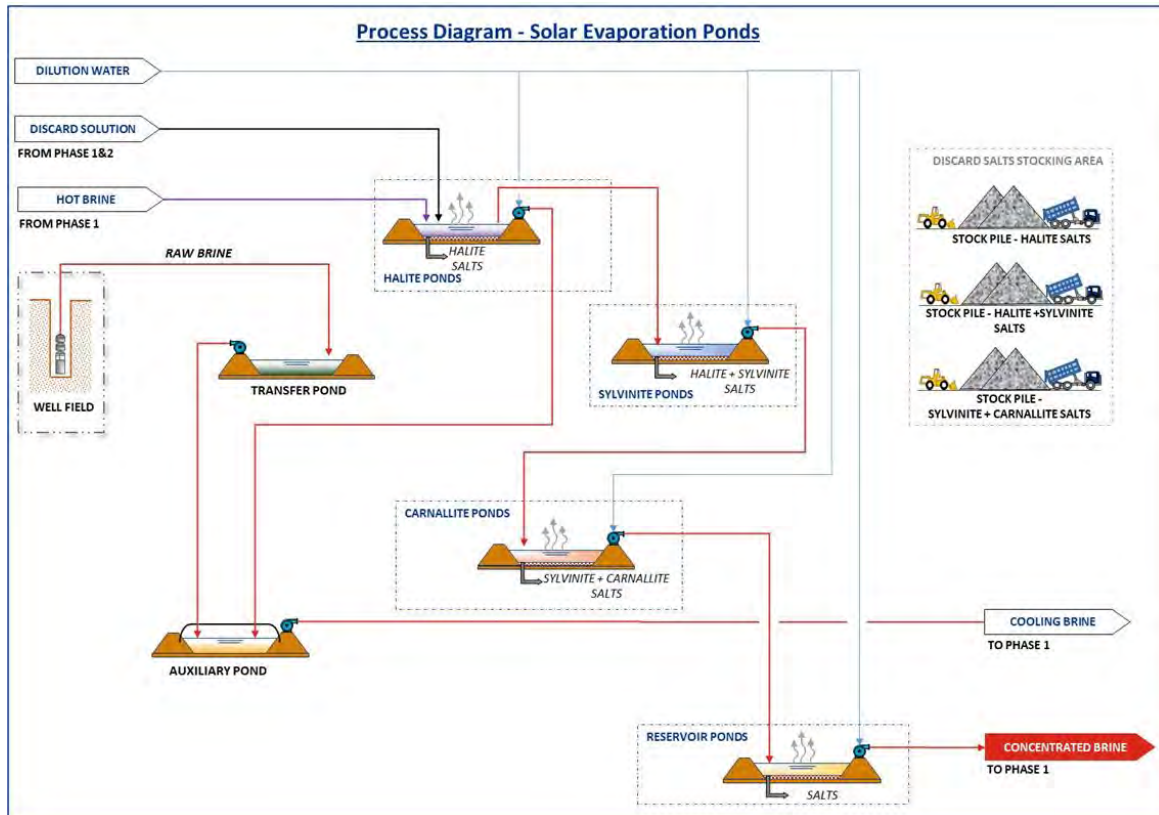
The concentrated lithium brine obtained from the evaporation ponds is pumped directly to reservoir ponds, which feed a Salt Removal Plant. This plant mainly removes calcium impurities as calcium chloride and tachyhydrite from the brine and generates a stable feed in terms of chemical composition to the Lithium Carbonate Plant. This is achieved through consecutive evaporation and crystallization steps. This process allows a higher and faster concentration of the lithium in the brine and reduces the lithium losses with the precipitated salts, thus increasing the overall efficiency.

The concentrated lithium brine obtained from the Salt Removal Plant is subsequently fed to the Lithium Carbonate Plant, where through processes of purification, ion exchange and filtration, remaining impurities such as boron, calcium and magnesium are removed. The lithium concentrated brine is then fed to a carbonation stage, where through the addition of soda ash, lithium carbonate

precipitates. This precipitated lithium carbonate is then fed to a centrifuge for water removal, and finally dried, and packed.

A simplified diagram of the process is presented in Figure 1-1 and a detailed description of the process is presented in Chapter 17.

Figure 1-1 General Process Diagram



Salt Removal Plant is required as the pilot evaporation tests indicated the high concentration of calcium, magnesium and lithium in the concentrated brine lowers the brine activity significantly and the eutectic end point of about 3-4% wt lithium is never reached at ambient concentrations. Additionally, concentrating to higher levels of about 1,5% wt in summertime, showed significant losses in lithium as lithium borates and entrapment in the crystallized salt in the ponds.

The risk that the brine might not reach the targeted lithium concentration in the ponds (3-4% wt) in a consistent and continues manner during the year, was the main driver to design the process for a concentration target of about 0.9% wt, which is proved it can be reached and maintained for a consistent and continuous feed to the Salt Removal Plant and Lithium Carbonate plant thereafter, thus increasing the overall efficiency by reducing the losses in salt entrainment, the consumption of chemical reagent and allowing water recovery during the process.

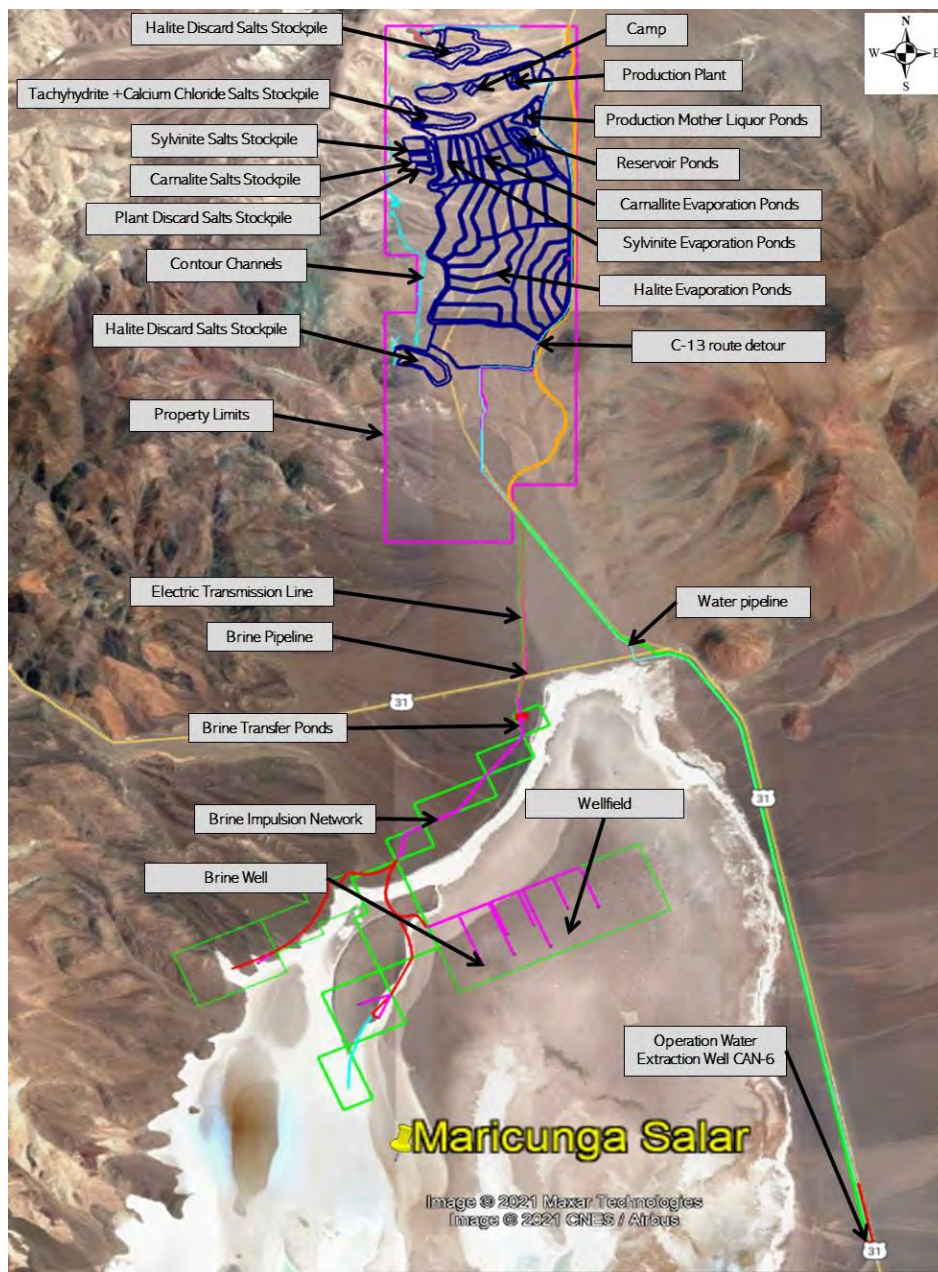
1.11 PROJECT INFRASTRUCTURE

The facilities that are considered for the project include mainly the following areas:

- Solar evaporation pond installations (transfer pumps, dilution water tanks, among others)
- Salt Removal Plant – (named also Phase 1)
- Lithium Carbonate Plant – (named also Phase 2)
- Utilities for process ancillary services (reagents, water, compressed air, steam boilers, among others)
- Installations for plant ancillary services (administration offices, laboratory, among others)
- Workers' camp and
- Temporary contractors' installations

All main installations are presented in Figure 1-2.

Figure 1-2 Project location presenting all main installations



Source: Worley – Google Earth

The brine production wellfield considers eleven (11) production wells operating concurrently at any time. The required annual average brine feed rate from the wellfield to the evaporation ponds is around 13,000 m³/d to support an annual average lithium carbonate production of 15,200 t over a 20-years mine-life. This feed will vary during the seasonal changes, increasing in the summer period due to a higher evaporation rate and decreasing in winter since evaporation will be lower.

The solar evaporation ponds area that MSB plans to build will be located north of the Maricunga Salar and will cover a total base area of 5.36 million m². These ponds will allow the brine to be concentrated in different steps. In addition, there will be approximately 1.6 million tonnes of discards salt that will be stockpiled at site, salts obtained from both the evaporation ponds and from the production plant.

The buildings of the plant area are designed according to the weather conditions of the site. These buildings are classified as follows:

Salt Removal Plant – Phase 1

- Building for evaporation and crystallization equipment
- Solvent extraction (SX) plant building

Lithium Carbonate Plant – Phase 2

- Building includes ion exchange, magnesium and calcium removal, solid / liquid separation, drying, packing and product storage.

Plant Services

- Reagent storage and/or preparation building, which includes the following building areas:
 - SX reagents storage and distribution
 - Hydrochloric acid storage and distribution
 - Caustic soda dilution, storage and distribution
 - Soda Ash storage (solid and liquid), preparation and distribution
 - Lime storage, preparation and distribution
 - Other minor reagents
- Fuel station.
- Air compressors room.
- Boilers room.
- Water Treatment Plant (to generate soft water).

The mining camp will have 2 platforms with a total area of 28,590 m². The facilities of the camp will be modular and will be connected by pedestrian and vehicular access. During the construction phase there will be 8 dorm buildings with a capacity for 1,200 people. This will reduce to 232 people during the operation phase that work on-site. All buildings will have a heating system, ventilation, power supply, networks, sanitary installations, fire detection and extinguishers according to DS594.

Electrical Energy

The Stage One Project has an average connected load of 13.7 MW of electrical power. The Electric Coordinator already gave MSB the authorization to connect to an existing 23 kV transmission line. MSB strategy is to build a new substation and reinforced the line.

Water

MSB has secured a water supply for the construction and operation stages of the project through a long-term lease agreement for the use of CAN-6 well. The use of the CAN-6 well is included in the Project RCA environment approval.

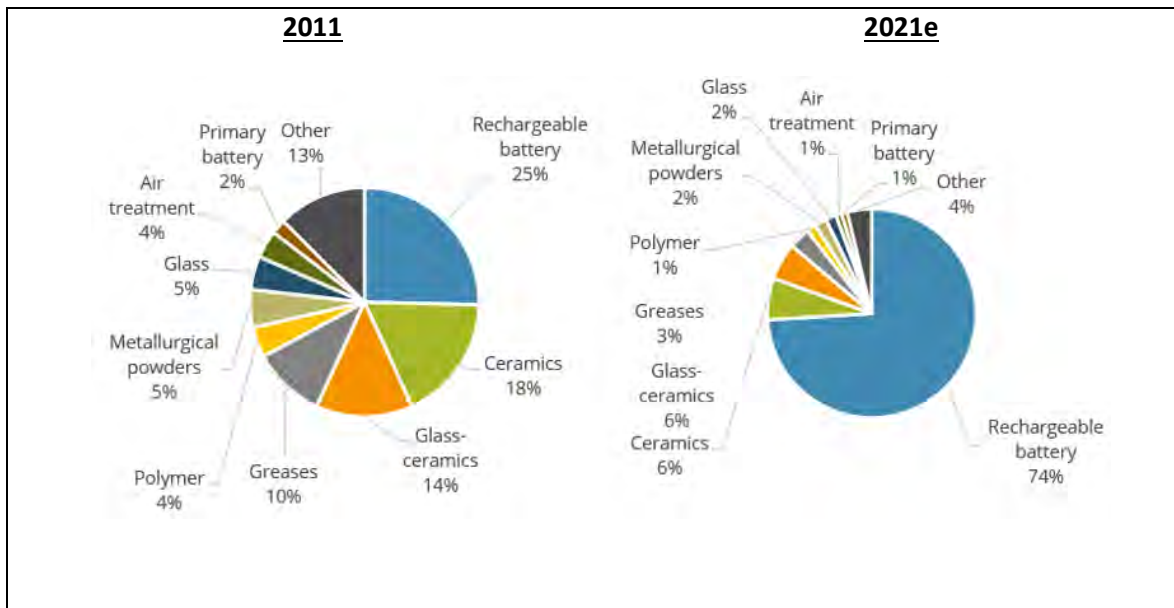
1.12 MARKET STUDIES AND CONTRACTS

1.12.1 CONSUMPTION

Demand growth for lithium since 2009 has been led by the rapidly increasing use of lithium in rechargeable battery applications in the form of lithium carbonate and more recently lithium hydroxide. From the rechargeable battery sector alone, growth has averaged 23.5%py between 2011 and 2021e, forming over 50% of lithium demand since 2017. Unlike most other major end-use applications, demand from rechargeable batteries continued to increase in 2020, despite disruption caused by the Covid-19 pandemic and related lockdowns.

The rechargeable battery sector accounted for 71% of lithium consumption in 2020, which is expected to increase to 74% in 2021. The rechargeable battery sector became the largest lithium consumer in 2008, and in 2015 accounted for over three times the volume consumed by the next largest sector, ceramics. The ceramics, glass-ceramics and glass industries formed the next largest end-use markets in 2021e, forming 6.4%, 5.7% and 1.6% of total demand respectively, with lithium greases forming 3.1% of total demand.

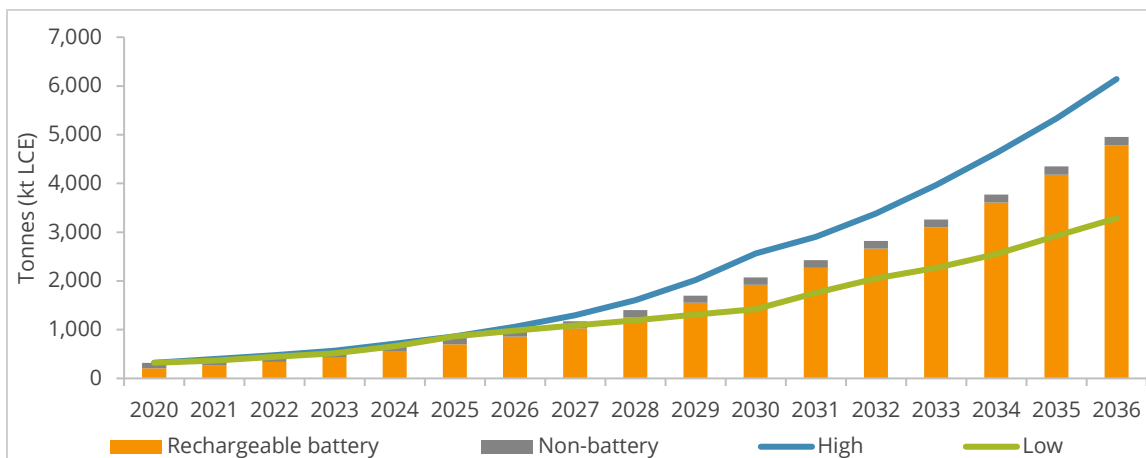
Figure 1-3 World: Consumption of lithium by first use, 2011 and 2021e (t LCE)



Source: Roskill

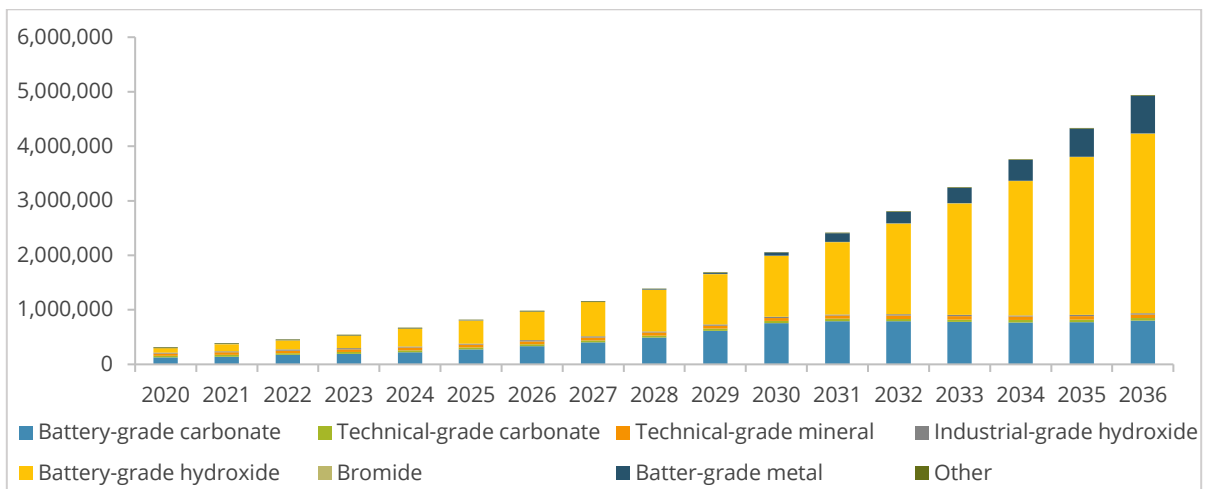
Under Roskill's base-case scenario, lithium demand is forecast to increase by 12.6%py in the period to 2036, reaching a total of 4.95Mt in 2036. In the 'High-case', forecast lithium demand is expected to increase by 20.1% CAGR in the period from 2021 to 2036, reaching a total of 6.14Mt LCE. Demand from non-battery applications is expected to form a diminishing proportion of lithium demand, with demand from such sectors decreasing from 31% in 2021 to 4% in 2036. Non-battery applications are expected to show continued demand growth of between 1-4%py over the period to 2036, aligned to growth in global and regional GDP and industrial production.

Figure 1-4 World: Forecast consumption of lithium by first use, 2020-2036 (000t LCE)



Source: Roskill

Figure 1-5 World: Forecast consumption of lithium by product, 2020-2036 (kt LCE)



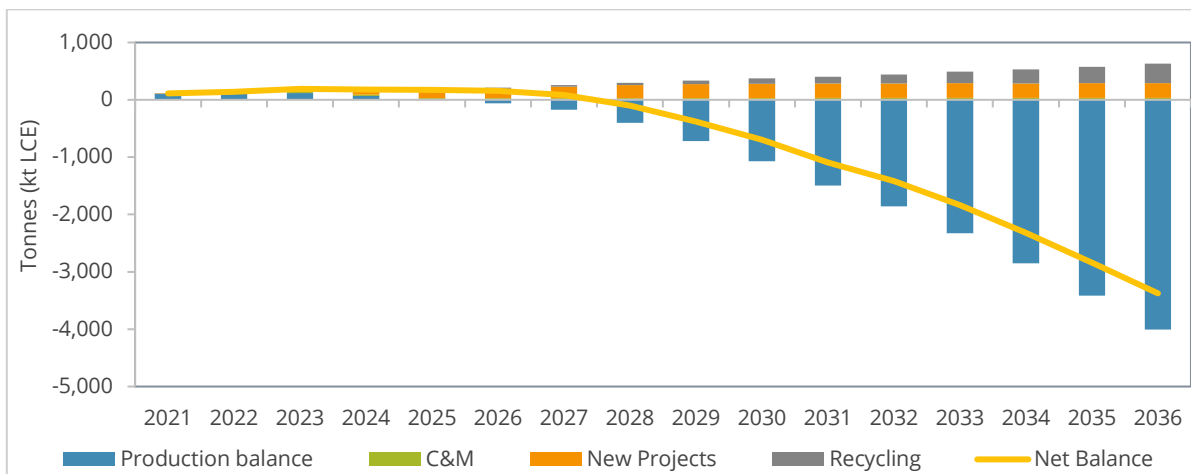
Source: Roskill

As a result of the strong growth in demand from rechargeable battery applications, demand for battery grade products is forecast to accelerate over the outlook horizon. Battery-grade lithium carbonate and hydroxide demand is forecast to increase by 18.8%py and 26.2%py respectively in the period from 2021 to 2031, with a further 0.2%py and 19.9%py increase respectively from 2031 to 2036. In 2036, battery-grade lithium carbonate and hydroxide demand are forecast at 802.3kt LCE and 3,288.1kt LCE respectively. Battery-grade metal will also grow above the industry average, as more is used in advanced lithium rechargeable batteries and primary batteries.

1.12.2 PROCESSING AND PRODUCTION

In 2021, global production of refined compounds is forecast to total 636.3kt LCE. Based on announced capacity expansions, refined production is forecast to increase at a CAGR of 7.9% to 2036. Under this scenario supply is forecast to surpass 1Mt LCE in 2024 before reaching 2Mt LCE by 2036. This represents more than a doubling of the expected output in 2021. Roskill forecasts battery-grade production to increase by 6.2% CAGR to 2036 reaching 1,057.7kt LCE under the base-case scenario. As a result of demand significantly outpacing that of refined supply Roskill forecast structural deficits to form in the market from the mid-2020s. The deficits are not definitive, however, and should be viewed as the “investment requirement” for additional supply.

Figure 1-6 Lithium chemical balance, 2021-2036 (kt LCE)



Source: Roskill

1.12.3 PRICES

The market saw growth in refined output outpace growth in demand in the 2018-2020 period with resultant stocks being built leading to lower prices. Roskill expects refined output and inventories to meet demand growth in 2021 with increasing pressure on the supply and demand balance for high quality battery-grade products.

From 2021, Roskill expects demand growth to return to higher levels – perhaps turbo-charged by government initiated Covid-19 economic recovery programmes – and with some capacity (built or under construction) temporarily or permanently off-line, and some brownfield/greenfield project development suspended, demand will start to stretch supply into 2022. Sentiment may well improve ahead of fundamentals, further incentivising prices, as has been witnessed in the downstream battery/EV sector even during 2020 as a “green” recovery is increasingly seen following the Covid-19 impact.

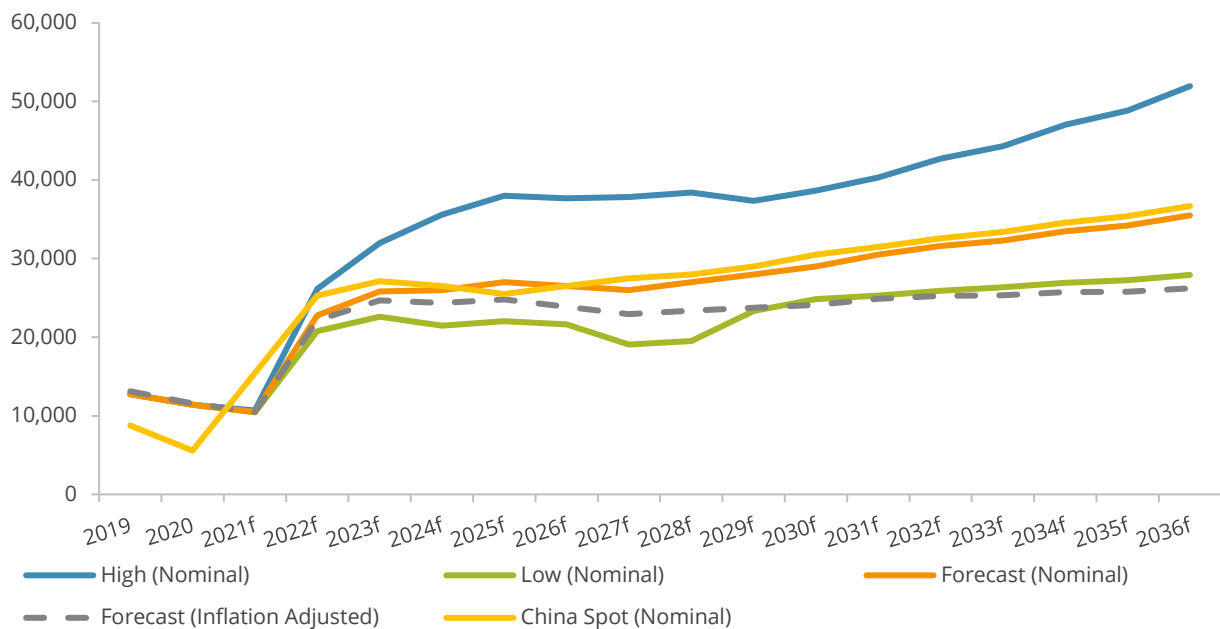
Roskill’s price forecast methodology for lithium is based on three main factors

- Production/margin cost curve
- Incentive pricing for expanded and new capacity
- Supply/demand balance and trends

Roskill expects marginal costs of refined lithium production (carbonate and hydroxide) to remain between US\$6,000-11,000/t LCE through 2036, depending on whether the very high cost of production from higher cost deposits enters the supply chain. This does not mean, however, that

prices will remain at or slightly above marginal cost, because to increase capacity to fulfil future demand the industry needs a price incentive – mining/refining projects being inherently risky to build and scale-up from a technical and economic perspective.

Figure 1-7: Average annual contract and spot price forecast for battery-grade lithium carbonate, 2019-2036 (US\$/t)



Source: Roskill

Note: Real prices adjusted to constant US dollars using United States GDP deflator data from the Federal Reserve and the International Monetary Fund's World Economic Outlook Database. Real prices adjusted to 2021\$.

Roskill forecast for contract battery-grade carbonate prices to average US\$23,609/t (constant 2021 US dollars) over the 2021-2036 horizon. Whereas for domestic China spot prices Roskill forecast an average of US\$24,683/t (constant 2021 US dollars) over the same time period.

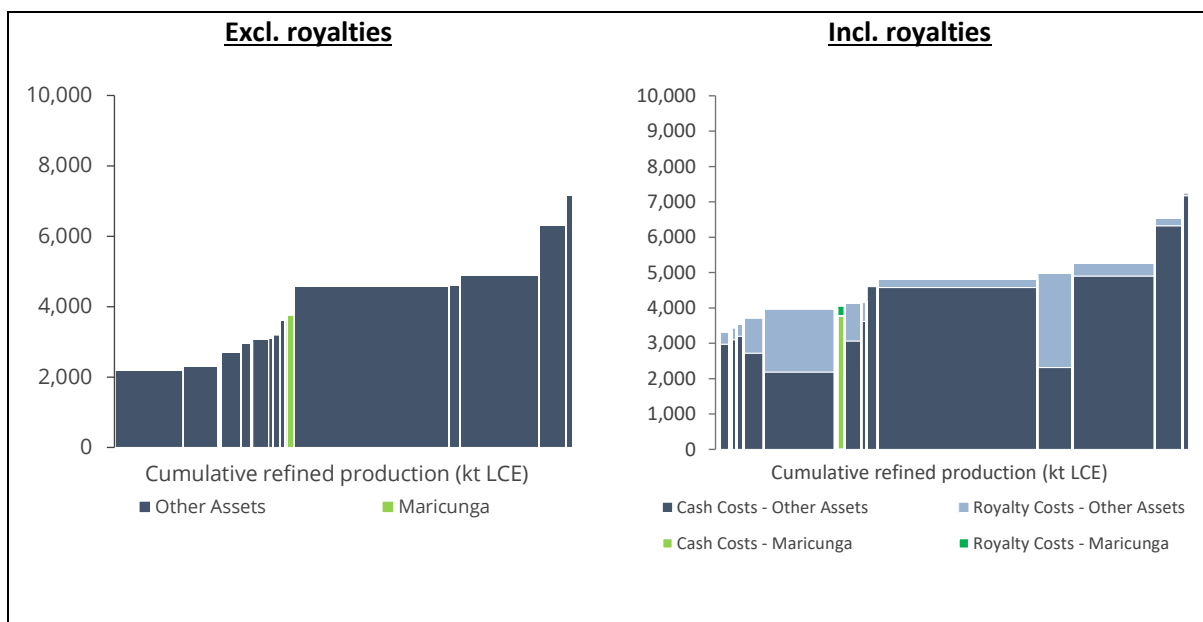
The commonly held view in the market is that battery-grade lithium carbonate commands a slightly higher price to technical-grade, typically around US\$500-1,000/t CIF, reflecting the purification and/or micronizing steps involved for most producers. However, there have been periods historically when technical-grade carbonate discounts have reversed. This has typically occurred in periods of severe supply tightness and/or negative sentiment for future availability.

1.12.4 COST

In 2021, brine producers continue to enjoy the lowest cost lithium carbonate production in the industry with costs typically around US\$4,150/t, within a range of US\$3,650/t to US\$4,850/t. In comparison, spodumene conversion plant costs are mostly in the range of US\$6,750/t to US\$9,150/t, although some fully integrated producers sit below this range aided by access to low-cost feedstock from Greenbushes. Chinese operations utilising lepidolite feedstocks have average lithium carbonate production costs of around US\$5,400/t.

Production costs in 2021 increased comparatively from 2020 for lithium carbonate derived from mineral sources. Costs for spodumene users increasing by around 18%, whilst the average y-o-y cost increase for refining from lepidolite feedstocks is around 1.5%. Looking forward, production costs for lithium carbonate derived from mineral concentrate feedstocks are expected to continue to increase as the market price of spodumene rises.

Figure 1-8: Lithium carbonate cash cost curve, 2021 (US\$/t LCE)



Source: Roskill

Minera Salar Blanco's Stage One Project has a number of competitive advantages which place the asset towards the centre of the carbonate cash cost curve. These include lower cost processing methods, lower cost of transportation and a lower cost of disposal of salts.

1.13 ENVIRONMENTAL STUDIES, PERMITTING AND SOCIAL OR COMMUNITY IMPACT.

MSB received the environmental approval for its Maricunga project on February 4, 2020, by Resolution N°94 considering the construction and operation of both, a 58,000 ton/year Potassium Chloride (KCL) Plant and a 20,000 ton/year Lithium Carbonate plant over a period of 20 years (KCL plant has not been included in this DFS). The EIA approved a brine extraction of 209 l/s, freshwater extraction of 35 l/s and all associated industrial facilities, including evaporation pond areas, brine pipelines and the campsite. The Environmental Impact Assessment (EIA), prepared by international consulting company Stantec (previously MWH), was submitted to the Chilean Environmental Assessment Service (SEA¹) in September 2018 and was the culmination of more than two years of field and desk work.

The process involved in-depth data gathering, a variety of environmental and engineering studies and monitoring campaigns which resulted in a comprehensive 11,400-page document, which included complete environmental baseline studies, hydrogeological modelling, human, archaeological and fauna and flora characterisation, and impact evaluation.

The EIA also included a lengthy process of social engagement with the Colla indigenous communities in the area. In addition, significant consultation took place with regional authorities and local organisations.

The EIA is the main environmental permit for construction and operation of the project and only several minor permits must be processed before construction.

Resolution N°94/2020 contains specific commitments that MSB must comply with, as mitigation and compensation measures.

¹ “Servicio de Evaluación Ambiental”.

1.14 CAPITAL AND OPERATING COST

1.14.1 CAPITAL EXPENDITURES – CAPEX

Capital expenditures are based on an average operating capacity of 15,200 TPY of lithium carbonate.

Capital equipment and construction costs have been obtained from solicited quotes to equipment manufacturers and construction companies. Considerable engineering progress has been achieved both on plant design and infrastructure requirements. Given this, Worley have confirmed a capital cost estimate accuracy within a +/- 11.1% range. Capital and operating cost estimates are expressed in fourth quarter 2021 US dollars.

Capital investment for the Project, including equipment, materials, indirect costs and contingencies during the construction period is estimated to be US\$ 626 million. Out of this total Direct Project Costs represent US\$ 419 million; Indirect Project Costs represent US\$ 145 million, and the Contingencies provision is US\$ 62 million. The indirect project costs represent 34.6% of Direct project costs, while the contingencies represent 11.1% of Direct plus Indirect project costs.

In addition, Sustaining Capital expenditures total US\$ 42 million over the 23-year evaluation period of the project, which includes a 2.5-year construction period and an operating life of 20 years. Maximum working capital requirements over the project horizon is US\$ 15.8 million.

Total capital expenditures are summarized in Table 1-7.

Table 1-7 Total Capital Expenditures

Area	Total Project	Projected Budget US\$ 000
	Direct Costs	
1000	Brine Extraction Wells	33,235
2000	Evaporation Ponds	89,878
5000	Salt Removal Plant	110,322
6000	Lithium Carbonate Plant	55,754
8000	General Services	83,953
9000	Infrastructure	45,814
	Total Direct Cost	418,957
	Total Indirect Cost	144,835
	Contingencies (11,1%)	62,581
	Total Capital Expenditures	626,372

1.14.2 OPERATING COST ESTIMATE

An operating cost estimate for an average of 15,200 TPY Li_2CO_3 capacity facility was prepared. This estimate is based upon process definition, laboratory work, tests at equipment suppliers and reagents consumption rates all provided or determined by MSB. Vendor quotations have been used for reagents costs. Expenses estimates, as well as manpower levels, are based on Worley's experience and information provided by MSB.

Table 1-8 Average Operating Costs

Average Operating Costs	US\$ / Tonne Li_2CO_3	Total 000 US\$
DIRECT COSTS		
Chemical Reactives and Reagents	1,099	16,704
Salt Harvesting	266	4,049
Energy	1,164	17,689
<i>Memo: - Electrical</i>	<i>342</i>	<i>5,206</i>
<i>- Thermal</i>	<i>821</i>	<i>12,483</i>
Manpower	518	7,867
Catering & Camp Services	132	1,999
Maintenance	358	5,443
Transport	181	2,756
OPERATIONAL CASH COSTS	3,718	56,506
INDIRECT COSTS		
General & Administration	146	2,220
INDIRECT COSTS SUBTOTAL	146	2,220
TOTAL PRODUCTION COSTS	3,864	58,726

As indicated in Table 1-8, energy costs -electrical and thermal- are the major operating cost of the project, closely followed by chemical reagents. Fuel consumed by the Salt Removal Plant is the major component of energy costs. Over 90% of the chemical reagents' costs correspond to soda ash and hydrochloric acid. Over 35,000 tonnes of soda ash are required to produce an average of 15,200 tonnes of Li_2CO_3 . Other important expense items are manpower, maintenance, and salt harvesting.

1.15 ECONOMIC ANALYSIS

The cash flow projection results in the following project economic metrics:

Table 1-9 Base Case Economic Results (full equity project funding)

ECONOMIC RESULTS		BEFORE TAXES	AFTER TAXES
NPV 6%	MM US\$	2,529	1,827
NPV 8%	MM US\$	1,971	1,412
NPV 10%	MM US\$	1,545	1,095
IRR	%	33.4%	29.3%
PAYOUT	Time	2 Y, 8 M	2 Y, 8 M

Table 1-10 Economic Results (50/50 debt / equity project funding)

ECONOMIC RESULTS		BEFORE TAXES	AFTER TAXES
NPV 6%	MM US\$	2,513	1,811
NPV 8%	MM US\$	1,984	1,425
NPV 10%	MM US\$	1,582	1,131
IRR	%	44.5%	39.6%
PAYOUT	Time	2 Y, 0 M	2 Y, 0 M

The above tables show that the project's economic metrics are very attractive, with the IRR for the full equity case being 29.3% on an after-tax basis and a project NPV (8%) of MMUS\$ 1,412. In this same case, investment pay out occurs at 2 years and 8 months after the end of the investment period. Given the project's high rate of return, including debt in the capital structure further improves these results, as shown in Table 1-10. Table 1-11 shows the main items included in the project's cash flow and which produce the above shown results.



Table 1-11 Project Summary Cash Flow Projection

Year Period	2023 1	2024 2	2025 3	2026 4	2027 5	2028 6	2029 7	2030 8	2031 9	2032 10	2037 15	2042 20	2044 22	2045 23	Totals
Revenues	-	-	-	195,521	344,814	384,853	389,906	395,987	407,734	414,120	377,767	416,846	416,846	432,478	7,665,936
Li2CO3 Battery Grade	-	-	-	100,218	275,427	347,010	352,806	358,241	369,383	375,201	342,207	377,608	377,608	391,768	6,828,137
Li2CO3 Technical Grade	-	-	-	95,302	69,387	37,843	37,100	37,745	38,351	38,919	35,560	39,238	39,238	40,710	837,799
Cost of Goods Sold	-	-	-	(34,903)	(53,147)	(58,430)	(63,112)	(63,112)	(63,112)	(63,112)	(57,640)	(61,744)	(61,744)	(63,386)	(1,174,520)
OPEX Li2CO3	-	-	-	(34,903)	(53,147)	(58,430)	(63,112)	(63,112)	(63,112)	(63,112)	(57,640)	(61,744)	(61,744)	(63,386)	(1,174,520)
Gross Margin	-	-	-	160,617	291,667	326,423	326,794	332,874	344,622	351,008	320,126	355,102	355,102	369,092	6,491,416
Gross Margin%				82%	85%	85%	84%	84%	85%	85%	85%	85%	85%	85%	85%
Other cash expenses				(2,545)	(7,411)	(8,488)	(7,268)	(7,467)	(7,861)	(8,211)	(7,070)	(8,265)	(8,174)	(30,949)	(170,006)
Current Royalties		-	-	(906)	(4,877)	(5,713)	(4,462)	(4,625)	(4,948)	(5,260)	(4,337)	(5,298)	(5,207)	(5,085)	(91,887)
Eventual Royalties (3% of Sales)		-	-	-	-	-	-	-	-	-	-	-	-	-	-
Communities		-	-	(1,173)	(2,069)	(2,309)	(2,339)	(2,376)	(2,446)	(2,485)	(2,267)	(2,501)	(2,501)	(2,595)	(45,996)
Mining Licenses & Water Rights		-	-	(352)	(352)	(352)	(352)	(352)	(352)	(352)	(352)	(352)	(352)	(352)	(7,040)
Insurance Policy for Rem Allowance - 0,5 %		-	-	(114)	(114)	(114)	(114)	(114)	(114)	(114)	(114)	(114)	(114)	(114)	(2,280)
Remediation		-	-	-	-	-	-	-	-	-	-	-	-	(22,803)	(22,803)
EBITDA	-	-	-	158,072	284,256	317,935	319,526	325,407	336,761	342,797	313,057	346,837	346,928	338,143	6,321,410
- Depreciation	-	-	-	(225,494)	(200,439)	(200,439)	(4,512)	(4,011)	(4,011)	(76)	(1,494)	(3,815)	(4,659)	(4,929)	(671,183)
- Amortization	-	-	-	(40,803)	-	-	-	-	-	-	-	-	-	-	(40,803)
Profit Before Taxes	-	-	-	(108,225)	83,816	117,495	315,014	321,396	332,750	342,721	311,563	343,021	342,269	333,214	5,609,424
Income Taxes (27%)	-	-	-	-	-	(25,133)	(85,054)	(86,777)	(89,843)	(92,535)	(84,122)	(92,616)	(92,413)	(89,968)	(1,514,545)
Profit After Taxes	-	-	-	(108,225)	83,816	92,362	229,960	234,619	242,908	250,186	227,441	250,406	249,856	243,246	4,094,880
+ Depreciation & Amortization	-	-	-	266,297	200,439	200,439	4,512	4,011	4,011	76	1,494	3,815	4,659	4,929	711,986
Operating After Tax Cash Flow	-	-	-	158,072	284,256	292,801	234,472	238,630	246,919	250,262	228,935	254,221	254,515	248,176	4,806,866
Non Operating Cash Flow	(71,855)	(335,071)	(247,014)	10,901	(3,117)	(1,988)	(15,340)	1,191	-	(231)	(1,939)	(4,260)	(5,104)	17,795	(676,526)
Initial Investment and Sustaining Capital	(65,621)	(311,694)	(249,057)	-	-	-	(12,534)	-	-	(211)	(1,899)	(4,220)	(5,064)	(5,064)	(676,045)
VAT on CAPEX and OPEX, net of refunds	(6,234)	(23,377)	5,950	19,627	(2,463)	(668)	(1,636)	1,191	-	(20)	(40)	(40)	(40)	7,424	(481)
Working Capital Variation	-	-	(3,907)	(8,725)	(654)	(1,321)	(1,171)	-	-	-	-	-	-	15,436	-
Cash Flow Before Interest and Tax	(71,855)	(335,071)	(247,014)	168,973	281,139	315,946	304,186	326,598	336,761	342,566	311,117	342,576	341,824	355,939	5,644,884
Accumulated Cash Flow (Before Interest and Tax)	(71,855)	(406,926)	(653,940)	(484,967)	(203,828)	112,118	416,304	742,902	1,079,663	1,422,229	3,013,042	4,604,934	5,288,945	5,644,884	
Financing cash flow	-	-	-	-	-	-	-	-	-	-	-	-	-	-	-
Before Tax Cash Flow	(71,855)	(335,071)	(247,014)	168,973	281,139	315,946	304,186	326,598	336,761	342,566	311,117	342,576	341,824	355,939	5,644,884
After Tax Cash Flow	(71,855)	(335,071)	(247,014)	168,973	281,139	290,813	219,132	239,821	246,919	250,031	226,996	249,960	249,411	265,971	4,130,340

1.16 CONCLUSIONS AND RECOMMENDATIONS

1.16.1 CONCLUSIONS

Based on the analyses and interpretation of the results of the exploration work carried out for the Stage One Project between 2011 and 2021, the following concluding statements are prepared:

- The entire MSB concessions in the Salar have been covered by exploratory drilling between 2011 and 2021 at an approximate borehole density of one exploration borehole per 1.5 km²; it is the opinion of the author that such borehole density is appropriate for the mineral resource estimate described herein.
- It is the opinion of the author that the Salar geometry, brine chemistry composition and the specific yield of the Salar sediments on the OCC have been adequately defined to a depth of 400 m to support the Measured and Indicated Resource estimate described in Section 14 and shown in Table 1-4.
- MSB was awarded a key regulatory license by the Chilean Nuclear Energy Commission (CChEN) to produce, market and export lithium products from Salar de Maricunga on March 9th, 2018 for an initial 88,885 t lithium metal or 472,868 t of LCE over a 30-year term.
- MSB received the environmental approval for its Maricunga project on February 4, 2020, by Resolution N°94 considering the construction and operation of both, a 58,000 ton/year Potassium Chloride (KCL) Plant and a 20,000 ton/year Lithium Carbonate plant over a period of 20 years (the KCL plant has not been included in this DFS).
- MSB has secured a water supply for the construction and operation stages of the Project through a long-term lease agreement for the use of CAN-6 well, that has all the water rights in place. MSB also has secured all environmental approvals for the operation of this supply. Based on the engineering and economic analysis of the project the following conclusions are presented:
- The CAPEX for the lithium carbonate 15,200 TPY Stage One Project is US\$ 626 million. This total is higher than for other similar size lithium carbonate projects as result of the requirement of a Salt Removal Plant, with the objective to maintain a consistent and continuous feed to the Lithium Carbonate plant, thus decreasing the operation risk and increasing the overall efficiency. It also must be mentioned that the Salt Removal Plant has the following advantages:
 - It allows ending the solar pond evaporation stage with a comparatively low lithium concentration brine (0.8% to 0.9%), given that in addition to Ca removal, substantial evaporation and concentration takes place at the above referred plant. Thus, if the Salt Removal Plant were not necessary, additional pond area would be required to obtain a concentrated brine suitable for the Lithium Carbonate Plant.
 - It allows recovery of part of the water contained in the brine, thus reducing the total water consumption.

- It allows extracting impurities (mainly calcium) contained in the brine without the use of chemical reagents.
 - It allows obtaining battery-grade lithium carbonate without adding a CO₂ purification stage.
- Total average unit operating cash cost for the Project is US\$ 3,718 per tonne of lithium carbonate. Again, this is relatively higher than some comparably sized lithium brine projects, the main reason being the energy cost associated with the Salt Removal Plant, but which has the advantages pointed out in the previous commentary.
- The project's economic results are very positive, with a full equity, after-tax base case that generates, an NPV (8%) of US\$ MM 1,412, an IRR of 29,3 % and pay-out period of 2 years and 8 months. On a pre-tax basis, the NPV (8%) is US\$ MM 1,971, resulting in a 33,4 % IRR. On a levered basis (50:50 debt/equity), after-tax NPV (8%) is US\$ MM 1,425, resulting in a 39.6 % IRR.
- The main reasons for the above results are the favourable outlook for lithium prices, as developed in Section 19, relatively low -27 %- corporate income tax rate in Chile, as well as an expected low royalty rate regime for MSB, due mostly to the special "grandfathered" conditions affecting the OCC MSB mining properties included in the Stage One Project.
- The project's sensitivity analysis carried out in sub section 22.8.2, which examines its results when base case assumptions can deviate from expected values. The outcome of this analysis indicates that the project is sensitive to the expected price of lithium carbonate. In this way, if lithium prices were to be permanently only 75 % of the base case projection, the project's NPV after-tax (8%) declines to US\$ MM 856 and IRR drops to 22,3 %. Conversely, the project's results improve very substantially - NPV after-tax (8%) US\$ MM 1,964 and IRR 35,3 % if lithium prices were to be permanently 125 % of the base case projection.
- The project is less sensitive to variations in the production level, since a 25% variation in this second parameter causes only a 12% variation in NPV. Maybe contrary to expectations, the project's NPV is very slightly sensitive to variations in CAPEX or OPEX, given that a 25% variation in each of these two parameters translates into, respectively, an 8% and a 6% change. This indicates project resilience in the face of possible negative CAPEX or OPEX scenarios.

1.16.2 RECOMMENDATIONS

- Completion of the detailed engineering needed to get the final permits to modify the course of Highway C-13, whose current routing runs through the project's pond farm, must be given priority given that solar evaporation pond construction is the most critical element in the project's construction plan. An initial approval was granted by the Infrastructure Ministry (Road Department) during Q4 2021 based on basic engineering.
- Given that the solar evaporation pond construction is a critical element for the project and given the very large pond surfaces that need to be covered with plastic liner, it is advisable to enter, as soon as possible, into a production contract with a reputable supplier of this critical material. Considering that it may be possible that one, or more, additional lithium brine projects might be in construction at the same time, straining plastic liner production capacity.
- As it was suggested in the PEA study in 2017, it is reasonable to postpone the investment in a KCl plant for a few years and reconsider the decision to build it if there is a clear improvement of its expected long-term pricing outlook.
- It is recommended that a new risks evaluation workshop be conducted before the start of the detailed engineering. This workshop will address safety, environmental, brine production and process issues.
- It is recommended that for the project's next stage, a cost reimbursable type EPC (Engineering, Procurement and Construction) contract, with the support of an Owner's Engineer is adopted. Another possible alternative would be an EPCM (Engineering, Procurement and Construction Management) contract. In either case, experience in lithium projects of the engineer/contractor is recommended.
- The Maricunga Salar is a mid-size salar and the mineral property in the salar is divided among four large holders (MSB being the one of the largest) and many other small holders. There will be a material advantage to the party that is able to progress its project faster, because the resource might not support another competitively sized lithium carbonate plant. Thus, if MSB can proceed quickly with this project, it may become "dominant" in the salar and might be in a position to acquire additional resources at favourable conditions.
- Explore the replacement of thermal energy by electrical renewable energy supply.
- To evaluate the increase of the power line capacity for the use of electrical boilers in the Salt Removal Plant.

2. INTRODUCTION

2.1 TERMS OF REFERENCE

The Stage One Project (herein the “Project”) (previously known as the Maricunga Lithium Project and Blanco Project) is owned and operated by Minera Salar Blanco S.A. (“Minera Salar Blanco or MSB”). This report was prepared by Worley and Atacama Water for MSB to provide a National Instrument 43-101 (“NI 43-101”) compliant Definitive Feasibility Study (“DFS”) of its Stage One Project located in Salar de Maricunga in the Atacama Region of northern Chile. This report provides an independent updated Mineral Reserve estimation and a technical appraisal of the economic viability of the production of an average of 15,200 TPY of lithium carbonate battery grade over 20-years mine-life from the lithium contained on the ‘Old Code’ mining concessions (OCC) owned by MSB, based on exploration work carried out to 400 m depth during 2021. The OCC are constituted under the 1932 Chilean Mining Code and do not require a special license from the Chilean Government (Contrato Especial de Operacion del Litio – CEOL) for the production and sale of lithium products. Resource estimates are for lithium and potassium contained in brine. The report was prepared under the guidelines of NI 43-101 and in conformity with its standards.

All items related to geology, hydrogeology, mineral resources and reserves were prepared by Atacama Water. Peter Ehren was responsible for preparing all technical items related to brine chemistry and mineral processing. Capital and Operating expenditures mentioned in this report were estimated by Worley, relying on quotations requested from equipment, chemicals and other suppliers, as well as from its project data base. Worley relied extensively on Minera Salar Blanco and its consultants, as cited in the text of the study and the references, for information on future prices of lithium carbonate, legislation and tax in Chile, as well as for general project data and information.

This report was reviewed by Mr. Marek Dworzanowski, CEng., BSc (Hons), HonFSAIMM, FIMMM of Worley, Mr. Peter Ehren, MSc, MAusIMM and Mr. Frits Reidel, CPG. Mr. Marek Dworzanowski, Mr. Peter Ehren and Mr. Frits Reidel are “qualified persons” (QP) and are independent of MSB as such terms are defined by NI 43-101.

2.2 SOURCES OF INFORMATION

Previous technical reports prepared for the Project include:

- Technical Report on the Maricunga Lithium Resource Update, Stage One. NI 43-101 Technical Report for MSB report dated 20th September 2021.
- 90 percent increase in measured & indicated resources for LPI’s Maricunga Stage One Lithium Project Lithium Power International JORC report dated 29th of September 2021.

- Technical Report: Definitive Feasibility Study of the MSB Lithium Project, III Region Chile. NI 43-101 Technical Report for Minera Salar Blanco prepared by WorleyParsons and FloSolutions, dated January 2019.
- Environmental Impact Assessment of the “Proyecto Blanco” of Minera Salar Blanco, prepared by Stantec, September 2018.
- Technical Report: Preliminary Assessment and Economic Evaluation of the Minera Salar Blanco Project Atacama Region, Chile. NI 43-101 Technical Report for Minera Salar Blanco prepared by Worley Parsons and FloSolutions, dated December 2017.
- Technical Report: Definitive Feasibility Study of the MSB Lithium Project, III Region Chile. NI 43-101 Technical Report for Minera Salar Blanco prepared by WorleyParsons and FloSolutions, dated January 2019.
- Maricunga Lithium Brine Project; 3.7-Fold Increase in Mineral Resource Estimate; Lithium Power International JORC report dated 12 July 2017.
- Technical Report on the Maricunga Lithium Project, Region III, Chile. NI 43-101 Technical Report for Bearing Resources prepared by Don Hains March 20, 2017.
- Technical Report on the Maricunga Lithium Project, Region III, Chile. NI 43-101 Technical Report for Li3 Energy Inc prepared by Don Hains and Frits Reidel April 17, 2012.
- Technical Report on the Salar de Maricunga Lithium Project, Northern Chile prepared for Li3. NI 43-101 Technical report prepared by Donald H Hains, Amended May 26, 2011.

The author was provided full access to the Project’s database including drill core and cuttings, drilling and testing results, brine chemistry and porosity laboratory analyses, aquifer testing results, geophysical surveys and all other information available from the work carried out on the Project area between 2011 and 2021. The documentation reviewed, and other sources of information, are listed at the end of this report in Section 27 References.

Numerous site visits were carried out to the Project area between 2011 and 2021. The author was closely involved with the work carried out during the 2011, 2015, 2016, 2017, 2018 and 2021 drilling and testing campaigns.

Chapters 1, 25 and 26 were prepared by Worley, Atacama Water and MSB. Chapters 2 to 4 were prepared by MSB and Atacama Water, chapters 5 through 12, 14, 15, 16 and 23 have been prepared by Atacama Water (Mr. Frits Reidel, CPG), Chapters 13 was prepared by Mr. Peter Ehren, MSc, MAusIMM CP, Chapter 17 was prepared by Worley, GEA and Mr. Peter Ehren. Chapters 18 and 21 were prepared by Worley. Chapters 19 was prepared by Roskill, a Wood Mackenzie Business. Chapters 20 was prepared by MSB and chapter 22 was prepared by MSB Consultant Daniel Briebe.

This report was reviewed by Mr. Marek Dworzanowski, CEng., BSc (Hons), HonFSAIMM, FIMMM of Worley, Mr. Peter Ehren, MSc, MAusIMM and Mr. Frits Reidel, CPG. Mr. Marek Dworzanowski, Mr. Peter Ehren and Mr. Frits Reidel are “qualified persons” (QP) and are independent of MSB as such terms are defined by NI 43-101.

2.3 UNITS

The metric (SI system) units of measure are used in this report unless otherwise noted. List of abbreviations is presented below. All currency in this report is US dollars (US\$) unless otherwise noted.

μ	micron	gr/ft3	grain per cubic foot	MVA	megavolt-amperes
°C	degree Celsius	gr/m3	grain per cubic metre	MW	Megawatt
°F	degree Fahrenheit	hr	hour	MWh	megawatt-hour
μg	microgram	ha	hectare	m3/h	cubic metres per hour
A	ampere	hp	horsepower	opt, oz/st	ounce per short ton
a	annum	in	inch	Oz	Troy ounce (31.1035g)
bbl	barrels	in2	square inch	Ppm	part per million
Btu	British thermal units	J	joule	Psia	pound per square inch absolute
C\$	Canadian dollars	k	kilo (thousand)	Psig	pound per square inch gauge
cal	calorie	kcal	kilocalorie	PWL	Pumping water level
cfm	cubic feet per minute	kg	kilogram	RL	relative elevation
cm	centimetre	km	kilometre	s	Second
cm2	square centimetre	km/h	kilometre per hour	Sy	Specific Yield
d	day	km2	square kilometer	St	short ton
dia.	diameter	Kt	Kilo tonne	Stpa	short ton per year
dm	decimetre	kVA	kilovolt-amperes	Stpd	short ton per day
dmt	dry metric tonne	kW	Kilowatt	SWL	Static water level
dwt	dead-weight ton	kWh	kilowatt-hour	T	metric tonne
ft	foot	L	Litre	Tpa	metric tonne per year
ft/s	foot per second	L/s	litres per second	Tpd	metric tonne per day
ft2	square foot	m	Metre	US\$	United States dollar
ft3	cubic foot	M	mega (million)	USg	United States gallon
g	gram	m2	square metre	USgpm	US gallon per minute
G	giga (billion)	m3	cubic metre	V	Volt
Gal	Imperial gallon	Min	Minute	W	Watt
g/L	gram per litre	MASL	metres above sea level	Wmt	wet metric tonne
g/t	gram per tonne	mm	Millimetre	yd3	cubic yard
gpm	Imperial gallons per minute	Mt	Mega tonne	Yr	Year

3. RELIANCE ON OTHER EXPERTS

The authors have relied on the following expert:

For the legal opinion on the status of the Project's mining claims the authors have relied on the following expert:

Mr. J.P. Bambach of the legal firm Philippi, Prietocarrizosa, Ferrero DU & Uria in Santiago, Chile.

For the purpose of this report, the authors have relied on ownership information provided by MSB. MSB has relied on a legal opinion by Philippi, Prietocarrizosa, Ferrero DU & Uria dated September 19, 2021 in respect to the legal title to the properties (Appendix I).

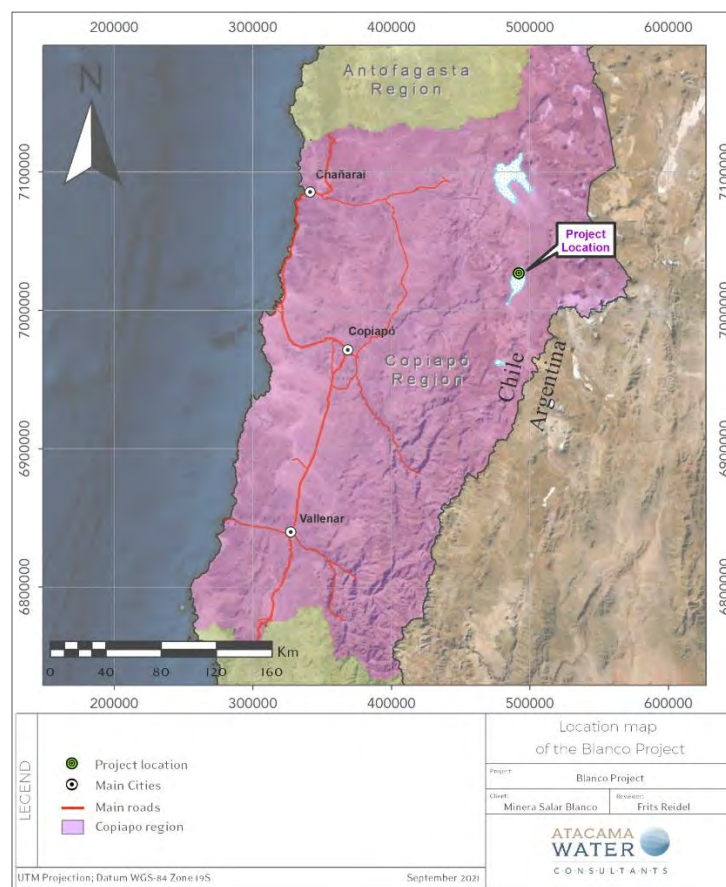
The authors also have relied on the topographic information regarding property locations provided by MSB and Philippi, Prietocarrizosa, Ferrero DU & Uria.

4. PROPERTY DESCRIPTION AND LOCATION

4.1 PROPERTY LOCATION

The Project is located approximately 170 km northeast of Copiapó in the III Region of northern Chile at an elevation of approximately 3,750 masl. Figure 4-1 shows the location of the Project. The property is more particularly described as being centred at approximately 492,000 mE, 7,025,000 mN (WGS 84 datum, UTM Zone 19). The Project covers 2,563 ha of mineralized ground in Salar de Maricunga, 100 ha just to the northeast of the Salar for camp and evaporation test facilities, and an additional 1,800 ha some eight km north of the Salar for the future construction of evaporation ponds, process and plant facilities.

Figure 4-1 Location map of the Project



4.2 TENURE

The mineralized area of the Project is comprised of the following mining concessions: *Litio 1-6* (1,438 ha), *Cocina 19-27* (450 ha), *Salamina*, *Despreciada*, and *San Francisco* (675 ha). Figure 4-2 shows the Project land tenure and concession boundaries in the northern part of Salar de Maricunga. Table 4-1 provides a detailed listing of the MSB concessions.

The *Cocina 19-27*, *San Francisco*, *Despreciada* and *Salamina* concessions, herein after referred to as the “Old Code” Concessions (OCC), were constituted under the 1932 Chilean mining law and have “grand-fathered” rights for the production and sale of lithium products; unlike the *Litio 1-6* concessions which were constituted under the 1983 Chilean mining law and require an additional government license for the production and sale of lithium. This definitive feasibility study updated is limited to the OCC.

Table 4-1 MSB mining concessions

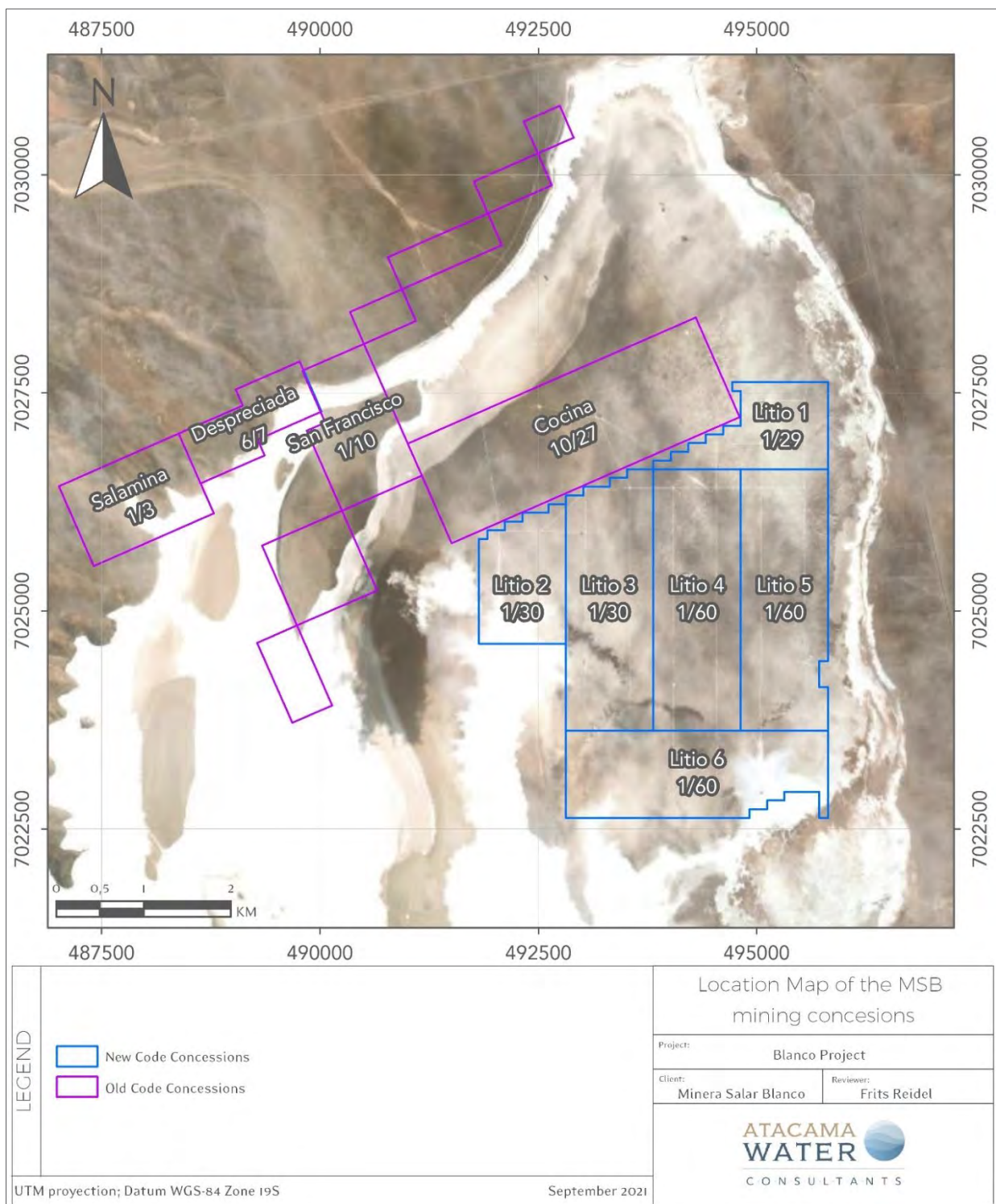
Property	Role Number	Area (ha)	Registered Owner	Mining Code
Litio 1, 1 al 29	03201-6516-4	131	MSB	1983
Litio 2, 1 al 30	0321-6517-2	143	MSB	1983
Litio 3, 1 al 58	03201-6518-0	286	MSB	1983
Litio 4, 1 al 60	03201-6519-9	300	MSB	1983
Litio 5, 1 al 60	03201-6520-2	297	MSB	1983
Litio 6, 1 al 60	03201-6521-0	282	MSB	1983
Cocina 19-27	03201-2110-19	450	MSB	1932
San Francisco 1 al 10	03201-0006-2	425	MSB	1932
Despreciada 6 al 7	03201-0007-0	100	MSB	1932
Salamina 1 al 3	03201-0005-4	150	MSB	1932
Blanco	N/A	1,800	MSB	1983
Camp	N/A	100	MSB	1983

Verification of the land titles and mining rights owned by MSB, was conducted by Juan Paulo Bambach Salvatore of the legal firm *Philippi Prietocarrizosa Ferrero DU & Uria* in Santiago. Mr. Bambach documented his legal opinion in a letter dated September 19, 2021 and concluded the following:

- Minera Salar Blanco S.A. (MSB) has been duly incorporated and is a validly existing company under the laws of Chile and is in good standing.

- MSB owns 100 percent of the Litio 1 through Litio 6, Cocina 19-29, San Francisco 1-10, Despreciada 6-7, Salamina 1-3, Blanco and Camp mining concessions as shown in Table 4-1.
- MSB has all necessary corporate faculties and authority to carry on its business as now conducted by it and to own its properties and assets.
- The Company currently has a portfolio of 10 Mining Concessions, as follows:
 - Old Legislation Exploitation Concessions (pertenencias)
 - 1983 Exploitation Concessions (pertenencias)
- All titles of the Mining Concessions set out in Table 4-1 are in good standing and there are no encumbrances on such Mining Concessions.
- MSB is empowered to conduct exploration activities on the Exploration Concessions, and exploration and development activities on the Mining Claims.
- By means of the Old Mining Chilean Legislation, MSB is entitled to explore and exploit lithium, fulfilling all legal requirements provided by the Chilean legislation.
- The 1983 Exploitation Concessions do not allow to explore nor exploit lithium, unless a Special Operation Contract for Lithium, CEOL is obtained, but do permit the exploration and exploitation of any other mining substances, whether metallic or non-metallic, for example potassium, where lithium may be a sub product. In other words, the 1983 Exploitation Concessions, do not entitle to appropriate the extracted lithium, but only other concessionable substances.
- According to the legal documentation reviewed, the Mining Concessions are valid and in force.
- To date, the granting processes of the applications under proceeding (the “Applications”) have been carried out according to the law, and they would not present defects that could lead to the expiration of the application.
- The Mining Concessions have no marginal records evidencing mortgages, encumbrances, prohibitions, interdictions or litigations.
- The Mining Concessions have all their last four periods of mining licenses duly paid.
- All the Mining Concessions have preferential rights over the relevant area. There are no mining concession nor mining rights held or filed by third parties challenging the rights and preference of the Mining Concessions.
- From a technical point of view and after having requested the review of the complete area by the expert in mining property Mr. Juan Bedmar, we can confirm that the location of the Mining Concessions is correct.

Figure 4-2 Location map of MSB mining concessions



4.3 HISTORY OF OWNERSHIP

- SLM Litio, a Chilean corporation, acquired the Litio 1-6 mining claims in 2004.
- On May, 2011, Li3 Energy Inc. (Li3 now Bearing Lithium) through its 100 % owned Chilean subsidiary Minera Li Energy (MLE) acquired its original interest in the Salar de Maricunga through the purchase of a 60 % interest in SLM Litio 1 through 6 (which are the legal entities holding the Litio 1-6 concessions).
- On November 5, 2013, Li3 announced an agreement with BBL SpA (now MSB SpA) for BBL to acquire 51% (a controlling stake) of MLE in return for specified funding for the company. On April 16, 2013, MLE acquired 100% of Cocina 19-27 mining concessions.
- On August 25, 2014, BBL purchased directly another 36 % interest in SML Litio 1-6 held by another third party. The remaining 4% interest in the Litio 1-6 claims is still held by a third party individual.
- On December 30, 2014, BBL acquired the option to buy the San Francisco, Despreciada and Salamina concessions from a local group (the Padilla Family).
- On September 2, 2015, BBL changed its name to Minera Salar Blanco SpA. During December 2015, Minera Salar Blanco SpA acquired directly the Blanco and Camp mining concessions.
- In 2016 MSB SpA (former BBL SpA), MLE and, Lithium Power International Ltd. agreed to form a new company, Minera Salar Blanco S.A, (MSB) to continue the development of the Blanco Project. At the same time, MSB SpA and Li3, shareholders of MLE, agreed to dissolve MLE. As a result, the ownership structure of MSB ended up with; LPI 50 %, Minera Salar Blanco SpA 32.3 %, and Li3 17.7 %. Through this agreement MSB holds 96 % interest in the Litio 1-6 concessions and 100 % in the Cocina, San Francisco, Despreciada and Salamina, Camp and Blanco concessions.
- On December 11, 2016, Bearing Lithium Corp. announced a binding agreement to acquire 100% of the common shares of Li3 and, as a result, assumed Li3's 17.7% interest in the MSB during 2017.
- During August 2018, Minera Salar Blanco SpA. sold 1.3534% of its shares. Both LPI and Bearing Lithium exercised its preferential rights resulting on LPI acquiring 1.00% and Bearing Lithium 0.3534 %. As a result, the ownership structure of MSB was; LPI 51 %, Minera Salar Blanco SpA. 30.98 %, and Bearing Lithium 18.02 %.
- On April 2019, MSB acquired the remaining 4% in the Litio 1-6 claims that were still held by a third party. After this transaction, MSB consolidated 100% of the ownership of the Litio 1-6 concessions.
- Different capital increases executed on MSB have taken the current ownership structure of the company to: LPI 51.55%, Minera Salar Blanco SpA. 31.31 %, and Bearing Lithium 17.14%.

4.4 ROYALTIES

Given that this project is based on developing exclusively MSB's lithium mining properties registered under the Chilean old mining law, it is MSB's interpretation of the relevant legislation that they are exempt from any special royalties on lithium carbonate production. In this case, production from these properties would be only subject to Law 20.026 of Specific Tax on mining activities. These royalties to be paid depend on both the facility's revenue level, and on the relation between lithium carbonate and copper prices. Royalties would amount to approximately US\$ 4.6 million per year. This is equivalent to about 1.2 % of yearly sales.

It should also be mentioned that a project to increase general mining royalties is under discussion in the Chilean Congress. Even though, as of today, nothing has been decided, two ideas are being put forward. The first one is to set a flat 3% royalty on net sales and the second proposition is to set a 5% royalty on Mining Margin. In the case of MSB, using the realizations that result from its production plan and Roskill's projected prices, the second alternative is equivalent to a 2.7% royalty on net sales. In both instances royalties to be paid by MSB would increase, however, as it will be shown in the Project Sensitivity sub section chapter 22, the impact on the project's profitability, as measured by NPV and IRR, will not be relevant for the Project.

4.5 ENVIRONMENTAL LIABILITIES

The author is not aware that the Project is subject to any material environmental liabilities.

4.6 OTHER SIGNIFICANT FACTORS AND RISKS

A number of normal risk factors are associated with the Project properties. These risks include but are not limited to the following. It is not anticipated they will affect access, title or the ability to perform work on the Salar de Maricunga:

- The risk of obtaining all the necessary licenses and permits on acceptable terms, in a timely manner or at all.
- Regulatory risks associated with the government revisions to regulations for exploitation of lithium.
- The risk of changes in laws and their implementation, impacting activities on the properties.
- The risk of activities on adjacent properties having an impact on the Project.

5. ACCESSIBILITY, CLIMATE, LOCAL RESOURCES, INFRASTRUCTURE AND PHYSIOGRAPHY

5.1 PHYSIOGRAPHY

The hydrographic basin of Salar de Maricunga covers 2,195 km² in the Altiplano of the III Region. The average elevation of the basin is 4,295 masl while the maximum and minimum elevations are 6,749 masl and 3,738 masl respectively. The Salar itself is located in the northern extent of the hydrographic basin and covers 142.2 km² (DGA 2009). The salar nucleus sit elevation of approximately 3,750 masl.

The principal surface water inflow into the lower part of basin occurs from Rio Lamas which originates in Macizo de Tres Cruces. Average flow in Rio Lamas (at El Salto) is measured at 240 l/s. All flows from the Rio Lamas infiltrate into the Llano de Cienaga Redonda (DGA 2009). The second largest inflow to the lower part of the basin occurs from Quebrada Cienaga Redonda. Average flow (at La Barrera) is measured at 20 l/s; all flow infiltrates in to the Llano de Cienaga Redonda (DGA 2009).

Laguna Santa Rosa is located at the southwest extent of the basin valley floor and is fed mainly locally by discharge of groundwater. Laguna Santa Rosa drains north via a narrow natural channel into the Salar itself. Additional groundwater discharge occurs along the path of this channel and surface water flow has been recorded at 200-300 l/s (DGA 2009). Tres Cruces National Park is located in the southern part of the Maricunga watershed and includes Laguna Santa Rosa.

5.2 ACCESSIBILITY

The Project is accessed from the city of Copiapó via National Highway 31. Highway 31 is paved for approximately 75 percent of the distance and is a well-maintained gravel surface road thereafter. National Highway 31 extends through to Argentina via the Paso San Francisco. Access to Maricunga from the city of El Salvador is via a well-maintained gravel surface highway. Occasional high snowfalls in the mountains may close the highways for brief periods during the winter.

5.3 CLIMATE

5.3.1 TEMPERATURE

The climate at the property is a dry, cold, high-altitude desert with cold, dry winters and dry summers. Summer temperatures range from 10°C – 20°C, with the winter daytime temperatures

averaging approximately 4°C – 0°C. The average annual temperature at Salar de Maricunga is estimated at 5-6 °C as shown in Figure 5-1 (DGA 2009).

Long-term historical temperature data are not available for the immediate Project area. The DGA maintained Lautaro Embalse meteorological station (1,110 masl) located 160 km southwest of the Project area has average monthly temperature records available for the period of 1966 through to date.

A weather station at the Lobo Marte Project site located in the southern extension of the Maricunga basin at an elevation of 4,090 masl, (30 km to the south of the Project) has average monthly temperature records available for the period of January 1997 to December 1998.

Table 5-1 shows average monthly temperature data for the Lobo Marte Project (Golder Associates 2011) while Figure 5-1 provides an isotherm map for the Salar de Maricunga region.

Table 5-1 Average monthly temperature at the Lobo Marte Project (°C)

Jan	Feb	Mar	Apr	May	Jun	Jul	Aug	Sep	Oct	Nov	Dec
8.5	6.6	6.5	2.5	-0.5	-5.0	-3.5	-2.5	-0.5	1.0	3.7	5.8

(re-elaborated after Golder Associates 2011)

5.3.2 PRECIPITATION

Precipitation in Salar de Maricunga may occur during the months of January and February as a result of “Bolivian winter” effects and during the months of June through September. The intensity of these annual rainfall patterns is significantly influenced by the El Nino-Southern Oscillation.

The nearest long-term historical precipitation records for the Project are available from DGA maintained meteorological stations at Las Vegas (70 km northwest) at an elevation of 2,250 masl and Pastos Grande (60 km WSW) at an elevation of 2,260 masl. No long-term historical precipitation records are available for the III Region above 2,500 masl elevation. Table 5-2 provides summary information of the Las Vegas and Pastos Grande stations.

Table 5-2 DGA Meteorological stations with long-term precipitation records

Station	BNA code	Basin	Elevation (masl)	Distance from Project	Record
Las Vegas	03210001-5	Rio Salado	2,250	70 km NW	1984 – to date
Pastos Grande	03441001-1	Rio Copiapó	2,260	60 km WSW	1966 – to date

Source: DGA, 2009

Additional rainfall records are available from selected weather stations that are part of the “Pilot System for the III Region” operated by the Catholic University of Chile (PUC) in conjunction with the DGA. Table 5-3 provides summary information for the Maricunga and Pedernales Sur weather stations.

Table 5-3 Selected PUC-DGA weather stations with partial precipitation records

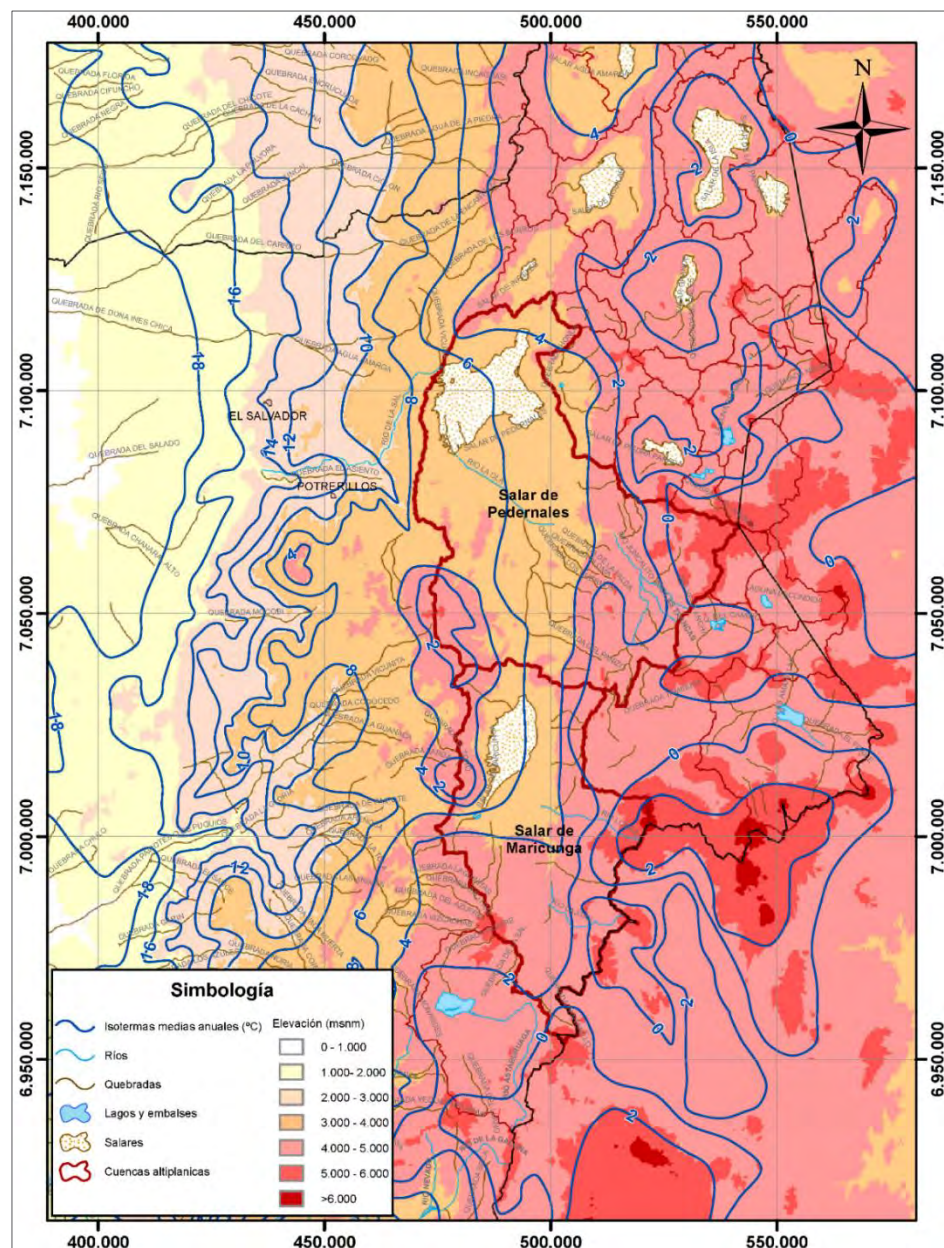
Station	Basin	UTM (WGS 84)		Elevation (masl)	Record
Maricunga	Maricunga	7,000,372 mN	486,326 mE	3,852	2007 – 2008
Pedernales Sur	Pedernales	7,049,016 mN	493,056 mE	3,774	2007 – 2008

Source: DGA, 2009

Figure 5-2a and 5-2b show monthly precipitation records for the Maricunga and Pedernales Sur weather stations for the 2007/8 period. It is believed that these data are representative of a relative dry year (DGA 2009).

Precipitation records collected at the Marte Lobo Project weather station during the 1997/1998 period show an annual cumulative precipitation (rainfall and snowfall water equivalent) of 451 mm (Golder Associates 2011). Further analyses of rainfall records of the III Region indicate that the 1997/8 cumulative precipitation coincides with a 100 year precipitation event. Additional precipitation data collected at the Marte and Lobo stations between 2009 and 2010 are shown in Figure 5-3.

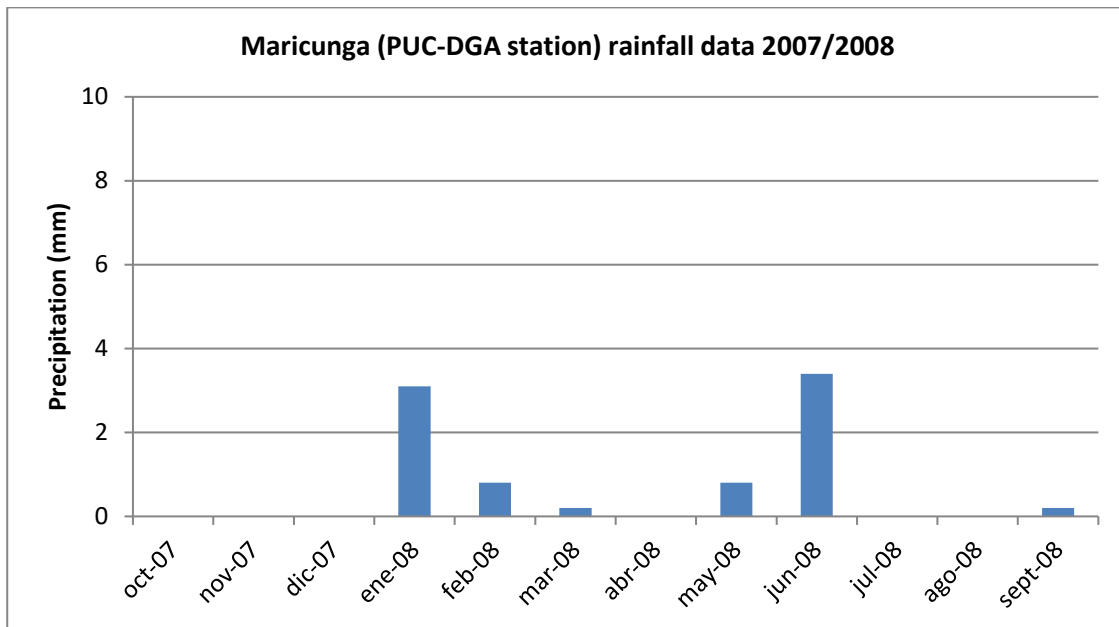
Figure 5-1 Isotherm map for Salar de Maricunga



Source: DGA 2009

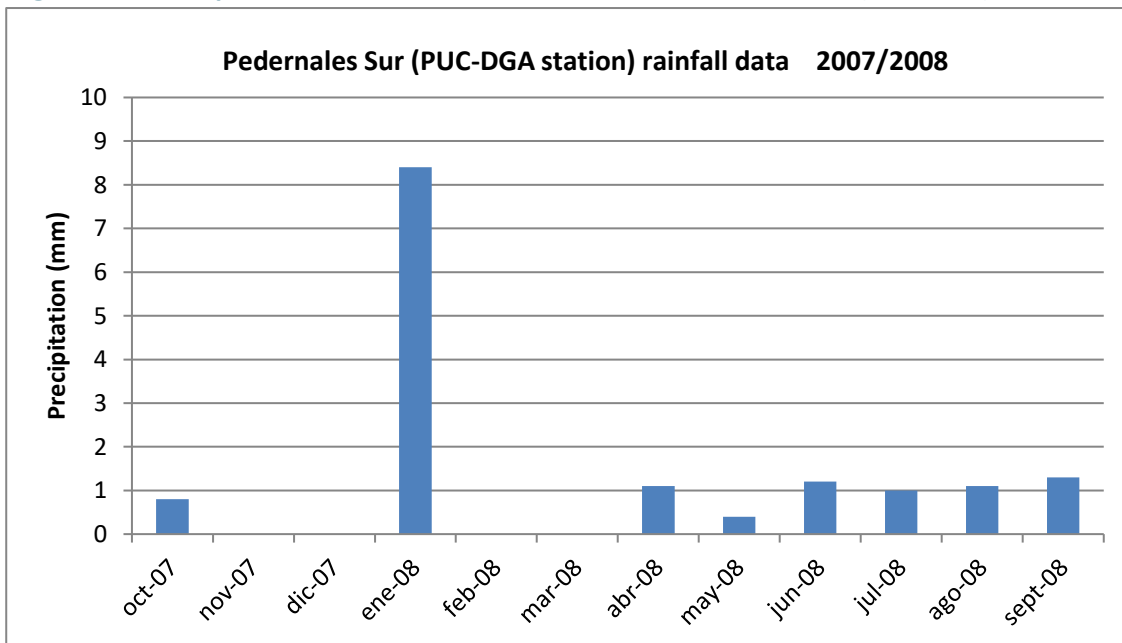
Average annual precipitation estimates were prepared as part the “Balance Hídrico de Chile” (DGA 1987). Figure 5-4 shows an isohyet map for the Salars of Maricunga and Pedernales. The map suggests that the average annual precipitation in Salar de Maricunga is 100 mm - 150 mm.

Figure 5-2a Precipitation data for the Maricunga weather station (PUC-DGA) 2007/2008



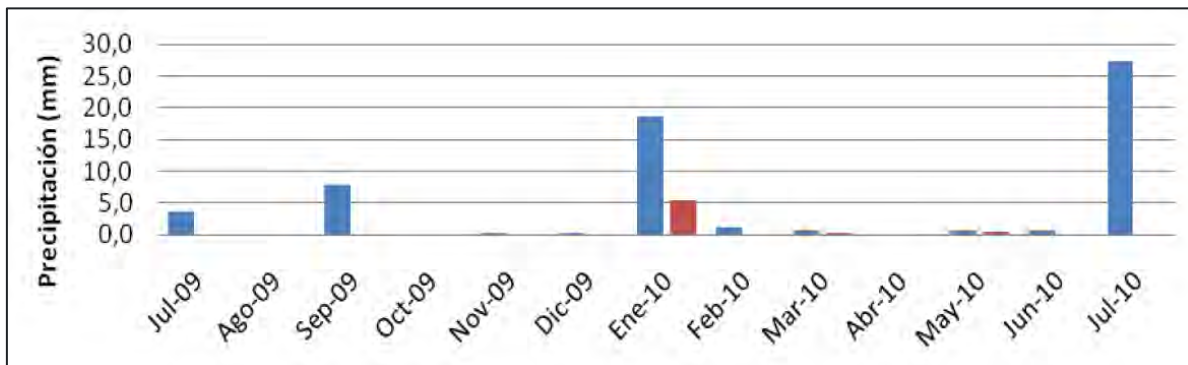
Source: DGA 2009

Figure 5-2b Precipitation data for the Pedernales Sur weather station (PUC-DGA) 2007/2008



Source: DGA 2009

Figure 5-3 Precipitation data from the Marte and Lobo stations 2009/2010



Source: AMEC 2011

DRA (1998) carried out a hydrogeological investigation for the Salar de Maricunga and Piedra Pomez areas and described the following precipitation – elevation relationship:

$$P = 0.038 \times H - 53$$

Where:

P is average annual precipitation (mm); and H is elevation (masl)

Using this correlation, the average annual precipitation for Salar de Maricunga is estimated at 90 mm.

The DGA (2006) carried out a hydrogeological investigation for Salar de Maricunga in which the following precipitation – elevation relationship was developed:

$$P = 0.1 \times H - 300$$

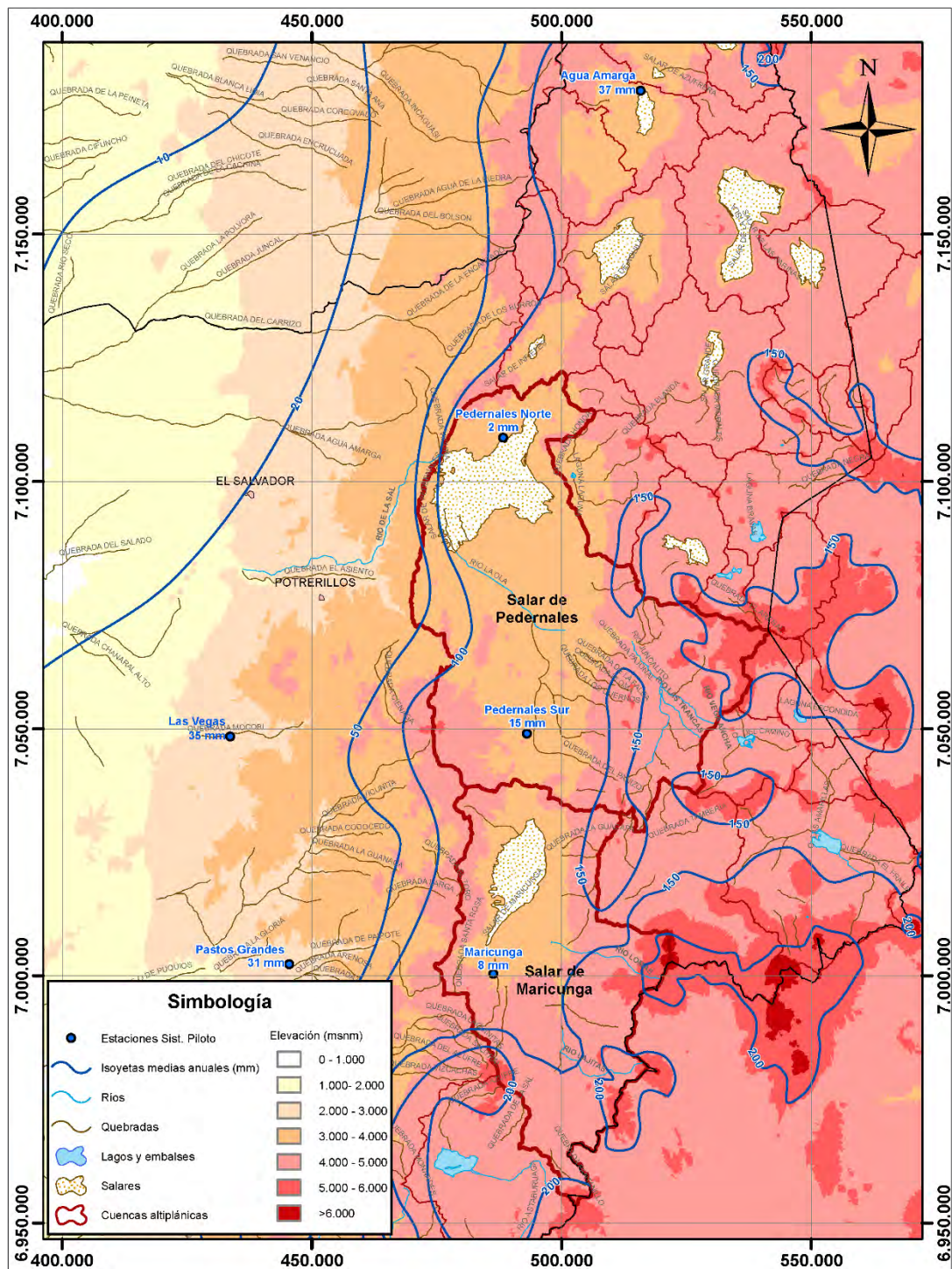
Where:

P is average annual precipitation (mm); and H is elevation (masl)

Using this correlation, the average annual precipitation for Salar de Maricunga is estimated at 75 mm.

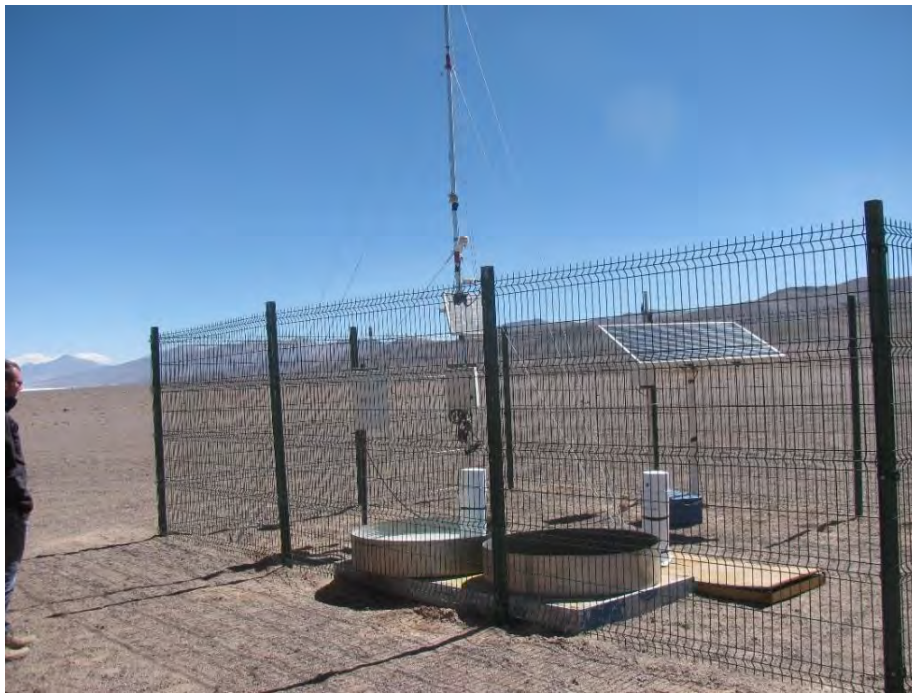
MSB installed a weather station in Salar de Maricunga in 2016 to validate the results of previous precipitation studies and third-party data sets (Figure 5-5). Figure 5-10 through Figure 5-13 show a summary of the data collected at the MSB station between 2016 and 2020.

Figure 5-4 Isohyet map for Salar de Maricunga



Source: DGA 2009

Figure 5-5 MSB weather station in the plant site area



5.3.3 SOLAR RADIATION

Solar radiation is the most important energy input for evaporation. Long-term solar radiation data are not available for Salar de Maricunga directly. Regional solar radiation estimates are shown in Figure 5-6 and suggest that solar radiation in Salar de Maricunga falls in the range of 1,700 – 1,900 KWh/m² per year. Partial solar radiation data are available from the Marte Lobo Project site and are reported in Amec 2011. Table 5-4 shows monthly records solar radiation records in Watts/m² for the Marte and Lobo stations.

Table 5-4 Monthly solar radiation data (W/M2) for the Marte and Lobo Stations

Month	Lobo			Marte		
	Min	Mean	Max	Min	Mean	Max
07/2009	0.0	194.2	974	s/d	s/d	s/d
08/2009	0.0	244.7	1,078.7	s/d	s/d	s/d
09/2009	0.0	324	1,164.1	0.0	299.9	1,019.2
10/2009	0.0	374.3	1,246.8	0.0	331.7	1,157.6
11/2009	0.0	394.7	1,217	0.0	387.8	1,171
12/2009	0.0	417.6	1,221	0.0	408.1	4,981
01/2010	0.0	397.4	1,229	0.0	386.8	1,154
02/2010	0.0	375.8	1,349	0.0	356.7	1,156
03/2010	0.0	328	1,132	0.0	312	1,019
04/2010	0.0	259.6	1,009	0.0	247.3	918
05/2010	0.0	193.6	866	0.0	187.1	825
06/2010	0.0	171.6	914	0.0	163.9	746.1
07/2010	0.0	198.6	785.1	0.0	196.8	796.8

Source: Modified from AMEC 2011

Figure 5-6 Solar radiation distribution in Chile

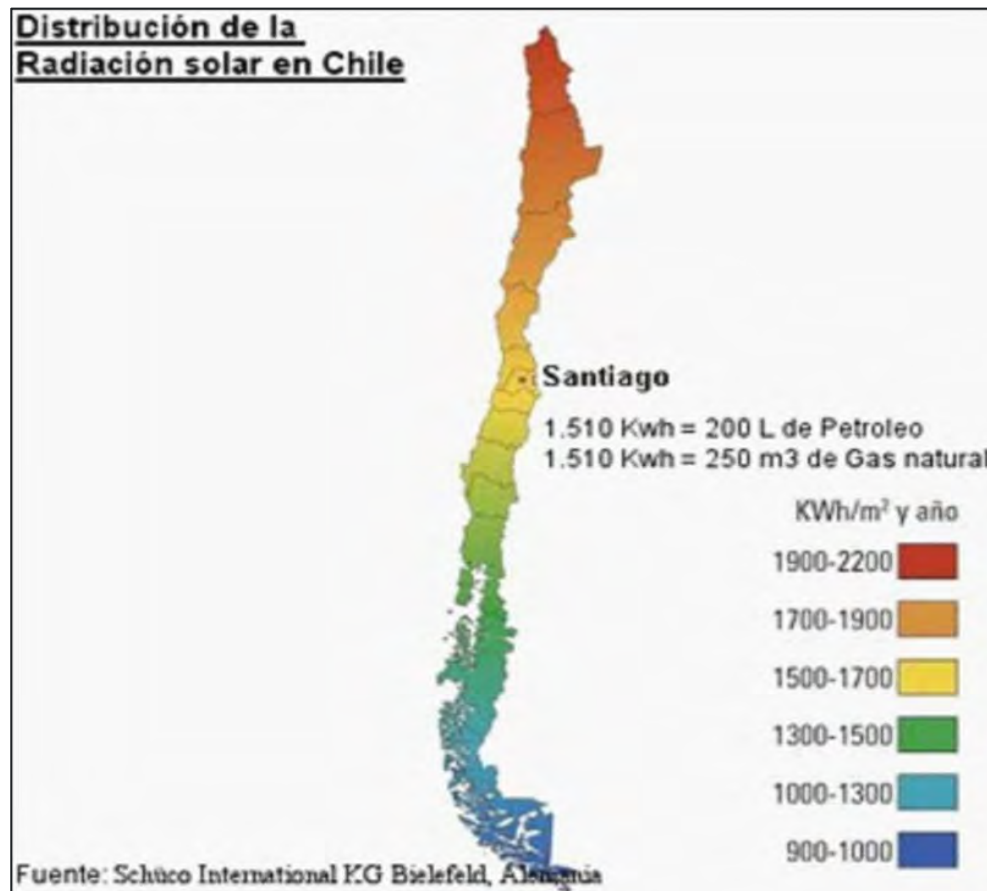
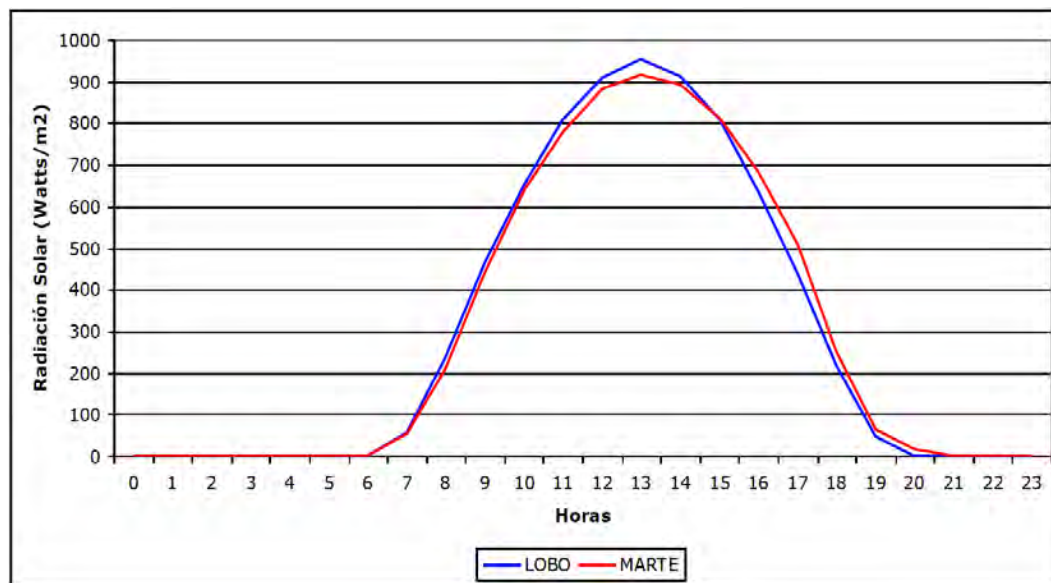


Figure 5-7 Average hourly solar radiation intensity at the Marte and Lobo stations 2009/2010



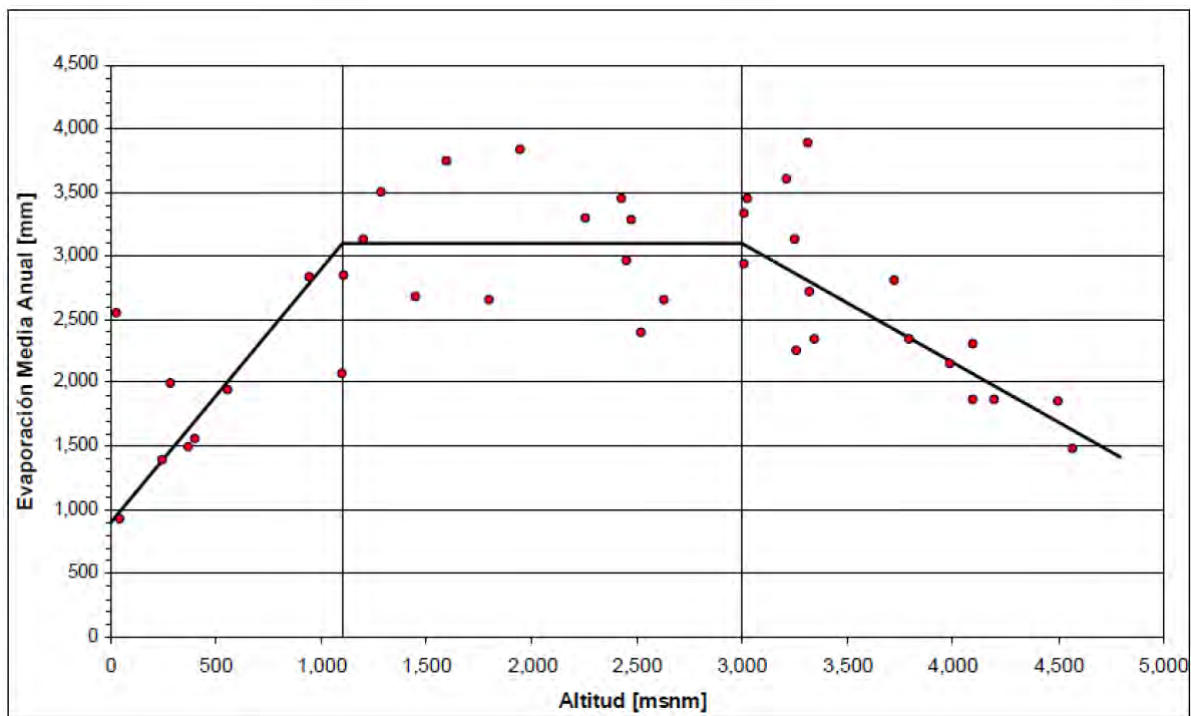
Source: AMEC 2011

The MSB weather station installed on site is collecting local solar radiation data in support of the evaporation tests that are currently in progress.

5.3.4 EVAPORATION

The DGA (2009) has developed a relationship between elevation and average annual pan evaporation based on pan evaporation records from some 40 stations across the I, II, and III Regions of northern Chile as shown in Figure 5-8. Based on this correlation the annual average pan evaporation rate for Salar de Maricunga is estimated at 2,400 mm.

Figure 5-8 Elevation versus average annual pan evaporation



Source: DGA 2009

A similar relationship between elevation and average annual pan evaporation has been described by Houston (2006) as follows:

$$MAE_{pan} = 4364(0.59 \times A)$$

Where: MAE_{pan} is mean annual pan evaporation (mm) and A is elevation (m) for stations above 1,000 masl.

Using this correlation, the mean annual pan evaporation rate for Salar de Maricunga is estimated at 2,150 mm.

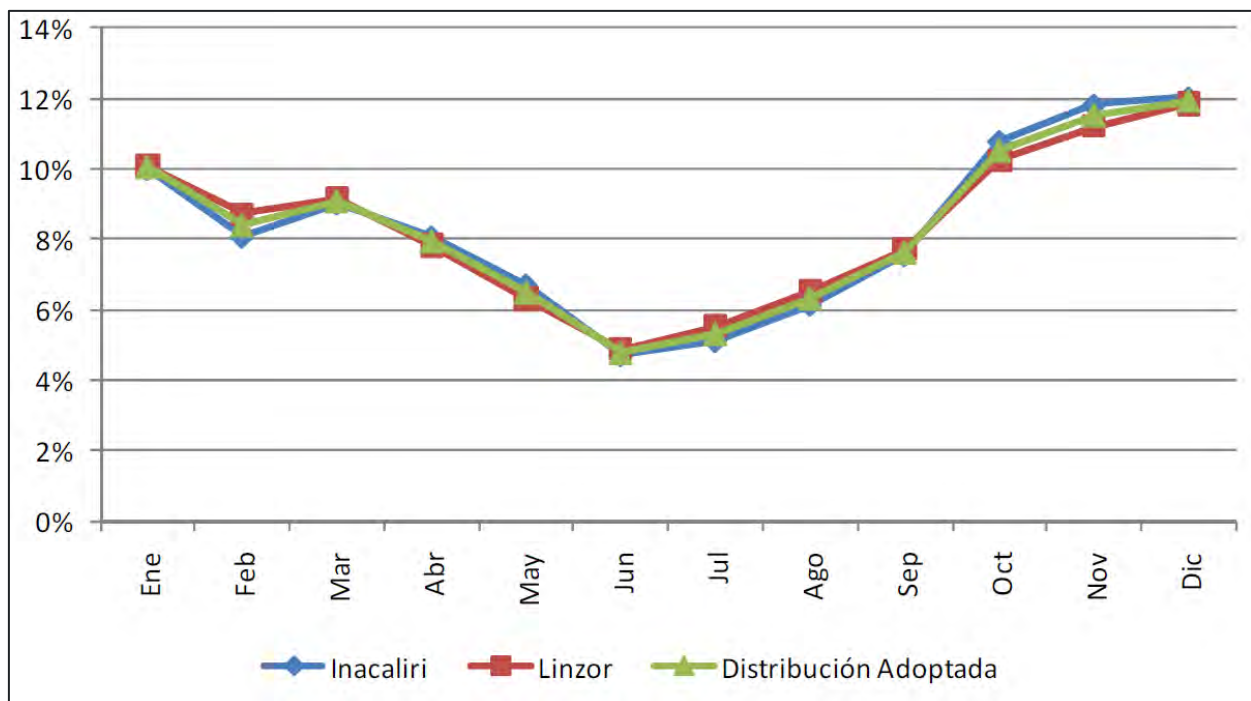
Houston (2006) further describes the effects of brine density on mean annual pan evaporation rates as:

$$MAE_{pan} = 10026 - 6993D; \text{ where } D \text{ is fluid density}$$

Applying this to Maricunga brine ($D = 1.2 \text{ g/ml}$), the annual average brine pan evaporation rate is estimated at 1,600 mm.

The DGA (2008) described the monthly distribution of average annual pan evaporation based on observations made from records (1977-2008) of the Linzor (4,096 masl) and Inacaliri (4,000 masl) stations in the II Region of northern Chile. Figure 5-9 summarizes this monthly distribution of the annual average pan evaporation (Golder Associates 2011).

Figure 5-9 Monthly distribution of average annual Pan Evaporation



Source: Golder Associates 2011

The DGA (2009) carried out a detailed field investigation program in Salar de Maricunga to establish evaporation rates as a function of soil type and depth to groundwater. Table 5-5 summarizes the findings of this investigation.

Table 5-5 Evaporation rates used for the Maricunga Basin water balance

Type	Mean annual evaporation rate (mm)
Open water	6.1
Humid soil	4.1
Vegas	2.1
Salar crust	1.8

Source: Modified from DGA 2009 and Golder 2011

MSB has installed several Class A evaporation pans (fresh water and brine) at the weather station and a series of test evaporation ponds adjacent to the camp site. These pans and test ponds are designed to validate previous evaporation studies and confirm evaporation pathways for lithium brine concentration.

Figure 5-10 Temperature - Blanco station (2016 –2020)

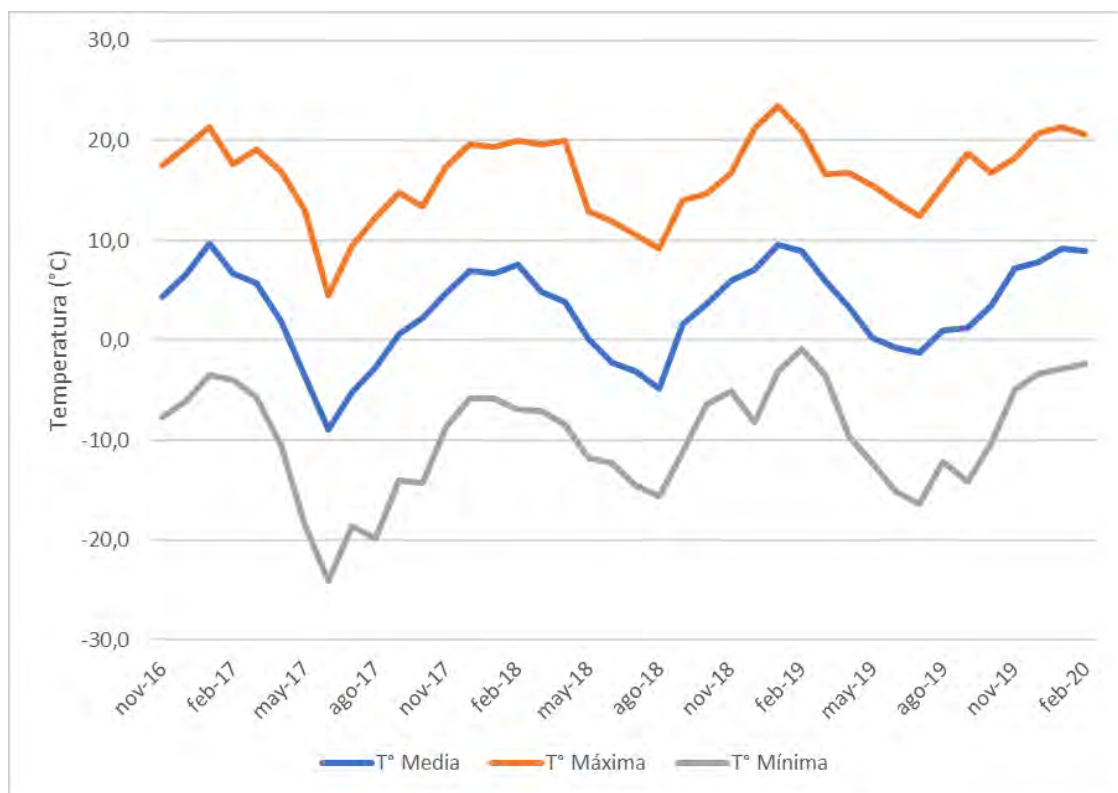


Figure 5-11 Precipitation - Blanco station (2016-2020)

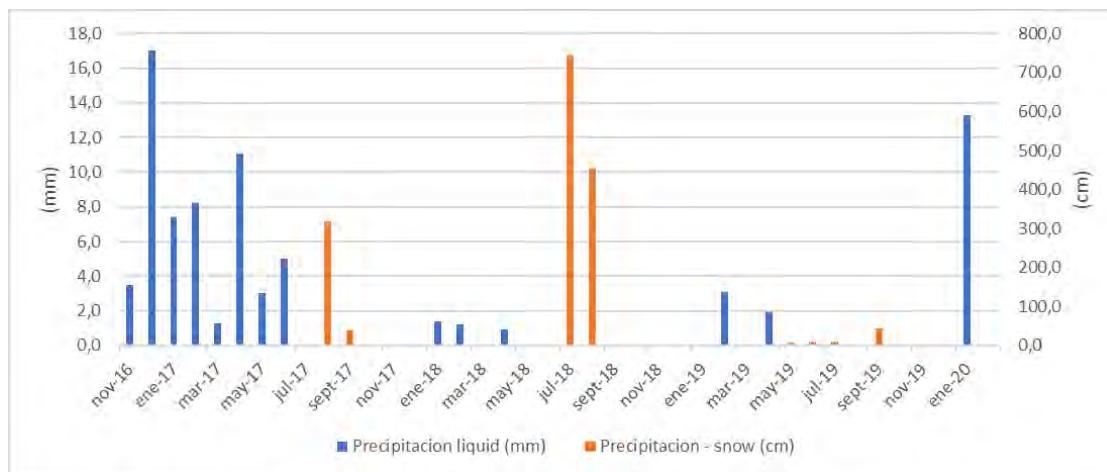


Figure 5-12 Fresh water Class A Pan Evaporation - Blanco Station 2016-2020

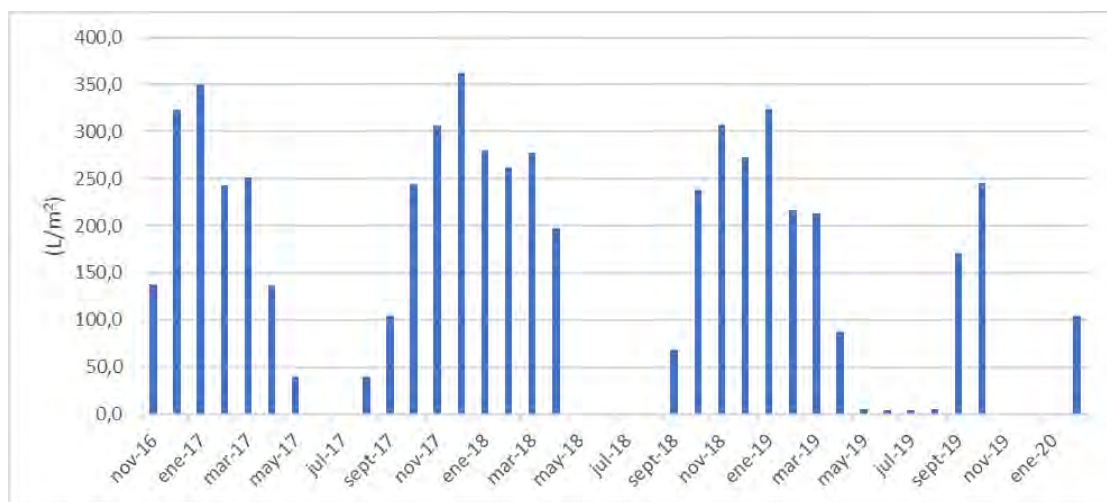
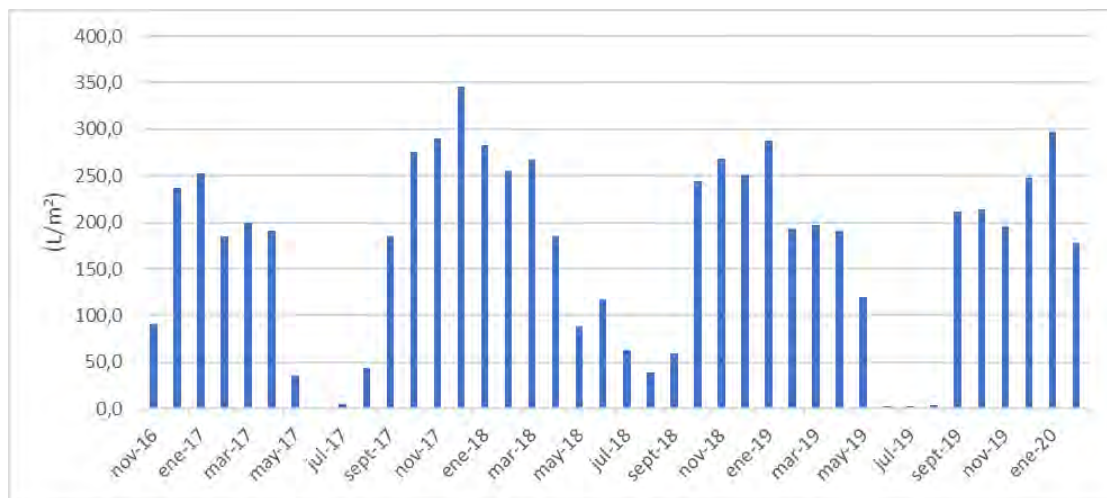


Figure 5-13 Diluted Brine Class A Pan Evaporation – Blanco Station (2016-2020)



5.4 LOCAL RESOURCES

Local resources are absent at the Salar. Copiapó is a major regional mining centre. Drilling contractors, drilling equipment, exploration tools and heavy mining equipment and machinery are all available.

5.5 INFRASTRUCTURE

Local infrastructure at the Salar includes National Highway 31 and an electrical power line running parallel to the highway. There is a customs post at the north end of the Salar that is staffed on a 24-hour basis.

Copiapó is a major city and provides a full range of services. Copiapó is serviced by daily flights with connections to Santiago and other major cities in Chile, as well as service to Argentina and Bolivia. The port of Caldera is located approximately 80 km west of Copiapó. The port has excellent dock facilities for general cargo, liquid fuel and bulk cargo. The port of Chañaral is located approximately 250 km from the Salar.

6. HISTORY

6.1 CORFO (1980'S)

CORFO, under the aegis of the Comité de Sales Mixtas, (CORFO, 1982) conducted a major study of the northern Chilean salars in the 1980s with the objective of determining the economic potential of the salars for production of potassium, lithium, and boron. CORFO undertook systematic hydrogeological and geological studies and sampling of the various salars. Exploration work at Salar de Maricunga consisting of sampling shallow pits (50 cm deep) covered the northern half of the Salar. It was determined that the phreatic level of the brine was at 15 cm below the Salar surface. Estimates of contained mineral resources were developed based on the assay results and assuming a constant porosity of 10% down to a 30 m depth. CORFO estimated lithium metal resources in Salar de Maricunga at 224,300 tonnes. This estimate does not comply with NI 43-101 standards.

CORFO currently does not control any mineral rights in Salar de Maricunga

6.2 PRIOR OWNERSHIP AND OWNERSHIP CHANGES

- SLM Litio, a Chilean corporation, acquired the Litio 1-6 mining claims in 2004.
- On May, 2011, Li3 Energy Inc. (Li3 now Bearing Lithium) through its 100 % owned Chilean subsidiary Minera Li Energy (MLE) acquired its original interest in the Salar de Maricunga through the purchase of a 60 % interest in SLM Litio 1 through 6 (which are the legal entities holding the Litio 1-6 concessions).
- On November 5, 2013, Li3 announced an agreement with BBL SpA (now MSB SpA) for BBL to acquire 51% (a controlling stake) of MLE in return for specified funding for the company. On April 16, 2013, MLE acquired 100% of Cocina 19-27 mining concessions.
- On August 25, 2014, BBL purchased directly another 36 % interest in SML Litio 1-6 held by another third party. The remaining 4% interest in the Litio 1-6 claims is still held by a third party individual.
- On December 30, 2014, BBL acquired the option to buy the San Francisco, Despreciada and Salamina concessions from a local group (the Padilla Family).
- On September 2, 2015, BBL changed its name to Minera Salar Blanco SpA. During December 2015, Minera Salar Blanco SpA acquired directly the Blanco and Camp mining concessions.
- In 2016 MSB SpA (former BBL SpA), MLE and, Lithium Power International Ltd. agreed to form a new company, Minera Salar Blanco S.A, (MSB) to continue the development of the Blanco Project. At the same time, MSB SpA and Li3, shareholders of MLE, agreed to dissolve MLE. As a result, the ownership structure of MSB ended up with; LPI 50 %, Minera Salar

Blanco SpA 32.3 %, and Li3 17.7 %. Through this agreement MSB holds 96 % interest in the Litio 1-6 concessions and 100 % in the Cocina, San Francisco, Despreciada and Salamina, Camp and Blanco concessions.

- On December 11, 2016, Bearing Lithium Corp. announced a binding agreement to acquire 100% of the common shares of Li3 and, as a result, assumed Li3's 17.7% interest in the MSB during 2017.
- During August 2018, Minera Salar Blanco SpA. sold 1.3534% of its shares. Both LPI and Bearing Lithium exercised its preferential rights resulting on LPI acquiring 1.00% and Bearing Lithium 0.3534 %. As a result, the ownership structure of MSB was; LPI 51 %, Minera Salar Blanco SpA. 30.98 %, and Bearing Lithium 18.02 %.
- On April 2019, MSB acquired the remaining 4% in the Litio 1-6 claims that were still held by a third party. After this transaction, MSB consolidated 100% of the ownership of the Litio 1-6 concessions.
- Different capital increases executed on MSB have taken the current ownership structure of the company to: LPI 51.55%, Minera Salar Blanco SpA. 31.31 %, and Bearing Lithium 17.14 %.

6.3 BRINE EXPLORATION WORK BY PREVIOUS OWNERS

6.3.1 LITIO 1-6 (2007)

An initial exploration program on the *Litio 1-6* concessions was carried out during February 2007 and consisted of the following components:

- 58 reverse circulation holes were drilled on a 500 m x 500 m grid to 20 m depth. Holes were 3.5" diameter and cased with either 40 mm PVC or 70 mm HDPE pipe inserted by hand to resistance. 232 brine samples were collected from these holes (using an airlift methodology) at 2 m to 10 m depth and 10 m to 20 m depth. The brine samples were analysed by Cesmec in Antofagasta.
- No NI 43-101 compliant resource estimate was prepared.

6.3.2 MLE / LI3- RESOURCE EVALUATION PROGRAM (2011/2)

Li3 carried out an initial brine resource investigation program on the *Litio 1-6* claims during 2011/2 that consisted of the following components:

- Six sonic boreholes (C-1 through C-6) were completed to a depth of 150 m. Undisturbed samples were collected from the sonic core at three meter intervals for porosity analyses

(318 samples). Brine samples were collected during the sonic drilling at three meter intervals for chemistry analyses (431 primary samples and 192 QA/QC samples). All sonic boreholes were completed as observation wells on completion of drilling.

- A total of 915 m of exploration RC drilling was carried out for the collection of chip samples for geologic logging, brine samples for chemistry analyses and airlift data to assess relative aquifer permeability. The RC boreholes were completed as observation wells for use during future pumping tests. Two test production wells (P-1 and P-2) were installed to a total depth of 150 m each for future pumping trials.
- A seismic tomography survey was carried out by GEC along six profiles (S1 through S6) for a total of 23 line km to help define basin lithology and geometry.
- Six test trenches adjacent to the sonic boreholes were completed to a depth of 3 m and 24-hour pumping tests were carried out in each trench.
- Evaporation test work was initiated on the Maricunga brine at the University of Antofagasta to evaluate the suitability of conventional brine processing techniques. Test work was also initiated by Li3's strategic partner to evaluate the application of proprietary technology on the recovery of lithium.
- Environmental baseline monitoring of flora, fauna, surface water and groundwater were initiated by consultants GHD.
- A NI 43-101 Technical report (Technical Report on the Maricunga Lithium Project, III Region, Chile, prepared for Li3 Energy by D. Hains and F. Reidel, dated April 17, 2012) was prepared on the lithium and potassium resources of the Litio 1-6 mining claims based on the results of the 2011 work program. Table 6-1 summarizes the resource estimate therein.

Table 6-1 Estimated mineral resources for the Litio 1-6 claims – April 9, 2012

	Lithium		Potassium	
	Measured	Inferred	Measured	Inferred
Area (km ²)	14.38	7.06	14.38	7.06
Depth interval (m)	0-150	150-180	0-150	150-180
Aquifer volume (km ³)	2.157	0.212	2.157	0.212
Avg grade (g/m ³)	50	50	360	360
Lithium metal (t)	107,850	10,590		
Potassium (t)			776,250	76,320

6.3.3 BBL- AMT GEOPHYSICS AND PUMPING TESTS (2015)

BBL carried out a field program during 2015 that consisted of the following components:

- An AMT / TEM geophysical survey was completed by Wellfield Services along 6 profiles across the Salar covering a total of 75 line km. 383 AMT sounding were collected at 200 m to 250 m station spacing; 15 TDEM soundings were carried out at the end and centre of each AMT profile. The purpose of the AMT survey was to help map the basin geometry and the fresh water / brine interface.
- Two long-term pumping tests were carried out on production wells P-1 (14 days) and P-2 (30 days) at 37 L/s and 38 L/s, respectively.
- The results of the 2015 program were reported in “Proyecto Blanco, Informe Tecnico, Programa de Pruebas de Bombeo 2015, Analisis y Resultados”, prepared for BBL SpA by Atacama Water in October 2015.

The results of the field program are discussed in further detail in Sections 7 and 9 herein.

6.3.4 MSB- RESOURCE AND RESERVE EVALUATION PROGRAM (2016/8)

MSB initiated a phased work program in August 2016 to complete a Definitive Feasibility Study (DFS) and Environmental Impact Assessment (EIA) for the Blanco Project. This program consisted of exploration drilling and well testing focused on the *Cocina, San Francisco, Salamina and Despreciada* claims and limited additional drilling on the Litio 1-6 mining claims. Sections 9 and 10 herein provide further details on this program. The results of this work resulted in an updated resource estimate to 200 m depth on all mining concessions of the Blanco Project as shown in Table 6-2 and a maiden reserve estimate for these concessions as shown in Table 6-3.

Table 6-2 Measured, Indicated and Inferred Lithium and Potassium Resources for the Blanco Project, December 24, 2018

	Measured (M)		Indicated (I)		M+I	
	Li	K	Li	K	Li	K
Property Area (km2)	18.88		6.43		25.31	
Aquifer volume (km3)	3.05		1.94		5	
Specific yield (Sy)	0.04		0.11		0.07	
Brine volume (km3)	0.13		0.21		0.35	
Mean grade (g/m3)	48	349	128	923	79	572
Concentration (mg/L)	1,175	8,624	1,153	8,306	1,167	8,500
Resource (tonnes)	146,000	1,065,000	244,000	1,754,000	389,000	2,818,000

Notes to the resource estimate:

1. CIM definitions (2014) were followed for Mineral Resources.
2. The Qualified Person for this Mineral Resource estimate is Frits Reidel, CPG
3. No cut-off values have been applied to the resource estimate.
4. Numbers may not add due to rounding.
5. The Measured and Indicated Resources are inclusive of those Mineral Resources modified to produce the Mineral Reserves.
6. The effective date is December 24, 2018

Table 6-3 Blanco Project Lithium Reserve Estimate (assuming 58% lithium process recovery efficiency), January 15, 2019

Concession area	Category	Year	Brine Vol	Ave Li conc	Li metal	LCE
			(Mm3)	(mg/l)	(tons)	(tons)
Old code	Proven	1-7	21	1,051	13,000	67,000
	Probable	1-18	42	1,068	26,000	140,000
Litio 1-6	Proven	7-14	14	1,184	10,000	51,000
	Probable	14-23	48	1,170	32,000	173,000
Total 20 yr DFS production	All	1-20	117	1,115	75,000	401,000
Total 23 yr production	All	1-23	125	1,117	81,000	430,000

Notes to the Reserve Estimate:

1. Blanco Project brine production initiates in Year 1 on the mining concessions constituted under old Chilean mining code and include the Cocina, San Francisco, Salamina, Despreciada concessions (the “Old Code concessions”). In Year 7 brine production switches to the Litio 1-6 concessions that were constituted under the 1983 (“new”) Chilean mining code and require a special operating license (CEOL) from the Chilean government. It is the opinion of the author that there is a reasonable expectation that MSB will obtain a CEOL, in advance of any brine production from the Litio 1-6 concessions.
2. The EIA for the Blanco Project was submitted to the Chilean Environmental Review Agency (SEA) in September 2018; it is the opinion of the author that there is a reasonable expectation that the final environmental approvals for the construction and operation of the Project will be obtained during 2019.
3. The Blanco Project Reserve Estimate includes an optimized wellfield configuration and pumping schedule to comply with environmental constraints and water level decline restrictions on the northeast side of the Salar over the total 23-year simulated brine production.
4. The total Mineral Reserves contain approximately four (4) percent of Li mass that is derived from outside of the Blanco Project property boundaries.
5. Lithium is converted to lithium carbonate (Li_2CO_3) with a conversion factor of 5.32.
6. The effective date for the Reserve Estimate is January 15, 2019.
7. Numbers may not add to due rounding effects.
8. Approximately 36 percent of the Measured and Indicated Resource are converted to Proven and Probable Reserves as brine feed from the production wellfield to the evaporation ponds without accounting for the lithium process recovery efficiency. The overall conversion from M+I Resources to Total Reserves including lithium process recovery efficiency is approximately 21 percent.

6.3.5 PREVIOUS WATER EXPLORATION IN SALAR DE MARICUNGA

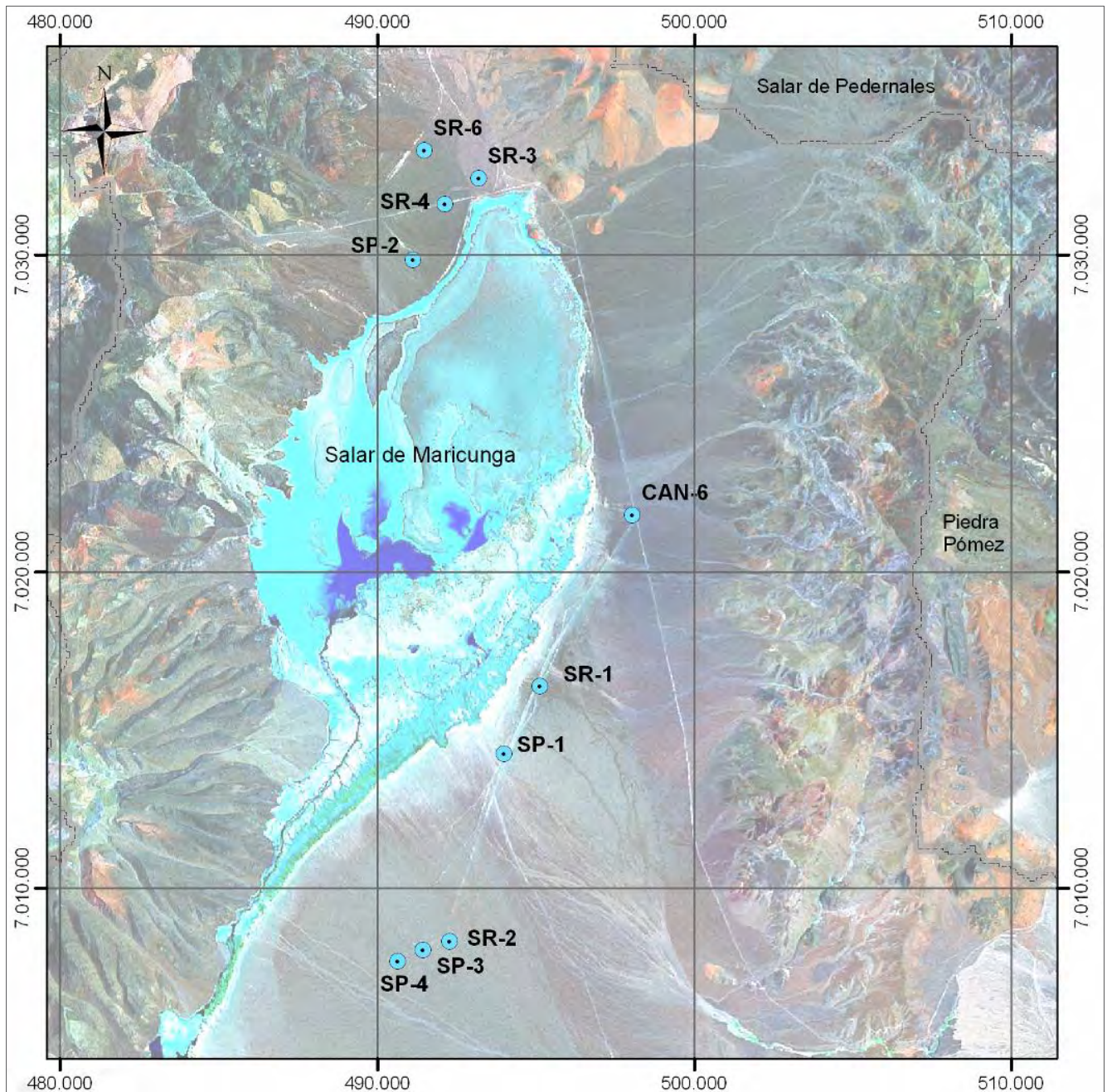
A significant amount of hydrogeological and water resources studies has been carried in the Maricunga basin in the past. Below is a list of work and references relevant to this investigation.

- Balance Hídrico de Chile, Dirección General de Aguas, 1987.
- Mapa hidrogeológico de la cuenca Salar de Maricunga: sector Salar de Maricunga, Escala 1:100.000, Región de Atacama. N° Mapa: M62.- Autor: Iriarte D., Sergio. SERNAGEOMIN, 1999.
- Mapa hidrogeológico de la Cuenca Salar de Maricunga: sector Ciénaga Redonda, escala 1:100.000, Región de Atacama. N° Mapa: M65. Venegas, M.; Iriarte, S. y Aguirre, I. SERNAGEOMIN, 2000.
- Geología del Salar de Maricunga, Región de Atacama, Escala 1:50.000. N° Mapa: M54.- Autor: Tassara O., Andrés. SERNAGEOMIN, 1997.

- Ref. 14 Mapa Hidrogeológico de la Cuenca Campo de Piedra Pómez-Laguna Verde.
- Región de Atacama, Escala 1:100.000. N° Mapa: M66.- Autor: Santibáñez I., Venegas M. Formato JPG. SERNAGEOMIN, 2005.
- Geoquímica de Aguas en Cuencas Cerradas: I, II y III Regiones de Chile, Volumen I, Síntesis. S.I.T N° 51, de los autores Risacher, Alonso y Salazar, Convenio de Cooperación DGA – UCN – IRD, 1999.
- Análisis de la Situación Hidrológica e Hidrogeológica de la Cuenca del Salar de Maricunga, III Región. DGA, Departamento de Estudios y Planificación (2006). S.D.T. N° 255.
- Hidrogeología Sector Quebrada Piedra Pómez. EDRA, 1999.
- Evaluation of the Hydrogeological Interconnection between the Salar de Maricunga and the Piedra Pomez Basins, Atacama Region, Chile; An Isotope and Geochemical Approach. Iriarte, Santibáñez y Aravena, 2001.
- Levantamiento Hidrogeológico para el Desarrollo de Nuevas Fuentes de Agua en Areas Prioritarias de la Zona Norte de Chile, Regiones XV, I, II, y III. Etapa 2 Sistema Piloto III Region Salares de Maricunga y Pedernales. Realizado por Departamento de Ingenieria Hidraulica y Ambiental Pontificia Universidad Catolica de Chile (PUC). SIT No. 195, Noviembre 2009.
- Hidrogeologia Campo de Pozos Piedra Pomez- Compania Minera Casale; prepared by SRK Consulting; May 2011.
- Linea Base Hidrogeologica y Hidrologica Marte Lobo y Modelo Hidrogeologico Cienaga Redonda – Kinross Gold Corporation; prepared by Golder Associates, June 2011.

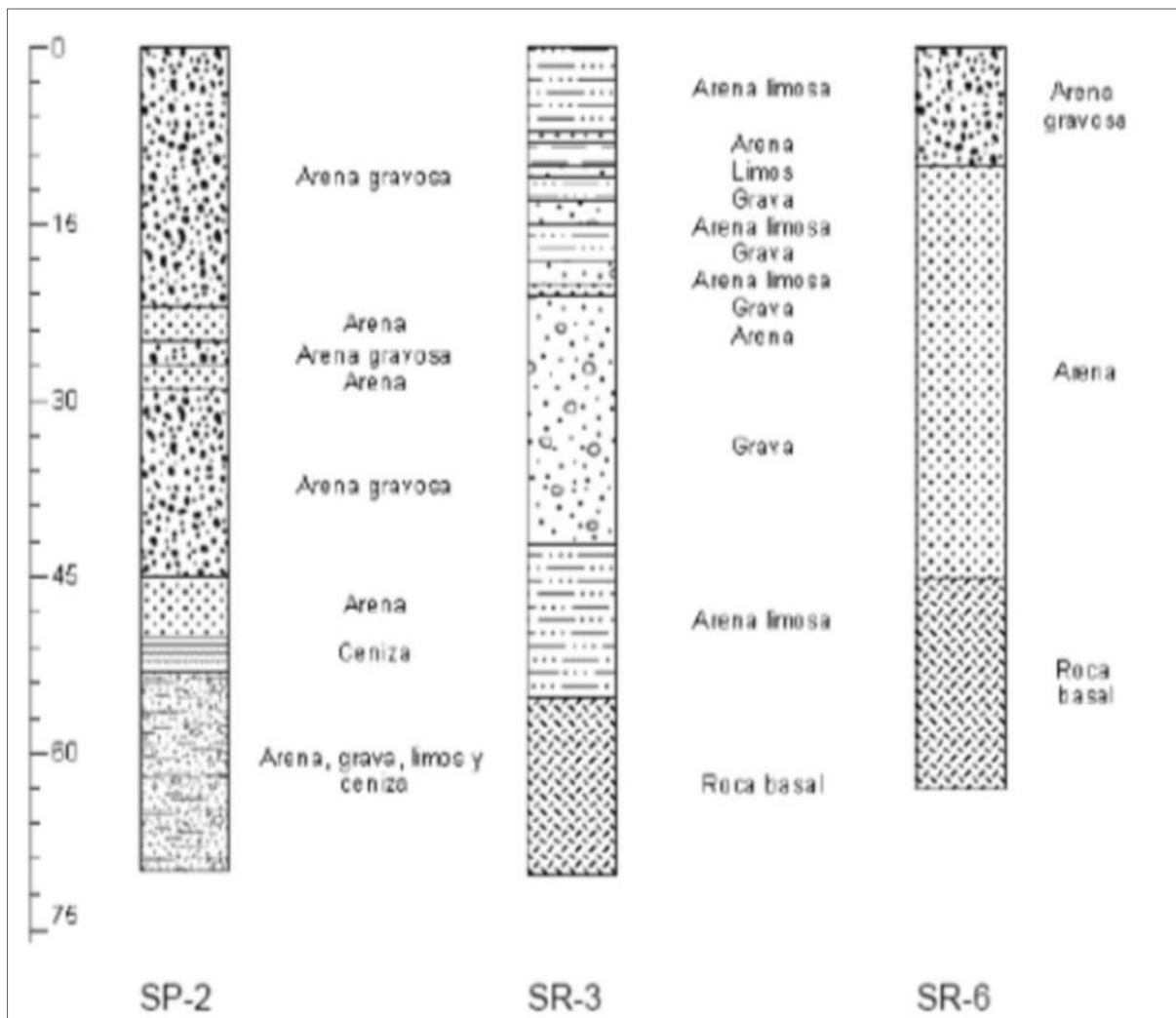
Compania Mantos de Oro and Chevron Minera Corporation of Chile carried out several water well drilling campaigns between 1988 and 1990 during which a total of 10 wells were installed around the perimeter of Salar de Maricunga as shown in Figure 6-1. Figure 6-2 and Figure 6-3 show the available lithological logs for these wells.

Figure 6-1 Location map of wells installed by Compania Mantos de Oro and Chevron 1988/1990



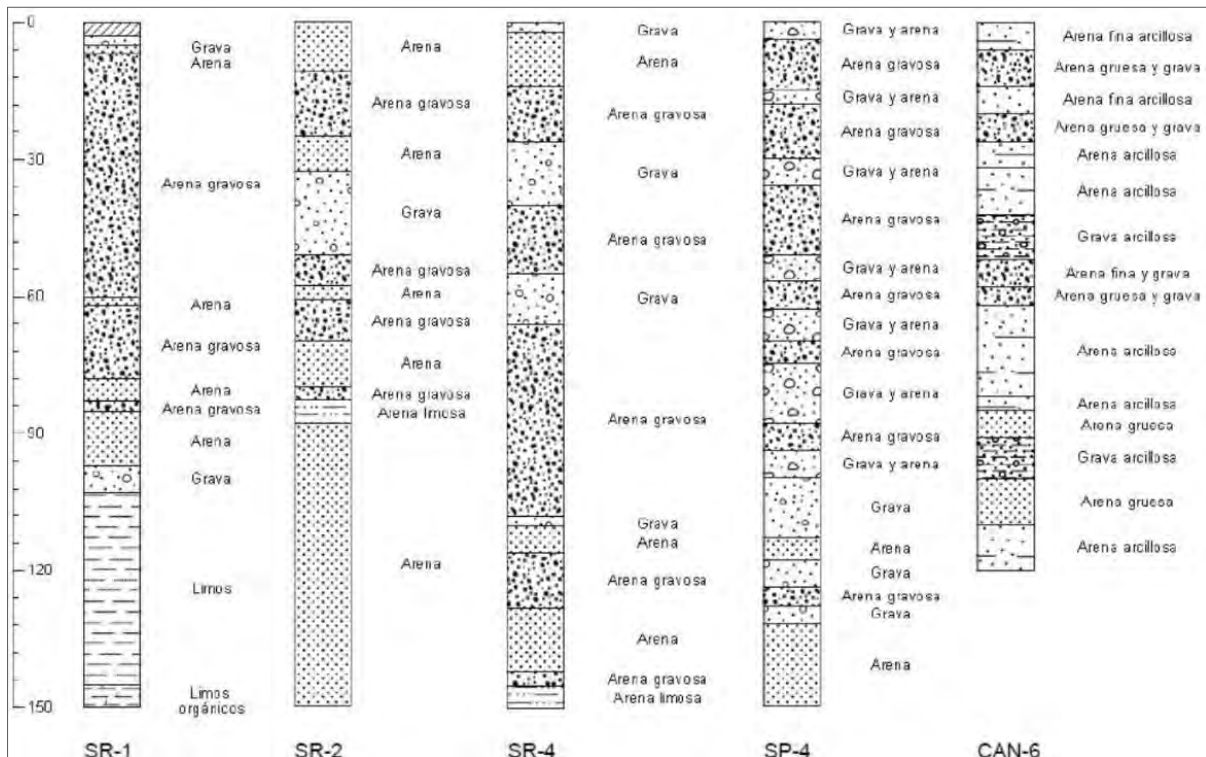
Source: DGA 2009

Figure 6-2 Lithological logs of Compania Mantos de Oro wells SP-2, SR-3 and SR-6



Source: DGA 2009

Figure 6-3 Lithological logs of Compania Mantos de Oro wells SR-1, SR-2, SR-4, SP-4 and Chevron well CAN-6



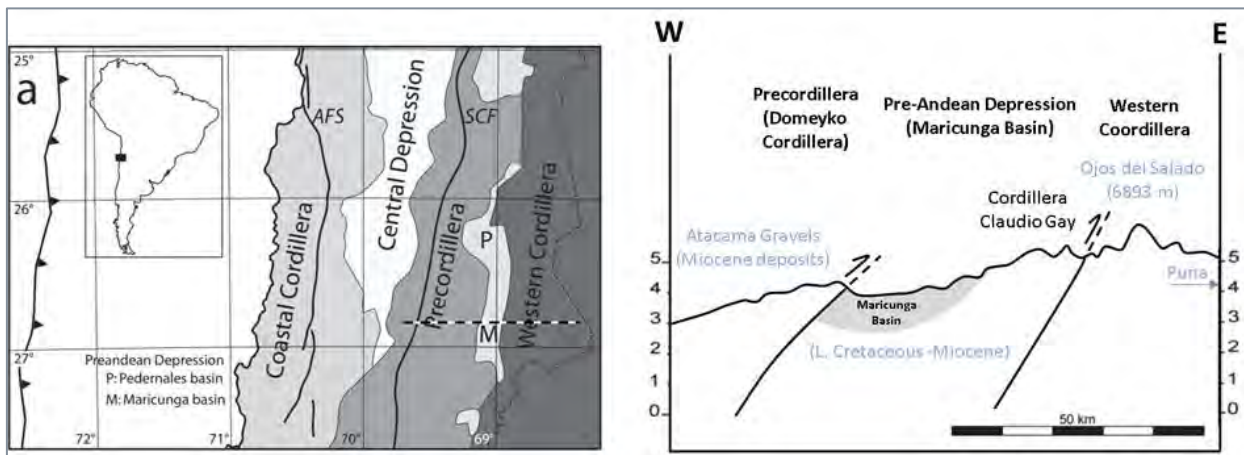
Source: DGA 2009

7. GEOLOGICAL SETTING AND MINERALIZATION

7.1 REGIONAL GEOLOGY

The Andean Cordillera in northern Chile is divided in five (Figure 7-1) well-defined morphotectonic units: The Coastal Cordillera and Central Depression, Precordillera (or Cordillera de Domeyko), Preandean depressions (Pedernales and Maricunga basins) and the Western Cordillera (where the Cordillera Claudio Gay separates the Western Cordillera from the Maricunga Basin). The Coastal Cordillera comprise the eroded remnants of Jurassic-early Cretaceous magmatic arc represented by large plutonic complexes, a Jurassic andesitic to basaltic volcanic sequence (La Negra Formation, Garcia, 1967), and Upper Jurassic-Early Cretaceous andesitic to dacitic lavas (Punta del Cobre Group Lara and Godoy, 1998). The main tectonic feature in the Coastal Cordillera is the Atacama Fault System, which originated in the Jurassic as a "trench-linked" structural system along the axis of the early Andean magmatic arc. Backarc Jurassic-early Cretaceous marine and continental sedimentary units appear further east in the Precordillera overlying Late Paleozoic igneous basement units (Cornejo et al., 1993). To the east, in the Precordillera, the Mesozoic back-arc sediments are intruded by Eocene sub volcanic stocks and porphyries and deformed by the Eocene Sierra del Castillo-Agua Amarga fault and Potrerillos Fault and Thrust Belt (Tomlinson et al., 1994; Mpodozis et al., 1995; Tomlinson et al., 1999) which form part of the regionally important Domeyko Fault system. Finally, The Cordillera Claudio Gay is an uplifted basement block, covered by Eocene-Miocene sedimentary and volcanic sequences (Mpodozis and Clavero, 2002).

Figure 7-1 Morphotectonic units of the Andean Cordillera in northern Chile

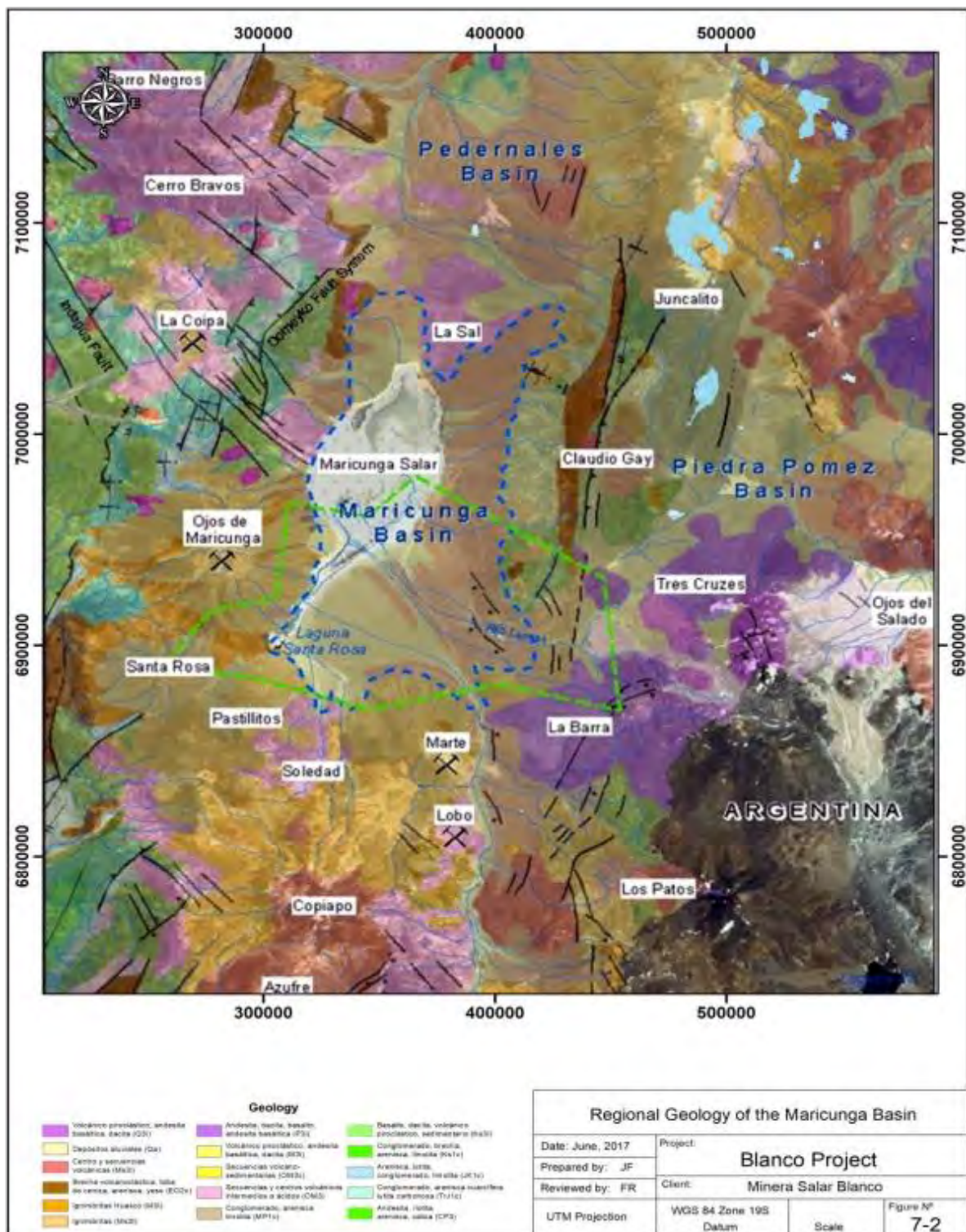


Modified from Nalpas (2008)

The Project is located in the Maricunga Basin within the pre-andean depression. Uplift and denudation should have produced a large amount of sediments during the Cenozoic era. Nevertheless, only the Maricunga and Pedernales Basins preserve a large amount of sediments

while in the Precordillera and Central Depression only a thin blanket of Miocene sediments (Atacama Gravels) forms the infill of a Tertiary paleovalley network (Sillitoe et al., 1968; Mortimer 1980 ; Riquelme, 2003; Gabalda et al., 2005). The geodynamic framework and geological evolution that makes possible the formation, thickening and preservation of the Maricunga basin is presented and summarized in five stages inside the project area as shown in Figure 7-2.

Figure 7-2 Regional Geology of the Maricunga Basin



First stage: Pre-Basin evolution (299 to 66 Ma)

The oldest outcrops near the Maricunga basin are related to a Late Paleozoic granitoids and rhyolites in the precordillera and the Claudio Gay cordillera (Mpodozis and Clavero, 2002), they are uplifted basement blocks that are overlain by Devonian to Carboniferous sandstones, shales and mudstones of the Chinchas Formation, abruptly covered by Triassic deposits corresponding to the continental El Mono Beds (Mercado 1982; Corneto et al. 1998), consisting of a thick succession of breccias and conglomerates with rhyolitic and andesitic clasts, and intercalations with huge boulders (1m in diameter), laminated black carbonaceous lacustrine shale and sandstones containing Triassic fauna, and matrix-supported conglomerated and sandstones. This succession is continuous with Early Jurassic marine deposits of the Montandón Formation.

Other Mesozoic formations are described near as the Pantanoso Formation or El Leoncito sequence. The Mesozoic cover is formed by sedimentary rocks, mainly arkosic sandstones and carbonaceous black shales of the late Triassic La Ternera Formation (Brüggen, 1950), Jurassic marine limestone and volcanic rocks of the Lautaro Formation, sandstone of the late Jurassic to early Cretaceous Quebrada Monardes Formation, and volcanoclastic rocks of the late Cretaceous Quebrada Seca Formation. The Mesozoic cover is capped by andesitic breccias and agglomerates of late Cretaceous to early Tertiary age.

Second stage: Early volcanic episode (66 to 21 Ma)

During this stage occurred the earliest volcanic episode of the Maricunga arc. This volcanic event erupted over a moderately dipping subduction zone through a crust that was likely near 40 km thick. These centres mark the frontal arc west of the backarc basalt. This is seen in the Cerros Bravos–Barros Negros centres that are located along a NW-trending sinistral strike-slip faults that are part of the Domeyko Fault System (Cornejo et al., 1993; Mpodozis et al., 1995; Tomlinson et al., 1999). K/Ar ages from these centres range from 25 to 21.7 Ma (Mpodozis et al., 1995; Tomlinson et al., 1999). Many of the dome complexes and associated tuff and pyroclastic breccia rings are hydrothermally altered. Epithermal, high-sulfidation, gold-silver and porphyry-style gold mineralization occurred during this stage at La Coipa, Esperanza, and La Pepa (Vila and Sillitoe, 1991; Mpodozis et al., 1995; Muntean and Einaudi, 2001).

Activity at the Cerros Bravos–Barros Negros centres began with the eruption of small-volume rhyodacitic ignimbrites that were subsequently covered by main stage pyroxene and hornblende-andesitic lava and block and ash deposits. Crystal-rich hornblende and dacitic domes were then emplaced in the cores of the stratovolcanoes. A series of subcircular domes that host the Esperanza epithermal gold and silver deposit (Vila and Sillitoe, 1991; Moscoso et al., 1993) were emplaced in an 8-km long belt along a reactivated NW-trending fault zone (Cornejo et al. 1993) on the

northeastern flank of Cerros Bravos. The domes at Esperanza are surrounded by a rhyolitic lapilli tuffs with K/Ar ages ranging from 24 to 20 Ma. Alteration ages range from 23 to 19 Ma (Sillitoe et al. 1991; Moscoso et al. 1993). The northeastern most domes are intruded by unaltered dacitic porphyry dikes with biotite K/Ar ages of 22.5 and 22.4 Ma (Cornejo et al., 1993; Kay et al., 1994).

A few kilometres at the south of Cerro Bravos, a multistage dome complex was emplaced at La Coipa. This complex is located where west-verging, north-trending thrusts (Domeyko Fault System) intersect the sinistral northwest-trending (Quebrada Indagua fault). The La Coipa dome cluster K/Ar ages range from 24.6 to 22.9 Ma (Zentilli 1974; Moscoso et al., 1993). The domes are surrounded by an extensive coeval blanket of intensely altered, coarse pyroclastic breccias, and poorly welded lapilli tuffs with biotite K/Ar ages of 24.7 and 24.0 Ma. Volcanism in the La Coipa region ended with the emplacement of middle Miocene domes (Mpodozis et al., 1995).

Third stage: Compressional and crustal thickening (21 to 17 Ma)

This stage begins with a virtual volcanic lull during a period of compressional deformation and crustal thickening. Evidence for compressional deformation is seen in the Cordillera Claudio Gay (Mpodozis and Clavero, 2002). The depositional regime changed dramatically as east-bearing, high-angle reverse faults uplifted the Late Paleozoic basement of the Cordillera Claudia Gay. Intense volcanism followed as large 20–19 Ma dome complexes with extensive block and ash-flow aprons erupted along the northern Cordillera Claudio Gay. These domes are covered by the widespread 18–19 Ma dacitic ignimbrite that has been correlated with the huge Rio Frio ignimbrite (Cornejo and Mpodozis, 1996). All these volcanic deposits are the base of the Maricunga basin.

In the middle Miocene, the Claudia Gay Cordillera was affected by the last compressional deformation in the region of the modern pre-Andean depression. Evidence for this deformation comes from the alluvial gravels interbedded with distal ignimbrites (K/Ar age of 15–16 Ma) in the Rio Lamas sequence. These gravels show progressive unconformities and intraformational folds indicative of synsedimentary deformation (Gardeweg et al., 1997; Mpodozis and Clavero, 2002).

Fourth stage: Stratovolcanic complexes (17 to 11 Ma)

The fourth stage was marked by the construction of voluminous, andesitic to dacitic stratovolcanic complexes along the length of the Maricunga arc. From north to south, these centres include the Ojos de Maricunga, Santa Rosa, Pastillitos volcanoes were emplaced during the initial stages at some centres. Most centres are little eroded and preserve much of their original form. The third stage ended with the emplacement of structurally controlled, shallow-level, quartz-dioritic stocks hosting gold and copper mineralization (Marte, and Lobo, gold porphyries; Vila and Sillitoe, 1991).

The largest group of middle Miocene volcanic centres in the Maricunga Belt is the cluster of stratovolcanoes to the west and south of the Salar de Maricunga. The northernmost of these centres is the well-preserved Ojos de Maricunga volcano (4985 m) with a basal diameter of 15 km and a central crater filled by a dacite dome dated at 15.8 ± 0.9 Ma (whole-rock K/Ar; Mpodozis et al., 1995). The slopes of the volcano are covered by unconsolidated hornblende andesite block and ash deposits that have yielded K/Ar ages from 16.2 ± 0.6 to 15.1 ± 0.7 Ma (Zentilli, 1974; Mpodozis et al., 1995) and a $^{40}\text{Ar}/^{39}\text{Ar}$ age of 14.5 ± 0.1 Ma (McKee et al., 1994). The block and ash deposits overlie two ignimbrites of uncertain origin. The older is a welded red tuff (60%–62% SiO_2) that is up to 100 m thick and has a whole-rock K/Ar age of 15.8 ± 0.8 Ma. The younger, which is exposed on the southwestern slope, is a slightly welded, pumice-rich biotite-bearing ignimbrite with biotite K/Ar ages of 14.3 ± 1.6 Ma and 13.7 ± 2.6 Ma (Zentilli, 1974).

Other middle Miocene volcanic centres to the south are principally made of hornblende- and pyroxene-bearing andesite. They include the Santa Rosa, Cerro Lagunillas, and Pastillitos, volcanoes. Blocks from a coarse blanket of reworked pyroclastic block and ash deposits on the slopes of the Santa Rosa cone have K/Ar ages of 15.4 ± 0.55 Ma (hornblende, McKee et al., 1994) and 13.8 ± 0.6 Ma (whole rock, González-Ferrán et al., 1985). Whole-rock K/Ar ages from a Cerro Lagunillas lava, a block from the Pastillitos centre, and a Cerro Las Cluecas lava range from 16.2 ± 0.6 to 15.9 ± 1.4 Ma (Mpodozis et al., 1995).

Fifth stage: Volcanic arc migration (11 to 4 Ma)

A radical change in the distribution of volcanic centres occurred during this stage as most of the volcanic activity at the north of Laguna Negro Francisco became concentrated in the silicic andesitic to dacitic Copiapó volcanic complex. Volcanic activity in the Maricunga Belt from 11 to 7 Ma was largely restricted to the Copiapó volcanic complex at the intersection of the northwest-trending Valle Ancho–Potrerillos fault system with the Maricunga Belt. The silicic andesitic to dacitic pyroclastic flows, domes, and lavas that make up the Copiapó complex cover an area of more than 200 km².

The Ojos del Salado volcanic region is located near the southern termination of the modern Central Volcanic Zone near 27°S latitude. This region is home to the Central Volcanic Zone arc and the late Oligocene to Miocene volcanic centres that erupted in the backarc of the Maricunga arc, which is over 40 km to the west. Between 9 and 6 Ma, the Maricunga arc volcanic activity dramatically decreased and then ceased as volcanism increased significantly in the backarc. By 4 Ma, the main frontal volcanic arc was essentially in the Ojos del Salado region. The distribution, age, and geochemistry of the Ojos del Salado region volcanic rocks reflect complex magmatic-tectonic interactions associated with arc migration, crustal thickening, and uplift (Mpodozis et al., 1996; Kay et al., 2006). Considering the modern subduction geometry and assuming that the magmatic front

of the Maricunga arc was located around 100 km above the subducting Nazca slab, a significant portion of the forearc crust and frontal arc lithosphere should have been removed from below this region after 8 Ma (Kay and Mpodozis, 2002; Kay et al., 2006).

The late Miocene to Pliocene is marked by the eruption of small-volume bimodal centres at the southern end of the Maricunga arc. These eruptions include ignimbrites associated with the fault-controlled Jotabeche rhyodacitic caldera and glassy mafic andesitic to andesitic Pircas Negras lavas emplaced along faults (Mpodozis et al., 1995; Kay et al., 1994). The chemistry (very high La/Yb ratios and Na₂O and Sr contents) of these magmas are uncommon in the central Andes and have been associated with a very thick crust and contamination of the mantle wedge by crustal material removed from the forearc by subduction erosion. Climatic conditions change from 9 to 10 Ma to a hyper-arid climate (Hartley and May, 1998), both sedimentation and erosion came to a halt. This is also attributed to an important change on the mass transfer regime that occurred between the Oligocene when all the sediments are exported out of the drainage system towards the ocean, and the Miocene, when the sediments started to accumulate along the drainage network (Nalpas et al., 2008).

7.2 LOCAL GEOLOGY

Based on the drilling campaigns carried out in the Salar between 2011 and 2021, eight major geological units were identified and correlated from the detailed geological logging of drill cuttings and undisturbed core to depths of up to 400 m. The correlation of the geological units between boreholes was further supported by borehole geophysical surveys (LithoSight). These geological units are composed of unconsolidated clastic, volcanoclastic, and evaporitic sediments. Only one borehole (S-29) near the western edge of the Salar reached bedrock at a depth of 213 m. The remaining bedrock topography has been interpreted from the results of surface geophysics surveys (including TEM/AMT and Gravity). Salar de Maricunga is a mixed style salar, with a halite nucleus of up to 34 m in thickness in the central northern part. The halite crust towards the southeast changes to borate and sulphate dominant facies. The halite unit is underlain by a clay-dominated lacustrine unit (previously referred to as the clay core). The clay is locally interbedded with silt and silty sands. The Salar is surrounded by relative coarse grained alluvial and fluvial sediments. These sedimentary fans demarcate the perimeter of the actual salar and at depth grade towards the centre of the Salar where they form the distal facies with an increase in sand and silt. At depth four unconsolidated units of volcanoclastic origin units have been identified. The volcanoclastic units are separated by a relatively thin and continuous sand unit which may be reworked material of the lower volcanoclastic unit. Figure 7-3 is a W-E Section through the Salar schematically showing the geological model.

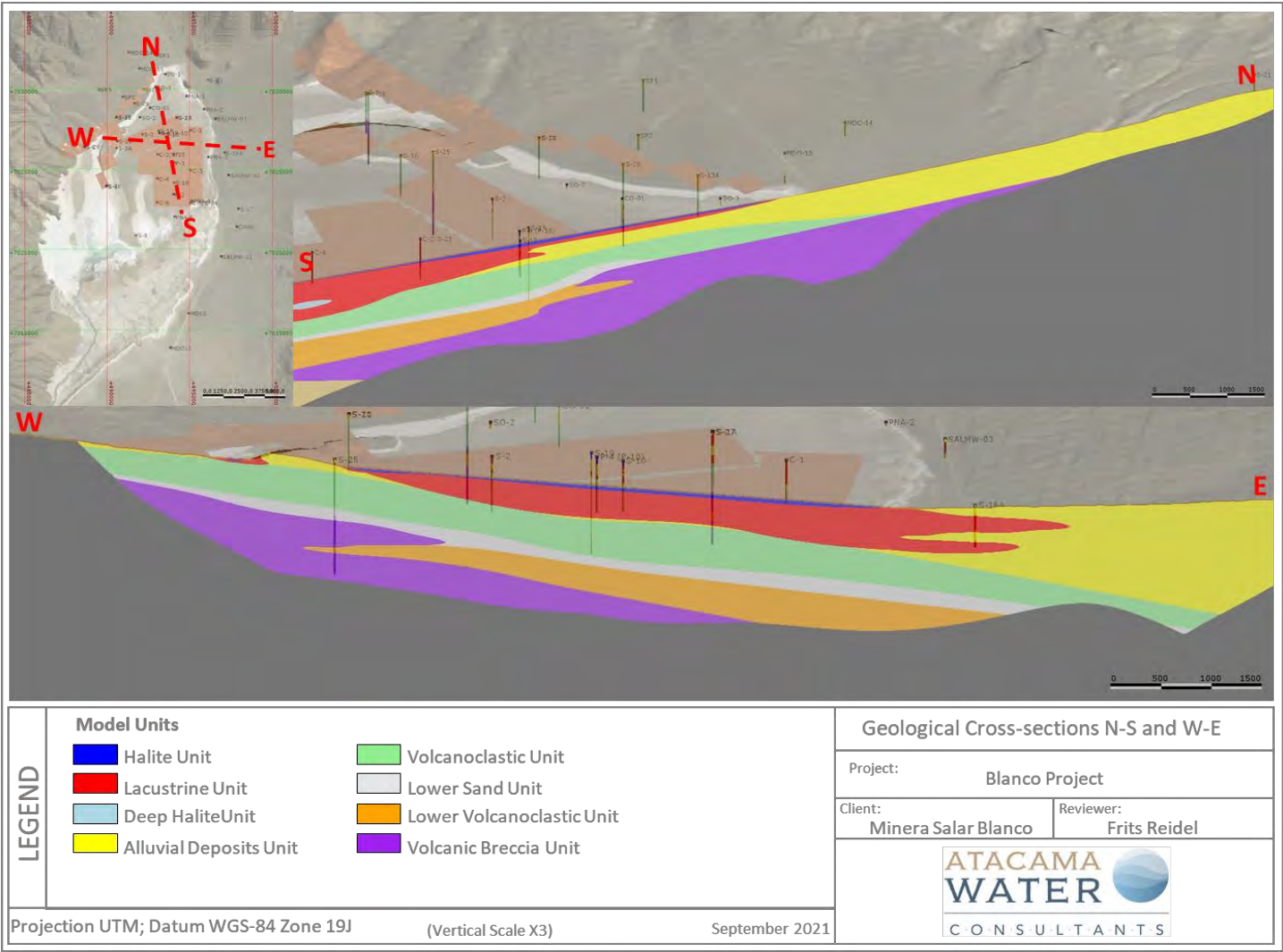
Upper Halite

The nucleus of the Salar is comprised of a halite crust. This unit is characterized by coarse translucent crystals of (1 to 10 mm) of euhedral halite as shown in Figure 7-4. Locally it has traces of interstitial clay and /or ulexite and minor thin strings of clay with halite.

The halite crust thickens towards the centre and north. The halite has a thickness of 30 m in borehole C-2 and 34 m in P-2. Halite pinnacles of up to 60 cm height have developed in the central part of the Salar (Rugosa crust) showing an absence of flooding in this area. In the south (holes S-8 and C-5) the halite unit has a thickness of approximately 1 m; and in the north (holes S-1A, C-1, S-10 and S-19) a thickness of approximately 6 m. Towards the edges of the Salar the crust thins, until it is a saline efflorescence surface that includes areas of re-solution and precipitation from rainwater or recent flooding. Figure 7-4 shows the lateral extent of the halite unit and an East – West section through the Salar.



Figure 7-3 General N-S and W-E Sections through the Maricunga geological model



Lacustrine unit (previously Clay Core)

Immediately below the halite crust, a thick deposit was identified that constitutes an eminently clayey body composed of reddish, green, and brown clays and few levels of black lake clay (Figure 7-5). Locally and close to the edges interspersed with fine sandy levels and towards the centre of the Salar with fine levels of halite. In contact with the most superficial halite unit, this unit presents numerous halite crystals (up to 50%) widespread within the clay matrix. This deposit reaches a depth of 180 m in the eastern sector (boreholes C-5 / S-24) and thins towards the lateral limits of the current lake/saline surface. The unit transcends the superficial limits of the Salar and extends below the Alluvial Deposits in the eastern sector of the basin (boreholes S-15 and S-16). Likewise, based on previous drilling by Minera Mantos de Oro (boreholes MDO-08, MDO-10, MDO-24 and CAN-6) it can be interpreted that in the southeast sector, below the fluvial fan of the Lamas River (Alluvial Deposits), the Lacustrine unit can also be identified at depth (Figure 7-5).

Deep Halite

A Deep Halite unit was identified between boreholes S-18 and C-3. This Deep Halite unit has a thickness of up to 30 m and was intersected at a depth of around 110 m; it is entirely contained within the Lacustrine unit (Figure 7-6). This unit is characterized by whitish, massively compacted halite with crystals of between 1 to 5 mm with interstitial clay and ulexite. A fine layer of black clay and some ulexite with a thickness of approximately 1 m was also identified in these two boreholes.

Alluvial Deposits

The previous geological model subdivided the alluvial deposits into several smaller subunits mainly based on its location within the basin. Now, given that the textural variations and porosity do not present large and clear variations, the sandy and gravel sediments of fluvial / alluvial origin are all grouped here into the Alluvial Deposit.

In general terms, the unit is characterized by a heterogeneous sequence of sediments with variable texture, alluvial and fluvial, dominated by clastic sediments consisting sub-rounded gravels (up to 5 cm) and sands. Fine grained sediment of silts and clays are also found within these alluvial deposits. This unit develops mainly along the edges of the Salar de Maricunga basin and pro-grades to depth towards the basin centre (Figure 7-7).

Towards the eastern margin of the Salar, this unit interbedded levels of sand, forms the foothills of the Cordillera de Claudio Gay. It can interfinger with the clayey and sandy units of the Lacustrine unit as observed in borehole S-16.

To the south, this unit includes the sediments of the Río Lamas fan (Figure 7-7) as identified in Mantos de Oro boreholes MDO-08, MDO-10, MDO-24 and CAN-6.

In the north-western part of the Salar the Alluvial Deposits include a series of W-E fluvial/alluvial fans associated with recent intermittent drainages and older drainage systems that form the limit of the basin in the area around Quebrada Caballo Muerto. The unit was encountered and correlated between boreholes S-11, S-13A, S-3A and S-10.

In the central part of the basin the Alluvial Deposits are overlain by the Lacustrine Deposits. The Alluvial Deposits here consist of gravels, sands and silty sands and is spatially interpreted as the distal part of NW Alluvium system that enters the Salar from the northwest. These deeper Alluvial Deposits are inter-fingered with the Lacustrine Deposits further east in the Salar. These deeper Alluvium Deposits are interpreted in part as reworked material of the underlying volcanoclastic sequences and were encountered in boreholes S-1A, S-2, S-10, S-19, C-1, C-2 y C-4.

Volcanoclastic

The Volcanoclastic Unit has been identified in numerous boreholes (C-1, C-2, P-1, S-1A, S-2, S-3A, S-5, S-6, S-10, S-11, S-13A, S-19, S-25, S-26, S-27, S-28 and S-29). The response in the down hole geophysics profiles (LithoSight™) is marked by a strong kick in Gamma Ray log and strong decrease in resistivity. This unit is characterized by a friable volcanoclastic breccia, matrix supported (tuff), with isolated subangular clasts (3-5%) of 1 to 15 mm gray, brown and reddish aphanitic clasts and numerous whitish pumice fragments in a light brown silty matrix (volcanic ash). It underlies the Alluvial and Lacustrine units and has a thickness up to 100 m (S-2) below the Lacustrine unit as shown in Figure 7-8. The unit is unconsolidated and is interpreted as a volcanic air-fall deposit.

Lower Sand Unit

This unit is a well-defined sand level, overlapping the lower volcanoclastic units that develop in the NW and central sectors of the basin (boreholes S-1A, S-3A, S-5, S-6, S-11, S-13A, S-19, S-25, S-26, S-27, S-28 and S-29) and is interpreted as a consequence of reworking of the underlying sequences. The Lower Sand is generally composed of medium to fine grained sand and locally of coarse to very fine sand with less than 2-5% silt and / or clay. Grains are sub-rounded with translucent crystals (qz) and minor gray, brown and reddish lithics. The unit has a general slope towards the centre of the basin and follows the volcanoclastic units above and below; it has an average thickness of approximately 40 m as shown in Figure 7-9.

Lower Volcanoclastic (LV)

The Lower Volcanoclastics was identified in boreholes S-19, S-25, S-26, S-27 and S-28 in the north-western sector of the Salar. This unit is a homogeneous volcanoclastic air-fall deposit to the upper Volcanoclastic Unit. It consists of very friable, medium to fine sand with little brown silt (ash) that is formed mainly of translucent crystals and to a lesser extent lithic gray and whitish pumice with very few altered biotites. The unit interfingers with the lower Volcanic Breccia Unit as shown in Figure 7-10 and as described below.

Volcanic Breccia

The Volcanic breccia was identified in the centre and WNW sector of the Salar in boreholes S-25, S-26, S-27, S-28 and S-29) immediately below the Lower Sand unit below 200 m as shown in Figure 7-10 and Figure 7-11. It is characterized by a breccia matrix of minor reddish phaneritic and aphanitic lithic fragments (lava) and a very fine sand silty-sized matrix with numerous biotite crystals. The lithic fragments are reworked and range in size from 0.30 cm and 1cm. Fine whitish, friable clasts (sub-rounded to subangular) can be identified throughout the sequence.

The Volcanic Breccia differs from the Lower Volcanoclastic unit in the amount of pumice fragment and the finer rock fragment size. The gamma ray response (LithoSight) also aids in differentiating between the two units.

Basement

The bedrock contact in Salar de Maricunga was modelled based on borehole data and results of the gravity geophysical surveys carried out by MSB, correlated with topography and imagery. Drilling results of boreholes S-19, S-25, S-26, S-27 and S-28 indicate that the depth to bedrock is more than 400 m in the north-central part of the Salar. Bedrock was encountered on the western margin of the Salar in borehole S-29 at a depth of 213 m. Information on regional Figure 7-12 shows the modelled/interpreted bedrock topography. The thickness of the basin fill increases towards the centre of the basin, reaching maximums of up to 1,500 m; the average thickness below the Project area is estimated to range between 400 m and 500 m.

Figure 7-4 Details of the Upper Halite unit

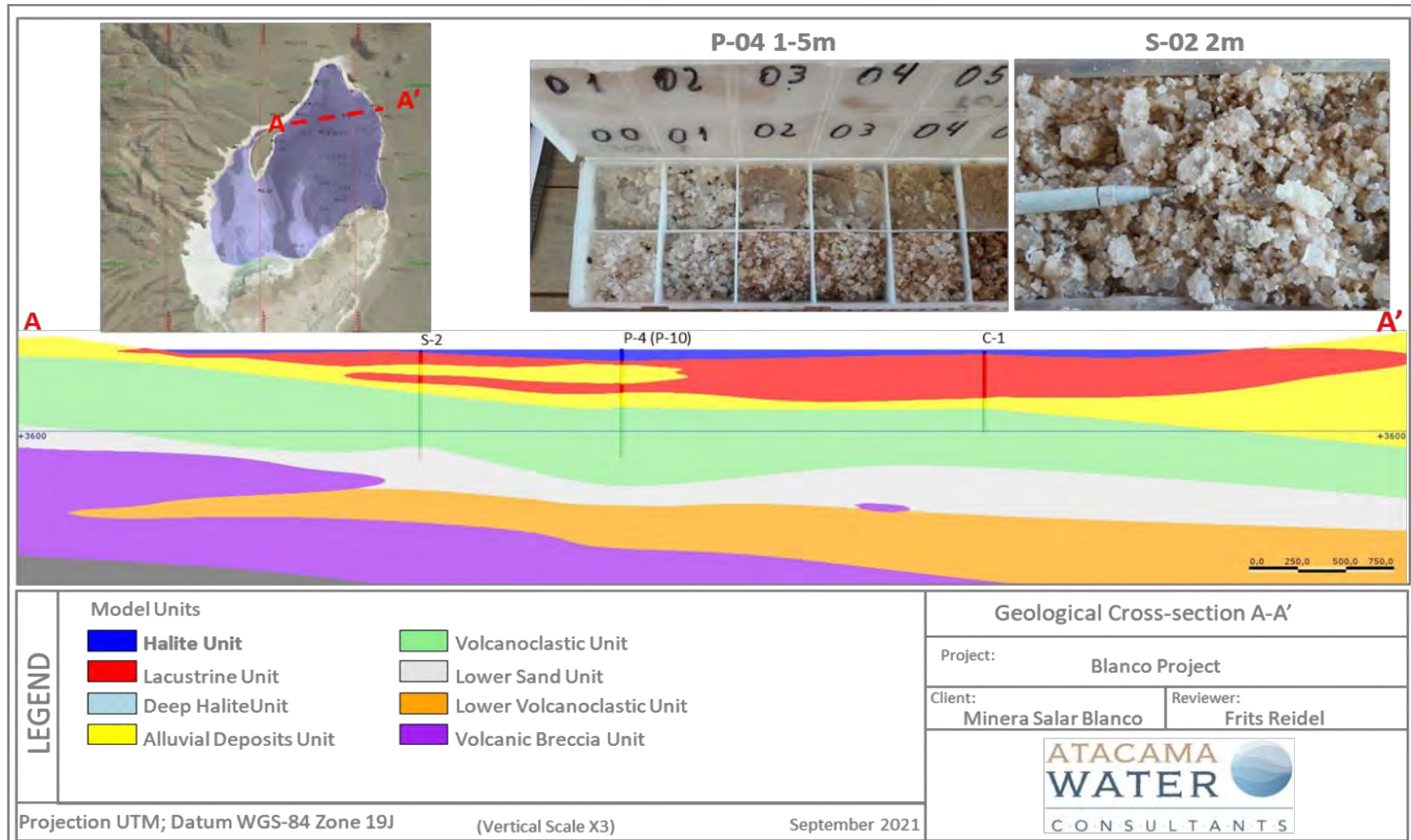


Figure 7-5 Details of the Lacustrine unit

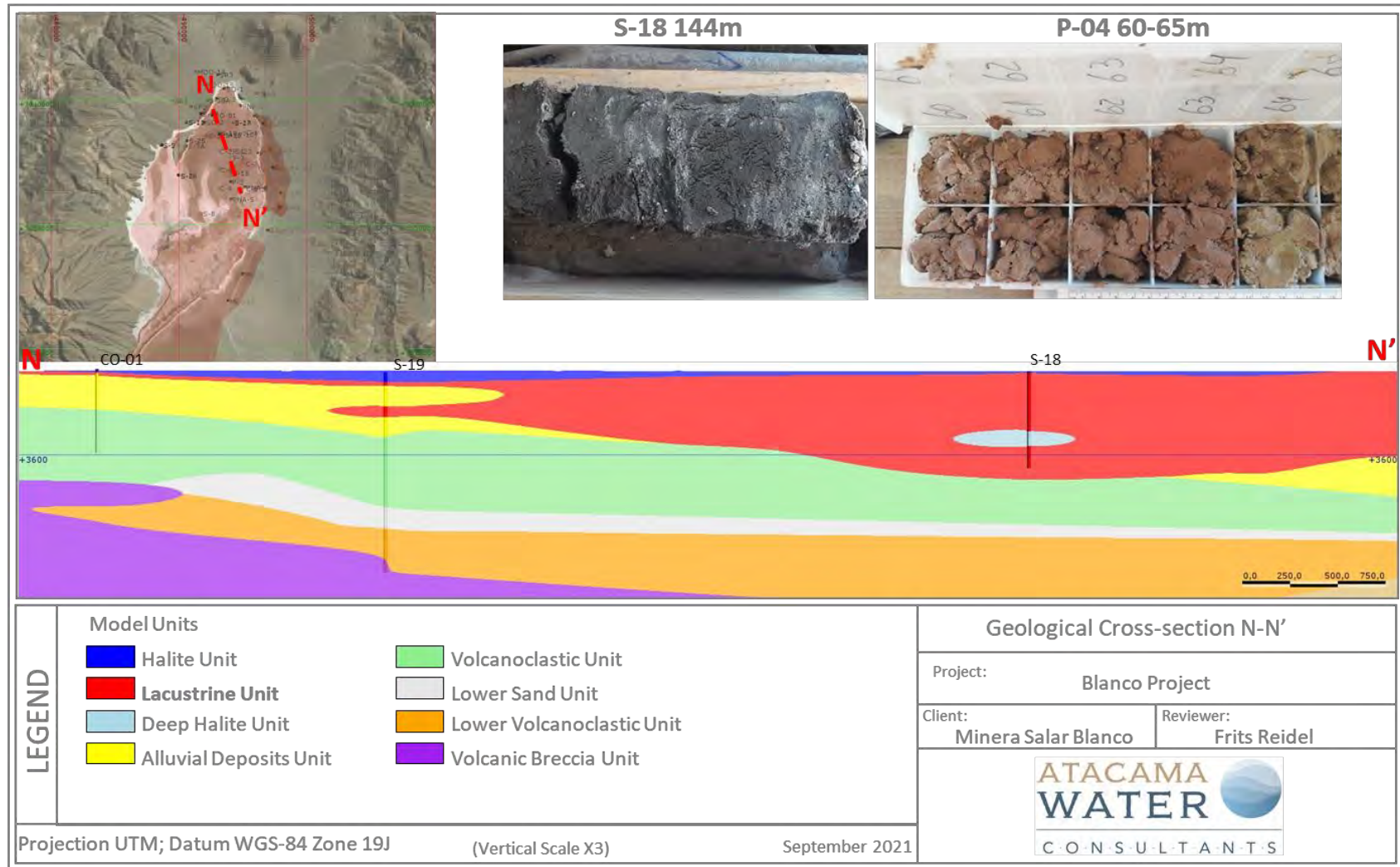


Figure 7-6 Details of the Deep Halite unit

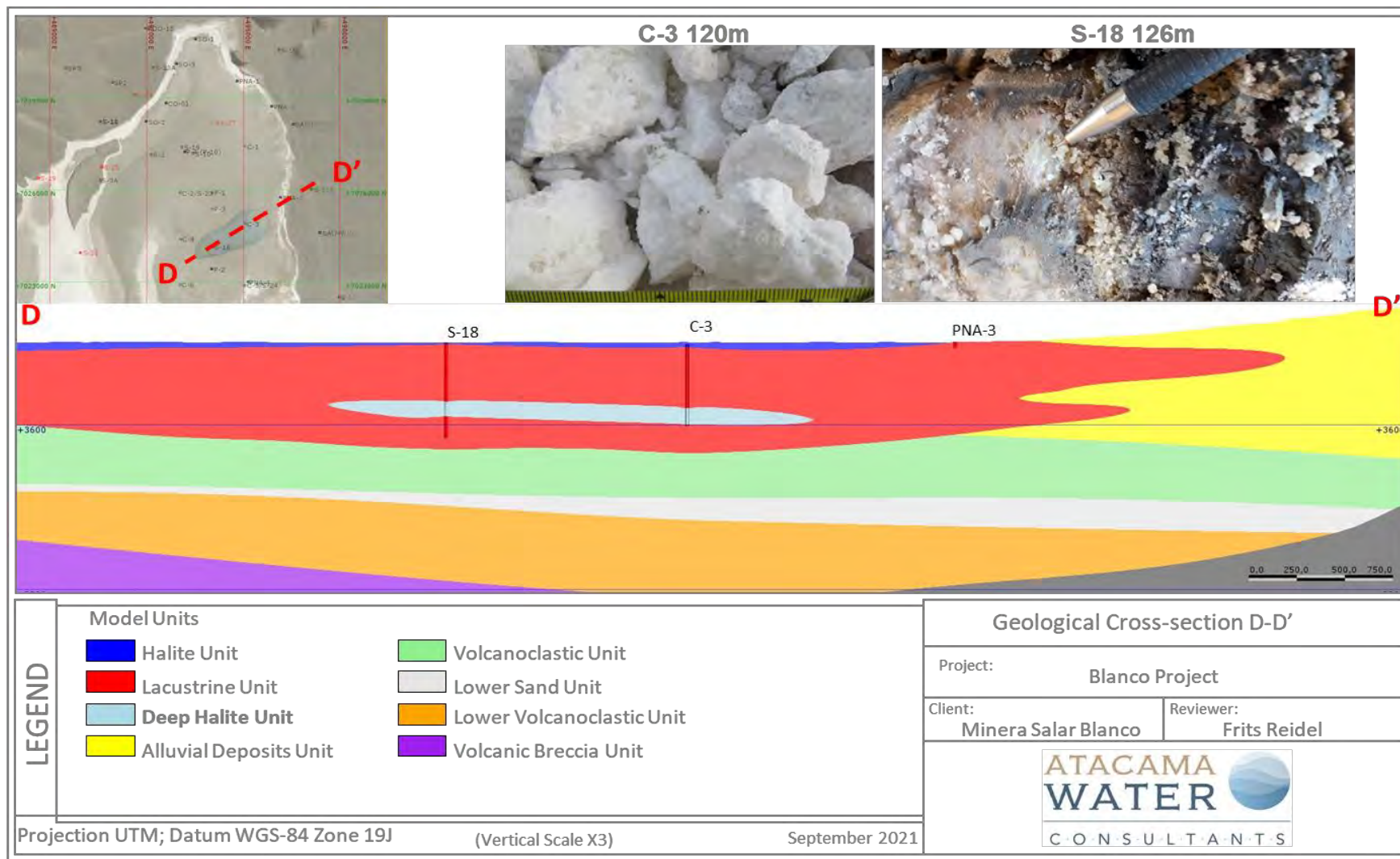


Figure 7-7 Details of the Alluvium Deposits

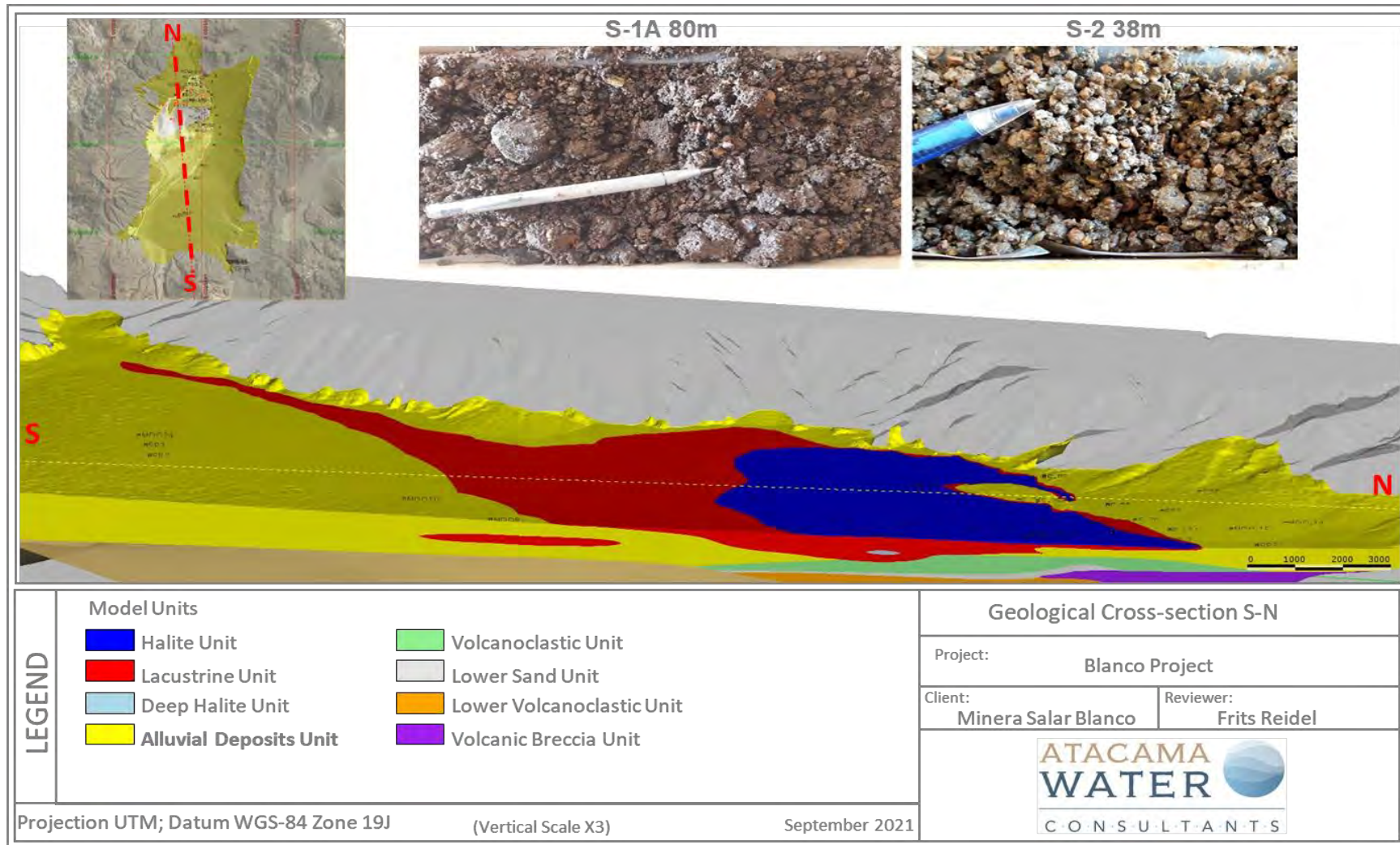


Figure 7-8 Details on the Volcanoclastic unit

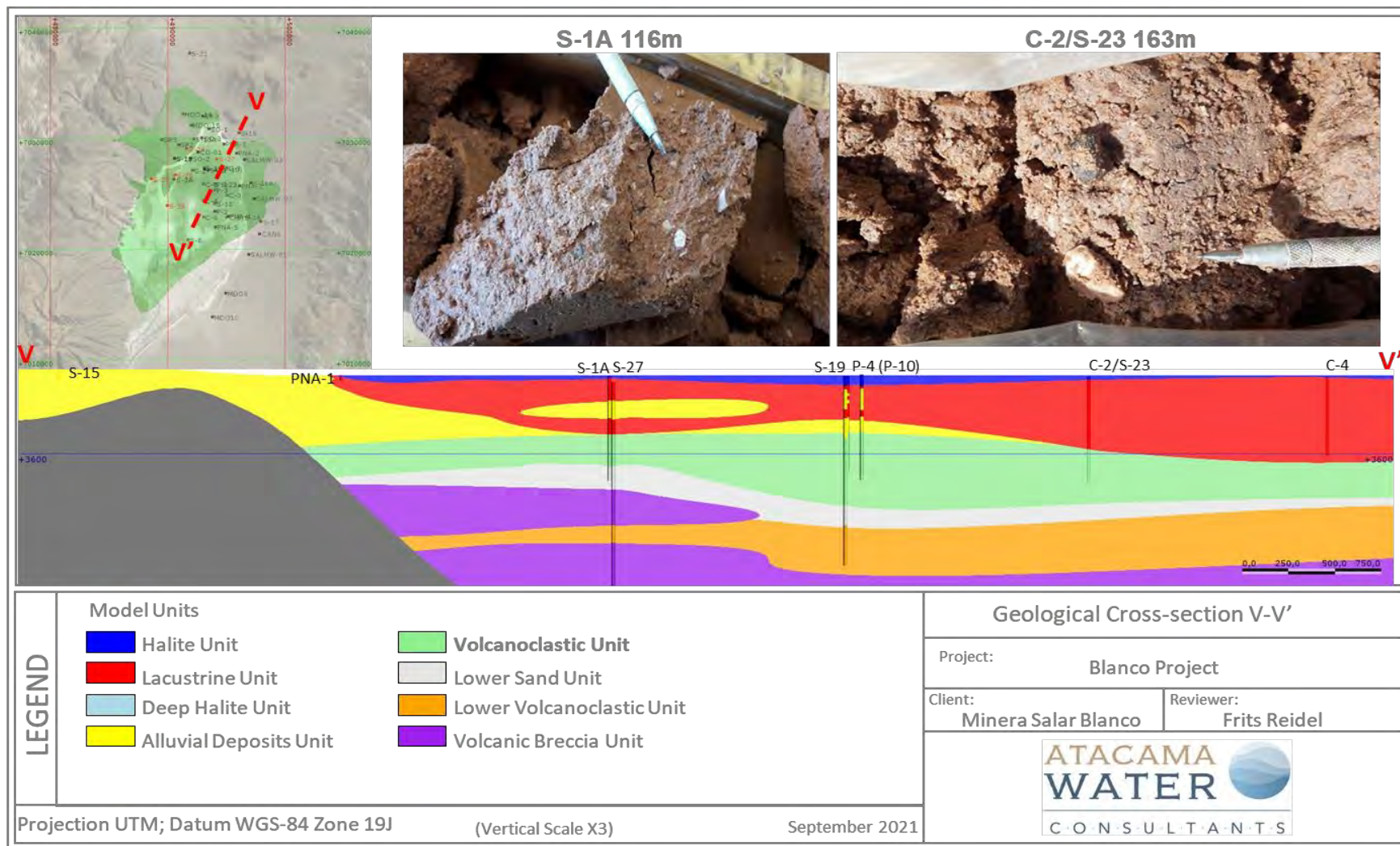


Figure 7-9 Details of the Lower Sand unit

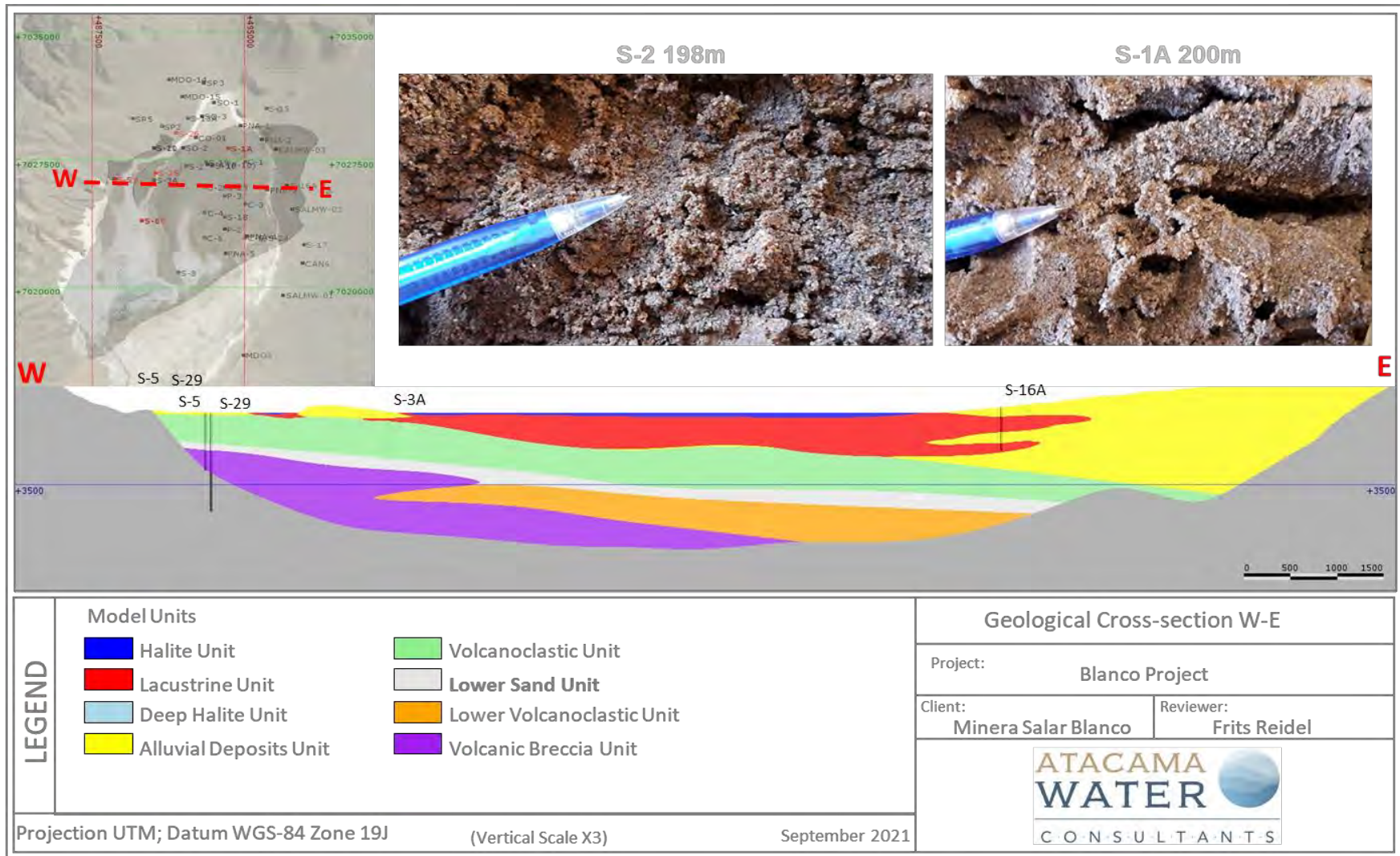


Figure 7-10 Details of the Lower Volcanoclastics unit

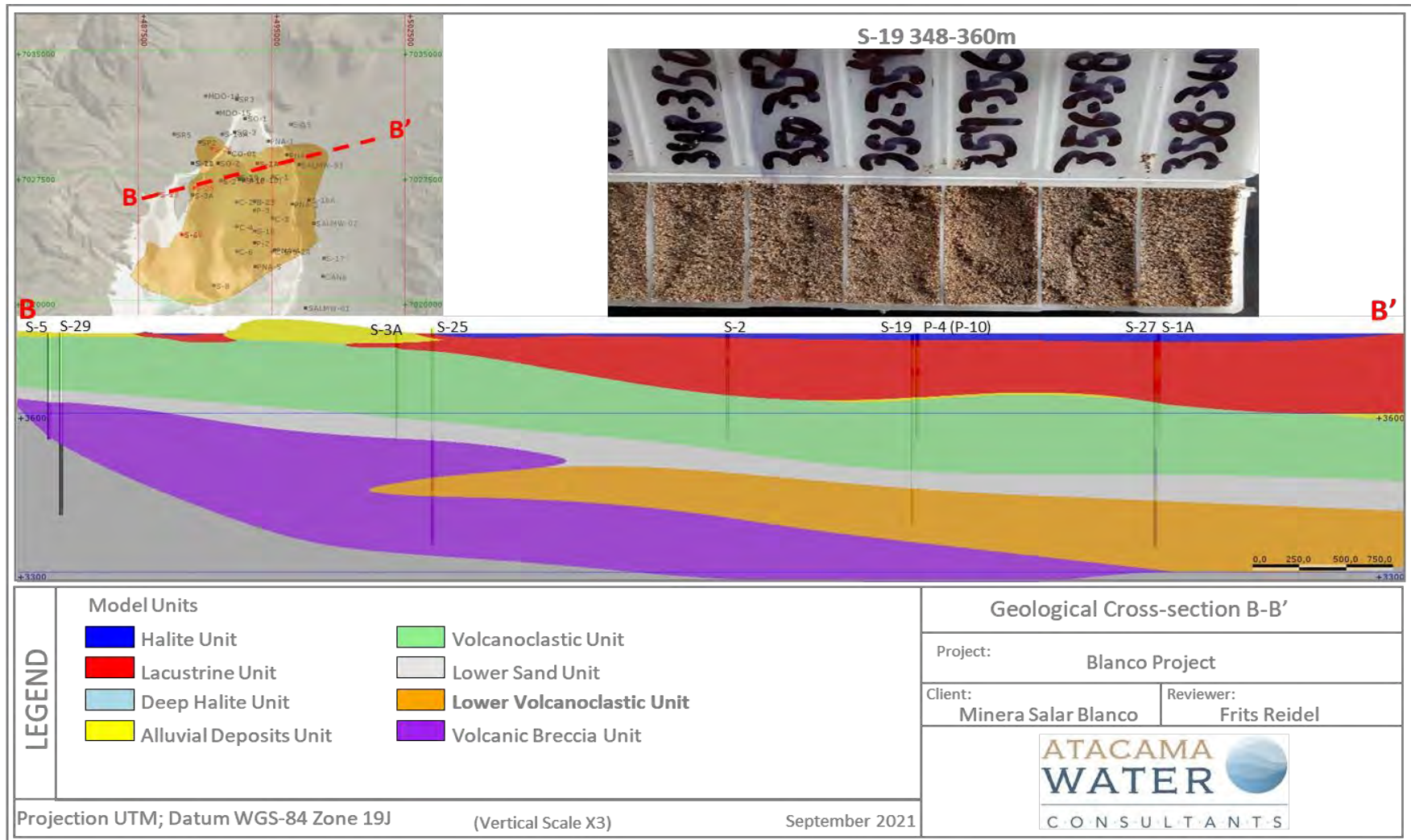
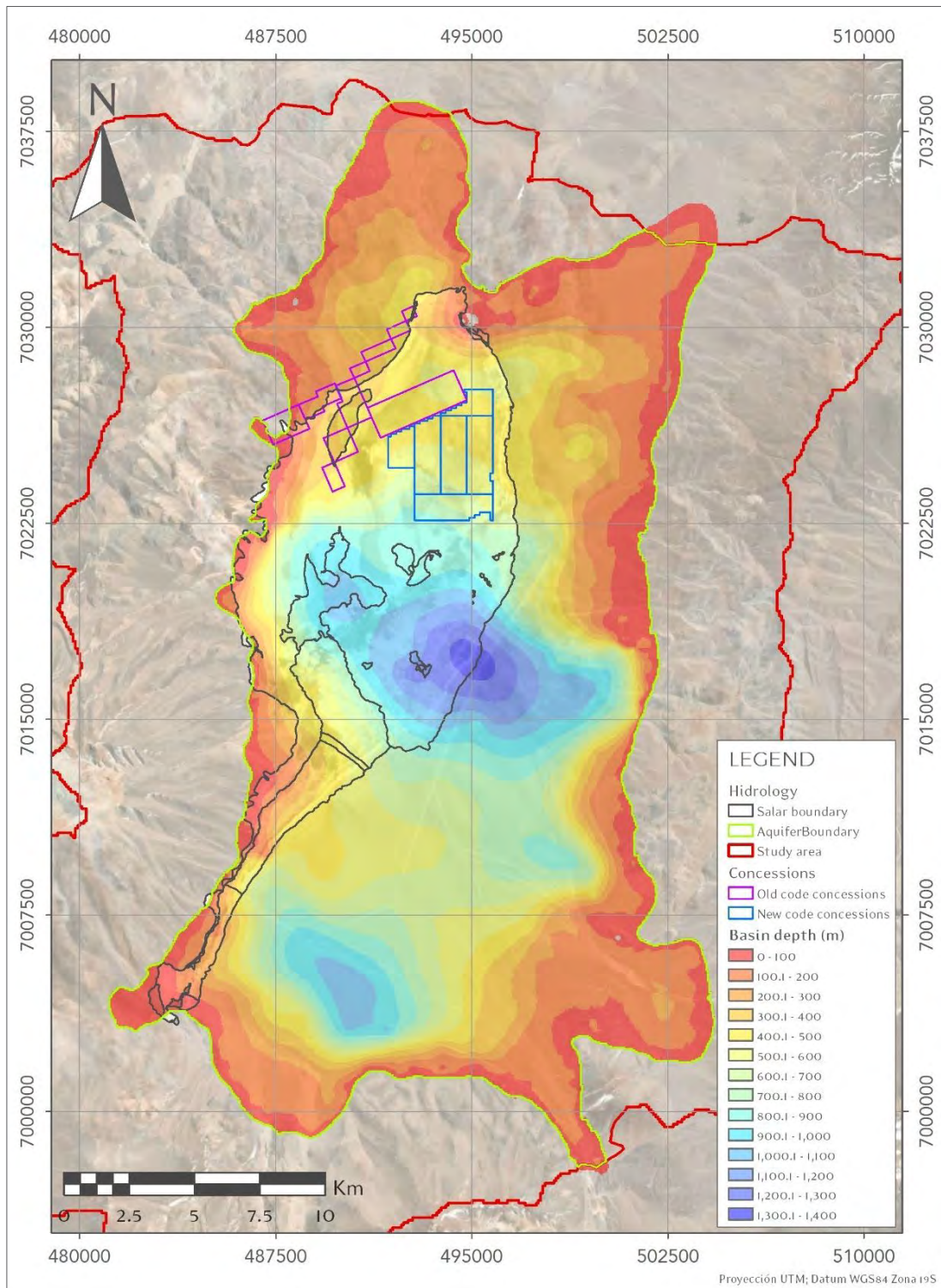


Figure 7-11 Details of the Volcanic Breccia Unit



Figure 7-12 Modelled depth to bedrock for Salar de Maricunga



7.3 MINERALIZATION

The brines from Maricunga are solutions nearly saturated in sodium chloride with an average concentration of total dissolved solids (TDS) of 311 g/L. The average density is 1.20 g/cm³. The other components present in the Maricunga brine are K, Li, Mg, Ca, SO₄, HCO₃ and B. Elevated values of strontium (mean of 359 mg/L) also have been detected.

Table 7-1 shows a breakdown of the principal chemical constituents in the Maricunga brine including maximum, average, and minimum values, based on 718 primary brine samples collected across all mining concessions (OCC and Litio 1-6) between 2011 and 2021.

Table 7-1 Maximum, average and minimum elemental concentrations of the Maricunga brine

	B	Ca	Cl	Li	Mg	K	Na	SO ₄	Density
Units	mg/L	mg/L	mg/L	mg/L	mg/L	mg/L	mg/L	mg/L	g/cm ³
Maximum	1,993	36,950	233,800	3,375	21,800	20,640	105,851	2,960	1.31
Average	572	12,847	192,723	1,122	7,327	8,142	87,106	711	1.20
Minimum	234	4,000	89,441	460	2,763	2,940	37,750	259	1.10

Figure 14-20 and Figure 14-21 show the kriged lithium and potassium concentration distribution in the Salar at approximately 30 m, 130 m, 230 m and 330 m depth. Typically, high and low concentrations of lithium and potassium are correlated. The kriged three-dimensional distribution of lithium and potassium concentrations were used in the updated resource model as further described in Section 14.

Brine quality is evaluated through the relationship of the elements of commercial interest, such as lithium and potassium, with those components that in some respect constitute impurities, such as Mg, Ca and SO₄. The calculated ratios for the averaged chemical composition are presented in Table 7-2.

Table 7-2 Average values (g/L) of key components and ratios for the Maricunga brine

K	Li	Mg	Ca	SO ₄	B	Mg/Li	K/Li	(SO ₄ +2B)/(Ca+Mg)*
8.14	1.12	7.33	12.85	0.71	0.57	6.53	7.23	0.092

*SO₄+2B/ (Ca+Mg) is a molar ratio

As indicated in Table 7-2, the brines from Maricunga have an Mg/Li ratio (6.5) very similar to the Atacama brine (6.4). However, Maricunga has a low sulphate content, which is illustrated by the very low molar ratio (SO₄+2B)/(Mg+Ca) that is also influenced by a relatively high calcium content.

This is an advantage as it will reduce lithium losses as lithium sulphate salts in the ponds for the conventional solar evaporation process. Treatment of the brine to remove the calcium would make the process similar to that utilized by SQM and Albermarle at Salar de Atacama.

As in other natural brines in the region, such as those of the Salar de Atacama and Salar del Hombre Muerto, the higher content of ions Cl^- , SO_4^{2-} , K^+ , Mg^{++} , Na^+ at Maricunga, allows a simplification for the study of crystallization of salts during an evaporation process. The known phase diagram (Janecke projection) of the aqueous quinary system (Na^+ , K^+ , Mg^{++} , SO_4^{2-} , Cl^-) at 25°C and saturated in sodium chloride (equilibrium data in the technical literature) can be used when adjusted for the presence of lithium in the brines. The Janecke projection of $\text{MgLi}_2\text{-SO}_4\text{-K}_2$ in mol % is used to make this adjustment. The Maricunga brine composition has been represented in this diagram (field of KCl), as shown in Figure 7-13 along with brine compositions from other salars. The Maricunga brine composition is compared with those of Silver Peak, Salar de Atacama, Salar del Hombre Muerto, Salar de Cauchari, Salar de Rincon and Salar de Uyuni in Table 7-3.

Figure 7-13 Comparison of brines from various salars in Janecke Projection

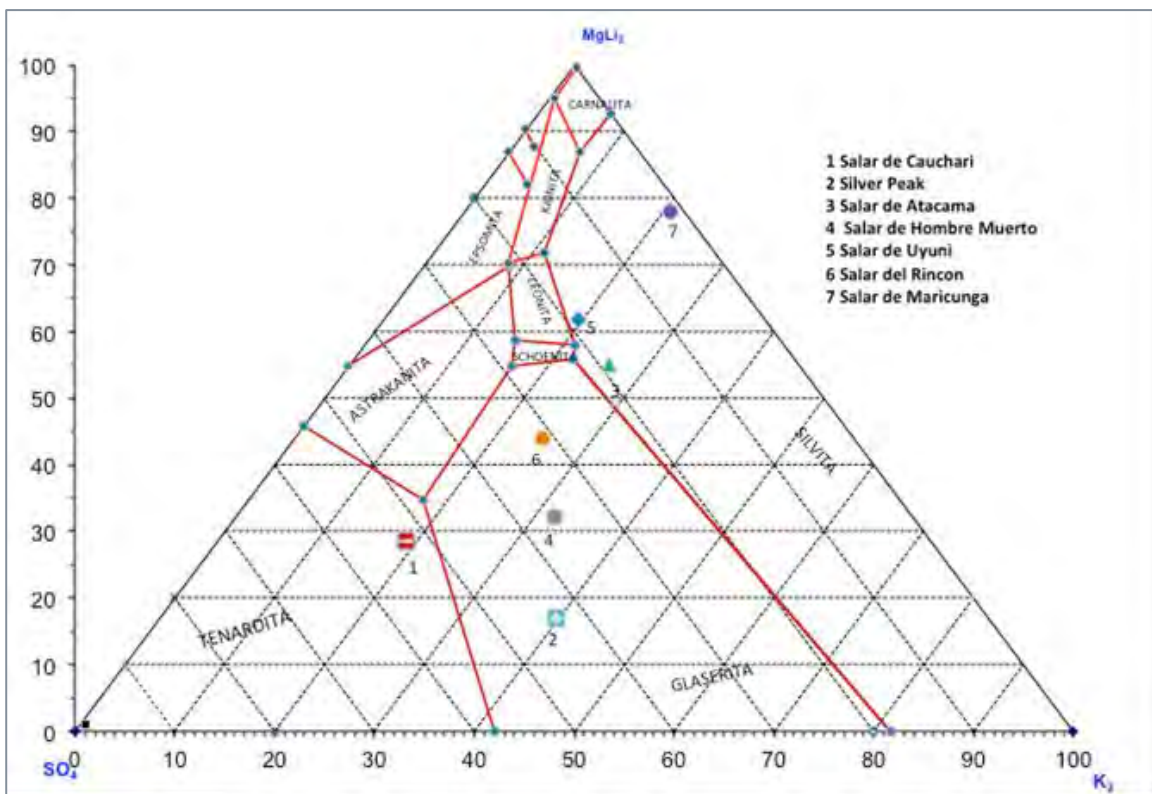


Table 7-3 Comparative chemical composition of various salars (weight %)

	Salar de Maricunga (Chile)	Silver Peak (USA)	Salar de Atacama (Chile)	Hombre Muerto (Argentina)	Salar de Cauchari (Argentina)	Salar del Rincon (Argentina)	Salar de Uyuni (Bolivia)
Na	7.10	6.20	7.60	9.79	9.55	9.46	8.75
K	0.686	0.53	1.85	0.617	0.47	0.656	0.72
Li	0.094	0.023	0.150	0.062	0.052	0.033	0.035
Mg	0.61	0.03	0.96	0.085	0.131	0.303	0.65
Ca	1.124	0.02	0.031	0.053	0.034	0.059	0.046
SO ₄	0.06	0.71	1.65	0.853	1.62	1.015	0.85
Cl	15.91	10.06	16.04	15.80	14.86	16.06	15.69
HCO ₃	0.039	n.a.	Traces	0.045	0.058	0.030	0.040
B	0.050	0.008	0.064	0.035	0.076	0.040	0.020
Density	1.200	n.a.	1.223	1.205	1.216	1.220	1.211
Mg/Li	6.55	1.43	6.40	1.37	2.52	9.29	18.6
K/Li	7.35	23.04	12.33	9.95	9.04	20.12	20.57
SO ₄ /Li	0.64	30.87	11.0	13.76	31.06	31.13	24.28
SO ₄ /Mg	0.097	23.67	1.72	10.04	12.33	3.35	1.308
Ca/Li	9.5	0.87	0.21	0.86	0.65	1.79	1.314

Source: Published data from various sources

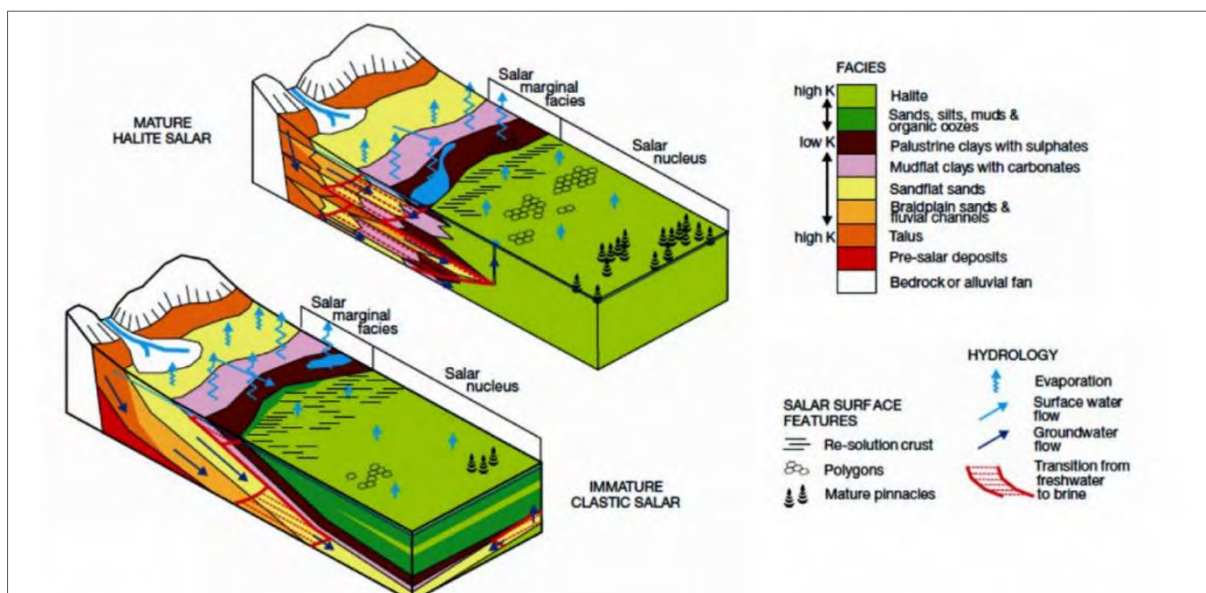
8. DEPOSIT TYPE

8.1 GENERAL

Salars occur in closed (endorheic) basins without external drainage, in dry desert regions where evaporation rates exceed stream and groundwater recharge rates, preventing lakes from reaching the size necessary to form outlet streams or rivers. Evaporative concentration of surface water over time in these basins leads to residual concentration of dissolved salts (Bradley et al., 2013) to develop saline brines enriched in one or more of the following constituents: sodium, potassium, chloride, sulphate, carbonate species, and, in some basins, metals such as boron and lithium.

Houston et al., 2011 identified two general categories of salars: 1) mature, halite dominant, and 2) immature, clastic dominant. Figure 8-1 shows the general conceptual model for each salar type.

Figure 8-1 Conceptual model for mature and immature salars showing the distribution of the facies and the main hydrogeological components. (Houston, et al., 2011.)



Source: Houston, et al., 2011

Immature salars are characterized by increased humidity (increased precipitation, less evaporation) and are more frequent at higher elevations and in the wetter northern and eastern parts of the region. They are characterized by alternate sequences of fine-grained sediments and evaporitic beds of halite and/or ulexite, indicating the changes in sediment supply due to variable tectonic and climate history (Houston, et al., 2011). Immature salars include Olaroz, Cauchari, Diablillos and Centenario.

Mature salars are less humid and tend to be more common in lower and drier areas of the region. They are characterized by a relatively thick and uniform sequence of halite deposits in variable sub-aquatic and sub-aerial conditions. Nevertheless, ancient floods leading to widespread silty clay deposits and volcanic fallout have led to thin intercalated beds that can be recognized in drill core and geophysical surveys. The central portion of Salar de Atacama is a typical mature setting.

Salar de Maricunga, is a mixed type. The northern part of Salar de Maricunga has a well-developed halite crust with a thickness of up to 34 m. This halite unit is underlain by clastic sediments. Brine is saturated in respect to halite. Progressively to the south clastic facies become dominant (Tassara, 1997). As described in Section 7.2, drilling within the Project properties has been able to identify the geometry of the clastic and halite dominant units. Pumping tests have been carried out to characterize the hydraulic behaviour of both the clastic and halite units as further described in Sections 9 and 10 below.

8.2 HYDROGEOLOGY

The salar is the topographic low point within the Maricunga Basin. The Salar itself is surrounded by alluvial fans which drain into the salar. The floor of the Salar in the north and northeast is composed of chloride facies consisting of flat halite crust (more recently flooded) and coarse irregular- and pinnacle shaped halite blocks (absence of recent flooding). The floor of the Salar in the southeast is composed of boric and sulphate facies. In the nucleus of the Salar the water table can be within approximately 5 cm of the surface.

Interpretation of drilling and testing results in the salar and the surrounding alluvial fans by MSB and other companies previously exploring for freshwater resources suggests the occurrence of several hydrogeological units of importance. Figure 8-2 is a hydrogeological section through the Salar showing the principal units and which are summarized as follows:

- Alluvial fans surrounding the salar. These are coarse grained and overall highly permeable units that drain towards the salar. Groundwater flow is unconfined to semi-confined; specific yield (drainable porosity) is high. Water quality in the fans on the east side of the salar is fresh to brackish.
- An unconfined to semi-confined Upper Halite aquifer can be identified in the northern part of the salar. This unit is limited in areal extent to the visible halite nucleus as observed in satellite images. This Upper Halite unit is highly permeable; has a medium drainable porosity; and contains high concentration lithium brine.
- The Lacustrine deposits (clay core). The lacustrine sediments underlie the upper halite aquifer in the centre of the Salar and extends to the east below the alluvial fans. This generally clay-dominated unit, with locally interbedded sand and silt layers, has an overall

low permeability and forms a hydraulic barrier for flow between the Upper Halite aquifer and the underlying clastic units (deeper sand gravel and Volcanoclastics aquifer). On the east side of the Salar fresh water in the alluvial fans sits on top of this unit; while brine is encountered in the clastic sediments underlying the unit. In the nucleus of the Salar the Lacustrine deposits contain high-concentration lithium brine.

- A deeper brine aquifer occurs in the gravel, sand and Volcanoclastics units underlying the lacustrine deposits. Below the nucleus of the Salar groundwater flow conditions in this deeper aquifer are confined. The deeper brine aquifer is relatively permeable and has a relatively high drainable porosity.

A groundwater monitoring network has been installed across the Maricunga basin and is part of the baseline monitoring program for the EIA. An updated conceptual hydrogeological model, including a water balance, was completed for the Maricunga basin. This conceptual model forms the basis for the three-dimensional numerical groundwater flow / transport model (FEFLOW code) used to estimate brine reserves and evaluate potential effects of the future brine abstraction.

Figure 8-2 W-E Hydrogeological cross section

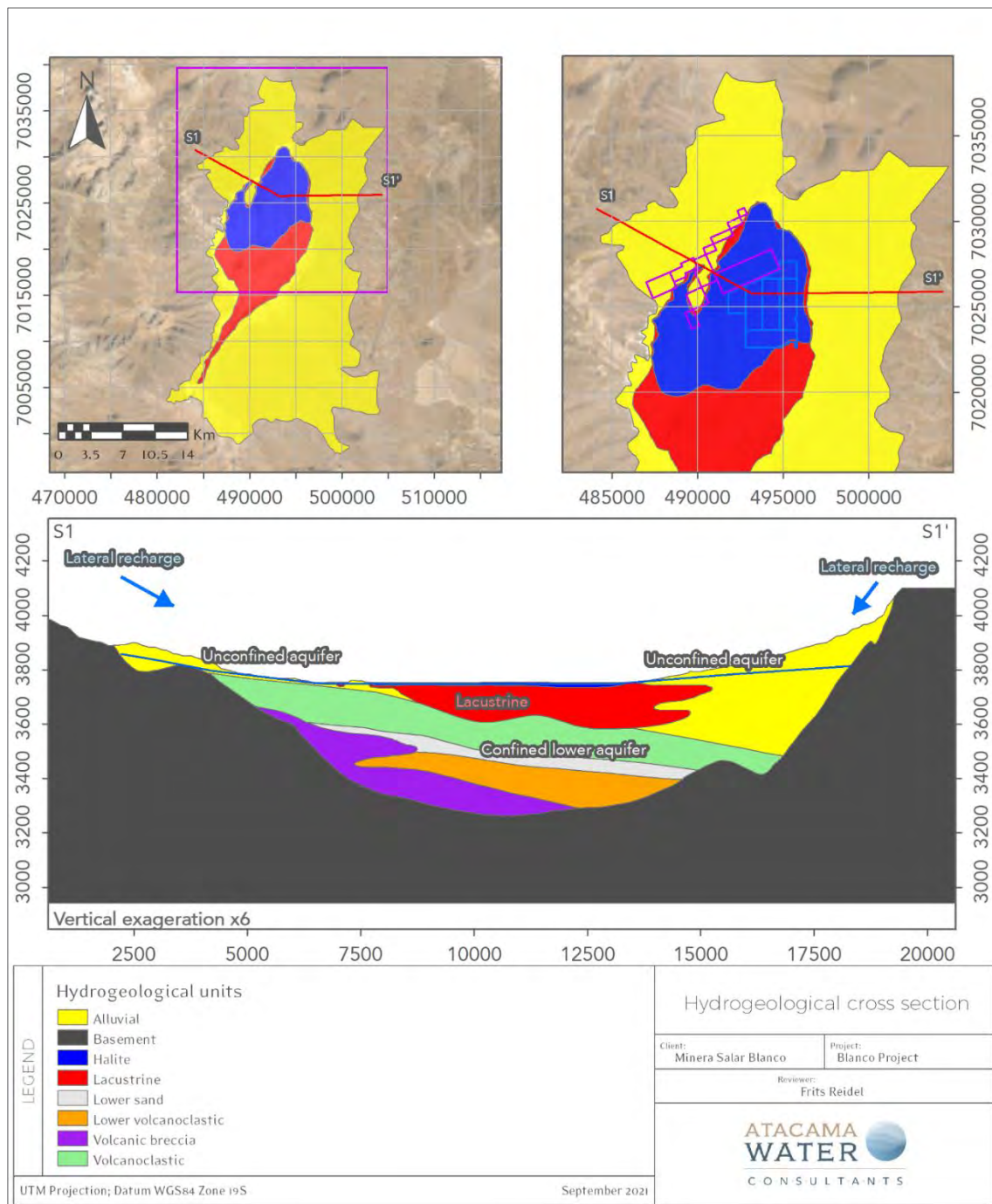
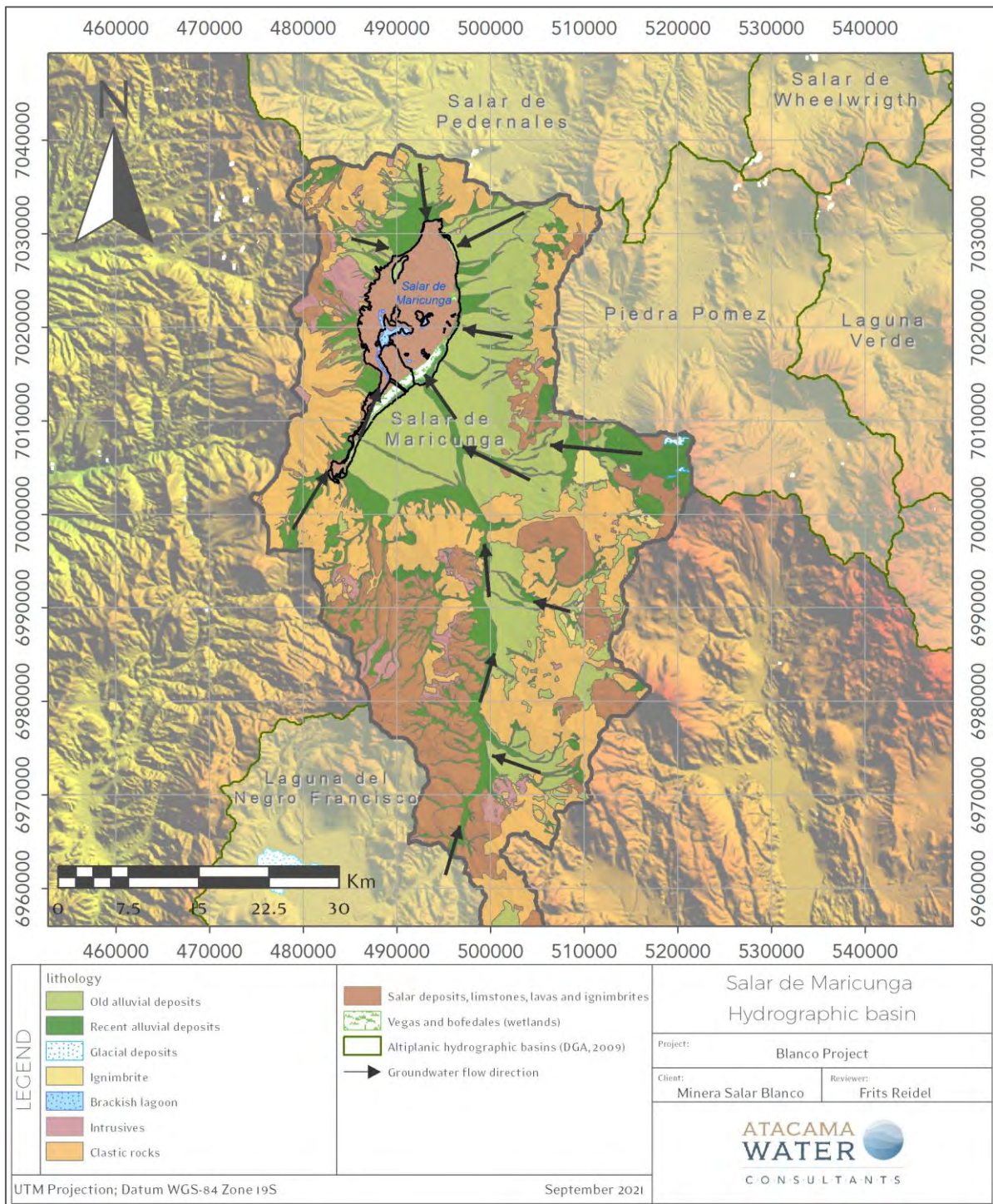


Figure 8-3 Salar de Maricunga hydrographic basin



Source: Modified from DGA 2009

8.3 WATER BALANCE

A water balance for Salar de Maricunga was prepared by Flosolutions (2018) as part of the conceptual hydrogeological model for the EIA and is summarized in Table 8-1. Figure 8-3 shows the general surface and groundwater flow patterns in the Salar de Maricunga watershed. Surface water flow generally only occurs at higher ground and infiltrates into the more permeable alluvial and fan sediments surrounding the Salar before reaching the Salar floor itself. The only surface water flow that occurs on the Salar floor is the natural discharge from Laguna Santa Rosa north towards the centre of the Salar. There is no surface water outflow from the Maricunga watershed. Groundwater flow patterns follow closely the surface water flow patterns. There are no known groundwater outflows from the Maricunga watershed.

Recharge to the Maricunga basin occurs through the direct infiltration of precipitation (709 l/s) and through lateral recharge from Río Lamas (264 l/s) and Ciénaga Redonda (436 l/s) catchments. The total average annual recharge to the Maricunga basin is estimated at 1,409 l/s or 44.5 million m³.

Discharge from the Maricunga basin is through seepage to streams and lakes, evaporation, evapotranspiration and groundwater pumping. The total average annual discharge through evaporation has been estimated at 1,348 l/s or 42.5 million m³.

According to DGA records, existing granted water rights in the Salar de Maricunga basin amount to 1,366 l/s; actual authorized usage by the Environmental Evaluation System (SEA) is estimated at 153 l/s; and actual usage is estimated at 40 l/s. Table 8-1 summarizes the water balance for the Salar de Maricunga watershed.

Table 8-1 Water Balance for the Salar de Maricunga Basin

Inflows	Average flow (l/s)
Recharge from precipitation	709
Lateral groundwater inflow from Rio Lamas basin	264
Lateral groundwater inflow from Cienega Redonda basin	436
Total inflows	1,409
Outflows	
Evaporation (diffuse seepage, ET and soil)	1,308
Actual abstraction (SEA authorised)	40
Total outflows	1,348
Balance (Inflows – Outflows)	61

Source: FloSolutions 2018

8.4 DRAINABLE POROSITY

Porosity is highly dependent on lithology. Total porosity is generally higher in finer grained sediments, whereas the reverse is true for drainable porosity or specific yield since finer grained sediments have a high specific retention. The lithology within the Salar is variable with halite and halite mixed units, clay and gravel-sand-silt-clay sized mixes spanning the full range of sediment types.

Based on the results of drainable porosity analyses carried out on 561 undisturbed samples from sonic and HQ core by GeoSystems Analysis, Daniel B Stephens and Associates, Corelabs, and the British Geological Survey it was possible to assign drainable porosity values to the specific lithological units encountered during the various drilling programs between 2012 and 2021 in the Salar. Table 8-2 summarizes the results of the porosity analysis. The analysis of drainable porosity is further discussed in Section 11.

Table 8-2 Results of drainable porosity analyses (2011-2021)

Lithology	Average
Halite	0.06
Lacustrine	0.02
Alluvial deposits	0.14
Volcanic breccia	0.13
Volcanoclastic	0.12
Lower sand	0.07
Lower volcanoclastic	0.08

8.5 PERMEABILITY

Permeability (or hydraulic conductivity) is also a parameter that is highly dependent of lithology. Generally finer grained and well-graded sediments have a lower permeability than coarser grained poorly graded sediments. The permeability of halite can be enhanced through fracturing and solutions features. MSB has carried out four pumping tests within the Salar and third parties have carried out numerous other pumping tests in the alluvial sediment surrounding the Salar. The results of the permeability calculations from these pumping tests are summarized in Table 8-3. The analysis of the pumping tests is further discussed in Section 10 below.

Table 8-3 Summary of permeability values

Unit	Description	K (m/d)
Halite	Confined and fractured	192-637
Lacustrine deposits	Clay with sands and gravels - confined	0.9-11
East Alluvium	Semi-confined to confined	1-10
West Alluvium	Unconfined to semi-confined	4-40
Lower alluvium	Confined	0.4-0.9
Volcanoclastic	Confined	0.4-0.9

9. EXPLORATION

9.1 OVERVIEW

This section provides a description of the exploration work that has been carried out for the Stage One Project between 2011 and 2021 by the various owners.

The following work was carried out on the *Litio 1-6* claims by MLE in 2011

- Seismic refraction tomography survey along 6 profiles for a total of 23 km to map lithological units and basin geometry.
- Construction of six test trenches to carry out 24 hour pumping trials to determine hydraulic parameters.

The following work was carried out by BBL in 2015:

- AMT / TEM survey along 6 profiles for a total of 75 km across the Salar to map basin geometry and the interface between freshwater and brine.
- Topographic survey between Laguna Rosa and the Project area to map hydraulic gradients.

The following work was carried out by MSB in 2016/7:

- Gravity survey along 6 profiles for a total of 75 km across the Salar to map basin geometry and bedrock topography.

9.2 GEOPHYSICAL SURVEYS

9.2.1 SEISMIC REFRACTION TOMOGRAPHY (2011)

Li3 contracted Geophysical Exploration and Consulting S.A. (GEC) from Mendoza Argentina to carry out a Seismic Refraction Tomography Survey to map lithological units and structure in the northern part of the Salar. A total of 23 line-km of seismic tomography data were collected along six lines as shown in Figure 9-1. Prior to the seismic data collection all lines were surveyed using a differential GPS system. All data collection work was completed in the field between September and December 2011.

A 24-bit, ultra-high resolution 20 kHz bandwidth (8 to 0.02 ms sampling), low distortion (0.0005%), low noise (0.2uV) GEODE Acquisition System was used for the collection of the seismic tomography data. Geophone (14Hz Geospace) spacing was 5 m; inline source spacing was 15 m and outline offsets were 30 m, 60 m, 90 m, 150 m, 250 m and 500 m. The spread data acquisition layout included

48 active channels. The seismic source for the surveys was a 150 kg trailer-mounted accelerated drop-weight. Recording length was 250/500 ms with a 1.0 ms sampling rate.

During the seismic data acquisition, data quality control and pre-processing of the geophysical data were carried out in the field with PC based processing and interpretation packages called “*Firstpix*” / *Gremix 15*” and “*Rayfract32*”. Final data processing with the “*Rayfract 32*” software included tomography inversion techniques *Delta TV* and WET or *Wave Eikonal Traveltime* as follows:

- Delta T-V method (after Gebrande and Mille, 1985): The Delta TV method is a pseudo 2D Inversion method that delivers a continuous 1D velocity versus depth model for all geophone stations. The method handles geological situations such as velocity gradients, linear increasing of velocity with depth, velocity inversions, pinching out layers and outcrops, faults and local velocity anomalies.
- WET or **Wave Eikonal Traveltime** Tomography processing. Wave propagation is modelled in a physically meaningful way with ray paths, using the output from the Delta-TV inversion as starting model. It handles geological situations, such as discontinuities velocity distributions and sharp vertical or horizontal velocity gradients. Quality control of geological models is performed by direct graphical comparison of the measured travel time data to those calculated from the model solution.

Figure 9-2 shows as an example of the result of the WET processing and inversion with the geological interpretation below along Profile 1 and is considered representative of the overall seismic survey results obtained. Data from the 2011 sonic and RC boreholes was included in the final interpretation. The seismic tomography survey provided valuable information on the vertical distinction and lateral continuity of lithological layers, however bedrock was not clearly detected along any of the profiles.

9.2.2 AMT / TEM (2015)

Six profiles of Audio Magnetotellurics were carried out across Salar de Maricunga to map the bedrock geometry and identify the interface between freshwater and brine along the perimeter of the Salar. The work was carried out by Wellfield Services Ltda. The survey consisted of 60.8 km of AMT profiles with a station spacing of 200 m and 14 km with a station spacing of 250 m. 360 stations were measured with scalar methodology and 23 stations were measured with the tensorial array. 15 TEM soundings were carried out at the ends of the AMT lines and at the intersection with Line 6. Figure 9-1 shows the location of the AMT profiles.

AMT data were collected in the range of 10,000 – 1 Hz and MT data in the range of 4 – 0,01 Hz to include the deeper portion of the frequency spectrum. Seven GPS synchronized systems were operated by two teams with data collection taking place overnight for a period of 15-18 hours at each station.

Due to logistical and climatic conditions (partial flooding of the Salar) the survey was carried out in 3 stages during March and April 2015. The AMT data were inverted into 2D resistivity models using the software WinGLink.

9.2.3 GRAVIMETRY

A gravity survey was carried out in the Salar along Profiles 1 - 6 (immediately over the AMT lines) as shown in Figure 9-1. Station spacing along Line 1 and 2 was 250 m, while station spacing along lines 3 to 6 was 500 m. Each station was surveyed in with a differential GPS with a precision of ± 5 cm. The gravity data was collected with a Scintrex micro-gravimeter Model CG-5 with resolution of 0.001mgals and with an automatic drift correction.

Data processing included the Free Air, Simple Bouguer, and Total Terrain corrections; the final product included final Bouguer anomaly maps and 2D inversion models. An average density contrast of 0.45 g/cc was used between the bedrock and the Salar basin fill sediments to prepare depth-to-bedrock models along each of the gravity profiles. The density contrast was based on results of laboratory (Universidad de Chile) density measurements on 18 rock samples collected in outcrop at the end of Lines 1 – 6 and the density measurements carried out by GSA on the basin fill sediments. The geological model described in Section 7 was used to constrain the geometry of the lithological units within the gravity interpretation. The gravity profiles were also overlain by the AMT resistivity sections to aid in the final depth-to-bedrock model. The final bedrock topography was kriged based on interpolation from the line profiles and is shown in Figure 7-13 above.

Figure 9-1 Location map of seismic refraction tomography, AMT and gravity profiles

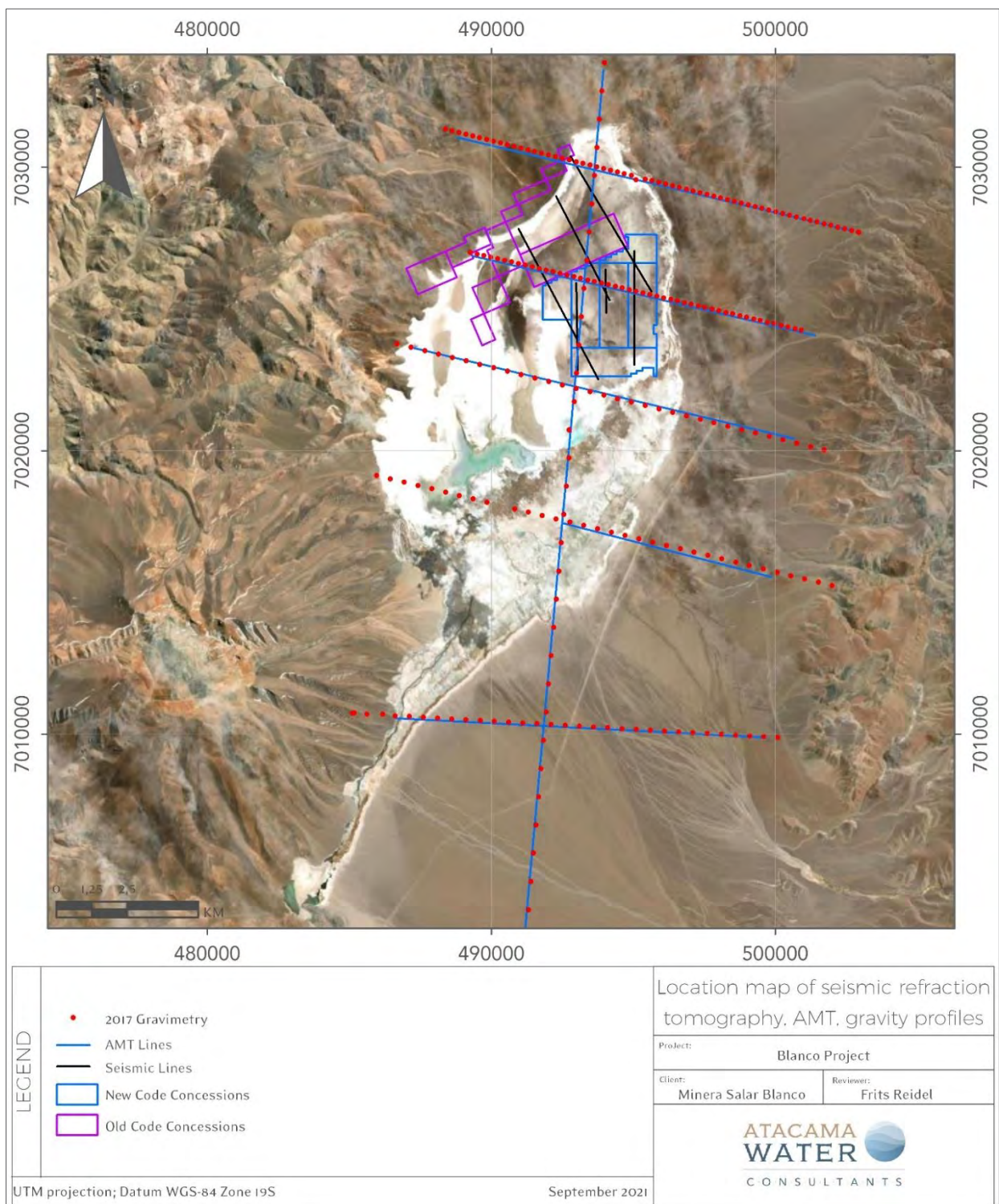
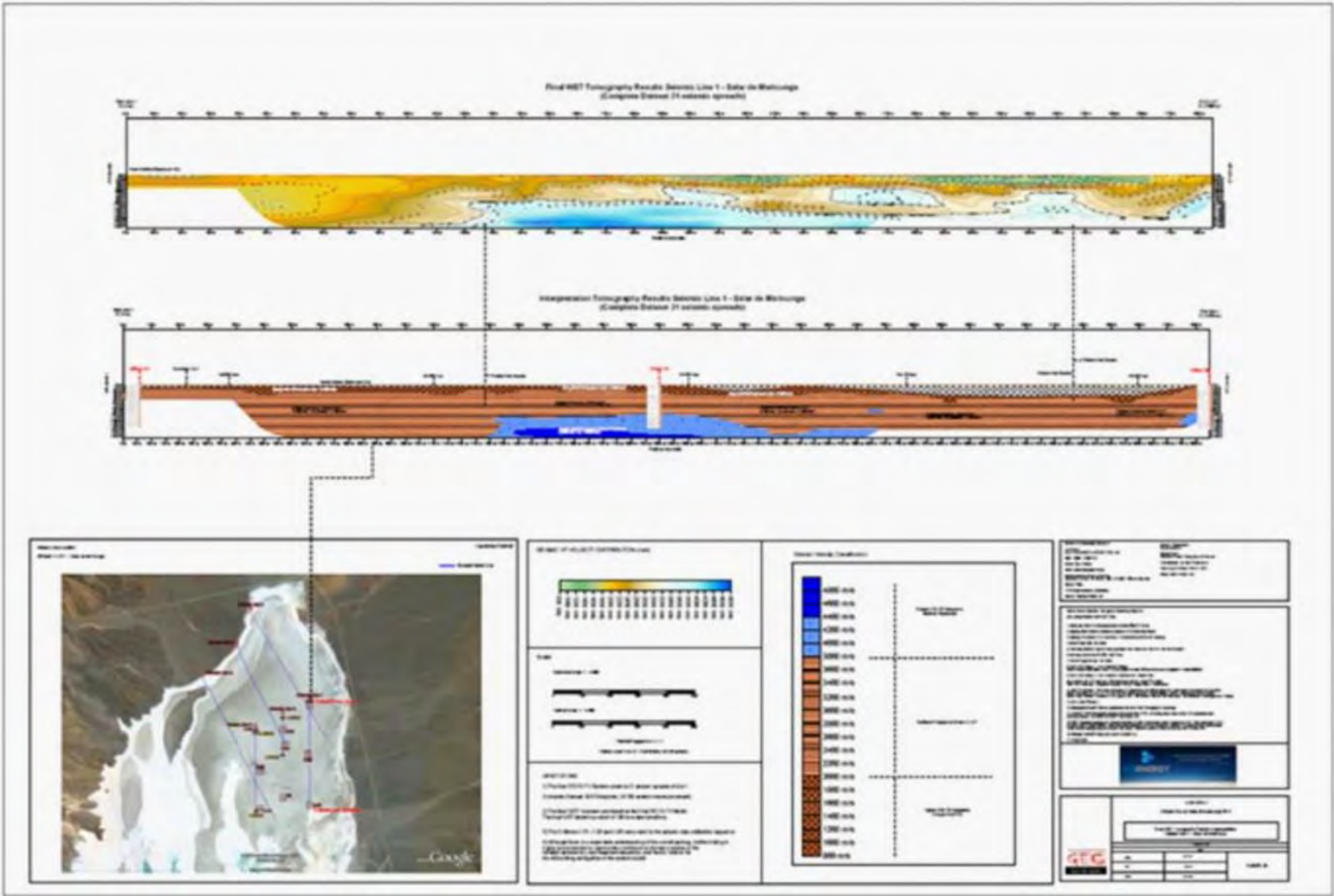




Figure 9-2 Seismic Tomography Line 1



9.3 TEST TRENCHING (2011)

Six test trenches (T1 through T6) were constructed in 2011 on *the Litio 1-6* tenements to test the feasibility of brine production from trenches as an alternative to brine production from production wells. One trench was installed adjacent to each sonic borehole C-1 through C-6. The trenches were dug at 3 m width to a depth of 2.5 m. Each trench was completed in generally massive (relatively competent) halite and the trench walls did not encounter stability problems as shown in Figure 9-3.

A 24-hour pumping test was carried out in each trench at a flow rate of 5 l/s using a sump pump. Water level responses during each pumping test were observed in a shallow monitoring well (36 m depth) adjacent to each trench that allowed for the calculation of aquifer parameters. Figure 9-3 through 9.4e show the water level response in each observation well and the associated pumping test analyses.

summarizes the results of the pumping test analyses. The relatively high S_y values obtained from the pumping tests are representative of the halite mix sediments and suggest enhanced porosity in the halite through dissolution and fracture features.

Figure 9-3 Test Trench T6 in the Upper Halite

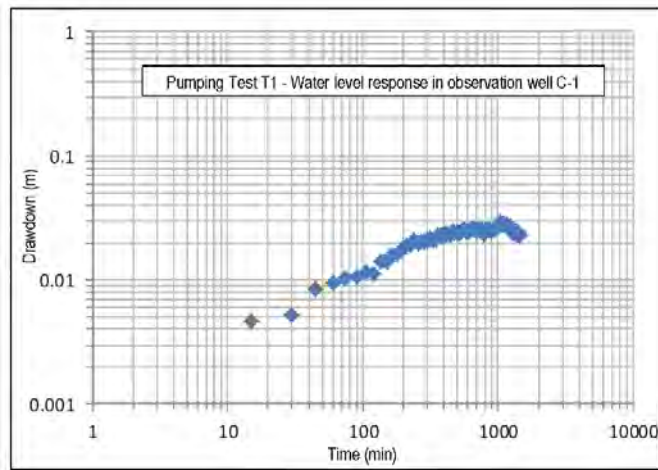


Table 9-1 Results of Trench pumping tests

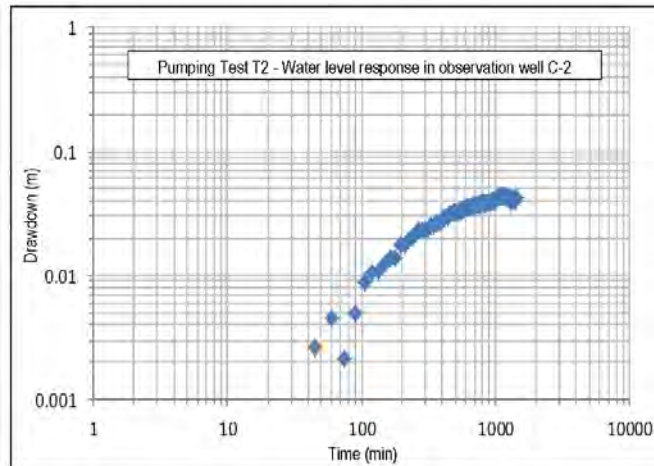
Trench	Hydraulic Conductivity (K) m/d	Specific Yield (S _y)
T1	208	0.24
T2	84	0.28
T3	145	0.24
T4	No water level response in piezometer	
T5	15	0.12
T6	45	0.04

The results of these tests indicate that the upper halite is highly permeable and that brine production from trenches is a feasible alternative to production wells from the upper meters of the upper halite.

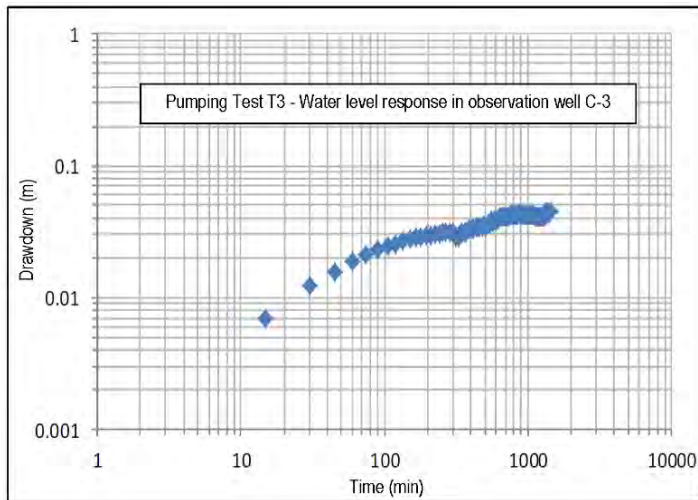
Figure 9-4a – 9.4e Pumping test analyses for Trench pumping tests T1, T2, T3, T5 and T6



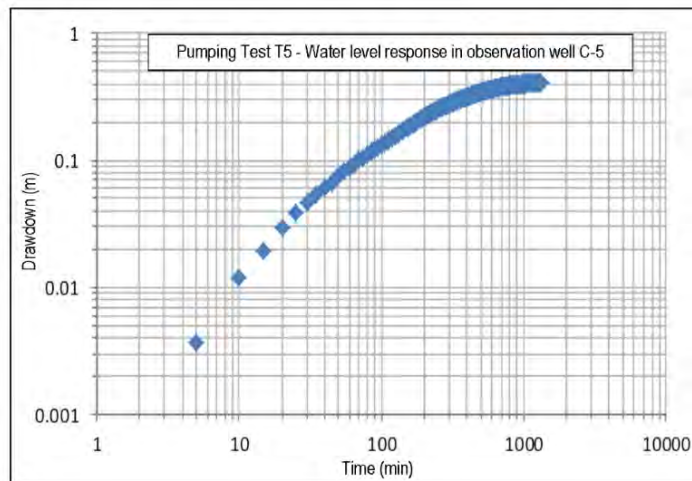
After Papadopoulos, 1967		
a	0.01	[]
1/u	100	[]
F(u)	1	[]
t	190	[min]
s	0.0055	[m]
r	12.9	[m]
Q	529	[m ³ /d]
KD	7513	[m ² /d]
Sy	0.24	[]



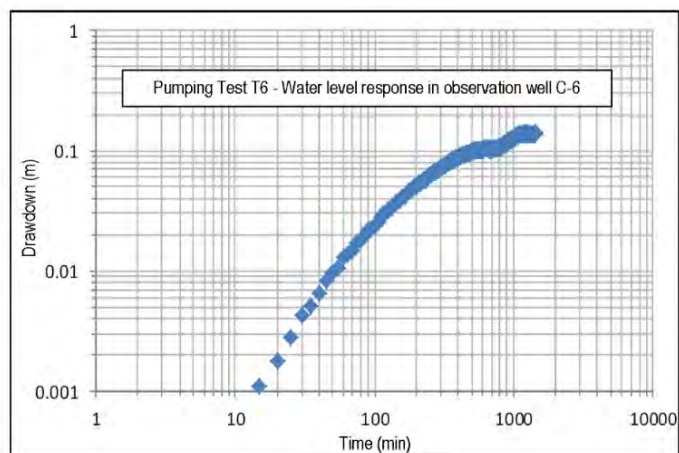
After Papadopoulos, 1967		
a	0.1	[]
1/u	10	[]
F(u)	1	[]
t	350	[min]
s	0.015	[m]
r	32.47	[m]
Q	573	[m ³ /d]
KD	3041	[m ² /d]
Sy	0.28	[]



After Papadopoulos, 1967		
a	0.1	[]
1/u	10	[]
F(u)	1	[]
t	35	[min]
s	0.009	[m]
r	14.6	[m]
Q	593	[m ³ /d]
KD	5237	[m ² /d]
Sy	0.24	[]



After Papadopoulos, 1967		
a	0.01	[]
1/u	100	[]
F(u)	1	[]
t	300	[min]
s	0.085	[m]
r	6	[m]
Q	562	[m ³ /d]
KD	526	[m ² /d]
Sy	0.12	[]



After Papadopoulos, 1967		
a	0.01	[]
1/u	100	[]
F(u)	1	[]
t	410	[min]
s	0.025	[m]
r	22.6	[m]
Q	518	[m ³ /d]
KD	1650	[m ² /d]
Sy	0.04	[]

10. DRILLING

10.1 OVERVIEW

Three principal drilling campaigns were carried, the first in 2011 on the *Litio 1-6* claims by MLE, a second and third on the properties by MSB between 2016 and 2021.

The objectives of each drilling campaign can be broken down into three general categories:

- 1) Exploration drilling on a general grid basis to allow the estimation of “in-situ” brine resources. The drilling methods were selected to allow for 1) the collection of continuous core to prepare “undisturbed” samples at specified depth intervals for laboratory porosity analyses and 2) the collection of depth-representative brine samples at specified intervals without contamination by drilling fluids. The 2011 campaign included six (6) sonic boreholes (C-1 through C-6) on the *Litio 1-6* claims. The 2016-2018 campaign included six (6) sonic boreholes (S-1, S-2, S-18 and S-20, S-23, and S-24) and eight (8) tricone /HWT boreholes (S-3, S-3A, S-5, S-6, S-10, S-11, S-13, and S-19). The 2021 campaign included five diamond core holes (S-25 through S-29).

On completion of drilling, each borehole was completed as a monitoring well with 2-inch diameter PVC blank and slotted casing, gravel pack and cement seal (except S-23 through S-29 were completed with 3-inch diameter PVC casing to facilitate future BRM logging). Figure 10-1 shows the location of the exploration boreholes.

- 2) Production- and monitoring well drilling. Test production wells were installed to carry out pumping tests to determine the hydraulic parameters of the Salar sediments and investigate the behaviour of the brine aquifer under pumping stress. Monitoring wells were installed adjacent to production wells to observe water levels changes during the pumping tests and in other locations to monitor baseline groundwater conditions around the Salar. Monitoring wells were drilled using the reverse circulation (air) drilling method (RC) to allow hydraulic test work. Production wells were installed using conventional rotary methods at large diameter. Production wells P-1 and P-2 along with piezometers P1-1, P1-2, P1-3, P1-4, P2-1, P2-2, P2-3, P2-5 and P-3 were installed in the 2011 campaign. Production well P-4 and monitoring wells S-7, S-8, S-12, S-15, S-16A, S-17, and S-21 were installed during the 2016/7 campaign. The analytical results of brine samples collected during the production and monitoring well drilling were not used in the resource model. Production well P-5 was drilled and completed in November 2021 and a long-term pumping test (30 days) will be completed by mid-January 2022.
- 3) Pumping tests. Long-term pumping tests were carried out on wells P-1 and P-2 during 2015 and on wells P-4 and P-2 (shallow) in 2017. A long-term pumping test is also schedule for well P-5 will be completed by mid-January 2022.

10.2 EXPLORATION DRILLING

10.2.1 SONIC DRILLING

Boart Longyear (BLY) was contracted to carry out sonic drilling for the collection of continuous core and brine samples for both the 2011 and 2018 programs. Sonic boreholes C1 through C6 were drilled to a depth of 150 m in 2011 and S-1A, S-2, and S-18 to depths of up to 200 m in 2016. Sonic hole S-20 was drilled as a twin hole to S-11 to a depth of 40 m to correlate porosity information. S-23 and S-24 were drilled to 200 m depth immediately adjacent to C-2 and C-5, respectively in 2018. Core recovery during all sonic drilling was consistently high and exceeded 90%.

The drilling equipment consisted of a BLY (SR-162 SRF 600T) sonic rig and support equipment utilizing a 4-inch diameter coring by 6-inch casing system. No drilling additives/fluids were used thereby preventing possible brine sample contamination. All holes were drilled vertically. The drilling was carried out in 1.5 m runs and core was collected in alternating plastic bags (1.5 m) and lexan core barrel liners (1.5 m). The retrieved lexan core liners were capped and sealed with tape at each end. All retrieved core was labelled with its borehole number and the drilling depth interval and stored in wooden core boxes. The 6-inch diameter casing was advanced at the end of each core run.

Brine samples were collected at 3 m intervals during the 2011 program and at 6 m intervals during 2016. Brine level measurements were made inside the drill casing to calculate the required volume of brine to be bailed from the hole prior to obtaining a brine sample. Up to three well volumes were bailed prior to collecting the final brine sample from the bottom of the hole. This procedure was repeated to total depth (TD).

On completion of drilling, each sonic borehole was completed as a monitoring well with 2-inch diameter PVC blank and slotted casing, gravel pack and cement seal (except S-23 and S-24 were completed with 3-inch diameter PVC casing to facilitate future BRM logging).

Figure 10-1 Location map of the boreholes (2011 - 2021 programs)

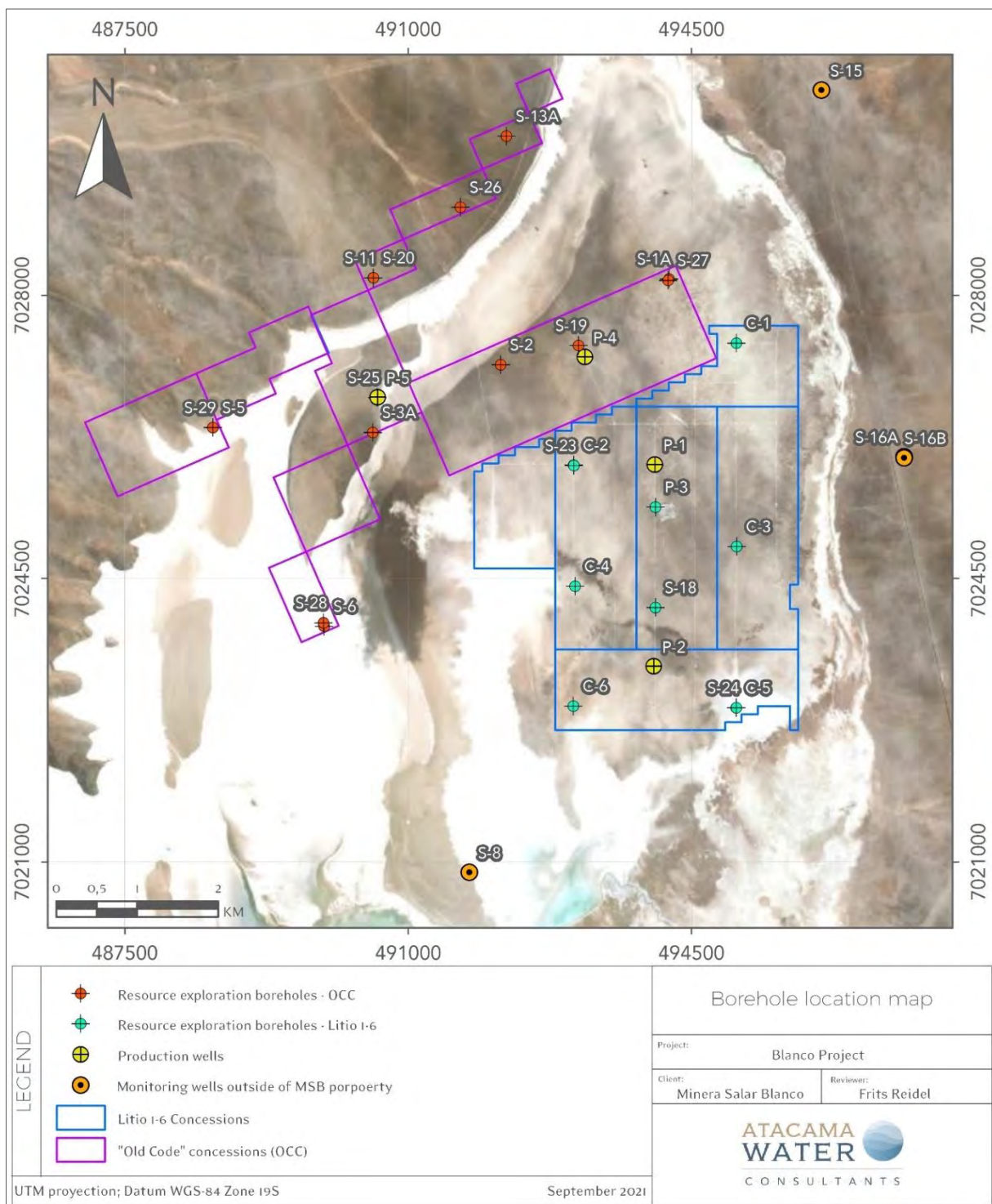


Table 10-1 Summary of 2011 – 2021 boreholes

Borehole	UTM N	UTM E	Elevation (masl)	TD (m)	Method	Year	Objective	Screened Interval	SWL
C1	7,027,408	495,052	3,747.51	150	Sonic	2011	Resource	Abandoned	na
C2	7,025,899	493,041	3,747.35	150	Sonic	2011	Resource	06-34	0.11
C3	7,024,895	495,056	3,746.86	150	Sonic	2011	Resource	03-26	0.12
C4	7,024,400	493,058	3,747.35	150	Sonic	2011	Resource	06-29	0.24
C5	7,022,900	495,045	3,746.58	150	Sonic	2011	Resource	06-11	0.15
C6	7,022,918	493,039	3,746.78	150	Sonic	2011	Resource	06-11	0.23
P1	7,025,904	494,043	3,747.25	150	Rotary	2011	Production	6-24;60-144	0.18
P1.1	7,025,891	494,032	3,747.59	150	DTRC	2011	Monitoring	60-149	0.72
P1.2	7,025,894	494,061	3,747.34	30	DTRC	2011	Monitoring	06-24	0.18
P1.3	7,025,905	494,032	3,747.69	70	DTRC	2011	Monitoring	54-66	0.37
P1.4	7,025,915	494,032	3,747.74	30	DTRC	2011	Monitoring	06-24	0.12
P2	7,023,422	494,030	3,746.22	150	Rotary	2011	Production	6-24; 66-144	0.25
P2.1	7,023,393	494,035	3,746.44	113	DTRC	2011	Monitoring	102-108	0.26
P2.3	7,023,410	494,030	3,746.38	30	DTRC	2011	Monitoring	12-30	0.2
P2.4	7,023,403	494,034	3,746.44	150	DTRC	2011	Monitoring	60-145	0.27
P2.5	7,023,397	494,061	3,746.60	150	DTRC	2011	Monitoring	60-145	0.77
P3	7,025,380	494,052	3,747.62	192	DTRC	2011	Monitoring	127-185	-0.37
S 1A	7,028,201	494,220	3,748.95	200	Sonic	2016	Resource	29-119	0.23
S 2	7,027,141	492,143	3,748.84	200	Sonic	2016	Resource	184-190	1.43
S-3	7,026,300	490,560	3,751.54	40	Tricone/HWT	2016	Resource	Abandoned	na
S-3A	7,026,306	490,563	3,751.53	200	Tricone/HWT	2016	Resource	Abandoned	na
S-5	7,026,366	488,590	3,750.17	200	Tricone/HWT	2016	Resource	182-188	1.55
S-6	7,023,913	489,964	3,749.09	200	Tricone/HWT	2016	Resource	184-195	3.09
S-8	7,020,871	491,753	3,748.72	40	Rotary	2016	Monitoring	28-34	1.18

Borehole	UTM N	UTM E	Elevation (masl)	TD (m)	Method	Year	Objective	Screened Interval	SWL
S-11	7,028,215	490,569	3,757.61	200	Tricone/HWT	2016	Resource	144-150	8.95
S-12	7,013,856	493,740	3,769.28	40	Rotary	2016	Monitoring	22-28	na
S-13	7,029,964	492,213	3,755.88	200	Tricone/HWT	2016	Resource	194-200	9.18
S-15	7,030,533	496,104	3,781.23	40	Rotary	2016	Monitoring	34-40	25.11
S-17	7,022,516	497,969	3,789.94	40	Rotary	2016	Monitoring	32-38	29.8
S-16A	7,026,005	497,122	3,769.89	150	Tricone/HWT	2016	Monitoring	50-62	11.3
S-16B	7,025,991	497,123	3,769.99	18	Tricone/HWT	2016	Monitoring	09-12	14.72
S-18	7,024,141	494,054	3,748.64	173	Sonic	2016	Resource	1160-172	2.58
S-19	7,027,381	493,104	3,748.17	360	Tricone/HWT	2016	Resource	196-208	2.98
S-20	7,028,217	490,569	3,757.64	40	Sonic	2016	QA/QC	Abandoned	na
S-21	7,037,751	491,855	3,863.06	85	Rotary	2016	Monitoring	72-84	dry
S-22	NA	NA			Not drilled				
S-23	7,025,899	493,041	3,747.35	200	Sonic	2018	Resource	0-200	0.10
S-24	7,022,900	495,045	3,746.58	200	Sonic	2018	Resource	0-200	0.15
P-4.1	7,027,224	493,194	3,748.81	200	Tricone/HWT	2016	Monitoring	160-172	2.26
P-4.2	7,027,242	493,172	3,748.65	2	Auger	2016	Monitoring	0-2	0.1
P-4.3	7,027,250	493,160	3,748.70	2	Auger	2016	Monitoring	0-2	0.12
P-4.4	7,027,265	493,139	3,748.74	2	Auger	2016	Monitoring	0-2	0.11
S-25	7,026,736	490,620	3,760.00	408.8	Rotary/DDH	2021	Resource	384.7-408.7	10.23
S-26	7,029,088	491,644	3,760.00	402.6	Rotary/DDH	2021	Resource	384.5-402.5	12.98
S-27	7,028,183	494,210	3,750.00	402.7	Rotary/DDH	2021	Resource	384.6-402.5	7.09
S-28	7,023,955	489,955	3,750.00	402.7	Rotary/DDH	2021	Resource	384.6-402.6	2.2
S-29	7,026,380	488,650	3,752.00	345.6	Rotary/DDH	2021	Resource	262.9-286.9	4.87

10.2.2 ROTARY TRICONE/HWT DRILLING

Eight (8) tricone /HWT boreholes (S-3, S-3A, S-5, S-6, S-10 or M-10, S-11, S-13, and S-19) were drilled as part of the 2016 program. Rotary drilling with HWT casing was substituted for conventional diamond drilling as core recovery of the coarse grained sediments on the western side of project area did not prove to be successful. The rotary drilling was carried out by AK drilling using an EDM rig. Rotary drilling was carried out using a 3-7/8 inch tricone bit, with sample recovery through the HWT casing to surface. Cuttings were collected at surface in cloth bags with representative sub-samples at 2 m intervals stored in labelled chip trays. Brine samples were collected at six meter intervals during the rotary drilling. The brine sampling methodology is further described in Section 11. Selected boreholes were completed as monitoring wells with blank and slotted PVC.

10.2.3 DIAMOND CORE DRILLING

Five (5) tricone / HQ/HWT core holes (S-24 through S-29) were drilled as part of the 2021 program on the OCC by Major Drilling. The five holes were drilled with tricone from ground surface to 200 m depth and cored at HQ diameter from 200 m to 400 m depth. HWT casing was installed during the drilling to provide hole stability and facilitate depth-representative brine sampling. Continuous HQ core was collected for geological logging and the preparation of 'undisturbed' sub-samples at 12 m intervals between 200 m and 400 m depth (with exception of S-29 which intercepted bedrock at 219 m depth). Brine samples were collected using bailer methodology at 12 m intervals during the core drilling between the 200 m - 400 m depth interval. The brine sampling methodology is further described in Section 11. The five boreholes were all completed as monitoring wells with blank and slotted 3-inch diameter PVC casing to facilitate BRM logging and future water level and brine chemistry monitoring.

10.3 MONITORING- AND PRODUCTION WELL DRILLING

10.3.1 REVERSE CIRCULATION (RC) DRILLING AND PIEZOMETER INSTALLATIONS (2011)

A total of 915 m of RC drilling (P1-1, P1-2, P1-3, P1-4, P2-1, P2-2, P2-3, P2-5 and P-3) was carried out for the collection of chip samples for geologic logging, brine samples for chemistry analyses and airlift data. Rock Drilling S.A. provided an Ingersoll Rand T3-W reverse circulation rig equipped with a 350 psi, 1000 cfm air compressor and support equipment. The exploration drilling was carried out at 5 ½-inch diameter using dual tube reverse circulation pipe and air; no additives/fluids were used during the drilling. Exploration drilling depths ranged from 30 m to 192 m. Chip samples were collected at 2 m intervals for geological logging, brine samples were collected at 3 m intervals

(directly from the cyclone) and airlift tests were completed at 6 m intervals. The RC exploration boreholes were completed as monitoring wells for use during the pumping tests. The distance between each monitoring well and the associated production well ranges from 10 m to 35 m. Table 10-2 shows the details of the RC exploration drilling completed.

10.3.2 PRODUCTION WELL DRILLING

Drilling of production wells P1 and P2 was carried out by Rock Drilling S.A. using the Ingersoll Rand T3-W rig in 2011. The wells were drilled in two passes at 11-inch and 17-inch diameter to a final total depth of 150 m using flooded reverse circulation (rotary) drilling. The wells were completed with a 10-inch diameter PVC production casing string in both the upper halite aquifer and the lower aquifer. The annulus of each test well was completed with gravel pack. Well development was carried out over a 72-hour period in each well using a double swab/airlift system. Table 10-2 shows the construction details of P-1 and P-2.

Production well P-4 was drilled by Hellema Holland Engineering using a Prakla rig. The well was drilled using conventional rotary drilling at 17.5-inch diameter to a depth of 180 m. The well was completed with screened 12-inch diameter PVC production casing in the lower aquifer between 70 m and 180 m depth. A bentonite / cement seal was installed (on top of the gravel pack) from ground surface to a depth of 56 m. Well development was carried out over a 48-hour period using a double swab/airlift system. Table 10-2 shows the construction details of P-4.

10.3.3 PIEZOMETER INSTALLATIONS- 2016

Piezometers S-7, S-8, S-12, S-15, S-16A, S-17, and S-21 were installed as part of the 2016 campaign. These monitoring wells were drilled using conventional rotary methodology to depths of up to 150 m. Fluid samples were taken at selected intervals during the drilling of the monitoring wells. The wells were completed with 2-inch diameter schedule 80 blank and screened PVC casing. A geomembrane filter was placed over the screened casing to prevent silting. No materials were installed in the annulus. Figure 10-1 shows the completion details of each of these installations.

10.4 PUMPING TESTS (2015 AND 2017)

Pumping tests were carried out on wells P-1, P-2, and P-4 between 2015 and 2017. Table 10-2 summarizes the construction details of each pumping test.

Figure 10-2 Collecting RC Airlift Flow Measurements (2011)

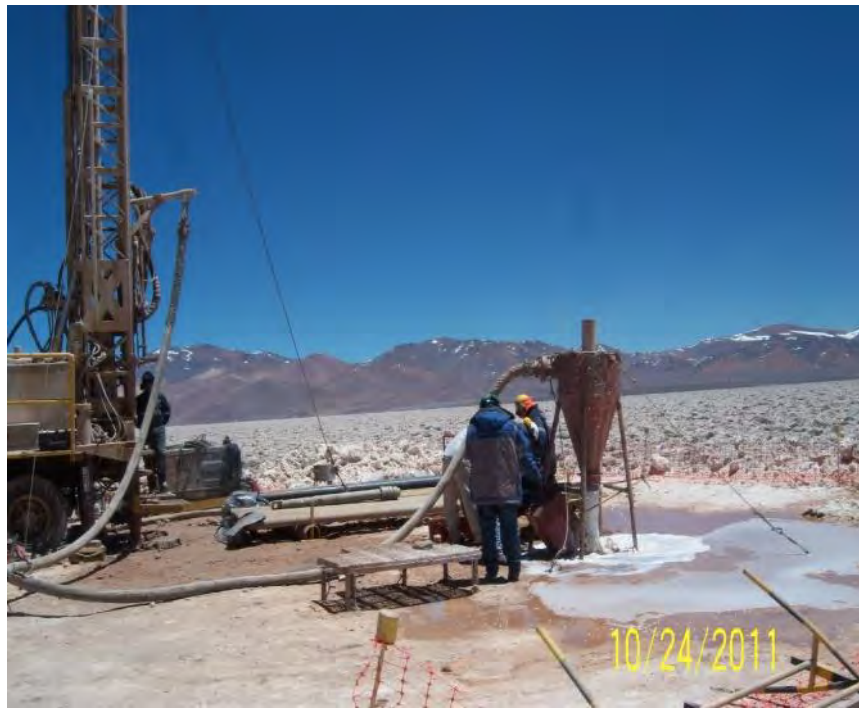


Figure 10-3 Installation of surface casing in well P-1 (2011)



Table 10-2 Wells P1, P2 and P4 pumping test layout

Well	Type	UTM E	UTM N	Screened interval (mbgs)	Unit
P-1 Test					
P-1	Pumping	494,043	7,025,903	0-12,18-24 ,60-144	Upper Halite and lower Alluvium
P1-1	Observation	494,032	7,025,890	60-149	Lacustrine and lower Alluvial
P1-2	Observation	494,061	7,025,893	7-24	Upper Halite
P1-3	Observation	494,032	7,025,905	55-66	Lacustrine
P1-4	Observation	494,031	7,025,915	7-24	Upper Halite
P-2 Test					
P-2	Pumping	494,030	7,023,422	0-16, 62-141	Upper Halite and lower Alluvial
P2-1	Observation	494,034	7,023,392	102-108	Lacustrine
P2-3	Observation	494,030	7,023,409	11-28	Upper Halite
P2-4	Observation	494,033	7,023,402	58-140	Lacustrine and lower Alluvial
P2-5	Observation	494,060	7,023,397	55-144	Lacustrine and lower Alluvial
P-4 Test					
P-4	Pumping	493,040	7,025,899	70-180	Lower alluvial and volcanoclastic
P4-1	Monitoring	495,055	7,024,994	170-182	Volcanoclastics
P4-2	Monitoring	493,057	7,024,400	0-2	Upper halite
P4-3	Monitoring	495,045	7,022,900	0-2	Upper halite
P4-4	Monitoring	493,038	7,022,917	0-2	Upper halite

P-1 Pumping test (2015)

Production well P-1 has two completion intervals: the upper completion between 6 and 24 m depth in the Upper Halite aquifer and the lower completion between 60 m and 144 m depth in the lower part of the Lacustrine unit and the under-lying lower Alluvial. Four monitoring wells (P1-1, P1-2, P1-3 and P1-4) are installed adjacent to well P-1 at radial distances from 11 to 20 m as shown in Figure 10-4 and Figure 10-5. Piezometers P1-2 and P1-4 are completed in the Upper Halite unit. Piezometer P1-3 is completed in a deeper halite layer within the Lacustrine unit and Piezometer P1-1 is completed in the lower part of the Lacustrine unit and the lower Alluvial sediment

A 14-day constant rate test was conducted at 38 L/s between May 31 and June 13, 2015, followed by recovery. Pumped brine was piped through a 1,200 m plastic line to a V-notch tank where final discharge took place on to the Salar as shown Figure 10-6. The pumping rate was measured by an inline flow meter, manual measurements and in the V-notch tank. Pressure transducers were installed in all piezometers and the V-notch tank to record water level responses during the test in addition to manual measurements. Observed water level responses to the test are shown in Figure 10-7. The curve fitting and interpretation results of the P-1 constant rate test are shown in Figure 10-8 and Table 10-3.

Figure 10-4 Layout of pumping test P-1 and P-2

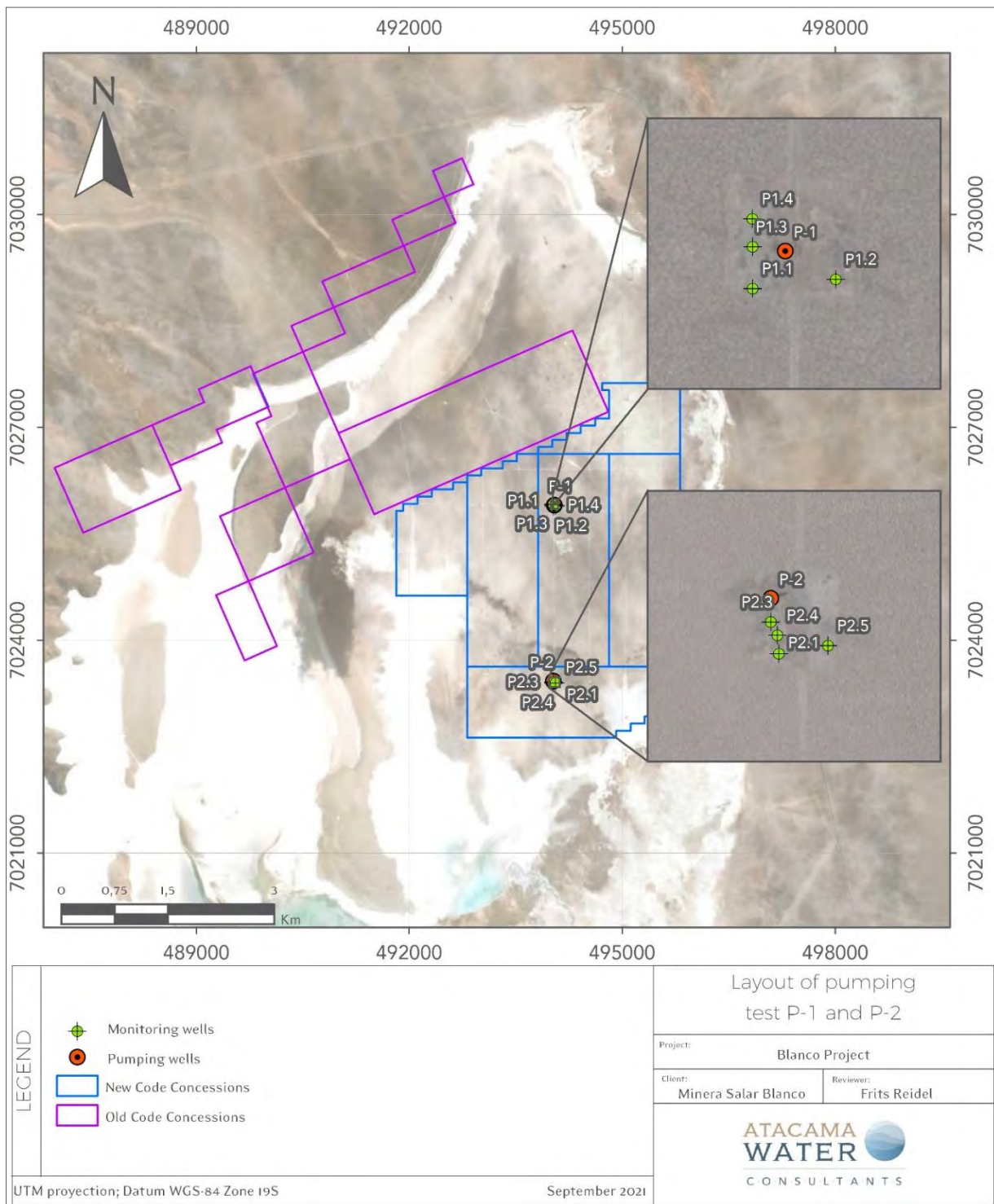


Figure 10-5 Pumping test P-1 layout

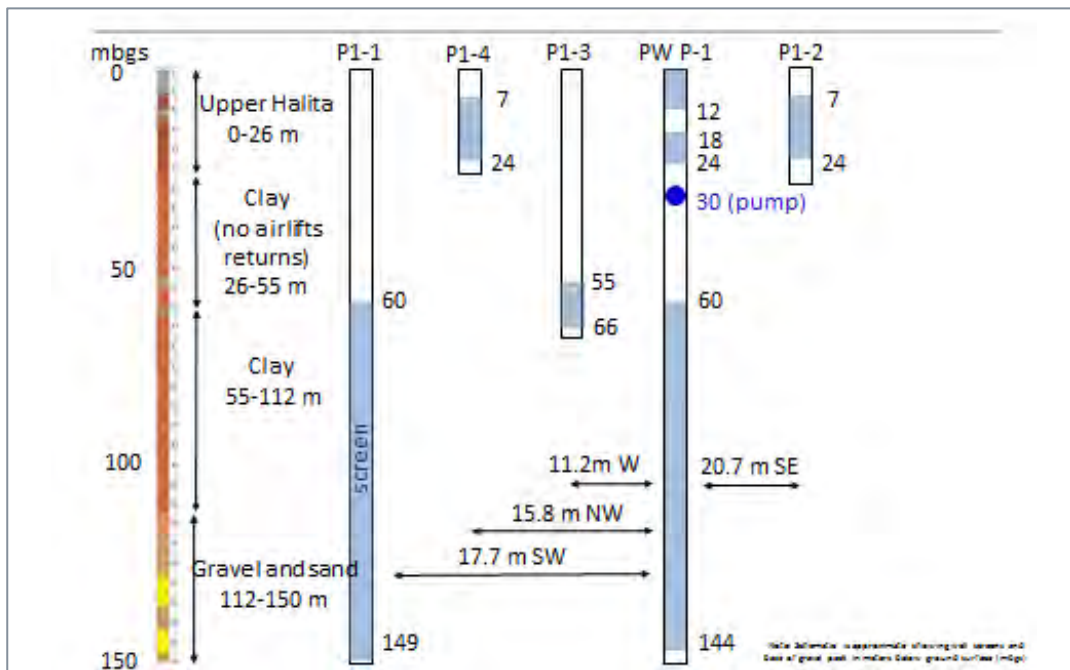


Figure 10-6 V-notch tank during P-1 constant rate test

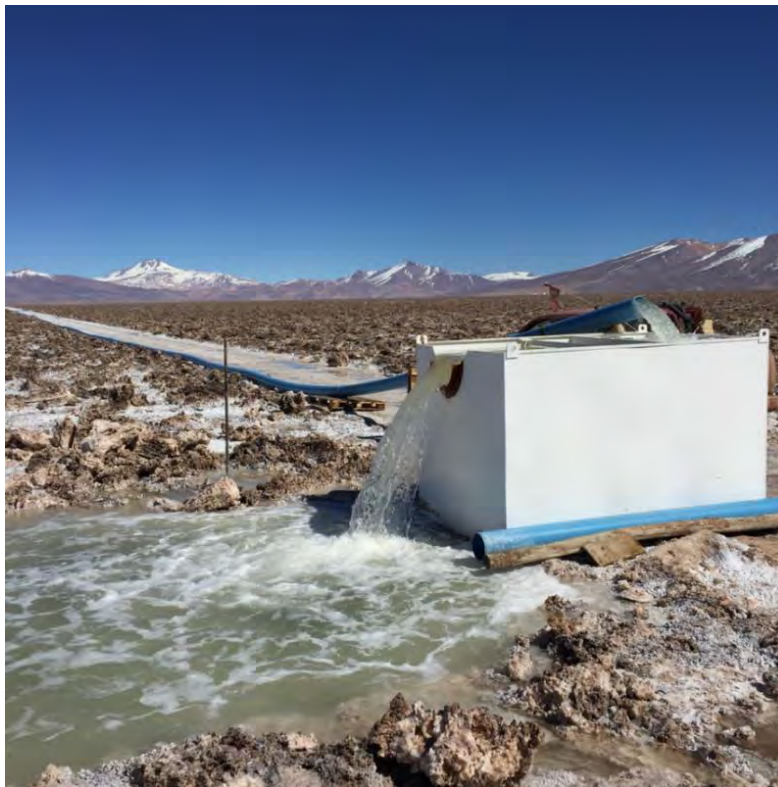
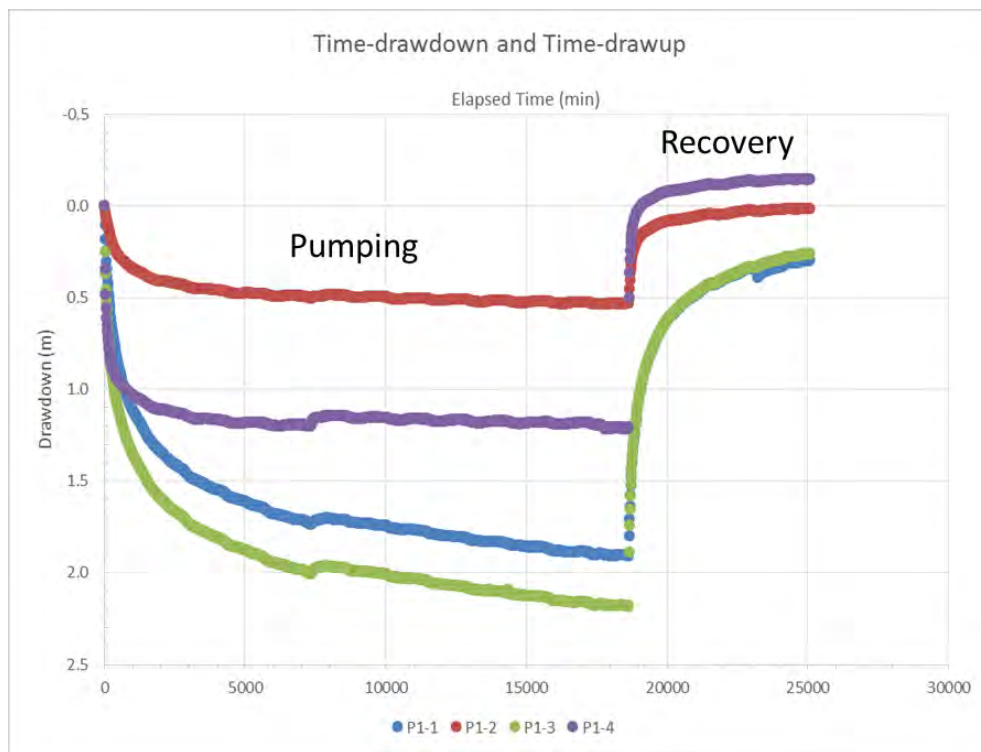


Figure 10-7 Water level responses P-1 constant rate test



Source: Atacama Water 2015b

Figure 10-8 P-1 pumping test interpretation

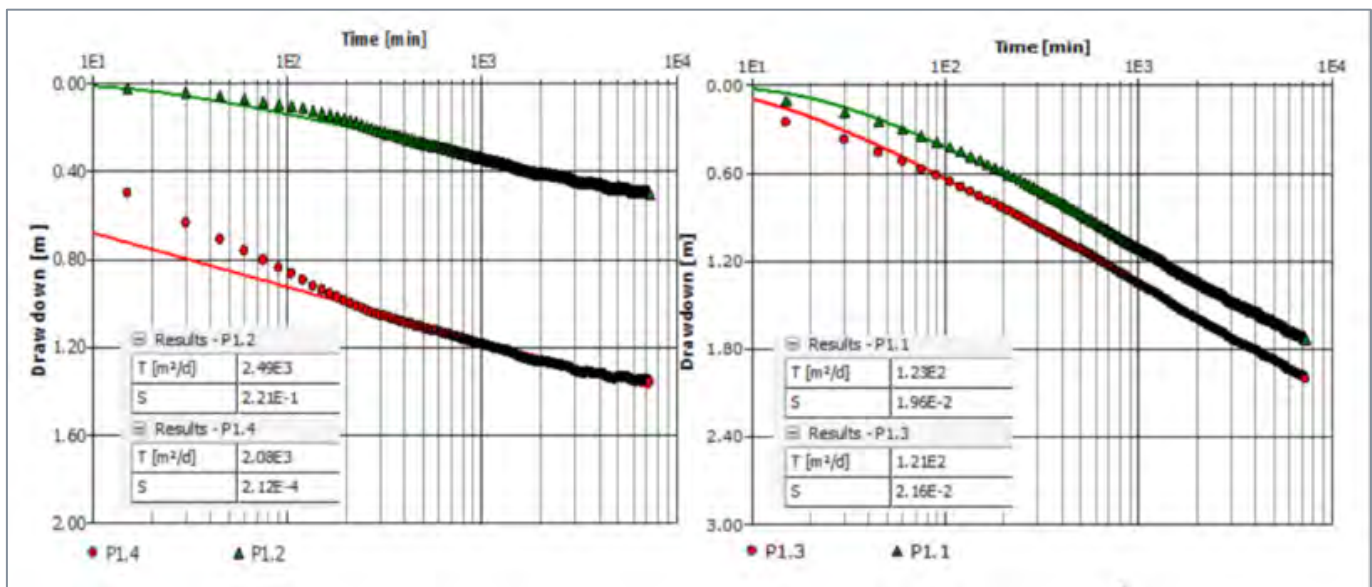
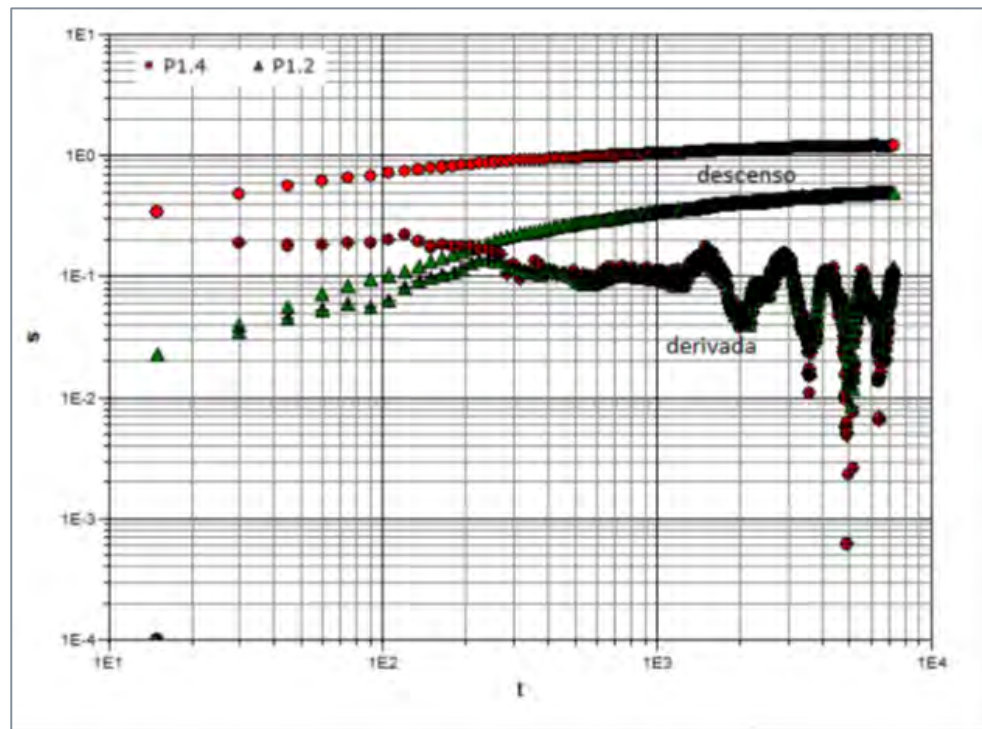


Table 10-3 P-1 pumping test results

Well	Unit	Max Drawdown (m)	Fit	T (m ² /d)	S(-)	K (m/d)*	Ss (1/m)
P-1.2	Upper Halite	0.531	Theis	2,490	2.21E-01	146.5	1.3E-02
P-1.4	Upper Halite	1.362	Theis	2,080	2.12E-04	122.4	1.2E-05
P-1.1	Lower aquifer	1.906	Theis	123	1.96E-02	1.4	2.2E-04
P-1.3	Lower aquifer	2.181	Theis	121	2.16E-02	11.0	2.0E-03

P-2 Pumping test (2015)

Production well P-2 has two completion intervals: the upper completion between 0 m and 16 m depth in the Upper Halite aquifer and the lower completion between 60 m and 144 m depth in the lower part of the Lacustrine deposits and the underlying lower Alluvial unit. Four monitoring wells (P2-1, P2-3, P2-4 and P2-5) are installed adjacent to well P-2 at radial distances from 12 m to 40 m as shown in Figure 10-5 and Figure 10-9. Piezometer P2-3 is completed in the Upper Halite unit. Piezometer P2-1, P2-4 and P2-5 are completed within the lower part of the Lacustrine deposits and the lower alluvial sediments.

A 30-day constant rate test was conducted at 37 L/s during July/ August 2015, followed by recovery. Pumped brine was piped through a 1,200 m plastic line to a V-notch tank where final discharge took place on to the Salar. The pumping rate was measured by an inline flow meter, manual measurements and in the V-notch tank. Pressure transducers were installed in all piezometers and the V-notch tank to record water level responses during the test in addition to manual measurements. Observed water level responses to the test are shown in Figure 10-10. The curve fitting and interpretation results of the P-2 constant rate test are shown in Figure 10-11 and Table 10-4.

Figure 10-12 shows the variation of lithium and potassium concentrations during the P-1 and P-2 pumping tests, which is within the range of laboratory analytical variability.

Figure 10-9 Pumping test P-2 layout

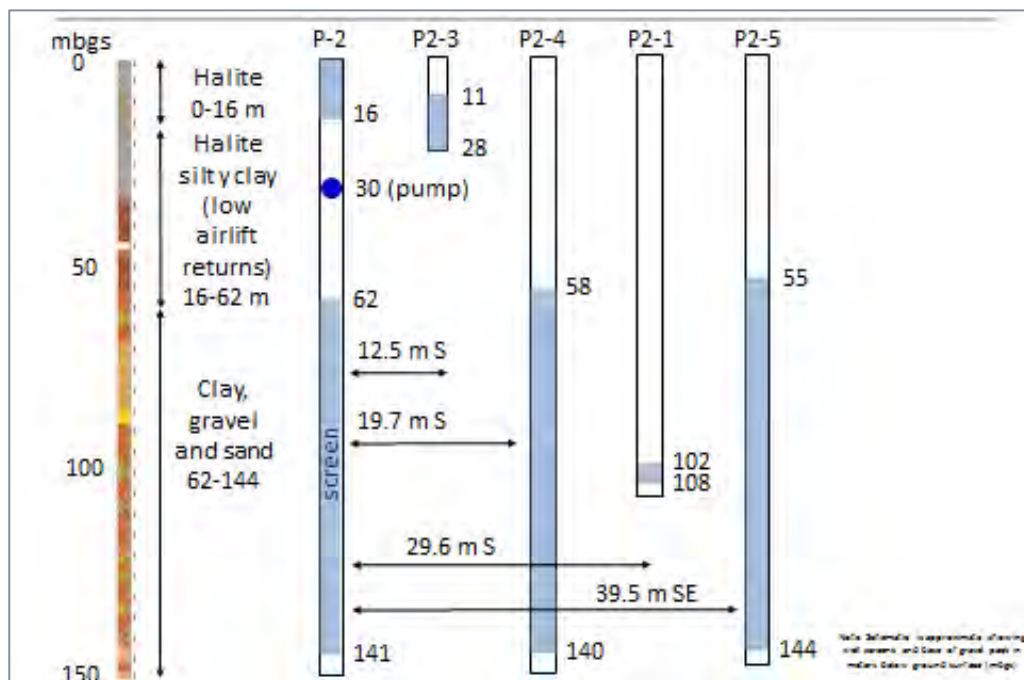


Figure 10-10 Water level responses P-2 constant rate test

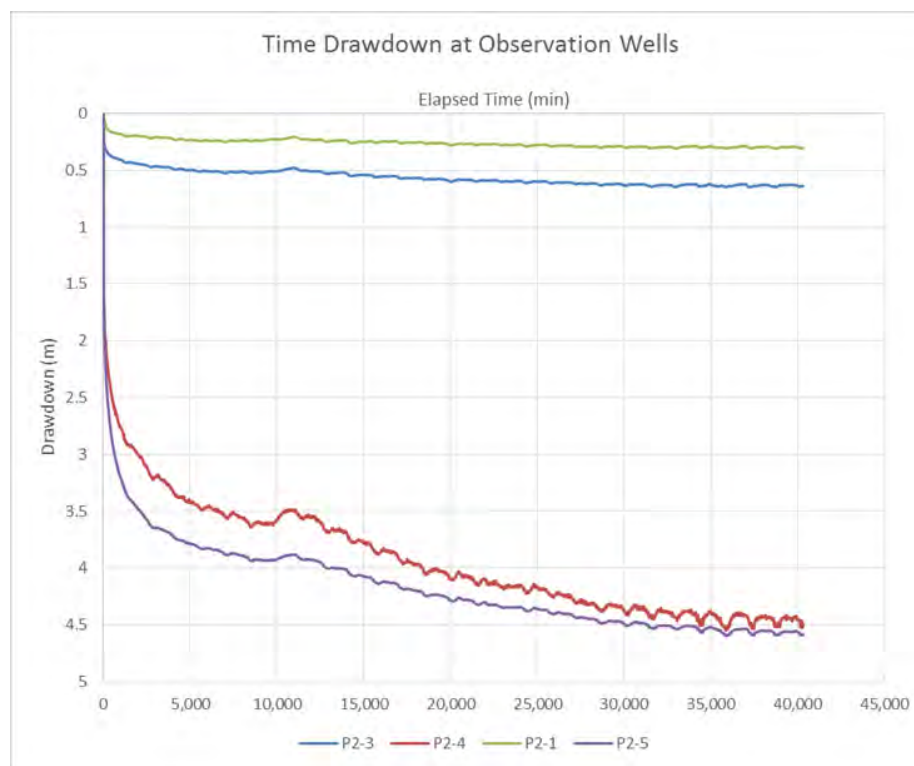


Figure 10-11 P-2 pumping test interpretation

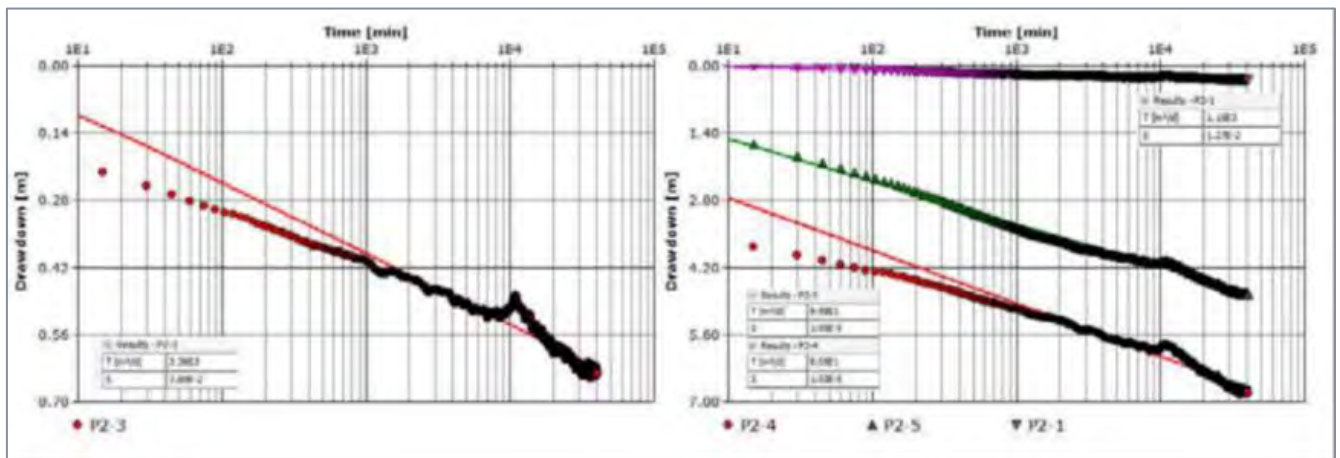
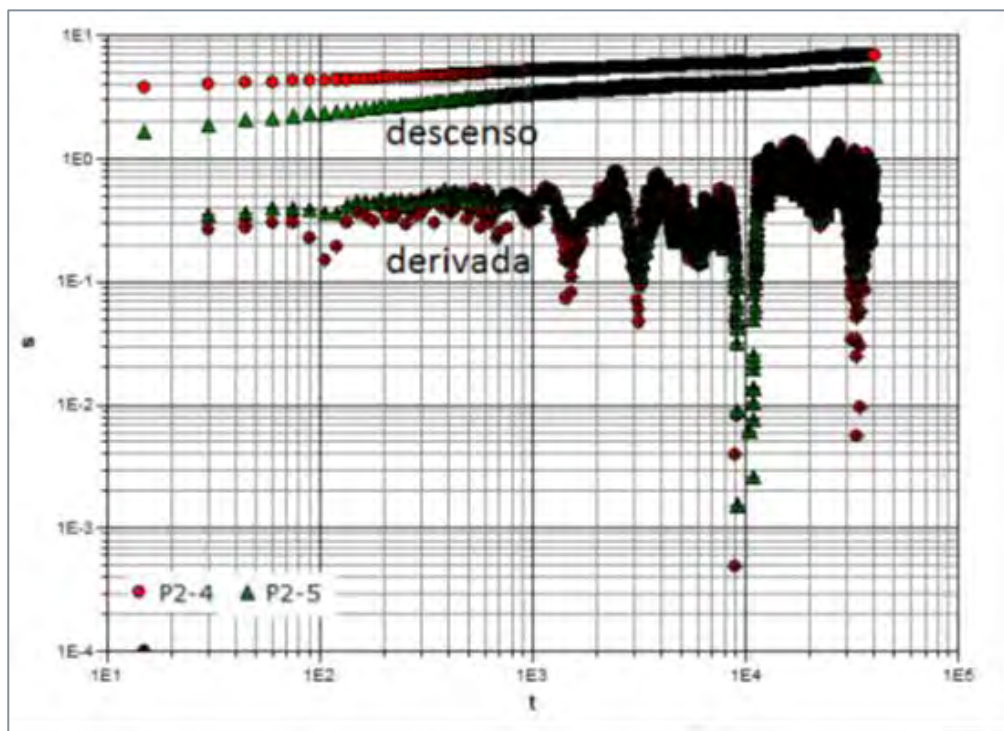
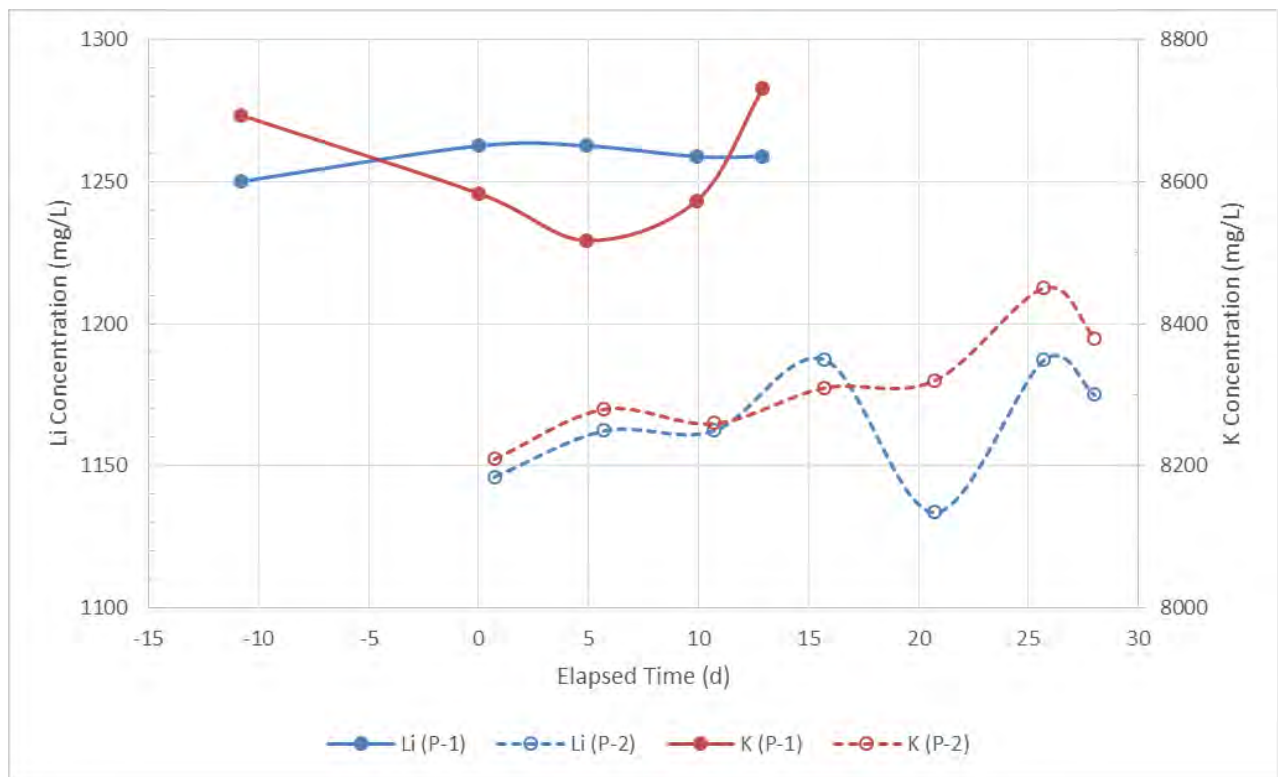


Table 10-4 P-2 pumping test results

Well	Unit	Max Drawdown (m)	Fit	T (m ² /d)	S(-)	K (m/d)*	Ss (1/m)
P-2.3	Upper Halite	0.637	Theis	3,360	7.89E-02	197.6	4.64E-03
P-2.1	Upper Halite-clay	0.299	Theis	1,150	1.27E-02	191.7	2.12E-03
P-2.5	Lacustrine/lower alluvial	4.723	Theis	99.8	1.95E-05	1.1	2.19E-07
P-2.4	Lacustrine/lower alluvial	6.795	Theis	80.5	1.03E-05	0.9	1.17E-07

Figure 10-12 Li and K concentrations during the P-1 and P-2 pumping tests



Source: Atacama Water 2015

P-2 Pumping test – shallow (2017)

A second pumping test was carried out on production well P-2 during 2017. During this test a packer was installed in the well at 40 m depth to isolate the deeper screened interval of the well and pump brine from just the Upper Halite unit. As expected, some brine still entered the upper section of the

well via upward vertical flow through the gravel pack. This second test was carried out at 45 L/s over a 7 day period during February 2017. Water level responses were measured in the adjacent monitoring wells (P2-1, P2-3, P2-4 and P2-5). The pumping rate was measured by an inline flow meter, manual measurements and in the V-notch tank. Pressure transducers were installed in all piezometers and the V-notch tank to record water level responses during the test in addition to manual measurements. Observed water level responses to the test are shown in Figure 10-13. The curve fitting and interpretation results of the second P-2 constant rate test are shown in Table 10-5.

Figure 10-13 Water level responses P-2 constant rate test (2017)

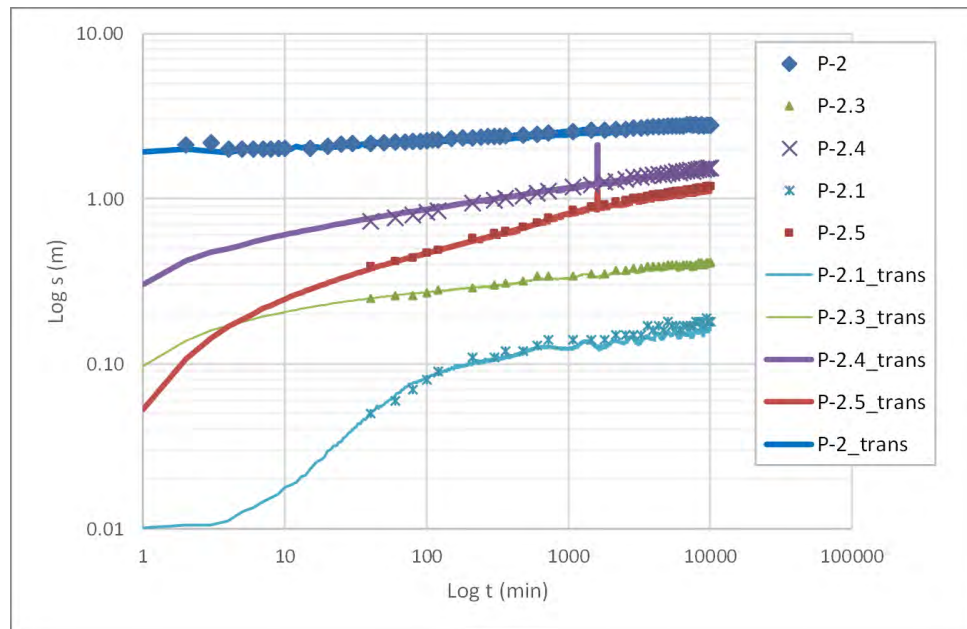


Table 10-5 P-2 pumping test results (2017)

Well	Unit	Max Drawdown (m)	Fit	T (m ² /d)	S(-)	K (m/d)*	Ss (1/m)	Sy (%)
P-2.1	Upper Halite	0.17	Neuman	287	7.00E-03	47.8	1.17E-03	19
P-2.3	Upper Halite and clay	0.4	Theis	10,830	6.00E-04	637.1	3.53E-05	
P-2.4	Lacustrine/lower Alluvial	2.12	Theis	96	1.00E-04	1.1	1.14E-06	
P-2.5	Lacustrine/lower Alluvial	1.14	Theis	95	3.80E-04	1.1	4.27E-06	

P-4 Pumping test (2017)

Production well P-4 is completed with screened casing from 70 and 180 m depth in sands and gravels of the lower Alluvial and volcanoclastic unit (lower aquifer). A bentonite and cement seal were installed in the annulus of the well between 57 m depth and ground surface so that no water from the upper aquifer (Upper Halite) could enter the well. Four monitoring wells (P4-1, P4-2, P4-3 and P4-4) are installed adjacent to well P-4 at radial distances from 10 to 40 m as shown in Figure 10-14. Piezometer P4-1 is completed in the Volcanoclastic unit, while piezometers P4-2, P4-3 and P4-4 are all shallow completions in the Upper Halite.

A 30-day constant rate test was conducted at 25 L/s during January / February 2017, followed by recovery. Pumped brine was piped through a 1,200 m plastic line to a V-notch tank where final discharge took place on to the Salar. The pumping rate was measured by an inline flow meter, manual measurements and in the V-notch tank. Pressure transducers were installed in all piezometers and the V-notch tank to record water level responses during the test in addition to manual measurements.

Observed water level responses to the test are shown in Figure 10-15. It should be noted that no water level responses were observed in shallow monitoring wells P4-2, P4-3 and P4-4. The curve fitting and interpretation results of the P-4 constant rate test are shown in Figure 10-16 and Table 10-6.

Figure 10-14 Pumping test P-4 layout

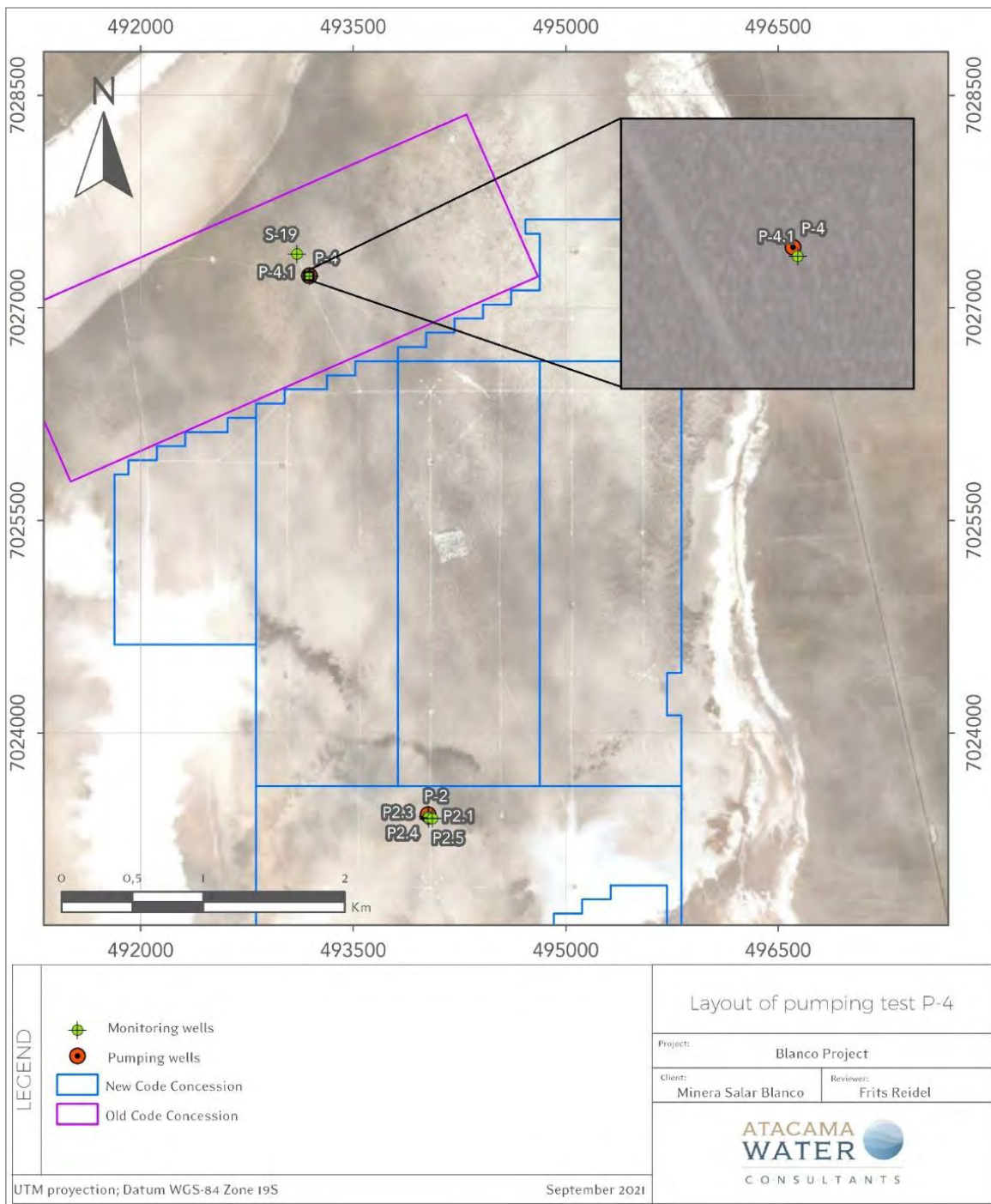


Figure 10-15 Water level responses P-4 constant rate test (2017)

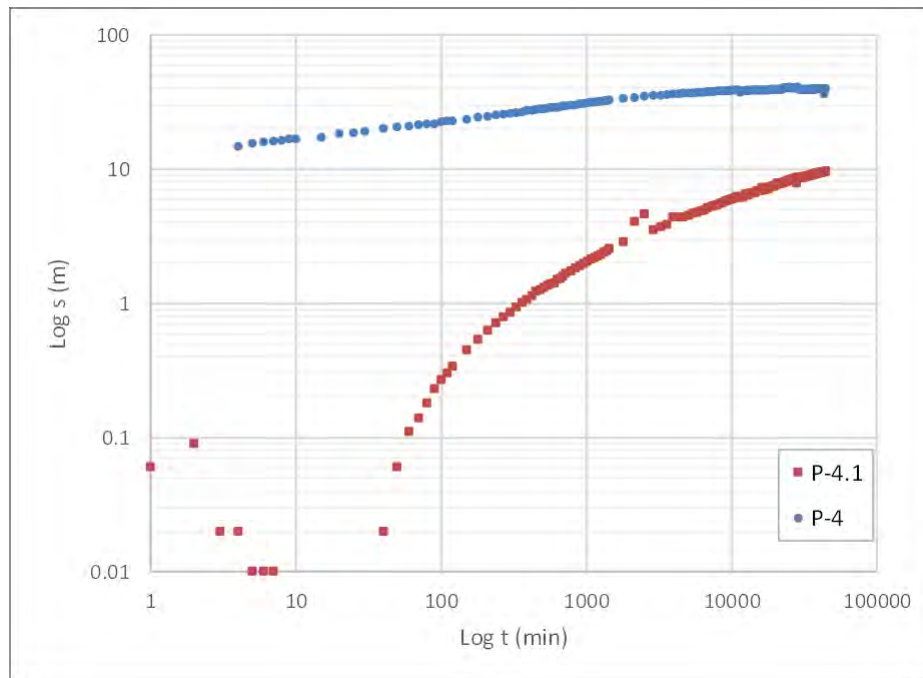


Figure 10-16 P-4 pumping test interpretation

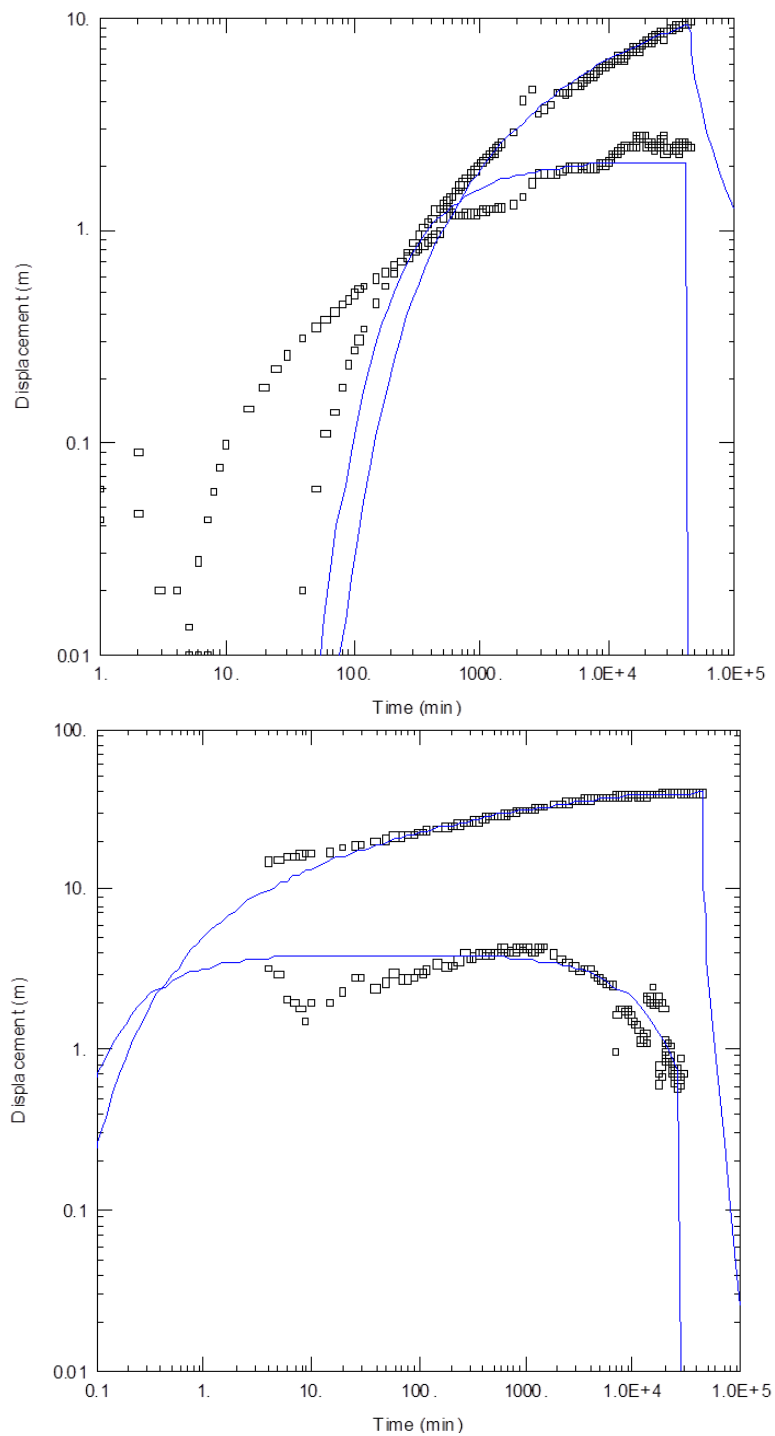


Table 10-6 P-4 pumping test results (2017)

Well	Unit	Max Drawdown (m)	Fit	T (m ² /d)	S(-)	K (m/d)	Ss (1/m)
P-4	Lower aquifer	40.73	Hantush	44		0.4	
P-4.1	Lower aquifer	9.58	Theis	82	4.00E-01	0.9	4.44E-03

Pumping test 2021-2022

A 30-day pumping test is being conducted in production well P-5 which is completed to 400 m depth in the lower brine aquifer. The test is being carried out at a pumping rate of 35 l/s; water level measurements are being made in adjacent monitoring well S-25. The pumping test started on 10th December 2021 and is scheduled to be completed by the second week of January 2022. Preliminary results show a maximum drawdown of 14,25 m in the pumping well suggesting a Specific Capacity (Sc) of 2,5 l/s/m

11. SAMPLE PREPARATION, ANALYSIS, AND SECURITY

11.1 SAMPLING METHODS

Sampling and sample preparation protocols for the sonic drilling and RC drilling programs in 2011 were developed by Frits Reidel, CPG, Don Hains, P.Geo, and Pedro Pavlovic, Chem Eng. All protocols were implemented at the start-up of the drilling programs in October 2011 under the supervision of Frederik Reidel, CPG and included extensive day to day training and supervision of Li3 field staff and experienced MWH hydrogeologists and field technicians. Frits Reidel, CPG was present throughout the drilling program on regular intervals to review the day to day execution of these protocols.

Sampling and sample preparation protocols for the 2016-2021 drilling programs were developed by Frits Reidel, CPG and Murray Brooker, PGeo. All protocols were implemented at the start-up of the drilling programs in October 2016 under the supervision of Frits Reidel, CPG. Both QP's were present throughout both drilling programs on regular intervals to review the day-to-day execution of these protocols. Mr Brooker was present at various times during the 2016 program but could not travel to assist supervising the 2021 program.

11.1.1 SAMPLING PROCEDURES – SONIC AND DIAMOND CORE DRILLING

Porosity samples

Sonic core was collected in 1.5 m lexan core liners in alternating 1.5 m intervals as described in Section 10 above. A 10 cm sub-sample was cut from the lexan core liner; caps were placed on each end of the porosity sub-sample and taped to prevent any fluid loss. The samples were labelled with the borehole number and depth interval. Each day the porosity samples were transferred to the workshop in the on-site camp where the samples were labelled with a unique sample number. Prior to shipping each sample was wrapped in bubble plastic to prevent disturbance during shipping.

285 porosity samples were shipped to Daniel B Stephens and Associates (DBS&A) Laboratory in the USA in 2011

32 porosity check samples were shipped to the British Geological Survey (BGS) in the UK in 2011

208 core samples were shipped to Geosystems Analysis (GSA) during the 2016-2018 drilling programs from which 28 samples were analysed by Corelabs as check samples.

HQ core was collected during the 2021 drilling program in each borehole in 1.5 m lengths from 200 m and 400 m depth from which sub-samples were prepared at 12 m intervals for laboratory drainable porosity analysis. These samples were handled similar to the Sonic samples as described

above. A total of 66 samples were shipped to GeoSystems Analysis Laboratory (GSA) from which 10 sub-samples were selected and prepared as check samples for analysis by Daniel B. Stevens & Associates Inc. (DBSA).

Brine Samples

Brine samples were collected at three-meter intervals during the 2011 sonic drilling where possible. Based on the experience from the 2011 program the brine sampling interval for the 2016-2018 programs was changed to 6 m and to 12 m for the 2021 campaign. In some cases where the formation permeability was low, it was not possible to collect a brine sample after a one hour waiting period. The borehole was purged by bailing up to three well volumes of brine from the drill casing as calculated from the water level measurement prior to collecting the final brine sample from the bottom of the hole. The final brine sample was discharged from the bailer into a 20-liter clean bucket from which three one-litre sample bottles were rinsed and filled with brine. Each bottle was taped and marked with the borehole number and depth interval. A small sub-sample from the bucket was used to measure field parameters (density, electric conductivity, pH and temperature) at the wellhead as shown in Figure 11-1.

Figure 11-1 Collection of field parameters of the brine samples at the wellhead



The samples were moved from the drill site to secure storage at the camp on a daily basis. All brine sample bottles are marked with a unique label. One sample bottle was stored as a permanent back-up sample in the on-site warehouse. One sample bottle was prepared for shipment and the third bottle was either used as a duplicate or discarded. No filtration was carried out on the brine samples prior to shipment to laboratories.

Figure 11-2 illustrates the porosity samples and brine samples storage facility.

Figure 11-2 Porosity and brine samples



11.1.2 SAMPLING PROCEDURES – RC DRILLING

RC drill cuttings (2011)

During RC drilling, rock chip and brine were collected directly from the cyclone. Drill cuttings were collected over two-meter intervals in plastic bags that were marked with the borehole number and depth interval. Sub-samples were collected from the plastic bag by the site geologist to fill chip trays (also at two-meter interval). At the end of each borehole all chip trays were removed to storage in the on-site office as shown in Figure 11-3. All plastic sample bags were stored in a secure on-site warehouse.

Figure 11-3 RC drill chip samples



RC brine sampling (2011)

Brine samples were collected at three-meter intervals during the RC drilling from the cyclone where possible. In some cases where the formation permeability was low, it was not possible to collect a brine sample. Brine samples were collected in three one-litre (rinsed) sample bottles. Each bottle was taped and marked with the borehole number and depth interval. A small sub-sample from the cyclone was used to measure field parameters (density, electric conductivity, pH and temperature) at the wellhead.

11.1.3 SAMPLING PROCEDURES- ROTARY / HWT DRILLING (2017)

Drill Cuttings

During the rotary drilling, cuttings were collected directly at the head of the borehole in cloth, flow-through bags that minimize the loss of fines but allow fluid to drain at 2 m intervals. The cloth bags were marked with the borehole number and depth interval. Sub-samples were collected from the bags by the site geologist to fill chip trays (also at two-meter interval). At the end of each borehole all chip trays were removed to storage in the on-site office. All sample bags were moved and stored in a secure warehouse in Copiapó.

196 rotary chip samples were shipped to Geosystems Analysis (GSA) in 2017 for physical properties analyses and consolidation tests.

Figure 11-4 Fluorescein tracer dye in the rotary drilling fluid



Brine sampling

A plug-type device connected to the wireline cable was used to purge the hole, rather than using a bailer. This consists of a very stiff rubber plug on a steel tool which is lowered down the hole. When this tool is pulled up from the base of the hole the rubber plug expands to flush within the drill rods, drawing brine up the drill rods above the plug, with the brine flowing out of the rods at surface. This works in a similar fashion to the bailer, but in a continuous mode, rather than numerous repetitions of lowering and raising a bailer.

In the case of the rotary drilling, it was not possible to lower the HWT casing to a meter above the base of the hole in some cases and consequently inflows from around the sides to the base of the hole could occur. The raising of the plug is likely to have had a suction effect around the base of the hole, stimulating inflows into the hole over a larger area than with the sonic drill holes.

Drilling fluids (in this case brine) are required during the rotary drilling to lift the cuttings out of the hole. The drilling fluid was mixed with a rhodamine / fluorescein tracer dye in portable tanks adjacent to the rig to distinguish the drilling fluid from the natural formation brine as shown in Figure 11-4. Purging of the drill hole was continued until no tracer dye was observed in the purged brine. Any trace of dye observed in brine samples was noted to indicate the potential for contamination with drilling fluid. Brine samples were collected in duplicate at every sampling interval and in triplicate at every fifth sampling interval.

11.2 BRINE ANALYSIS AND QUALITY CONTROL RESULTS

11.2.1 ANALYTICAL METHODS

The University of Antofagasta in northern Chile was selected as the primary laboratory to conduct the assaying of the brine samples collected as part of the 2011 – 2018 drilling programs. The laboratory of the University of Antofagasta is not ISO certified, but it is specialized in the chemical analysis of brines and inorganic salts, with extensive experience in this field since the 1980s, when the main development studies of the Salar de Atacama were begun. Other clients include SQM, FMC, LAC, and Orocobre.

Alex Stewart Argentina in Mendoza, Argentina was used for the analysis of external check samples during the 2011 drilling campaign, while NOA Alex Stewart Argentina in Jujuy was used for external check samples during 2016 – 2018 campaigns. This laboratory is accredited to ISO 9001 and operates according to Alex Stewart Group standards consistent with ISO 17025 methods at other laboratories.

Table 11-1 lists the basic suite of analyses requested from both laboratories. Both used the same analytical methods based on the Standard Methods for the Examination of Water and Wastewater, published by American Public Health Association (APHA) and the American Water Works Association (AWWA), 21st edition, 2005, Washington DC. The University of Antofagasta used Atomic Absorption Spectrometry (AAS) for the determination of lithium, potassium, magnesium and calcium. Alex Stewart (Mendoza) employed Inductively Coupled Plasma (ICP), which is generally used for a large suite of elements (multi-elemental analysis), including the detection of trace metals. ASA included 10 elements in the determination with this analytical technique: B, Ba, Ca, Fe, K, Li, Mg, Mn, Na, and Sr.

**Table 11-1 List of analyses requested from the University of Antofagasta and Alex Stewart
 Argentina SA Laboratories**

Analysis	University of Antofagasta	Alex Stewart	Method
Chemical-Physical Parameters			
Total Dissolved Solids	SM 2540-C	SM 2540-C	Total Dissolved Solids Dried at 180°C
PH	SM 4500-H+B	SM 4500-H+B	Electrometric Method
Density	CAQ – 001DS	IMA-28	Pycnometer
Alkalinity	SM 2320-B	SM 2320-B	Acid-Base Titration
Inorganic Parameters			
Boron (B)	CAQ – 005 BS	ICP - OES	Acid-Base Titration
Chlorides (Cl)	SM 4500-Cl-B	SM 4500-Cl-B	Argentometric Method
Sulphates (SO4)	SM 45002-D (Drying of residue)	SM 45002-C (Ignition of Residue)	Gravimetric Method
Dissolved Metals			
Sodium (Na)	SM 3111 B	ICP-OES 10	Direct Aspiration-AA or ICP Finish
Potassium (K)	SM 3111 B	ICP-OES 10	Direct Aspiration-AA or ICP Finish
Lithium (Li)	SM 3111 B	ICP-OES 10	Direct Aspiration-AA or ICP Finish
Magnesium (Mg)	SM 3111 B	ICP-OES 10	Direct Aspiration-AA or ICP Finish
Calcium (Ca)	SM 3111 B	ICP-OES 10	Direct Aspiration-AA or ICP Finish

11.2.2 ANALYTICAL QUALITY ASSURANCE AND QUALITY CONTROL (“QA/QC”) 2011 PROGRAM

A full QA/QC program for monitoring accuracy, precision and potential contamination of the entire brine sampling and analytical process was implemented. Accuracy, the closeness of measurements to the “true” or accepted value, was monitored by the insertion of standards, or reference samples, and by check analysis at an independent secondary laboratory.

Precision of the sampling and analytical program, which is the ability to consistently reproduce a measurement in similar conditions, was monitored by submitting blind field duplicates to the primary laboratory. Contamination, the transference of material from one sample to another, was measured by inserting blank samples into the sample stream at site. Blanks were barren samples on

which the presence of the main elements undergoing analysis has been confirmed to be below the detection limit.

Approximately 31 % of the 623 samples submitted for chemical analysis during the 2011 campaign were quality control samples. The QA/QC procedures adopted for the Project are discussed below, and included the following:

Three standards (A, B and C) were inserted at a frequency of 1 in 15 samples (1/3 of each type of standard, randomly inserted). The specially prepared samples were submitted to five laboratories as a Round Robin (each analysing five 1-L sub-samples from each type of standard) to establish an accepted mean and standard deviations for the analytical variables. These three standards were prepared from Maricunga brine and each with a different dilution factor.

The University of Antofagasta made an internal check on overall analytical accuracy for the primary constituents of the brine by using ion balance. This calculation was checked and the ratio of measured to calculated TDS was added as another procedure for checking the correctness of analyses.

Duplicate samples at a frequency of 1 in 10 samples in the analysis chain were submitted to the University of Antofagasta as unique samples (blind duplicates) to monitor precision.

Stable blank samples (distilled water) were inserted at a frequency of 1 in 30 samples to measure cross contamination.

Duplicates at a frequency of 1 in 10 samples and including blind control samples (a total of 70 samples), were submitted to the secondary laboratory (Alex Stewart in Mendoza) as check samples (external duplicates).

11.2.3 ANALYTICAL ACCURACY 2011 PROGRAM

Anion-Cation balance

The anion-cation balance was used as a measure of analytical accuracy. The anion and cation sums, when expressed as equivalents or milliequivalents per litre, must balance in an ideally perfect analysis, because mixtures of electrolytes are electrically neutral. The term meq/L is defined as:

$$\text{Meq/L} = (\text{mg/l} \times \text{valence number} / \text{molecular weight of ion})$$

The charge balance is expressed as a percentage, as follows:

$$\% \text{Difference} = ((\sum \text{Cations} - \sum \text{Anion}) / (\sum \text{Cations} + \sum \text{Anion})) \times 100,$$

Although this test does not monitor individual elements, it is recommended by APHA-AWWA-WPCF in their Standard Methods, 21st edition, 2005 (1030 E) as a procedure for checking correctness of water analyses. The typical criterion for acceptance is a maximum difference of 5 %, which is used by the University of Antofagasta as well as by Alex Stewart.

The performance of the University of Antofagasta in the analyses of 431 primary samples and 61 duplicates show a balance within 2 %, i.e. much less than the maximum acceptable difference of 5 %. All the check samples analysed by Alex Stewart had a balance within a value of 5 %.

Measured versus calculated TDS

Measured versus calculated Total Dissolved Solids (TDS) was used as a second evaluation test of analytical accuracy. The recommended ratio according to the APHAA/AWWA/WPCF Standard Method should be between 1.0 and 1.2. Results for the submitted samples to the University of Antofagasta (431 primary samples plus 61 duplicates) ranged from 0.983 to 1.043, with 10 % of the samples below the acceptable ratio (1.0) and most of these between 0.994 and 1.0. This is considered as a very good performance given the high dissolved solids content of the brine.

Based on the results detailed above, the authors are of the opinion that the sample analytical results are reliable and accurate.

Certified analytical standards

Three standard reference samples, prepared at site with original brine (Standard A, 100% natural brine; Standard B, 80 %; Standard C, 60 %, dilution with distilled water) were used in the sampling program. Sets of randomized replicates were sent in a Round Robin analysis program to five laboratories (15 sub-samples to each lab) to determine the certified values used to monitor the accuracy of analyses. Statistics were done on the Round Robin assay results and the standard reference samples certified for the elements that met the criteria of having a global Relative Standard Deviation (RSD) of near 5 % or less.

The results of the standards analyses for Li, K and Mg are summarized in Table 11-2. This table lists the statistics, number of samples exceeding the acceptable failure criteria of the mean \pm 2 standard deviations, and the relative standard deviation (RSD) for each standard. Standard analyses at the

University of Antofagasta indicate very acceptable accuracy. There are only two exceptions: one failure for potassium analysis of the Standard A and one failure for Mg analysis of the Standard B. Each of these failures is not significant. Table 11-2 shows the relative standard deviation values (measure of precision) for the University of Antofagasta analyses range from 1.36 to 2.67, indicating very good analytical reproducibility for the standard analyses conducted at the primary laboratory. Based on the analysis detailed above, the authors are of the opinion that the lithium, potassium and magnesium analyses are accurate. There is also a good reproducibility or precision in the assay values reported by the University of Antofagasta for these three elements.

Table 11-2 Standards analysis results from U. Antofagasta (2011)

Standard	A	B	C
Statistics	Li (mg/l)		
Count	14	14	14
Min	1,095	855	675
Max	1,150	950	725
Mean	1,128	914	699
Standard Deviation	15.3	21.9	14.2
Mean \pm 2 Standard Deviation			
Mean + 2SD	1,159	958	728
Mean - 2SD	1,098	870	671
No of Failures >2SD	0	0	0
Relative Standard Deviation			
RSD	1.36	2.40	2.04
Statistics	K (mg/l)		
Count	14	14	14
Min	7,896	6,291	4,883
Max	8,510	6,830	5,215
Mean	8,090	6,533	5,033
Standard Deviation	157.8	142.7	87.3
Mean \pm 2 Standard Deviation			
Mean + 2SD	8,405	6,818	5,207
Mean - 2SD	7,774	6,247	4,858
No of Failures >2SD	1	0	0
Relative Standard Deviation			
RSD	1.95	2.18	1.74
Statistics	Mg (mg/l)		
Count	14	14	14
Min	6,875	5,588	4,275
Max	7,450	6,225	4,600
Mean	7,169	5,915	4,487
Standard Deviation	148.4	157.7	101.8
Mean \pm 2 Standard Deviation			
Mean + 2SD	7,466	6,231	4,691
Mean - 2SD	6,872	5,600	4,284
No of Failures >2SD	0	1	0
Relative Standard Deviation			
RSD	2.07	2.67	2.27

Check analyses

Checks analyses were conducted at Alex Stewart located in Mendoza, Argentina. About 15 % of external duplicates (61 samples) were submitted. In addition, some blanks and standard control samples were inserted to monitor accuracy and potential laboratory bias. The total number of

samples in the batch was 70. The standards indicated acceptable accuracy and precision for Li and K.

Statistical analysis of the 61 pairs of check sample assay values was conducted using Reduction-to-Major-Axis (“RMA”) multiple linear regressions for Li, K and Mg. StatGraphics software was used for this analysis. The results are summarized in Table 11-3.

Table 11-3 Check assays (U. Antofagasta vs. Alex Stewart): RMA regression statistics

Maricunga Project - RMA Parameters							
Element	R2	Pairs	m	Error (m)	B	Error (b)	Bias
Li (mg/l)	0.98223	61	0.8598	0.01511	832.787	192.822	14.02%
K (mg/l)	0.98675	61	10.207	0.01539	521.422	141.618	-2.07%
Mg (mg/l)	0.97183	61	10.978	0.02433	-217.714	206.109	-9.78%

The R-squared statistic is the indicator of the quality of the fit. High values of this coefficient reflect a good fit and low values a poor fit.

The bias, which is a measure of accuracy (the higher the bias, the lower the accuracy), is calculated as $\text{Bias (\%)} = 1 - \text{RMAS}$ where RMAS is the slope (m) of the Reduction-to-Major-Axis regression line of the secondary laboratory ICP values (ASA) versus the primary laboratory AAS values (University of Antofagasta) for each element. Because of different analytical finish, in general the University of Antofagasta obtained a little higher assay values for lithium and a little lower for potassium and magnesium, as shown in Table 11-4.

Precision in Table 11-4 was assessed through the Relative Percent Difference or Relative Error, defined as the absolute value of the difference between two similar analyses, and divided by the average between these two assays. Precision of the external duplicate analyses is acceptable for Li, K and Mg. Eighty-eight per cent of the Li assays are within $\pm 10\%$ of one another (ASA considers acceptable 10% RPD for check samples analysed in the same lab).

Based on the analysis detailed above, the authors are of the opinion that the check assays indicate that the lithium and potassium concentrations determined for the primary sample assays are suitable for use in a resource calculation.

Table 11-4 Check assays between the University of Antofagasta and Alex Stewart

Statistics	UA Li	ASA Li	UA K	ASA K	UA Mg	ASA Mg
	(mg/l)	(mg/l)	(mg/l)	(mg/l)	(mg/l)	(mg/l)
Count	61	61	61	61	61	61
Min	470	447	3,828	4,123	2,838	3,030
Max	1,850	1,697	13,750	14,396	13,200	14,574
Mean	1,240	1,149	8,946	9,654	8,199	8,783
Std Dev	304	264	2,152	2,209	2,146	2,390
Precision		7.5		7.8		7.6
% Bias		14.02		-2.07		-9.78
Correlation		0.98		0.99		0.97
%<10%		88		85		87
%<15%		98		100		98

Sample Duplicate Analyses

Sixty-one duplicate samples were collected in the field to confirm the overall sampling precision and shipped also to the University of Antofagasta laboratory. Table 11-5 lists the statistics, as well as the calculated precision, bias, correlation and percent of duplicate analyses with results within 5% of one another. The bias and correlation were calculated through RMA plots, constructed with StatGraphics software. The duplicate analysis repeated exceedingly well, as was shown in these RMA plots.

Table 11-5 Duplicate analyses from the University of Antofagasta

Statistics	Li	Duplicate Li	K	Duplicate K	Mg	Duplicate Mg
	(mg/l)	(mg/l)	(mg/l)	(mg/l)	(mg/l)	(mg/l)
Count	61	61	61	61	61	61
Min	470	470	3,853	3,918	3,031	3,006
Max	1,938	1,95	13,506	13,519	14,425	14,25
Mean	1,261	1,265	9,098	9,09	8,444	8,445
Std Dev	298	299	2,159	2,134	2,107	2,09
Precision		1.17		1.25		1.31
% Bias		0.03		1.42		1.07
Correlation		0.99		0.99		0.99
%<5%		100		100		95

Assay results for duplicate samples at the U. Antofagasta indicate excellent precision (within 5 % or less) for Li, K and Mg. Bias between duplicates and main samples are within 2 % and correlation is high ($R^2=0.9938$ to 0.9950) for the three elements.

Sample Contamination

Potential sources of sample contamination are related to sample mis-ordering errors or insufficient washing of analytical equipment between samples. A field blank consisting of distilled water was inserted into the sample stream 20 times. New plastic bottles were used in all the cases to avoid eventual contamination with brine samples.

Results reported by the University of Antofagasta indicate <0.05 mg/l (detection limit for lithium) in most blank samples. However, there are four results, corresponding to the last two sample batches with 0.07 (2), 0.08 and 0.09 mg/l for lithium. This reveals that some small contamination with brine was produced in the manipulation of the plastic bottles, either at the project site, or in the lab. This issue is not considered to detract from the validity of the overall sampling and assay results and the use of the assay results in resource estimates.

11.2.4 ANALYTICAL QUALITY ASSURANCE AND QUALITY CONTROL ("QA/QC") 2016-2018 PROGRAM

A total of 363 primary brine samples were analysed from the 2016-2018 drilling campaigns. An additional 133 brine samples from pumping tests and baseline monitoring were analysed. These primary analyses were supported by a total 166 QA/QC analyses consisting of:

- 49 standard samples (7 %),
- 89 duplicates (13 %) and
- 28 blank samples (4 %).

In addition to evaluation of standards, field duplicates and blanks the ionic balance (the difference between the sum of the cations and the anions) was evaluated for data quality. Balances are generally considered to be acceptable if the difference is < 5 % and were generally < 1 %. No samples were rejected as having > 5 % balances. The results of standard, duplicate and blank samples analyses are considered to be adequate and appropriate for use in the resource estimation described herein.

11.2.5 ANALYTICAL ACCURACY 2016-2018 PROGRAM

Anion-Cation balance

The performance of the University of Antofagasta in the analyses of 328 main samples and 32 duplicates show a balance within 5 %. All the check samples analysed by Universidad de Antofagasta had a balance within a value of 2 %.

Measured versus Calculated TDS

Measured versus calculated Total Dissolved Solids (TDS) was used as a second evaluation test of analytical accuracy. The recommended ratio according to the APHAA/AWWA/WPCF Standard Method should be between 1.0 and 1.2. Results for the submitted samples to the University of Antofagasta (308 main samples plus 30 duplicates) ranged from 0.97 to 1.02, with 9 % of the samples below the acceptable ratio of 1.0, and most of these between 0.99 and 1.0. This is considered as a very good performance given the high dissolved solids content of the brine.

Results for the submitted samples to the external laboratory (30 duplicate samples) ranged from 0.98 to 1.14, with only one sample below the acceptable ratio of 1.0, and most of these between 1.02 and 1.14. This is considered as a good performance given the high dissolved solids content of the brine.

Based on the results detailed above, the authors are of the opinion that the sample analytical results are reliable and accurate.

Certified Analytical Standards

Two standard reference samples, SRM-1 and SRM-2 were used in the sampling program. Sets of randomized replicates were sent in a Round Robin analysis program to five laboratories to determine the certified values used to monitor the accuracy of analyses. Statistics were done on the Round Robin assay results and the standard reference samples certified for the elements that met the criteria of having a global Relative Standard Deviation (RSD) of near 5 % or less. Overall, the performance of University of Antofagasta laboratory and the external laboratory were satisfactory.

The results of the standards analysis for Li, K and Mg, are summarized in Table 11-6. This table lists the statistics, number of samples exceeding the acceptable failure criteria of the mean \pm 2 standard deviations, and the relative standard deviation (RSD) for each standard. Standard analyses at the University of Antofagasta indicate an acceptable accuracy. There is one failure for Li and K analysis, and 2 failures for Mg analysis of the Standard SRM-1, and there is no failure for Li analysis and one

failure for K and Mg analysis of Standard SRM-2. Overall these failures are not significant. Table 11-6 shows the relative standard deviation values (measure of precision) for the University of Antofagasta analyses range from 1.3 to 2.4, indicating very good analytical reproducibility for the standard analyses conducted at the primary laboratory. Based on the analysis detailed above, the authors are of the opinion that the lithium, potassium and magnesium analyses are accurate. There is also a good reproducibility or precision in the assay values reported by the University of Antofagasta for these three elements.

Table 11-6 Standards analysis results from U. Antofagasta (2016-2018)

Statistics	Li (mg/l)	
Standard	SRM-1	SRM-2
Count	16	15
Min	476	1,040
Max	500	1,087
Mean	486	1,059
Standard Deviation	7	15
Mean \pm 2 Standard Deviation		
Mean + 2SD	499	1,090
Mean - 2SD	473	1,029
No of Failures >2SD	1	0
Relative Standard Deviation		
RSD	1.4	1.4

Statistics	K (mg/l)	
Standard	SRM-1	SRM-2
Count	16	15
Min	6,150	7,760
Max	6,630	8,540
Mean	6,341	7,986
Standard Deviation	123	195
Mean \pm 2 Standard Deviation		
Mean + 2SD	6,588	8,377
Mean - 2SD	6,094	7,596
No of Failures >2SD	1	1
Relative Standard Deviation		
RSD	1.9	2.4

Statistics	Mg (mg/l)	
Standard	SRM-1	SRM-2
Count	16	15
Min	4,415	5,915
Max	4,730	6,250
Mean	4,557	6,052
Standard Deviation	69	81
Mean \pm 2 Standard Deviation		
Mean + 2SD	4694	6214
Mean - 2SD	4420	5890
No of Failures >2SD	2	1
Relative Standard Deviation		
RSD	1.5	1.3

Check Analyses

Checks analyses were conducted at Alex Stewart located in Mendoza, Argentina. A total of 28 samples were submitted. In addition, some blanks and standard control samples were inserted to monitor accuracy and potential laboratory bias. The total number of samples in the batch was 35. The standards indicated acceptable accuracy and precision for Li and K.

Statistical analysis of the 28 pairs of check sample assay values was conducted using Reduction-to-Major-Axis ("RMA") multiple linear regressions for Li, K and Mg. StatGraphics software was used for this analysis. The results are summarized in Table 11-7.

In general, there is an acceptable correlation between the main samples and the external duplicates, with R2 ranging from 0.919 to 0.955.

The bias is below 5 % with the highest bias (0.55 %) for lithium, lower bias (-3.79 and -3.23) for potassium and magnesium, indicating that the UoA obtained a little higher assay values for lithium and a little lower for potassium and magnesium, as shown in Table 11-7.

Precision of the external duplicate analyses is acceptable for Li, K and Mg. Eighty-three per cent of the Li assays are within ± 15 % of one another.

Table 11-7 Check assays between the University of Antofagasta and Alex Stewart

Statistics	UA Li	ASA Li	UA K	ASA K	UA Mg	ASA Mg
	(mg/l)	(mg/l)	(mg/l)	(mg/l)	(mg/l)	(mg/l)
Count	28	28	28	28	28	28
Min	660	566	4,52	4,446	3,88	3,456
Max	1,626	1,517	12,62	12,833	11	10,675
Mean	1,015	931	7,744	7,642	6,308	6,064
Std Dev	248	246	1,982	2,053	1,702	1,755
Precision		9.43		5.83		5.94
% Bias		0.55		-3.79		-3.23
Correlation		0.955		0.919		0.955
%<10%		63		77		80
%<15%		83		83		90

Based on the analysis detailed above, the authors are of the opinion that the check assays indicate that the lithium and potassium concentrations determined for the primary sample assays are suitable for use in a resource calculation.

Sample Duplicate Analyses

Thirty-two (32) duplicate samples were collected in the field to confirm the overall sampling precision and shipped also to the University of Antofagasta laboratory. Table 11-8 lists the statistics, as well as the calculated precision, bias, correlation and percent of duplicate analyses with results within 5 % of one another. The bias and correlation were calculated through RMA plots, constructed with StatGraphics software. The duplicate analysis repeated exceedingly well.

Table 11-8 Duplicate analyses from the University of Antofagasta

Statistics	Li	Duplicate Li	K	Duplicate K	Mg	Duplicate Mg
	(mg/l)	(mg/l)	(mg/l)	(mg/l)	(mg/l)	(mg/l)
Count	32	32	32	32	32	32
Min	523	516	2,94	2,94	3,215	3,3
Max	3,375	3,342	20,64	20,02	21,8	21,76
Mean	1,123	1,121	8,079	8,101	7,074	7,101
Std Dev	511	511	3,22	3,12	3,37	3,351
Precision		1.79		1.96		1.47
% Bias		0.15		-3.21		-0.58
Correlation		0.997		0.995		0.998
%<5%		93		93		97

Assay results for duplicate samples at the U of Antofagasta indicate excellent precision (within 5 % or less) for Li, K and Mg. Bias between duplicates and main samples are within 3 % and correlation is high ($R^2=0.995$ to 0.998) for the three elements.

Sample Contamination

A field blank consisting of distilled water was inserted into the sample stream 21 times. New plastic bottles were used in all the cases to avoid eventual contamination with brine samples. Results reported by the University of Antofagasta indicate <0.05 mg/l (detection limit for lithium) in all of the blank samples. This indicates no lithium contamination during all the sampling and analysis stages.

11.2.6 ADDITIONAL QA/QC ANALYSIS 2016-2018 PROGRAM

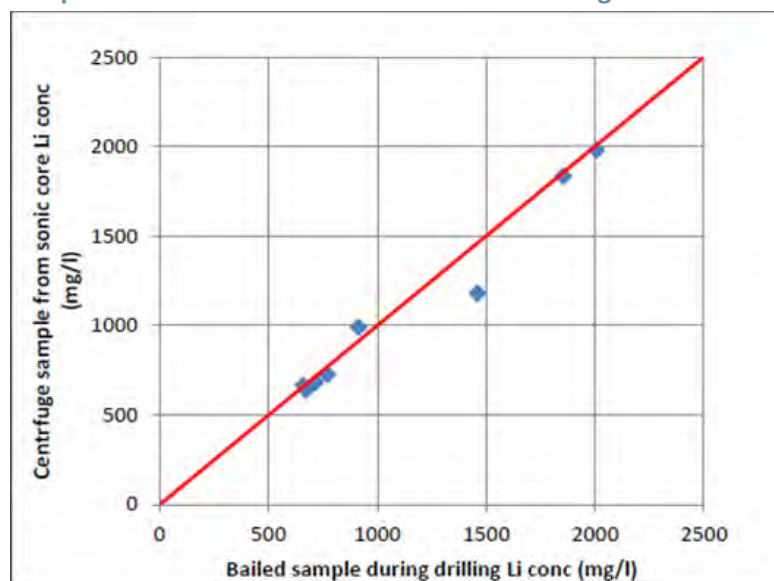
A comparison was carried out between centrifuged brine samples from sonic core and bailed brine samples collected during sonic drilling. Eight sonic cores were centrifuged at 1/3 bar by Corelabs and the released brine was collected and shipped to University of Antofagasta in small sealed glass

containers for Li concentration analysis. Table 11-9 shows the selected core samples (borehole and depth interval) with the analysis of the Li concentration of the centrifuged brine and the Li concentration of the bailed brine sample during the sonic drilling at the same depth interval. Figure 11-5 shows the comparison between the bailed and the centrifuged brine samples. The two methodologies show a good correlation.

Table 11-9 Comparison of lithium concentrations in centrifuge and bailed brine samples

Borehole	Depth (m)	Centrifuge Li (mg/l)	Bailed Li (mg/l)
S-1	5	1,834	1,854
S-1	11	990	913
S-1	19	1,980	2,006
S-2	11	1,180	1,460
S-2	89	664	660
S-2	110	725	770
S-2	134	639	670
S-2	152	681	716

Figure 11-5 Comparison of lithium concentrations in centrifuge and bailed brine samples



11.2.7 ANALYTICAL QUALITY ASSURANCE AND QUALITY CONTROL ("QA/QC") 2021 PROGRAM

Andes Analytical Assay SpA laboratory (AAA) was used as the primary analytical laboratory because the UoA laboratory had limitations on its production capacity due to COVID 19 related restrictions. UoA was therefore used as the secondary/external laboratory for the analysis of check samples

A total of 92 primary brine samples were analysed from the 2021 drilling campaign. These primary analyses were supported by a total 36 QA/QC analyses consisting of:

- 10 standards (7 %),
- 20 duplicates (14 %) and
- 6 blank samples (4 %).

In addition to the evaluation of standards, field duplicates, and blanks, the ionic balance was evaluated for data quality. Balances are generally considered to be acceptable if the difference is < 5 % and were generally < 1 %. The results of standard, duplicate and blank samples analyses are considered to be adequate and appropriate for use in the resource estimation described herein.

11.2.8 ANALYTICAL ACCURACY 2021 PROGRAM

Anion-Cation balance

The performance of the AAA in the analyses of 92 main samples and 10 duplicates show a balance within 2 %, and all the check samples analysed by University of Antofagasta within a value of 2 %.

Certified Analytical Standards

As in previous campaigns two standard reference samples, SRM-1 and SRM-2 were used in the sampling program. Sets of randomized replicates were sent in a Round Robin analysis program to four laboratories to determine the certified values used to monitor the accuracy of analyses. The standard reference samples certified for the elements met the criteria of having a global Relative Standard Deviation (RSD) of near 5 % or less. Overall, the performance of AAA and the external laboratory (UoA) was satisfactory.

The results of the standards analyses for Li, K and Mg, are summarized in Table 11-10. This table lists the statistics, number of samples exceeding the acceptable failure criteria of the mean ± 2 standard deviations, and the relative standard deviation (RSD) for each standard. Standard analyses by AAA

indicate an acceptable accuracy. No failure was observed for Li, K and Mg for both standards (SMR-1 and SMR-2).

Table 11-10 shows the relative standard deviation values (measure of precision) for the AAA analyses range from 8.1 to 14. Based on the analysis detailed above, the authors are of the opinion that the lithium, potassium and magnesium analyses are accurate. There is also a good reproducibility or precision in the assay values reported by the AAA for these three elements.

Table 11-10 Standards analysis results from AAA (2021)

Statistics	Li (mg/l)	
Standard	SRM-1	SRM-2
Count	6	6
Min	424	902
Max	536	1148
Mean	480.8	1031.8
Standard Deviation	41.4	88.7
Mean \pm 2 Standard Deviation		
Mean + 2SD	564	1209
Mean - 2SD	398	854
No of Failures >2SD	0	0
Relative Standard Deviation		
RSD	8.6%	8.6%
Statistics	K (mg/l)	
Standard	SRM-1	SRM-2
Count	6	6
Min	5,217	7,664
Max	7,362	9,118
Mean	6,548	8,177
Standard Deviation	721	606
Mean \pm 2 Standard Deviation		
Mean + 2SD	7,989	9,388
Mean - 2SD	5,106	6,966
No of Failures >2SD	0	0
Relative Standard Deviation		
RSD	11.0%	7.4%
Statistics	Mg (mg/l)	
Standard	SRM-1	SRM-2
Count	6	6
Min	3,835	5,355
Max	5,628	7,359
Mean	4,657	6,183
Standard Deviation	653	810
Mean \pm 2 Standard Deviation		
Mean + 2SD	5,964	7,802
Mean - 2SD	3,350	4,563
No of Failures >2SD	0	0
Relative Standard Deviation		
RSD	14.0%	13.1%

Check Analyses

Check analyses were conducted at UoA. Nine drill samples were analysed in addition to five blank and standard samples to monitor accuracy and potential laboratory bias. The standards indicated acceptable accuracy and precision for Li and K.

Statistical analysis of the 9 pairs of check sample assay values was conducted using linear regressions for Li, K and Mg. The results are summarized in Table 11-11.

Table 11-11 Check assays between AAA and UoA

Statistics	Li	Duplicate Li	K	Duplicate K	Mg	Duplicate Mg
	(mg/l)	(mg/l)	(mg/l)	(mg/l)	(mg/l)	(mg/l)
Count	9	9	9	9	9	9
Min	663	710	4,788	5,315	4,068	4,650
Max	1,325	1,200	10,796	9,875	9,271	8,025
Mean	870	854	6,511	6,530	5,833	5,681
Std Dev	209	145	1,929	1,382	1,653	986
Correlation		0.9807		0.9859		0.9534
%<10%		89		67		44

Based on the analysis detailed above, the authors is of the opinion that the check assays indicate that the lithium and potassium concentrations determined for the primary sample assays are acceptable for use in a resource calculation.

Sample Duplicate Analyses

Ten (10) duplicate (drill) samples were analysed by AAA to confirm the overall sampling precision Table 11-12 shows the statistics of internal duplicates. Precision of the internal duplicates were evaluated through the relative error (ER <5% for internal duplicates). The results of the duplicate analyses show a very good precision.

Table 11-12 Duplicate analyses at AAA laboratory

Statistics	Li	Duplicate Li	K	Duplicate K	Mg	Duplicate Mg
	(mg/l)	(mg/l)	(mg/l)	(mg/l)	(mg/l)	(mg/l)
Count	10	10	10	10	10	10
Min	655	670	4,977	4,951	4,294	4,202
Max	1,022	1,012	7,838	7,824	7,742	7,710
Mean	858	848	6,211	6,187	5,733	5,674
Std Dev	127	120	1085	1,107	1,152	1,155
Correlation		0.9904		0.9933		0.9966
%<5%		100		100		100

Sample Contamination

A field blank consisting of distilled water was inserted into the sample stream 7 times. New plastic bottles were used in all the cases to avoid eventual contamination with brine samples. Results reported by AAA indicate Li concentrations of <5 mg/l (quantification limit for lithium) in four of the blank samples. Three samples showed values over the quantification limit (a maximum of 19 mg/l) within the acceptable limit of 5 times. This suggests that there was no lithium contamination during the sampling and laboratory analysis stages.

11.3 DRAINABLE POROSITY ANALYSIS AND QUALITY CONTROL RESULTS

11.3.1 DBSA 2011

Daniel B. Stevens & Associates Inc. in Albuquerque, New Mexico (DBSA) was selected as the primary laboratory for determination of drainable porosity (or specific yield) on the 2011 sonic core samples from boreholes C-1 through C-6. DBSA also undertook analysis of particle size, density and other physical properties of the core samples. DBSA received a total of 285 core samples which had been initially prepared by Li3 staff at the field camp on the Salar. All samples were prepared and shipped to DBSA as detailed in section 11.1 of this report. On receipt of samples at DBSA, the samples were treated in one of three ways in preparation for determination of Relative Brine Release Capacity. These were:

- The entire intact sample was used,

- An intact sub-sample was obtained by cutting the original sample acetate sleeve with a chop saw,
- An intact sub-sample was obtained by pushing a smaller diameter testing ring into the original sample.

All but six samples received were subject to RBRC testing. The six samples not used for RBRC testing were considered to be too brittle or crumbly to obtain an appropriate sub-sample. Thirty-four (34) verification tests (duplicates) were also performed, for a total of 313 RBRC tests. After completion of RBRC tests, 30 samples were selected for particle size analysis.

Relative Brine Release Capacity Test

The Relative Brine Release Capacity test predicts the volume of solution that can be extracted from an unstressed geologic sample which is equivalent to drainable porosity. The test method is briefly described below:

Undisturbed samples from the site are saturated in the laboratory using site specific brine solution. The bottom of the samples is then attached to a vacuum pump using tubing and permeable end caps and are subjected to a suction of 0.2 to 0.3 bars for 18 to 24 hours. The top end cap is fitted with a one-gallon air bladder which allows enough drainage while inhibiting continuous atmospheric air flow. The vacuum system permits testing multiple samples simultaneously in parallel. The samples are then oven dried at 60 °C.

Based on the density of the brine, the sample mass at saturation, and the sample mass at 'vacuum dry', the volumetric moisture (brine) contents of the samples are calculated. The difference between the volumetric moisture (brine) content of the saturated sample and the volumetric moisture (brine) content of the 'vacuum dry' sample is the "relative brine release capacity".

This methodology has been widely accepted by companies involved in the lithium brine exploration activities and is regarded as being a suitable method for determination of Specific Yield (Houston, 2011).

DBSA also undertook several verification tests related to RBRC testing. These included the following:

- "Remolded" samples in cases where there was insufficient intact original material for secondary testing. Samples were prepared for testing by remolding the material to target the initial density after the initial testing was performed.

- Samples designated as 'Sub-sample #2' were prepared for testing by obtaining a separate intact sub-sample from the original core.
- Samples designated as 'Day 1' and 'Day 2' are the same sub-sample, only the time the sample was subjected to vacuum suction was varied (18-24 hours and 36-28 hours, respectively).

Particle Size Analysis

After RBRC testing, thirty (30) of the samples were chosen to be used for particle size analysis (PSA). The samples were chosen with the intent to represent each of the material types present in the sample batch. Several of the sample results indicate discontinuity between the physical particle size analysis and the hydrometer analysis due to high clay and/or salt content.

DBSA employed the following standard test methods for determination of other physical properties of the samples:

- Dry Bulk Density: ASTM D7263
- Moisture Content: ASTM D7263
- Calculated Porosity: ASTM D7263
- Particle Size Analysis: ASTM D422
- USDA Classification: ASTM D422, USDA Soil Textural Triangle

DBSA relied upon the brine solution density (1.20) provided by Li3 in calculating the volumetric moisture (brine) content. Particle densities of the samples were calculated based on the assumption that the samples were 100% saturated after the saturation stage of the test procedure. The calculated particle density was then used to calculate the total porosity of each of the samples. Volume measurements for each sample were obtained at the “as received”, “saturated”, and “vacuum dry” conditions. It is noted that due to irregularities on the sample surfaces, volume measurements should be considered as estimates.

A total of 20 samples tested were noted to have questionable integrity (QI) relative to the in-situ conditions described by Li3. For sands, silts, and clays a ‘questionable integrity’ designation indicates that the sample may, or may not, accurately represent in-situ conditions (material appeared loose initially) relative to presumed in-situ conditions. For halite cores a ‘questionable integrity’ designation indicates that the sample core had grooves, pits, or other void spaces that may, or may not, be a result of the sampling technique employed. For halite cores a ‘questionable integrity’ may indicate that some dissolution has occurred during testing.

RBRC test results

Drainable porosity is largely dependent on lithology which is highly variable as observed from the drilling results. Figure 11-6 shows a plot of total porosity vs drainable porosity based on the results of the DBSA analyses. Therefore, based on visual inspection and particle size analyses the samples were grouped in three types as follows: 1) a halite mix, 2) a silt-clay mix and 3) a sand mix. **Table 11-13** shows the results of the laboratory drainable porosity analyses.

Figure 11-6 DBSA laboratory specific yield (Sy) analyses against total porosity

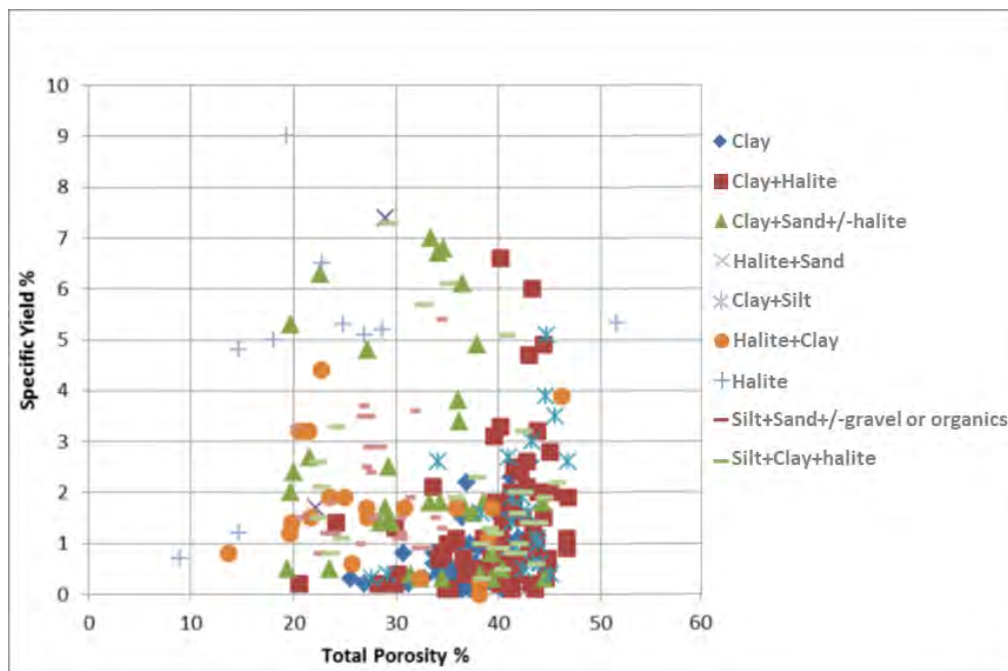


Table 11-13 Results of laboratory specific yield (Sy) analyses

	Sy - Halite mix	Sy - Silt-clay mix	Sy - Sand mix
Number of samples	56	195	29
Max	0.203	0.066	0.310
Min	0.002	0.001	0.015
Mean	0.034	0.012	0.061
Standard Deviation	0.038	0.011	0.058

British Geological Survey QA/QC tests 2011

Thirty (30) sonic core samples were shipped to the British Geological Survey (BGS) for determination of porosity and specific yield as a check against the DBSA results. The samples were duplicates of samples shipped to DBSA for RBRC testing. Samples were initially centrifuged to release pore fluid to determine Sy in "as received conditions". The chemistry of released pore fluid was analysed as a double check against UoA and ASA results and found to be similar. The samples were then re-saturated and allowed to drain (similar to the RBRC test) and then oven dried to obtain total porosity values.

Results of the BGS test work showed significantly higher drainable porosity values than reported by DBSA, as shown in Figure 11-7, however DBSA shows significantly higher total porosity values (Figure 11-10). It is possible that the DBSA testing methodology systematically under-estimates drainable porosity for finer grained sediments (clay and silt).

Figure 11-7 Comparison of BGS and DBSA specific yield (Sy) analyses

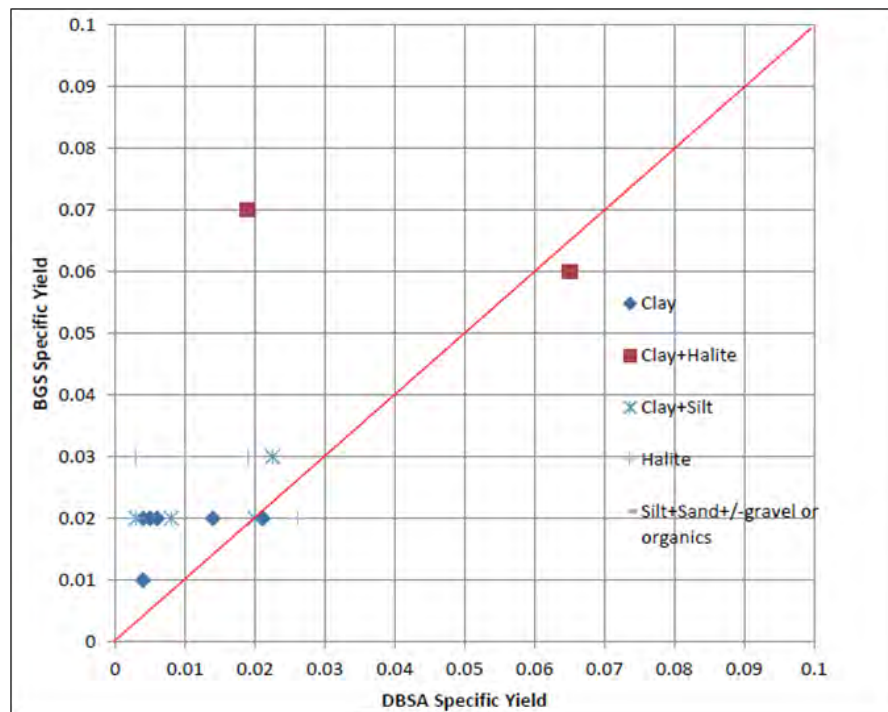
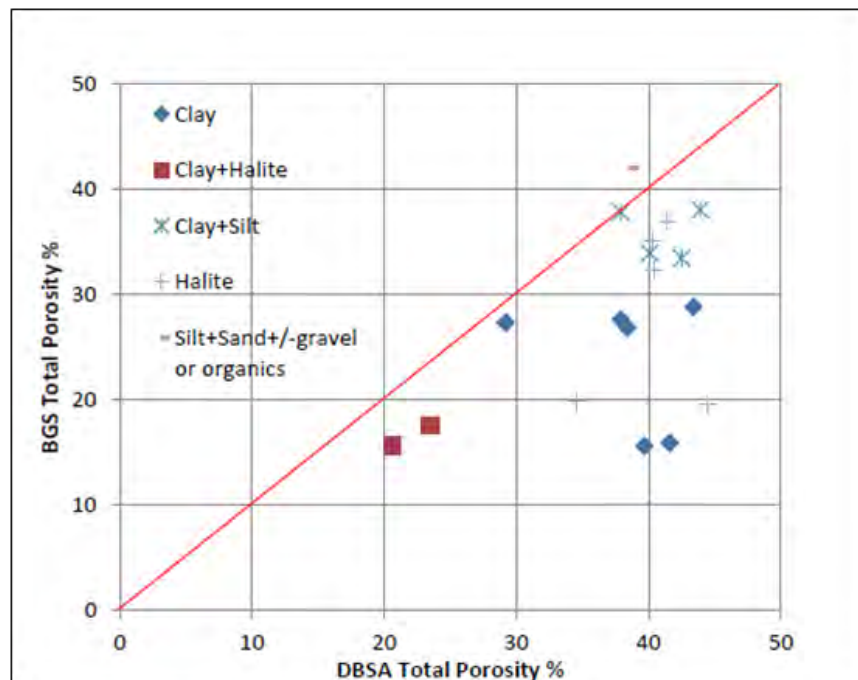


Figure 11-8 Comparison of BGS and DBSA total porosity (Pt) analyses



11.3.2 GSA 2016-2018

The Relative Solution Release Curve (RSRC) method was used by the GSA Laboratory (Tucson, AZ) to determine S_y and P_t . A subset of paired samples was tested using the Centrifuge Moisture Equivalent of Soils (Centrifuge) method by Core Laboratories (Houston, TX). The goals of the test work were to provide S_y and P_t values for each sample and summary statistics of S_y and P_t values by lithological group; to compare the results from the core and tri-cone samples; and to compare the S_y and P_t values for paired sonic core samples derived from the RSRC and Centrifuge methods. Table 11-14 shows an overview of the laboratory test work performed by GSA.

Table 11-14 GSA laboratory tests performed

Test Type	Sample Type and Number	Test Method	Testing Laboratory	Standard
Physical	184 Core samples	Bulk Density	GSA Laboratory, (Tucson, AZ)	ASTM D2937-10
	49 Tri-cone samples			
	29 Tri-cone samples	1-D Consolidation	Pattison Engineering and Geo-Logic Associates, (Tucson, AZ)	ASTM D2435
Hydraulic	28 Core samples	Centrifuge Moisture Equivalent of Soils	Core Laboratories (Houston, TX)	Modified ASTM D425-17
		Estimated Total Porosity	GSA Laboratory (Tucson, AZ)	MOSA Part 4 Ch. 2, 2.3.2.1
	184 Core samples	Estimated Field Water Capacity		MOSA Part 4 Ch. 3, 3.3.3.2
	49 Tri-cone samples			Modified ASTM D6836-02
		Relative Solution Release Capacity (RSRC)		MOSA Part 4 Ch. 3, 3.3.3.5

190 10-cm diameter intact sonic drill intact core samples (core) from boreholes S-1A, S-2, S-18, S-20, S-23, and S24 and 196 unconsolidated tri-cone samples from boreholes S-3A, S-5, S-6, S-11, S-13, and S-19 were received by GSA. The core samples which ranged in length from 10 to 20 cm, were received wrapped in cellophane and bubble-wrap in a re-sealable bag or in a clear, lexan sleeve with end caps duct-taped; the tri-cone rotary samples were in plastic bags.

Table 11-15 lists the lithology of the samples received. For interpretation of RSRC and Centrifuge method results, samples were classified into the following categories: clay-dominated, sand-dominated, gravel-dominated, halite, ulexite, and volcanoclastic material.

Table 11-15 Sample lithology and GSA classification

Lithology Code	Lithology	Number of Sonic Core Samples	Number of Tri-cone Samples	GSA Material Classification
C	Clay	51	1	Clay dominated
C+H	Clay and halite	4		Clay dominated
SC	Sandy clay	5		Clay dominated
S	Sand	4	92	Sand dominated
SS	Silty sand	10	9	Sand dominated
CS	Clayey sand	7	4	Sand dominated
CG	Clayey gravel	7		Gravel dominated
SG	Sandy gravel	15	7	Gravel dominated
H	Halite	8	3	Halite
H+C	Halite and clay	12		Halite
U	Ulexite	5		Ulexite
V	Volcanoclastic	42	80	Volcanoclastic

Sample Preparation

Undisturbed 10 cm diameter by 10 to 20 cm length sonic core samples were prepared to fit into HQ (6.35 cm diameter by 2.5 cm length) stainless steel liners by driving the liners into the in-tact sonic cores using a hydraulic press in order to maintain the core sample bulk density. The soil cores were carefully trimmed to the same height and width as the liners. Care was taken to reduce core handling that could modify the physical structure of the core and effect porosity and drainage measurements. The core samples were prepared using identical procedures for the RSRC and Centrifuge methods, except the samples for the Centrifuge method were prepared in 3.8 cm diameter and 5 cm length stainless steel sleeves. Seventeen core samples appeared to contain a significant amount of material greater than 0.63 cm in diameter. The bulk density of these in-tact cores were measured (ASTM D2937-10) and then the material was re-packed into a 15 cm diameter Tempe cell for RSRC testing.

It was not possible to test six of the S-18 borehole core samples: 2 H, 1 V, and 1 H+C cores from 120 m to 127 m depth and 1 U and 1 C core from 152 m to 155 m depth, because these cores were dominated by solid salt crystals and could not be prepared for testing. Figure 11-9 shows the rejected samples.

Figure 11-9 Rejected core samples



To seal the stainless-steel liner of the HQ samples, a pre-wetted micro-pore membrane (rated 760 mbar air entry) was placed into a bottom PVC cap and top cap was added and the sample was sealed air-tight with gaskets and connectors between both PVC caps.

The HQ core assembly was then saturated with a brine solution prepared to mimic the Maricunga brine solution (specific gravity = 1.2 g/cm³). Saturation was achieved by repetitively applying solution from the bottom of the assembly and then applying vacuum (30 to 50 mbar) from the top of the core to assist the saturation. The core samples for the Centrifuge method were prepared by immersing the core samples into brine solution for 24 hours and allowing the solution to saturate from the bottom. The 15 cm cells and HQ core assemblies packed with tri-cone samples were slowly injected with the brine solution from the bottom of the assembly until the material was saturated. The 15-cm cells and HQ core assemblies packed with tri-cone samples saturated quickly, so no vacuum was needed. Any standing brine solution was carefully removed prior to starting the test.

Relative Solution Release Capacity (RSRC) Sample Testing

HQ core samples and the 15-cm diameter repacked core samples were tested in the GSA laboratory using the RSRC method to measure the amount of brine that may be released under gravity drainage conditions from saturated porous media (i.e. the specific yield, Sy). The RSRC is based on the

moisture retention characteristic method using the Tempe cell design (Modified ASTM D6836-02). Total porosity (Pt) is also measured in the RSRC method.

Each core assembly was transferred to a test rack for the pressure extraction procedure as shown in Figure 11-10. Three pressure steps were applied to each core assembly: the first step was applied without pressure for a day and any free water due to over saturation was removed from this step. Two sequential pressure steps, 120 mbar and 333 mbar (estimated field water capacity, MOSA Part 4 Ch. 3, 3.3.3.2), were used to approximate brine solution release at. The 120 mbar pressure step was maintained for two days and the 333 mbar was continued for another two to four days. Core assemblies were weighed prior to saturation, after saturation, and then two to three times daily to determine loss of brine solution content over time. Samples were oven dried after the final step to determine Pt (MOSA Part 4 Ch. 2, 2.3.2.1). Pt was calculated as:

$$I - (\text{Bulk density} / \text{Particle density})$$

Brine solution release volumes at the 120 mbar and at 333 mbar pressure steps were estimated as the difference of the brine weight divided by the brine specific gravity (1.2 g/cm^3) between the initial cell assembly mass and the mass after each pressure plate step (MOSA Part 4 Ch3, 3.3.3.5). The solution release volume (specific yield) from saturation to 333 mbar can be considered to approximate the maximum solution drainage under gravity/pumping conditions and was calculated as follows:

$$S_y = (w_s - w_{333 \text{ mbar}}) / (A \times L \times B_{sg})$$

Where: w_s is the saturated weight, $w_{333 \text{ mbar}}$ is the weight at 333 mbar, A is sample area, L is sample length, and B_{sg} is the specific gravity of the brine solution.

One hundred and eighty-four (184) core samples were measured for Pt and S_y using the RSRC method.

Figure 11-10 Relative Solution Release Capacity (RSRC) HQ core sample testing



Centrifuge Moisture Equivalent of Soils Sample Testing

The repeatability of S_y and P_t measurements was assessed by testing 28 paired samples using the RSRC method by GSA and the Centrifuge Moisture Equivalent of Soils (Centrifuge) method by Core Laboratories (Houston, TX). GSA packed all of the samples in stainless steel sleeves, saturated them with a brine solution prepared to mimic the Maricunga brine solution, and shipped to Core Laboratories. The sample pairs were of adjacent sections of the same core section and thus reflect similar lithologies as closely as possible, although there is no way of repeating the analysis on exactly the same sample.

Saturated samples were weighed, placed in a low-speed centrifuge for four hours, and then removed from the centrifuge and weighed for a second time. The centrifuge speed was selected to produce suction on the samples equivalent to 330 mbar. Specific yield was calculated as described in Section 11.3.3 Cores were oven dried at a low temperature for five days to determine the residue brine content and bulk density. Particle density was measured using Boyle's Law on oven-dried samples. P_t was calculated as above.

GSA Drainable Porosity Results

In order to assess the relationship between the porosity parameters (P_t and S_y) and lithology, samples were classified into the following categories: clay-dominated, sand-dominated, gravel-dominated, halite, ulexite, and volcanoclastic material as shown in Table 11-16. Histograms and normal distributions for the GSA core data are shown in

Figure 11-13 by category and a summary of the data is given in Table 11-16. Figure 11-14 and Figure 11-15 compare all the P_t and S_y data, respectively, by borehole as measured by GSA and Core Laboratories.

P_t generally increases from gravel-dominated material (lowest porosity) to sand and then clay-dominated material (highest porosity). Volcanoclastic material also had high P_t values, similar to the gravel-dominated material. The halite material had low P_t values, similar to gravel-dominated material, but three halite samples could not be tested because they contained cemented salt crystals. Only five ulexite samples were tested; these also had low porosity (mean = 0.35). Mean values were in good agreement with literature values for these types of sediments (Morris and Johnson, 1967).

In contrast, S_y increased with increasing particle size; therefore, the gravel-dominated material showed the highest S_y values, followed by sand and then clay-dominated material with the lowest S_y values. The volcanoclastic material showed similar S_y values to the gravel-dominated material. The halite samples had intermediate S_y values similar to the sand-dominated material, but not all of the halite samples could be tested because some were cemented and solid, and therefore would have little to no S_y . Ulexite material had lower S_y values than the sand-dominated material.

Mean values for S_y were in good agreement with literature values for these types of sediments (Johnson, 1967). The halite samples showed a relatively wide range of P_t values. There was a relatively wide range of S_y values for the gravel-dominated, volcanoclastic, and halite material. The gravel-dominated material included clayey-gravels, which had lower S_y values than the sandy gravels.

Figure 11-11 GSA specific yield vs GSA total porosity

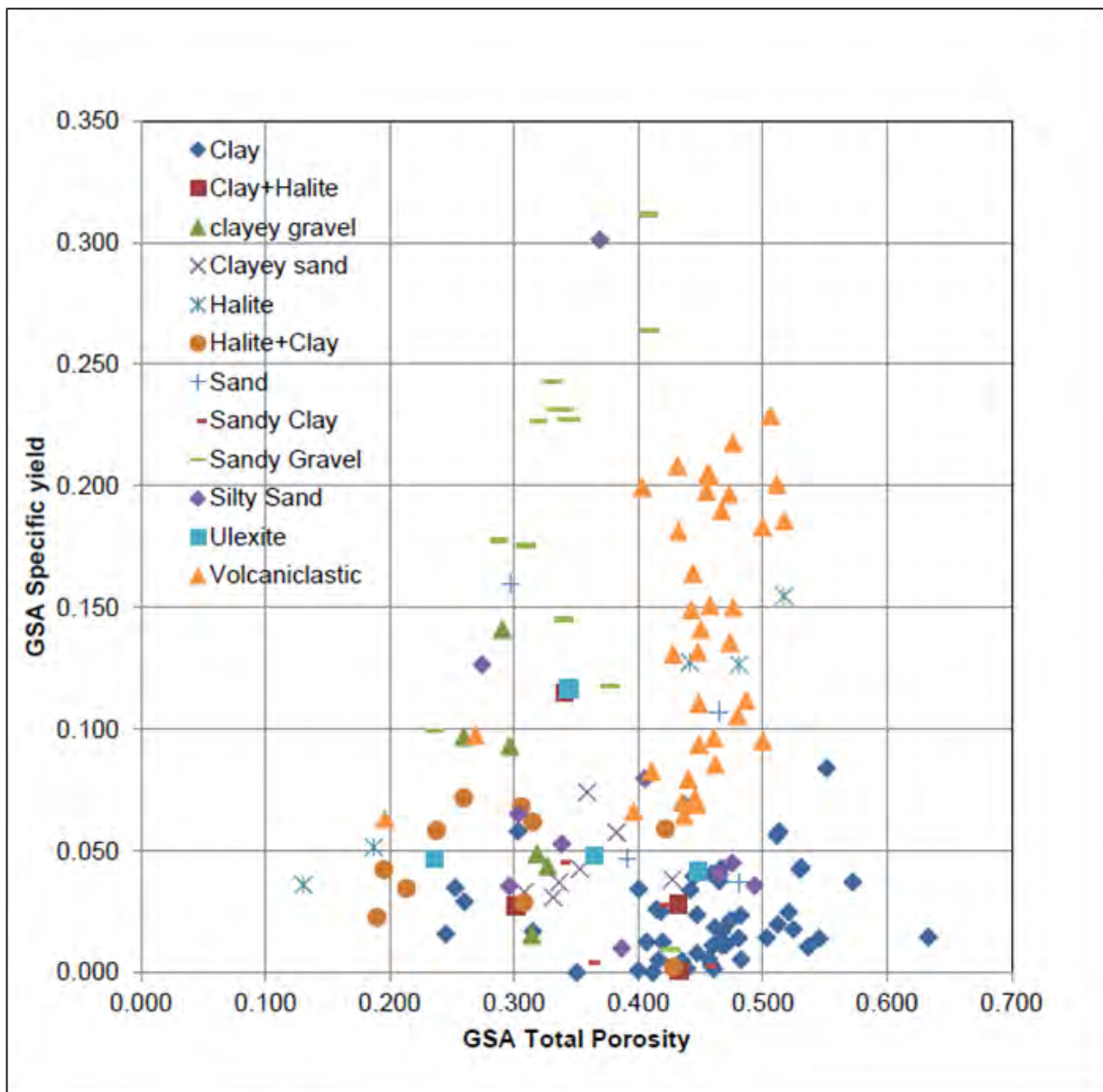


Figure 11-12 Lithologically classified Pt and Sy distributions and statistics

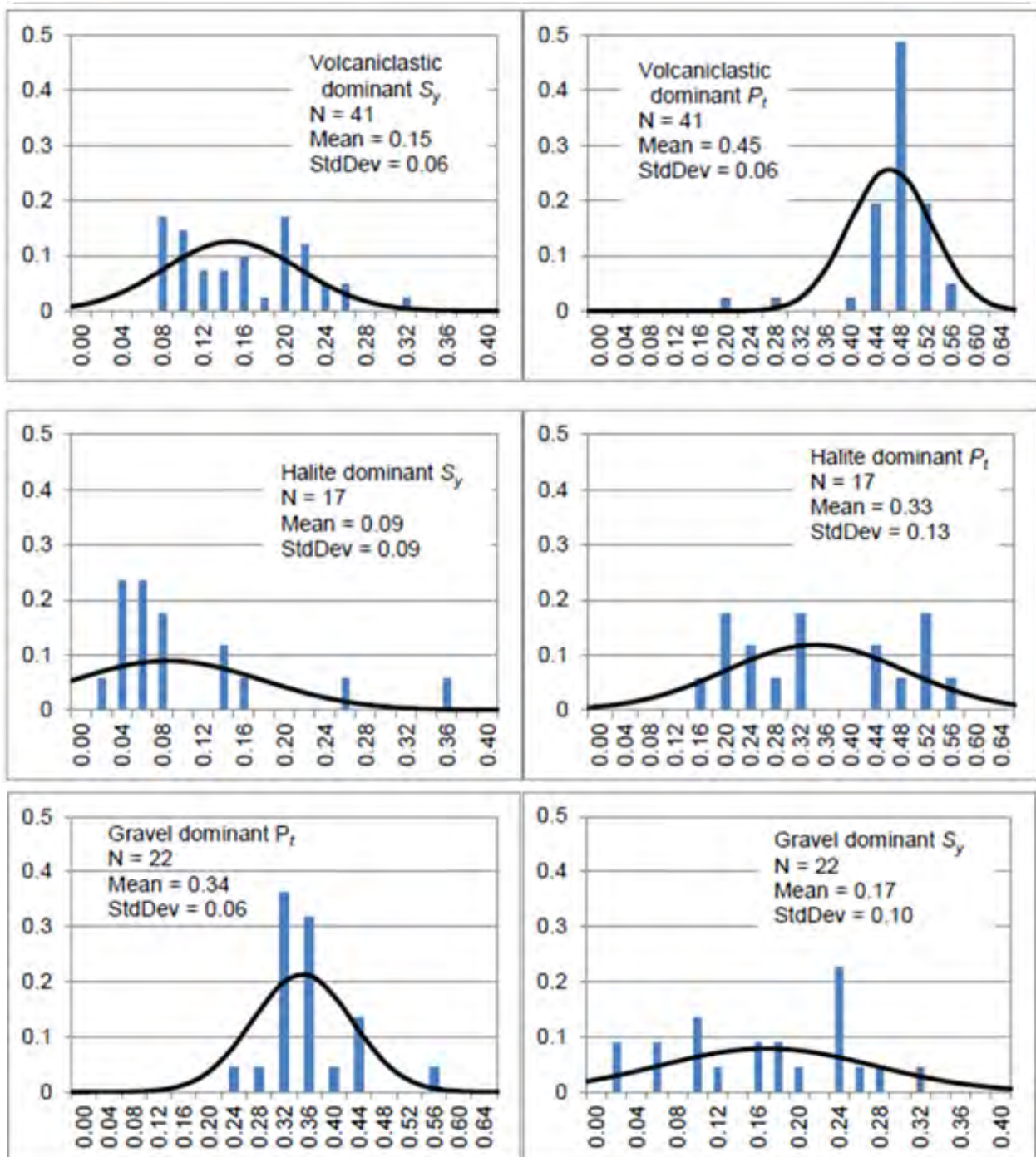


Table 11-16 Summary of total porosity and specific yield by lithological group and laboratory

Lithological Group	Core Lab Total Porosity (Pt)			GSA Total Porosity (Pt)			Core Lab Specific Yield (Sy)		GSA Specific Yield (Sy)	
	N	Mean	StdDev	N	Mean	StdDev	Mean	StdDev	Mean	StdDev
Clay dominated	6	0.53	0.05	59	0.44	0.08	0.02	0.03	0.03	0.04
Sand dominated	3	0.45	0.08	21	0.38	0.07	0.05	0.04	0.07	0.06
Gravel dominated	3	0.32	0.02	22	0.34	0.06	0.10	0.07	0.17	0.10
Volcanoclastic	13	0.46	0.05	41	0.45	0.06	0.13	0.05	0.15	0.06
Halite	2	0.35	0.08	17	0.33	0.13	0.07	0.05	0.09	0.09
Ulexite	1	0.49	N/A	5	0.35	0.09	0.04	N/A	0.05	0.04

Figure 11-13 Comparison of total porosity estimated by GSA using RSRC method and Core laboratory using the Centrifuge method

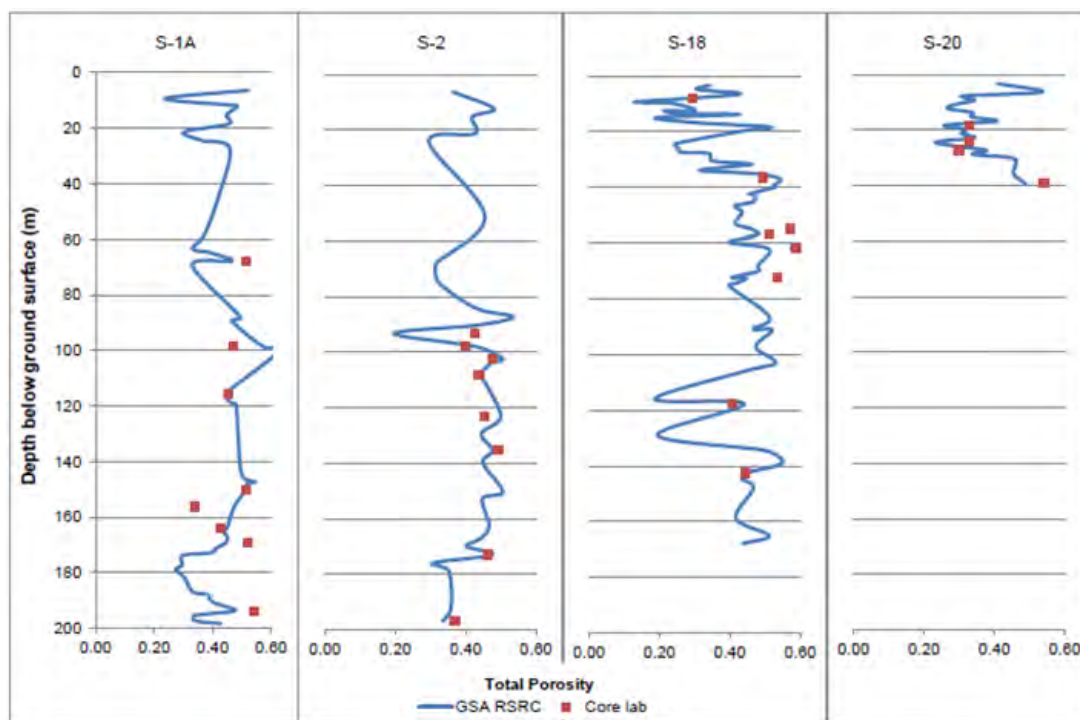
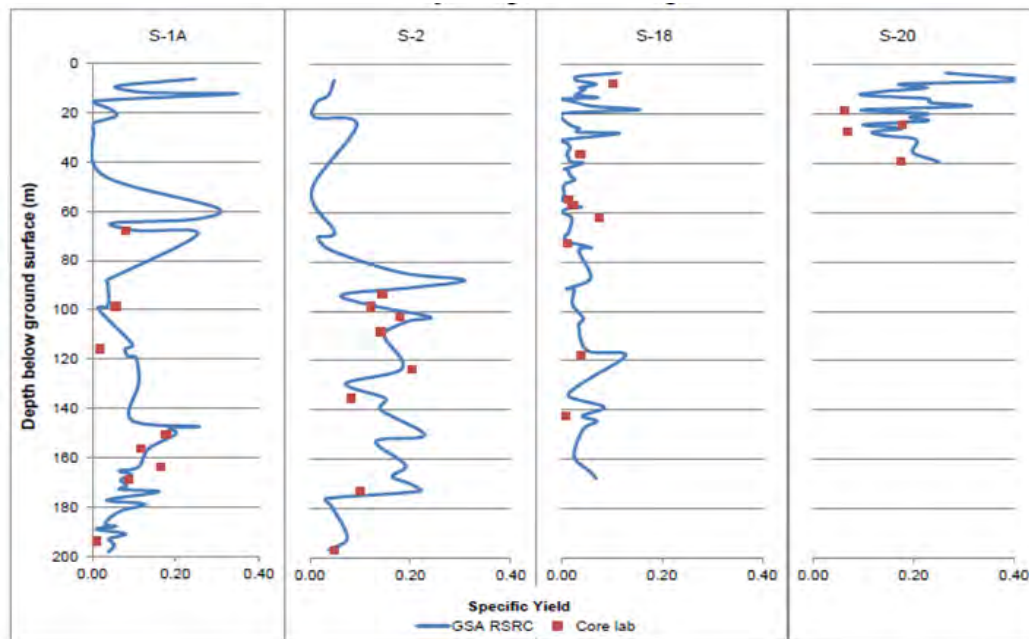


Figure 11-14 Comparison of specific yield estimated by GSA using RSRC method and Core laboratory using the Centrifuge method



11.3.3 QUALITY CONTROL – GSA AND CORE LABORATORY DETERMINATIONS OF SY AND PT

Table 11-17 provides summary statistics and Figure 11-16 compares the measured Sy (drainable porosity) values by lithological category between the laboratories. There is good agreement between the specific yield data ($R^2 = 0.62$); correlation is lower between the total porosity data ($R^2 = 0.39$). The Sy values measured by GSA are in general similar or slightly higher than the Sy measured by Core Laboratories, except for the clay samples, where the results from GSA were slightly lower than the Core Laboratories results. The largest difference in the paired results was for volcanoclastic material.

Table 11-18 provides summary statistics and Figure 11-17 compares the measured total porosity Pt values by lithology between the laboratories. The Pt was frequently higher measured by Core Laboratories compared to GSA.

Table 11-17 Comparison of Sy values between GSA and Corelabs

	Clay Dominated		Sand Dominated		Gravel Dominated		Halite		Ulexite		Volcanoclastic	
	Core	GSA	Core	GSA	Core	GSA	Core	GSA	Core	GSA	Core	GSA
N	7	7	3	3	3	3	1	1	1	1	13	13
Mean	0.03	0.02	0.05	0.06	0.10	0.10	0.10	0.13	0.04	0.04	0.13	0.15
St Dev.	0.02	0.02	0.04	0.04	0.07	0.01	N/A	N/A	N/A	N/A	0.05	0.06
Average Relative Difference %	3%		21%		1%		21%		11%		13%	

Figure 11-15 Comparison of Sy values between GSA and Corelabs

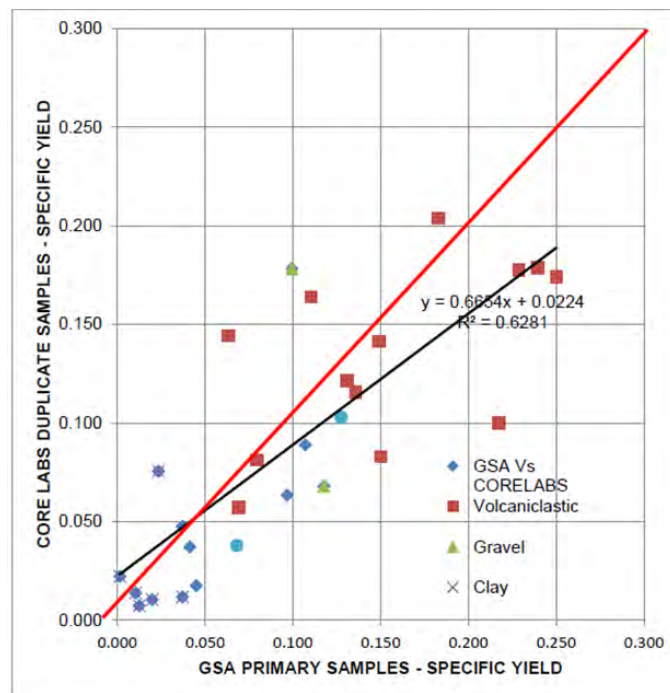
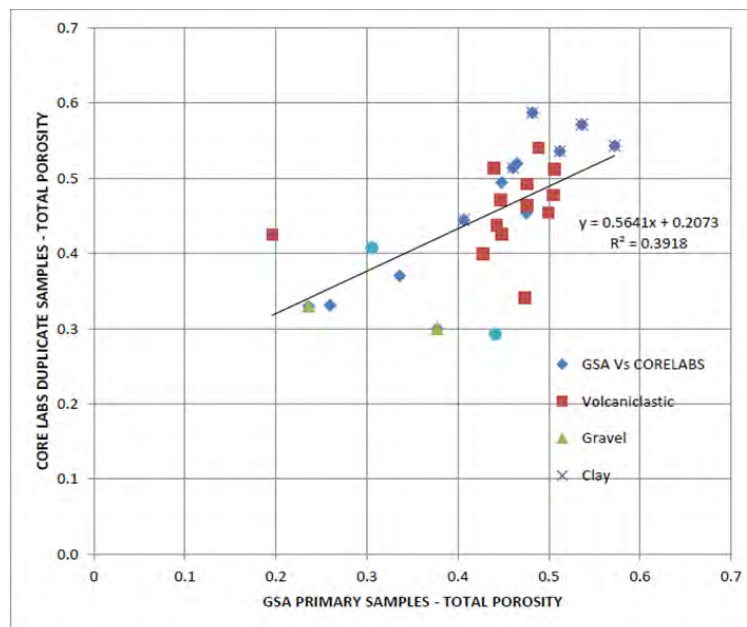


Table 11-18 Comparison of Total Porosity between GSA and Corelabs

	Clay Dominated		Sand Dominated		Gravel Dominated		Halite		Ulexite		Volcanoclastic	
	Core	GSA	Core	GSA	Core	GSA	Core	GSA	Core	GSA	Core	GSA
N	7	7	3	3	3	3	1	1	1	1	13	13
Mean	0.51	0.47	0.45	0.43	0.32	0.29	0.29	0.44	0.49	0.45	0.46	0.45
St. Dev.	0.07	0.09	0.08	0.08	0.02	0.08	N/A	N/A	N/A	N/A	0.05	0.08
Average Relative Difference %	10%		5%		10%		40%		10%		2%	

Figure 11-16 Comparison of Total Porosity between GSA and Corelabs



11.3.4 GSA 2021

GSA Drainable Porosity Results

The GSA Laboratory (Tucson, AZ) performed the Relative Solution Release Curve (RSRC) to determine S_y and P_t , using the same methodology as it had done in the 2016-18 campaign and as described above in Section 11.3.3. On this occasion, a total of 66 HQ core samples were shipped to the GSA laboratory from boreholes S-25 through S29. Table 11-19 summarizes the samples analysed and the results obtained from the 2021 test work. Table 11-20 shows the results of the laboratory test work based on lithology.

Table 11-19 Summary of samples analysed for Porosity and Sy in GSA Laboratory (2021)

Borehole ID	Depth From (m)	Depth To (m)	Porosity (cm ³ /cm ³)	Specific Yield (cm ³ /cm ³)	Borehole ID	Depth From (m)	Depth To (m)	Porosity (cm ³ /cm ³)	Specific Yield (cm ³ /cm ³)
S-25	210.00	210.15	0.416	0.135	S-27	234.30	234.70	0.169	0.043
S-25	247.05	247.20	0.305	0.078	S-27	246.30	246.70	0.312	0.049
S-25	263.60	263.70	0.358	0.287	S-27	258.30	258.70	0.333	0.027
S-25	275.55	275.70	0.371	0.141	S-27	270.30	270.70	0.426	0.252
S-25	288.65	288.80	0.277	0.085	S-27	282.30	282.70	0.490	0.229
S-25	300.65	300.80	0.322	0.078	S-27	294.30	294.70	0.325	0.063
S-25	312.65	312.80	0.352	0.178	S-27	318.30	318.70	0.276	0.048
S-25	324.65	324.80	0.378	0.126	S-27	330.30	330.70	0.311	0.210
S-25	336.65	336.80	0.400	0.143	S-27	342.30	342.70	0.260	0.094
S-25	342.85	343.00	0.314	0.188	S-27	354.30	354.70	0.347	0.225
S-25	348.65	348.80	0.397	0.140	S-27	366.30	366.70	0.159	0.055
S-25	360.65	360.80	0.388	0.165	S-27	378.30	378.70	0.211	0.074
S-25	372.65	372.80	0.386	0.065	S-27	402.30	402.70	0.244	0.116
S-25	396.65	396.80	0.375	0.071	S-28	210.30	210.70	0.444	0.093
S-25	408.65	408.80	0.364	0.054	S-28	222.30	222.70	0.293	0.017
S-26	222.45	222.60	0.359	0.087	S-28	234.30	234.70	0.343	0.057
S-26	234.45	234.60	0.357	0.058	S-28	246.30	246.70	0.423	0.052
S-26	246.50	246.60	0.389	0.094	S-28	258.30	258.70	0.320	0.145
S-26	258.45	258.60	0.354	0.064	S-28	270.30	270.70	0.288	0.183
S-26	270.45	270.60	0.409	0.074	S-28	282.30	282.70	0.342	0.261
S-26	282.45	282.60	0.282	0.174	S-28	294.30	294.70	0.240	0.153
S-26	294.45	294.60	0.284	0.112	S-28	306.30	306.70	0.325	0.181
S-26	306.45	306.60	0.189	0.063	S-28	318.30	318.70	0.360	0.231
S-26	318.45	318.60	0.319	0.192	S-28	330.30	330.70	0.331	0.127
S-26	330.45	330.60	0.338	0.220	S-28	342.30	342.70	0.344	0.123
S-26	354.45	354.60	0.319	0.181	S-28	354.30	354.70	0.335	0.165
S-26	366.45	366.60	0.219	0.189	S-28	366.30	366.70	0.368	0.201
S-26	378.45	378.60	0.293	0.143	S-28	378.30	378.70	0.332	0.057
S-26	390.45	390.60	0.345	0.198	S-28	390.30	390.70	0.229	0.075
S-26	402.45	402.60	0.044	0.006	S-28	402.30	402.70	0.341	0.051
S-27	210.30	210.70	0.408	0.192	S-29	225.20	225.60	0.184	0.051
S-27	222.30	222.70	0.014	0.009	S-29	344.10	344.40	0.021	0.002

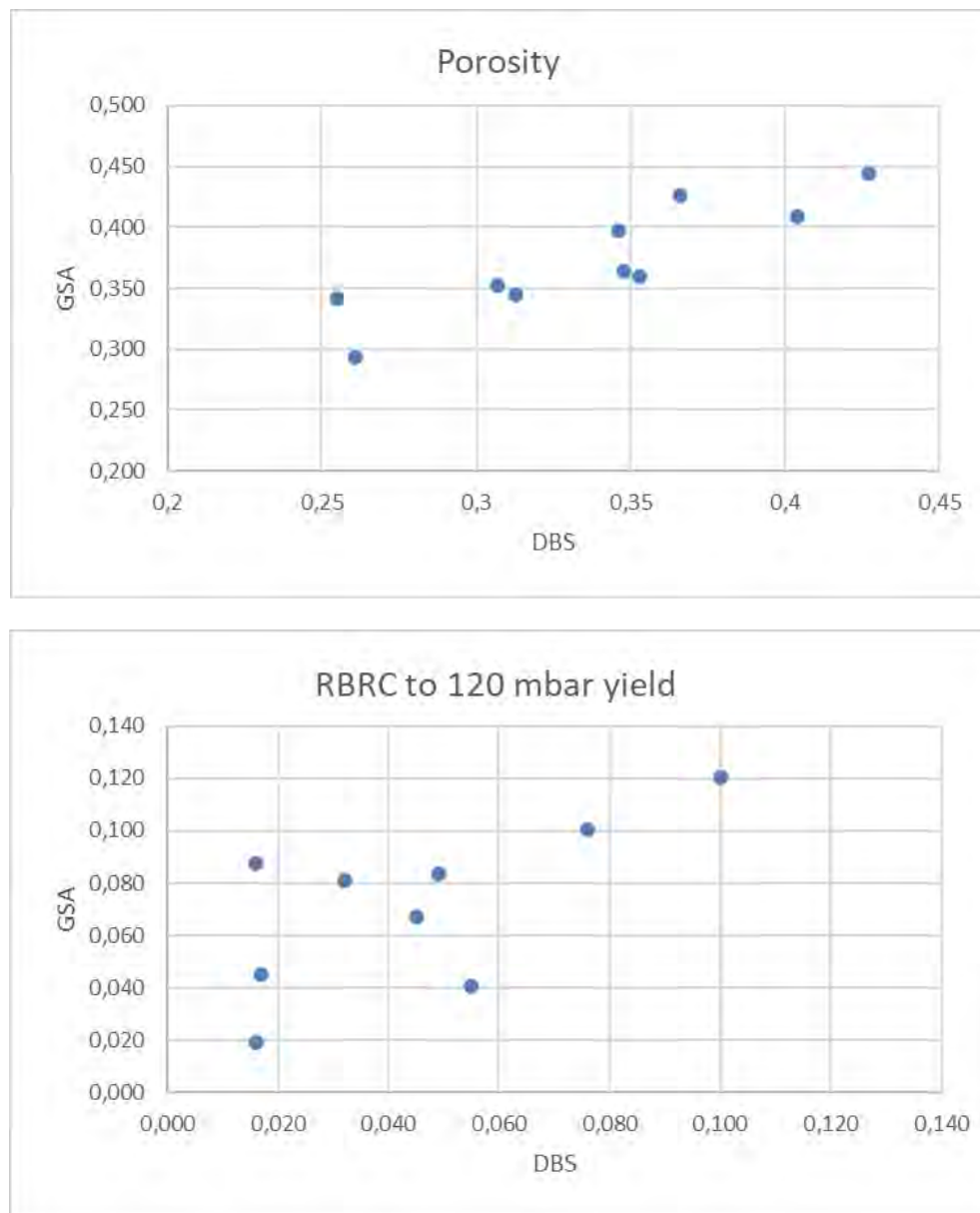
Table 11-20 Summary of GSA drainable porosity analyses by lithology (2021 samples)

Geological Unit	N	Mean	Min	Max	St. Dev.
Lower Sand	3	0.10	0.02	0.19	0.09
Lower Volcanoclastic	51	0.13	0.01	0.29	0.07
Volcanic Breccia	8	0.07	0.05	0.13	0.03
Basement	2	0.03	0.00	0.05	0.03

Quality Control – GSA and DBS Determinations of Sy and Pt

Ten samples were selected from the 2021 GSA batch to perform an inter-laboratory check analysis by Daniel B. Stevens & Associates Inc. (DBSA) using its RBRC methodology. The check analyses included total porosity and RBRC (specific yield). The results of the check analyses show a certain degree of correlation between the analyses of both laboratories. The observed differences can be assumed due to the high vertical geological variability of the sediments or DBSA testing methodology systematically under-estimates drainable porosity for finer grained sediments (clay and silt) as described on section 11.3.1. Figure 11-17 shows the comparison of total porosity Pt and drainable porosity values between the laboratories.

Figure 11-17 Comparison of total and drainable porosities between GSA and DBSA



12. DATA VERIFICATION

The author, Frederik Reidel was involved with the planning, execution, and oversight of the 2011-2021 drilling and testing programs for the Stage One Project in Salar de Maricunga. The author was responsible for developing drilling and sampling methodologies and the implementation of field sampling protocols. The author spent a significant amount of time in the field during all field campaigns overlooking the implementation and execution of drilling, testing, and sampling protocols.

The author was responsible for the oversight and analysis of the QA/QC programs related to brine sampling and laboratory brine chemistry analysis as well as the laboratory porosity analysis. A significant amount of QA/QC protocols were implemented for the brine chemistry and drainable porosity analysis programs that allowed continuous verification of the accuracy and reliability of the results obtained. As described in Section 11 no issues were found with the results of the brine and porosity laboratory analysis. It is the opinion of the author that the information developed and used for the brine resource estimate herein is adequate, accurate and reliable.

13. MINERAL PROCESSING AND METALLURGICAL TESTING

13.1 BACKGROUND – LI3 / MLE 2011 EXPLORATION PROGRAM

In order to study the phase chemistry of the Maricunga brine, the initial step for designing a lithium recovery process, a simulated lab solar evaporation test work was conducted at the University of Antofagasta, northern Chile. Two batch wise evaporation tests at laboratory scale were carried out at a relatively constant temperature of 20 °C. The natural brine was used in the first test and in the second one a treated brine with sodium sulphate, to remove most of the high calcium content that characterizes the Maricunga brine. Both tests provided information on the nature of the crystallized salts along the different stages of an evaporation process, which has been useful for process simulations.

A summary of the experimental procedure and the main results of both tests are presented below.

13.2 EXPERIMENTAL PROCEDURE

A total brine feed of 192.04 kg was used in the first test (natural brine), distributed in four fiberglass glass reinforced plastic pans, each of 75.5 cm diameter and 12.3 cm height. The brine evaporation takes place at a temperature of 20 °C into a thermally insulated chamber (3.5 m long by 1 m wide by 0.8 m high), where a fan with variable speed propels air. Temperature, air speed and relative humidity, are measured through a data acquisition system to monitor the evaporation. This evaporation chamber operates continuously (24 hours) with air having relative humidity of 60 % to 75 %.

The amount of salt deposited in the pans, weighed by a digital scale, was used to define each stage (harvest) of evaporation, as well as determining the cumulative percentage of evaporated water. Samples of the solution and the salts after filtration were collected from every stage for chemical analysis and X-ray diffraction.

When the concentration of the Maricunga brine increases and the brine volume has diminished significantly, the evaporation is continued in another insulated chamber (1.18 m long by 0.70 m wide by 0.46 m high). The concentrated brine has a much lower brine activity (vapor pressure of the brine divided by the vapor pressure of the water), which results in lower evaporation rates.

The second chamber operates continuously with dehumidified air, which circulates through three PVC columns containing silica gel as drying agent. Under these conditions, the air can reach a relative humidity of the order of 40 %. When the silica gel gets saturated, heating in a dryer at 120 °C activates it for re-use.

As per the brine treated previously with anhydrous sodium sulphate (10 % excess was used to precipitate 88.7 % of Ca++), a total of 156.04 kg, distributed in three pans, was fed to the evaporation system. Table 13-1 shows the composition of the natural brine and treated brine used in the evaporation test work.

Table 13-1 Chemical composition (% weight) of brines used in the test work

Brine	Na	K	Li	Ca	Mg	Cl	SO ₄	H ₃ BO ₃	HCO ₃	Density
Natural	7.81	0.676	0.0933	0.743	0.616	16.44	0.059	0.216	0.044	1.21
Treated	8.59	0.547	0.0927	0.102	0.578	16.10	0.440	0.234	0.040	1.21

A general view of the two evaporation chambers is shown in Figure 13-1.

Figure 13-1 General view of evaporation chambers



13.3 RESULTS OF THE EVAPORATION TESTS

The natural brine was concentrated up to 0.925 % lithium and 3.95 % magnesium in twelve stages of evaporation, being a 69.1 % cumulative evaporation. The treated brine was concentrated up to 1.98 % lithium and 6.08 % magnesium in nine stages of evaporation, with a cumulative evaporation of 68 %. Due to the low activity of the concentrated brine, it was necessary to increase the evaporation temperature to 30 °C during the last stages of both tests. Table 13-2 and Table 13-3 show the changes in the chemical composition of the untreated brine as well as the wet salt composition after every harvest (12) of the pans. Table 13-3 also shows a mass balance (crystallized salts, solution and evaporated water) referred to the initial weight of brine for each evaporating stage at 20 °C. The brine has been concentrated until the end of the carnallite field.

Table 13-2 Brine compositions during evaporation of the untreated brine

Brine									Density 20°C kg/l	Activity, 20°C (Vpbrine /Vpwater)
Mg %	Ca %	Na %	K %	Li %	Cl %	SO4%	B %	H2O %		
0.616	0.743	7.810	0.676	0.093	16.440	0.059	0.038	73.525	120.761	0.775
1.080	1.300	6.150	1.220	0.167	16.560	0.062	0.069	73.392	121.768	*
1.280	1.710	5.370	1.490	0.204	17.600	0.040	0.090	72.216	122.526	*
1.790	2.340	4.030	1.990	0.280	18.220	0.040	0.114	71.196	123.663	*
2.500	3.160	1.900	2.620	0.394	20.260	0.010	0.158	68.998	126.965	*
2.650	3.520	1.480	2.430	0.423	20.390	0.010	0.169	68.928	126.902	0.606
2.690	3.580	1.480	2.380	0.431	20.500	0.020	0.171	68.748	127.017	0.618
3.130	4.110	0.868	1.910	0.508	22.220	0.020	0.204	67.030	128.485	0.570
3.389	4.540	0.506	1.500	0.561	22.940	0.037	0.216	66.311	*	*
3.417	5.165	0.366	0.907	0.655	24.040	0.022	0.245	65.183	132.527	0.398
3.263	5.550	0.347	0.873	0.685	24.660	0.005	0.247	64.370	131.376	0.518
3.570	5.670	0.299	0.679	0.709	25.120	0.018	0.257	63.678	132.864	0.404
3.950	7.630	0.086	0.088	0.925	30.670	0.000	0.268	56.383	137.405	0.292

* No measurements

The density and activity of the brine along the concentration process is also indicated. Additionally, the moisture of the crystallized salts after harvesting and filtration of the solution is included in Table 13-3.

Table 13-3 Salts compositions during evaporation of the untreated brine

	Salts kg	Brine kg	Evapor kg	Mg %	Ca %	Na %	K %	Li %	Cl %	SO4 %	B %	H2O %	Mois %
Brine feed		192.04											
Harvest 1	19.91	117.91	54.22	0.069	0.122	36.210	0.082	0.009	57.890	0.136	0.008	5.47	4
Harvest 2	8.85	84.09	26.10	0.135	0.296	35.430	0.282	0.016	56.520	0.360	0.014	6.95	4
Harvest 3	6.04	61.23	16.76	0.182	0.248	35.670	0.312	0.021	56.600	0.170	0.018	6.78	5
Harvest 4	5.05	41.43	14.74	0.220	0.351	34.970	1.815	0.033	57.690	0.250	0.013	4.66	4
Harvest 5	0.74	39.00	1.58	0.080	0.109	37.230	0.128	0.013	58.920	0.380	0.016	3.12	3
Harvest 6	0.12	37.46	1.35	0.378	0.528	20.560	16.940	0.060	50.790	0.110	0.026	10.61	9
Harvest 7	1.29	31.92	4.98	0.426	0.536	17.940	21.440	0.066	50.960	0.150	0.035	8.45	8
Harvest 8	0.78	17.78	2.70	5.556	0.709	6.890	11.830	0.042	40.100	0.092	0.041	34.74	5
Harvest 9	2.68	21.22	4.30	6.410	0.665	6.480	10.590	0.037	40.730	0.058	0.069	34.96	4
Harvest 10	0.24	6.21	1.39	7.425	0.779	2.370	10.670	0.089	37.770	0.034	0.054	40.81	8
Harvest 11	0.97	16.64	3.16	5.660	3.090	2.580	7.010	0.263	33.040	0.129	0.919	47.31	3
Harvest 12	1.64	12.27	2.72	6.670	3.920	1.730	5.060	0.362	36.420	0.001	0.173	45.66	14

Table 13-4 shows the main estimated crystallized salts in each harvest according to mineralization calculated by chemical assay and X-ray diffraction analysis.

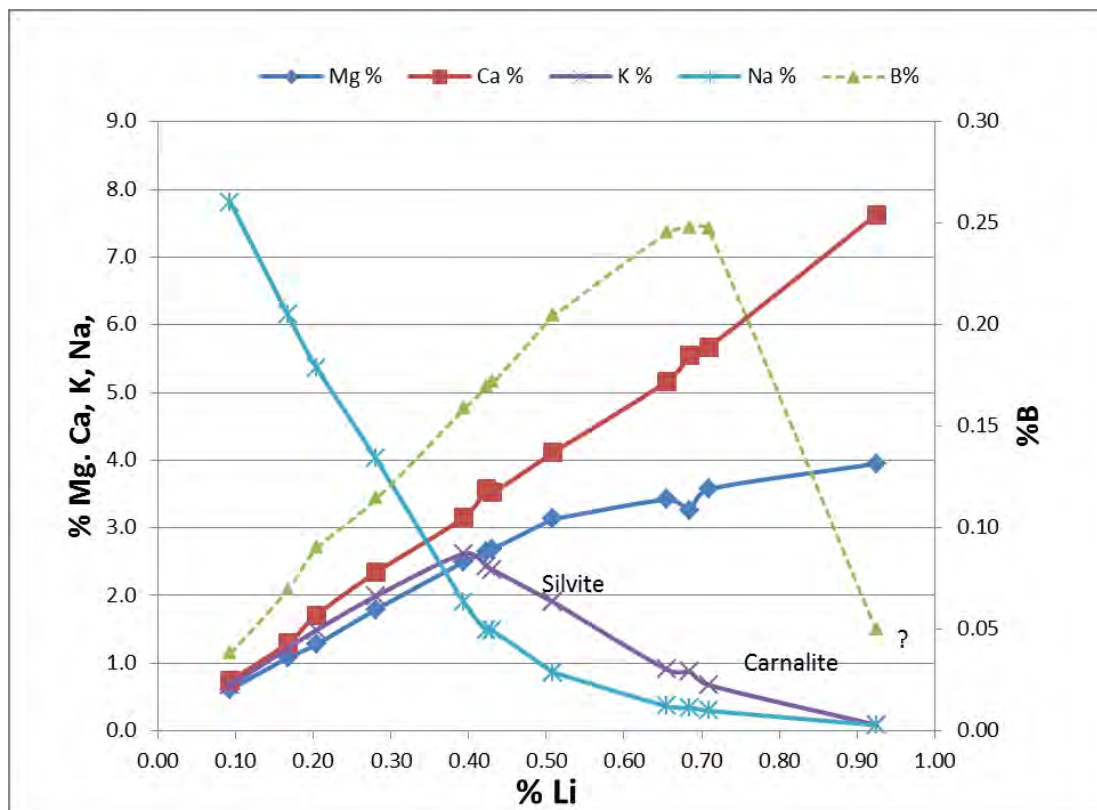
Table 13-4 Crystalized Salts in the harvest

	NaCl	KCl	CaSO ₄ .2H ₂ O and/ or Na ₂ Ca(SO ₄) ₂	KCl*MgCl ₂ *H ₂ O	CaCl ₂ *2MgCl ₂ *12H ₂ O	CaB ₆ O ₁₀ *6H ₂ O
Harvest 1	1		1			
Harvest 2	1		1			
Harvest 3	1		1			
Harvest 4	1		1			
Harvest 5	1	1	1			
Harvest 6	1		1			
Harvest 7	1	1	1			
Harvest 8	1		1			
Harvest 9	1	1	1			
Harvest 10	1		1	1		
Harvest 11	1		1	1	1	
Harvest 12	1		1	1	1	1

According to the salt composition, harvests 11 and 12 should have tachyhydrite; however, analysing the brine evaporation curves of the ions presented by K/Li and Ca/Mg pairs, it is expected that this salt has not yet been crystallized, and the author suspects that the calcium and lithium are still entrained in the brine within the harvested salts.

Figure 13-3 illustrates the complete evaporation curve for the untreated brine.

Figure 13-2 Evaporation curves plotted versus % Li in the brine



The results of the brine evaporation, after treatment with sodium sulphate to remove most of the calcium, are presented in Table 13-5 and Table 13-6.

Table 13-5 Brine composition during evaporation of the treated brine

Brine									Density 20 °C Kg/l	Activity 20 °C (Vpbr /Vpwater)
Mg	Ca	Na	K	Li	Cl	SO ₄	B	H ₂ O		
%	%	%	%	%	%	%	%	%	%	
0.578	0.102	8.590	0.547	0.093	16.100	0.440	0.041	73.509	1.20787	*
0.984	0.108	7.910	1.110	0.154	16.590	0.510	0.062	72.572	1.21019	*
1.240	0.127	7.160	1.404	0.199	16.910	0.600	0.079	72.281	1.2273	0.664
1.540	0.077	6.270	1.800	0.261	16.980	0.650	0.101	72.321	1.21899	0.706
1.920	0.088	5.140	2.250	0.325	17.230	0.730	0.129	72.188	1.22507	0.693
2.600	0.141	3.910	3.000	0.428	18.130	0.860	0.168	70.763	1.23517	0.535
3.130	0.030	2.730	3.007	0.514	18.510	1.000	0.178	70.901	1.23518	0.443
4.705	0.013	1.050	2.007	0.764	20.620	1.380	0.305	69.156	*	*
6.771	0.016	0.160	0.133	1.130	25.960	0.466	0.571	64.793	1.31812	0.248
6.080	0.012	0.093	0.062	1.980	28.080	0.084	0.721	62.888	1.32492	*

Table 13-6 Wet salt compositions during evaporation of the treated brine

	Salts kg	Brine kg	Evap kg	Mg %	Ca %	Na %	K %	Li %	Cl %	SO ₄ %	B %	H ₂ O %	Moist %
Brine feed		156.24											
Harvest 1	16.87	95.42	43.90	0.070	0.592	36.410	0.088	0.010	57.630	0.740	0.006	4.454	3
Harvest 2	6.27	70.38	18.60	0.139	0.290	35.020	0.171	0.021	55.670	0.770	0.012	7.907	8
Harvest 3	3.92	47.28	19.10	0.128	0.241	36.510	0.160	0.020	56.730	0.730	0.016	5.465	5
Harvest 4	2.94	30.84	6.40	0.791	1.052	20.540	13.51	0.127	49.740	0.620	0.066	13.55	2
Harvest 5	1.43	23.39	6.00	0.141	0.318	37.120	11.55	0.022	59.230	0.990	0.019	1.943	1
Harvest 6	2.34	15.24	5.80	0.259	0.338	30.180	7.820	0.020	56.000	0.950	0.027	4.406	2
Harvest 7	2.10	4.15	1.80	5.556	0.709	6.890	11.83	0.042	40.100	0.092	0.041	34.74	3
Harvest 8	0.56	6.36	4.00	6.004	0.088	2.830	8.430	1.840	31.670	0.217	0.085	37.50	3
Harvest 9	2.51	2.56	1.29	9.910	0.009	0.247	0.230	0.599	32.380	0.836	0.605	55.18	12

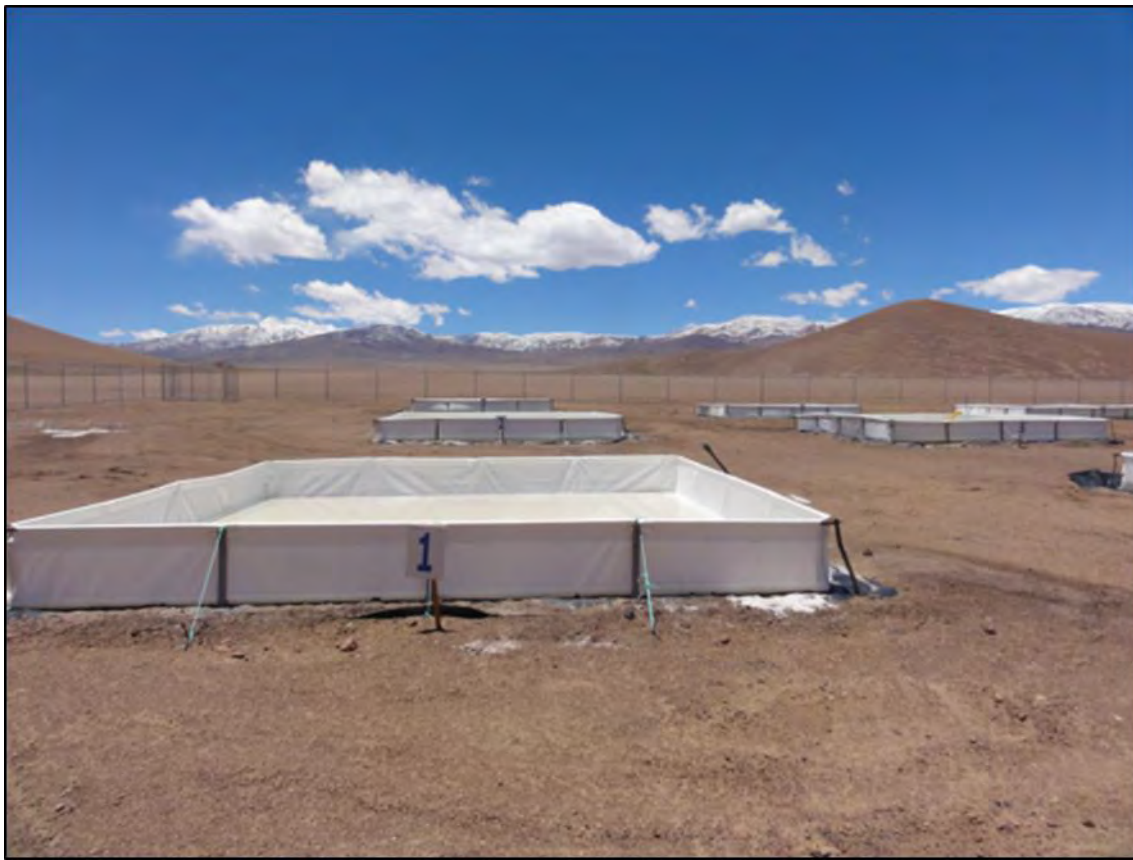
13.4 POSCO PROCESS TESTS – 2012/13

Pilot plant evaluation of the POSCO direct extraction process was undertaken in late 2012 – early 2013. The POSCO process is a proprietary process for direct extraction and recovery of lithium from brine. Details of the process were not made available to MSB. The test work used brine recovered from trenches on the Litio 1-6 claims, with the brine being processed in a pilot plant established at Copiapó. POSCO reported the process test work was successful but did not provide details of the results to MSB. Subsequent to 2013, POSCO decided not to pursue further evaluation of the use of the process at Maricunga. The reasons for the POSCO decision are unknown.

13.5 2016 AND 2018 EVAPORATION POND TESTS

A series of evaporation pond tests were initiated by MSB in late 2016 using brine from Well P1. During the Q4/16 a total of ten trial evaporation ponds were constructed in series in order to measure the precipitation of salts, the evolution of brine, and evaporation rates over a minimum one-year period to determine the optimal processing methodology and process flow sheet for the extraction of lithium, potassium, and other by-products. The evaporation pond test site is illustrated below.

Figure 13-3 MSB evaporation ponds



The average grade of the brine fed from the pump well to the first of the evaporation test ponds was 1,260 mg/l lithium and over an initial 9-month period, the brine concentration increased seven-fold to 8,600 mg/l lithium on a continuous basis and up sixteen-fold to 20,460 mg/l on a batch basis. In addition, sodium chloride (NaCl), potassium chloride (KCl) and carnallite ($\text{KCl} \cdot \text{MgCl}_2 \cdot 6\text{H}_2\text{O}$) as well as a small fraction of calcium chloride hexahydrate ($\text{CaCl}_2 \cdot 6\text{H}_2\text{O}$) crystallized as by-products. In all ponds very small amounts of gypsum ($\text{CaSO}_4 \cdot 2\text{H}_2\text{O}$) are identified. The behaviour of the ions in the brine is given in Figure 13-5. and confirms the test work at the University of Antofagasta in 2011. The potassium solubility is lower as the ponds at 4000 m operate at a significantly lower temperature than the test work done at Antofagasta, which was carried out at 20°C. At higher lithium concentrations boron becomes saturated, most likely as calcium borates, and slowly the values are reduced or maintained constant. Strontium is crystallized as a salt and very strongly reduces its solubility at higher lithium concentration.

Figure 13-4 MSB harvesting of salts



Sampling and assay procedures for the pond evaporation tests incorporated the following:

- Collection of brine samples on a periodic basis to measure brine properties such as chemical analysis, density, brine activity, etc. Samples were assayed at the University of Antofagasta using the same methods and QA/QC procedures as for brine samples collected from drill holes and from pumping tests.
- Collection of precipitated salts from the ponds for chemical analysis to evaluate the evaporation pathways, brine evolution as well as physical and chemical properties of the salts.

Figure 13-5 Evaporation curves plotted versus % Li of pilot ponds compared with test work realized in University of Antofagasta 2011 (UA)

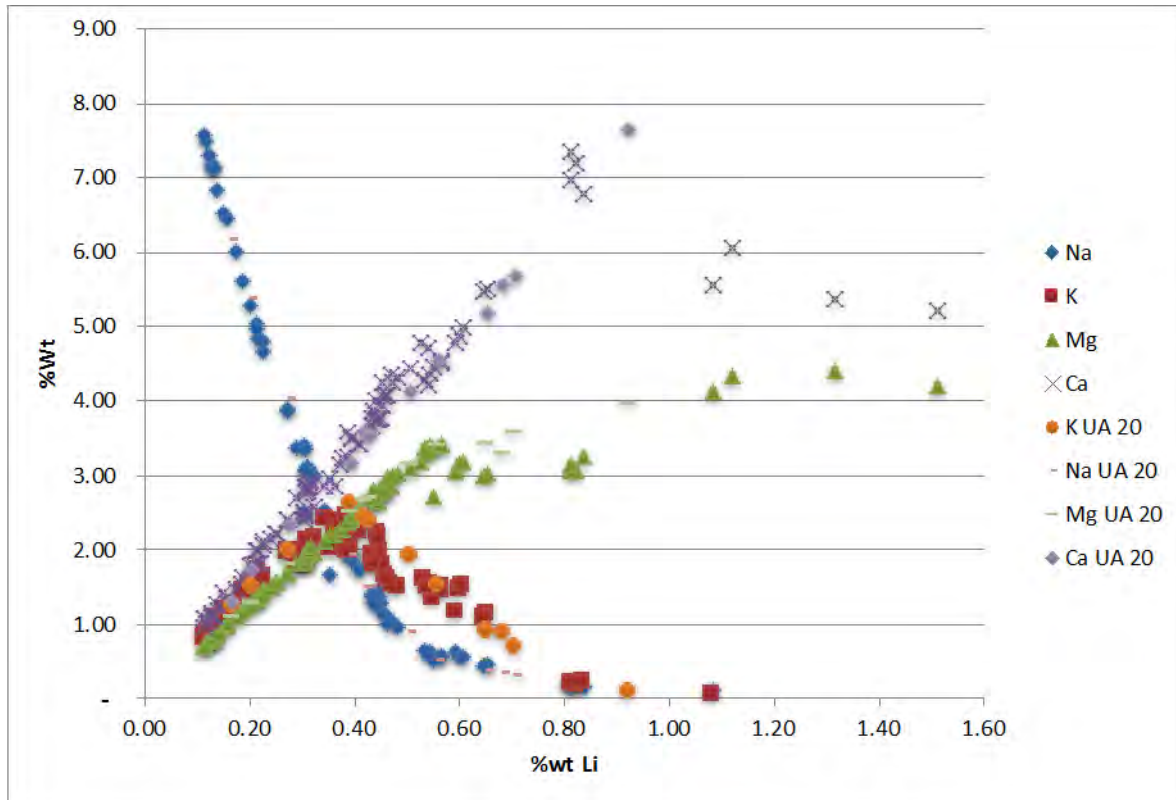
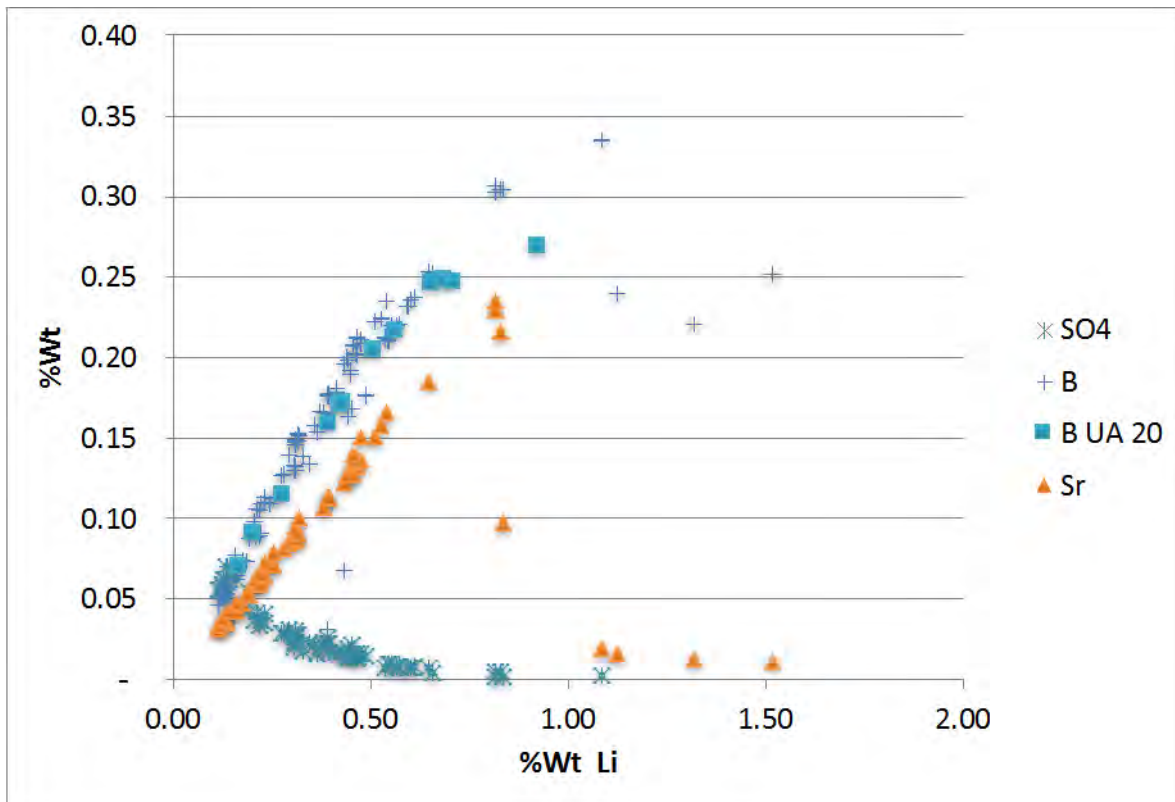


Figure 13-6 Evaporation curves plotted versus % Li of pilot ponds compared with testwork realized at University of Antofagasta 2011 (UA)



13.6 2017 AND 2018 SALT REMOVAL AND LITHIUM CARBONATE TESTS

The concentrated brine that was produced in the pilot ponds was tested at the University of Antofagasta through processes of evaporation and crystallization, which allows the concentration of the lithium contained in the brine, and at the same time enables the elimination of impurities from the brine in the form of tachyhydrite and calcium chloride.

In the Janecke diagram below (Figure 13-7) some of the test results are represented and it can be observed how lithium is concentrated by evaporation and cooling as it moves in the direction that represents the lithium chloride concentration. Lithium can be concentrated with values above 4.5% Li, with Ca lower than 3% and Mg lower than 1.5%.

Based on this concept, for detailed process design and equipment specification, the concentrated lithium brine was tested by the technology provider GEA to concentrate the brine up to slightly above 4% lithium and subsequently remove boron using solvent extraction, followed by calcium and

magnesium removal by precipitation as calcium carbonate and magnesium hydroxide respectively. Then from the purified lithium brine, lithium carbonate solids are precipitated by the addition of soda ash.

Further optimization testing was done by GEA with brine produced from the pilot ponds at the Salar de Maricunga.

The testwork was divided in the Salt Removal Plant as follows:

1. Two stage preconcentration (Falling film evaporator)
2. Cooling crystallization of tachyhydrite (Vacuum cooling unit)
3. Crystallization of tachyhydrite and $\text{CaCl}_2 \times 2 \text{H}_2\text{O}$ (Evaporation and crystallization unit)
4. Acidification and cooling crystallization of $\text{CaCl}_2 \times 6\text{H}_2\text{O}$ and boric acid (Surface cooling crystallization)

And the Lithium Carbonate Plant as follows:

1. Solvent extraction of boron
2. Precipitation of CaCO_3
3. Precipitation of $\text{Mg}(\text{OH})_2$ and CaCO_3
4. Final removal of calcium, magnesium and heavy metals by ion exchange resins
5. Li_2CO_3 precipitation crystallization (Li_2CO_3 crystallizer)
6. Li_2CO_3 resuspension and solid- liquid separation unit including washing

13.6.1 RESULTS OF SALT REMOVAL PLANT

It was observed that there is no danger of tachyhydrite crystallization in the falling film evaporator up to a solution composition at 100°C of 5.9 wt.-% LiCl 23.4 wt.-% CaCl_2 15.8 wt.-% MgCl_2 .

Up to 11.3 wt.-% lithium chloride, the flash cooling stages produce only tachyhydrite and traces of sodium chloride and strontium chloride at 40°C. The saturation concentrations of 31.0 wt.-% for CaCl_2 and 6.4 wt.-% for MgCl_2 were at a level of 11.4 wt.-% LiCl. To minimize lithium losses, crystal washing with saturated or almost saturated wash solution is absolutely necessary. Tachyhydrite from vacuum cooling crystallization contained 7.3 wt.-% adhering mother liquor. This product was washed with 17 wt.-% wash solution (referred to as the wet crystals) in the centrifuge, so that the amount of adhering mother liquor could be reduced down to 2.6 wt.-%.

The evaporation stage at 57°C produces tachyhydrite and calcium chloride dihydrate. During the tests it was found out that dewatering of tachyhydrite is much easier than dewatering of $\text{CaCl}_2 \times 2\text{H}_2\text{O}$. The amount of adhering mother liquor to tachyhydrite was around 7 wt.-%. For $\text{CaCl}_2 \times 2\text{H}_2\text{O}$ plus tachyhydrite about 17 wt.-% was determined. To minimize the lithium losses, the evaporation stage will be divided into two crystallization and separation steps. One stage should

crystallize tachyhydrite and the second stage should crystallize a mixture of tachyhydrite plus $\text{CaCl}_2 \cdot 2\text{H}_2\text{O}$. Due to co-crystallization, exact splitting of them is not possible.

Both products should be washed with 40 wt.-% wash solution (referred to as the wet crystals) in the centrifuge.

It was noticed that the condensates of this test work had high conductivities as well as high pH values. With the increasing concentration factor this effect became stronger. The analysis showed that the condensates contained some hydrochloric acid.

For safe process control it is absolutely necessary to adjust the lithium concentration in the evaporation stage to a fixed level. Large deviations in the ratio between lithium, calcium and magnesium can cause co-crystallization of lithium chloride in the surface cooling stage. Small deviations can be compensated for by the amount of added water.

Before the cooling crystallization of $\text{CaCl}_2 \cdot 6\text{H}_2\text{O}$ the solution was slightly diluted to provide the water for the calcium chloride crystals, avoiding co-crystallization of lithium chloride and also acidified to remove the boron as boric acid.

At 30 wt.-% LiCl only 7.3 wt.% CaCl_2 and 1.2 wt.% MgCl_2 were soluble. Also, the solubility of boric acid was reduced to approximately 0.9 wt.%. Boric acid crystallized as fine solids and it was not possible to separate them completely by centrifugation. Here an additional filtration step is required for fines removal. The low magnesium concentration is also very positive for further processing in the lithium carbonate plant.

13.6.2 RESULTS OF LITHIUM CARBONATE TESTING

Several process routes were tested and it turned out that, based on chemical consumptions, the best process steps are those already mentioned above. Solvent extraction tests were executed by SGS, GEA and Technoforce. All tests confirmed that boron can easily be removed with iso-octanol as the extractant and kerosene as the diluent.

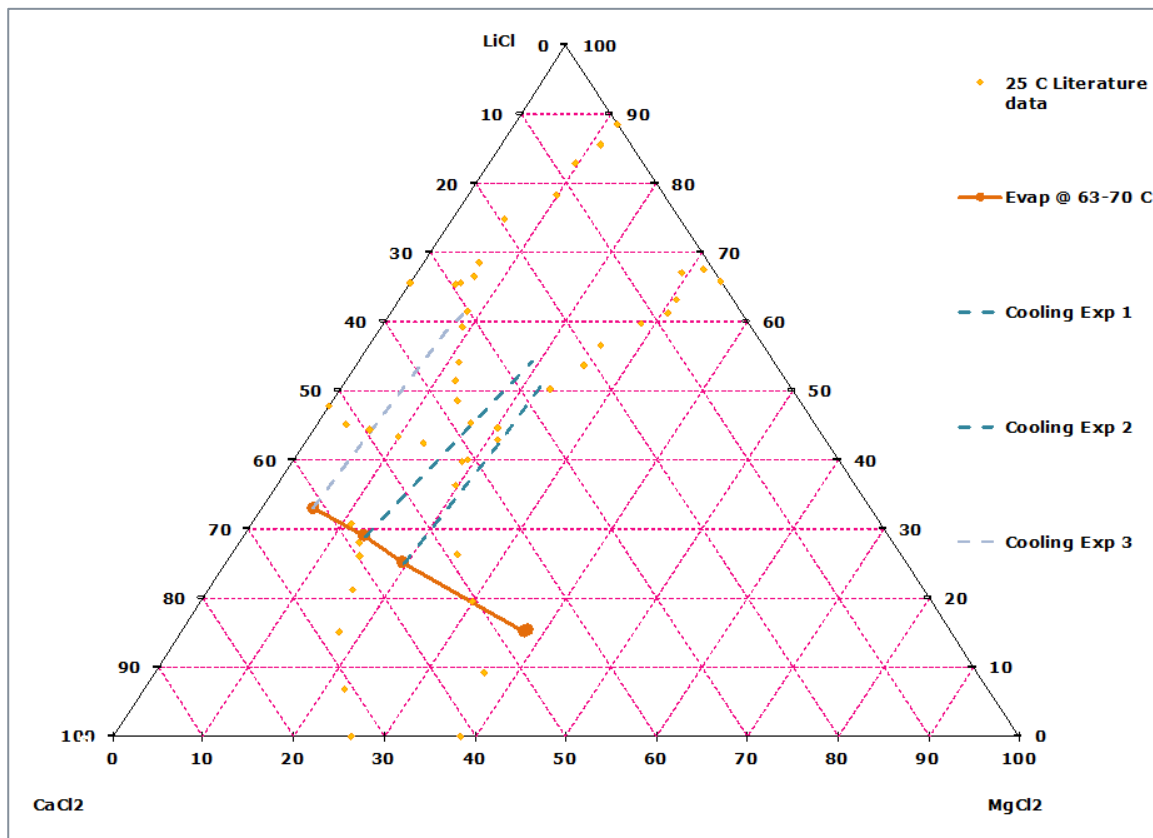
Initially the precipitation of calcium and magnesium was executed in two steps at 40 and 80 °C.

Finally, it was concluded that the best approach is to remove the calcium as calcium carbonate in a primary stage and to remove the magnesium as magnesium hydroxide in a secondary stage, followed up by ion exchange to remove final calcium and magnesium values.

The treated solution was so pure that the Li_2CO_3 precipitation crystallization could follow. The process was simulated by semi-continuous operation in order to add the calculated amount of Na_2CO_3 solution (102% of stoichiometric) dropwise at 85°C. After the retention time of two hours,

the separation of the suspension took place. The crystals were washed 4 times with water (100 % referred to the amount of wet filter cake) on the filter at ambient temperature, resulting in very high-grade lithium carbonate solids, fulfilling completely the target quality set by MSB.

Figure 13-7 Evaporation and cooling curves plotted in a Janecke projection of testwork realized at University of Antofagasta 2011 (UA)



13.7 2019, 2020 AND 2021 SALT REMOVAL AND LITHIUM CARBONATE TESTS

During the years of 2019, 2020 and 2021 semi pilot testwork was mainly concentrated on the equipment selection. GEA together with its subsuppliers conducted extensive testwork in order to specify the equipment and its optimal design, with a focus on operability and operational risk.

One of the findings is that the cooling operation significantly improves when boron is removed upfront. The boron is removed by crystallisation and solvent extraction. The crystallisation of boric acid was tested by GEA. The boron removal with solvent extraction was extensively pilot plant tested by Metso Outotec. The process that is traditional and conventional for boric acid was used.

The testwork was focussed on the Salt Removal Plant as follows:

1. Two stage preconcentration (Falling film evaporator)
2. Cooling crystallization of tachyhydrite (Vacuum cooling unit)
3. Crystallization of tachyhydrite and $\text{CaCl}_2 \times 2 \text{H}_2\text{O}$ (Evaporation and crystallization unit)
4. Acidification and cooling crystallization of boric acid (Crystallization unit)
5. Solvent extraction of boric acid
6. Cooling crystallization of $\text{CaCl}_2 \times 6\text{H}_2\text{O}$ (Surface cooling crystallization)

and the Lithium Carbonate Plant as follows:

7. Precipitation of $\text{Mg}(\text{OH})_2$ and CaCO_3
8. Final removal of remaining boron, calcium, magnesium and heavy metals by ion exchange resins
9. Li_2CO_3 precipitation crystallization (Li_2CO_3 crystallizer)
10. Li_2CO_3 resuspension and solid- liquid separation unit including washing

The cooling crystallization of tachyhydrite and crystallization of tachyhydrite and $\text{CaCl}_2 \times 2 \text{H}_2\text{O}$ were repeated during this period by GEA and the salts were centrifuged by Sieb Technik confirming initial results with slightly better washing of the crystals. This way the feed stock was generated for new acidification of the brine with hydrochloric acid and cooling to form boric acid. This boric acid was filtered and tested with equipment supplier OFS to specify the filter equipment. The boric acid was easily filterable, but there was some lithium loss due to brine entrainment, leaving room for improvement as cake washing was not tested.

A continuous 100 hours boron solvent extraction pilot plant was run successfully, containing five extraction stages and four stripping stages. The organic phase contained iso octanol and kerosene. The extraction stage mixers were operated at 28-31 °C. The extraction stages had a pH of 2.5-3.5. Boron concentration in the brine feed was 5.2 g/L and boron in the E5 raffinate was mostly <6 mg/L. The lithium loss to strip product was <0.2 % of the lithium in brine solution.

The boron free lithium brine was now cooled. The equipment performance was significantly improved and the same lithium chloride of 30 wt% was achieved. The centrifuge and washing performance tested by Sieb Technik was improved, resulting in higher lithium recovery.

In order to simplify the process, the calcium carbonate and the magnesium hydroxide precipitation steps were combined and tested with positive results. Due to the higher amount of calcium carbonate in the precipitate, subsequent filtration was improved.

Figure 13-8 Extraction stages E1-E5 at 26 h after start-up



Eurodia conducted a detailed ion exchange study with the main objective an adequate equipment design for the project. The study covered the removal of boron and of divalent cations, especially calcium, magnesium and strontium, from a pre-treated brine prior to the lithium carbonate precipitation.

Several resins with different functional groups were tested in the initial phase to determine the most suitable for divalent cations removal for this application. Aminophosphonic resins were much more efficient than the iminodiacetate resin which has shown very low capacity. Results have shown that the purification is limited by strontium removal. Tested resins have low capacity for strontium removal and strontium leakage starts early during the production. This is leading to short production cycles and consequently to potential high lithium losses. Decreasing the strontium concentration in the feed helped to increase the cycle time and decrease the lithium losses.

During the second phase, several productions have been done with two columns in series in order to simulate an industrial set up. The first column is used to remove totally the calcium and magnesium and a part of the strontium. The second column is used as a polishing stage, to remove the leaking part of the strontium. Thanks to the analysis of the regeneration effluent, it was also possible to estimate lithium losses, which are expected to be around 0.6%.

Four resins have been tested in the first phase to determine the most suitable for the boron removal in terms of capacity and reaction rate. A series of tests were done to simulate an industrial operation with two columns in series. Initially results showed that the amount of boron fixed by the resin can be much higher than estimated in phase 1. This difference is explained by the change of the production flowrate between the two phases. Regeneration has been studied by analysing the acidic regeneration effluents. As expected for a boron selective resin, no lithium losses were observed during regeneration.

14. BRINE RESOURCE ESTIMATES

14.1 OVERVIEW

The essential elements of a brine resource determination for a salar are:

- Definition of the aquifer geometry,
- Determination of the drainable porosity or specific yield (Sy) of the hydrogeological units in the salar, and
- Determination of the concentration of the elements of interest.

Resources may be defined as the product of the first three parameters. The use of specific yield allows the direct comparison of brine resources from the widest range of environments.

Aquifer geometry is a function of both the shape of the aquifer, the internal structure and the boundary conditions (brine / freshwater interface). Aquifer geometry and boundary conditions can be established by drilling and geophysical methods. Hydrogeological analyses are required to establish catchment characteristics such as ground and surface water inflows, evaporation rates, water chemistry and other factors potentially affecting the brine reservoir volume and composition in-situ. Drilling is required to obtain samples to estimate the salar lithology, specific yield and grade variations both laterally and vertically.

14.2 RESOURCE MODEL DOMAIN AND AQUIFER GEOMETRY

The resource model domain is constrained by the following factors:

- The top of the model coincides with the brine level in the Salar that was measured in the monitoring wells shown in Table 10-1.
- The lateral boundaries of the model domain are limited to the area of the MSB 'Old Code' mining concessions.
- The bottom of the model domain coincides with the modelled basement from the geological model or the depth of 400 m when the basement is not present.

14.3 SPECIFIC YIELD

Specific yield is defined as the volume of water released from storage by an unconfined aquifer per unit surface area of aquifer per unit decline of the water table.

The specific yield values used to develop the resources are based on results of the logging and hydrogeological interpretation 17 sonic-and HQ core holes, results of drainable porosity analyses carried out on 520 undisturbed valid core samples GeoSystems Analysis, Daniel B Stephens and Associates, Corelabs, BGC, and four pumping tests. The boreholes within the measured and indicated resource areas are appropriately spaced at a borehole density of one bore per 1.5 km². Table 14-1 shows the drainable porosity values assigned to the different geological units for the resource model.

Table 14-1 Drainable porosity values applied in the resource model

Unit	Count	Sy Average	Sy Low	Sy Max	Sy Std. Dev
Halite	6	0.06	0.05	0.12	0.028
Lacustrine	323	0.02	0	0.15	0.023
Deep Halite	8	0.06	0.01	0.13	0.044
Alluvial Deposits	31	0.14	0	0.31	0.097
Lower Sand	20	0.06	0.01	0.19	0.046
Volcanoclastics	72	0.12	0	0.31	0.073
Lower Volcanoclastics	7	0.08	0.05	0.18	0.046
Volcanic Breccia	52	0.13	0.01	0.29	0.070

14.4 BRINE CONCENTRATIONS

The distributions of lithium and potassium concentrations in the model domain are based on a total of 718 brine chemistry analyses (not including QA/QC analyses). Table 14-2 shows a summary of the brine composition below all mining concessions (OCC and Litio 1-6).

Table 14-2 Summary of brine chemistry composition

Units	B mg/L	Ca mg/L	Cl mg/L	Li mg/L	Mg mg/L	K mg/L	Na mg/L	SO4 mg/L	Density g/cm ³
Maximum	1,993	36,950	233,800	3,375	21,800	20,640	105,851	2,960	1.31
Average	572	12,847	192,723	1,122	7,327	8,142	87,106	711	1.20
Minimum	234	4,000	89,441	460	2,763	2,940	37,750	259	1.10

14.5 RESOURCE CATEGORY

The CIM Council (May 10, 2014) adopted the following definition standards for minerals resources:

Inferred Mineral Resource

An Inferred Mineral Resource is that part of a Mineral Resource for which quantity and grade or quality are estimated on the basis of limited geological evidence and sampling. Geological evidence is sufficient to imply but not verify geological and grade or quality continuity.

An Inferred Mineral Resource has a lower level of confidence than that applying to an Indicated Mineral Resource and must not be converted to a Mineral Reserve. It is reasonably expected that the majority of Inferred Mineral Resources could be upgraded to Indicated Mineral Resources with continued exploration.

An Inferred Mineral Resource is based on limited information and sampling gathered through appropriate sampling techniques from locations such as outcrops, trenches, pits, workings and drill holes. Inferred Mineral Resources must not be included in the economic analysis, production schedules, or estimated mine life in publicly disclosed Pre- Feasibility or Feasibility Studies, or in the Life of Mine plans and cash flow models of developed mines. Inferred Mineral Resources can only be used in economic studies as provided under NI 43-101.

There may be circumstances, where appropriate sampling, testing, and other measurements are sufficient to demonstrate data integrity, geological and grade/quality continuity of a Measured or Indicated Mineral Resource, however, quality assurance and quality control, or other information may not meet all industry norms for the disclosure of an Indicated or Measured Mineral Resource. Under these circumstances, it may be reasonable for the Qualified Person to report an Inferred Mineral Resource if the Qualified Person has taken steps to verify the information meets the requirements of an Inferred Mineral Resource.

Indicated Mineral Resource

An Indicated Mineral Resource is that part of a Mineral Resource for which quantity, grade or quality, densities, shape and physical characteristics are estimated with sufficient confidence to allow the application of Modifying Factors in sufficient detail to support mine planning and evaluation of the economic viability of the deposit.

Geological evidence is derived from adequately detailed and reliable exploration, sampling and testing and is sufficient to assume geological and grade or quality continuity between points of observation.

An Indicated Mineral Resource has a lower level of confidence than that applying to a Measured Mineral Resource and may only be converted to a Probable Mineral Reserve.

Mineralization may be classified as an Indicated Mineral Resource by the Qualified Person when the nature, quality, quantity and distribution of data are such as to allow confident interpretation of the geological framework and to reasonably assume the continuity of mineralization. The Qualified Person must recognize the importance of the Indicated Mineral Resource category to the advancement of the feasibility of the project. An Indicated Mineral Resource estimate is of sufficient quality to support a Pre-Feasibility Study which can serve as the basis for major development decisions.

Measured Mineral Resource

A Measured Mineral Resource is that part of a Mineral Resource for which quantity, grade or quality, densities, shape, and physical characteristics are estimated with confidence sufficient to allow the application of Modifying Factors to support detailed mine planning and final evaluation of the economic viability of the deposit.

Geological evidence is derived from detailed and reliable exploration, sampling and testing and is sufficient to confirm geological and grade or quality continuity between points of observation.

A Measured Mineral Resource has a higher level of confidence than that applying to either an Indicated Mineral Resource or an Inferred Mineral Resource. It may be converted to a Proven Mineral Reserve or to a Probable Mineral Reserve.

Mineralization or other natural material of economic interest may be classified as a Measured Mineral Resource by the Qualified Person when the nature, quality, quantity and distribution of data are such that the tonnage and grade or quality of the mineralization can be estimated to within close limits and that variation from the estimate would not significantly affect potential economic viability of the deposit. This category requires a high level of confidence in, and understanding of, the geology and controls of the mineral deposit.

14.6 RESOURCE MODEL METHODOLOGY AND CONSTRUCTION

The resource estimation for the Project was developed using the Stanford Geostatistical Modelling Software (SGeMS) and the geological model as a reliable representation of the local lithology. In order to incorporate the geological model as secondary information in the interpolation, kriging was used within strata, which consisted of stratifying the resource model based on the geological model. Kriging interpolation within each specific stratum is sequentially performed using a semi-variogram

model and the closest primary data samples within the stratum. The method assumes that the stratification is delimited by accurate geological boundaries and true changes in soil type. The following steps were carried out to calculate the lithium and potassium resources.

- Definition of the block model (9,419,505 blocks) and block size (x=50 m, y=50 m, z=1 m). The block size has been chosen for being representative of the thinner units within the geological model.
- Definition of regions or strata based on the geological model.
- Generation of histograms, probability plots and box plots for the Exploratory Data Analysis (EDA) for lithium and potassium for each region. No outlier restrictions were applied, as distributions of the different elements do not show anomalously high values. Calculation of the experimental variograms with their respective variogram models for lithium and potassium in three orthogonal directions. Variography revealed that the variogram model is axisymmetric with respect to the z coordinate direction; the variogram model is isotropic in the horizontal direction and anisotropic in the vertical.
- For each region, interpolation of lithium and potassium concentrations for each block in mg/L using ordinary kriging with the variogram models. The distribution of brine concentration does not follow lithological boundaries, therefore, no hard boundaries are considered within the geological units for the estimation.
- Validation using a series of checks including comparison of univariate statistics for global estimation bias, visual inspection against samples on plans and sections, swath plots in the north, south and vertical directions to detect any spatial bias.
- Calculation of total resources using the average drainable porosity value for each geological unit, based on the boreholes data and results of the laboratory drainable porosity analysis as shown in Table 14-1.

14.6.1 UNIVARIATE STATISTICAL DESCRIPTION

The univariate statistical description of lithium and potassium concentrations are based on histograms, probability plots and box plots. Table 14-3 presents a summary of the univariate statistics of potassium and lithium. As described in the methodology, these statistics contain the information of all geological units. The mean concentration of potassium is 7.3 times of the lithium. Both exhibit the same degree of variability with a coefficient of variation of 0.31 and 0.33 for the potassium and lithium, respectively. Distributions are positively skewed. The concentrations of potassium range between 2,940 mg/L and 20,640 mg/L, and the concentrations of lithium range between 460 mg/L and 3,375 mg/L.

Table 14-3 Summary of univariate statistics of potassium lithium and potassium

	Li mg/l	K mg/l
Valid N	718	718
Mean	1,123	8,142
Minimum	460	2,940
Maximum	3,375	20,640
Variance	124,038	5,947,876
Std.Dev.	352	2,439
Coef.Var.	0.33	0.31
Skewness	0.97	0.74
Std.Err. - Skewness	0.09	0.09
Kurtosis	2.52	0.72
Std.Err. - Kurtosis	0.18	0.18

Figure 14-1 shows the lithium and potassium distribution and their expected normal distribution. Results show that the data do not strictly follow a normal distribution. However, the figures permit to identify a straight line, indicating that although the data fail the normality tests, the distribution is close to a Gaussian shape. This gives confidence in the kriging estimate of the concentrations when the data follow a multivariate normal distribution.

Figure 14-2 shows the histogram of potassium and lithium concentrations. The distribution is slightly bimodal, but close to a Gaussian shape in general. In terms of a bivariate statistical description, it is important to note that potassium and lithium concentrations are highly correlated. Figure 14-3 shows the scatter plot of lithium versus potassium concentrations. The graph shows a clear correlation between both concentrations, with a correlation coefficient of 0.95 obtained with 718 pairs of data.

Figure 14-1 Lithium and potassium distribution

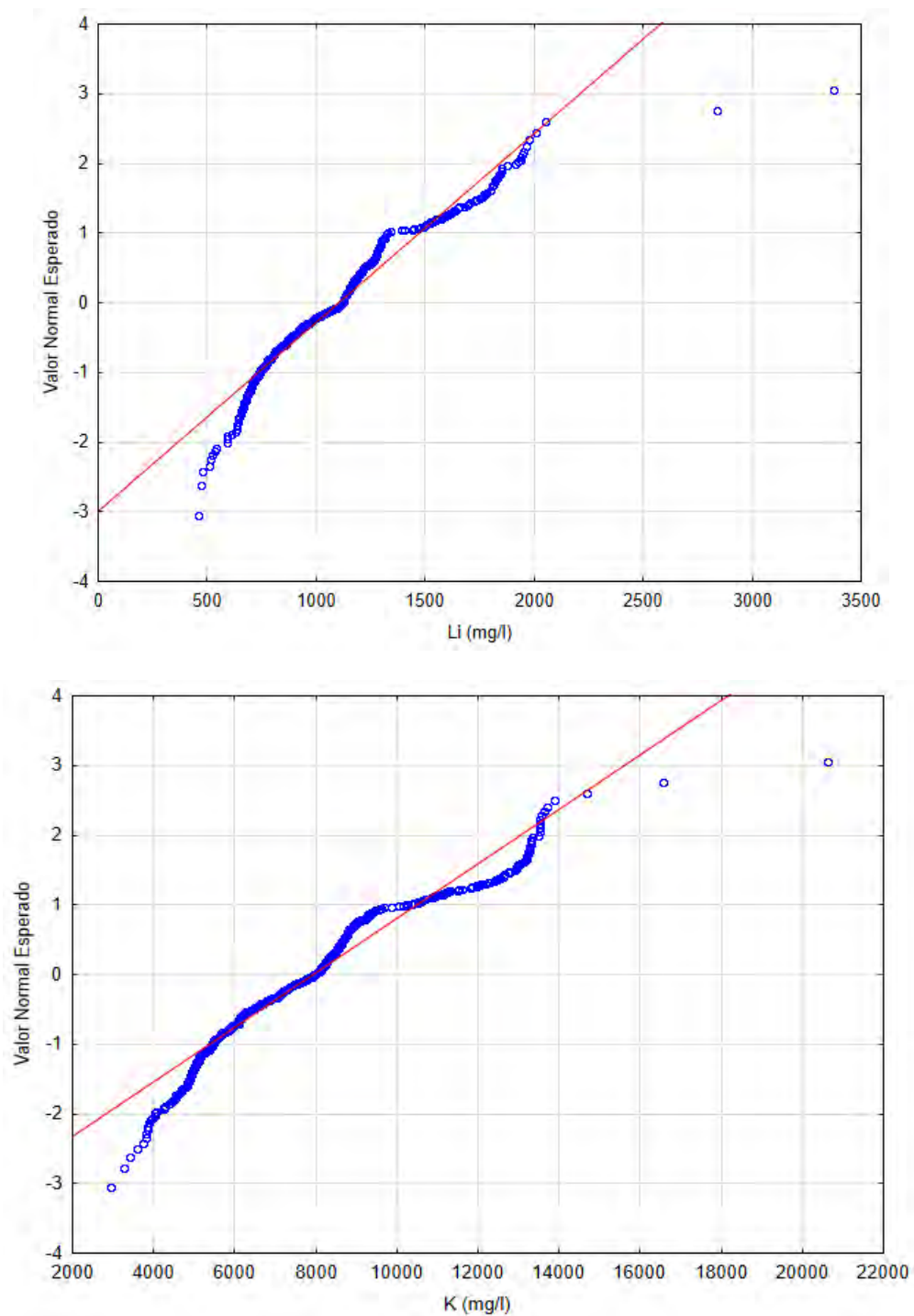


Figure 14-2 Histogram of potassium and lithium concentrations

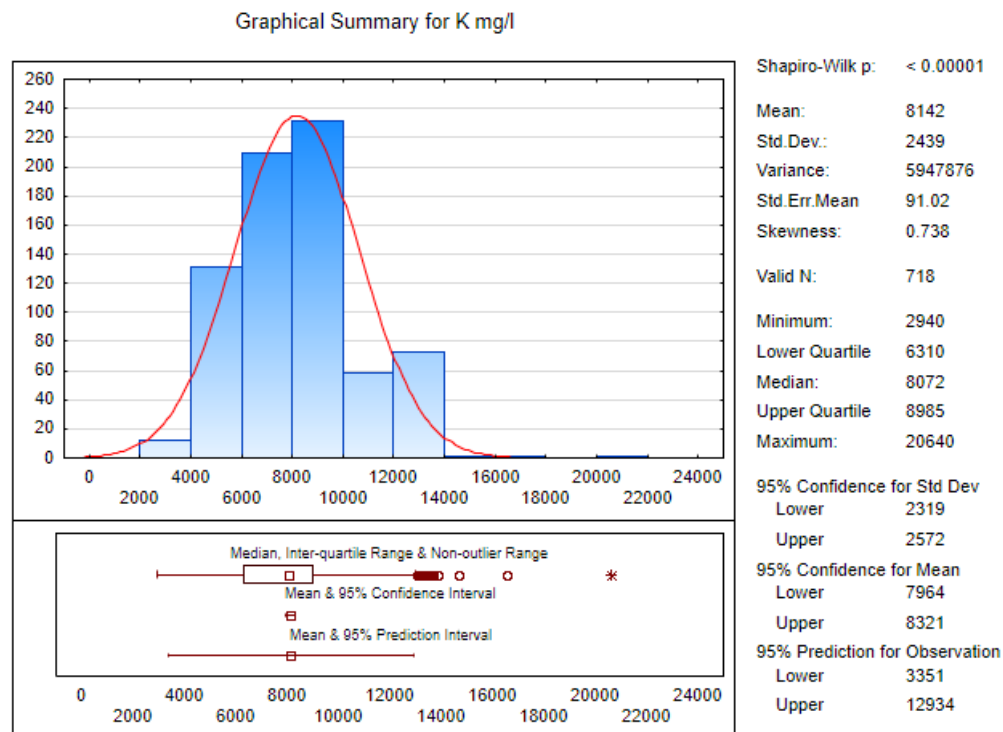
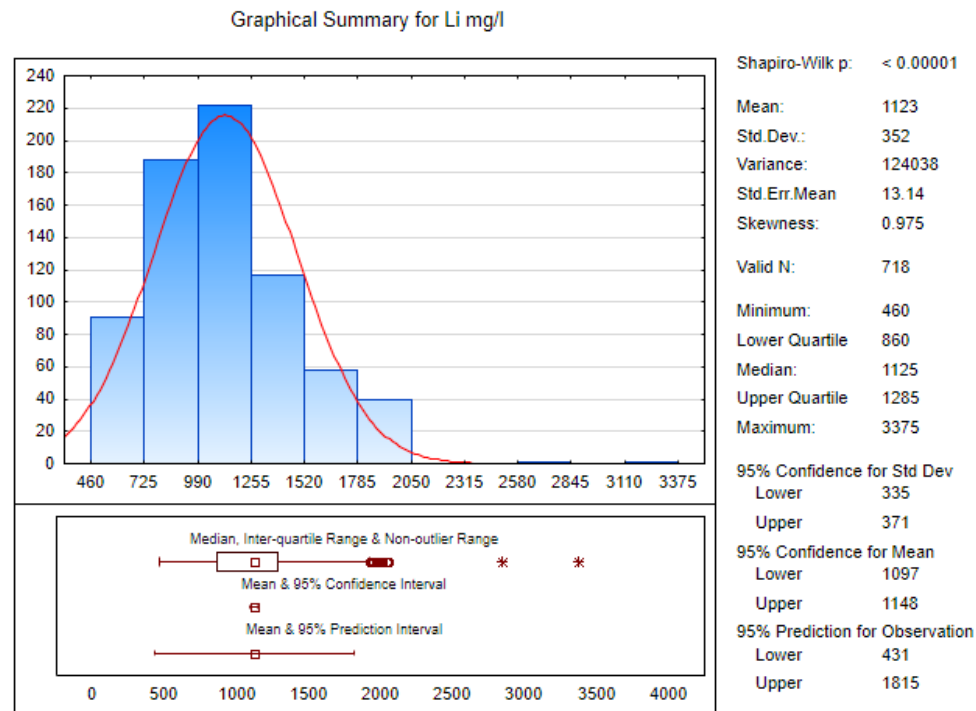
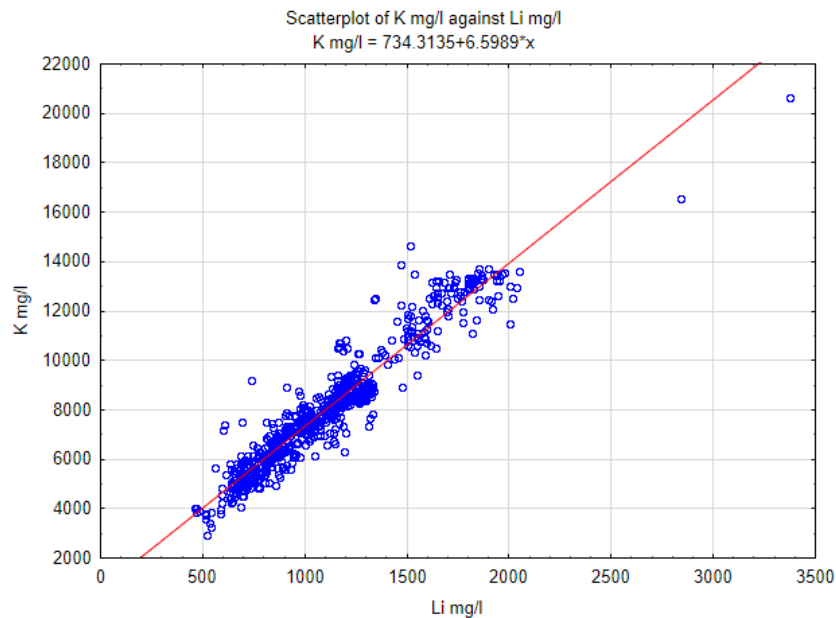


Figure 14-3 Scatter plot of lithium versus potassium concentrations



14.6.2 VARIOGRAPHY

The spatial correlation for the lithium and potassium concentrations were reviewed using experimental variograms with the parameters shown in Table 14-4. Variogram models are axisymmetric with multiple structures characterized by a horizontal range a_h and a vertical range a_z . Consequently, for each region, the spatial variability was modelled using two experimental directions. Lithium and potassium concentrations are expressed in mg/L. The variograms are expressed in mg/l squared. In general, a good correlation was found between the sample concentrations of lithium and potassium in all regions. Consequently, results show that the lithium and potassium concentrations can be represented by the same fundamental structures.

Table 14-4 Parameters for the calculation of the experimental variograms

Variogram Parameters				Tolerance	
Lag (m)	Max. No. Of Lags	Azimuth (°)	Dip (°)	Bandwidth (m)	Angular (°)
400	50	-45	0	500	45
400	50	-135	0	500	45
3	40	0	90	25	89

The volcanoclastic and volcanic breccia units were represented by the sum of an exponential and a Gaussian variogram. In this case, two structures are needed to represent the vertical variability of the concentrations. The exponential variogram describes the short-scale spatial continuity with a vertical range of $a_z=12$ m, which contrasts with a range of $a_h=2500$ m in the horizontal direction. This means that the ratio of anisotropy is $a_h/a_z=208$, which expresses that the geological system is highly stratified as can be observed in sedimentary formations. The second structure reflects the appearance of more variability in the vertical direction at larger scales.

$$\gamma_{Li}(h) = 17000\gamma_{EXP}(a_h = 2500, a_z = 12) + 40000\gamma_{Gauss}(a_h = 2500, a_z = 220)$$

$$\gamma_K(h) = 680000\gamma_{EXP}(a_h = 2500, a_z = 12) + 1630000\gamma_{Gauss}(a_h = 2500, a_z = 120)$$

The alluvial deposit and lower sand units were represented by an anisotropic spherical variogram. The range in the vertical direction is 10 m and in the horizontal direction 2000 m. The total contribution and anisotropy ratio are similar to the previous units but the vertical variogram model does not reflect multiple structures. Instead, the experimental variogram shows a clear asymptote after a range of 10 m.

$$\gamma_{Li}(h) = 60300\gamma_{Sph}(a_h = 2000, a_z = 10)$$

$$\gamma_K(h) = 2400000\gamma_{Sph}(a_h = 2000, a_z = 10)$$

The halite and deep halite units can be represented by two structures; the sum of an exponential and a Gaussian variogram model. In this case, lithium and potassium follow a similar heterogeneous structure but with markedly different spatial continuity. Lithium is more homogeneous than potassium in the vertical direction. The small-scale variability of lithium exhibits a vertical range of 105 m, which is much larger than that of potassium ($a_z=15$ m). A similar effect is seen in the horizontal direction but less pronounced. Lithium has a horizontal range of 2700 m, which compares with a range of 600 m for potassium. In sum, this expresses that the variability of potassium concentrations in these formations is much higher than lithium.

$$\gamma_{Li}(h) = 6500\gamma_{Gauss}(a_h = 2700, a_z = 2700) + 8000\gamma_{Exp}(a_h = 2700, a_z = 105)$$

$$\gamma_K(h) = 3585000\gamma_{Gauss}(a_h = 600, a_z = 600) + 592000\gamma_{Exp}(a_h = 600, a_z = 15)$$

The Lacustrine geological unit is mostly composed of clay. The variogram model are represented by the sum of two Gaussian models. The second Gaussian model represents the vertical large-scale variability which is manifested in the vertical variogram with a monotonous increase after 20 m. The range of correlation for the lithium and potassium concentration in the horizontal direction is 2500 m and 2700 m, respectively.

$$\gamma_{Li}(h) = 45000\gamma_{Gauss}(a_h = 2500, a_z = 20) + 152000\gamma_{Gauss}(a_h = 2700, a_z = 160)$$

$$\gamma_K(h) = 1845000\gamma_{Gauss}(a_h = 2700, a_z = 20) + 6132000\gamma_{Gauss}(a_h = 2700, a_z = 160)$$

The experimental variograms for lithium and potassium with their respective variogram models are shown from Figure 14-4 to Figure 14-9.

The lithium and potassium concentrations were estimated within each specific region (geological unit) using the corresponding variogram models and the closest concentration data samples within the region. The interpolation methodology for estimating lithium and potassium was Ordinary Kriging (OK), whenever possible and Simple Kriging otherwise. The estimation was carried out separately for each parameter using their respective variogram models as appropriate.

Figure 14-4 Horizontal experimental variogram and variogram model for lithium within the alluvial deposits and lower sand

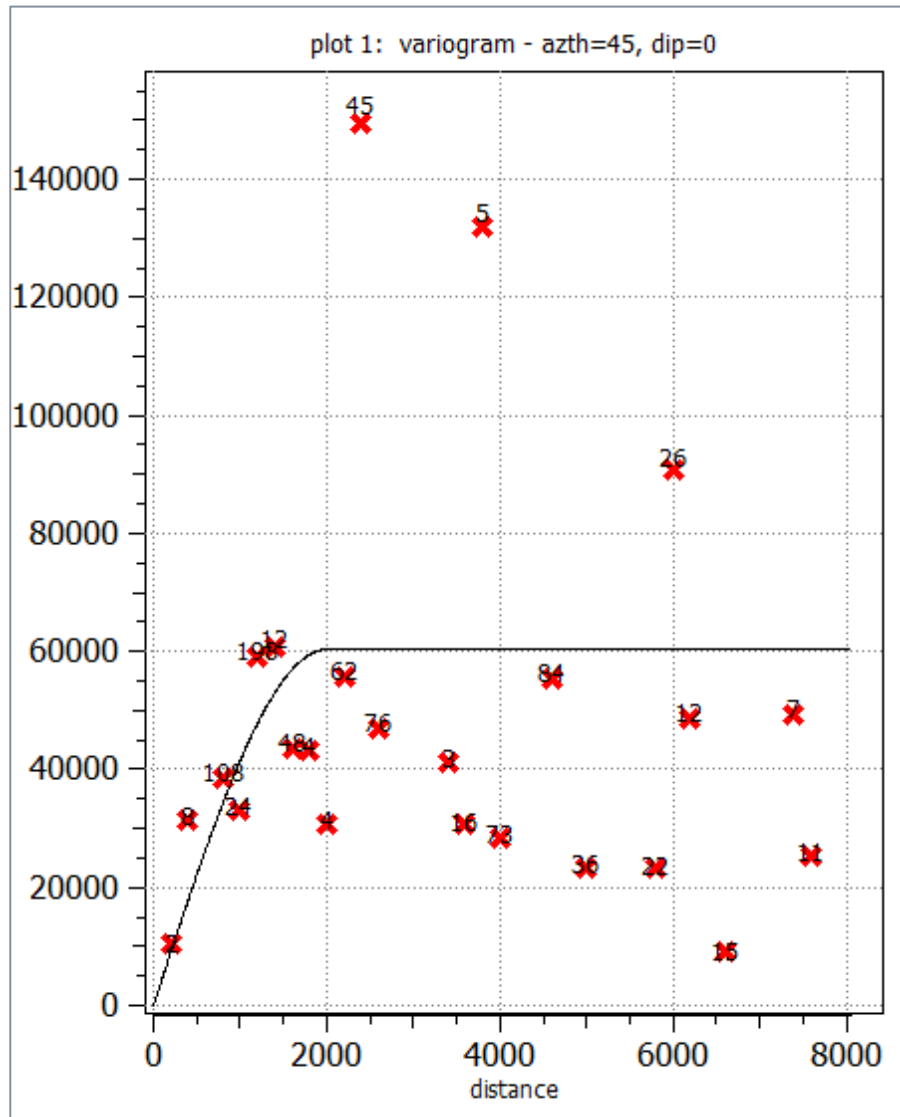


Figure 14-5 Horizontal experimental variogram and variogram model for lithium within the Lacustrine region

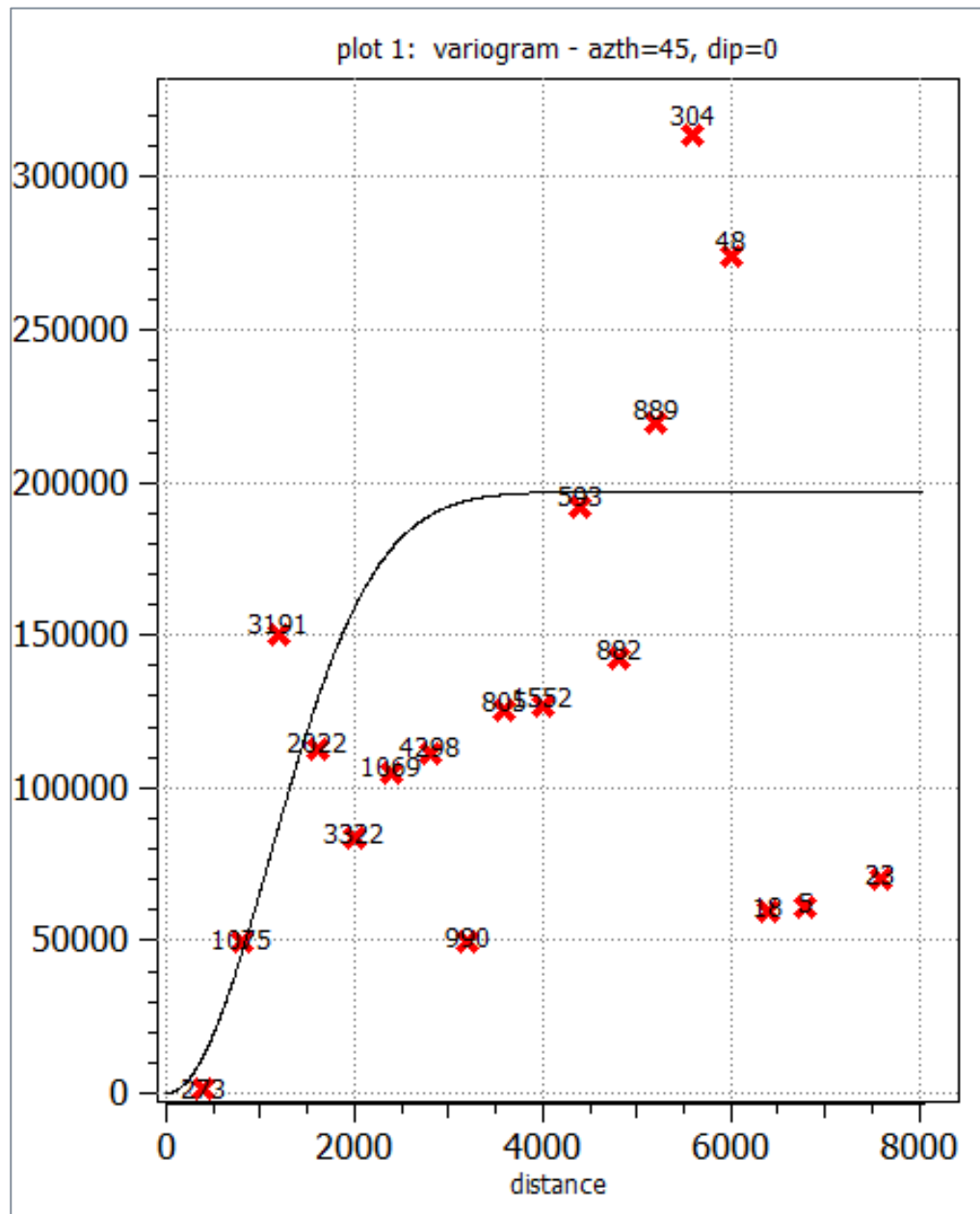


Figure 14-6 Horizontal experimental variogram and variogram model for lithium within the halite and deep halite region

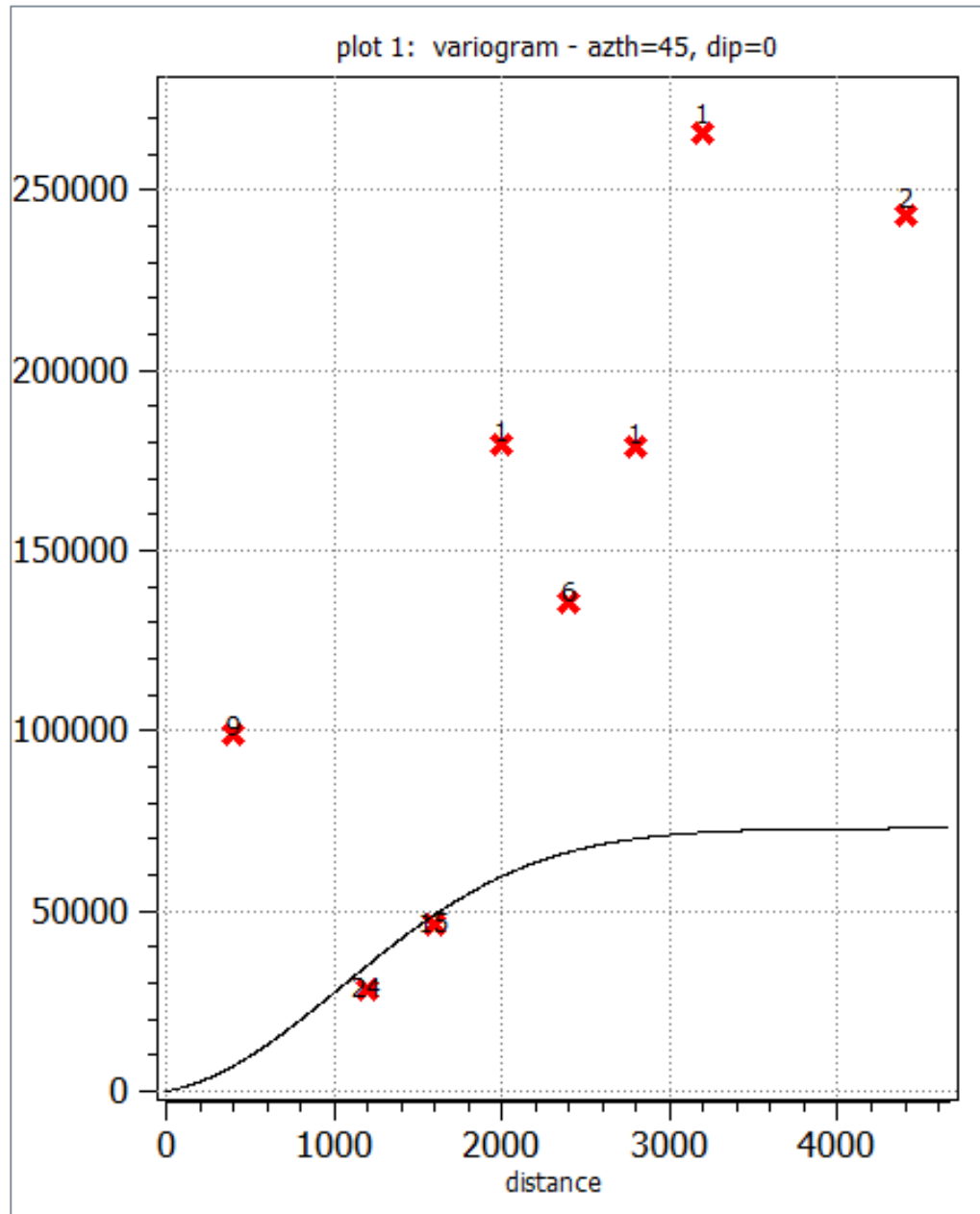


Figure 14-7 Horizontal experimental variogram and variogram model for lithium within the volcanoclastic, lower volcanoclastic and volcanic breccia

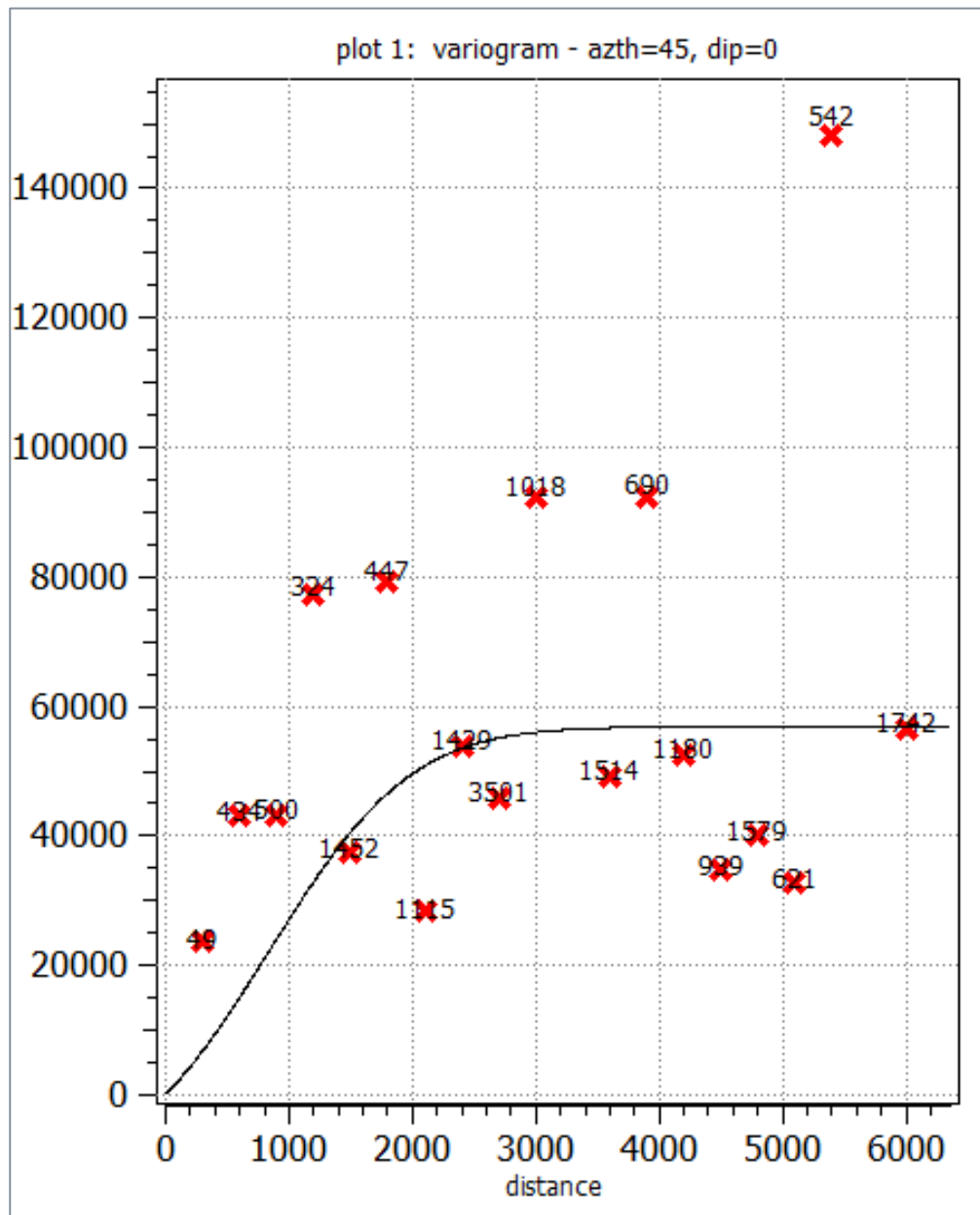


Figure 14-8 Vertical experimental variogram and variogram model for lithium within the alluvial deposits and lower sand

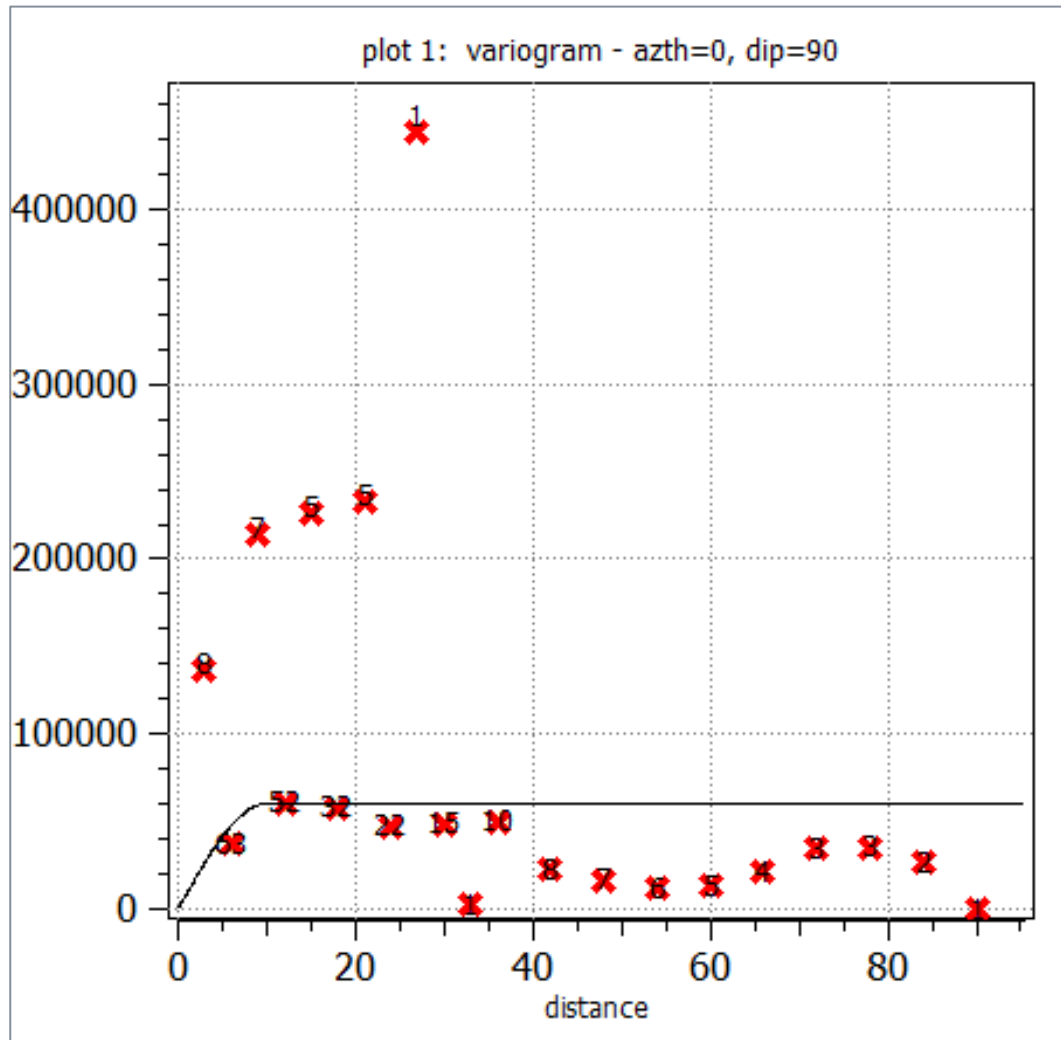


Figure 14-9 Vertical experimental variogram and variogram model for lithium within the Lacustrine region

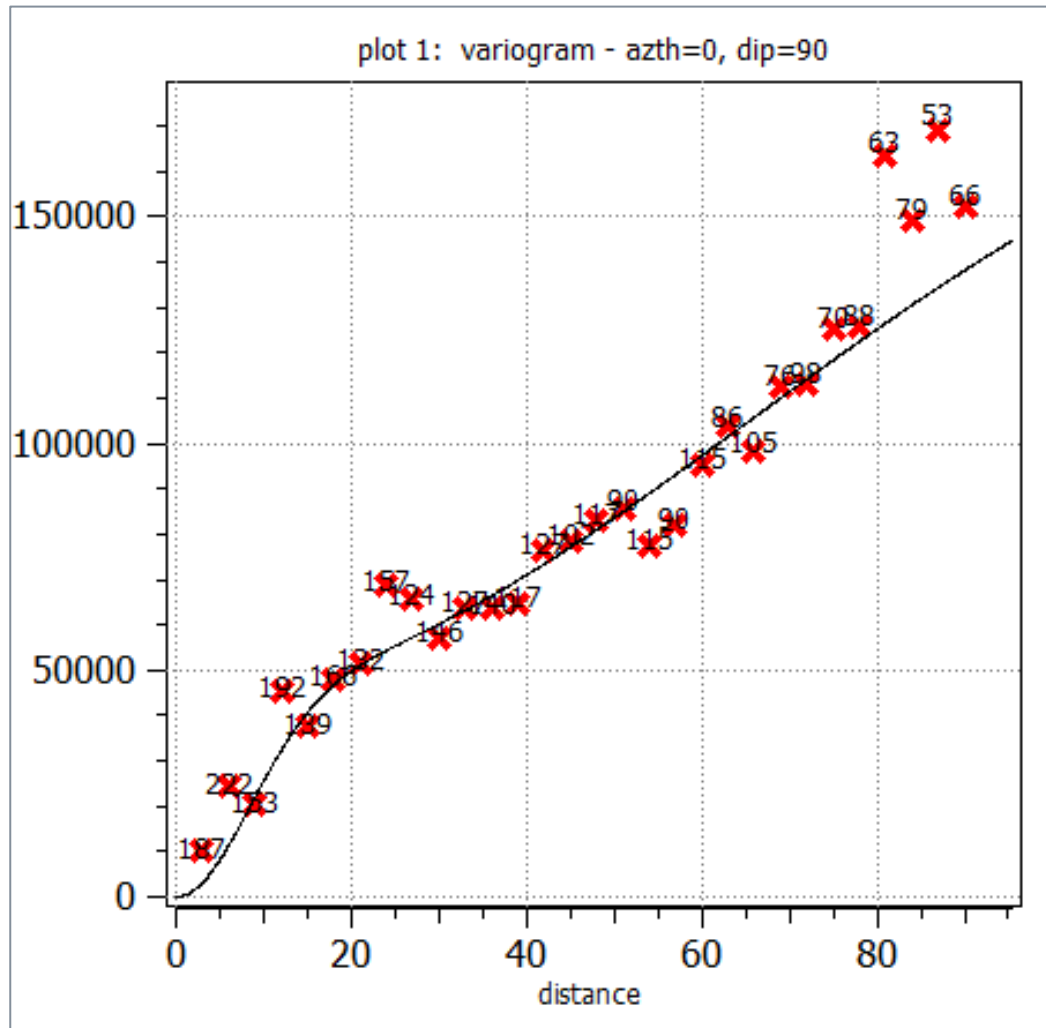


Figure 14-10 Vertical experimental variogram and variogram model for lithium within the halite and deep halite region

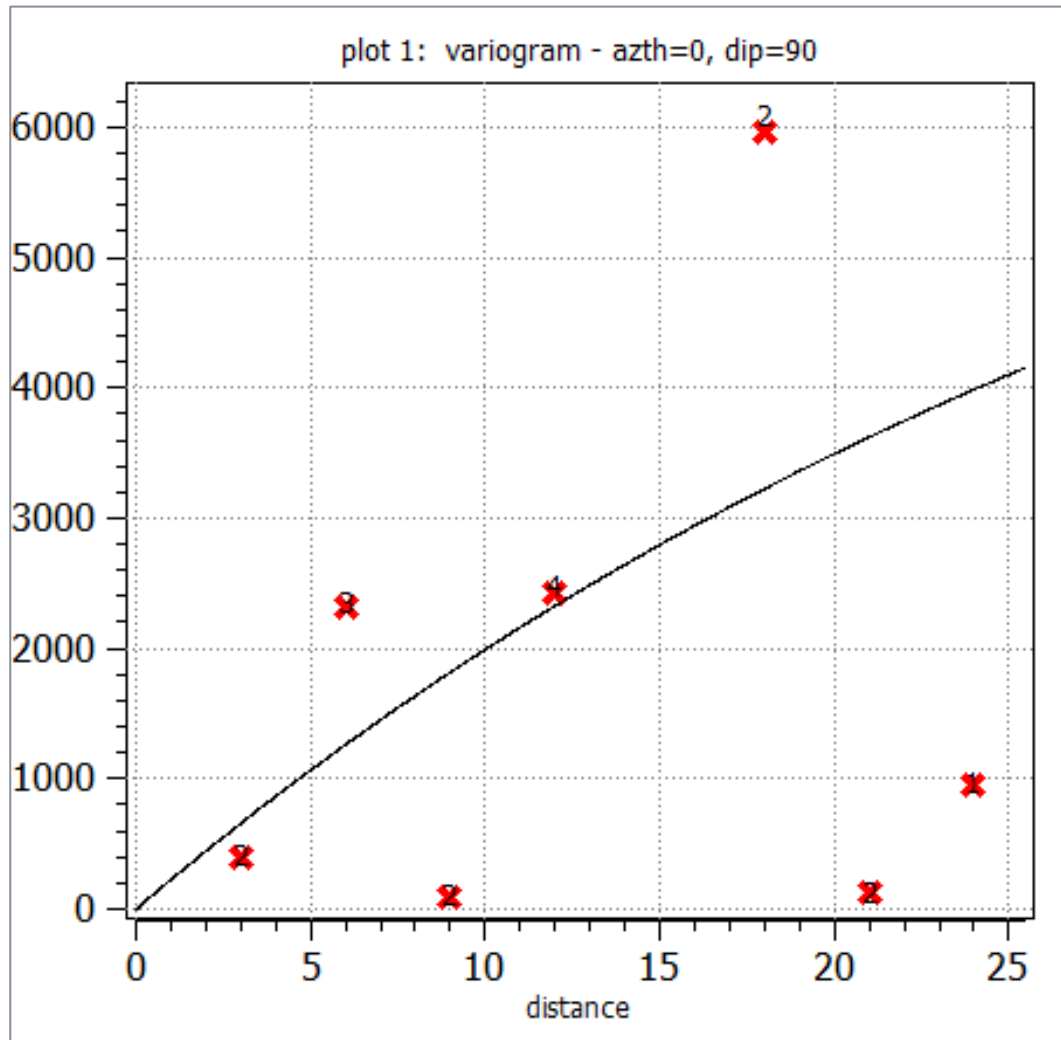


Figure 14-11 Vertical experimental variogram and variogram model for lithium within the volcanoclastic, lower volcanoclastic and volcanic breccia

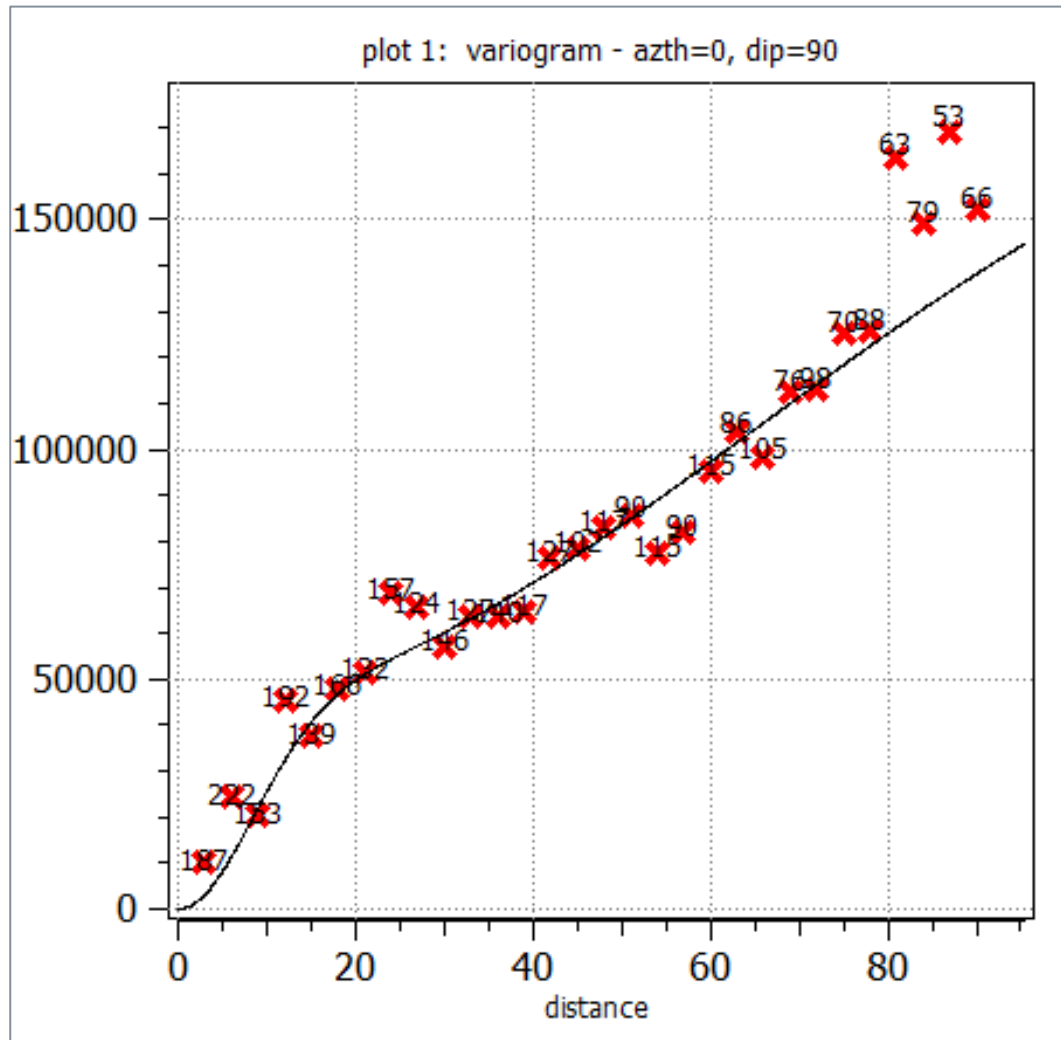


Figure 14-12 Horizontal experimental variogram and variogram model for potassium within the alluvial deposits and lower sand

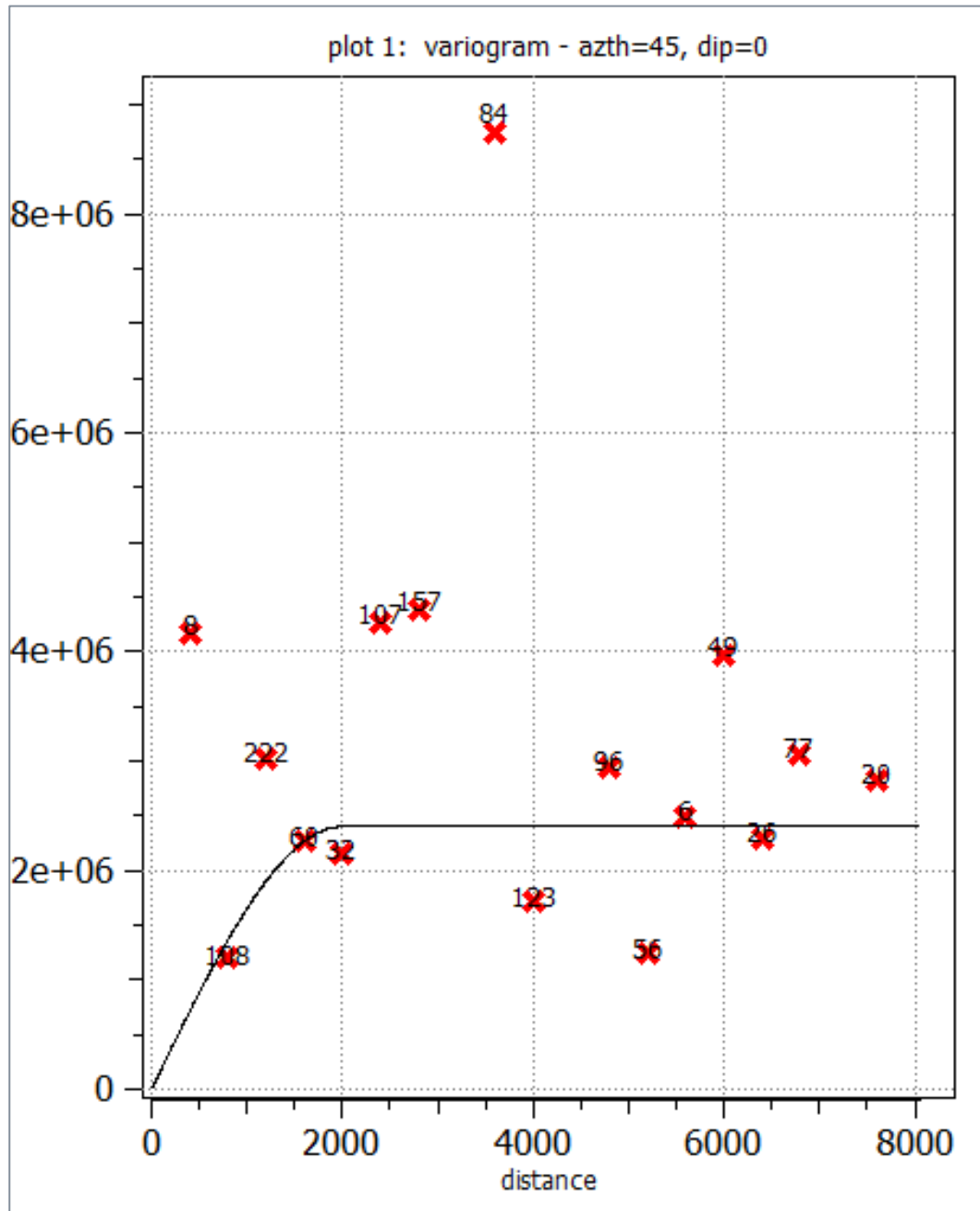


Figure 14-13 Horizontal experimental variogram and variogram model for potassium within the Lacustrine region

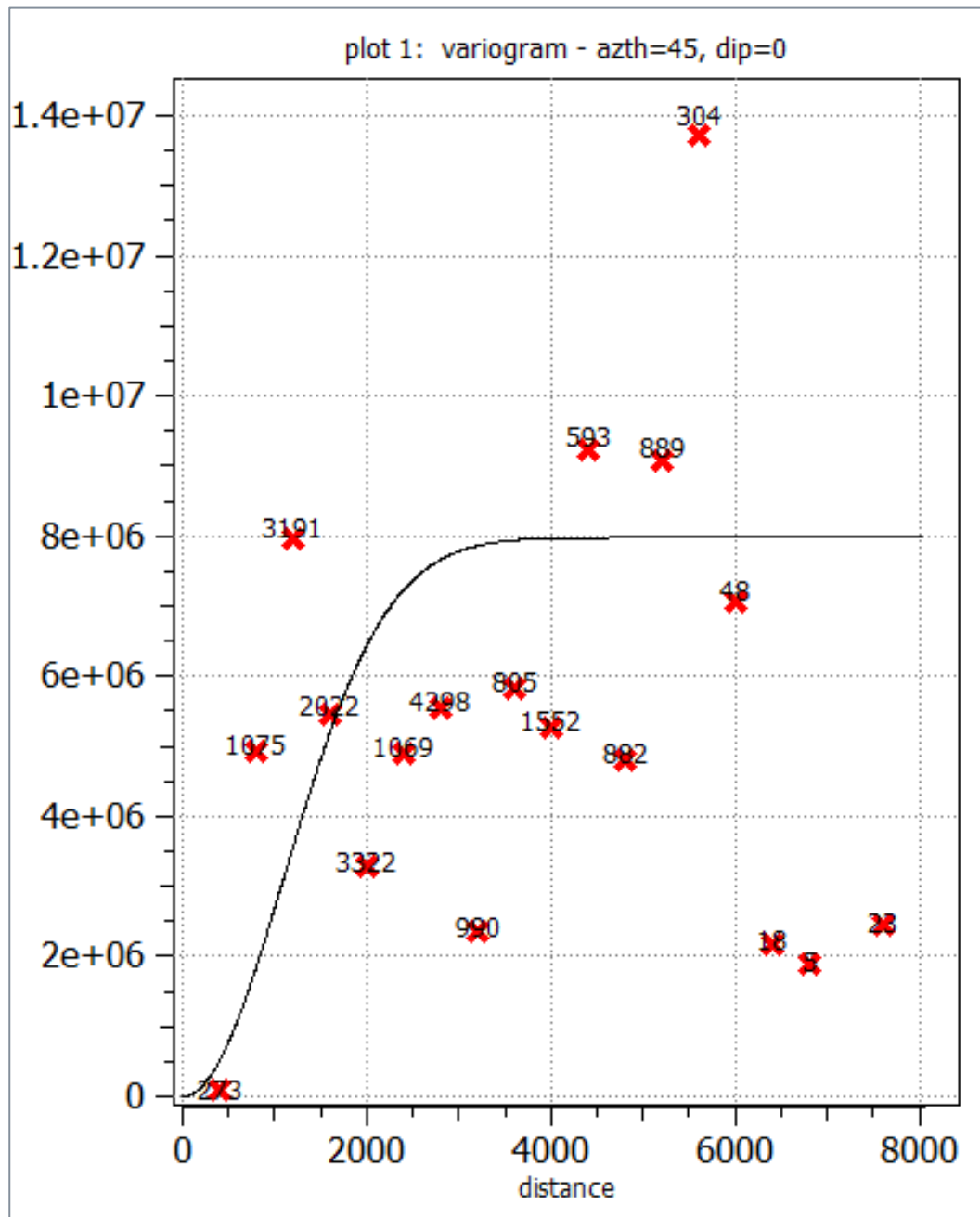


Figure 14-14 Horizontal experimental variogram and variogram model for potassium within the halite and deep halite region

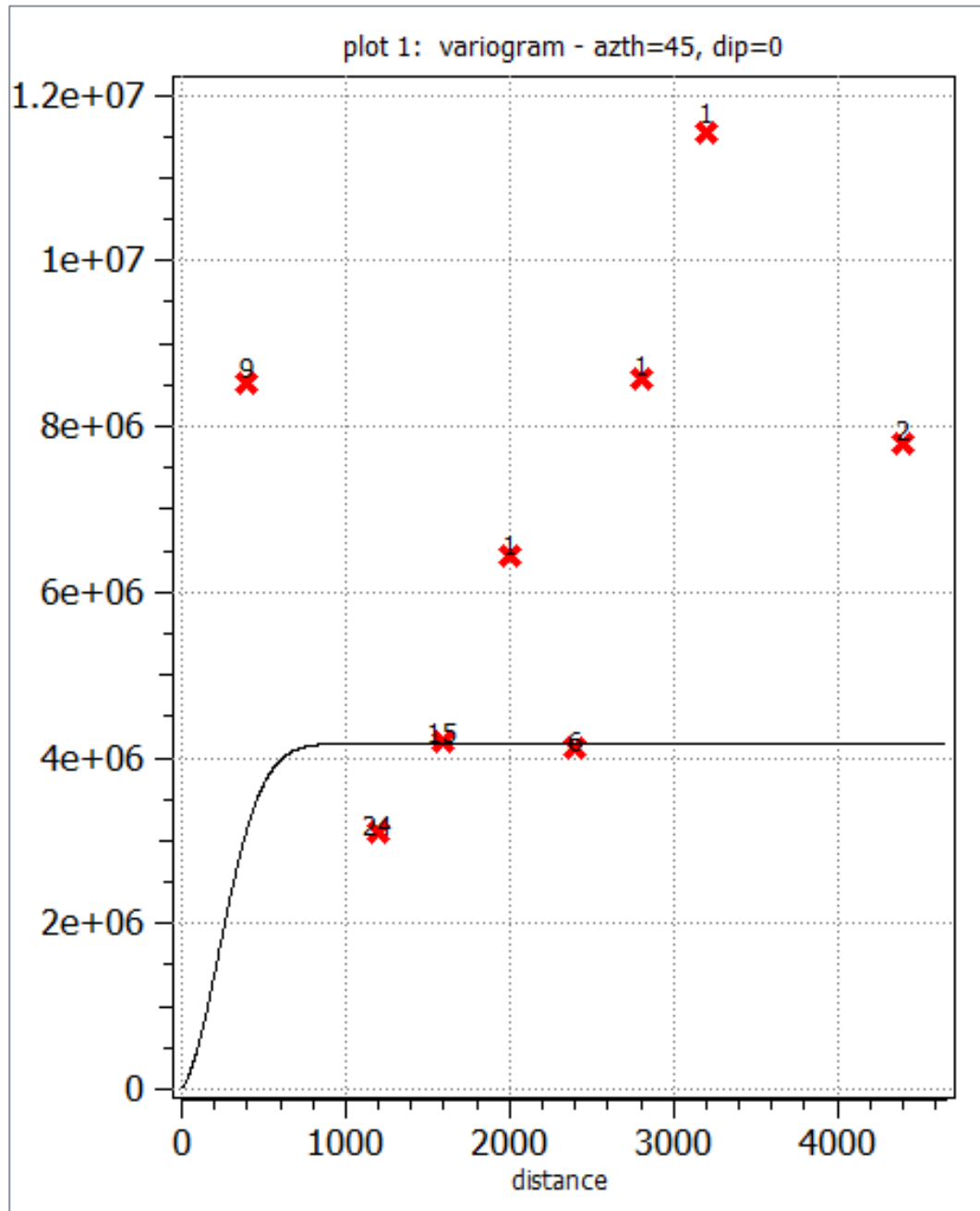


Figure 14-15 Horizontal experimental variogram and variogram model for potassium within the volcanoclastic, lower volcanoclastic and volcanic breccia

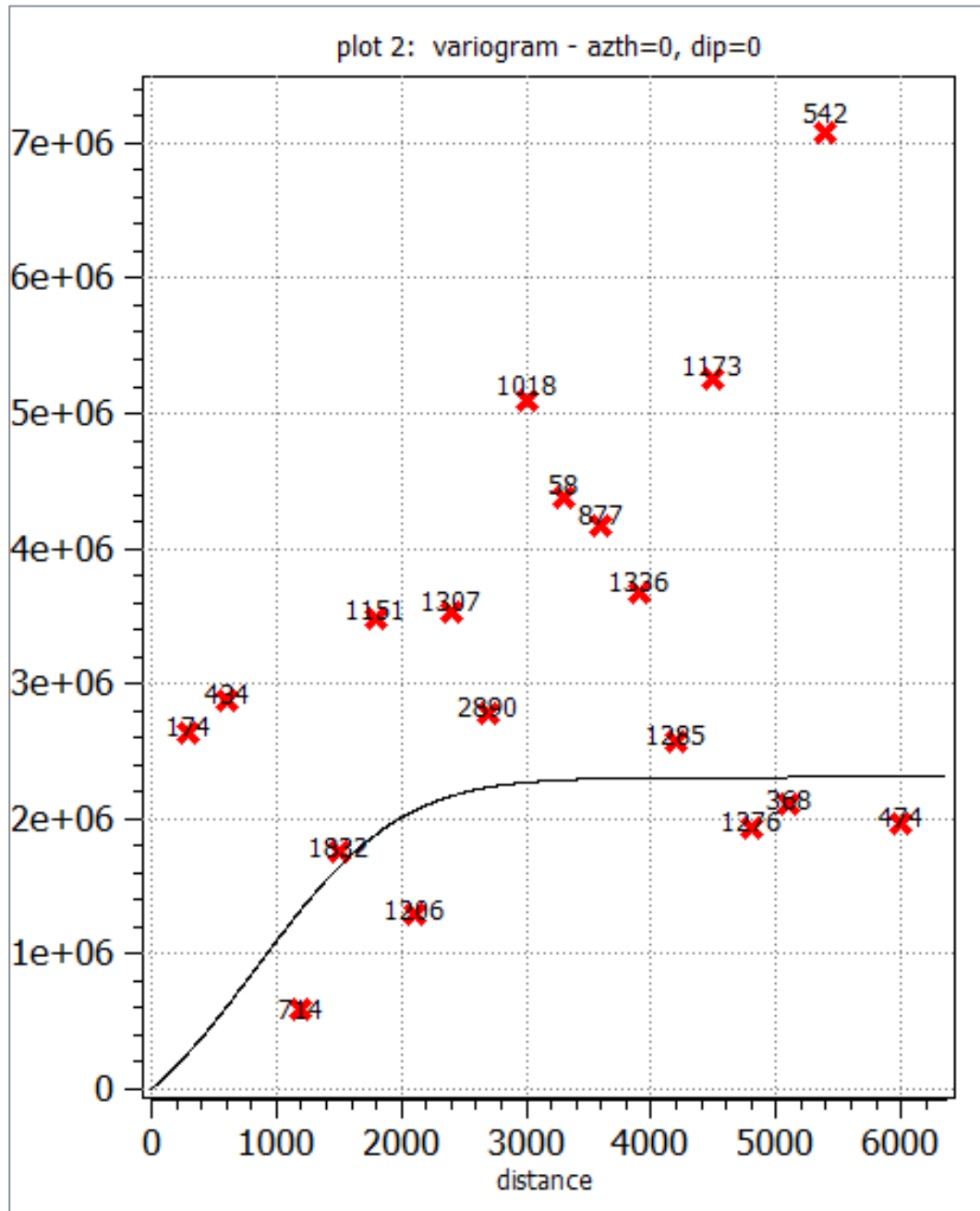


Figure 14-16 Vertical experimental variogram and variogram model for potassium within the alluvial deposits and lower sand region

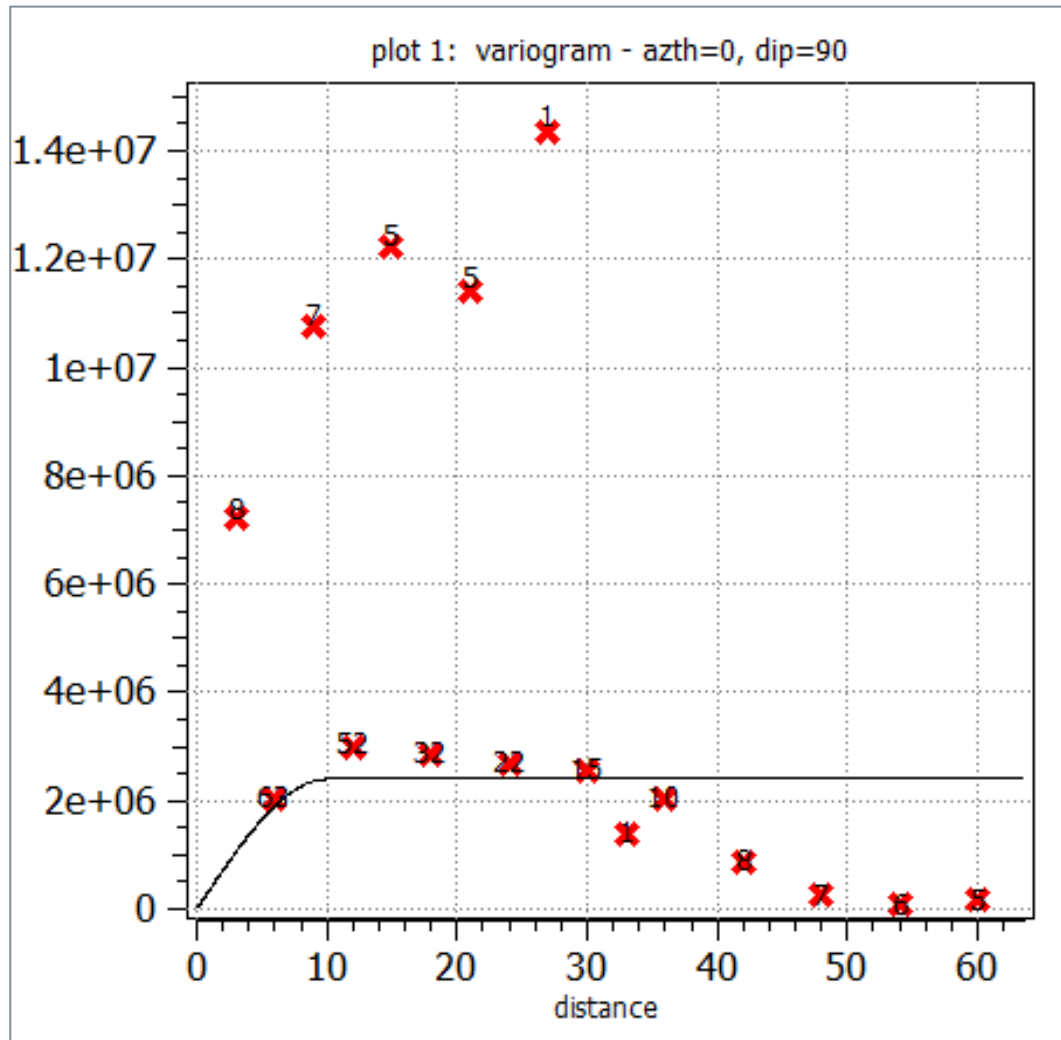


Figure 14-17 Vertical experimental variogram and variogram model for potassium within the Lacustrine region 11

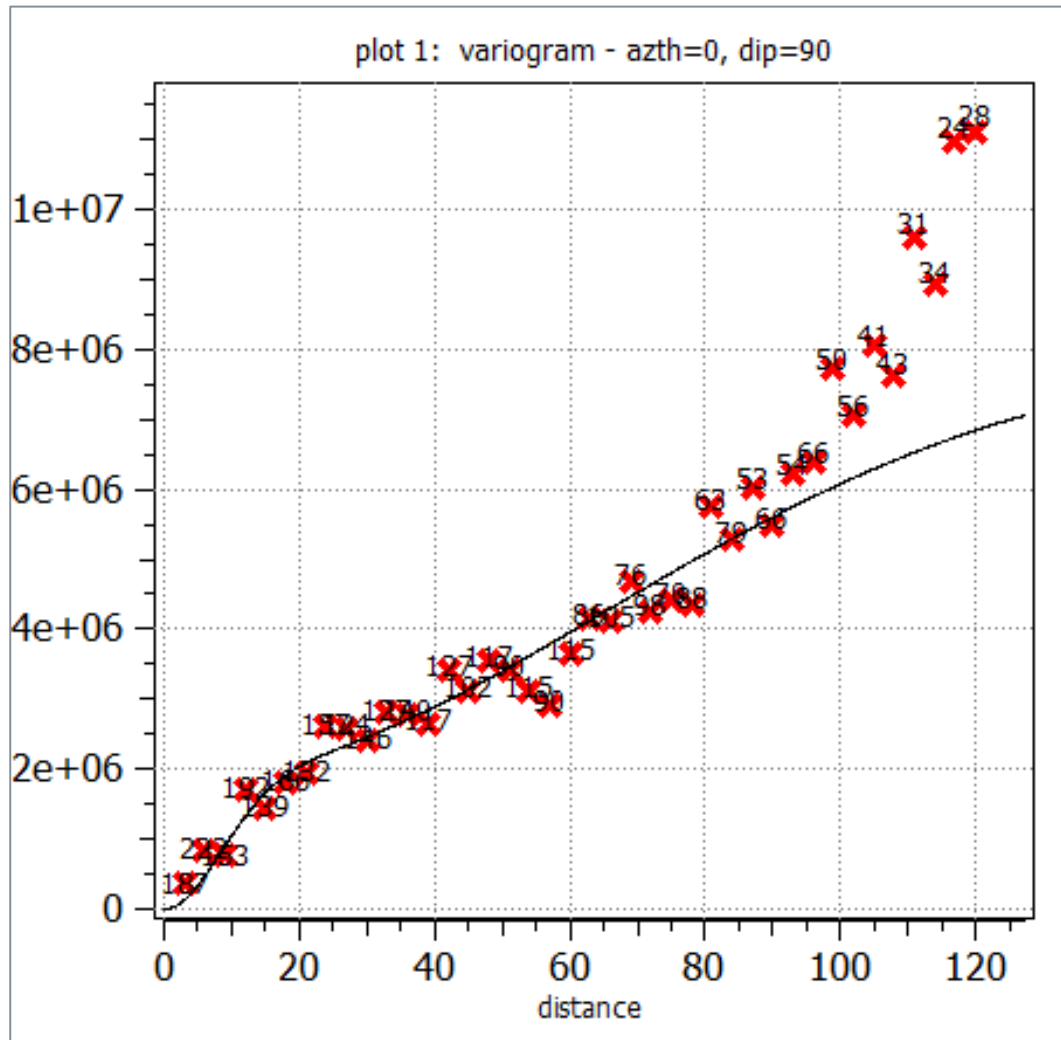


Figure 14-18 Vertical experimental variogram and variogram model for potassium within the halite and deep halite region

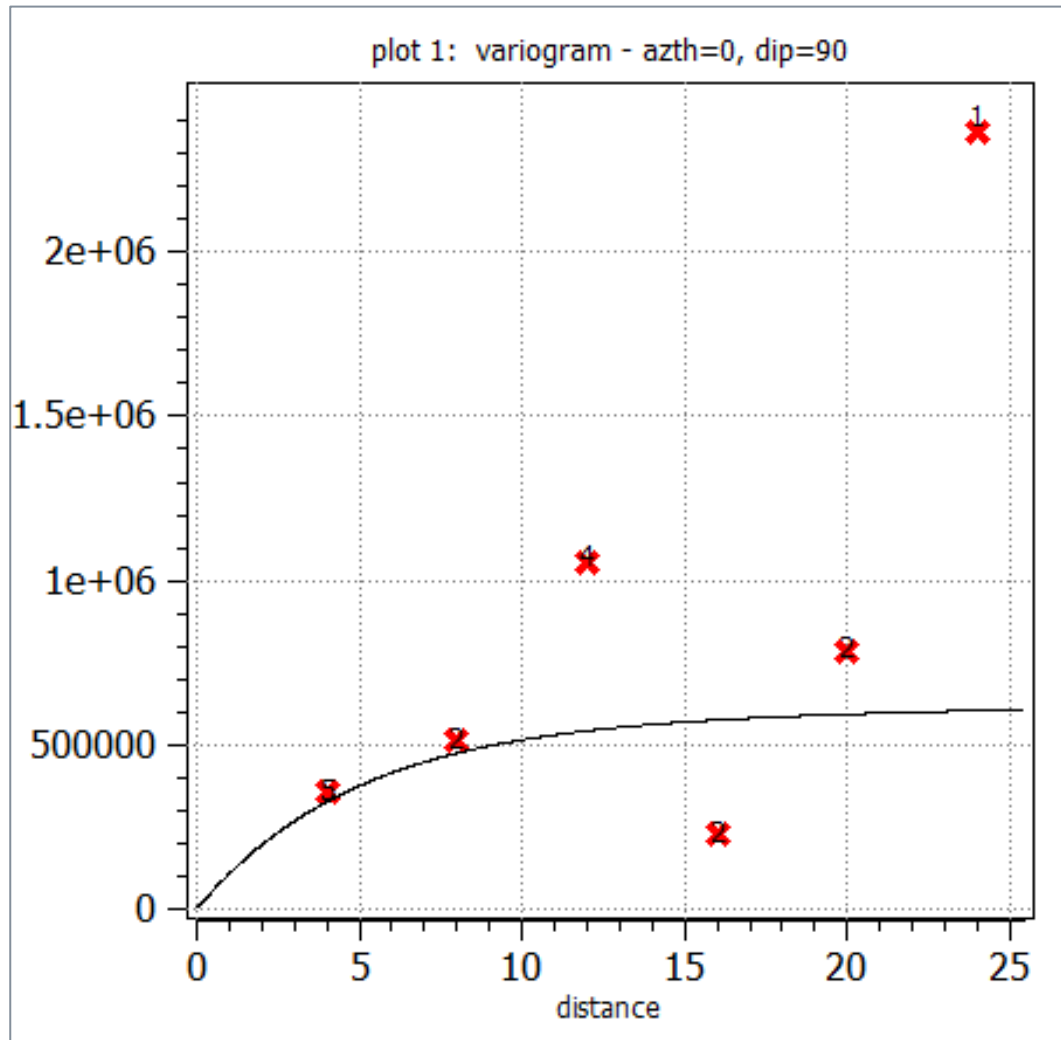


Figure 14-19 Vertical experimental variogram and variogram model for potassium within the volcanoclastic, lower volcanoclastic and volcanic breccia

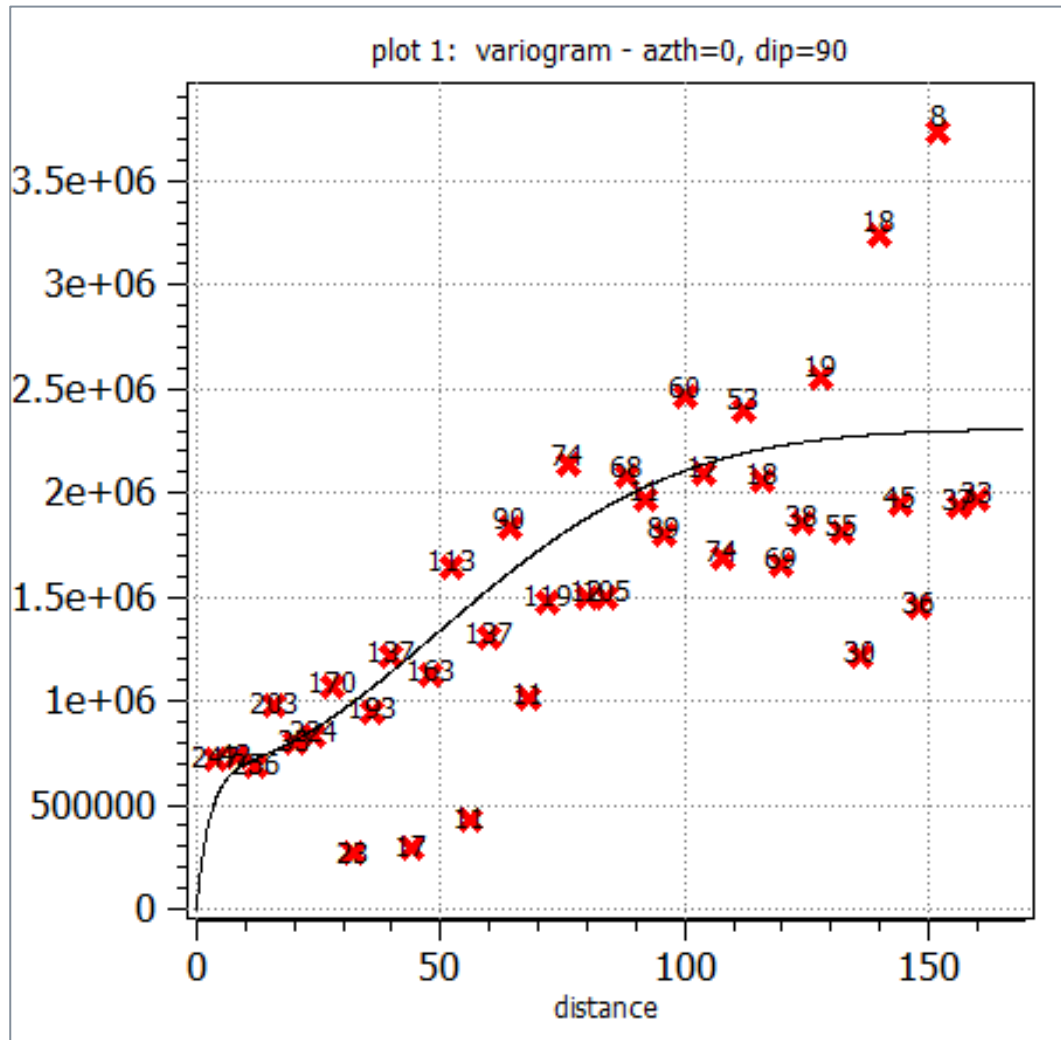


Figure 14-20 Lithium concentration distribution

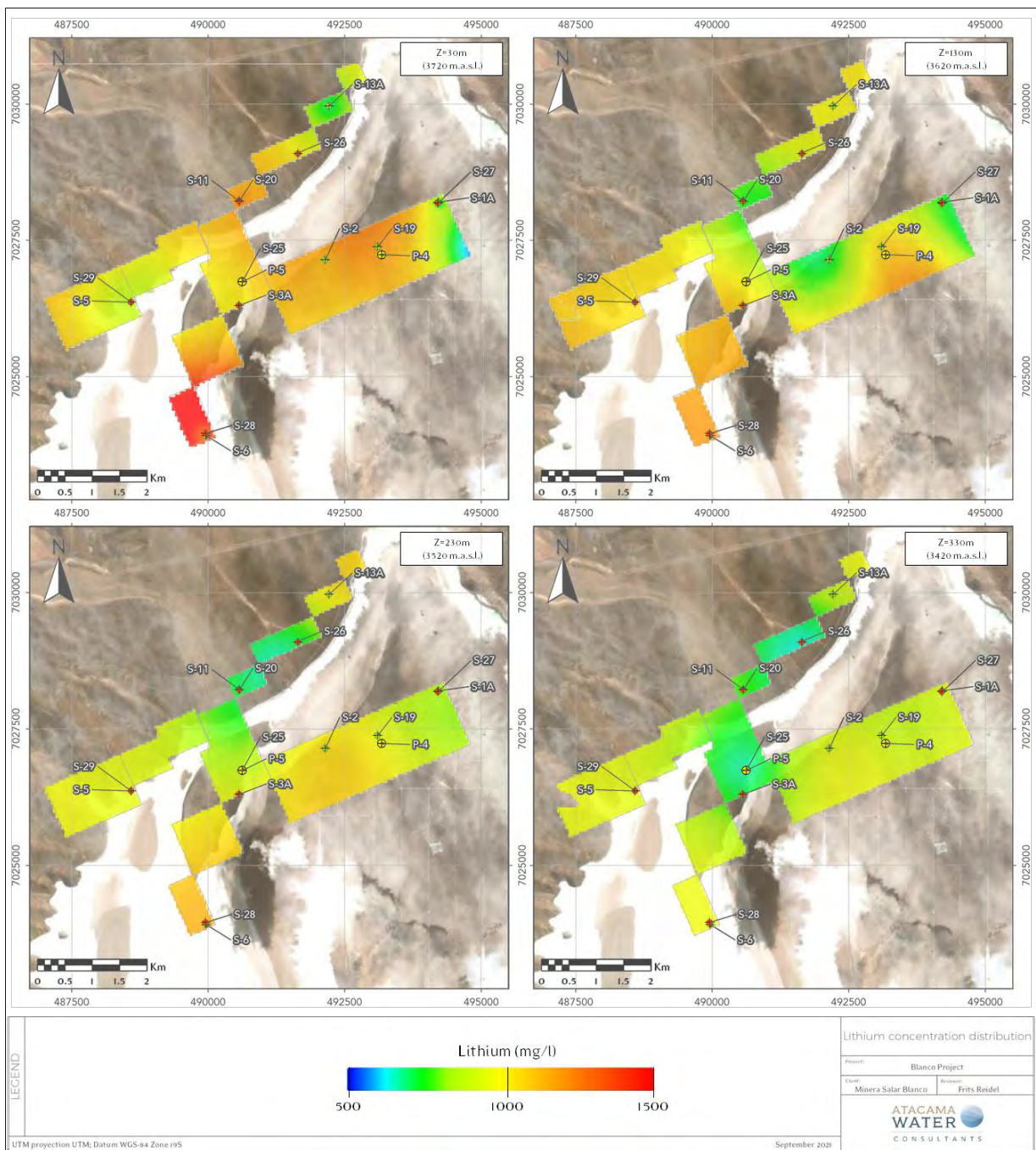
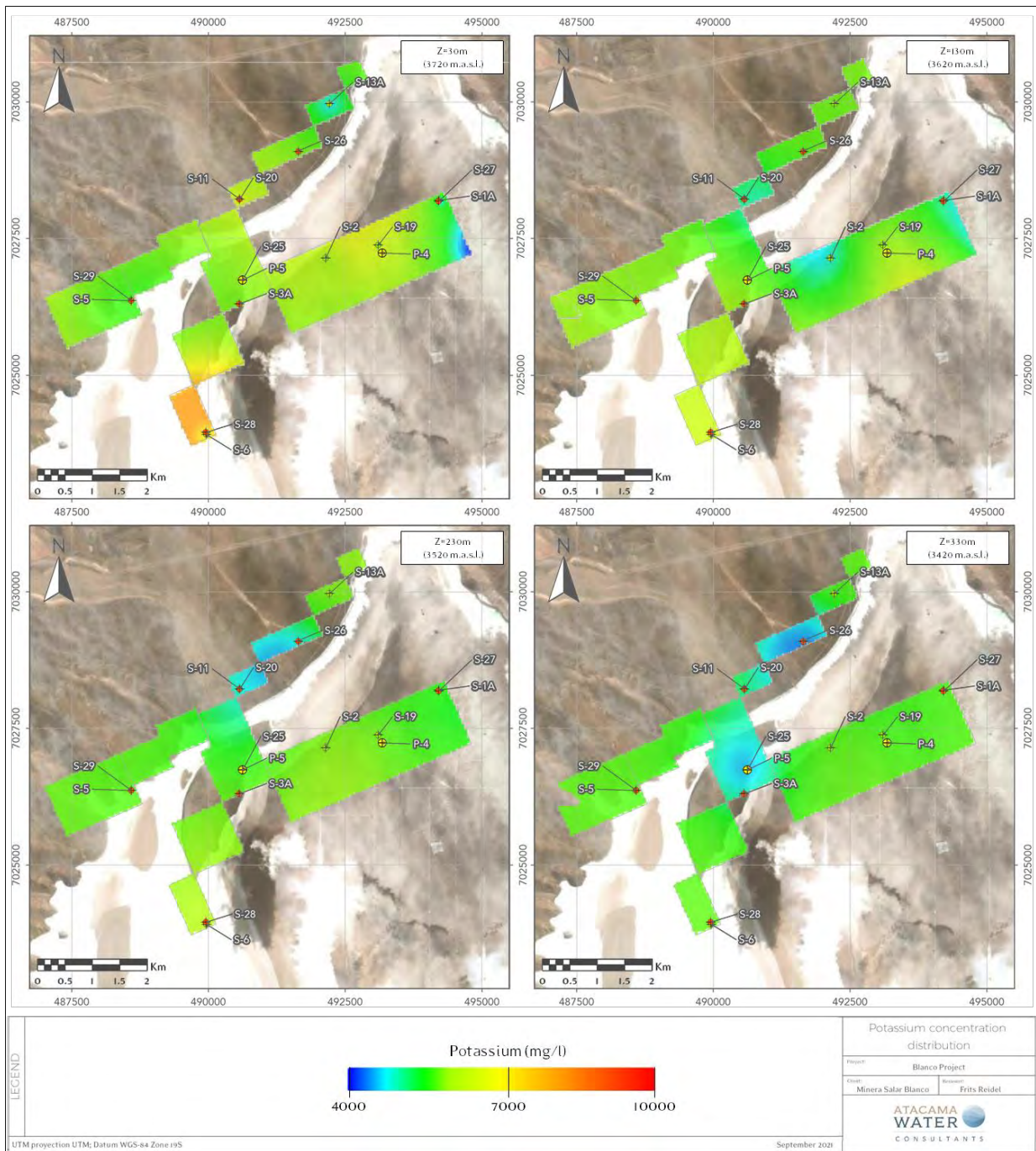


Figure 14-21 Potassium concentration distribution



14.7 GRADE ESTIMATE

The grade estimates of lithium and potassium in each block inside the model were calculated applying the following operation:

$$R_i = C_i \times Sy_i$$

Where: i is the indice of the block, going from 1 to 9,419,505

R_i : Grade value to be assigned (g/m³)

C_i : Concentration value assigned from the estimation (mg/L)

Sy_i : Specific yield value assigned from the estimation (%)

Figure 14-22 through Figure 14-24 show N-S, W-E, and NW-SE sections through the resource model with lithium grade distributions in g/m³. The resource classification was made within the limits of the block model. The Measured and Indicated Resource areas are shown in Figure 14-25.

Figure 14-22 3D lithium grade distribution in comparison to the geological model

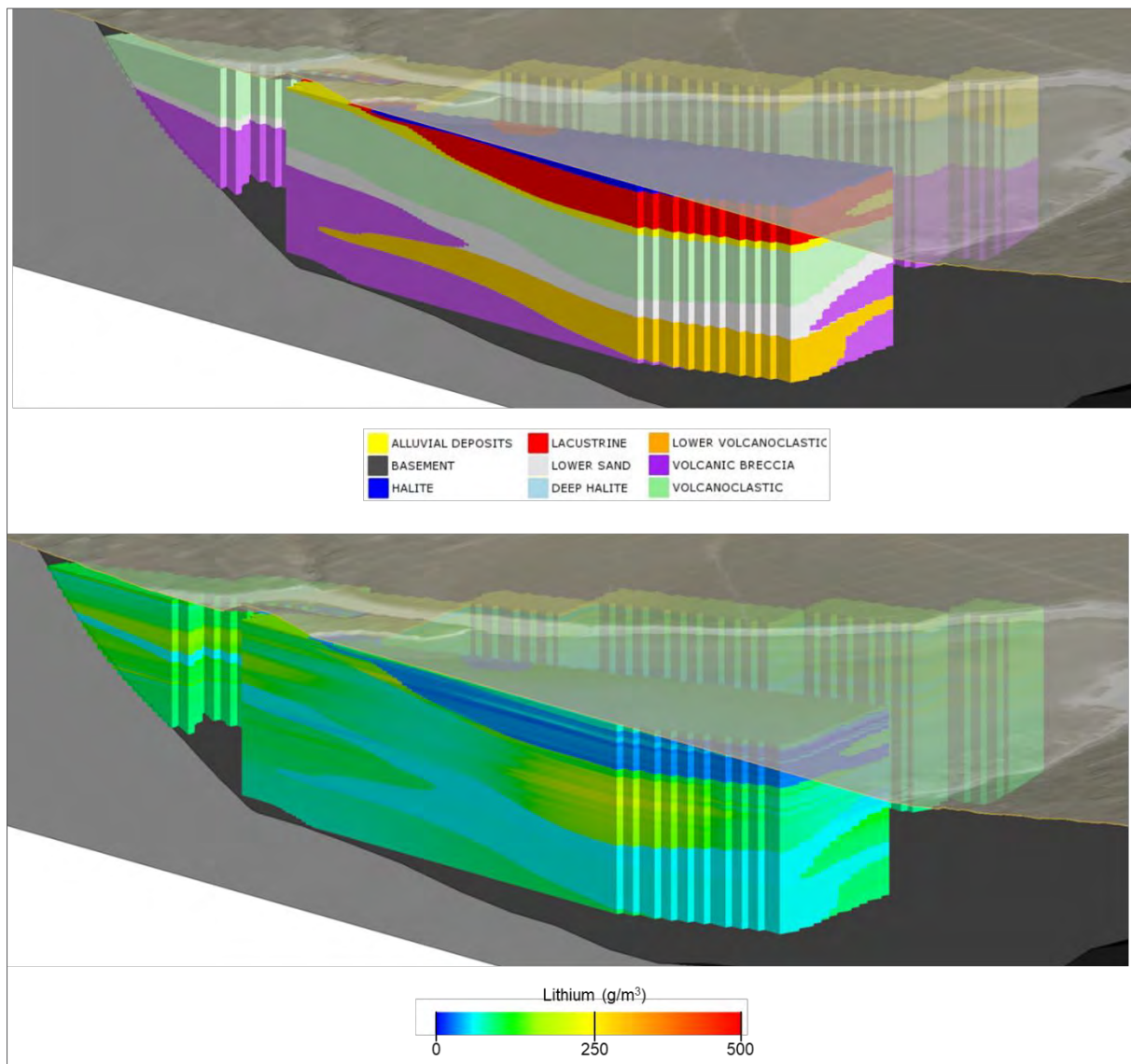


Figure 14-23 N-S section through the resource model showing the lithium grade distribution

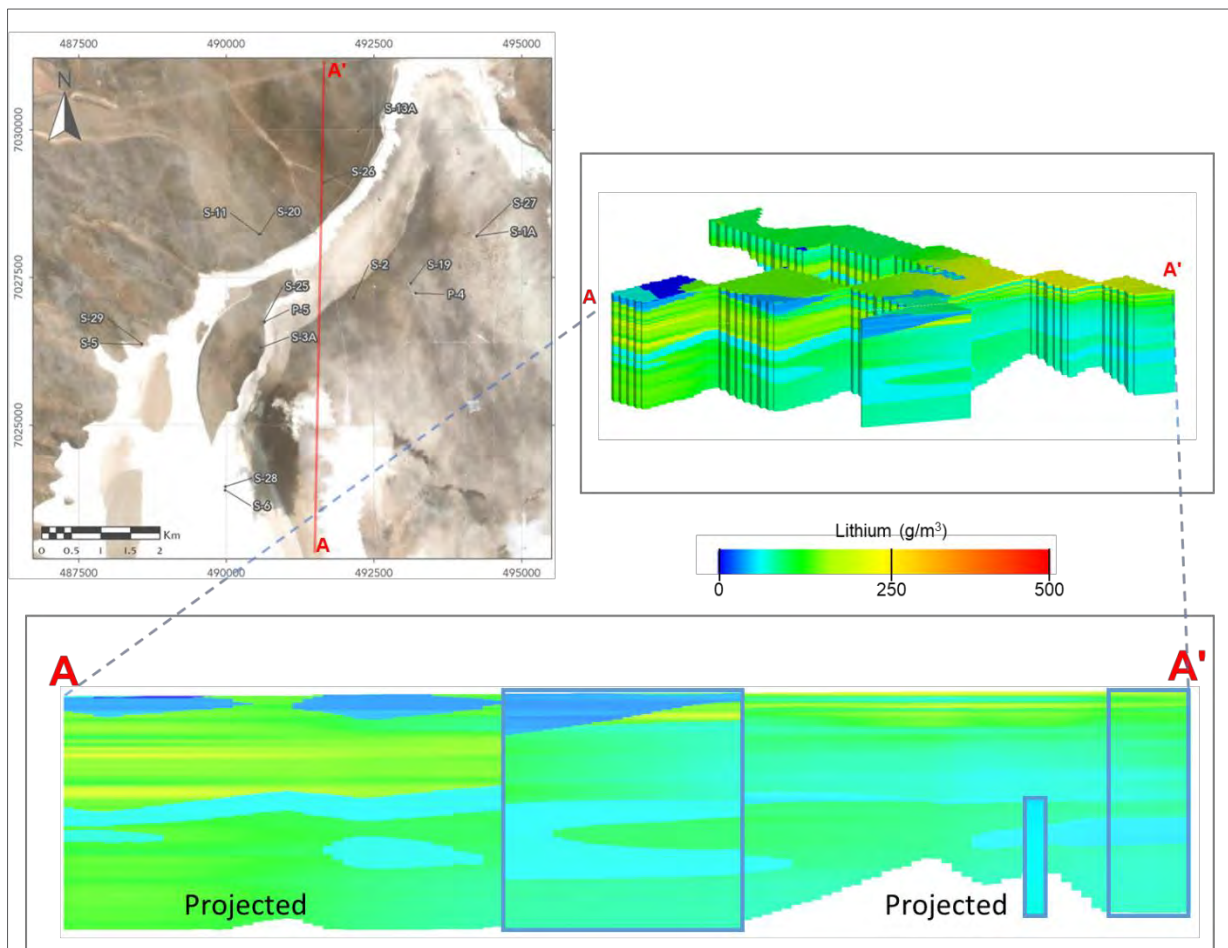


Figure 14-24 W-E section through the resource model showing the lithium grade distribution

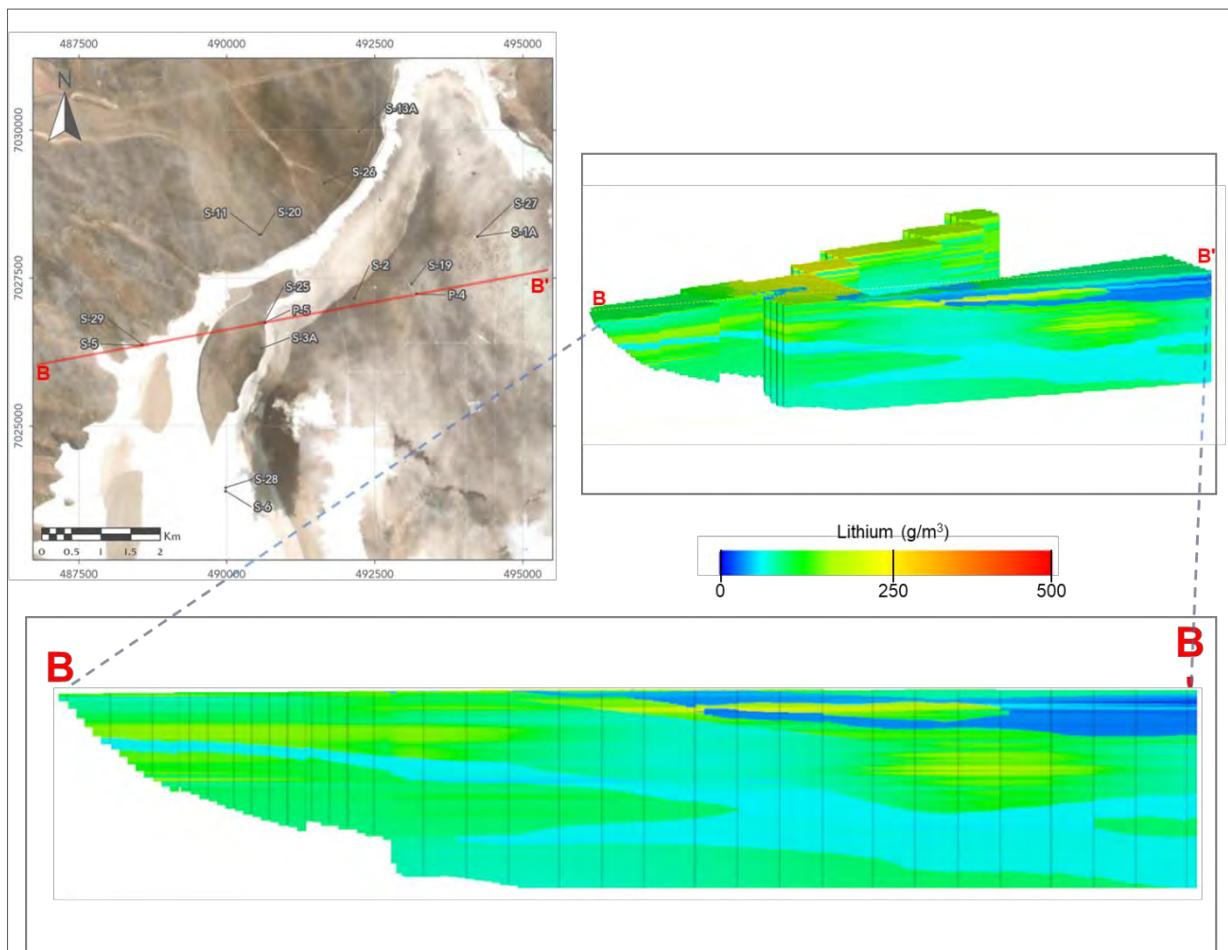


Figure 14-25 SW-NE section through the resource model showing the lithium grade distribution

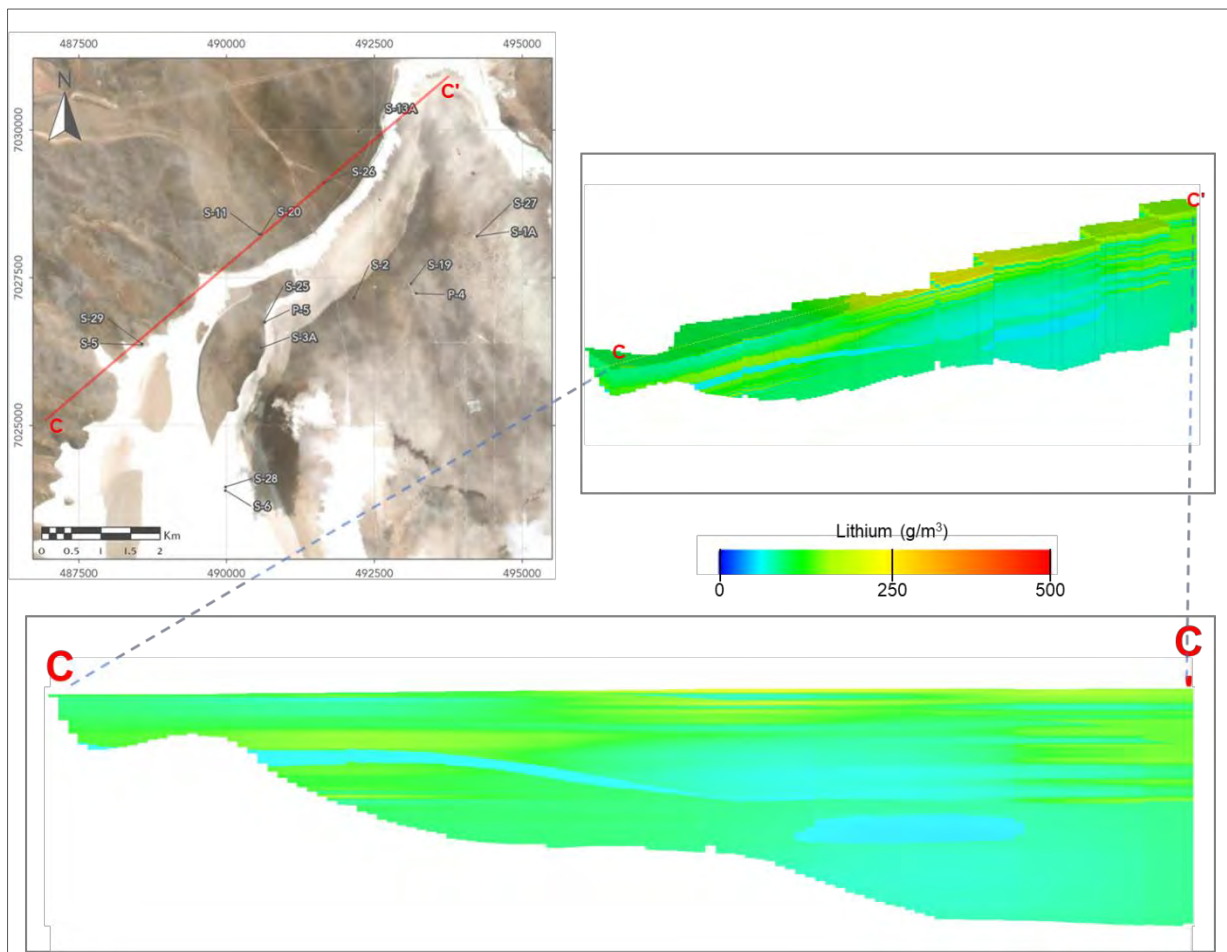
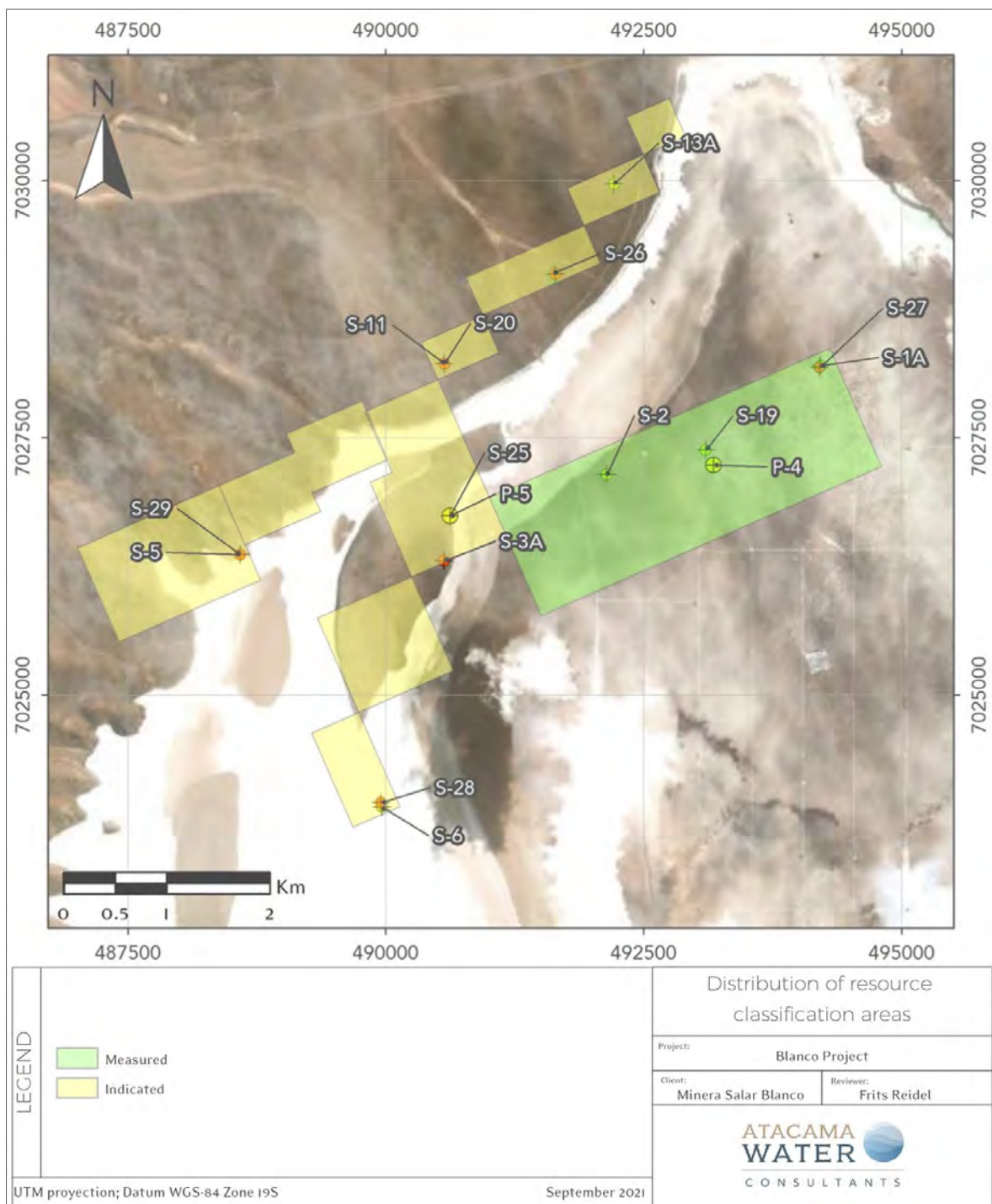


Figure 14-26 Distribution of resource classification areas



14.8 RESOURCE ESTIMATE

The resource estimate for the Stage One Project was prepared in accordance with the guidelines of National Instrument 43-101 and uses the best practices methods specific to brine resources. The lithium and potassium resources are summarized in Table 14-5. The effective date for the estimate is September 20, 2021.

Table 14-5 Lithium and Potassium Measured and Indicated Resources of the Stage One Project – ‘Old Code’ Concessions - dated September 20, 2021

	Measured (M)		Indicated (I)		M+I	
	Li	K	Li	K	Li	K
Area (Km ²)	4.5		6.76		11.25	
Aquifer volume (km ³)	1.8		1.8		3.6	
Mean specific yield (Sy)	0.09		0.12		0.1	
Brine volume (km ³)	0.162		0.216		0.378	
Mean grade (g/m ³)	87	641	111	794	99	708
Concentration (mg/l)	968	7,125	939	6,746	953	6,933
Resource (tonnes)	154,500	1,140,000	203,500	1,460,000	358,000	2,600,000

Notes to the resource estimate:

1. CIM definitions were followed for Mineral Resources.
2. The Qualified Persons for this Mineral Resource estimate is Frits Reidel, CPG
3. No cut-off values have been applied to the resource estimate.
4. Numbers may not add due to rounding
5. The effective date is September 20, 2021

Table 14-6 shows the mineral resources of the OCC expressed as lithium carbonate equivalent (LCE) and potash (KCl).

Table 14-6 Stage One (OCC) mineral resources expressed as LCE and KCL

	M+I Resources	
	LCE	KCL
Tonnes	1,905,000	4,950,000

1. Lithium is converted to lithium carbonate (Li₂CO₃) with a conversion factor of 5.32.
2. Potassium is converted to potash with a conversion factor of 1.91
3. Numbers may not add due to rounding

It should be noted that the OCC M+I Resources described in Table 14-5 and Table 14-6 are in addition to the M+I Resources (2018) of 184 Kt Lithium (979 Kt LCE) in the Litio 1-6 concessions to a depth of 200 m.

It is the opinion of the author that the Salar geometry, brine chemistry composition and the specific yield of the Salar sediments have been adequately characterized to support the Measured and Indicated Resource estimate for the Project herein.

It is the opinion of the author the resource estimated and described in the current report meet the requirements of reasonable prospects for eventual economic extraction, as defined in Form 43-101F1. The resource described herein has similar lithium concentrations, chemical composition and hydraulic parameter values (drainable porosity values between 0.02 and 0.14 and hydraulic conductivities values between 0,5 m/d and 300 m/d) to resources currently in commercial production such as those in Salar de Atacama or Salar de Olaroz (located in the Puna region of Northern Argentina). The hydraulic parameters of the resource area determined from the results of the pumping tests suggest that it is reasonable to expect brine extraction by a conventional production wellfield at a commercially viable rate, while the geochemical characteristics of the brine suggest that conventional processing techniques may be employed to produce saleable lithium products in an economically profitable manner.

These conventional processing techniques are employed in most lithium brine operations, including the two operations at Salar de Atacama (Chile), one at Salar de Olaroz (Argentina), and one at Clayton Valley (USA).

15. MINERAL RESERVE ESTIMATES

This section presents a numerical groundwater flow and transport model developed for the Stage One Project to evaluate the brine mineral reserve for the Stage One Project. The modelling work was carried out by DHI in Lima, Peru under close supervision of Atacama Water and the QP. The essential elements of a brine reserves determination for a Salar are:

- Construction of a three-dimensional groundwater flow and transport model
- Steady state and transient calibration of the model
- Predictive simulation of brine extraction

The calibrated reserve model is used to simulate a brine extraction system that will meet the brine feed requirements for the evaporation ponds for an annual lithium carbonate (LCE) production target of 15 kilotons per year (ktpy) over a 20-year project life. It is assumed that the Project has a lithium process recovery efficiency of 65%. Therefore, to meet the LCE target production rate of 15 ktpy, the brine abstraction from the production wellfield in the Salar needs to be at a rate of 23.1 ktpy approximately. The reserve model predicts that the proposed brine wellfield can extract an annual average of 24 ktpy of LCE for 20 years implying an average production rate of 15.2 ktpy.

This section describes the construction and calibration of the numerical model and summarizes the results of the brine production simulations and the reserve estimate.

15.1 MODEL DOMAIN

The model domain shown in Figure 15-1 encompasses the unconsolidated sediments of the Maricunga basin. It extends from the Salar de Maricunga, in the west central portion of the domain, to the upper reaches of the alluvial fans in the catchments feeding the Salar. The topographic elevation of the model domain ranges from 3,745 meters above sea level (masl) at the Salar to 4,230 masl in the northeast corner of the domain. The base of the model has an elevation of 3,145 m, for a maximum simulated sediment thickness beneath the Salar of 600 m.

15.2 MESHING AND LAYERING

The horizontal refinement of the model consists of triangular prisms elements with elemental diameters ranging from approximately 7 m in the pumping test sites up to 227 m at the outer edges of the model domain. The total average element size is 81 m and for the concession area 45 m with a maximum element size of 84 m (Figure 15-1). Local refinement was added around the production wells used to simulate the pumping tests for transient calibration. The layer thickness is variable from depth and increases from the top to the bottom of the model (Figure 15-2). The model layers

can be classified in 4 different zones of layer thickness that range from 6.5 m for the two top layers up to 41 m for the layers below 400 m depth (Table 15-1). The model has a total of 2,304,325 active nodes and 4,366,999 active elements distributed between 29 active layers.

Table 15-1 Layer distribution

Zone	Layers	Thickness (m)	Total Thickness (m)
1	2	6.5	13
2	14	13	182
3	8	25	200
4	5	41	205
Total	29	-	600

Figure 15-1 Model domain and mesh element size

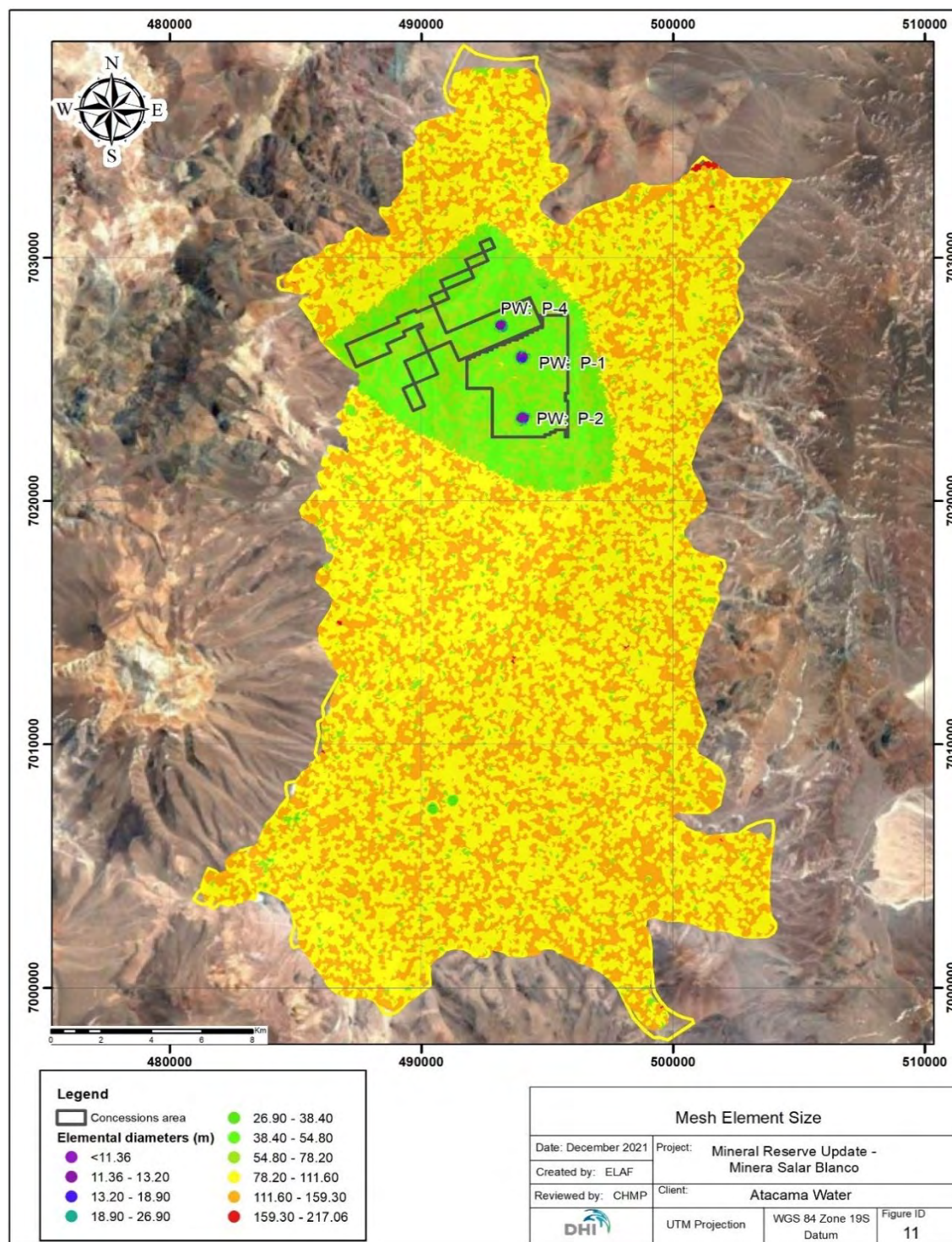
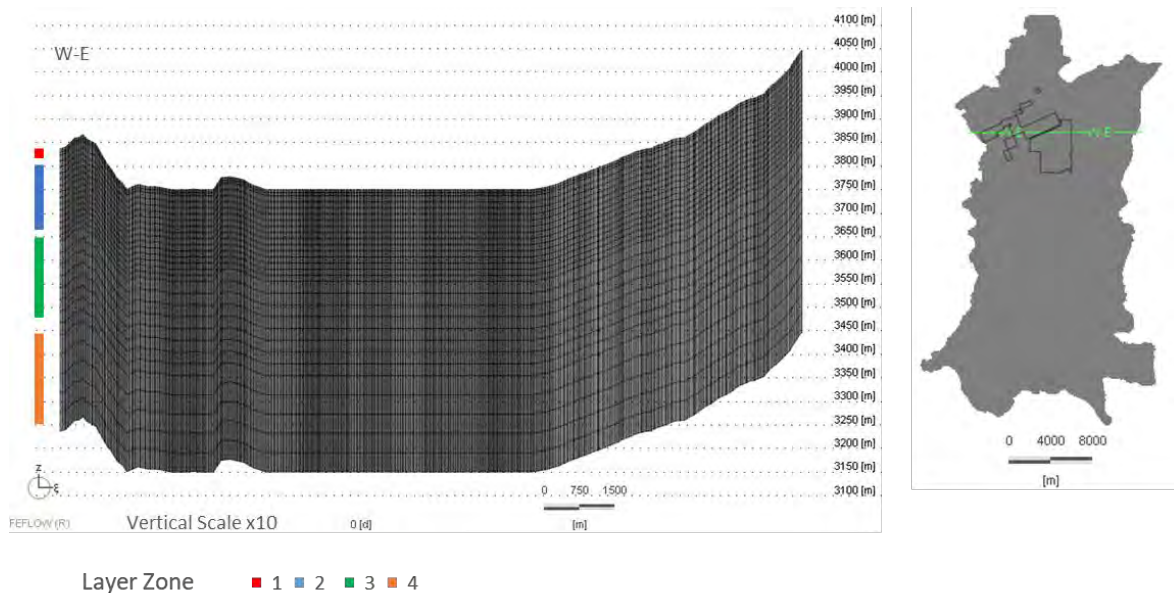


Figure 15-2 Mesh vertical extension

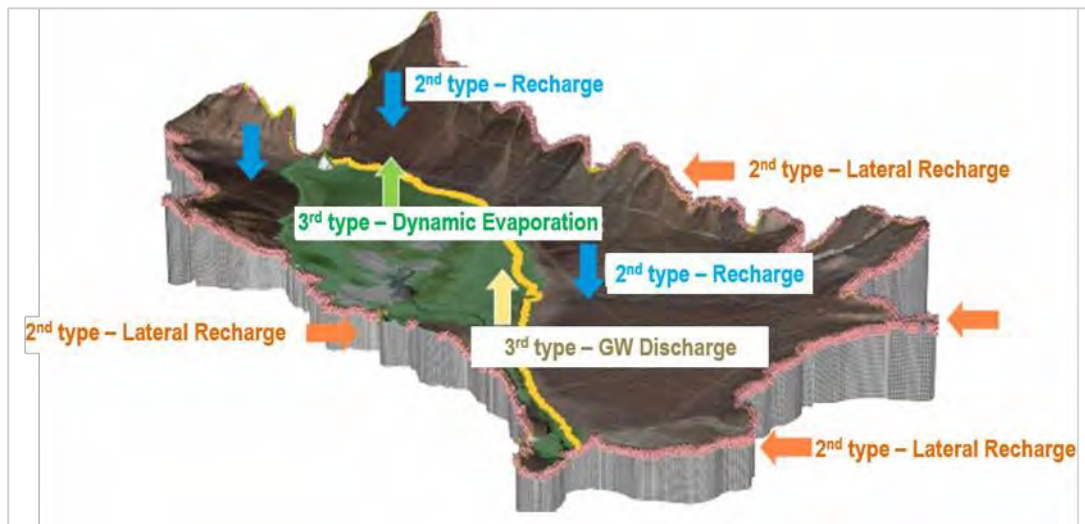


15.3 FLOW BOUNDARY CONDITIONS

The model boundary conditions are presented in Figure 15-3. Two primary groundwater inflow processes occur in the Maricunga Salar: surface recharge by direct precipitation and lateral recharge from the surrounding catchments. The groundwater natural outflow occurs at lower elevations only through evapotranspiration both from land surface and surface water.

The lateral recharge boundary conditions were applied to the outer boundaries in all the slices of the model, except for the inactive basement elements. Where a lateral recharge boundary is not defined, the model edge is treated as a no-flow boundary. Evapotranspiration and surface recharge boundary conditions were applied to Layer 1. The bottom of the model domain was treated as a no-flow boundary.

Figure 15-3 Model boundary conditions (WorleyParsons, 2019)



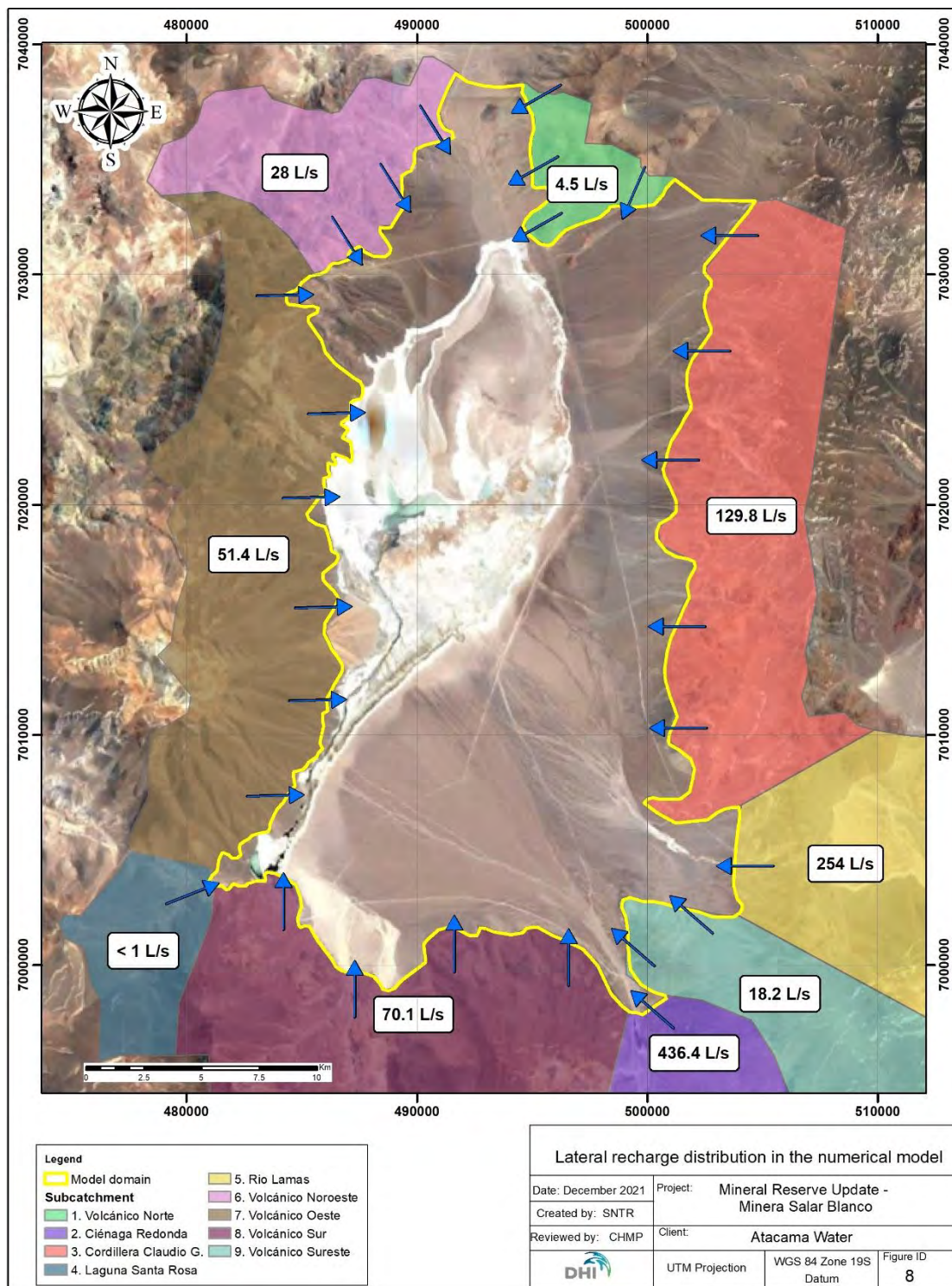
15.3.1 DIRECT RECHARGE

Recharge was applied only to the alluvial fan materials, at a rate of 32.3 mm/y, for a total of 405 L/s. The recharge area coincides with the areal extent of the unconsolidated sediments (discarding basement outcrops). Recharge on top of the Salar was discarded as it was assumed that this is assumed to be an area of net groundwater discharge (Figure 15-3).

15.3.2 CATCHMENT INFLOWS

In addition to direct recharge, the Maricunga Salar receives indirect recharge as lateral groundwater recharge that is generated by the eight upstream catchments surrounding the Maricunga Basin (Figure 15-4). The catchment inflows were treated as flux (second type) boundary conditions. Inflow rates range from 4.5 l/s from the North Volcanic basin located north of the Salar to 436 L/s from the Ciénaga Redonda catchment located southeast of the Salar. The total inflow in the model as lateral recharge is 990 L/s.

Figure 15-4 Indirect, lateral recharge to Salar de Maricunga from the surrounding catchments



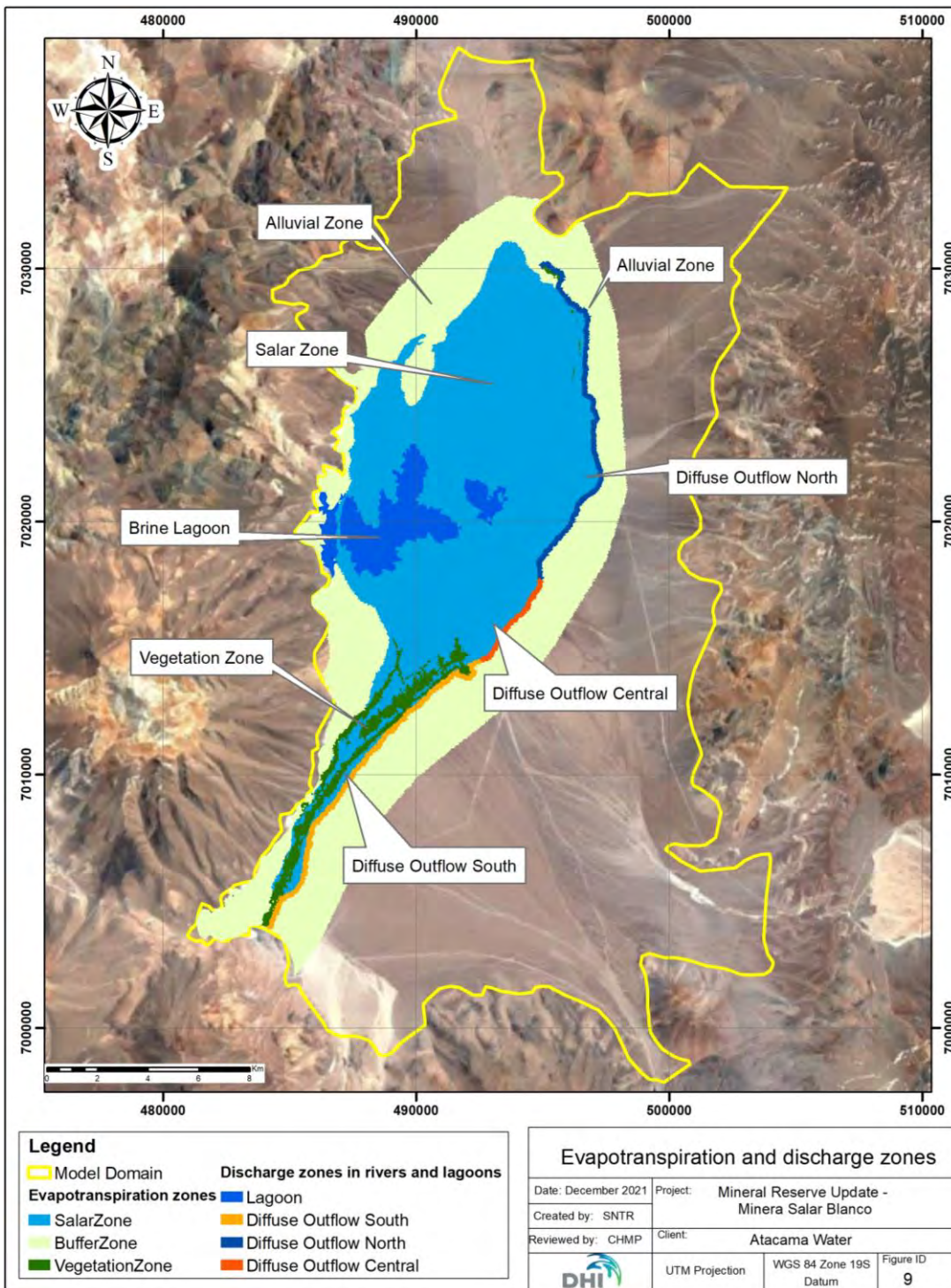
15.3.3 EVAPOTRANSPIRATION AND DIFFUSE GROUNDWATER DISCHARGE

Evapotranspiration and diffuse groundwater discharge are simulated with the Fluid-transfer boundary condition (Figure 15-5) as follows:

- 1- Zone 1. The head reference of the Fluid-transfer boundary condition is set 2 m below the ground surface and a minimum head constraint exist at the same elevation. The evapotranspiration rate decreases linearly with depth from ground surface to a depth of 2 m, at which point, the evapotranspiration rate is set to equal zero. This zone includes the conceptual evapotranspiration areas of vegetation, Salar and the alluvial buffer located in the lower topographic area of the alluvium deposits.
- 2- Zone 2. The Maricunga Salar hosts areas of surface water during the wet season. These areas are located along the eastern and southern margin of the Salar, where brine and freshwater come in contact at the downgradient edge of the alluvial fans. Conceptually, freshwater discharge is driven by the presence of the lacustrine unit, at the Salar margins (WorleyParsons, 2019). Three groundwater discharge zones were defined as diffuse outflow or stream zone that are classified between north, central and south. The geometry of this zone is conditioned by lacustrine outcrop in the centre of the Salar.

The magnitude of the steady state evapotranspiration was calibrated using target evapotranspiration fluxes from the conceptual water balance (WorleyParsons, 2019). The value of maximum evapotranspiration transfer rate in each zone was adjusted during the calibration such that the total evapotranspiration distribution matched the conceptual water budget.

Figure 15-5. Evapotranspiration and diffuse groundwater discharge zones



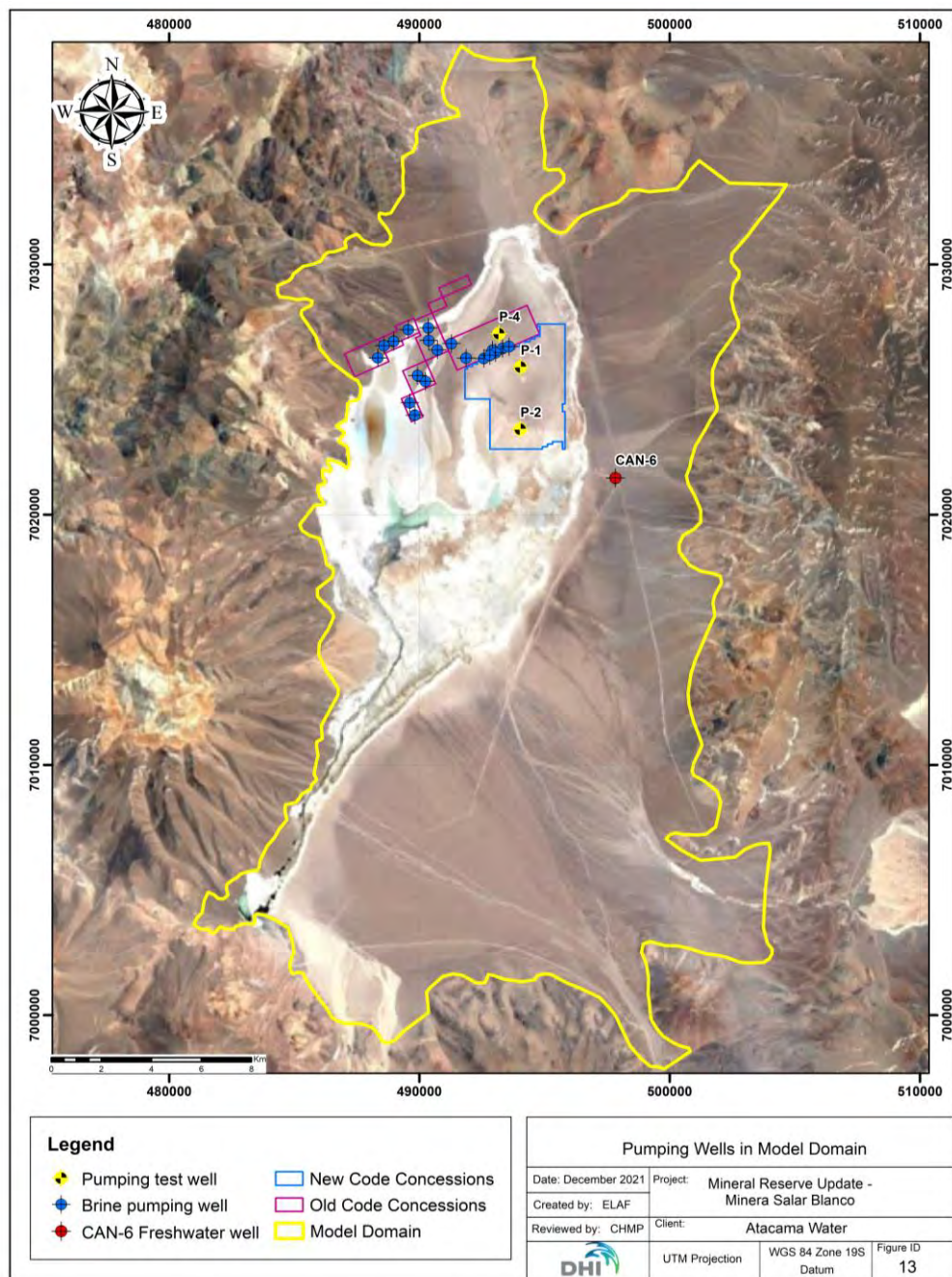
15.3.4 PUMPING WELLS

Pumping tests were completed in production wells, P-1, P-2, and P-4 (Figure 15-6). These wells were simulated with a series of individual well boundary conditions in the numerical model and their location and flow rates are described in Section 15.7.2. There are two existing water supply wells, MDO-23 and MDO-24, in the south-central area of the model domain, that operated in the past as part of the Mantos de Oro water supply system; currently they are not under operation. Given that the water levels have practically recovered to pre-pumping levels (Golder Associates, 2011), these wells were not part of the steady state or transient calibration runs.

In addition, MSB has permitted a freshwater supply well CAN-6 shown in Figure 15-6. CAN-6 was simulated as a series of vertically stacked well boundary nodes within the FEFLOW model in the predictive simulations. The flow rate from CAN-6 is 10 L/s over the duration of the mine life.

The brine production wellfield was simulated with 23 well boundary conditions also shown in Figure 15-6, located in the centre of the Upper Halite aquifer or the deep brine aquifers below the Lacustrine unit. These wells and their pumping rates are discussed in the reserve estimation presented in Section 15.9.

Figure 15-6 Pumping wells in the model domains



15.4 HYDROGEOLOGICAL UNITS AND PARAMETERS

15.4.1 MAIN HYDROGEOLOGICAL UNITS

The hydrogeological units were derived from the Leapfrog geological model. Eleven primary hydrogeological units were defined for the new reserve model:

- Upper Alluvium: Alluvial fans surrounding the Salar. In the model and for calibration purposes, this unit is divided into 19 different zones.
- Lower Alluvium: Alluvial material mainly located below the Upper Alluvium in the east part of the model and below the Lacustrine unit.
- Upper Halite: Upper shallow aquifer located in the centre of the Salar.
- Deep Halite: This is a secondary unit due to its extension that is located within the lacustrine unit. Deep Halite has lower hydraulic conductivity than Upper Halite.
- Lacustrine: The low permeability unit is represented by the Lacustrine unit in the centre of the Salar area. It underlies and surrounds the Upper Halite and close to the Salar margins occurs in outcrop and covers a significant area in the southern part of the Salar.
- Lower Sand: This is relatively minor unit underlies the Volcanoclastic unit and occurs mainly in the northern part of the model domain. It has a thickness between 30 m and 60 m.
- Volcanoclastic: This unit is located mainly in the northwest area of the model domain. It underlies the Upper Alluvium unit and the Lacustrine unit in the Salar. It hosts the deep brine aquifer below the Project area.
- Volcanic Breccia: This unit is located in the Northern part of the model domain and underlies the Upper Alluvial, Volcanoclastic and Lower Volcanoclastic units. This unit forms part of the deep brine aquifer.
- Lower Volcanoclastic: The extension of the Lower Volcanoclastic unit is restricted to the northern part of the Salar and represents a deep unit underlying the Lower Sand and surrounded by the Volcanic Breccia. This unit is part of the deep brine aquifer.
- Basal Sediments: This unit underlies all the previous units from a depth of approximately 300 m down to the basement in the centre and southern areas of the Salar and is also part of the deep brine aquifer.
- Basement: This unit represents the impermeable bedrock of the sedimentary basin and is inactivated in the model.

For the calibration process, subunits were defined to improve the match between the observed and simulated heads. A total of 36 hydrogeological property zones are defined in the model. The main hydrogeological zones that exist at ground surface—i.e., in Layer 1 of the model—are shown in

Figure 15-7 and Figure 15-8. A complete list for all the hydrogeologic units is presented in Table 15-2, along with conceptual values of hydraulic conductivity and storage reported in WorleyParsons, 2019.

Figure 15-7. Surface hydrogeological units

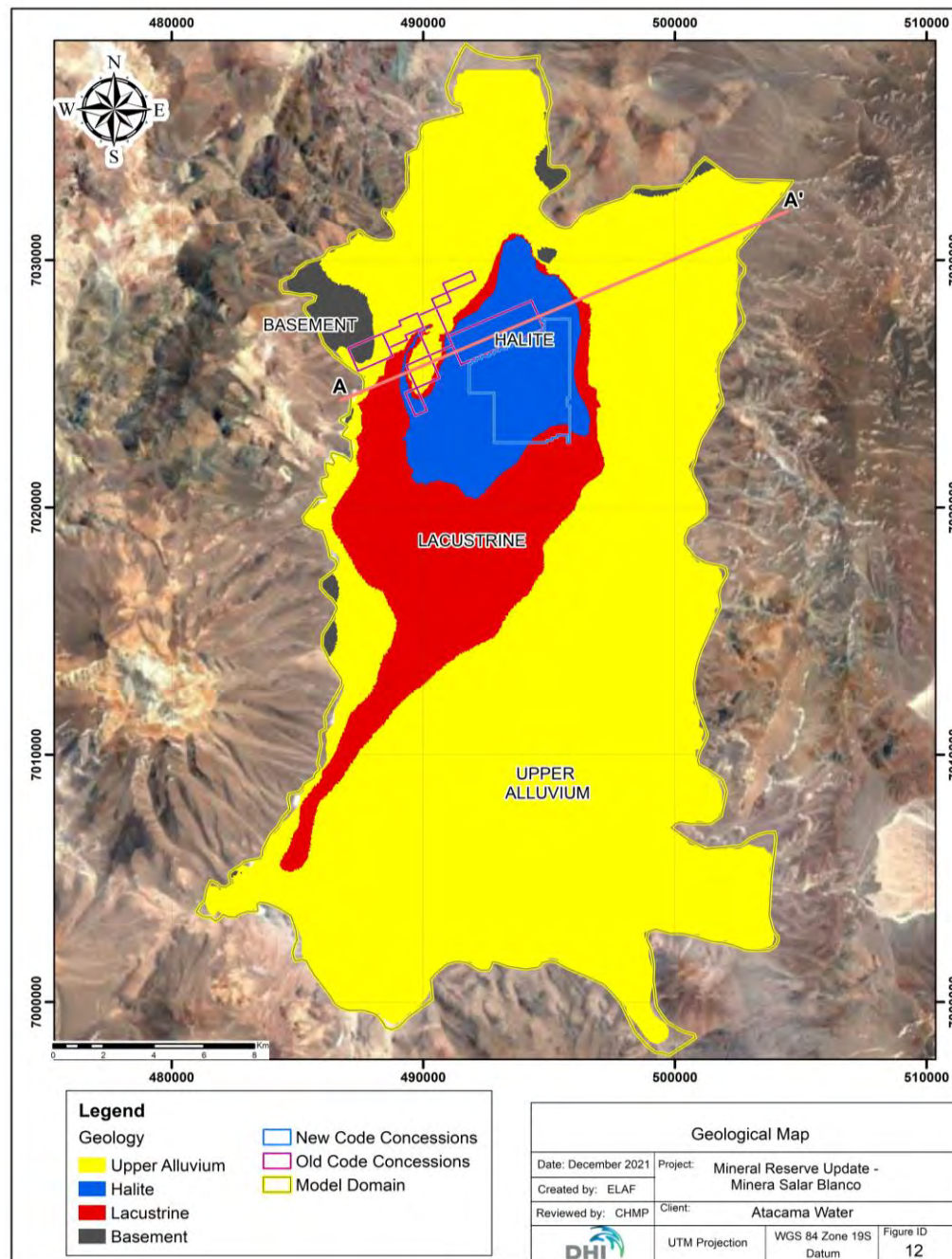


Figure 15-8 Geological units in cross section

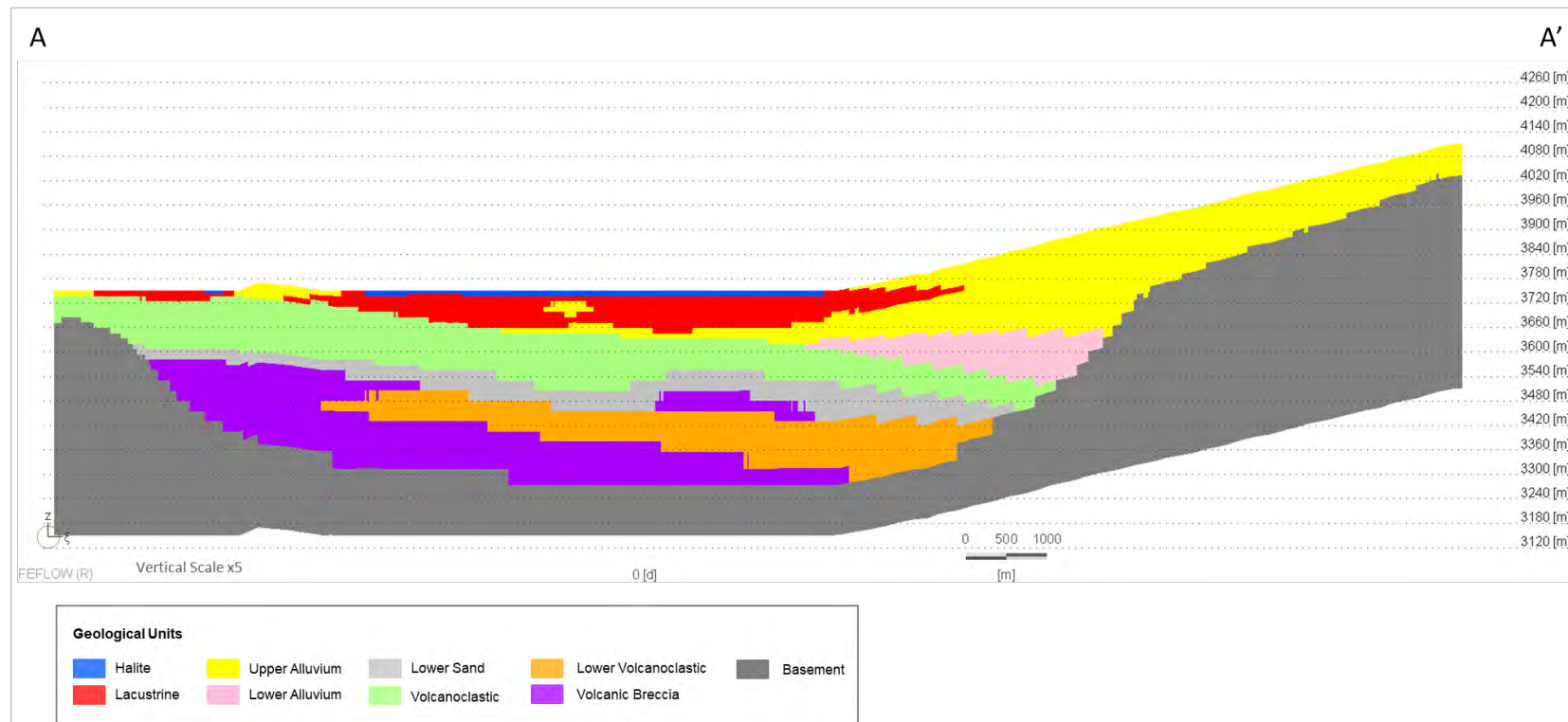


Table 15-2. Saturated hydraulic parameter values

ID	UG	Conceptual K (m/d)	Conceptual Ss (1/m)	Conceptual Sy
1.1all	Upper Alluvium	0.1 - 10	1.0E-05 - 1.0E-03	13.5%
1.2all	Upper Alluvium	0.1 - 10	1.0E-05 - 1.0E-03	13.5%
1.3all	Upper Alluvium	0.1 - 10	1.0E-05 - 1.0E-03	13.5%
1.4all	Upper Alluvium	0.1 - 10	1.0E-05 - 1.0E-03	13.5%
1.5all	Upper Alluvium	30 - 280	1.0E-05 - 1.0E-03	13.5%
1.6all	Upper Alluvium	30 - 300	1.0E-05 - 1.0E-03	13.5%
1.7all	Upper Alluvium	30 - 280	1.0E-05 - 1.0E-03	13.5%
1.8all	Upper Alluvium	30 - 280	1.0E-05 - 1.0E-03	13.5%
1.9all	Upper Alluvium	10 - 280	1.0E-05 - 1.0E-03	13.5%
1.19all	Upper Alluvium	0.1 - 40	1.0E-05 - 1.0E-03	13.5%
1.19all_sat	Upper Alluvium	0.1 - 40	1.0E-05 - 1.0E-03	13.5%
1.11all	Upper Alluvium	0.1 - 40	1.0E-05 - 1.0E-03	13.5%
1.11all_sat	Upper Alluvium	0.1 - 40	1.0E-05 - 1.0E-03	13.5%
1.12all	Upper Alluvium	0.1 - 40	1.0E-05 - 1.0E-03	13.5%
1.13all	Upper Alluvium	0.1 - 40	1.0E-05 - 1.0E-03	13.5%
1.14all	Upper Alluvium	0.1 - 40	1.0E-05 - 1.0E-03	13.5%
1.15all	Upper Alluvium	0.1 - 40	1.0E-05 - 1.0E-03	13.5%
1.16all	Upper Alluvium	0.1 - 40	1.0E-05 - 1.0E-03	13.5%
1.17all	Upper Alluvium	0.1 - 40	1.0E-05 - 1.0E-03	13.5%
1.18all	Upper Alluvium	0.1 - 40	1.0E-05 - 1.0E-03	13.5%
1.21all	Lower Alluvium	0.1 - 1	1.0E-05 - 1.0E-03	13.5%
1.22all	Upper Alluvium	0.1 - 40	1.0E-05 - 1.0E-03	13.5%
2bse	Basal Sediments	0.001 - 2.5	1.0E-07 - 1.0E-03	-
3dha	Deep Halite	0.0001 - 0.01	1.0E-07 - 1.0E-03	6.0%
4hal	Halite	100 - 640	1.0E-07 - 1.0E-03	6.3%
5lac	Lacustrine	0.0001 - 0.01	1.0E-07 - 1.0E-03	1.9%
5.1lac	Lacustrine	0.01 - 10	1.0E-07 - 1.0E-03	1.9%
5.2lac	Lacustrine	0.01 - 10	1.0E-07 - 1.0E-03	1.9%
5.3lac	Lacustrine	0.01 - 10	1.0E-07 - 1.0E-03	1.9%
5.4lac	Lacustrine	100 - 640	1.0E-07 - 1.0E-03	1.9%
5.5lac	Lacustrine	100 - 640	1.0E-07 - 1.0E-03	1.9%
5.6lac	Lacustrine	100 - 640	1.0E-07 - 1.0E-03	1.9%
6lsa	Lower Sand	0.1 - 2.5	1.0E-07 - 1.0E-03	6.5%
7lvo	Lower Volcanoclastic	0.1 - 2.5	1.0E-07 - 1.0E-03	7.9%
8vbr	Volcanic Breccia	0.1 - 2.5	1.0E-07 - 1.0E-03	13.1%
9vo	Volcanoclastic	0.1 - 2.5	1.0E-07 - 1.0E-03	11.8%

15.4.2 UNSATURATED PARAMETERS

The Feflow model was run using a variably saturated configuration. Feflow's modified van Genuchten parameterization was used. This formulation makes use of this pressure-saturation relationship:

$$S_e = \left(\frac{\theta - \theta_r}{\theta_s - \theta_r} \right) = \left[\frac{1}{1 + (\alpha\psi)^n} \right]^m \quad 1$$

where S_e is the effective saturation, θ is the volumetric moisture content; θ_s is the volumetric moisture content at the water table ($\theta_s = S_{sat}\phi$, where S_{sat} is the saturation fraction at zero pressure, and ϕ is the porosity); ψ is the matric pressure head, or the negative pressure head; and θ_r , α , n and m are fitting parameters. The first fitting parameter, θ_r , is called the residual moisture content and denotes a theoretical minimum moisture state. The second fitting parameter, α , is approximately equal to the "air entry pressure head", the matric head at which a saturated soil begins to desaturate. The other two fitting parameters are exponents.

The modified van Genuchten relative hydraulic conductivity relationship is as follows:

$$K_r = \left(\frac{\theta - \theta_r}{\theta_s - \theta_r} \right)^\delta = \left[\frac{1}{1 + (\alpha\psi)^n} \right]^{m\delta} \quad 2$$

where K_r is the relative hydraulic conductivity and δ is an exponent. The decoupling of m and n and the addition of δ adds flexibility to the modified van Genuchten model relative to the van Genuchten (1980) relationship. In addition, the modified relationship does not possess a portion of the pressure- hydraulic conductivity curve in which hydraulic conductivity becomes constant with pressure under very dry conditions. The parameters used in the Feflow model are shown in Table 15-3. Also shown in the table are the effective specific yield values for each hydrogeological unit.

Table 15-3. Unsaturated parameter values

Hydrogeological Unit	Porosity	Sr	α (1/m)	n	m	ξ	Effective Sy	Conceptual Sy
Upper Alluvium	0.25	0.15 - 0.3	0.001 - 0.9	1.45 - 1.5	0.28 - 0.33	2 - 2.5	0.13 - 0.19	0 - 0.31
Lower Alluvium	0.25	0.30	0.001 - 0.5	1.50	0.33	2.00	0.10 - 0.16	0 - 0.31
Deep Halite	0.40	0.10	0.12 - 0.15	1.19	0.15	7.00	0.05 - 0.17	0.01 - 0.13
Halite	0.35	0.25	0.001 - 0.5	1.35	0.25	4.00	0.12 - 0.21	0.05 - 0.12
Lacustrine	0.40	0.10	0.001 - 0.5	0.19 - 1.35	0.15 - 0.25	7.00	0.05 - 0.18	0 - 0.15
Lower Sand	0.25	0.30	0.001 - 0.5	1.50	0.33	2.00	0.10 - 0.16	0.01 - 0.19
Lower Volcanoclastic	0.25	0.30	0.001 - 0.5	1.50	0.33	2.00	0.10 - 0.16	0.05 - 0.18
Volcanic Breccia	0.25	0.30	0.50	1.50	0.33	2.00	0.10 - 0.16	0.01 - 0.29
Volcanoclastic	0.20	0.00	0.50	1.50	0.33	2.00	0.12 - 0.17	0 - 0.31

15.4.3 LITHIUM TRANSPORT PARAMETERS

In addition to groundwater flow, the FEFLOW model also considers mass to simulate the transport of lithium in support of the mineral reserve estimate. Specific model parameters such as longitudinal, horizontal, and transverse dispersivity were defined as follows: longitudinal dispersivity was set to a constant value of 50 m and the horizontal and vertical transverse dispersivity values were set to 5 m.

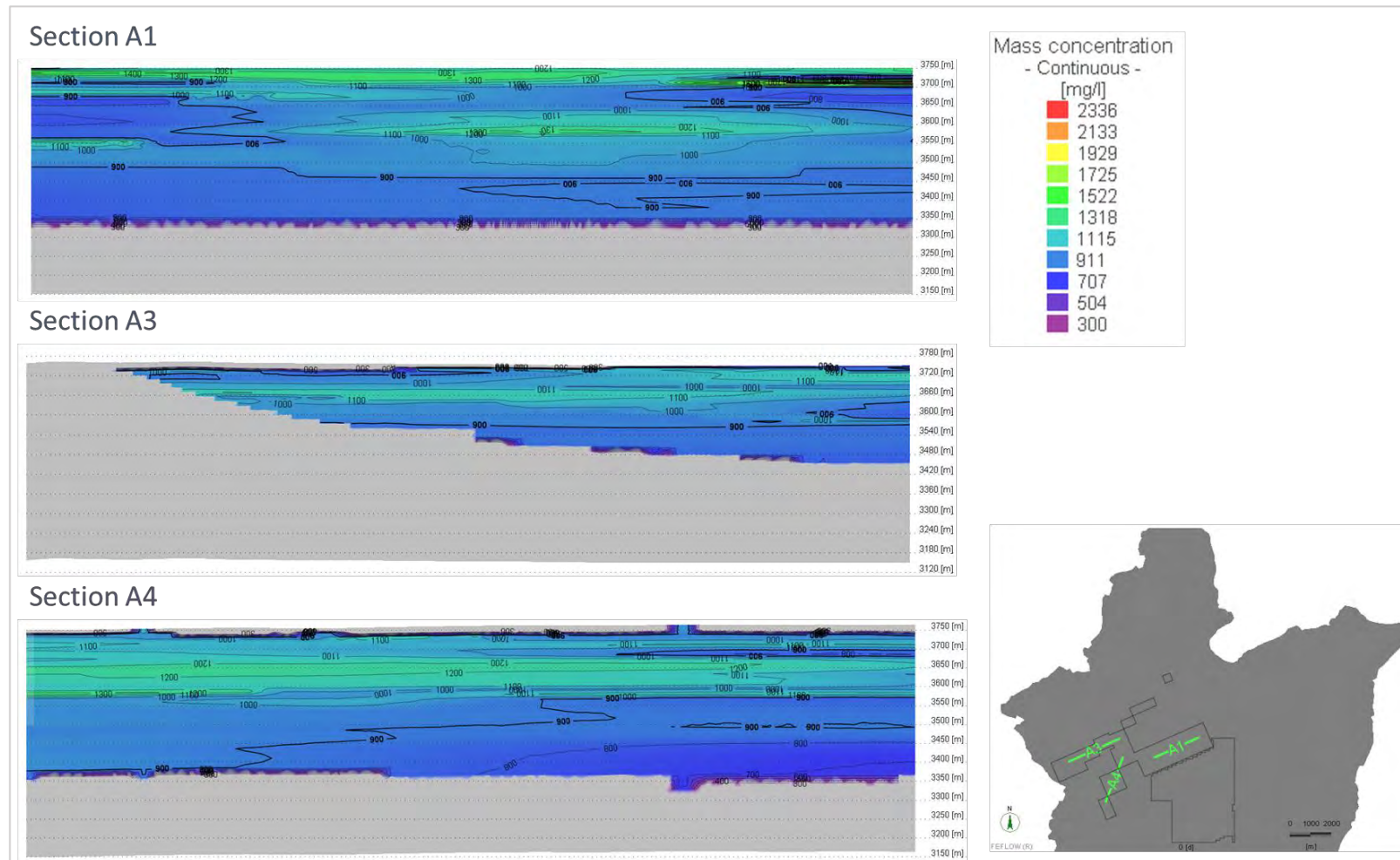
The initial concentration of lithium for the reserve estimate simulations was based on the Measured and Indicated resources provided by the resource model (Atacama Water, 2021). In the reserve assessment, the lithium present under the MSB properties was treated separately from brine present at the start of operations outside of the MSB property. The reserve estimate is classified between Proven and Probable respectively. The Proven reserve is considered as the measured resource that can be extracted from Year 1 to 7 and the rest is classified as Probable. The initial lithium concentration distribution is shown in Figure 15-9.

The effective porosity for the mass transport simulations was based on the conceptual specific yield and is shown in Table 15-4.

Table 15-4. Effective porosity for transport simulations

Unit	Effective Porosity
Upper Alluvium	0.11
Lower Alluvium	0.11
Basal Sediments	0.07
Deep Halite	0.06
Halite	0.06
Lacustrine	0.02
Lower Sand	0.07
Lower Volcanoclastic	0.08
Volcanic Breccia	0.12
Volcanoclastic	0.11

Figure 15-9. Initial distribution of lithium concentration



15.5 DENSITY CONSIDERATIONS

The hydrogeological system in the Maricunga Salar is strongly influenced by density-driven flow. Groundwater in the Salar can be classified by their density. The endmembers of this classification are fresh water and brine. Apart from the hydraulic gradient, this differences in density also control the regional flow directions and, therefore, the distribution of the water balance components. In the numerical model, the consideration followed by the previous model for mineral reserve estimates has been maintained (WorleyParsons, 2019). This assumes a single density value that corresponds to fresh water for all the hydrogeological systems. This simplification mainly causes in the model a greater hydraulic gradient between the fresh water and brine systems that would represent a conservative scenario for dilution of the lithium concentrations.

15.6 SOLVER AND CONVERGENCE CRITERIA

The flow solver used in the FEFLOW runs is the Algebraic Multigrid Methods for Systems (SAMG) solver with a maximum of 50 AMG cycles and 200 PCG iterations. The transport equation was also solved with the SAMG solver with these settings. A root mean squared (RMS) Euclidian L2 error tolerance of 3×10^{-5} , with a maximum of 12 outer iterations. Mass matrices were computed using a lumped mass configuration. The convective form of the transport solution was applied.

15.7 CALIBRATION METHODOLOGY

The flow model was calibrated for steady state and transient conditions to (1) fit the static water levels, (2) match the conceptual water balance, and (3) simulate head drawdowns from different pumping tests. A combination of manual and automated calibration was completed for both calibration processes. For the automated calibration, Feflow's built-in version of the PEST parameter optimization program, FePest, was applied. This section describes the calibration methodology. Calibration results are presented in Section 15.8.

15.7.1 STEADY STATE CALIBRATION

In the steady state calibration, the hydraulic conductivities and the transfer coefficients used to simulate evapotranspiration and diffuse groundwater discharge (Section 15.3.3) were calibrated to fit the observed heads and the conceptual flow values that represent evapotranspiration.

15.7.1.1 CALIBRATION TARGETS

Water level measurements are selected in 73 observation wells for the steady state calibration (Figure 15-10). Table 15-5 lists these head observation points and the measured target water level.

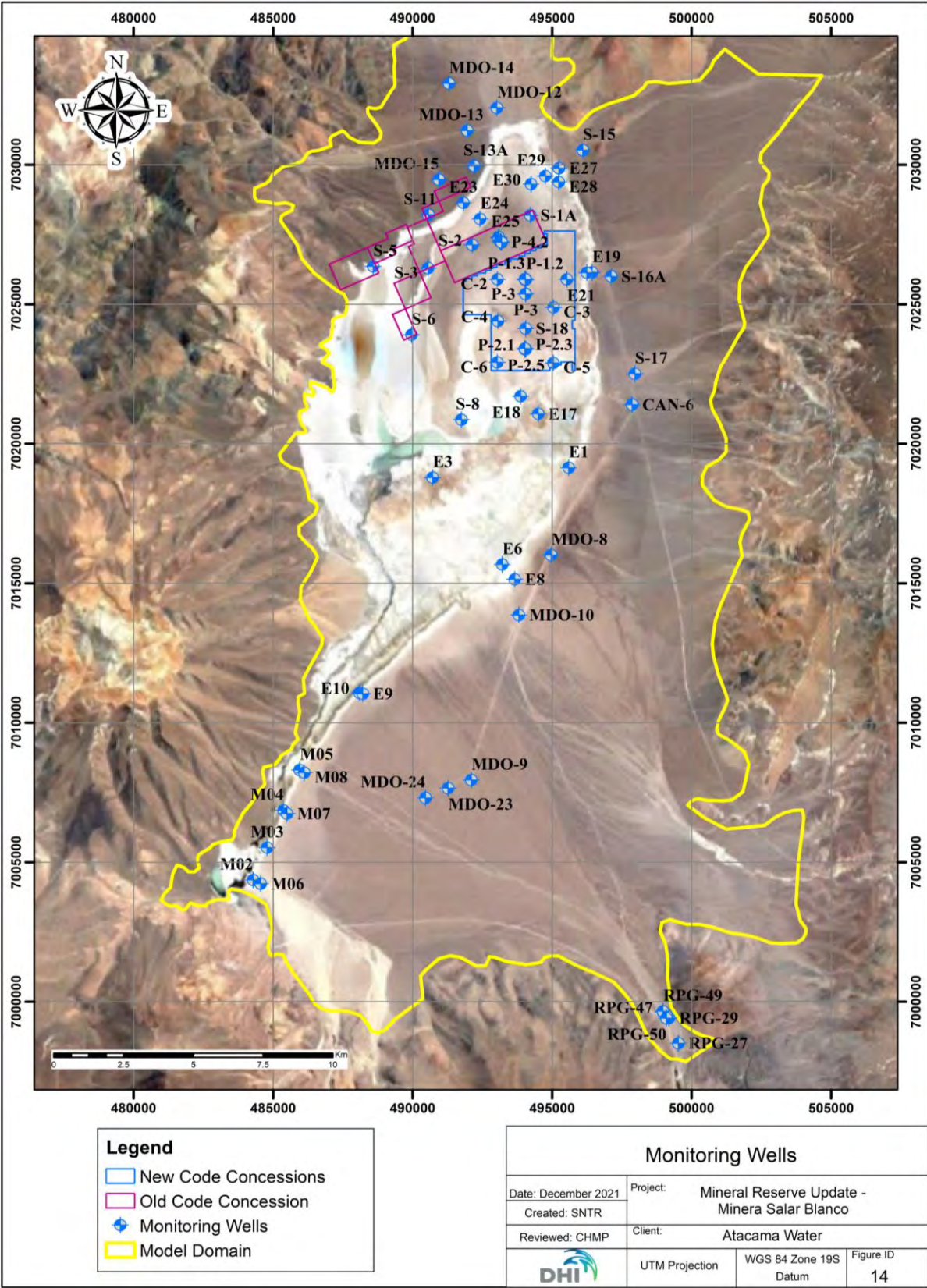
Table 15-5. Observation wells for steady state calibration

Well	Easting (WGS84)	Northing (WGS84)	Top of Casing Elevation (DEM)	Piezometric Head Target (masl)
C-2	493,045	7,025,903	3,741.51	3,749.86
C-3	495,057	7,024,898	3,750.67	3,749.91
C-4	493,060	7,024,406	3,750.78	3,749.81
C-5	495,051	7,022,904	3,750.57	3,749.93
C-6	493,039	7,022,924	3,750.88	3,749.86
P-1.1	494,035	7,025,894	3,750.71	3,749.49
P-1.2	494,064	7,025,896	3,750.71	3,749.88
P-1.3	494,035	7,025,908	3,750.80	3,749.88
P-1.4	494,035	7,025,918	3,750.83	3,749.97
P-2.1	494,061	7,023,401	3,750.71	3,749.91
P-2.3	494,033	7,023,407	3,750.63	3,749.92
P-2.4	494,035	7,023,398	3,750.64	3,749.91
P-2.5	494,061	7,023,402	3,750.81	3,749.59
P-4.1	493,194	7,027,224	3,750.71	3,748.24
P-4.2	493,172	7,027,242	3,750.23	3,749.89
P-4.3	493,160	7,027,251	3,750.23	3,749.88
P-4.4	493,140	7,027,265	3,750.34	3,749.88
S-11	490,569	7,028,217	3,759.57	3,749.95
S-13A	492,213	7,029,964	3,757.79	3,748.04
S-18	494,054	7,024,142	3,749.98	3,745.64
S-19	493,105	7,027,381	3,750.71	3,747.85
S-1A	494,220	7,028,201	3,750.25	3,749.36
S-2	492,143	7,027,141	3,750.75	3,747.76
S-5	488,590	7,026,366	3,752.06	3,749.87

Well	Easting (WGS84)	Northing (WGS84)	Top of Casing Elevation (DEM)	Piezometric Head Target (masl)
S-6	489,964	7,023,912	3,750.67	3,746.23
S-8	491,754	7,020,871	3,750.72	3,749.43
S-3	490,563	7,026,306	3,753.01	3,749.74
E20	496,245	7,026,138	3,750.08	3,749.60
E21	495,532	7,025,902	3,749.58	3,749.48
E18	493,876	7,021,712	3,750.12	3,749.24
E3	490,720	7,018,799	3,750.78	3,749.18
P-3	494,054	7,025,383	3,750.69	3,750.34
MDO-12	493,021	7,032,048	3,759.50	3,752.36
MDO-13	491,961	7,031,235	3,772.43	3,753.67
MDO-14	491,306	7,032,925	3,777.25	3,754.60
MDO-15	490,948	7,029,482	3,774.87	3,751.79
E27	495,248	7,029,884	3,752.26	3,752.13
E28	495,243	7,029,390	3,750.07	3,750.07
E29	494,761	7,029,606	3,750.17	3,750.17
E30	494,247	7,029,313	3,750.24	3,750.14
E23	491,826	7,028,648	3,750.99	3,750.70
E24	492,421	7,028,065	3,750.28	3,750.20
E25	493,084	7,027,415	3,750.24	3,750.16
E19	496,435	7,026,152	3,752.19	3,751.81
E17	494,507	7,021,081	3,750.88	3,750.75
S-15	496,103	7,030,534	3,783.09	3,757.50
M05	485,956	7,008,319	3,760.40	3,759.89

Well	Easting (WGS84)	Northing (WGS84)	Top of Casing Elevation (DEM)	Piezometric Head Target (masl)
E1	495,596	7,019,150	3,755.06	3,755.03
E6	493,219	7,015,682	3,755.58	3,755.53
E10	488,097	7,011,084	3,758.65	3,758.65
E9	488,219	7,011,050	3,759.78	3,758.99
S-16A	497,122	7,026,005	3,771.74	3,762.38
S-17	497,968	7,022,516	3,792.01	3,762.01
MDO-8	494,966	7,016,018	3,769.61	3,761.94
MDO-10	493,815	7,013,872	3,771.89	3,763.60
MDO-9	492,109	7,007,956	3,812.23	3,764.90
MDO-23	491,275	7,007,666	3,807.73	3,764.84
CAN-6	497,869	7,021,411	3,782.71	3,762.47
M02	484,288	7,004,376	3,763.07	3,762.98
M03	484,789	7,005,534	3,762.46	3,761.80
M04	485,384	7,006,873	3,761.51	3,761.42
M06	484,559	7,004,241	3,764.29	3,763.61
M07	485,504	7,006,753	3,762.67	3,761.89
M08	486,122	7,008,223	3,761.36	3,760.47
E8	493,662	7,015,155	3,761.63	3,760.64
MDO-24	490,468	7,007,320	3,803.30	3,765.28
RPG-49	498,978	6,999,669	3,916.91	3,871.20
RPG-27	499,528	6,998,523	3,927.59	3,880.70
RPG-47	498,977	6,999,649	3,917.86	3,871.00
RPG-48	499,111	6,999,494	3,919.31	3,873.30
RPG-50	499,101	6,999,421	3,919.32	3,873.30
RPG-29	499,190	6,999,427	3,919.47	3,874.50
RPG-46	499,074	6,999,670	3,917.40	3,871.30

Figure 15-10. Location of head observation wells for steady state calibration



In addition to head targets, targets of water flux from the conceptual water balance were weighted in the FePest calibration. Table 15-6 lists the flux calibration targets for the different water balance components. All groundwater outflow in the model is related to evapotranspiration. This process is classified in three different types depending on the outflow process. The diffuse discharge to surface water is characteristics of the wet season and is derived from groundwater. An estimated 488 L/s of groundwater seepage feeds these surface water features. This outflow is simulated in the model through the stream zone that represents the diffuse groundwater discharge between the fresh water and brine systems. Evaporation from bare soil plus evapotranspiration in vegetated areas together account for an estimates 820 L/s of groundwater losses in the Maricunga basin.

Table 15-6. Flux targets for the steady state calibration

Component	Flow Target (L/s)
Evapotranspiration from vegetation	370
Evaporation from bare soil (Salar and alluvium)	450
Diffuse groundwater discharge into surface water in and around Salar	488

15.7.1.2 CALIBRATION PARAMETERS

A total of 43 parameters were calibrated for the steady state head and flow solution: 36 parameter zones were applied for calibration of saturated hydraulic properties and 7 zones for the out- transfer rate that affects the evapotranspiration outflow. The hydraulic properties parameters were later further calibrated in the transient calibration described in the following section.

15.7.2 TRANSIENT CALIBRATION

15.7.2.1 TRANSIENT CALIBRATION APPROACH

Data from three pumping tests carried out in production wells P-1, P-2, and P-4 were used for the transient calibration of hydraulic conductivity and specific storage. The locations of the pumping wells and adjacent observation wells are shown in Figure 15-11. Table 15-7 shows the head observation wells.

The P1, P2, and P-4 pumping test duration were 13, 28, and 31 days, respectively. The pumping test flow rates ranged from 25 l/s in the P-4 to 38 l/s in the P-1. The pumping rates were distributed along the model layers within the screen interval according to the conceptual transmissivity of each of the corresponding units. The P-1 pumping test occurred in the Upper Halite, Lacustrine and Volcanoclastic units. The P-2 pumping test occurred in the Upper Halite and Lacustrine units. Geological logs indicate that the Lacustrine unit encountered in wells P1 and P-2 contain isolated, non continues layers of higher permeability clayey sand, clayey gravel sand clay lenses. The P-4 pumping test was designed to measure the hydraulic properties of the Volcanoclastic unit. The three pumping tests were modelled simultaneously in one single

numerical model, below the lacustrine unit. It was assumed that no significant interference occurs between them as observed in the field due to the well spacing and the relative short pumping period.

Figure 15-11. Pumping test locations

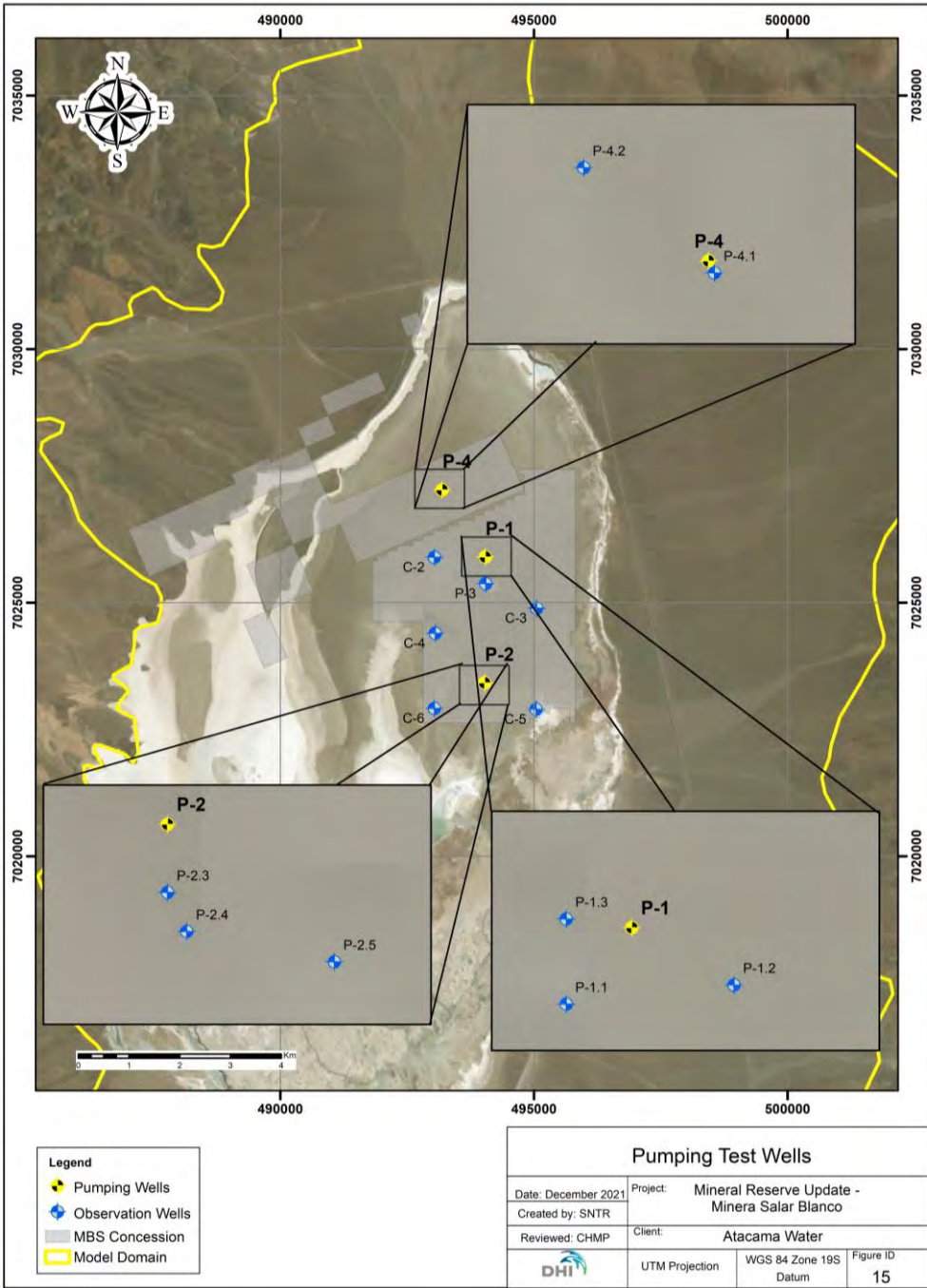


Table 15-7. Observation wells for pumping tests

Observation Well	Screened Interval (mbgs)	Hydrogeologic Unit	Distance from Pumping Well (m)
P-1.1	60 - 149	Volcanoclastic	17
P-1.2	6 - 24	Halite	20
P-1.3	54 - 66	Lacustrine	11
C2	6 - 34	Lacustrine	1004 (P-1)
C3	3 - 26	Halite	1432 (P-1)
C4	6 - 29	Lacustrine	1383 (P-2)
C5	6 - 11	Lacustrine	1141 (P-2)
C6	6 - 11	Halite	1113 (P-2)
P-2.3	12 - 30	Halite	12
P-2.5	60 - 145	Lacustrine	39
P-3	127 - 185	Lacustrine	524 (P-1)
P-4.1	160 - 172	Volcanoclastic	18
P-4.2	0 - 2	Halite	10

During transient calibration of the P1 and P-2 pumping test the model response was focused on the P-1.2 and P-2-3 observation wells as they are both completed in the Upper Halite, from which initial brine production will occur. In the P4 pumping test calibration, both observation wells P-4.1 and P-4.2 were considered with the same priority. The observation wells C-2, C-3, C4, C5 and C6 are located more than 1,000 m from the P-1 and P-2 productions wells and did not show a water level response during the pumping tests.

15.8 CALIBRATION RESULTS

15.8.1 STEADY STATE CALIBRATION

15.8.1.1 CALIBRATED PARAMETERS

Table 15-8 presents the final calibrated hydraulic conductivity values. For model consistency, the specific zones calibrated for the pumping tests in the transient model were incorporated to the steady state model. The calibrated hydraulic conductivities are within the conceptual range specified in the calibration.

Table 15-8. Calibrated hydraulic conductivities

ID	UG	UG DFS 2019	Calibrated Hydraulic Conductivity (m/d)		
			K _H	K _V	Conceptual Range
1.1all	Upper Alluvium	East Alluvial Fan a	0.85	0.10	0.1 - 10
1.2all	Upper Alluvium	East Alluvial Fan b	0.49	0.09	0.1 - 10
1.3all	Upper Alluvium	East Alluvial Fan c	1.55	0.14	0.1 - 10
1.4all	Upper Alluvium	East Alluvial Fan a	2.08	0.10	0.1 - 10
1.5all	Upper Alluvium	Río Lamas Alluvial Fan	30.00	3.00	30 - 280
1.6all	Upper Alluvium	Río Lamas Alluvial Fan Ctr	30.00	3.00	30 - 300
1.7all	Upper Alluvium	Río Lamas Alluvial Fan N	30.00	13.57	30 - 280
1.8all	Upper Alluvium	Río Lamas Alluvial Fan S	30.00	3.00	30 - 280
1.9all	Upper Alluvium	Upper Río Lamas Alluvial Fan	10.00	1.00	10 - 280
1.19all	Upper Alluvium	Northeast Alluvial Fan a	3.42	1.59	0.1 - 40
1.191all	Upper Alluvium	Northeast Alluvial Fan a	4.00	0.01	0.1 - 40
1.11all	Upper Alluvium	Northeast Alluvial Fan	1.41	0.35	0.1 - 40
1.111all	Upper Alluvium	Northeast Alluvial Fan	4.00	0.01	0.1 - 40
1.12all	Upper Alluvium	Northwest Alluvial Fan	8.82	1.04	0.1 - 40
1.13all	Upper Alluvium	Northwest Alluvial Fan a	8.36	1.14	0.1 - 40
1.14all	Upper Alluvium	Northwest Alluvial Fan b	16.31	2.09	0.1 - 40
1.15all	Upper Alluvium	Northwest Alluvial Fan c	8.30	2.01	0.1 - 40
1.16all	Upper Alluvium	Northwest Alluvial Fan d	5.09	0.67	0.1 - 40
1.17all	Upper Alluvium	West Alluvial Fan	9.64	2.10	0.1 - 40
1.18all	Upper Alluvium	West Alluvial Fan a	15.26	1.57	0.1 - 40
1.21all	Lower Alluvium	Lower Alluvium	0.45	0.05	0.1 - 1
1.22all	Upper Alluvium	Northwest Alluvial Fan a & b	8.00	0.01	0.1 - 40
2bse	Basal Sediments	Basin Fill Sediments	0.42	0.19	0.001 - 2.5
3dha	Deep Halite	Clay Core	0.01	0.00	0.0001 - 0.01
4hal	Halite	Upper Halite	232.00	3.30	100 - 640
5lac	Lacustrine	Clay Core	0.01	0.01	0.0001 - 0.01
5.1lac	Lacustrine	Sandy Clay (P-1)	2.75	1.19	0.01 - 10
5.2lac	Lacustrine	Clayey Sand (P-2)	0.50	0.50	0.01 - 10
5.3lac	Lacustrine	Clayey Gravel (P-2)	0.50	0.50	0.01 - 10
5.4lac	Lacustrine	Upper Halite	0.01	0.01	100 - 640
5.5lac	Lacustrine	Upper Halite	232.00	33.14	100 - 640
5.6lac	Lacustrine	Upper Halite	232.00	33.14	100 - 640
6lsa	Lower Sand	Lower Sand	0.75	0.23	0.1 - 2.5
7lvo	Lower Volcanoclastic	Lower Sand	0.30	0.24	0.1 - 2.5
8vbr	Volcanic Breccia	Lower Sand	1.07	0.25	0.1 - 2.5
9vo	Volcanoclastic	Lower Sand	0.22	0.01	0.1 - 2.5

The lowest transfer rate coefficient for evapotranspiration is $1.00\text{E}10^{-4} \text{ d}^{-1}$ for the Salar halite. In the Lacustrine unit, the calibrated evapotranspiration transfer rate coefficient is $2.79\text{E}10^{-4} \text{ d}^{-1}$. The evapotranspiration rate coefficient for the alluvial fan areas is from $8.92\text{E}10^{-4} \text{ d}^{-1}$, and the calibrated evapotranspiration rate coefficient for the vegetated zone in the southwestern portion of the model domain is $2.35\text{E}10^{-3} \text{ d}^{-1}$. Figure 15-12 presents the zonally averaged evaporation rate from the calibrated model, using the transfer rate coefficients in Table 15-9.

The calibrated transfer rate coefficients for diffuse groundwater discharge are higher than the transfer rate coefficients for evapotranspiration. This is due to the relationship with the zones of preferential regional discharge controlled by the change in topography between the alluvial and Salar nucleus areas. The part of the Salar margin with the highest transfer rate coefficient is the central zone that coincides with the alluvial fan from the Río Lamas (Figure 15-13).

Table 15-9. Calibrated transfer rate coefficients

Evapotranspiration Zone	Transfer Rate (1/d)	Evapotranspiration (mm/d)
Halite	$1.00\text{E}10^{-4}$	0.22
Lacustrine	$2.79\text{E}10^{-4}$	
Vegetation	$23.50\text{E}10^{-4}$	2.75
Alluvial Fan	$8.92\text{E}10^{-4}$	0.24
Groundwater Diffuse Discharge Zone	Transfer Rate (1/d)	-
North	$165\text{E}10^{-4}$	-
Central	10	-
South	$136\text{E}10^{-4}$	-

Figure 15-12. Calibrated evapotranspiration rates

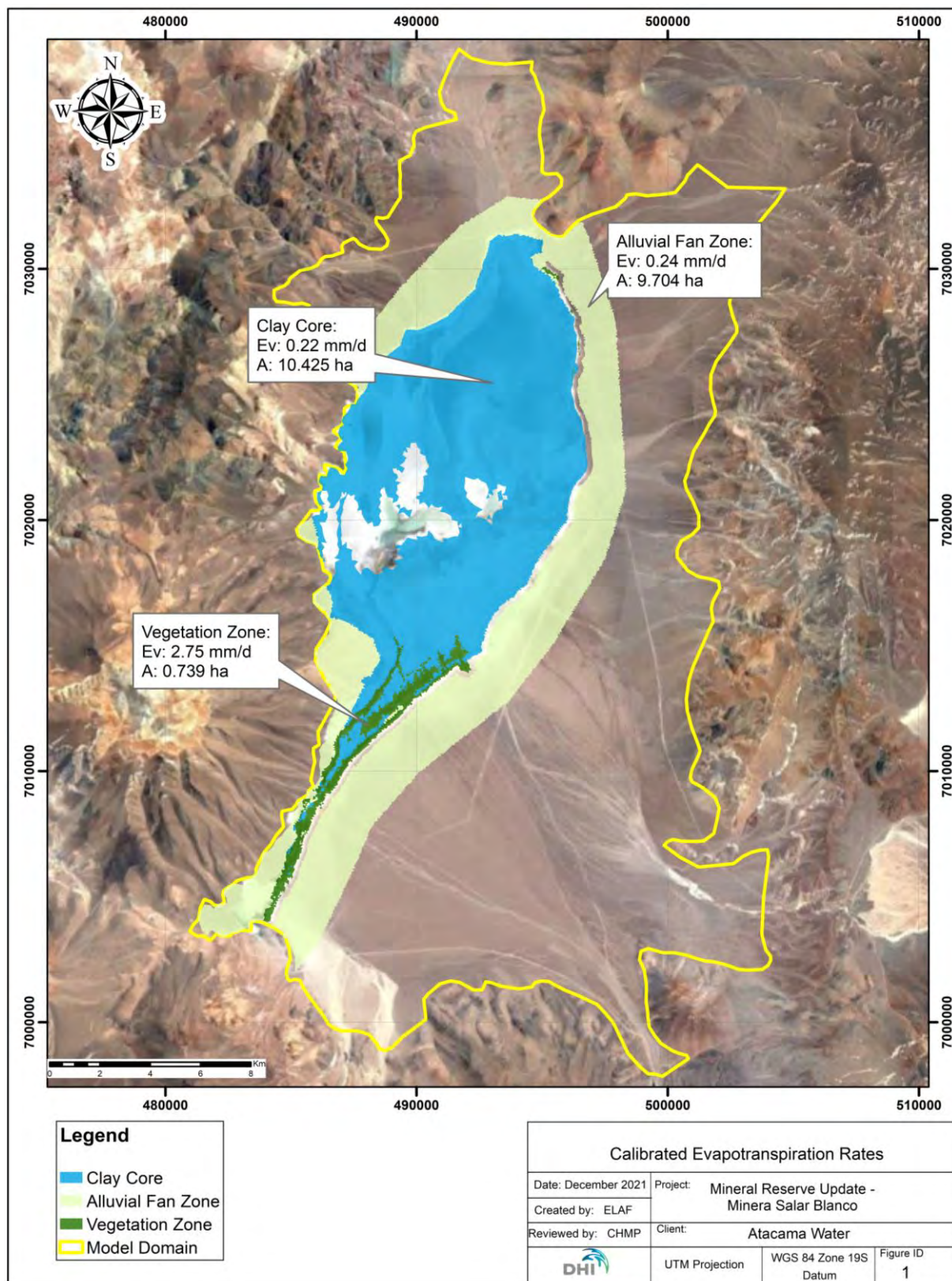
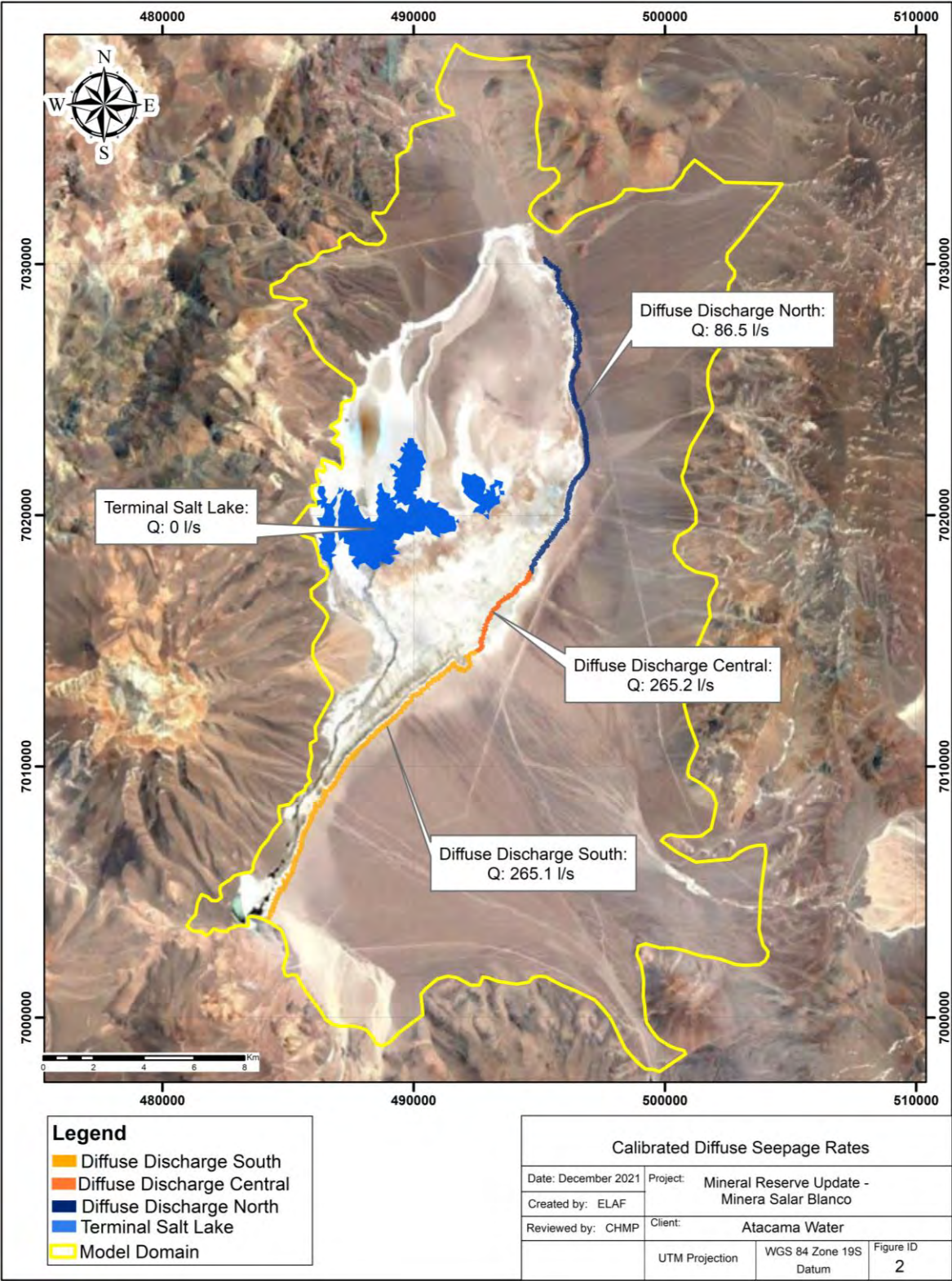


Figure 15-13 Calibrated diffuse seepage rates



15.8.1.2 CALIBRATION TO HEADS

Figure 15-14 shows the simulated steady state water table. Figure 15-15 presents a map-view of the calibration residuals and Figure 15-16 and Figure 15-17 display the calibration statistics. The mean residual head for the steady state calibrated model is -0.8 m and the mean absolute residual (MAE) is 2.8 m. The head error in percentage is presented as the normalized root mean squared error (NRMSE) and corresponds to 4.8%.

The results of the steady state calibration are classified between two groups of observation targets that were differently weighted for the calibration process. The main target group include 66 wells located in the lower parts of the Salar (Zone 1). A secondary group of 7 wells include the observation points in the Cienaga Redonda area (Zone 2). These wells are at a higher elevation than the Salar group and due to the greater distance to the project area were not the objective for calibration. The distribution of head residuals in the Salar group ranges from -1.7 m to 4.9 m with a trend distribution that slightly overestimates heads. The 68% of wells in this group have a head residual that ranges from -0.8 m to 0.6 m. The general head error for the Salar group corresponds to an average residual of 0.4 m, MAE of 1 m, and NRMSE of 7.4%.

Simulated Water Table - Premining

Date: December 2021	Project: Mineral Reserve Update - Minera Salar Blanco
Created: ELAF	
Reviewed: RMD	Client: Atacama Water
UTM Projection	WGS 84 Zone 19S Datum
	Figure ID 3

Calibration - Residuals Map

Legend

Residual

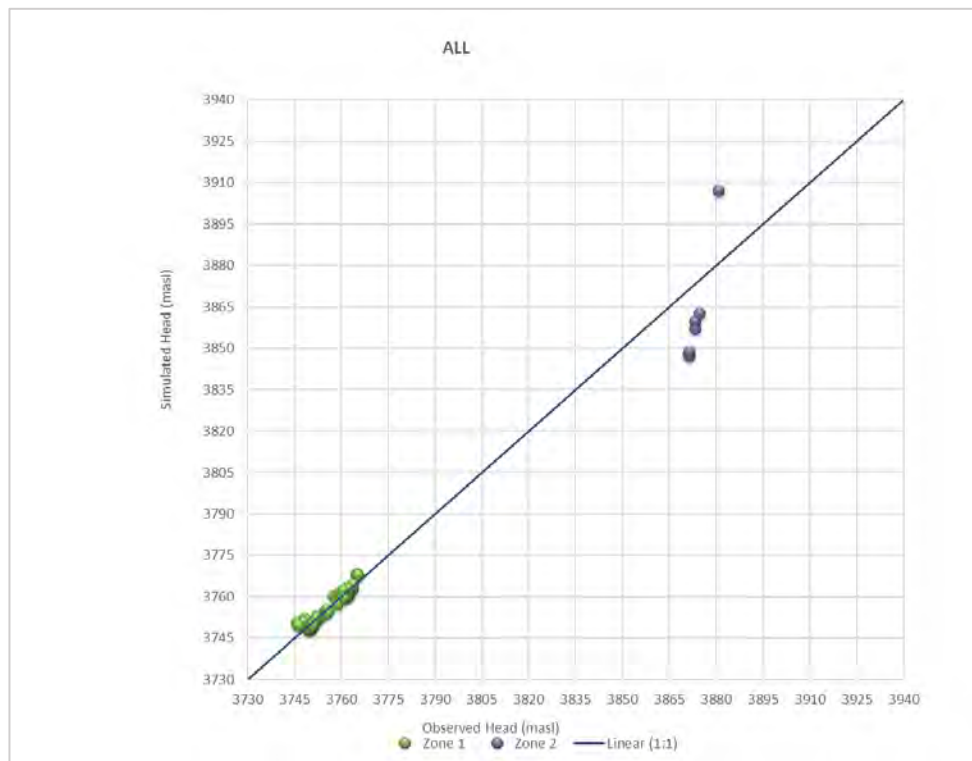
- 28.42 - -2.00
- 1.99 - -1.00
- 0.99 - -0.50
- 0.49 - 0.00
- 0.01 - 0.50
- 0.51 - 1.00
- 1.01 - 1.50
- 1.51 - 2.00
- 2.01 - 2.50
- 2.51 - 4.07

Model Domain

Map Information

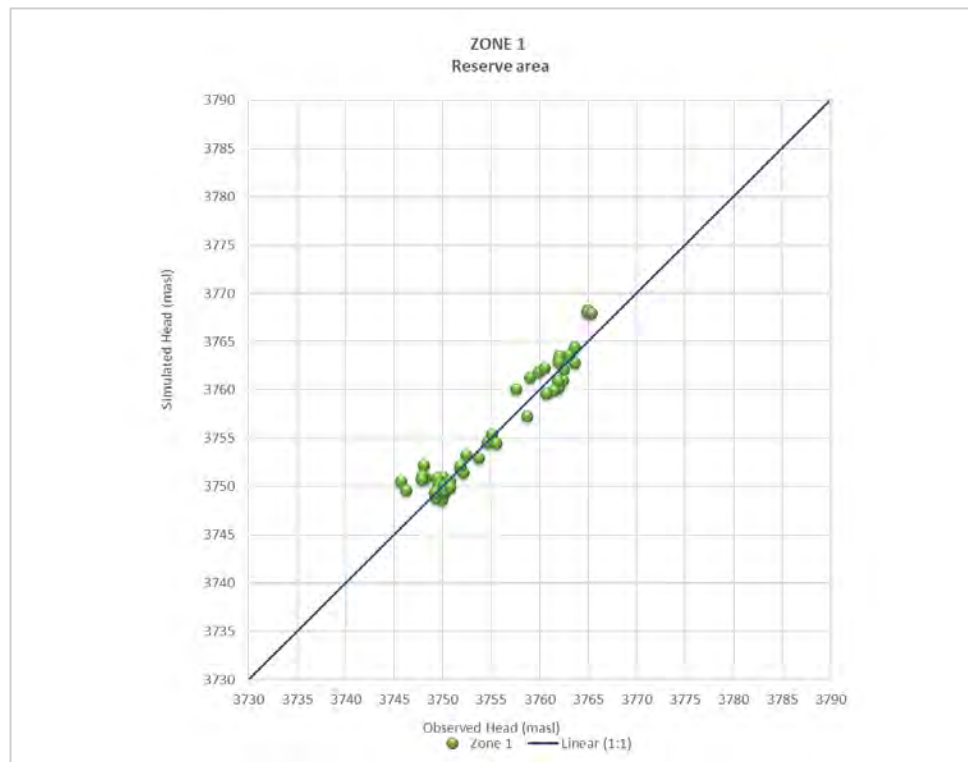
Date: December 2021	Project: Mineral Reserve Update - Minera Salar Blanco
Created: ELAF	Client: Atacama Water
Reviewed: RMD	UTM Projection
	WGS 84 Zone 19S
	Datum
	Figure ID 4

Figure 15-16. Observed vs. simulated water levels – entire model domain



Summary of Calibration Statistics	
73	Number of Wells
-0.8	Residual Mean (m)
2.8	Mean Absolute Error (m)
6.4	Root Mean Square Error (m)
4.8%	Normalized Root Mean Squared Error

Figure 15-17. Observed vs. simulated water levels – reserve area



Summary of Calibration Statistics	
66	Number of Wells
0.4	Residual Mean (m)
1.0	Mean Absolute Error (m)
1.5	Root Mean Square Error (m)
7.4%	Normalized Root Mean Squared Error

Table 15-10. Observed and simulated water levels

Well	Well Group	Measured Water Level (masl)	Simulated Water Level (masl)	Residual (m)	Absolute Residual (m)
C-2	Project	3,749.86	3,749.47	-0.39	0.39
C-3	Project	3,749.91	3,749.48	-0.43	0.43
C-4	Project	3,749.81	3,749.21	-0.60	0.60
C-5	Project	3,749.93	3,748.64	-1.29	1.29
C-6	Project	3,749.86	3,749.17	-0.69	0.69
P-1.1	Project	3,749.49	3,750.07	0.58	0.58
P-1.2	Project	3,749.88	3,749.54	-0.34	0.34
P-1.3	Project	3,749.73	3,749.82	0.09	0.09
P-1.4	Project	3,749.97	3,749.54	-0.43	0.43
P-2.1	Project	3,749.91	3,749.80	-0.11	0.11
P-2.3	Project	3,749.92	3,749.23	-0.69	0.69
P-2.4	Project	3,749.91	3,749.79	-0.12	0.12
P-2.5	Project	3,749.59	3,749.80	0.21	0.21
P-4.1	Project	3,748.24	3,750.92	2.68	2.68
P-4.2	Project	3,749.89	3,749.68	-0.21	0.21
P-4.3	Project	3,749.88	3,749.68	-0.20	0.20
P-4.4	Project	3,749.89	3,749.69	-0.20	0.20
S-11	Project	3,749.95	3,751.02	1.07	1.07
S-13A	Project	3,748.04	3,752.16	4.12	4.12
S-18	Project	3,745.64	3,750.54	4.90	4.90
S-19	Project	3,747.85	3,751.16	3.31	3.31
S-1A	Project	3,749.36	3,750.86	1.50	1.50
S-2	Project	3,747.76	3,750.74	2.98	2.98
S-5	Project	3,749.87	3,749.76	-0.11	0.11
S-6	Project	3,746.23	3,749.58	3.35	3.35
S-8	Project	3,749.43	3,749.17	-0.26	0.26
S-3	Project	3,749.74	3,749.44	-0.30	0.30
E20	Mini-Piezometer	3,749.60	3,750.16	0.56	0.56
E21	Mini-Piezometer	3,749.48	3,749.63	0.15	0.15
E18	Mini-Piezometer	3,749.24	3,748.89	-0.35	0.35
E3	Mini-Piezometer	3,749.18	3,749.41	0.23	0.23
P-3	Project	3,750.34	3,750.15	-0.19	0.19
MDO-12	MDO	3,752.36	3,753.24	0.88	0.88
MDO-13	MDO	3,753.67	3,752.98	-0.69	0.69
MDO-14	MDO	3,754.60	3,754.54	-0.06	0.06
MDO-15	MDO	3,751.79	3,751.90	0.11	0.11
E27	Mini-Piezometer	3,752.13	3,751.47	-0.66	0.66
E28	Mini-Piezometer	3,750.07	3,750.07	0.00	0.00
E29	Mini-Piezometer	3,750.17	3,749.84	-0.33	0.33
E30	Mini-Piezometer	3,750.14	3,750.10	-0.04	0.04
E23	Mini-Piezometer	3,750.70	3,750.60	-0.10	0.10
E24	Mini-Piezometer	3,750.20	3,749.76	-0.44	0.44
E25	Mini-Piezometer	3,750.16	3,749.71	-0.45	0.45
E19	Mini-Piezometer	3,751.81	3,752.15	0.34	0.34
E17	Mini-Piezometer	3,750.75	3,749.93	-0.82	0.82

Well	Well Group	Measured Water Level (masl)	Simulated Water Level (masl)	Residual (m)	Absolute Residual (m)
S-15	Project	3,757.50	3,760.08	2.58	2.58
M05	Project	3,759.89	3,761.89	2.00	2.00
E1	Mini-Piezometer	3,755.03	3,755.35	0.32	0.32
E6	Mini-Piezometer	3,755.53	3,754.48	-1.05	1.05
E10	Mini-Piezometer	3,758.65	3,757.31	-1.34	1.34
E9	Mini-Piezometer	3,758.99	3,761.33	2.34	2.34
S-16A	Project	3,762.38	3,760.98	-1.40	1.40
S-17	Project	3,762.01	3,763.49	1.48	1.48
MDO-8	MDO	3,761.94	3,760.27	-1.67	1.67
MDO-10	MDO	3,763.60	3,762.86	-0.74	0.74
MDO-9	MDO	3,764.90	3,768.32	3.42	3.42
MDO-23	MDO	3,764.84	3,768.09	3.25	3.25
CAN-6	Project	3,762.47	3,762.11	-0.37	0.37
M02	Project	3,762.98	3,763.59	0.61	0.61
M03	Project	3,761.80	3,760.93	-0.87	0.87
M04	Project	3,761.42	3,759.96	-1.46	1.46
M06	Project	3,763.61	3,764.44	0.83	0.83
M07	Project	3,761.89	3,762.91	1.02	1.02
M08	Project	3,760.47	3,762.32	1.85	1.85
E8	Mini-Piezometer	3,760.64	3,759.66	-0.98	0.98
MDO-24	MDO	3,765.28	3,767.95	2.67	2.67
RPG-49	Ciénaga Redonda	3,871.20	3,847.44	-23.76	23.76
RPG-27	Ciénaga Redonda	3,880.70	3,906.99	26.29	26.29
RPG-47	Ciénaga Redonda	3,871.00	3,848.26	-22.74	22.74
RPG-48	Ciénaga Redonda	3,873.30	3,857.10	-16.20	16.20
RPG-50	Ciénaga Redonda	3,873.30	3,859.92	-13.38	13.38
RPG-29	Ciénaga Redonda	3,874.50	3,862.65	-11.85	11.85
RPG-46	Ciénaga Redonda	3,871.30	3,848.86	-22.44	22.44

15.8.1.3 CALIBRATION TO FLOWS

The calibrated water balance components are shown in Table 15-11. The simulated total inflow is different to the conceptual target--i.e., the simulated flow of 1,393 L/s simulated is within 1% of the conceptual target of 1,398 L/s.

The sum of evapotranspiration and diffuse discharge is balanced with the sum of the direct and lateral recharge. Field data and the conceptual model were not able to account for 100% of the groundwater discharges. In the calibrated numerical model, the shortfall in groundwater discharge was derived primarily via diffuse groundwater discharge at the brine-freshwater contact, where intermittent surface water is observed. The reserve model predicts 27% more diffuse groundwater discharge than accounted for in the conceptual water balance.

Table 15-11. Simulated water balance

Inflow / Outflow	Conceptual Model (L/s)	Numerical Model (L/s)	Difference (L/s)
Rio Lamas + Cienaga redonda recharge	690	690	0
Other sub-basins recharge	303	298	5
Precipitation recharge	405	405	0
Total IN	1398	1394	4
Evapotranspiration from Vegetation Zone	370	235	135
Evapotranspiration from Salar + Alluvial	450	540	-90
Diffuse Zone	488	617	-129
Total OUT	1308	1393	-85

15.8.2 PUMPING TEST CALIBRATION

15.8.2.1 CALIBRATED PARAMETERS

The calibrated specific storage values in the transient calibration are listed in Table 15-12. The hydraulic conductivity was also calibrated at this stage and the calibrated values for this parameter were described in section 15.7.1.2.

Table 15-12. Calibrated specific storage

Hydrogeological Subunit	Calibrated Specific Storage (1/m)
Upper Alluvium	1.0×10^{-4}
Lower Alluvium	1.3×10^{-4}
Basal Sediments	1.0×10^{-4}
Deep Halite	5.0×10^{-6}
Halite	1.0×10^{-3}
Lacustrine	5.0×10^{-5}
Lower Sand	1.3×10^{-4}
Lower Volcanoclastic	1.3×10^{-4}
Volcanic Breccia	1.3×10^{-4}
Volcanoclastic	5.0×10^{-4}

15.8.2.2 PUMPING TEST P-1

The simulation of the Well P-1 considers two different screen intervals. The shallow interval extends from model layer 2 to 4 in the lower and upper parts of the Halite and Lacustrine units respectively. However, layer 3 was modified locally around P-1 (500 m radius) to better reflect the locally observed geology in the P-1 well log (which was underestimated in the Leapfrog model) and which accounts for 92% of the total well discharge. A second screen interval extends deeper from model layer 6 to 14 in the Lacustrine and Volcanoclastic units. At the top of this interval, a local higher permeability zone of sandy clay is considered within the Lacustrine unit.

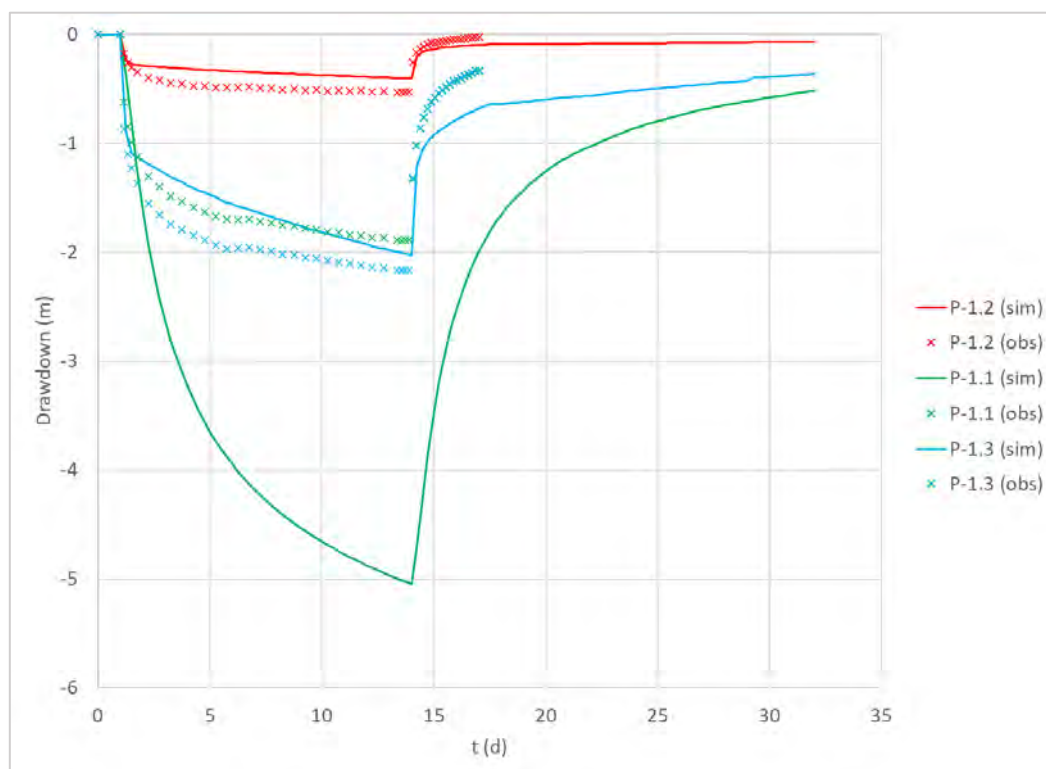
The maximum simulated drawdowns are shown in Table 15-13. The observed and simulated drawdowns at the observation wells for the P1 pumping test are shown in Figure 15-18.

Table 15-13. P-1 Test maximum simulated and observed drawdown values

Pumping Well	Observation Well	Maximum Simulated Drawdown (m)	Maximum Observed Drawdown (m)
P-1	P-1.1	5.05	1.90
	P-1.2	0.40	0.53
	P-1.3	2.03	2.17

At the end of the pumping period, the simulated drawdown matches closely the observed drawdowns for the P-1.2 and P-1.3 observation wells. For the P-1.1 observation well, the model is overestimating drawdown and simulates a head level that is approximately 3 m below the observed data. This well is in the Volcanoclastic unit like the P-4.1 observation well of the P4 pumping test site. Both observation wells show different hydrogeological behaviour despite they are screened in the volcanoclastic unit. The greater relevance considered for P-4.1 in the calibration process affected the head residual of P-1.1. The confidence of P-1.1 data is also affected by its relatively long screen that extends partially between the Lacustrine and Volcanoclastic unites compared with P-4.1 that has a local screen interval of approximately 10 m exclusively in the Volcanoclastic unit.

Figure 15-18. P-1 Test simulated and observed drawdowns



15.8.2.3 PUMPING TEST P-2

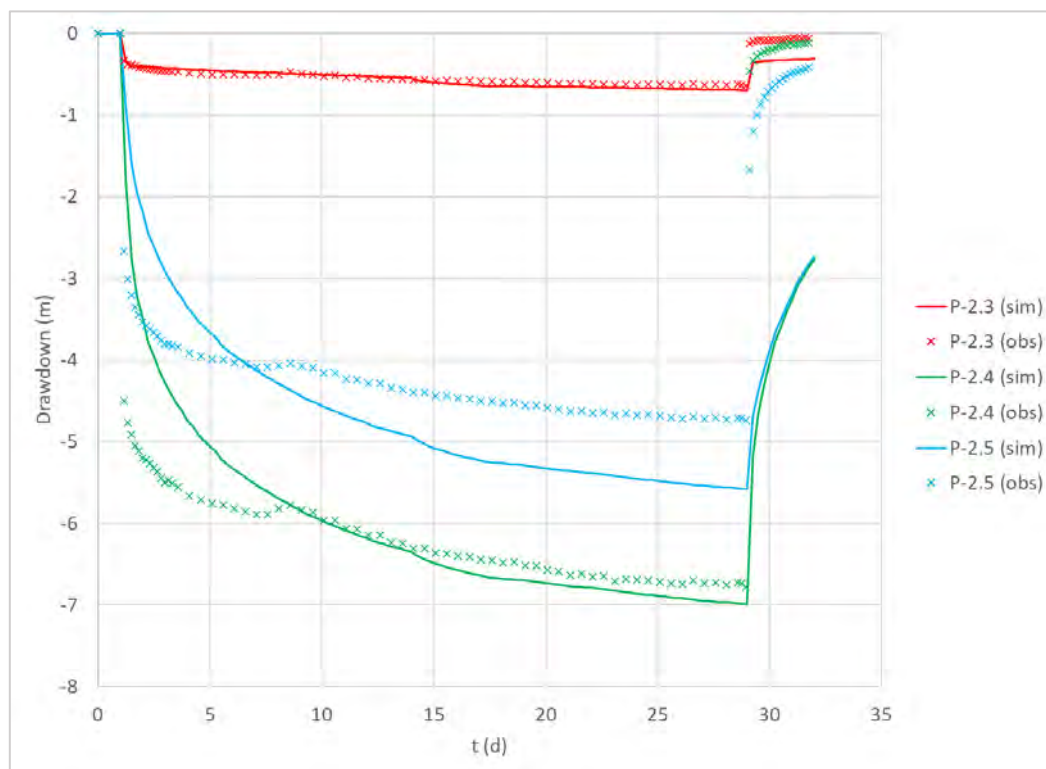
Water level responses during the P-2 pumping test were monitored in observation wells P-2.3, P-2.4 and P-2.5. P-2.3 in the Halite unit represents the priority calibration target. P-2.4 and P-2.5 are in Lacustrine unit with locally high permeability zones. The pumping is located at two different depths similarly to the P-1 configuration. The 92% of the discharge is applied to the shallower screen of approximately 20 m that extend at the bottom of the Halite unit. The Halite unit was extended down to layer 3 in the model mesh similarly to the P-1 modification. The rest of the discharge comes from the deeper screen interval in the Lacustrine unit with local high permeability zones.

The maximum simulated drawdowns are shown in Table 15-14. The observed and simulated drawdowns at the priority observation wells are shown in Figure 15-19 for the P2 pumping test. The simulated water level responses for the P-2 observation points are in general consistent with the observed data, especially for the priority well P-2.4 that has a maximum drawdown 0.2 m below the maximum observed drawdown. This residual is slightly greater in P-2.5 and P-2.3 with a magnitude of up to approximately 0.8 m (P-2.5). These wells also have more uncertainty due to the geometry and hydraulic properties of the higher permeability zone within the Lacustrine unit. The observation wells outside the pumping test site, C2, C3, C4, C5 and C6, show in some cases a slight response to the pumping that causes a residual of up to 6 cm (C2) with respect to the null response observed in the field. This is a conservative result that would overestimate the drawdown caused by future brine production.

Table 15-14. P-2 Test maximum simulated and observed drawdown values

Pumping Well	Observation Well	Maximum Simulated Drawdown (m)	Maximum Observed Drawdown (m)
P-2	C2	0.06	0.00
	C3	0.04	0.00
	C4	0.00	0.00
	C5	0.00	0.00
	C6	0.09	0.00
	P-2.3	0.70	0.64
	P-2.4	6.99	6.78
	P-2.5	5.58	4.74
	P-3	0.03	0.00

Figure 15-19. P-2 Test simulated and observed drawdowns



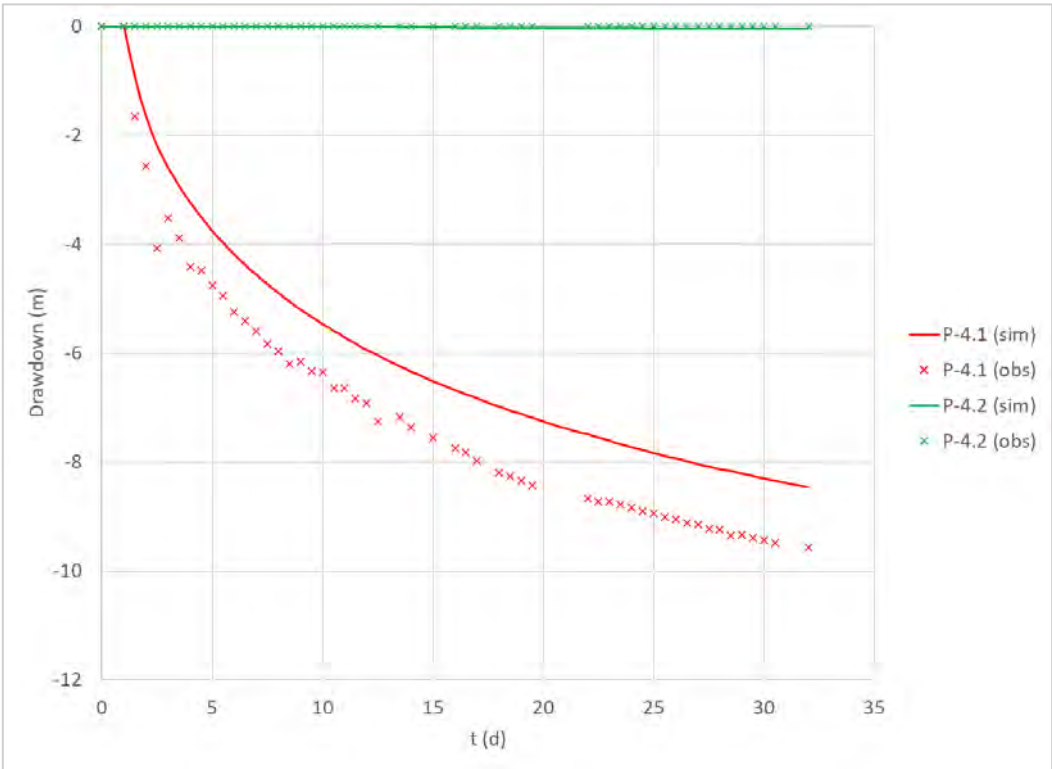
15.8.2.4 PUMPING TEST P-4

Water levels response during the P-4 pumping test were observed in observation wells P-4.1 (Volcanoclastic) and P-4.2 (Halite). The maximum simulated and observed drawdown in these wells is shown in Table 15-15. The observed and modelled water level responses are shown in Figure 15-20.

Table 15-15. P-4 Test maximum simulated and observed drawdown values

Pumping Well	Observation Well	Maximum Simulated Drawdown (m)	Maximum Observed Drawdown (m)
P-4	P-4.1	8.46	9.57
	P-4.2	0.05	0.00

Figure 15-20. P-4 Test simulated and observed drawdowns



15.9 BRINE RESERVE ANALYSIS

15.9.1 APPROACH

The numerical model, calibrated to steady state and transient flows and heads, was used for the Stage One reserve estimate over a 20-year brine extraction period. The reserve analysis takes the form of a transient groundwater flow and transport simulation, beginning with the initial steady state head distribution (Figure 15-14) and the initial lithium concentration distribution (Figure 15-9) from the resource estimate (Atacama Water, 2021). Water supply well CAN-6 with a flow rate of 10 l/s is included in the simulation.

Required brine wellfield production is 180 l/s during the first two years to fill the evaporation ponds. The target LCE extraction rate is 23.1 ktpy that corresponds to 15.0 ktpy assuming a plant efficiency of 65%. The location and pumping rates of active extraction wells vary from year to year to maximize lithium concentrations and minimize the extraction of brines originating from outside the MS concessions.

The brine production wellfield is located within the Old Code concessions. The brine extraction is simulated from either the shallow Halite aquifer or the deep brine aquifer below the Lacustrine unit. For the latter, the production interval is either from the base of the Lacustrine unit down to 200 m depth or from 200 m to 400m depth.

15.9.2 WELLFIELD LAYOUT

Figure 15-21 shows the well locations for the Stage One brine production wellfield. The wellfield configuration includes 19 production wells where 11 wells will be operating concurrently at every time. Two wells are completed in the Upper Halite aquifer, while the remaining wells are completed in the lower brine aquifer below the Lacustrine. Table 15-16 lists the coordinates of the brine extraction wells.

The brine wellfield production rate is 180 l/s during the first two years, then decreases for the rest of the production period with interannual variability between 120 l/s and 152 l/s as shown in Figure 15-22. Table 15-17 shows the detailed brine production schedule over the 20-year Project life.

Figure 15-21 Layout of the Stage One brine production wellfield

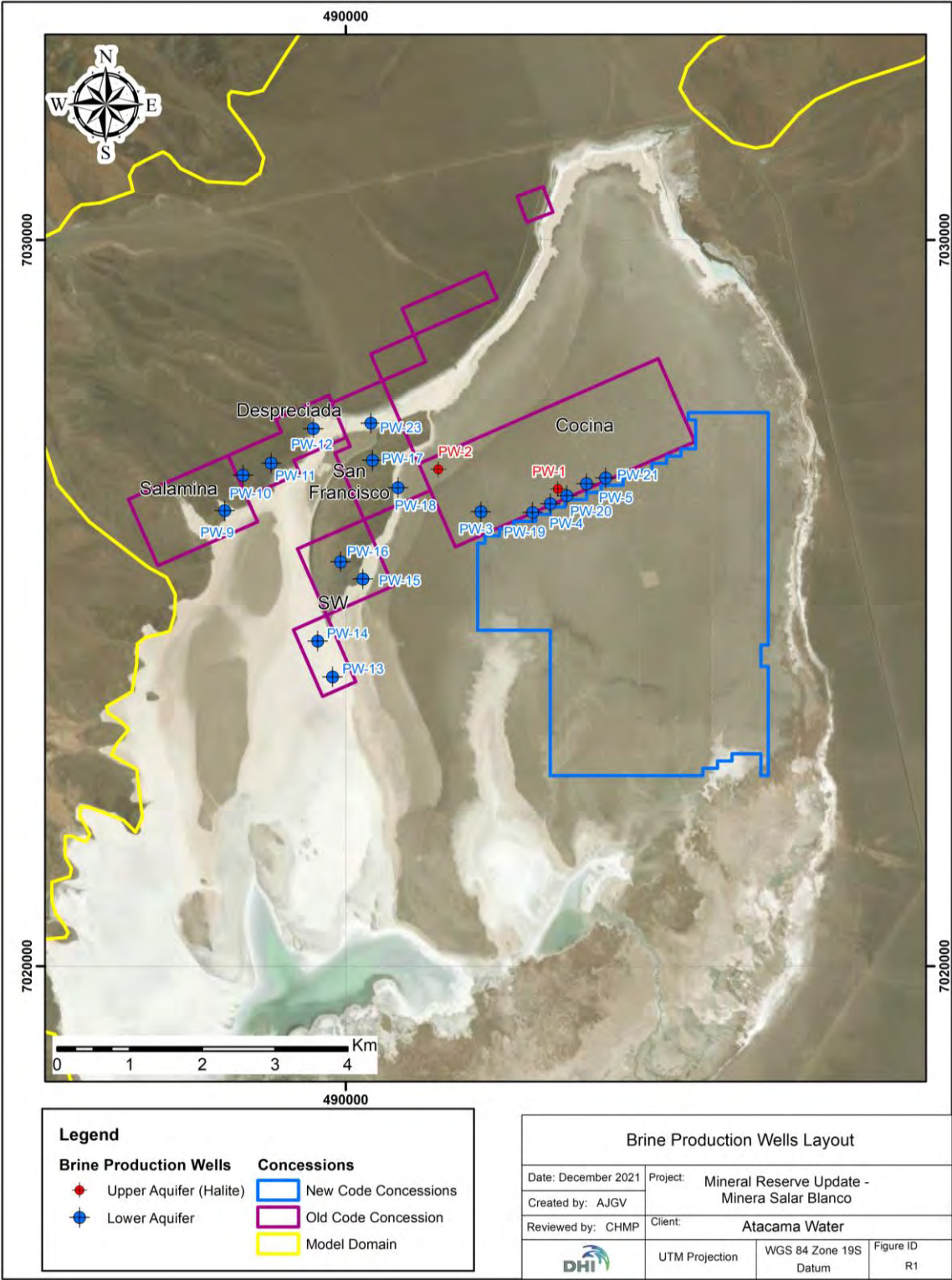




Table 15-16. Summary of production well construction details

Well	Concession	Aquifer Unit	UTM Northing (m)	UTM Easting (m)	Pumping Rate (L/s)	Screen Interval (m) ¹	Static Water Level (mbgs)	Pumping Water Level (mbgs) ²	Drawdown (m) ²
PW-1	Cocina	Halite	492921	7026573	15 to 18	0/6.5	0.7	1.4	-0.8
PW-2	Cocina	Halite	491275	7026844	13.7	0/6.5	0.8	3.1	-2.3
PW-4	Cocina	Lower Aquifer	492817	7026368	15 to 18	110/250	-0.3	9.3	-9.6
PW-5	Cocina	Lower Aquifer	493313	7026644	15 to 18	110/280	-0.6	7.7	-8.3
PW-19	Cocina	Lower Aquifer	492572	7026247	13.7 to 18	120/290	-0.2	22.4	-22.6
PW-20	Cocina	Lower Aquifer	493043	7026479	13.7 to 18	120/290	-0.4	24.2	-24.7
PW-3	Cocina	Lower Aquifer	491861	7026256	13.7 to 15	110/250	0	21.9	-21.9
PW-21	Cocina	Lower Aquifer	493579	7026724	15 to 18	120/300	-0.9	2.9	-3.8
PW-9	Salamina	Lower Aquifer	488335	7026273	15 to 18	51/121	1.7	5.8	-4.2
PW-10	Despreciada	Lower Aquifer	488587	7026761	13.7 to 15	59/159	8.6	17.8	-9.2
PW-11	Despreciada	Lower Aquifer	488971	7026927	13.7	55/205	4.5	21.7	-17.2
PW-12	Despreciada	Lower Aquifer	489556	7027400	13.7	50/250	-0.4	15.5	-15.9
PW-23	San Francisco	Lower Aquifer	490347	7027479	13.7	50/200	-0.4	17.3	-17.7
PW-13	SW	Lower Aquifer	489819	7023981	7.5 to 18	60/250	0.4	3.7	-3.3
PW-14	SW	Lower Aquifer	489612	7024477	13.7 to 18	50/230	0.6	4.6	-4
PW-15	SW	Lower Aquifer	490236	7025332	13.7 to 18	50/230	0.1	17.8	-17.6
PW-16	SW	Lower Aquifer	489928	7025567	7.5 to 13.7	63/223	13.8	32.4	-18.6
PW-17	San Francisco	Lower Aquifer	490368	7026966	13.7 to 15	66/216	15.5	37.3	-21.8
PW-18	San Francisco	Lower Aquifer	490719	7026587	13.7 to 15	50/200	0.1	18.5	-18.4

1 Initial/final screen depth

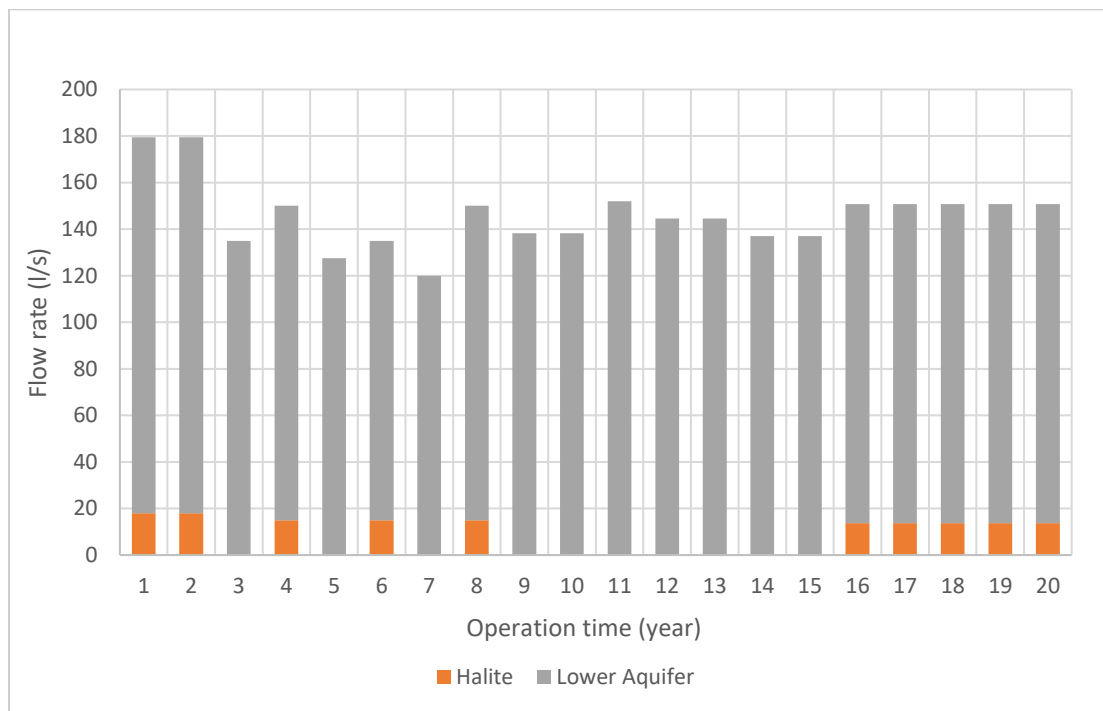
2 Computed head at the centre of the screen



Table 15-17 Simulated Stage One brine pumping schedule

Wells	Average production rate per year (L/s)																			
	1	2	3	4	5	6	7	8	9	10	11	12	13	14	15	16	17	18	19	20
PW-1	18	18	-	15	-	15	-	15	-	-	-	-	-	-	-	-	-	-	-	-
PW-2	-	-	-	-	-	-	-	-	-	-	-	-	-	-	-	13.7	13.7	13.7	13.7	13.7
PW-4	18	18	15	15	15	-	-	-	-	-	-	-	-	-	-	-	-	-	-	-
PW-5	18	18	15	15	15	-	-	-	-	-	-	-	-	-	-	-	-	-	-	-
PW-19	18	18	15	15	15	15	15	15	13.7	13.7	13.7	13.7	13.7	13.7	13.7	13.7	13.7	13.7	13.7	13.7
PW-20	18	18	15	15	15	15	15	15	13.7	13.7	13.7	13.7	13.7	13.7	13.7	13.7	13.7	13.7	13.7	13.7
PW-3	-	-	-	-	15	15	15	15	13.7	13.7	13.7	13.7	13.7	13.7	13.7	13.7	13.7	13.7	13.7	13.7
PW-21	18	18	15	15	15	15	15	15	-	-	-	-	-	-	-	-	-	-	-	-
PW-9	18	18	15	15	15	15	-	-	-	-	-	-	-	-	-	-	-	-	-	-
PW-10	-	-	-	-	-	-	15	15	13.7	13.7	13.7	13.7	13.7	13.7	-	-	-	-	-	-
PW-11	-	-	-	-	-	-	-	-	13.7	13.7	13.7	13.7	13.7	13.7	13.7	13.7	13.7	13.7	13.7	13.7
PW-12	-	-	-	-	-	-	-	-	-	-	13.7	13.7	13.7	13.7	13.7	13.7	13.7	13.7	13.7	13.7
PW-23	-	-	-	-	-	-	-	-	-	-	-	-	-	-	13.7	13.7	13.7	13.7	13.7	13.7
PW-13	18	18	15	15	7.5	7.5	7.5	7.5	7.5	7.5	7.5	-	-	-	-	-	-	-	-	-
PW-14	18	18	15	15	7.5	7.5	7.5	7.5	7.5	7.5	7.5	7.5	7.5	-	-	-	-	-	-	-
PW-15	18	18	15	15	7.5	7.5	7.5	7.5	13.7	13.7	13.7	13.7	13.7	13.7	13.7	13.7	13.7	13.7	13.7	13.7
PW-16	-	-	-	-	-	7.5	7.5	7.5	13.7	13.7	13.7	13.7	13.7	13.7	13.7	13.7	13.7	13.7	13.7	13.7
PW-17	-	-	-	-	-	-	-	15	13.7	13.7	13.7	13.7	13.7	13.7	13.7	13.7	13.7	13.7	13.7	13.7
PW-18	-	-	-	-	-	15	15	15	13.7	13.7	13.7	13.7	13.7	13.7	13.7	13.7	13.7	13.7	13.7	13.7
Total (l/s)	180	180	135	150	128	135	120	150	138	138	152	145	145	137	137	151	151	151	151	151

Figure 15-22. Stage One annual brine production rates



15.9.3 LCE PRODUCTION SIMULATIONS

The Stage One model simulations predict that 479 kt of LCE will be produced by the production wellfield over the 20-year period. The annual production profile of LCE contained in the pumped brine is shown in Figure 15-23. The annual LCE content in the pumped brine exceeds 30 kt during Year 1 and 2 and averages above 23 kt for Year 3 through Year 20.

The lithium concentration in the produced brine evolves over the 20 years period as shown in Figure 15-24. The average lithium concentration is predicted to remain above 1,000 mg/L until Year 6 and varies between 948 mg/l to 1,011 mg/l between Year 7 and Year 20.

The model simulations indicate that 94 % of the LCE is derived from the lower brine aquifer and 6% from the Upper Halite.

Since some brine wells may be located close to the border of MSB properties, there is the risk that some brine may be drawn from neighboring properties. FEFLOW model assumes a very limited percentage of lithium mass throughout a 20-year mine-life of the project coming from outside of MSB owned mining concessions.

Figure 15-23 Stage One LCE contained in the pumped brine

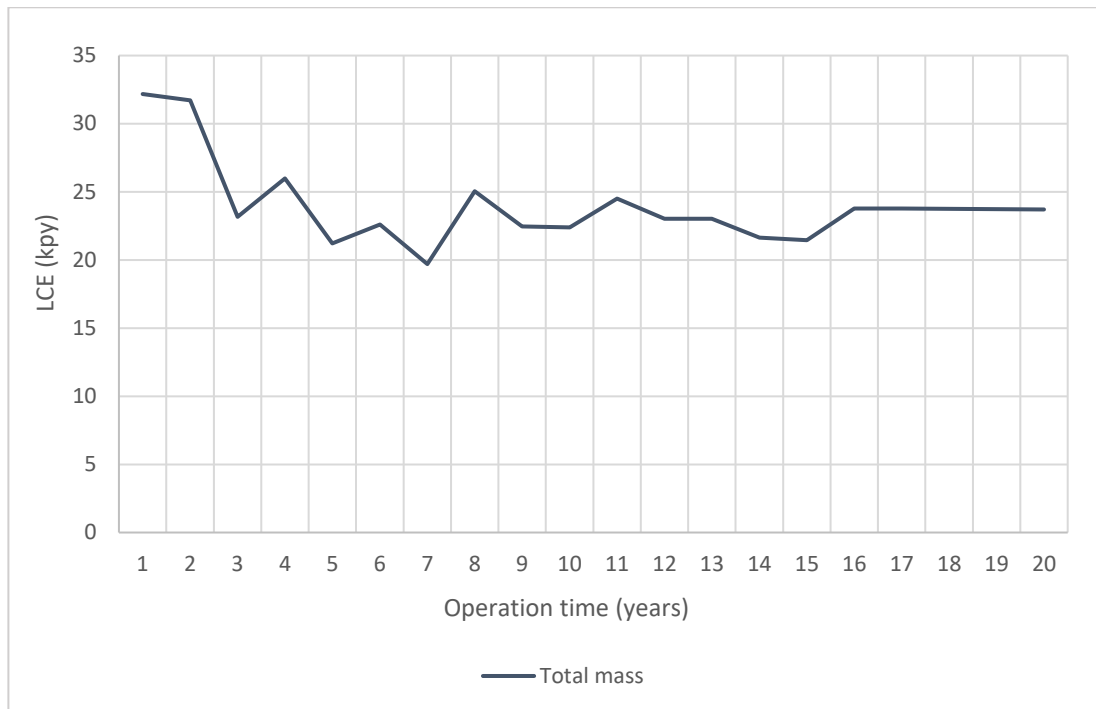
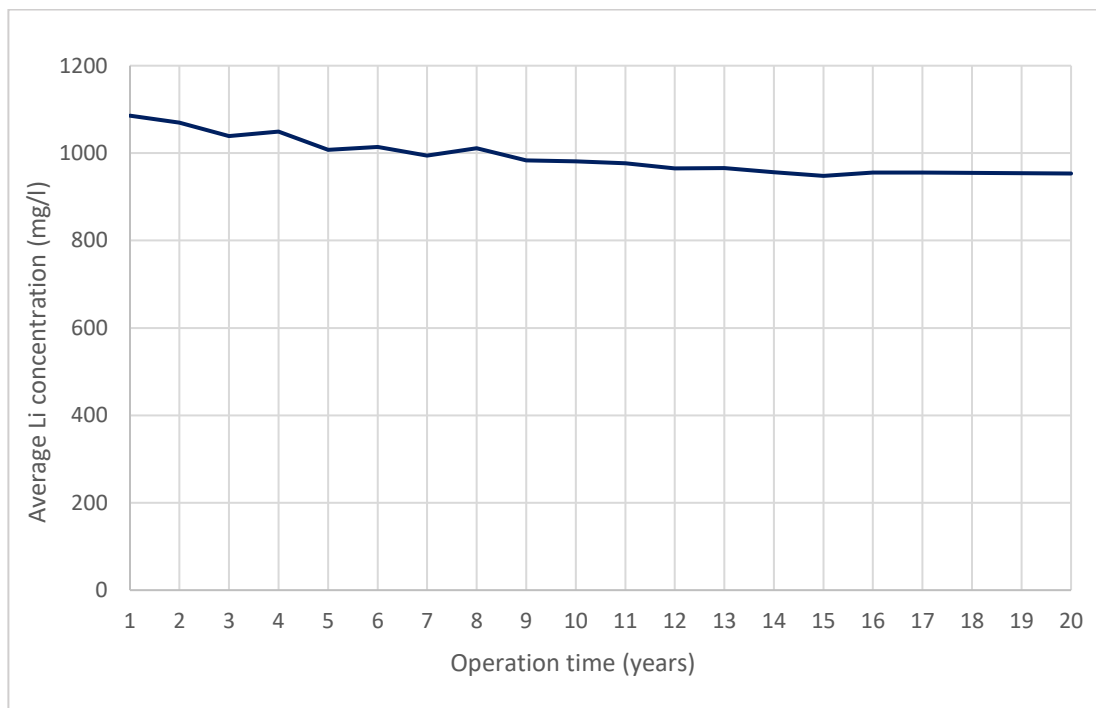


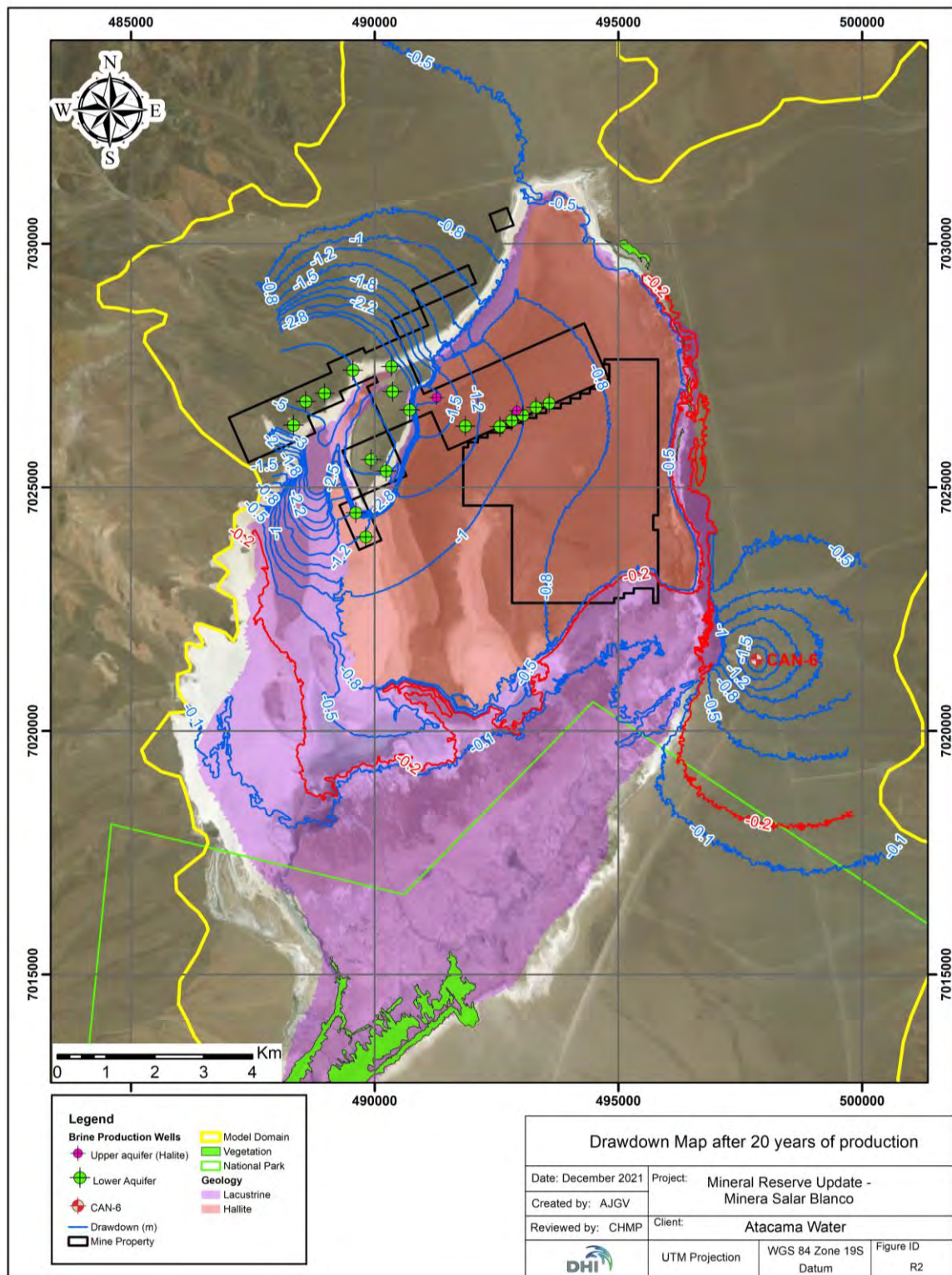
Figure 15-24. Average lithium concentration of wellfield production



15.9.4 WATER TABLE PREDICTIONS

The simulated water level responses after 20 years of brine production is shown in Figure 15-25. This is the simulated drawdown in the layer 1 of the model. There are two water table depressions, one centred around the Stage One brine production wellfield and the other centred around freshwater supply well CAN-6. The maximum water table depression around either of the two pumping zones does not exceed 5 m. The Lacustrine unit acts as a hydraulic barrier between the deep brine aquifer and the shallow water table.

Figure 15-25. Predicted drawdown after Year 20



15.9.5 RESERVE ESTIMATE

The reserve estimate for the Stage One Project was prepared in accordance with the guidelines of National Instrument 43-101 and uses the best practices methods specific to brine resources (Atacama Water, 2021). The lithium reserves are summarized in Table 15-18 and Table 15-19.

Table 15-18. Stage One Brine Mining Reserve for pumping to ponds

Category	Year	Brine Vol (Mm3)	Ave Li conc (mg/l)	Li metal (tonnes)	LCE (tonnes)
Proven	1-7	19	1,024	14,000	75,000
Probable	1-7	13		19,000	102,000
Probable	8-20	60	950	57,000	302,000
All	1-20	92	976	90,000	479,000

Table 15-19. Stage One Brine Production Reserve for Lithium Carbonate production (assuming 65% lithium process recovery efficiency)

Category	Year	Brine Vol (Mm3)	Ave Li conc (mg/l)	Li metal (tonnes)	LCE (tonnes)
Proven	1-7	19	1,024	9,000	49,000
Probable	1-7	13		12,000	66,000
Probable	8-20	60	950	37,000	196,000
All	1-20	92	976	58,000	311,000

Notes to the Reserve Estimate:

1. The Stage One Reserve Estimate includes an optimized wellfield configuration and pumping schedule to comply with environmental constraints and water level decline restrictions as part of the environmental approval document (RCA) issued by the Chilean Environmental Agency.
2. Lithium is converted to lithium carbonate (Li_2CO_3) with a conversion factor of 5.32
3. The qualified Person for the Mineral Reserve estimate Frits Reidel, CPG
4. The effective date for the Reserve Estimate is December 22, 2021.
5. Numbers may not add due to rounding effects.
6. Approximately 25 percent of the Measured and Indicated Resources are converted to Proven and Probable Reserves as brine feed from the production wellfield to the evaporation ponds without accounting for the lithium process recovery efficiency. The overall conversion from M+I Resources to Total Reserves including lithium process recovery efficiency of 65% is approximately 16 percent.

16. MINING METHODS

16.1 GENERAL DESCRIPTION

The production process starts with the brine extraction wells in the Salar.

Results of the pumping tests on the Stage One Project (as described in Section 10 above) indicate that brine abstraction from the Salar will take place by installing and operating a conventional brine production wellfield. Brine from the individual production wells will be fed into two collection/transfer ponds in the northwest of the Salar. From there it will be pumped, using a booster pumping station, through the main trunk pipeline up to the evaporation ponds some 12 km to the north in the general plant area.

The brine composition and lithium concentrations of the OCC indicate that an average of 15,200 TPY of lithium carbonate production will require an average annual brine feed rate of 12,960 m³/d or 150 l/s. The predicted evolution of the lithium concentration over the life of the wellfield operation is shown in Figure 15-24.

16.2 WELLFIELD LAYOUT

Results of the Stage One Project pumping tests and the reserve model simulations indicate that pumping rates of individual brine production wells will range between 8 l/s and 18 l/s. The detailed wellfield operation schedule is shown in Table 15-17. Well completion depths will vary between 40 m (upper brine aquifer) and 400 m (lower brine aquifer). The brine production wells will be completed with 12-inch diameter stainless steel production casing and equipped with 380 V submersible pumping equipment. Table 15-16 provides the planned location and construction details of the production wells. It is projected that a total of 19 wells will be required over the life of the Project. However, no more than 11 wells will be operating at a single time. Permanent power will be delivered to the wellfield area through a mid-range power line.

Brine discharge from each wellhead will be piped through 8-inch diameter HDPE feeder pipelines to two central collection/transfer ponds in the northwest of the Salar. A 12 km length, 20-inch diameter steel / HDPE main trunk pipeline will be installed between the collection/transfer ponds and the evaporation ponds area. A booster pumping station will be installed at the bottom of the main trunk line adjacent to the collection ponds to pump the brine up to the evaporation ponds (130 m lift).

17. RECOVERY METHODS

17.1 OVERVIEW

The facilities have been designed to produce an average of 15,200 TPY of lithium carbonate (Li_2CO_3) battery grade over a 20-year mine-life

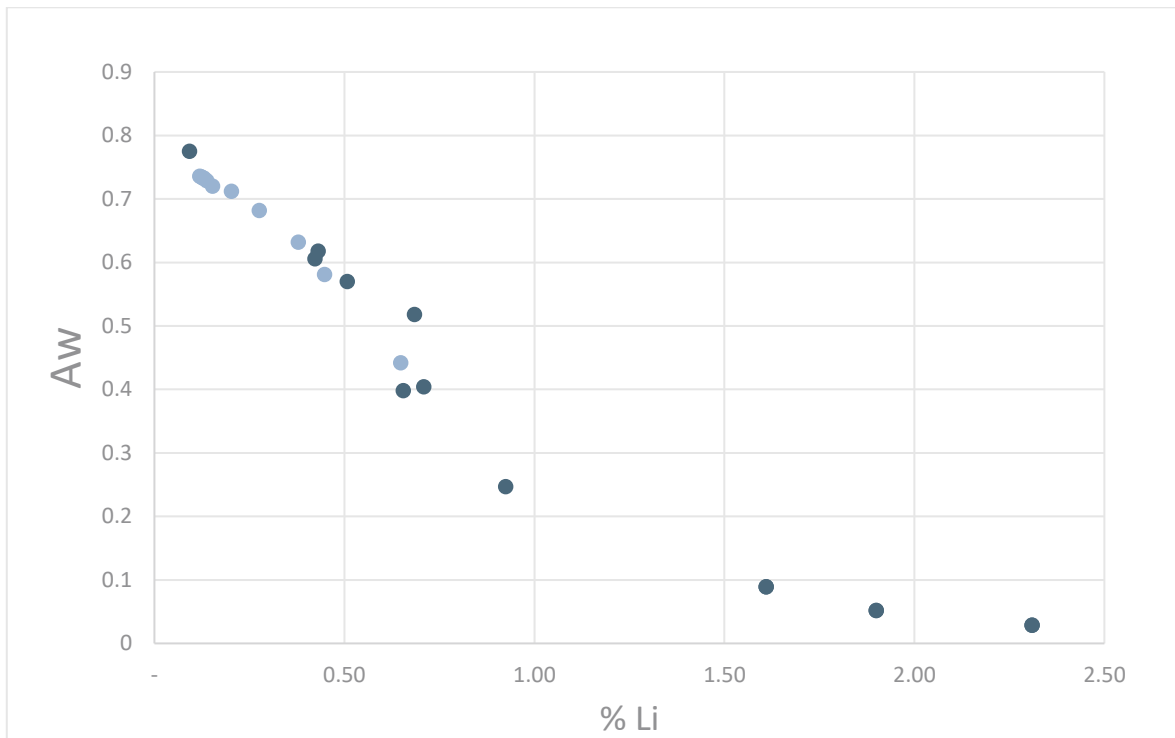
The raw material for the production of lithium carbonate is extracted from MSB's mineral properties in the salar. This brine is fed to evaporation ponds where various salts precipitate, such as halite, sylvinite and carnallite. Enriched Li^+ ion brine is obtained as a result of the evaporation stage and then pumped to the production plant.

This lithium-rich brine is fed to the Salt Removal Plant - Phase 1 to remove most of the calcium, boron and magnesium and remove boron through purification steps to further concentrate lithium in the brine. This brine is then pumped to the Lithium Carbonate Plant – Phase 2, which consists of purification steps for calcium and magnesium removal, a precipitation step for lithium carbonate, and steps for solid liquid separation. Finally, the final product is dried and packaged and stored in a warehouse for dispatch to the final client, as required.

Salt Removal Plant is required as the pilot evaporation tests indicated the high concentration of calcium, magnesium and lithium in the concentrated brine lowers the brine activity significantly and the eutectic end point of about 3-4% wt lithium is never reached at ambient concentrations (see Figure 17-1). Additionally, concentrating to higher levels of about 1,5% wt in summertime, showed significant losses in lithium as lithium borates and entrapment in the crystallized salt in the ponds.

The risk that the brine might not reach the targeted lithium concentration in the ponds (3-4% wt) in a consistent and continues manner during the year, was the main driver to design the process for a concentration target of about 0.9% wt, which is proved it can be reached and maintained for a consistent and continuous feed to the Salt Removal Plant and Lithium Carbonate plant thereafter, thus increasing the overall efficiency by reducing the losses in salt entrainment, the consumption of chemical reagent and allowing water recovery during the process.

Figure 17-1 Water Activity versus % Li in the tested brine



A general process flow diagram for the evaporation ponds and the production plant may be seen in Figure 17-2. For more details on the process, a complete process block diagram is presented in Figure 17-3 with the main inlet and outlet streams of the process, and more details are provided in the following sub-chapters.

Figure 17-2 General Process Diagram

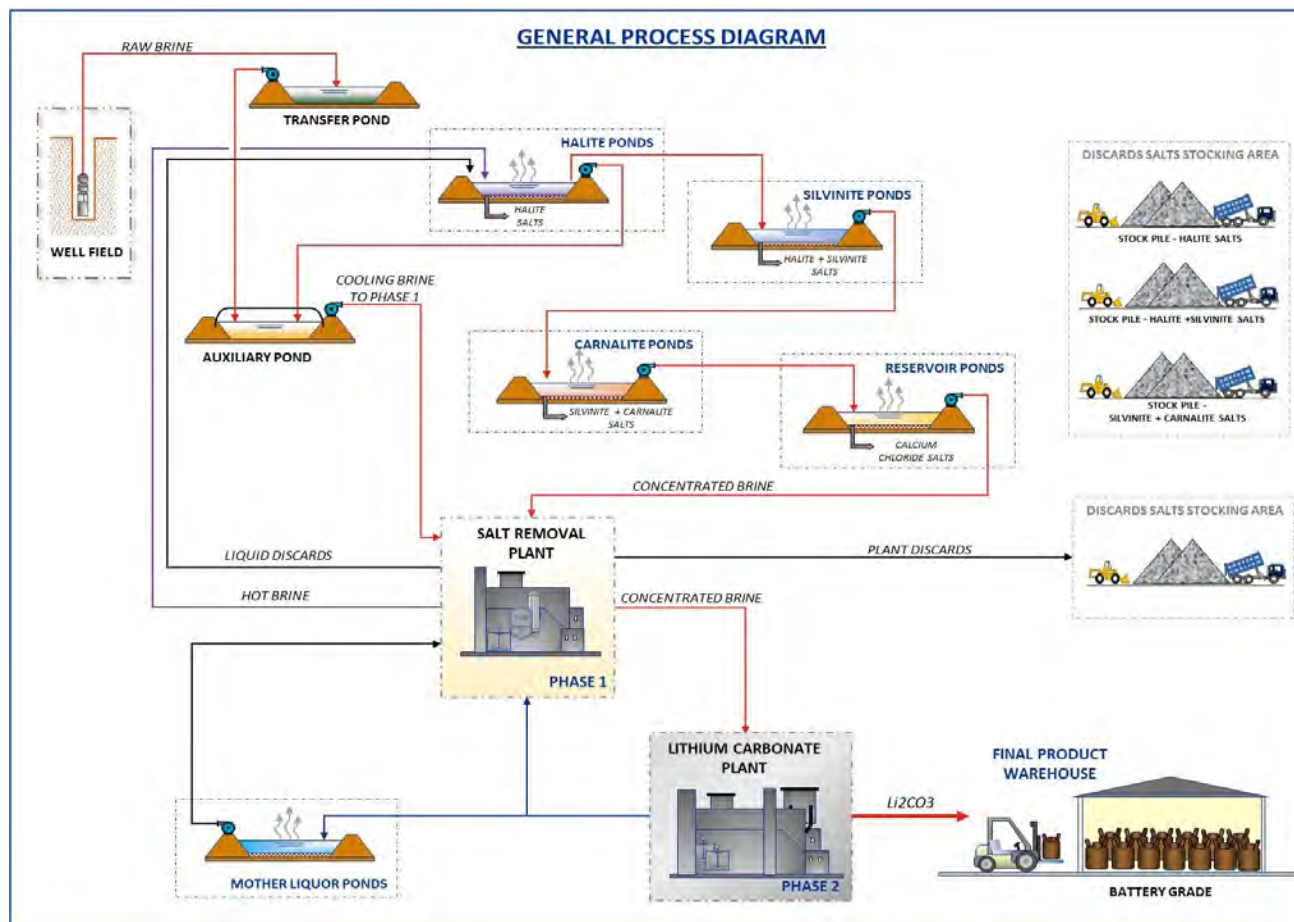
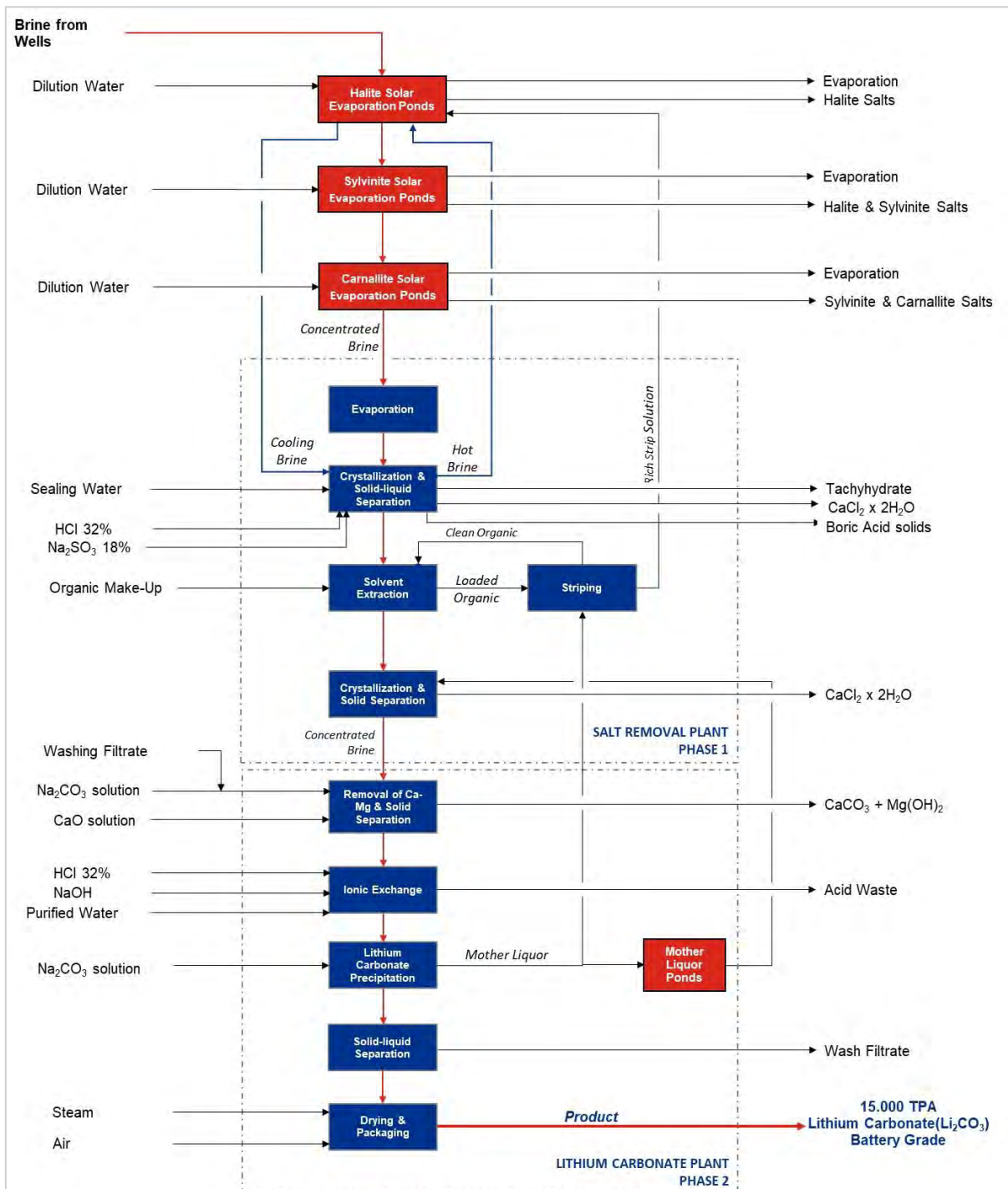


Figure 17-3 Process Block Diagram



17.2 OPERATION OF THE SOLAR EVAPORATION PONDS

The solar evaporation ponds are a group of concentration facilities that cover an extensive area and take advantage of the natural water evaporation effect as well as the solar radiation to concentrate the brine in the required element. The water evaporation rate depends on four main factors: solar radiation, the relative air humidity, wind speed and temperature changes. These four factors are favourably present in the Salar de Maricunga area.

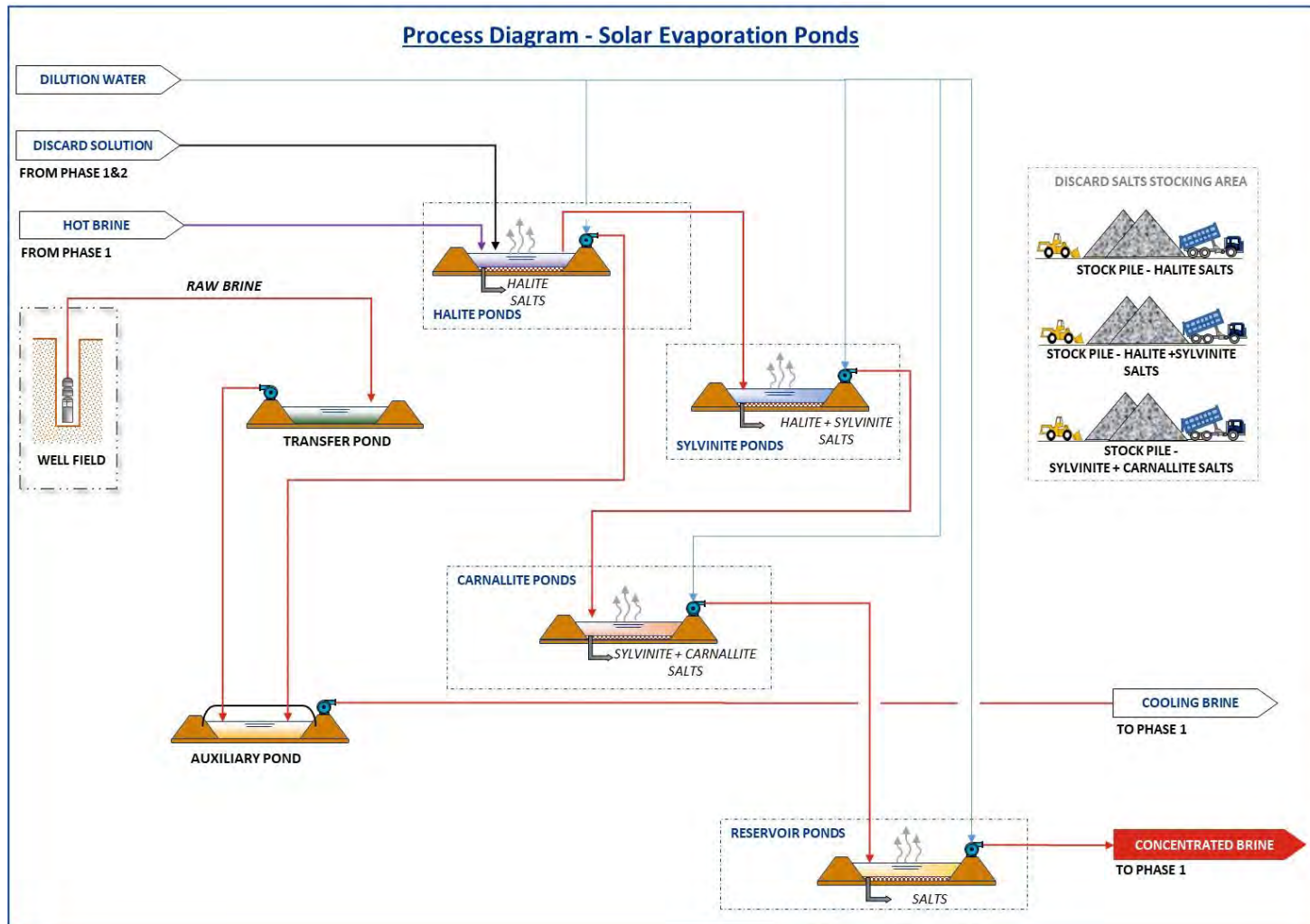
The solar evaporation ponds are simple structures of a very large size and shallow depth, located a few kilometres from the salt flat. Material from the area is used to construct the walls of each pond. They are covered by a geomembrane to guarantee impermeability and avoid leakage. Ponds operate in a sequence, where the first pond is fed with fresh brine, and the last pond is fed with concentrated brine from the previous evaporation ponds. In the specific case of this project, fresh brine from the production wells, which has a lower temperature, is firstly fed to the production plant to act as cooling brine. The outlet of the cooling brine from the production plant has a higher temperature than the fresh brine and will be sent to the first evaporation pond to continue with the evaporation process.

As mentioned above, each solar evaporation pond is interconnected with the following ponds in a downstream series. Due to the topography of the area where the evaporation ponds will be located, in most cases there will be a difference in altitude between the bottom of each pond. This allows the brine to be transported from a pond to the next one, using a communicating channel system through open pipelines as well as transfer channels covered with HDPE, making the most of the gravitational energy to carry out the transportation. In those cases when this is not possible, pumping is used.

The system behaves like a crystallization or salt separation mechanism through water evaporation and ion elimination through salt precipitation, using the brine's natural saturation property. In this way, salts precipitate when the brine reaches its saturation point and the resulting brine, with a higher lithium concentration, is transported to the next pond, as indicated previously. Precipitated salt must be harvested (extracted) from the ponds when it reaches pre-defined levels. Approximately 5,400,000 tons of brine are treated in the evaporation ponds annually. Concentrated brine from the last evaporation pond is pumped to a group of reservoir ponds, which act as a storage unit for concentrated brine before pumping it to the production plant, as well as a buffer pond for the seasonal variations of brine in the system. Due to the size and definition of the reservoir ponds, carnallite and calcium chloride salts also precipitate in these ponds, which will be harvested.

From the reservoir ponds, concentrated brine is fed to the production plant – Salt Removal Plant – Phase 1. Figure 17-4 presents a general diagram of the solar evaporation ponds.

Figure 17-4 Evaporation Ponds Diagram



The generation of harvested salts is shown in Table 17-1.

Table 17-1 Annual generation of salts from evaporation ponds

Compound/type	Annual production (TPY)
Pond Salts generated	
Halite (with 10% entrained brine)	978,406
Sylvinite (with 10% entrained brine)	81,697
Carnallite (with 10% entrained brine)	151,756
Calcium chloride (with 10% entrained brine) (from reservoir ponds)	160,757

Harvested salts are deposited in authorized stocking areas and separated by the type of salt, depositing them directly on the stocking ground using the same machinery used for harvesting.

Fresh brine coming from the auxiliary pond is also fed to the Salt Removal Plant as cooling brine at a temperature between -4.5 and 7°C (depending on the season of the year), which is then returned to the evaporation ponds, specifically Halite pond H-15, with a higher temperature of 22,8°C to start with the evaporation process, all present in Figure 17-4.

17.3 SALT REMOVAL PLANT – PHASE 1

For the main process, after all the evaporation process of the brine through all halite, sylvinite and carnallite ponds, concentrated brine from the reservoir ponds is fed to the Salt Removal Plant or Phase 1 to continue brine purification and lithium concentration. Here calcium and magnesium are removed from the brine in the form of tachyhydrite and calcium chloride salts. Boron is also removed using solvent extraction. These steps allow the further concentration of the Li^+ ion in the brine. This plant generates a more concentrated brine feed to the lithium carbonate plant, thus improving the plant's efficiency and producing a final material that will have improved market potential. This plant also recovers condensates that are reused within the process, thus reducing industrial water consumption.

The removal of these impurity elements is achieved through a sequence of processes, which are presented in Figure 17-5 and Figure 17-6.

The concentrated brine from the ponds firstly feeds an evaporation stage, which allows the formation of tachyhydrite salts which are separated from the brine using solid-liquid separation equipment. Brine is then fed to a stage of crystallizers, to further allow the formation of tachyhydrite, which is also then separated from the brine using solid-liquid separation equipment.

The brine is then fed to a second stage of crystallizers, where calcium chlorides will be formed, and will be removed in a subsequent solid-liquid separation stage. Brine is then fed to a boric acid crystallizer, and if pH reaches lower values, sodium sulphate (Na_2SO_3) is added to reduce bromine formation and avoid corrosion damages of the equipment. The addition of hydrochloric acid is also considered, to generate the precipitation of boric acid in the process, which is also removed using solid-liquid separation equipment.

The lithium concentrated brine then feeds a solvent extraction stage, where boron is removed from the brine using a selective extractant and diluent mixture. The boron extraction stages are carried out with an acidic pH and using the reagent mixture to transfer the boron from the aqueous phase (brine) to the organic phase. The stripping stages to remove the boron from the organic phase are carried out with a basic pH, obtaining a boron rich solution to be sent to the discard tank. The boron free brine is sent to the next stage. Sodium Sulphite is used in this stage if needed to control the pH of the brine.

The boron free brine is fed to a third and final stage of crystallizers, to remove the remaining calcium present in the brine as calcium chloride salts, which will be separated from the brine using a solid-liquid separation stage. The lithium concentrated brine with a low content of calcium and magnesium is stored in intermediate storage tanks to feed the Lithium Carbonate Plant – Phase 2.

All discard solids generated from Phase 1 are transported to disposal stockpiles that are designed according to the environmental requirements. The generation of discard salts from Phase 1 are shown in Table 17-2.

Table 17-2 Annual generation of discard salts from Phase 1

Compound/type	Annual production (TPY)
Phase 1 discard salts generated	
Tachyhydrite + Calcium Chloride (with 13% moisture)	304,491
Boric acid cake (with 50% moisture)	10,915

Figure 17-5 Simplified Salt Removal Plant Process Diagram (1/2)

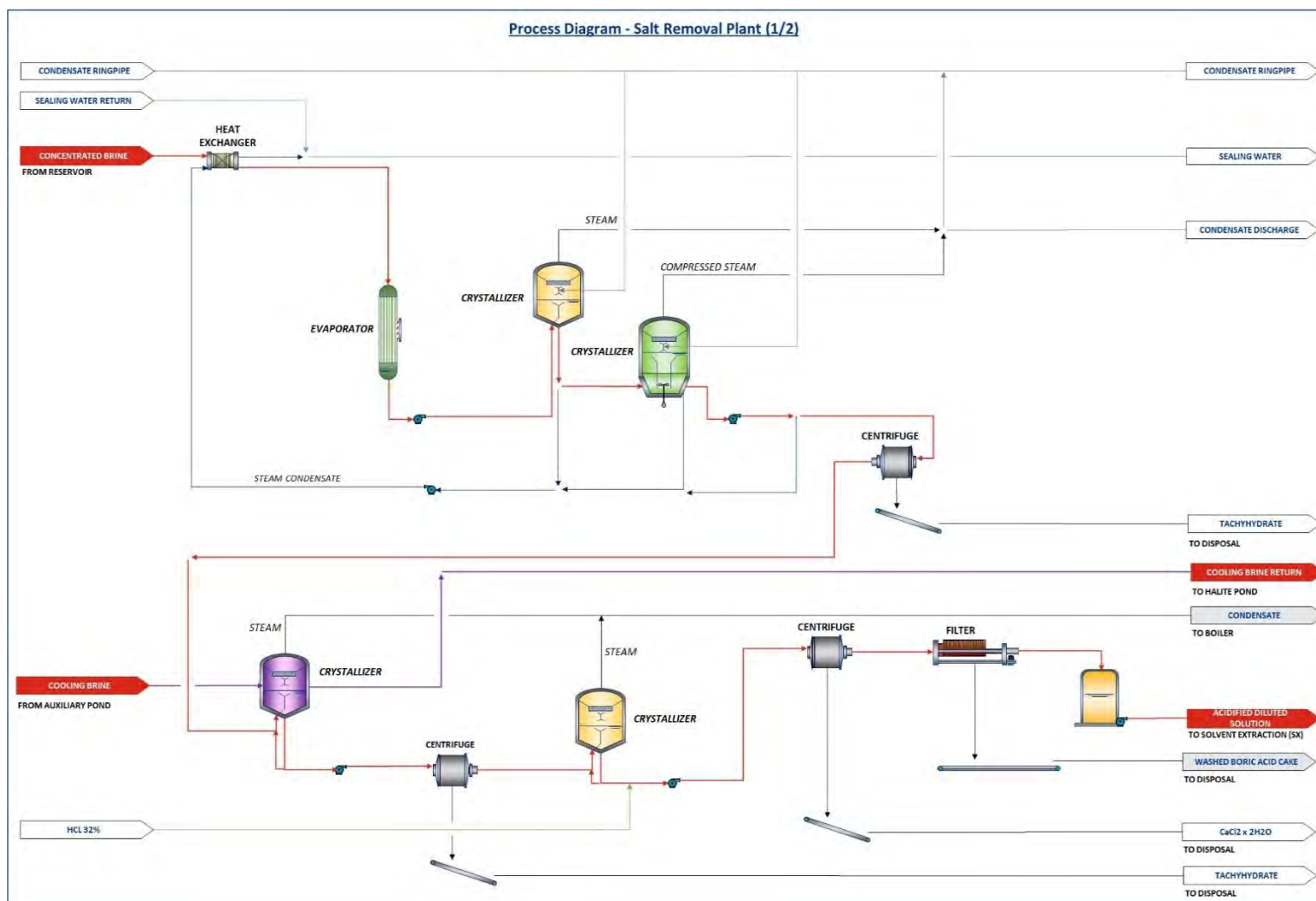
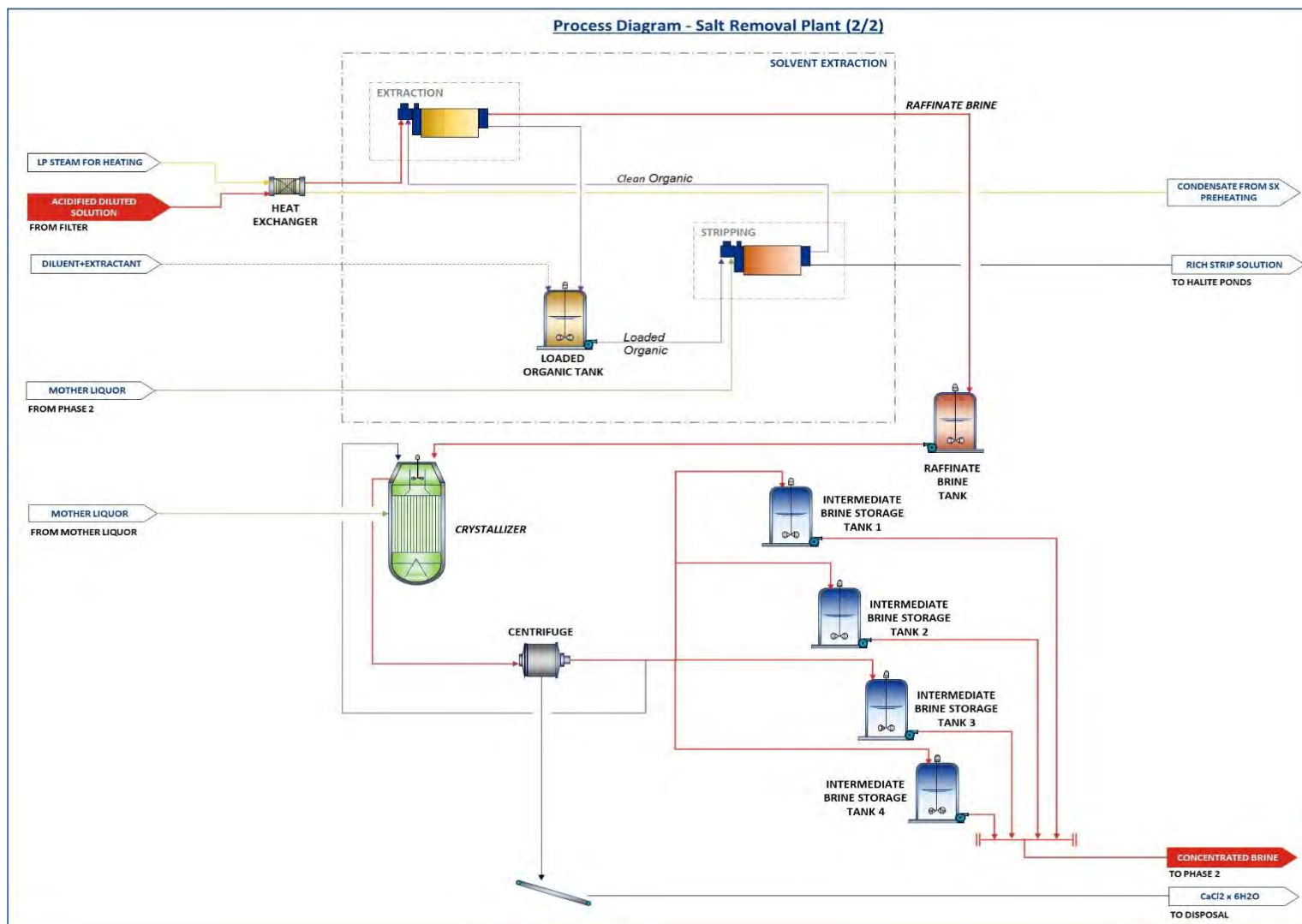


Figure 17-6 Simplified Salt Removal Plant Process Diagram (2/2)



17.4 LITHIUM CARBONATE PLANT

The Lithium Carbonate Plant, also known as Phase 2, is a chemical plant that receives concentrated brine from the Salt Removal Plant. This lithium rich brine also contains concentrations of impurity elements. These elements must be removed from the brine to generate a lithium carbonate product of high purity, in accordance with the international standards of the industry.

The elimination of the impurity elements is achieved through the processes such as mixing in reactors with specific reagents, as well as through ion exchange. The lithium carbonate is then precipitated in specific reactors with the aid of a soda ash solution, and finally, the lithium carbonate precipitate is dewatered and dried. This process is presented as a general scheme in Figure 17-7 and Figure 17-8.

For the elimination of the remaining contaminants present in the brine, the first stage is a reduction of calcium/magnesium. This is carried out using a recirculation of the mother liquor, milk of lime and a soda ash solution. These are all mixed in reactors with the concentrated brine from Phase 1 at 60 °C. This mixture promotes the formation and precipitation of calcium carbonate (CaCO_3) and magnesium hydroxide ($\text{Mg}(\text{OH})_2$), which are separated from the concentrated lithium brine using solid-liquid separation equipment. All solids obtained from this stage are sent to discard stockpiles and the brine with a residual amount of calcium is transferred to the next stage.

To assure the final elimination of all contaminants, an ion exchange stage is used. The concentrated brine is contacted with specific resins in ion exchange columns, removing any remaining impurities, and generating a contaminant free brine, which is sent to the next stage. All solutions generated in this stage are recirculated within the process or sent to the water treatment plant.

The contaminant free brine enters the carbonation stage, where it is placed in contact with a soda ash solution. The formation of lithium carbonate using soda ash is optimum at temperatures close to 80 °C, allowing the precipitation of the lithium carbonate in a solid state.

The pulp obtained from the carbonation stage is processed in solid/liquid separation equipment, where the product is also washed. The dewatered lithium carbonate is transported to a dryer. After drying, the lithium carbonate is packed into separate maxi bags and stored in a final product warehouse and is later delivered to clients as required.

The discard solids generated from Phase 2 are mainly calcium carbonate and magnesium hydroxide, which are transported to specific disposal stockpiles located within the project properties, and that are designed according to the environmental requirements. The generation of discard salts from Phase 2 are shown in Table 17-3.

Table 17-3 Annual generation of discard salts from Phase 2

Compound/type	Annual production (TPY)
Phase 2 discard salts generated	
Calcium Chloride and Magnesium Hydroxide (with 51% moisture)	16,150

Figure 17-7 Simplified Lithium Carbonate Plant Process Diagram (1/2)

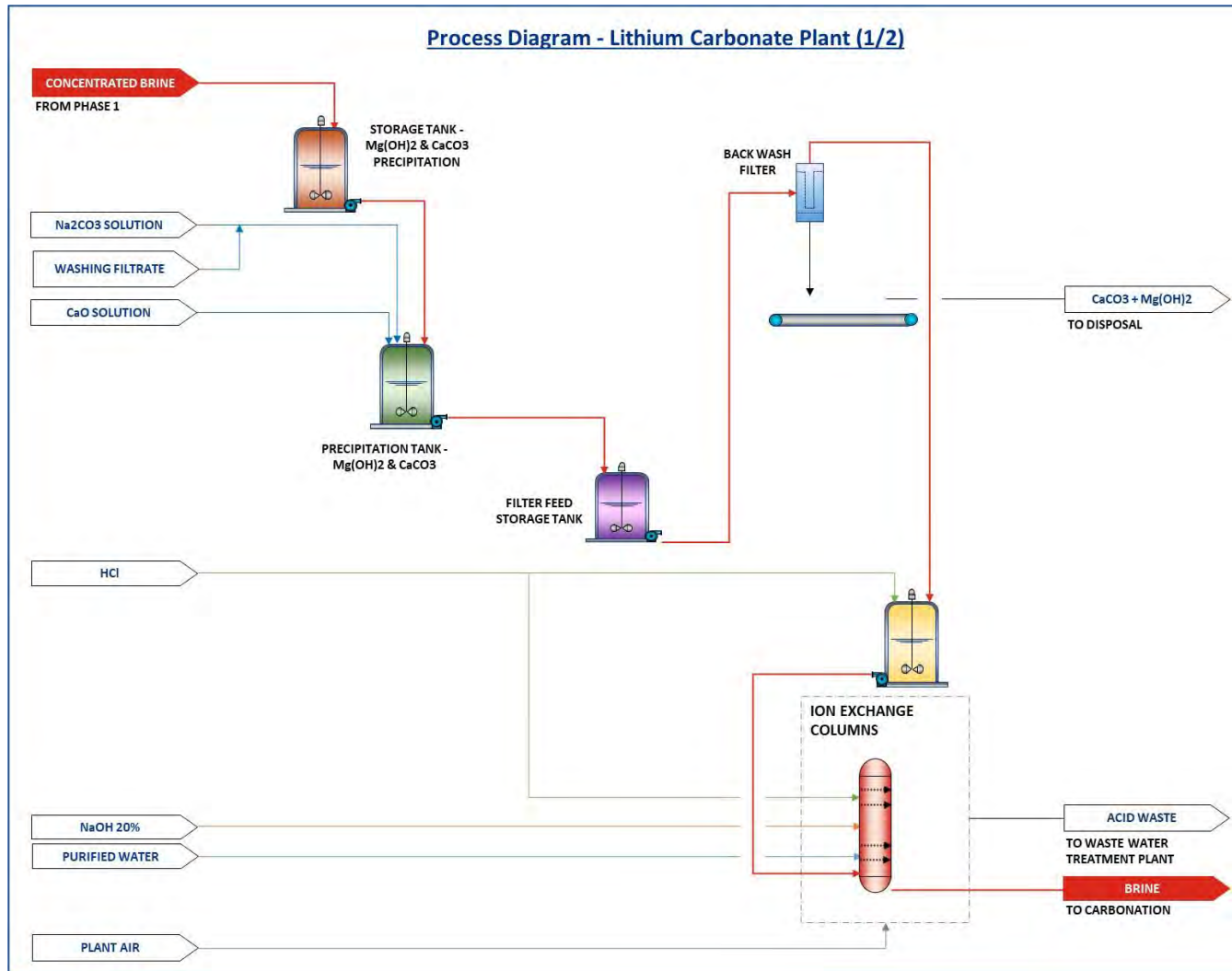
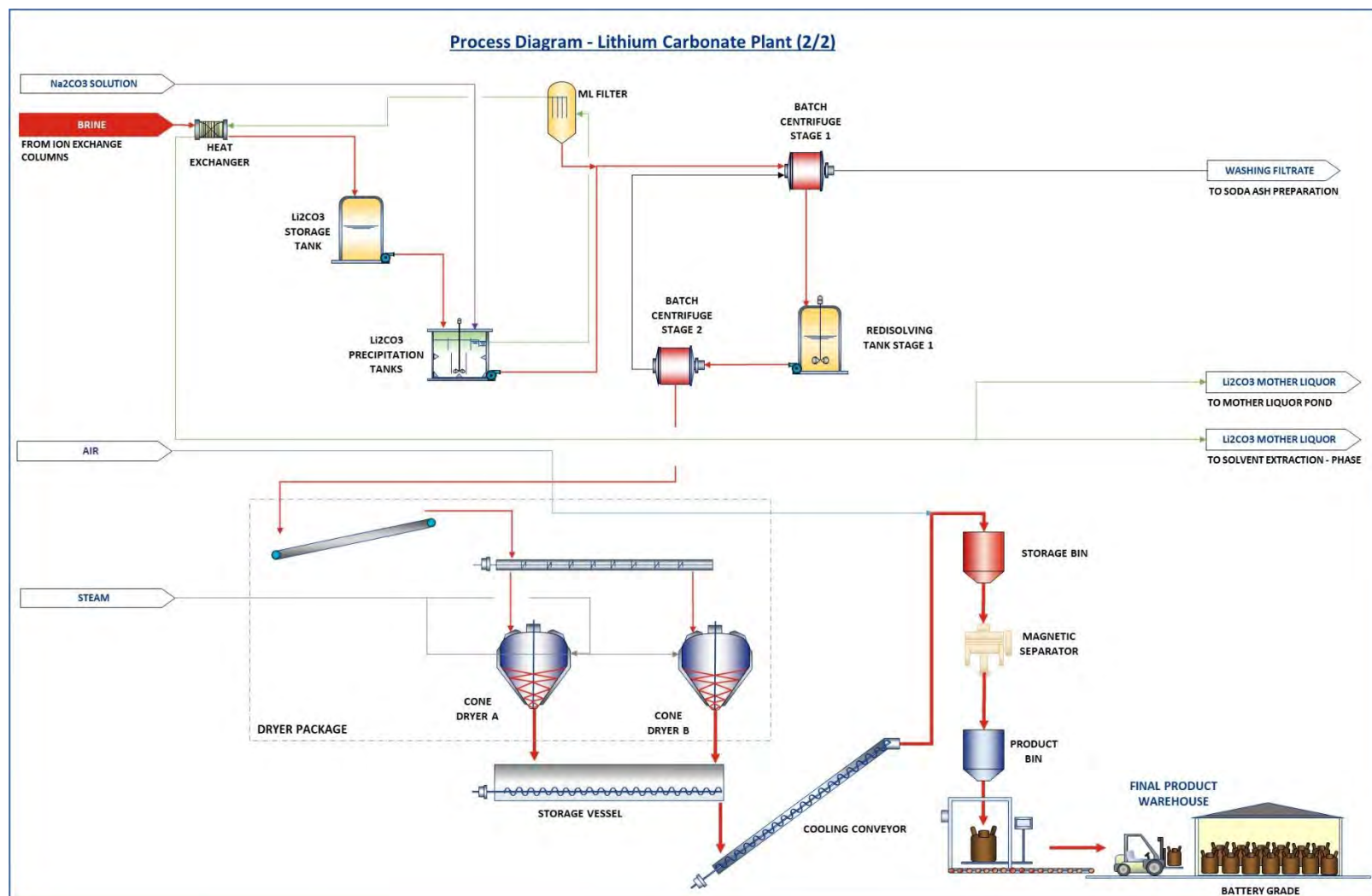


Figure 17-8 Simplified Lithium Carbonate Plant Process Diagram (2/2)



17.5 REAGENTS FOR THE PROCESS

To achieve the required lithium carbonate quality, specific reagents must be used in the process. Table 17-4 presents the annual consumption of each reagent, as well as the concentration in which reagent will be required in the process.

Table 17-4 Reagents used in the process

Reagent	Chemical formula	Annual consumption (TPY)
Lime	CaO (solid)	1,411
Soda Ash	Na ₂ CO ₃ (solid)	35,320
Caustic Soda	NaOH (20%)	2,826
Hydrochloric Acid	HCl (32%)	14,342
Sodium sulphite	Na ₂ SO ₃ (solid)	137
Flocculant	N/A	18
Solvent extraction diluent	N/A	50
Solvent extraction extractant	N/A	22.5

It is to note that Table 17-4 includes all reactants used regularly in the process, as well as other reactants that are required occasionally for equipment cleaning purposes, or for process control. The main reagents to be used are detailed in the following sections.

17.5.1 PREPARATION OF SODA ASH SOLUTION

Soda ash is one of the main reagents used in the Lithium Carbonate Plant. A consumption of 35,320 TPY of this product is expected. This reagent is prepared in a plant specifically designed for this purpose, transforming it from the solid state in which it is purchased to a 28% concentrated solution, the concentration at which it is added to the process. For its preparation, recycled water from the process is mixed in a tank with soda ash solids. This tank contains an excess amount of soda ash, assuring a saturated solution. The temperature of the system is controlled by heating the recycled water. The solution is later transported to the soda ash storage tanks and is ready for use in the process.

17.5.2 PREPARATION OF CALCIUM HYDROXIDE

Lime, which is slaked with water to generate calcium hydroxide, is the reagent that is used in the lithium carbonate plant for magnesium hydroxide precipitation. The process considers a total lime consumption of 1,411 TPY in the lithium carbonate plant. The milk of lime system will be installed near the stage where it is applied.

17.6 WATER PURIFICATION

This process includes the re-utilization of process water at various points, but the injection of fresh water (or industrial water) is still necessary in certain stages of the process. Process water is treated in a treatment plant which uses mainly a reverse osmosis operation, which will generate the required water quality for the process. The treatment of the industrial water is meant to avoid the entry of contaminants to the process.

17.7 LITHIUM CARBONATE PLANT SOLID WASTE MANAGEMENT

As previously described, the solid discards generated from the process are mainly solid salts harvested from the evaporation ponds, as well as solid discards generated from the Salt Removal Plant (Phase 1) and Lithium Carbonate Plant (Phase 2). The main discards generated in the Salt Removal Plant are tachyhydrite and calcium chloride salts, while the main discards generated in the Lithium Carbonate Plant are calcium carbonate (CaCO_3) and magnesium hydroxide (Mg(OH)_2). All discards generated from Phase 1 and 2 are sent, using trucks, to separate discard piles. The total amount of solids generated from both plants are stated in previous sections of this chapter.

18. PROJECT INFRASTRUCTURE

18.1 OBJECTIVE

This section describes the infrastructure required for Stage One Project.

The project includes the following physical areas:

- Brine production wellfield in the Salar.
- Evaporation ponds.
- Plant Facilities
- Utilities.

The brine production wells area will be located in the Salar de Maricunga, at 3,760 masl.

Figure 18-1 Location of Salar de Maricunga



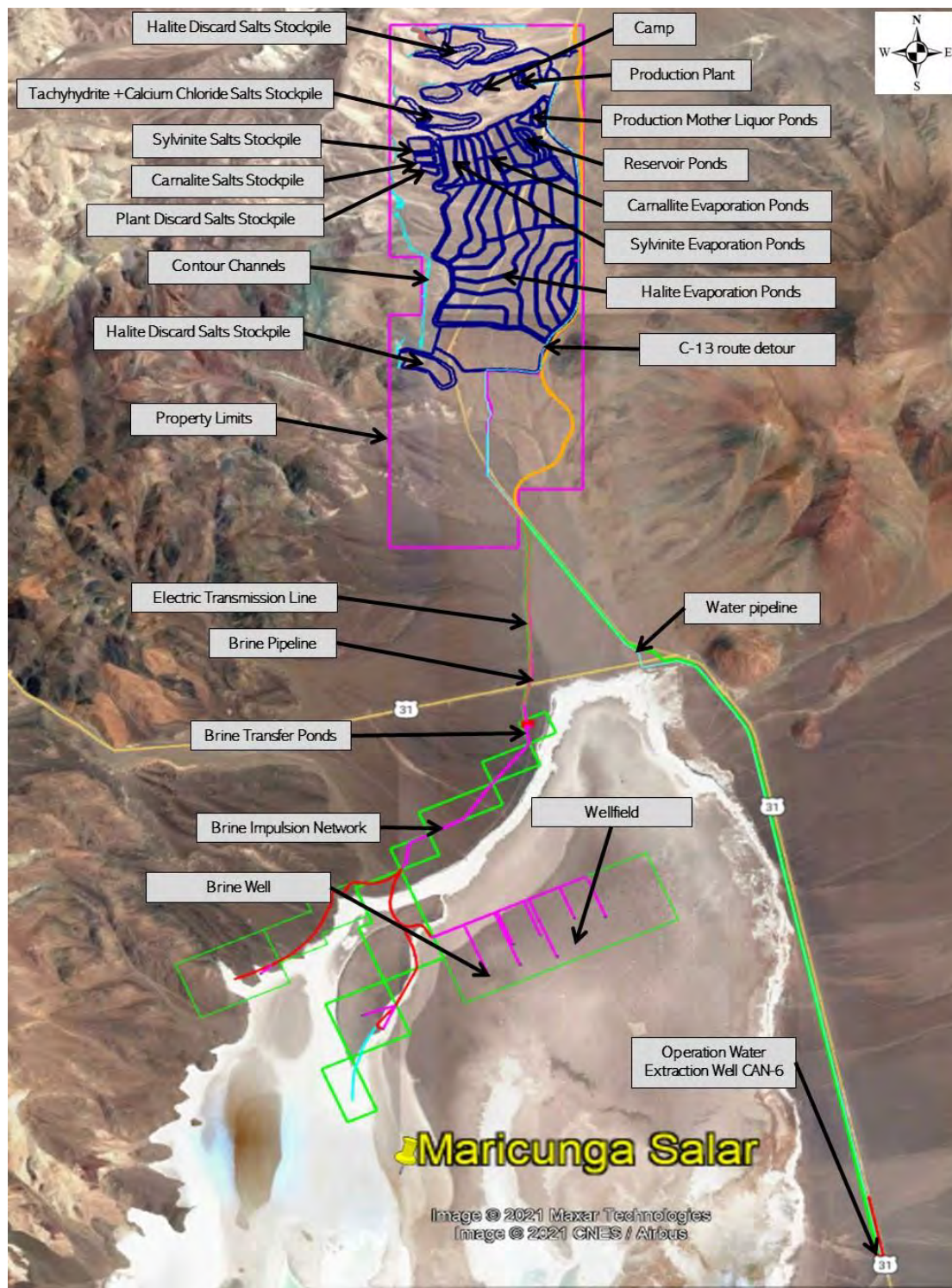
The facilities that are considered for the project include mainly the following areas:

- Solar evaporation pond installations (transfer pumps, dilution water tanks, among others)
- Salt Removal Plant – (named also Phase 1)
- Lithium Carbonate Plant – (named also Phase 2)
- Utilities for process ancillary services (reagents, water, compressed air, steam boilers, among others)
- Installations for plant ancillary services (administration offices, laboratory, among others)
- Workers' camp
- Temporary contractors' installations

All main installations are presented in Figure 18-2.

The solar evaporation ponds area that MSB plans to build will be located north of the Maricunga Salar and will cover a total base area of 5.36 million m². These ponds will allow the brine to be concentrated in different steps. In addition, there will be approximately 1.6 million tonnes of discards salt that will be stockpiled at site, salts obtained from both the evaporation ponds and from the production plant.

Figure 18-2 Project location presenting all main installations



Source: Worley – Google Earth

18.2 PROJECT ACCESS

The main road access to the Project corresponds to existing route C-173, which is well maintained and a mining road for the area. The Project includes a modification of this route, being an extension of approximately 8 km until reaching the Project.

As presented in Figure 18-3, Route C-173 can be accessed from Route 5, which is a Chilean main highway that runs from north to the south of the country, taking route C-13 east until reaching Diego de Almagro, and then continuing east on route C-13, then following Route C-163 and route C-177, until reaching Route C- 173 and heading south until reaching the Project location, which is around 220 km along this complete route.

Figure 18-3 Project Access from Route 5



Source: Worley – Google Earth

Figure 18-4 presents access to the Project from Paipote and Copiapó, located south of Diego de Almagro. Copiapó has the facility of reaching Route 5 directly as well as having a national airport. From Copiapó and Paipote, route C-17 must be taken in a north direction, for around 150 km, until reaching Diego de Almagro. To reach the Project from Diego de Almagro, the same route must be taken as described in Figure 18-3.

Figure 18-4 Project Access from Copiapó-Paipote



Source: Worley – Google Earth

Figure 18-5 presents access from Antofagasta, a city located in the second (II) region of Chile, which is located north of Diego de Almagro. Antofagasta also has an international airport as well as being one of the main ports of Chile. To reach the Project from Antofagasta, route 5 must be taken south for around 400 km, until reaching route C-13 and driving east for 50 km until reaching Diego de Almagro. To reach the Project from Diego de Almagro, the same route must be taken as described in Figure 18-3.

Figure 18-5 Project Access from Antofagasta



Source: Worley – Google Earth

18.3 TEMPORARY INSTALLATIONS

The project contemplates the requirement of temporary and permanent facilities. In particular, the mining camp consists of temporary and permanent elements, according to the stage of the project's life cycle. Temporary facilities will be mainly used during the construction of the Project, while permanent facilities will be used throughout the complete life of the Project.

18.3.1 CONTRACTORS INSTALLATIONS

Temporary contractors' installations will be placed in different areas near working fronts for the main contractors, all focused mainly on the construction of the Project. The temporary installations include areas such as:

- Offices
- Warehouses
- Workshops
- Storerooms
- Dining rooms
- Dressing rooms
- Sanitary facilities
- Concrete plant
- Aggregate plant
- Non-hazardous and domestic industrial waste management areas
- Hazardous waste area
- Other facilities

18.4 PERMANENT INSTALLATIONS

18.4.1 BRINE PRODUCTION WELLFIELD

The brine production wellfield considers eleven (11) production wells that will be drilled in the Salar. The required average annual brine feed rate from the wellfield to the evaporation ponds is around 13,000 m³/d to support an average annual lithium carbonate production of 15,200 t. This feed will vary during the seasonal changes, increasing in the summer period due to a higher evaporation rate and decreasing in winter since evaporation will be lower.

The extraction wells will be electrically fed with channelling at ground level, using isolated cable ducted in galvanized steel conduit.

18.4.2 TRANSFER PONDS AND PUMPING STATION.

As presented in Figure 18-2, two (2) transfer ponds will be located northwest of the Maricunga Salar, which will include a pumping station. The objective of these ponds is receiving brine from all production wells, homogenizing the brine and pumping it through a pipeline of around 10 km to the auxiliary pond located at the evaporation ponds area.

18.4.3 AUXILIARY POND

This pond is located next to the first Halite Pond (H-15) and its objective is to receive and store brine before pumping it as cooling brine to the process plant (Phase 1). This pond will be covered with a plastic liner, to avoid evaporation of water from the brine, as well as reducing the temperature increase in the brine. This pond will be lined at its base with an HDPE liner, to avoid leakages.

18.4.4 EVAPORATION PONDS

The function of the evaporation pond is concentrating the lithium contained in the brine extracted from the salar. This happens through evaporating the water from the brine with solar radiation and promoting the precipitation of different elements within the brine as salts (halite, sylvinite and carnallite). The construction of the ponds will be done by cut and fill so as to level the ground and build the pond walls. The ponds will be lined at their base with an HDPE liner or similar membrane for waterproofing.

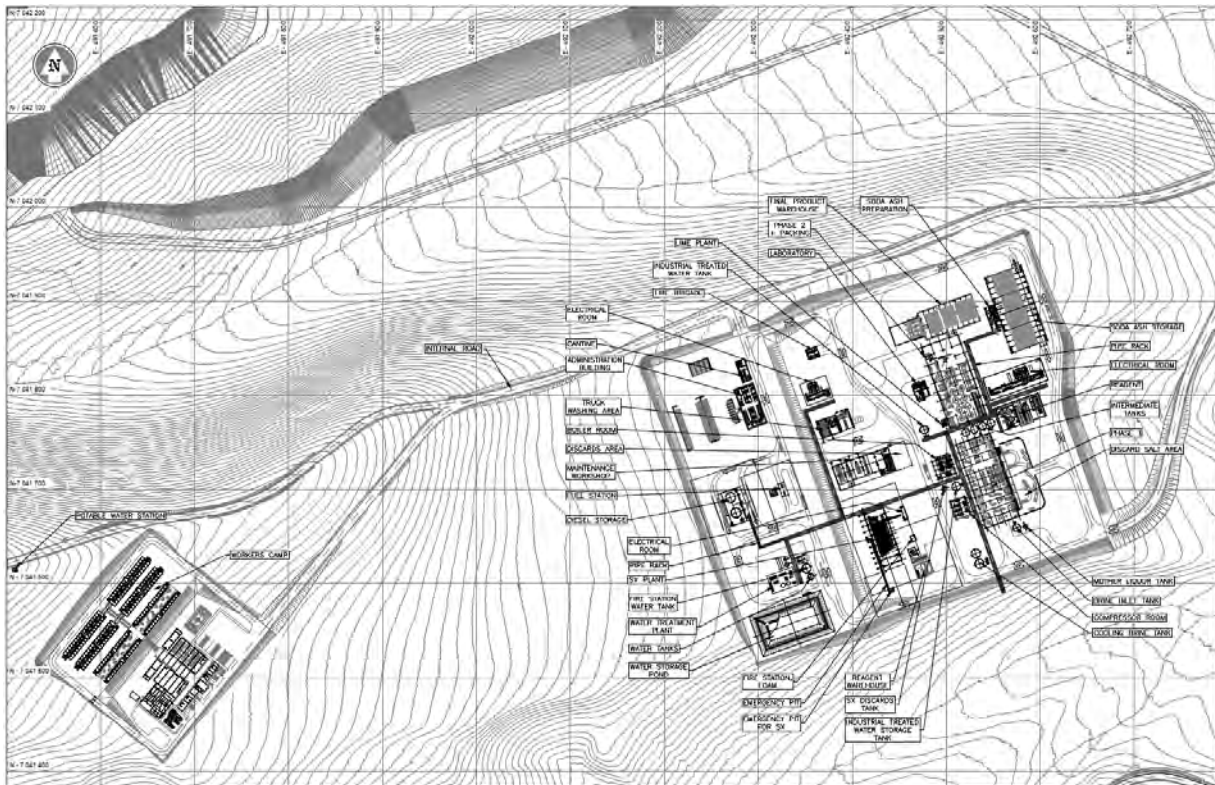
Due to the topography of the area where the evaporation ponds will be located, brine transfer from one pond to the next is mainly done by gravity. However, when this is not possible, a pumping station will be installed. All pumping stations will have power supply through an aerial network.

All ponds will have access roads for monitoring and maintenance activities. In addition, contour channels will be constructed where required in order to divert the rain waters of the zone.

18.4.5 PROCESS PLANTS

All the installations and facilities considered for the Project are presented in Figure 18-6 and described below:

Figure 18-6 Project Plants Installations



Source: Worley

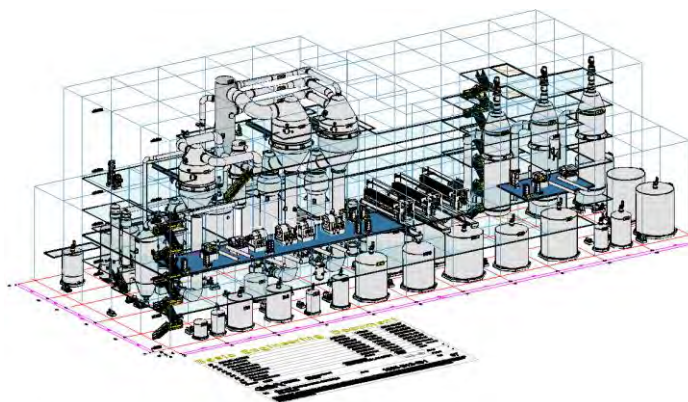
18.4.5.1 INDUSTRIAL BUILDINGS

The buildings of the plant area are designed according to the weather conditions of the site. These buildings are classified as follows:

Salt Removal Plant – Phase 1

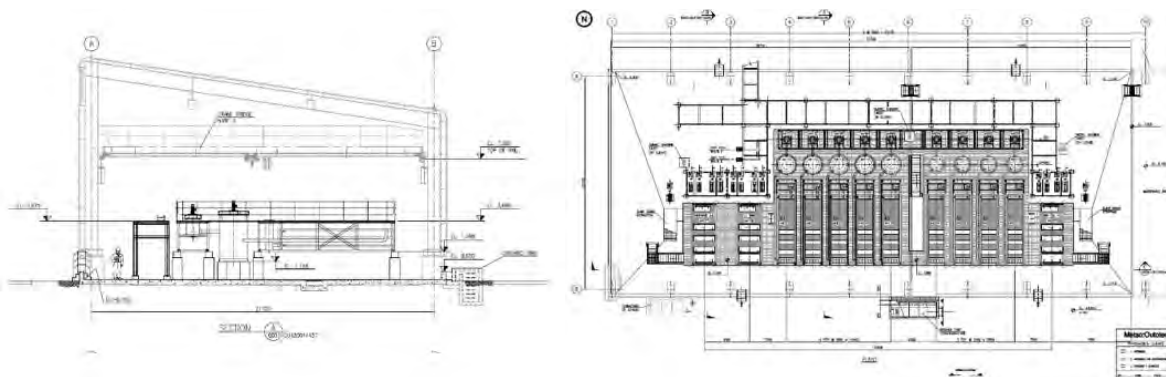
- Building for evaporation and crystallization equipment
- Solvent extraction (SX) plant building

Figure 18-7 Basic Engineering 3D Salt Removal Plant



Source: GEA Messo

Figure 18-8 Metso Outotec Solvent Extraction

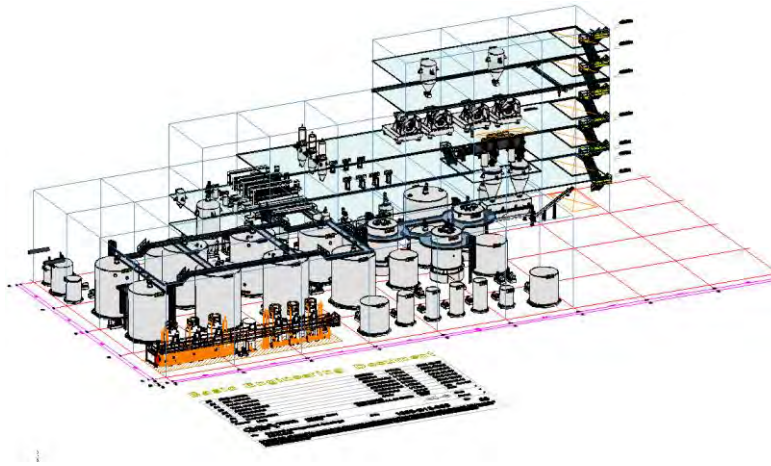


Source: Metso Outotec

Lithium Carbonate Plant – Phase 2

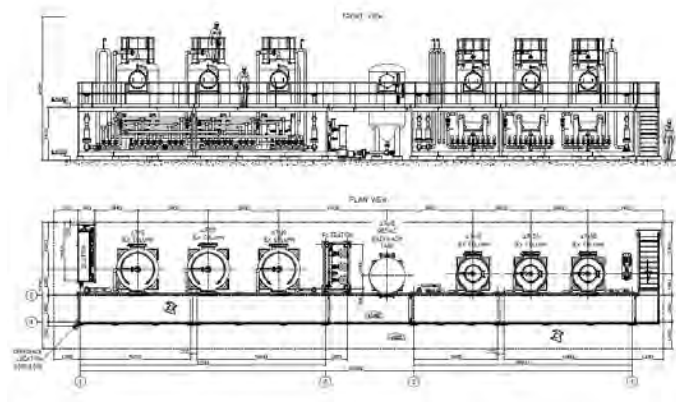
- Building includes ion exchange, magnesium and calcium removal, solid / liquid separation, drying, packing and product storage.

Figure 18-9 Basic Engineering 3D Lithium Carbonate Plant



Source: GEA Messo

Figure 18-10 Eurodia Ionic Exchange

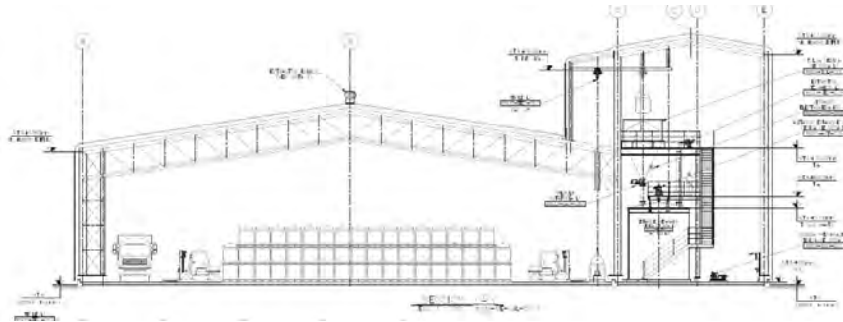


Source: Eurodia

Plant Services

- Reagent storage and/or preparation building, which includes the following building areas:
 - SX reagents storage and distribution
 - Hydrochloric acid storage and distribution
 - Caustic soda dilution, storage and distribution
 - Soda Ash storage (solid and liquid), preparation and distribution
 - Lime storage, preparation and distribution
 - Other minor reagents
- Fuel station.
- Air compressors room.
- Boilers room.
- Water Treatment Plant (to generate soft water).

Figure 18-11 Soda Ash storage (solid and liquid), preparation and distribution



Source: Worley

18.4.5.2 ELECTRICAL ROOMS

Three electrical rooms are considered for the Phase 1 and 2 plants and one for the camp. In addition, backup generators will be available for both the critical equipment in the plants as well as for the camp.

18.4.5.3 CONTROL ROOMS

One control room is considered and will be located in the interior of the industrial buildings.

18.4.6 AUXILIARY INSTALLATIONS

18.4.6.1 ACCESS CONTROL CHECKPOINT

The control checkpoint at the main entrance will include the following facilities: admission control office, luggage control room, induction room, vehicles parking and toilets for visitors and internal plant staff.

18.4.6.2 ADMINISTRATION BUILDING

The administration building includes the company's administrative offices, meeting rooms and a server room. This building will be located in the plant area and the construction will be in accordance with the rest of the buildings in the plant. Cafeteria and dining room areas will be considered inside the administration building, for the use of all personnel.

18.4.6.3 LABORATORY

Within the plant there will be a Process Quality Control Laboratory, which will allow chemical analysis, grain-size analysis and moisture analysis in order to ensure the correct operation of the process and product quality control.

18.4.6.4 PARKING AREAS

Two parking zones for buses, vans and pick-up trucks are considered, one of them prior to the access control, of approximately 2,200 m², and another by the administrative building, of approximately 1,643 m².

18.4.6.5 WEIGHING STATION

The project includes a weighing station for trucks, of approximately 420 m².

18.4.6.6 TRUCK WORKSHOP

The truck workshop includes the following facilities:

- Lubricants storage area
- Office area
- Truck washing area and water tank
- Electrical workshop
- Mechanical workshop
- Minor and major equipment workshop
- Sludge degreasing treatment plant

- Parking garage
- Waste yard

18.4.6.7 WASTE WATER TREATMENT PLANT (WWTP)

A WWTP is considered for the project to treat all water generated from both the plants and the camp. For the construction phase, it will be able to service up to 1,200 persons and in the operation phase it will reduce to 400 persons.

18.4.6.8 INDUSTRIAL WASTE YARDS AND ROOMS

The project includes a temporary yard for non-hazardous waste and a closed area for the hazardous waste. Each type of waste will be transported to an authorized landfill site.

18.4.6.9 FIRE PROTECTION SYSTEM

The fire system will consider a large water storage tank that feeds the fire protection wet network. It also includes a pumping system (electric and diesel) to maintain a constant pressure in the fire water network and guarantees the water supply, according to the National Fire Protection Association (NFPA).

A separate and special foam fire protection system will be installed in the solvent extraction plant and will also be constructed and maintained according to the National Fire Protection Association (NFPA).

18.5 MINING CAMP

The mining camp will have 2 platforms with a total area of 28,590 m². The facilities of the camp will be modular and will be connected by pedestrian and vehicular access.

18.5.1 DORMS

During the construction phase there will be 8 dorm buildings with a capacity for 1,200 people. This will reduce to 232 people during the operation phase that work on-site. All buildings will have a heating system, ventilation, power supply, networks, sanitary installations, fire detection and extinguishers according to DS594.

The dorms will have 3 types of bedrooms, one bedroom with an individual bathroom, double bedrooms with a shared bathroom and triple bedrooms with a shared bathroom.

18.5.2 DINING ROOM

It includes all the facilities for 400 people seated. It will have a heating system, ventilation, sanitary installations, fire detection and extinguishers according to DS594.

18.5.3 RECREATION AREAS

The camp includes recreation rooms equipped with TV, pool table and lounge area; a multisport court (baby soccer, basketball and volleyball) and a fitness centre.

18.5.4 POLYCLINIC

The polyclinic is equipped with a reception room for first aid, beds, resuscitation equipment (defibrillation), utensils and medicines, bathrooms for patients and another for medical personnel, nursing office, dormitory for paramedics, and storage for cleaning supplies. It also includes an exclusive parking area for the ambulance.

18.6 SERVICES

18.6.1 ELECTRICAL ENERGY

The Project has an average connected load of 13.7 MW of electrical power. The Electric Coordinator already gave MSB the authorization to connect to an existing 23 kV transmission line. MSB strategy is to build a new substation and reinforced the line. Below, Figure 18-12, shows the existing line's route and the proposed location for MSB's connection to the line.

Figure 18-12 Transmission Line Route



18.6.2 WATER

MSB has secured the water supply during the construction and operation of the project through a long-term lease agreement for the use of Can-6 water well. Also, that the use of this water well has been environmentally approved in the EIA.

18.6.2.1 POTABLE WATER

The supply of potable water for the construction phase will be carried out by tank trucks of 30 m³ capacity and distributed into storage tanks in the camp and in the industrial and administrative buildings.

During the operation phase the water of well CAN- 6 will be purified and will supply the water for the camp and the plants that can be used for showers and restroom facilities. All potable water will be available using bottles of water located in different areas of the plants.

18.6.2.2 INDUSTRIAL WATER

The project will require industrial water for the following purposes:

- Plant process
- Moistening the earthwork material
- Dust control in work fronts

The water will be pumped from the well CAN-6, which is located south of the salar, to an industrial water transfer tank that is installed near the well. From there the water will be pumped to a water pond located nearby the production plants, from where a Water Treatment Plant (WTP) will be fed. A reverse osmosis plant will be used for the WTP. This plant will feed tanks that will supply water to the process and purify the water for the restrooms of the plants and camp. The waste stream from the reverse osmosis plant will be used as dilution water for the transfer pumps in the evaporation ponds (to reduce salt scaling within the pumps).

18.6.2.3 DIESEL FUEL

The project includes diesel fuel storage and a loading facility. The fuel used by light vehicles, trucks, machinery and heavy equipment is estimated at approximately 90 m³/month during operations. The machinery includes salt harvest transport trucks, harvested salts handling trucks, soda ash transport trucks, among others.

In the production plant, diesel will be used mainly for steam boilers. This consumption is estimated at approximately 1,500 m³/month. The diesel supply will be provided through tanker trucks that will feed two storage tanks, each with a 700 m³ capacity.

18.7 ENGINEERING DELIVERABLES

In order to develop CAPEX and OPEX values, procurement quoted main equipment, supplies, materials, freight costs, and construction contracts. For this purpose, quotations for each unit to be quoted were requested to three suppliers. Procurement also carried out a study of the conditions for imports of supplies and services to facilitate the purchases. Technical and commercial evaluations were made for all quotations received.

Critical equipment was defined, being those which have long delivery times and those that are required to begin construction.

The following table summarizes the work carried out by the engineering team of WP and GEA:

Table 18-1 Worley Engineering Deliverables

Area	Li ₂ CO ₃ Drawings	Li ₂ CO ₃ Documents	TOTAL
General	0	8	8
Process	14	6	20
Mechanical	24	2	26
Civil	32	5	37
Structural	51	8	59
Piping	46	9	55
Electrical	15	7	22
Instrumentation	6	7	13
Ac of supply and/or Equip. Quotes	0	50 (Note 1)	50
Total	188	102	290

Note 1: Equipment quotes include all packages defined for this stage.

Table 18-2 GEA Engineering Deliverables

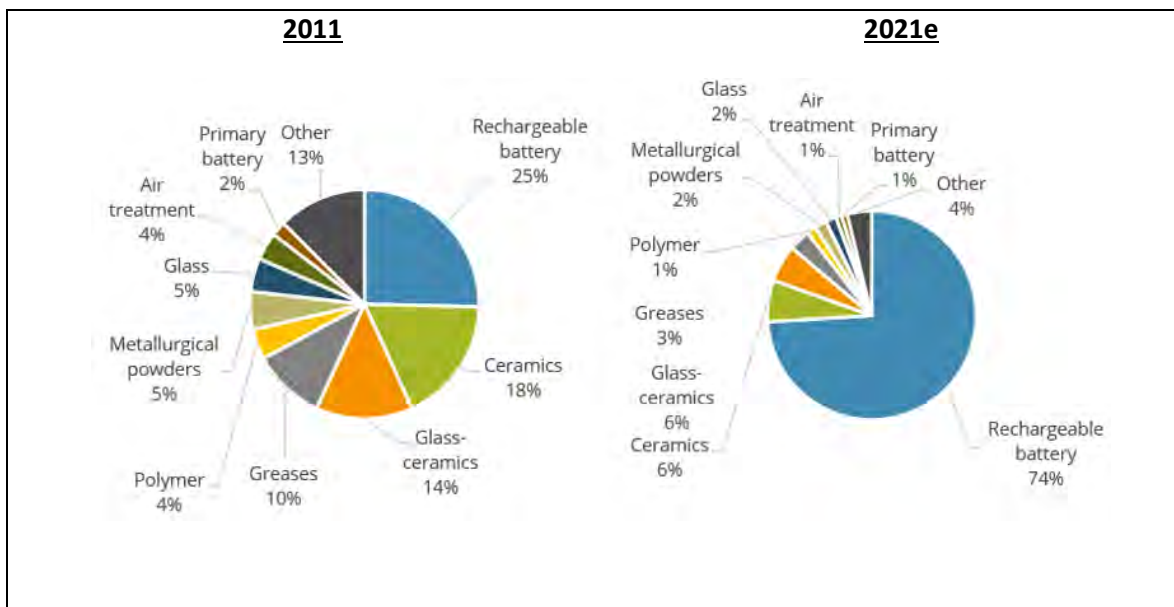
Area	Drawings	Documents	TOTAL
General description		1	1
Process description		2	2
Operating conditions		1	1
Description of the function of the plant		2	2
Instrumentation		8	8
Interlockings		2	2
Automatics		3	3
Safety installations		3	3
Block flow diagram phase	2		2
PFD	2		2
PID	2		2
Layout	8	2	10
Equipment Specifications		243	243
Piping		3	3
Valves		1	1
Insulation		1	1
Electrical consumers		2	2
Total	14	274	288

19. MARKET STUDIES AND CONTRACTS

19.1 CONSUMPTION

Demand growth for lithium since 2009 has been led by the rapidly increasing use of lithium in rechargeable battery applications in the form of lithium carbonate and more recently lithium hydroxide. From the rechargeable battery sector alone, growth has averaged 23.5%py between 2011 and 2021e, forming over 50% of lithium demand since 2017. Unlike most other major end-use applications, demand from rechargeable batteries continued to increase in 2020, despite disruption caused by the Covid-19 pandemic and related lockdowns.

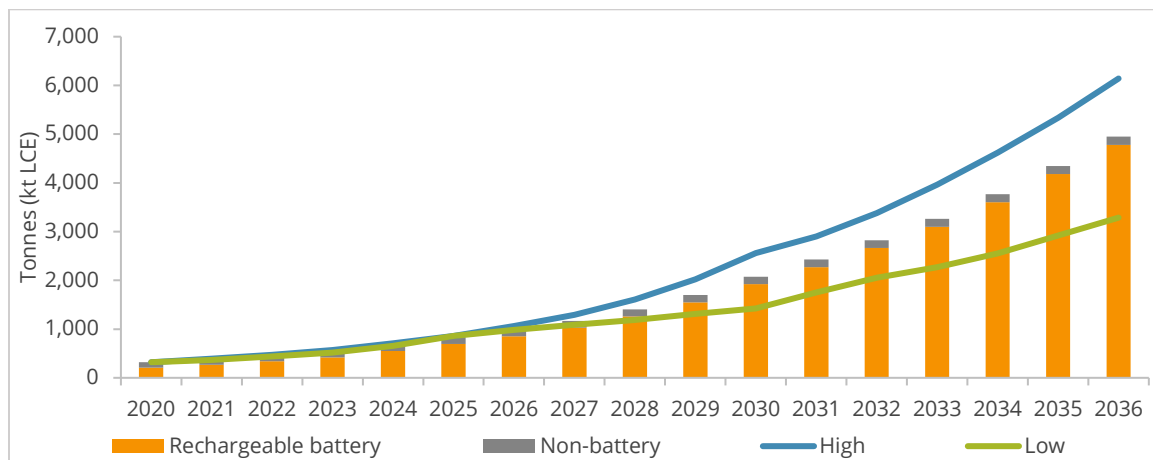
Figure 19-1 World: Consumption of lithium by first use, 2011 and 2021e (t LCE)



Source: Roskill

The rechargeable battery sector accounted for 71% of lithium consumption in 2020, which is expected to increase to 74% in 2021. The rechargeable battery sector became the largest lithium consumer in 2008, and in 2015 accounted for over three times the volume consumed by the next largest sector, ceramics. The ceramics, glass-ceramics and glass industries formed the next largest end-use markets in 2021e, forming 6.4%, 5.7% and 1.6% of total demand respectively, with lithium greases forming 3.1% of total demand.

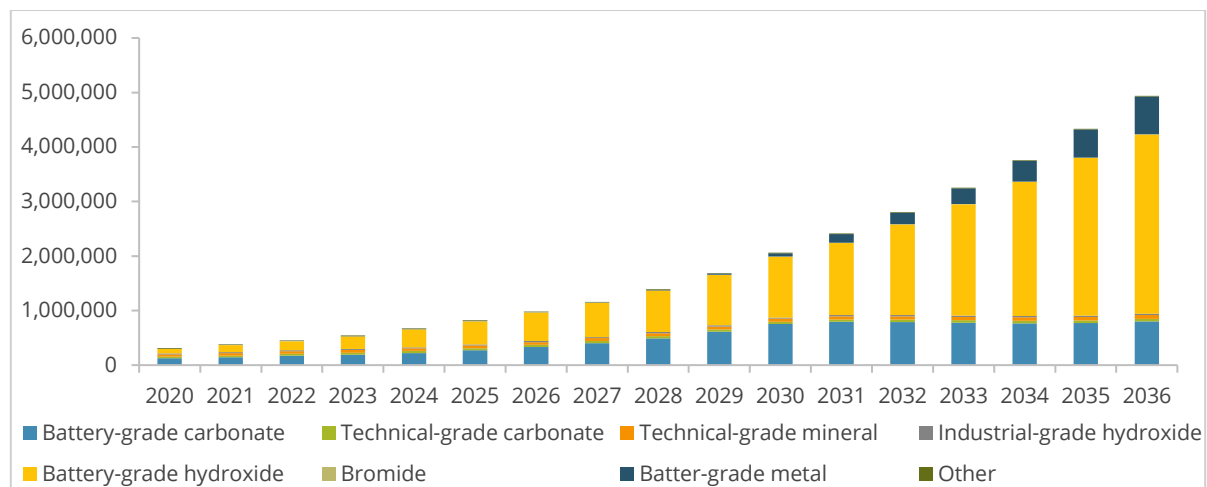
Figure 19-2 World: Forecast consumption of lithium by first use, 2020-2036 (000t LCE)



Source: Roskill

Under Roskill's base-case scenario, lithium demand is forecast to increase by 12.6%py in the period to 2036, reaching a total of 4.95Mt in 2036. In the 'High-case', forecast lithium demand is expected to increase by 20.1% CAGR in the period from 2021 to 2036, reaching a total of 6.14Mt LCE. Demand from non-battery applications is expected to form a diminishing proportion of lithium demand, with demand from such sectors decreasing from 31% in 2021 to 4% in 2036. Non-battery applications are expected to show continued demand growth of between 1-4%py over the period to 2036, aligned to growth in global and regional GDP and industrial production.

Figure 19-3 World: Forecast consumption of lithium by product, 2020-2036 (kt LCE)



Source: Roskill

As a result of the strong growth in demand from rechargeable battery applications, demand for battery grade products is forecast to accelerate over the outlook horizon. Battery-grade lithium

carbonate and hydroxide demand is forecast to increase by 18.8%py and 26.2%py respectively in the period from 2021 to 2031, with a further 0.2%py and 19.9%py increase respectively from 2031 to 2036. In 2036, battery-grade lithium carbonate and hydroxide demand are forecast at 802.3kt LCE and 3,288.1kt LCE respectively. Battery-grade metal will also grow above the industry average, as more is used in advanced lithium rechargeable batteries and primary batteries.

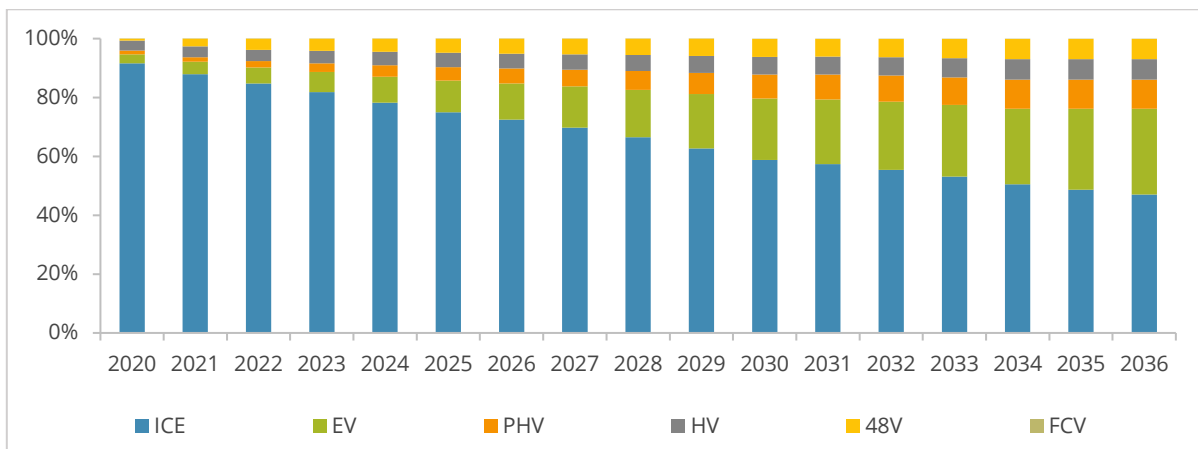
The preference in the automotive sector to increase vehicle range will inevitably shift battery production toward nickel-rich chemistries, which in turn will see demand for lithium hydroxide increase faster than demand for lithium carbonate. This responds to problems arising from gassing and moisture increase in the cathode powder when using lithium carbonate. While lithium hydroxide also has drawbacks as it increases the pH value of powders, it is more advantageous in cathode chemistries with nickel content over 60-80% of the cathode weight. Overall, the division of demand between battery-grade lithium carbonate and hydroxide going forward depends on a number of factors, including:

- Cathode material type produced/consumed
- Cathode manufacturer/process
- Cost and availability

19.1.1 LITHIUM-ION BATTERY MARKET

The lithium-ion battery cell market was estimated to be worth over US\$26Bn in 2020, with consumption totalling 231GWh, representing a 25% year-on-year increase over 2019. The Li-ion batteries market is expected to grow faster than any other rechargeable battery technology reaching a total demand of 5.7TWh by 2036 with a CAGR of 23%. Increasing demand for electrified vehicles is widely supported by government subsidies on one hand and plans of banning ICE vehicle sales on the other, that partially will come in power starting from middle of decade. Such policies are forecast to have a significant impact on EV penetration rates by the mid-2020s. Roskill forecast internal combustion engine (ICE) market share of global passenger vehicle sales to decrease from around 90% in 2020 to 45% in 2036.

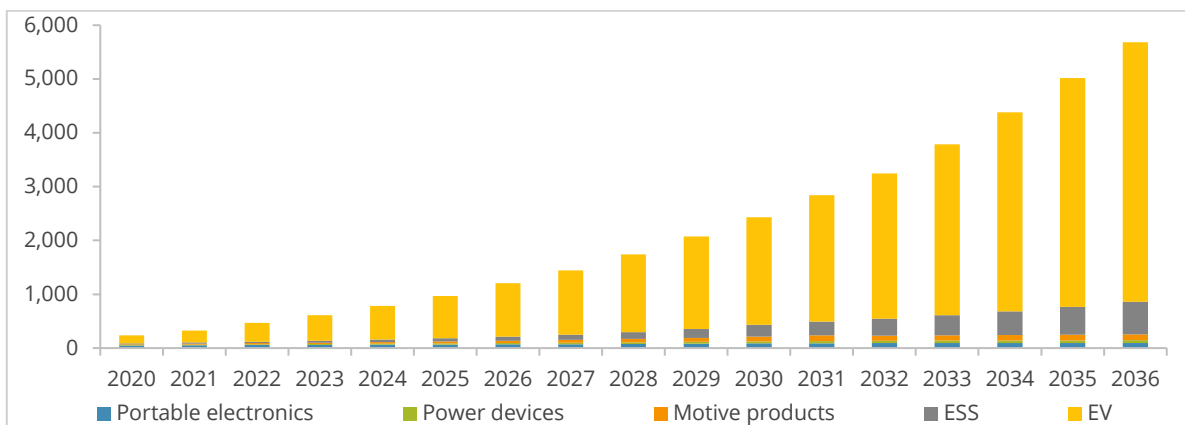
Figure 19-4: Global penetration rate of electric passenger vehicles, 2020-2036 (% of sales)



Source: Roskill

By 2036, Roskill forecast battery demand from automotive sector to reach 4.8TWh. The key reason behind the transition towards battery-powered cars has been stringent regulation on transport emissions, which is expected to further constrain current transport air pollution limits. By 2021, all major automotive markets had pledged to move towards de-carbonized economies, implying further tightening of ecological regulation in the field of emissions.

Figure 19-5: World Li-ion battery use by market, 2020-2036 (GWh)



Source: Roskill

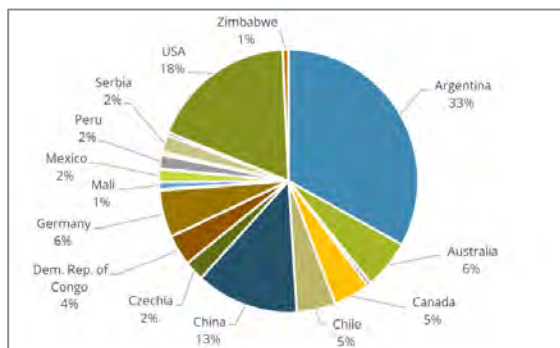
Some applications using Li-ion battery technology are not mature, such as in the motive and ESS categories, though Roskill expect strong growth in market penetration rates especially in the motive category (for example: forklifts, electric scooters, e-bikes, recreational and commercial drones), driven by the fall in Li-ion battery technology costs. ESS applications, especially in the grid segment, are expected to grow rapidly thanks to lower renewable energy costs, albeit from a low market size.

19.2 RESOURCES, PROCESSING AND PRODUCTION

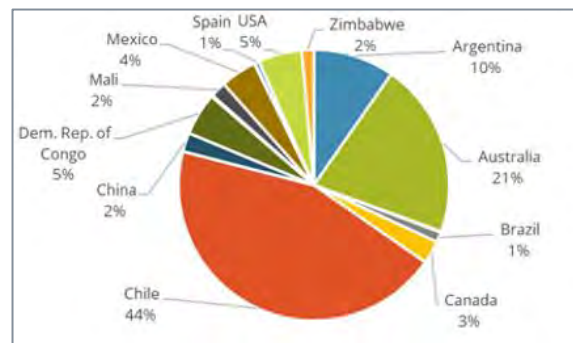
There are five naturally occurring sources of lithium, of which the most developed are lithium pegmatites and continental lithium brines. Other sources of lithium include oilfield brines, geothermal brines and clays. Roskill has catalogued mineral resources reported by lithium project developers (including projects on care and maintenance) and operators, and together these are estimated to contain 291.8Mt LCE, while reserves stand at 104.25Mt LCE.

Figure 19-6 Global lithium resources and reserves by country, 2021

Resources

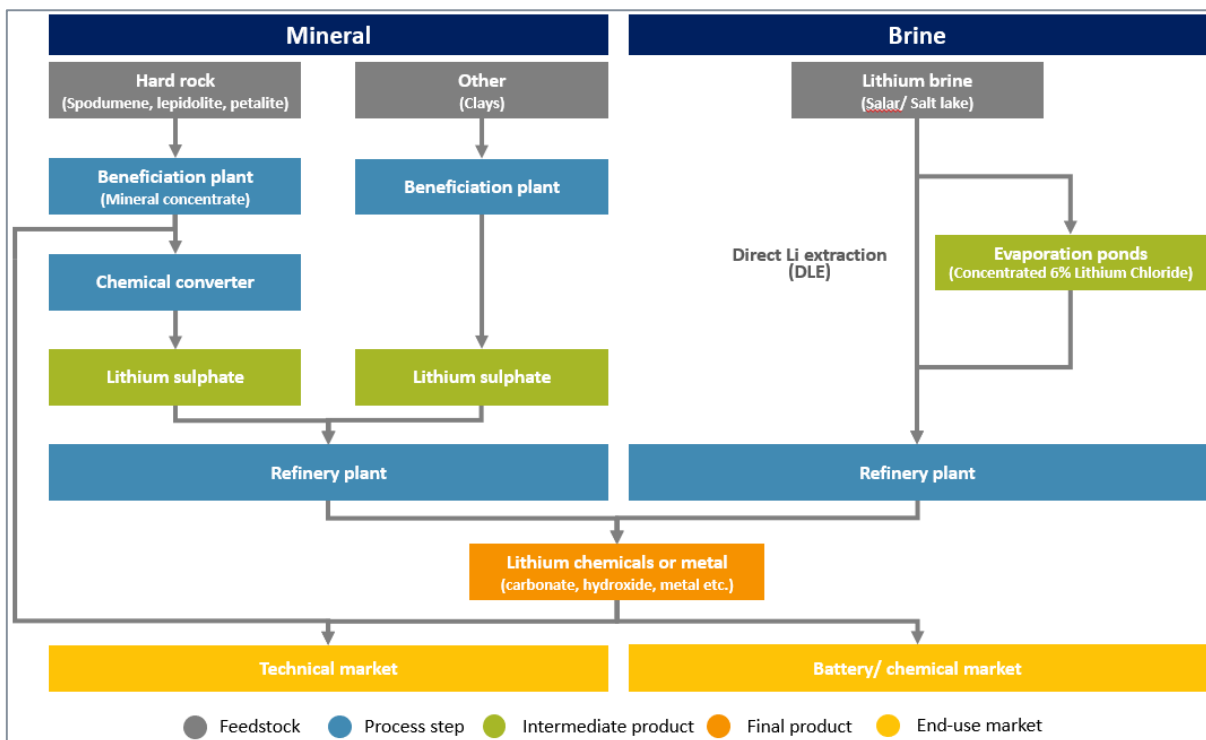


Reserves



Brine operations and projects are the largest contributors to project resources, with 169.8Mt LCE reported, accounting for 58.2% of the global total. Mineral projects formed 36.2% with clay projects forming 5.7%.

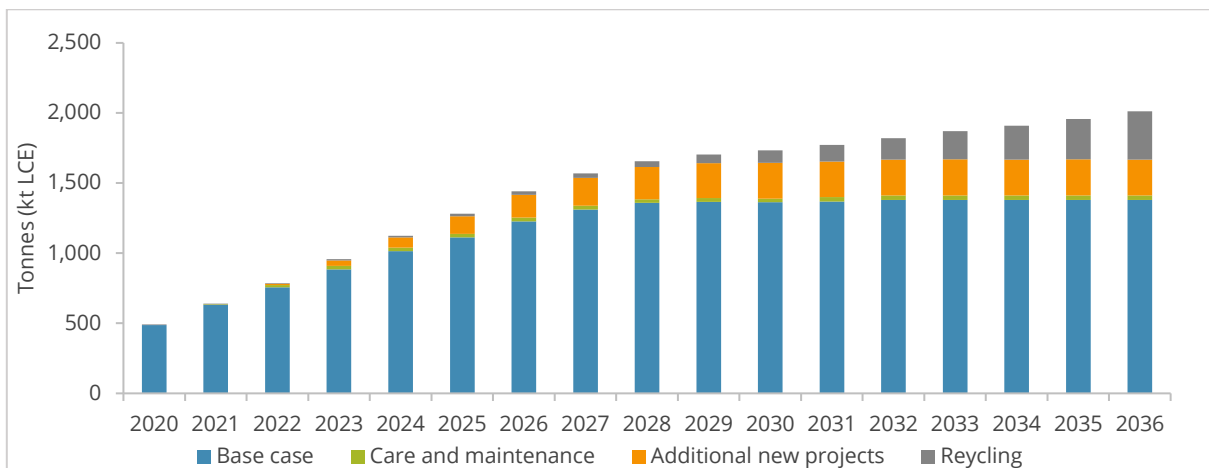
Figure 19-7: Simplified overview of mine-to-product flow



Source: Roskill

Lithium is extracted as either a mineral ore or brine, with concentration to a processible mineral feedstock through physical processing and a processible brine feedstock largely through evaporation, although other methods are also used. Mineral concentrates may be consumed directly by industry or used to produce downstream lithium compounds through chemical conversion. During the mineral conversion process, mineral feedstock is calcined and reacted with sulphuric acid, and the leachate processed into carbonate or hydroxide. As mineral feedstock can be converted directly into lithium hydroxide, but brine only to carbonate or chloride, the lithium industry is generally pursuing the mineral route for future hydroxide production and brine for carbonate production.

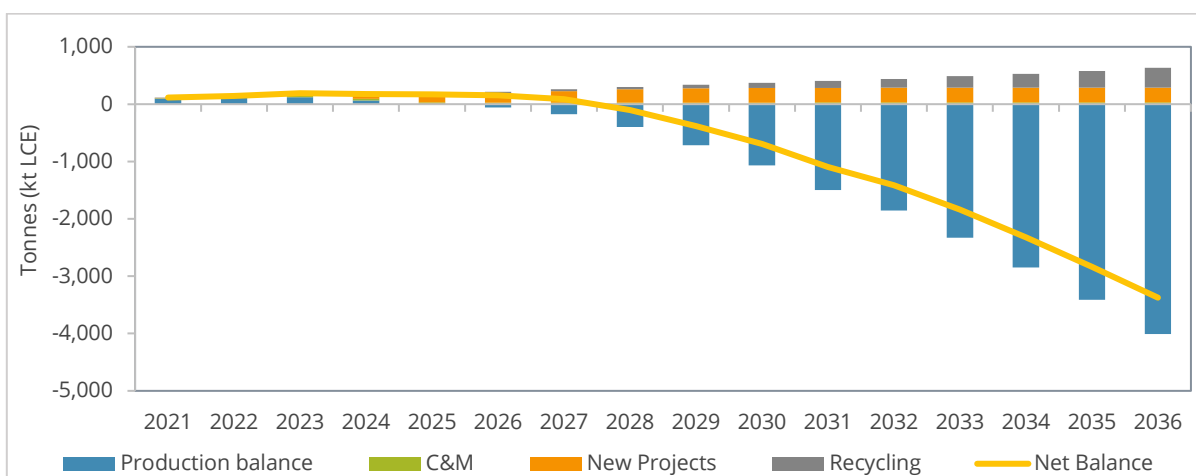
Figure 19-8 World: Forecast refined supply for lithium, 2020-2036 (kt LCE)



Source: Roskill

In 2021, global production of refined compounds is forecast to total 636.3kt LCE. Based on announced capacity expansions, refined production is forecast to increase at a CAGR of 7.9% to 2036. Under this scenario supply is forecast to surpass 1Mt LCE in 2024 before reaching 2Mt LCE by 2036. This represents more than a doubling of the expected output in 2021. Roskill forecast battery-grade production to increase by 6.2% CAGR to 2036 reaching 1,057.7kt LCE under the base-case scenario. As a result of demand significantly outpacing that of refined supply Roskill forecasts structural deficits to form in the market from the mid-2020s. The deficits are not definitive, however, and should be viewed as the “investment requirement” for additional supply.

Figure 19-9 Lithium chemical balance, 2021-2036 (kt LCE)



Source: Roskill

19.3 PRICES

The market saw growth in refined output outpace growth in demand in the 2018-2020 period with resultant stocks being built leading to lower prices. Roskill expects refined output and inventories to meet demand growth in 2021 with increasing pressure on the supply and demand balance for high quality battery-grade products.

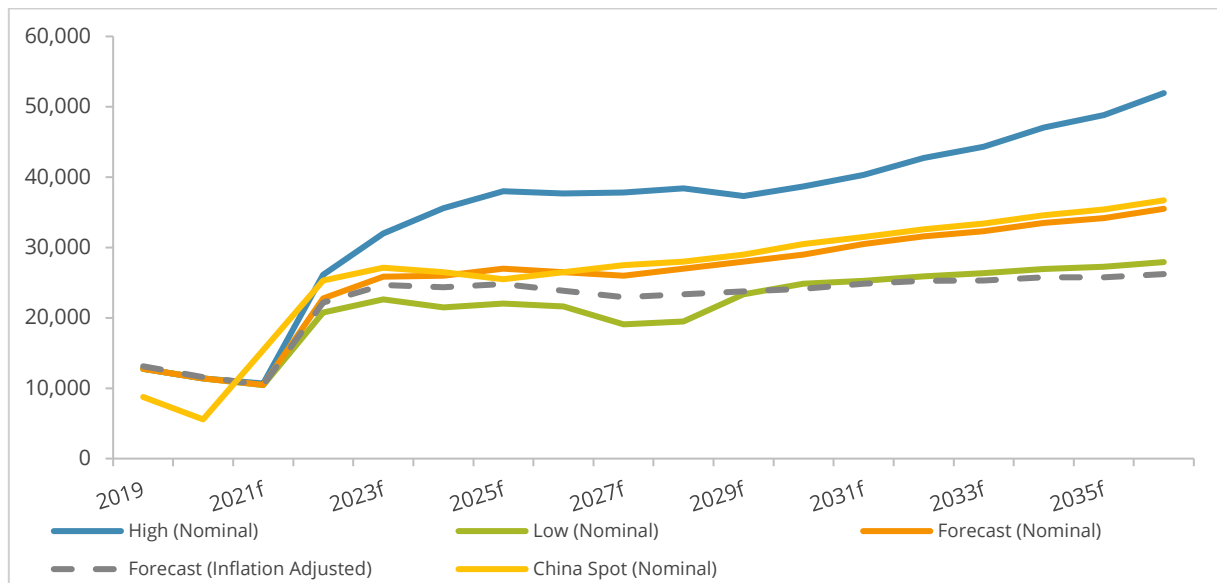
From 2021, Roskill expects demand growth to return to higher levels – perhaps turbo-charged by government initiated Covid-19 economic recovery programmes – and with some capacity (built or under construction) temporarily or permanently off-line, and some brownfield/greenfield project development suspended, demand will start to stretch supply into 2022. Sentiment may well improve ahead of fundamentals, further incentivising prices, as has been witnessed in the downstream battery/EV sector even during 2020 as a “green” recovery is increasingly seen following the Covid-19 impact.

Roskill’s price forecast methodology for lithium is based on three main factors:

- Production/margin cost curve
- Incentive pricing for expanded and new capacity
- Supply/demand balance and trends

Roskill expects marginal costs of refined lithium production (carbonate and hydroxide) to remain between US\$6,000-11,000/t LCE through 2036, depending on whether the very high cost of production from higher cost deposits enters the supply chain. This does not mean, however, that prices will remain at or slightly above marginal cost, because to increase capacity to fulfil future demand the industry needs a price incentive – mining/refining projects being inherently risky to build and scale-up from a technical and economic perspective.

Figure 19-10: Average annual contract and spot price forecast for battery-grade lithium carbonate, 2019-2036 (US\$/t)



Source: Roskill

Note: Real prices adjusted to constant US dollars using United States GDP deflator data from the Federal Reserve and the International Monetary Fund's World Economic Outlook Database. Real prices adjusted to 2021\$.

Roskill forecast for contract battery-grade carbonate prices to average US\$23,609/t (constant 2021 US dollars) over the 2021-2036 horizon. Whereas for domestic China spot prices Roskill forecast an average of US\$24,683/t (constant 2021 US dollars) over the same time period.

The commonly held view in the market is that battery-grade lithium carbonate commands a slightly higher price to technical-grade, typically around US\$500-1,000/t CIF, reflecting the purification and/or micronizing steps involved for most producers. However, there have been periods historically when technical-grade carbonate discounts have reversed. This has typically occurred in periods of severe supply tightness and/or negative sentiment for future availability.

Table 19-1 Average annual price forecast trend for technical-grade lithium carbonate, (US\$/t), 2021 to 2036

	Contract Asia		China spot	
	Nominal	Real (inflation adjusted)	Nominal	Real (inflation adjusted)
2019	11,728	12,065	7,530	7,747
2020	6,200	6,302	6,200	6,302
2021	8,034	8,034	14,514	14,514
2022	18,422	17,955	23,762	23,159
2023	20,960	20,029	25,478	24,346
2024	25,300	23,701	27,100	25,388
2025	24,600	22,594	25,900	23,788
2026	25,200	22,691	26,500	23,862
2027	26,200	23,129	27,500	24,276
2028	26,500	22,935	27,300	23,627
2029	26,500	22,485	28,500	24,182
2030	27,500	22,876	30,100	25,039
2031	28,500	23,243	31,200	25,445
2032	29,500	23,587	32,300	25,826
2033	30,200	23,673	33,000	25,868
2034	31,300	24,054	34,200	26,283
2035	32,000	24,110	35,000	26,371
2036	33,200	24,524	36,300	26,814
Avg. 2021-36	25,870	21,851	28,666	24,299

Note: Real prices adjusted to constant US dollars using United States GDP deflator data from the Federal Reserve and the International Monetary Fund's World Economic Outlook Database Real prices adjusted to 2021\$

Technical-grade lithium carbonate contract prices are expected to follow the same trend as battery-grade, with average prices trending similarly over the long-term. In the medium to long term, Roskill expect the price of technical-grade lithium carbonate to be driven largely by the price of battery-grade lithium hydroxide. The growth in demand for the latter product will increasingly be using technical-grade lithium carbonate as a feedstock for upgrading to battery-grade lithium hydroxide. Longer term this use will exceed the demand from industrial markets and price setting is considered likely to change as a result.

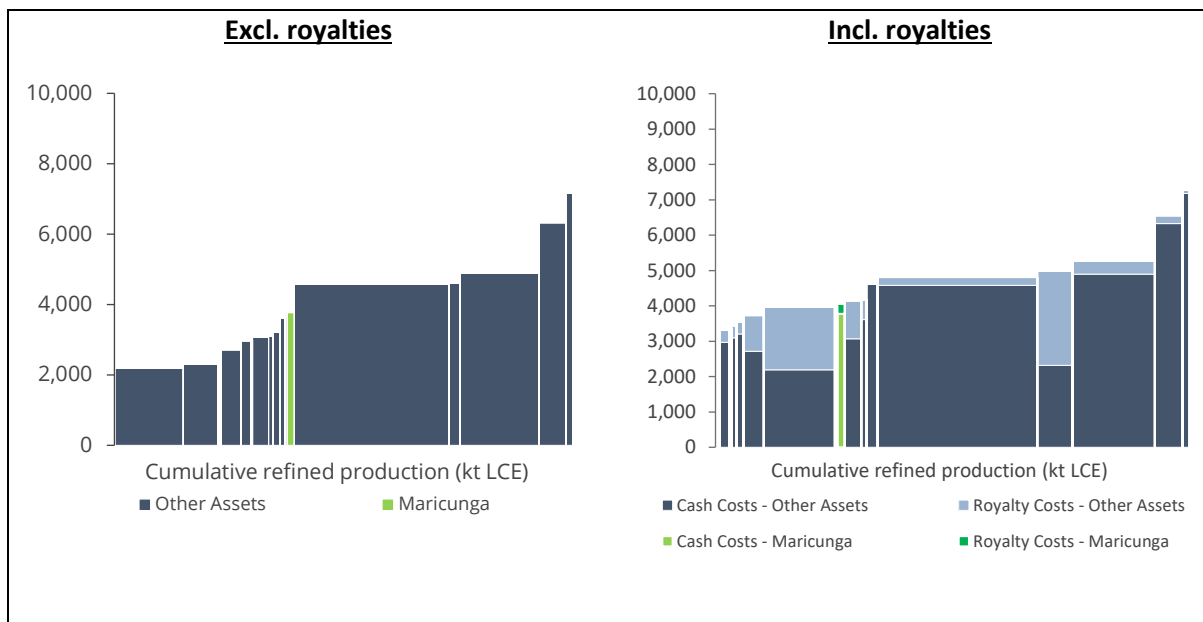
There are a number of factors outside of supply, demand and cost fundamentals which are considered likely to have an impact on lithium prices over the coming years. Several risks unique to the battery raw materials or lithium market also have the potential to impact pricing as witnessed since H2 2018. Numerous key factors underpin the price forecast presented above. These include, but are not limited to, global economic growth, supply-chain impact of Covid-19, changes to the cost of production (energy, labour and raw materials), shipping and FX rates, stockpiling, and technological developments.

19.4 COSTS

In 2021, brine producers continue to enjoy the lowest cost lithium carbonate production in the industry with costs typically around US\$4,150/t, within a range of US\$3,650/t to US\$4,850/t. In comparison, spodumene conversion plant costs are mostly in the range of US\$6,750/t to US\$9,150/t, although some fully integrated producers sit below this range aided by access to low-cost feedstock from Greenbushes. Chinese operations utilising lepidolite feedstocks have average lithium carbonate production costs of around US\$5,400/t.

Production costs in 2021 increased comparatively from 2020 for lithium carbonate derived from mineral sources. Costs for spodumene users increasing by around 18%, whilst the average y-o-y cost increase for refining from lepidolite feedstocks is around 1.5%. Looking forward, production costs for lithium carbonate derived from mineral concentrate feedstocks are expected to continue to increase as the market price of spodumene rises.

Figure 19-11: Lithium carbonate cash cost curve, 2031 (US\$/t LCE)



Source: Roskill

Minera Salar Blanco's Maricunga project has a number of competitive advantages which place the asset towards the centre of the carbonate cash cost curve. These include lower cost processing methods, lower cost of transportation and a lower cost of disposal of salts.

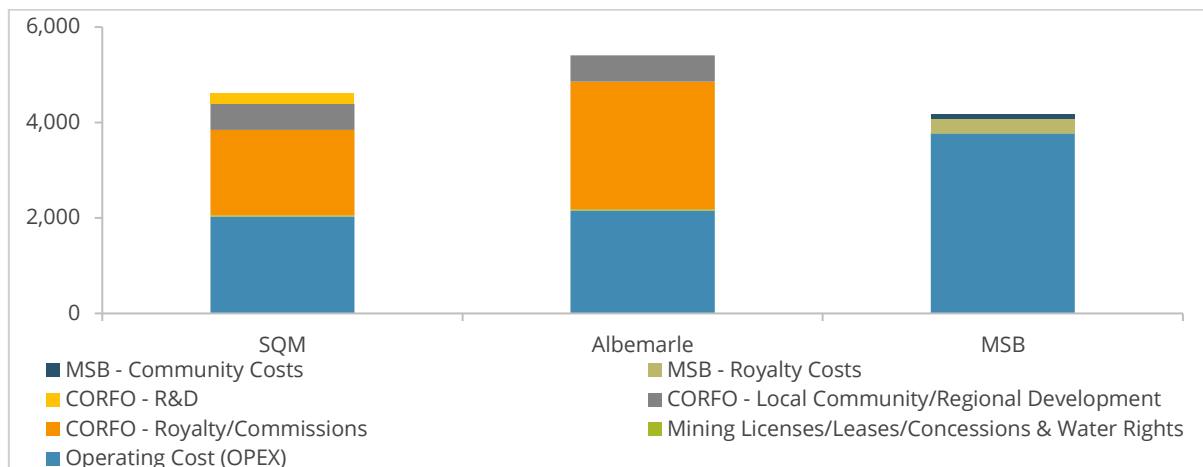
Although it does not currently affect the project costs, the currently scheduled Maricunga production average of up to 15.2 ktpy LCE is lower than the 50ktpy LCE production threshold for the additional 3% ad valorem royalty proposed in a bill presented to the Chilean Chamber of Deputies in March 2020 and advanced to the Senate in August 2021. Should the imposition of this royalty

come to pass, production at Maricunga would not be impacted, whereas operations in the Atacama, considering their expected future production, are highly likely to be.

Maricunga's brine reserves have an average grade of 1,117mg/l Li. This is a lower grade than other operating brine projects in Chile, namely Atacama (Albemarle) and Atacama (SQM) at 2,000mg/l Li. However, the brine grade at Maricunga is generally much more favourable than at operating Chinese brine projects, which typically have lithium concentrations in the range of 36-190mg/l. Roskill identifies nine other lithium brine projects currently under development, all of which are located in Argentina. The brine grade for these projects ranges from 321-750mg/l Li – considerably lower than at Maricunga.

While Maricunga benefits from lower scheduled production volumes by avoiding increased royalties, the smaller reserves mean the asset does not benefit from operating cost reductions imparted by economies of scale such as those achieved at the larger-capacity brine operations in the Atacama operated by SQM and Albemarle.

Figure 19-12: Lithium carbonate production costs in Chile, including royalties, 2031 (US\$/t LCE)



Source: Roskill; SQM; Albemarle; Minera Salar Blanco.

Note: 1 - It is assumed that the agreement between SQM and CORFO, due to expire in 2030, is renewed without material changes.

2 - Royalty and sales commission rates are based on Roskill's price forecasts for refined lithium products.

3 - A portion of Albemarle's commissions are paid into a fund for R&D.

20. ENVIRONMENTAL STUDIES, PERMITTING AND SOCIAL OR COMMUNITY IMPACT.

20.1 ENVIRONMENTAL STUDIES AND PERMITTING

MSB received the environmental approval for its Maricunga project on February 4, 2020, by Resolution N°94 considering the construction and operation of both, a 58,000 ton/year Potassium Chloride (KCL) Plant and a 20,000 ton/year Lithium Carbonate plant over a period of 20 years (KCL plant has not been included on this DFS). The EIA approved a brine extraction of 209 l/s, freshwater extraction of 35 l/s and all associated industrial facilities, including evaporation pond areas, brine pipelines and the campsite. The Environmental Impact Assessment (EIA), prepared by international consulting company Stantec (previously MWH), was submitted to the Chilean Environmental Assessment Service (SEA²) in September 2018 and was the culmination of more than two years of field and desk work.

The process involved in-depth data gathering, a variety of environmental and engineering studies and monitoring campaigns which resulted in a comprehensive 11,400-page document, which included complete environmental baseline studies, hydrogeological modelling, human, archaeological and fauna and flora characterisation, and impact evaluation.

The EIA also included a lengthy process of social engagement with the Colla indigenous communities in the area. In addition, significant consultation took place with regional authorities and local organisations.

The EIA is the main environmental permit for construction and operation of the project and only several minor permits must be processed before construction.

Resolution N°94/2020 contains specific commitments that MSB must comply with, as mitigation and compensation measures.

² "Servicio de Evaluación Ambiental".

20.2 ENVIRONMENTAL BASELINE STUDY

A summary of the environmental baseline studies and monitoring activities are described as follows. The baseline study covers the project site area, environmental influence area, and the main routes that will be used during construction and operation.

The baseline study includes: climate and meteorology, air quality, noise and vibrations, geology, geomorphological and geological risks, hydrology, hydrogeology, water balance, soil, flora, fauna, archaeology, landscape, tourism and facilities, and human environment.

20.2.1 CLIMATE AND METEOROLOGY

A detailed description of the Climate and Methodology for the Salar and Project area is presented in Chapter 5 of this FS report.

20.2.2 AIR QUALITY

Air quality was measured with MSB's air quality monitoring station, which was installed along with the weather station (Figure 20-1). The air quality conditions in the area surrounding the Project site are good, as no emitting sources exists in the area, and consequently, do not show any latency or saturation levels. According to the measurements between January 2017 to December 2018, the average breathable particulate material (PM) in the project area is as follows:

- PM₁₀ = 12.3 µg/m³N.
- PM_{2.5} = 2.3 µg/m³N.

Figure 20-1 Weather and Air Quality Monitoring Station – MSB



Source: MSB

20.2.3 NOISE

Background noise levels were measured at the Project Site and at the roads that will be used by the project (Figure 20-2). Measurements for fauna sensitive receptors were conducted at the site and at the Salar (Figure 20-3).

The potential sensitive noise receivers are located at the existing custom facilities “*Complejo Fronterizo San Francisco*”, the future project camp and the communities that are adjacent to the routes that will be used by the project. Background noise levels were recorded for human receptors are as follows:

- Human receptors: During the day, the Continuous Sound Pressure Level (Leq) of background noise obtained fluctuates between 34 and 71 dBA and during the night, it fluctuates between 31 and 63 dBA.
- Fauna receptors: The measurements were lower than the referenced 85 dBZ, an international used reference to determine effects on wild fauna.

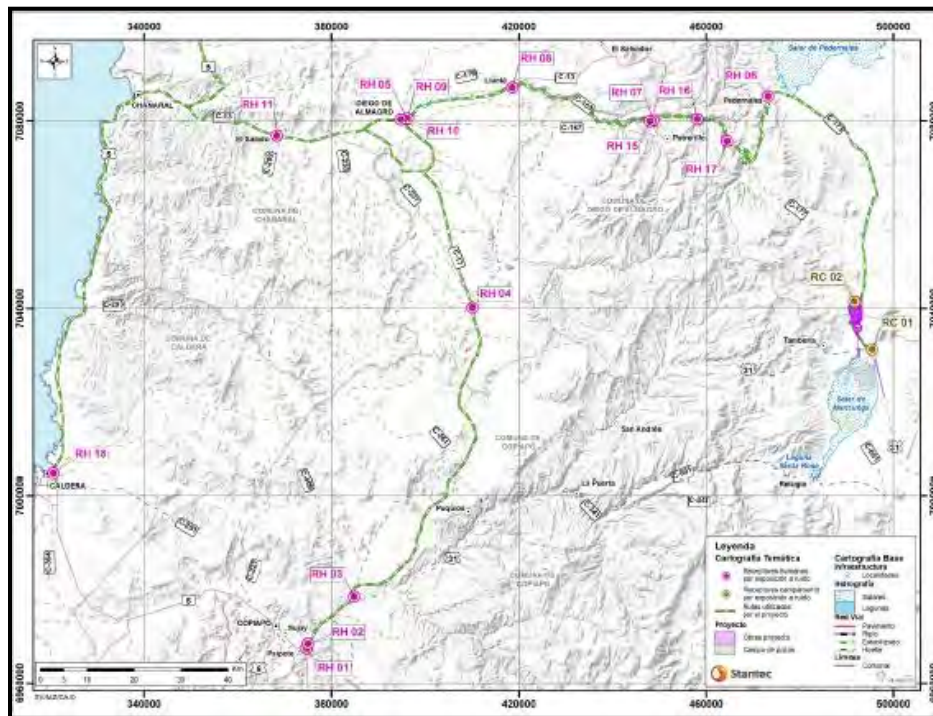
In addition, sound pressure level projections on sensitive receivers (both human and fauna) living in the area, were conducted for the EIA.

20.2.4 VIBRATIONS

Background vibration measurements were conducted to obtain vertical acceleration. These measurements were recorded at the same measurement point for noise. All measurements were below the threshold of human perception.

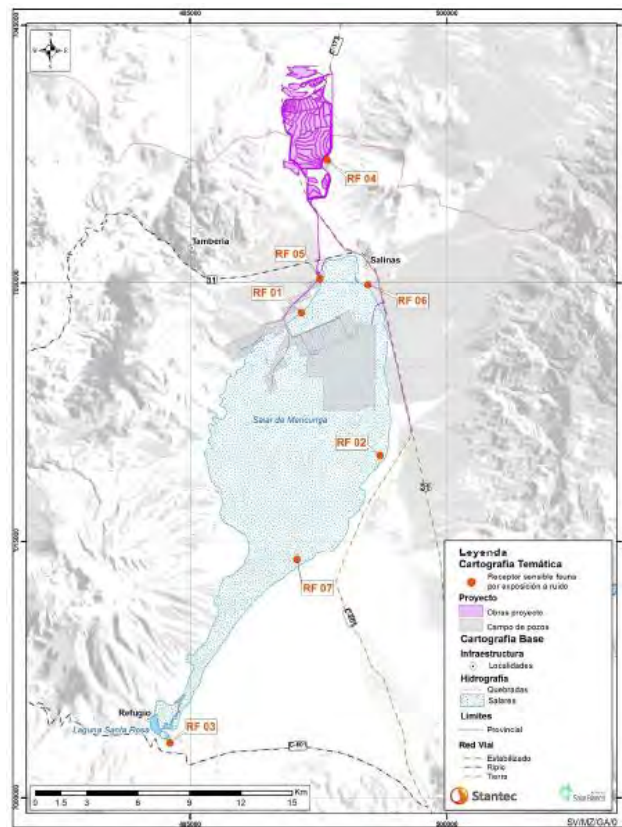
In addition, vibration projections that were recorded for the EIA, were below the threshold of human perception.

Figure 20-2 Measurement Locations for Noise and Vibration for Humans



Source: Stantec

Figure 20-3 Measurement Locations for Noise and Vibration for Fauna



Source: Stantec

20.2.5 GEOLOGY, GEOMORPHOLOGICAL AND GEOLOGICAL RISKS

The local geology of the Project area is comprised mainly of alluvial deposits from fans composed of gravels and blocks of low rounding. A detailed description of the geology of the Salar is presented in Chapter 7 of this FS report.

The geomorphological pattern corresponds to the geomorphological unit called "*Salares Trench Prealtiplánicos*", in which forms of lithostructural modelling and water and fluvial modelling were identified, as well as forms of gentle slopes and the salar depression.

The geological risks identified include earthquakes, volcanic activity and morphodynamical processes, such as floods and mud or debris flows.

20.2.6 SOILS

MSB conducted an edaphological study, which included the excavation of test pits to characterize the soil profile, texture and structure at the project site. It was determined that the soil is comprised mainly of sands with gravel from the alluvial fan. The gravels are mostly angular due to sand friction and erosion. Topsoil is minimal and therefore unable to support vegetation. There are, however, certain areas located at the edges of the Salar de Maricunga which accumulate fine material and water due to poor drainage; these sectors support endemic vegetation.

20.2.7 HYDROGEOLOGY AND WATER BALANCE

The hydrogeology and water balance of Salar de Maricunga have been described in detail in Chapter 8 of this DFS.

20.2.8 ARCHAEOLOGICAL HERITAGE AND PALAEOONTOLOGY

A total of 51 archaeological finds (AM) were detected during the baseline study, 12 of which were assigned to the pre-Hispanic period, 8 to the historical period and 30 registered as indeterminate.

A paleontological desktop study was completed, resulting in the identification of a geological unit (*Los Chinchos formation*) with the potential for geological remains. During prospecting, no geological remains were discovered.

In the geological unit of recent alluvial deposits, remains were identified that belongs to a Jurassic marine unit that emerges approximately 10 km from the place of origin.

20.2.9 LANDSCAPE

Two landscape units, UP1 and UP2, were identified (Figure 20-4). The visual quality of the UP1 landscape is highlighted in the Salar de Maricunga, with unique biophysical and structural attributes. The second landscape unit (UP2) is considered to be of average visual quality, since it presents more homogeneous characteristics and does not have any features that diminish the visual quality of the landscape. Based on the above analysis, the Project is considered to be in an area that has visual landscape value.

Figure 20-4 Landscape Units UP1 and UP2



Source: Stantec

20.2.10 BIODIVERSITY AND NATURAL SCENERY

The area surrounding the project site is part of the main tourism circuit of the region, due to the interesting landscape. It was classified into two groups by Sernatur, the Chilean Government Agency for Tourism:

- Protected Areas and Priority Sites for Conservation
 - National Park Nevado Tres Cruces; and
 - Ramsar Complex Site Laguna del Negro Francisco and Laguna Santa Rosa.
- Natural Scenery Sites
 - Zones of Tourism Interest (ZOIT) - Salar de Maricunga and Ojos del Salado;
 - Priority Tourism Areas (PTA) - Ojos del Salado in the Cordillera de Atacama and Desierto y Puna in the Atacama Desert.
 - “Route of the Six Thousand” - a tourist Route developed by Sernatur that has more than twenty peaks over 6000 masl and has the highest active volcano in the world (Ojos del Salado) at 6,893 masl;
 - Scenic Routes - A section of the Patrimonial Route N° 26 “El Derrotero de Atacama” and a section of the “Path of Chile”; and
 - Hot Springs - Laguna Verde and Cascadas del Río Lamas.

20.2.11 TERRITORIAL USE AND PLANNING

On a regional level, the majority of the territory does not have any current land use. The land use is categorized as follows:

- 50.88% of the land is categorized as “Use VIII”, which means it has no agricultural, livestock and/or forestry value; and
- 49.12% of the land is un-categorized.

The soil on the edges of the Salar de Maricunga was identified as Category V, which means it is very susceptible to flooding.

The Community Development Plans (PLADECOS) for the Copiapó and Diego de Almagro districts, highlight mining for Copper, Gold and Silver as part of the main economic activities for these districts. Mining is the main livelihood of the populated centres of Diego de Almagro and El Salado.

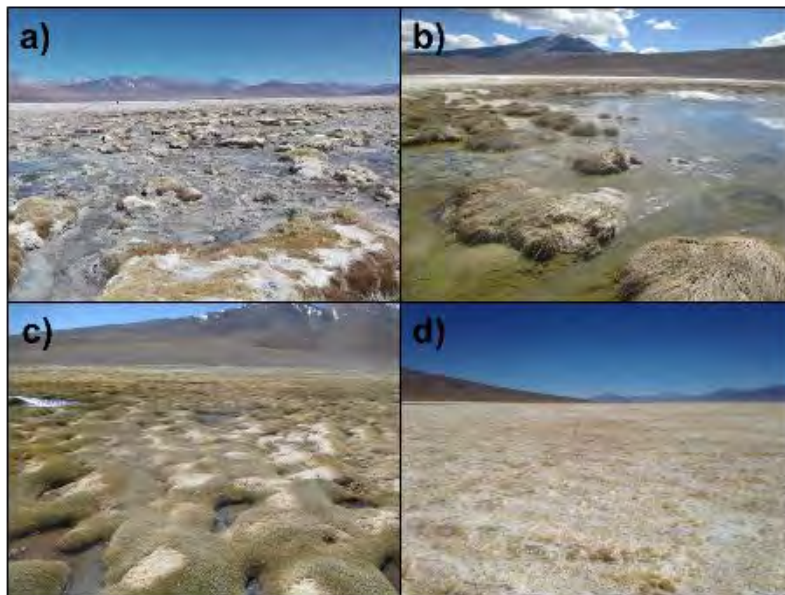
20.2.12 FLORA, VEGETATION AND FAUNA

According to the flora and vegetation characterization results of the study area, 29 species were detected, of which 60% are grassy brushes, 38.7% are bushes and 20.2% are endemic (grassy meadows and wetlands).

Most of the vegetation is found on the edges of the Salar de Maricunga. The most important are the endemic vegetation, of which 7.8 ha are grassy meadows and 12.4 ha are wetland vegetation (Figure 20-5). This 20.2 ha corresponds to 0.12% of the total study area.

Within the project area of influence, there are no flora or vegetation species under the official conservation category. Some protected species have been recorded near the Santa Rosa Lagoon, but they will not be disturbed by the project, as there will be no development activities close to this sector.

Figure 20-5 Endemic Vegetation on Shore of Salar de Maricunga



a and b) Formation of isolated individuals and groups of species within the unit; c and d) Homogenous formations of the vegetation coverings (bare soil, water and halite between the vegetation cover). Source: Stantec

According to the fauna characterization results, a total of 37 species were recorded (2 reptiles, 25 birds and 10 mammals).

Figure 20-6 Vulnerable Reptiles and Endangered Mammals



A) Liolaemus rosenmanni (lagartija de Rosenmann); B) Liolaemus patriciaturrae (Lagartija de Patricia Iturra). Vicugna (vicuña); B) Lama guanicoe (guanaco);

20.2.13 AQUATIC CONTINENTAL ECOSYSTEMS

The following aquatic organisms are present in the lagoons of the Maricunga salt lake:

- Phytobenthos: Bacillariophyceae class;
- Zoobenthos: Harpacticoida class;
- Diatoms: 48 species recorded (Nitzschia, Amphora, Pseudostaurosira and Navicula class);
- Plankton: Harpacticoida; and
- Phytoplankton: Bacillariophyceae class.

20.2.14 SOCIAL AND COMMUNITY

The influence area of the Project includes the districts of Copiapó (where Salar de Maricunga is located), Diego de Almagro (where the Lithium Carbonate plant will be located), Caldera and Chañaral (crossed by reagent supply and final products trucks), in the region of Atacama and the communities of María Elena (also crossed by trucks), Antofagasta and Mejillones (where Antofagasta Port and Angamos Port are located) in the Antofagasta region.

The closest indigenous communities to the Salar de Maricunga are Colla Communities in the district of Diego de Almagro whose relationship with the Project comes from the use of existing roads that cross through the territories. MSB has a proactive approach in its relationship with the local communities and other stakeholders in the Atacama Region.

The Colla indigenous communities mentioned above correspond to, Colla Community Chiyagua, Colla Community Quebrada El Jardín and Colla Community Geoxcultuxial. The Colla communities use the pastures, flooded meadows and areas with plenty of potable water for pasturing their livestock. The Colla have traditionally built their homes adjacent to these areas, which include the road C-13 used by the project.

20.3 WASTE AND TAILING MANAGEMENT

Different types of precipitated salt will be harvested during the ponds evaporation process and transported to stockpiles for storage. Halite salts will be stored in a separate stockpile, whereas, sylvinite and carnallite will be stockpiled together for use in the future Potassium Chloride Plant (not included in this FS).

Waste generated by the Salt Removal Plant includes calcium chloride-tachyhydrite salts, which are transported by truck from the salt removal plant and stockpiled.

The estimated amount of salt to be harvested during the entire Project operation phase is approximately 20,550,000 m³ of halite salt and 6,208,000 m³ of calcium chloride-tachyhydrite salts. For more information on the waste of the evaporation process and lithium carbonate production see Chapter 17 of this FS.

The waste generated by the project (domestic, construction, maintenance, non-hazardous and hazardous waste) will be handled in accordance with the current regulations of Chile.

21. CAPITAL AND OPERATING COSTS

21.1 CAPITAL COST ESTIMATE

21.1.1 CAPITAL EXPENDITURES – CAPEX

Capital expenditures are based on an average operating capacity/production of 15,200 tonnes of lithium carbonate per year (20 years mine-life). Potash production, which had been considered at the PEA stage, has been deferred until conditions in this particular market improve significantly. Since enough sylvinites and carnallite salts to operate a potash plant are naturally produced in the evaporation ponds, and are harvestable from year 4 onwards, MSB will review the decision to build a potash plant a few years into the future. Thus, at this stage, all MSB efforts are concentrated on becoming a lithium carbonate producer, for which demand is expected to continue growing at a very fast rate, as determined in Section 19 of this report.

Capital equipment and construction costs have been obtained from solicited quotes to equipment manufacturers and construction companies. As indicated in Sections 16 to 18, considerable engineering progress has been achieved both on plant design and infrastructure requirements. Given this, Worley have confirmed a capital cost estimate accuracy within a +/- 11.1% range.

Capital and operating cost estimates are expressed in fourth quarter 2021 US dollars. No provision has been included to offset future cost escalation since expenses, as well as revenue, are expressed in constant US dollar terms.

The capital cost estimate includes direct and indirect costs for:

- Brine production wellfields and pipeline delivery system
- Evaporation ponds
- Salt removal plant
- Lithium carbonate plant
- General services
- Infrastructure

Capital investment for the Project, including equipment, materials, indirect costs and contingencies during the construction period is estimated to be US\$ 626 million. Out of this total Direct Project Costs represent US\$ 419 million; Indirect Project Costs represent US\$ 145 million, and the

Contingencies provision is US\$ 62 million. The indirect project costs represent 34.6% of Direct project costs, while the contingencies represent 11.1% of Direct plus Indirect project costs.³

In addition, Sustaining Capital expenditures total US\$ 42 million over the 23-year evaluation period of the project, which includes a 2,5-year construction period and an operating life of 20 years. Maximum working capital requirements over the project horizon is US\$ 15.8 million.

Total capital expenditures are summarized in Table 21-1.

Table 21-1 Total Capital Expenditures

Area	Total Project	Projected Budget US\$ 000
	Direct Costs	
1000	Brine Extraction Wells	33,235
2000	Evaporation Ponds	89,878
5000	Salt Removal Plant	110,322
6000	Lithium Carbonate Plant	55,754
8000	General Services	83,953
9000	Infrastructure	45,814
	Total Direct Cost	418,957
	Total Indirect Cost	144,835
	Contingencies (11,1%)	62,581
	Total Capital Expenditures	626,372

21.1.2 BRINE PRODUCTION WELLFIELD AND PIPELINE DELIVERY SYSTEM

As indicated in Section 16, brine abstraction from the Salar will take place by installing and operating a conventional brine production wellfield. Brine from the individual production wells will be fed into two collection/transfer ponds in the northwest of the Salar. From there it will be pumped, using a booster pumping station, through the main trunk pipeline up to the evaporation ponds some 12 km to the north in the general plant area.

It is projected that a total of 19 brine wells will be required over the life of the Project. However, no more than 11 wells will be operating at a single time. Production wells will be completed with 12-inch diameter stainless steel production casing and equipped with 380 V submersible pumping

³ Above total includes initial spares but excludes plant first fills. The latter were included as a separate item in the cash flow and total US\$3.9 million.

equipment. Permanent power will be delivered to the wellfield area through a mid-range power line.

Brine discharge from each wellhead will be piped through 8-inch diameter HDPE feeder pipelines to two central collection/transfer ponds in the northwest of the Salar. A 12 km length, 20-inch diameter steel / HDPE main trunk pipeline will be installed between the collection/transfer ponds and the evaporation ponds area. A booster pumping station will be installed at the bottom of the main trunk line adjacent to the collection ponds to pump the brine up to the evaporation ponds (130 m lift).

Table 21-2 Brine Production Wellfield Cost Estimate

1000 Brine Extraction Wells	Projected Budget 000 US\$
Well drilling and construction	9,763
Pumps and Mechanic Equipment	1,798
Piping	13,261
Electrical supply and distribution	7,348
Instrumentation	1,065
Total	33,235

21.1.3 EVAPORATION PONDS

Evaporation ponds comprise 4 types, namely solar evaporation ponds proper, lithium brine reservoirs, mother liquor pond and an auxiliary pond. They are extensive shallow areas, with a depth of 2 or 4m depending on the type of pond. Brine transfer from one pond to the next will be by means of gravity overflow. In those sectors in which the topography of the sector is not favourable, transfer will be done by pumping.

Six lithium brine reservoirs will be installed at the end of the circuit, where concentrated brine from the evaporation ponds will accumulate, for later transfer to the production area for further processing.

The solar evaporation ponds have a surface of approximately 5,160,000 m², the lithium brine reservoirs have a combined area of approximately 116,000 m², the mother liquor pond and auxiliary pond have an approximate area of 90.300 m² and 441 m² respectively.

All the ponds have a waterproofing system, which considers the incorporation of an HDPE or similar liner, with resistance to impacts and punctures.

Table 21-3 Evaporation Ponds Cost Estimate

2000 Evaporation Ponds	Projected Budget 000 US\$
Earthworks	45,845
Liners	35,595
Mechanical Equipment	3,783
Piping	2,754
Electrical supply and distribution	1,578
Instrumentation	323
Total	89,878

21.1.4 SALT REMOVAL PLANT

Given the prevailing temperature, wind and solar radiation characteristics of the Maricunga Salar, as well as its brine composition, chemical process designers have reached the conclusion that in order to accelerate brine concentration, and remove its high calcium content, it is advisable to install a salt removal plant. This will receive solar concentrated brine from the reservoir and will subject it to additional concentration by means of evaporation and crystallization. Input for the plant will be approximately 52 m³/h of concentrated brine. Output from the plant is directed to the Lithium Carbonate Plant.

The technology, equipment and construction supervision for the Salt Removal Plant is being provided by GEA Messo, part of GEA Aktiengesellschaft of Düsseldorf, Germany (GEA).

Table 21-4 Salt Removal Plant Cost Estimate

5000 Salt Removal Plant	Projected Budget 000 US\$
Concrete	7,680
Steel Structures	15,936
Mechanic Equipment	73,704
Piping	5,153
Electrical supply and distribution	1,066
Instrumentation	3,138
Water cooling system	3,646
Total	110,322

21.1.5 LITHIUM CARBONATE PLANT

Concentrated brine from the Salt Removal Plant will be sent to the Lithium Carbonate Plant. By means of a series of continuous processes, these being solvent extraction, calcium and magnesium removal, ion exchange, filtering and washing, the remaining contaminants present in the brine, mainly boron, magnesium and calcium, will be removed. The purified lithium brine will undergo carbonation, precipitating lithium carbonate, after which it will be dewatered, dried, micronized and packaged as battery grade lithium carbonate.

The facilities that make up the plant comprise a total area of approximately 7,200 m². This includes a solvent extraction building⁴, a brine purification building which covers magnesium and calcium removal as well as ion exchange circuits, and the lithium carbonate building which includes a wet area, filtering, drying, packaging and storage of the final product.

Table 21-5 Lithium Carbonate Plant Cost Estimate

6000 Li₂CO₃ Plant	Projected Budget 000 US\$
Stripping - SX Plant	14,269
Calcium and Magnesium Removal	14,455
Ion Exchange	4,067
Carbonation	3,186
Filtering and Washing	6,069
Drying	9,600
Packaging and Storage	4,108
Total	55,754

21.1.6 GENERAL SERVICES

The main auxiliary services required by the salt removal and lithium carbonate process plants are water supply storage and distribution, fuel storage and distribution, electrical supply and distribution, and soda ash storage and preparation.

⁴ The solvent extraction circuit is located within the Salt Removal Plant, however, its cost was transferred to the Lithium Carbonate Plant for comparative purposes, since in the majority of lithium projects, the cost of this unit is part of the Lithium Carbonate Plant.

Table 21-6 General Services Cost Estimate

8000 General Services	Projected Budget 000 US\$
Fuel Storage and Distribution	2,521
Water Supply, Storage and Distribution	13,106
Electric Power Supply and Distribution	41,522
Steam Boiler Unit	3,054
Fire Protection System	6,241
Plant and Instrumentation Air Supply	1,731
Reagents Storage and Distribution	15,777
Total	83,953

21.1.7 INFRASTRUCTURE AND EQUIPMENT

The project infrastructure and equipment include the following areas:

- Construction and Operation Camp
- Internal Roads and C-13 route by-pass
- Products warehouse.
- Auxiliary services.
- Workers' camp.
- Temporary contractors' installations

In addition, there will be approximately 23 million m³ of stockpiles and discards ponds, originating from evaporation pond harvesting and from process plant discard streams.

Table 21-7 Infrastructure and Equipment Cost Estimate

9000 Infrastructure	Projected Budget 000 US\$
Auxiliary plant buildings	15,154
Access control and security	636
Camps and Facilities	16,860
Internal roads	4,954
Sanitary works	6,045
Electrical and Piping mains	2,164
Total	45,814

21.1.8 INDIRECT COST

The Project strategy for construction considers an EPC Contract with reimbursable cost at unit prices. Indirect expenses include the project is owner's cost, transportation fees, insurance policies, third party services, vendor representations and spare parts. Also included are field engineering and commissioning, as well as ramp up and first pond filling.

Table 21-8 Indirect Costs

Indirect Costs	Projected Budget US\$ 000
EPC Contract	16,999
Field Engineering and Commissioning	5,460
Freight, Insurance and Customs Fees	9,005
Third Party Services	4,069
Vendor Reps	3,333
Spare Parts (Commissioning and 1st year operation)	3,721
Owner's Cost	10,321
Indirect Cost EPC Contract	12,113
Overheads and Profits EPC Contract	29,291
Indirect Cost Subcontractor	50,522
Total Indirect Costs	144,835

21.1.9 EXCLUSIONS

The following items are not included in this estimate:

- Sunk and legal costs
- Special incentives and allowances
- Escalation
- Interest and financing costs
- Start-up costs beyond those specifically included
- Additional exploration expenses

21.1.10 CURRENCY

All values are expressed in fourth quarter 2021 US dollars; the exchange rate between the Chilean peso and the US dollar has been assumed as CHP\$ 800 / US\$; no provision for escalation has been included since both revenues and expenses are expressed in constant dollars. A US dollar Euro rate of 0,88 has also been used in some calculations.

21.2 OPERATING COST ESTIMATE

This section presents the main elements of the estimated operating expenses for the Stage One Project.

An operating cost estimate for a 15,200 TPY Li_2CO_3 average capacity facility was prepared. This estimate is based upon process definition, laboratory work, tests at equipment suppliers and reagents consumption rates all provided or determined by MSB. Vendor quotations have been used for reagents costs. Expenses estimates, as well as manpower levels, are based on Worley's experience and information provided by MSB. Energy prices -mainly electricity and diesel fuel- and reagents prices correspond to expected costs for products delivered at the project's location.

21.2.1 OPERATING EXPENSES SUMMARY – OPEX

The average operating expenses are summarized in the following table:

Table 21-9 Average Operating Costs

Average Operating Costs	US\$ / Tonne Li_2CO_3	Total 000 US\$
DIRECT COSTS		
Chemical Reactives and Reagents	1,099	16,704
Salt Harvesting	266	4,049
Energy	1,164	17,689
<i>Memo: - Electrical</i>	<i>342</i>	<i>5,206</i>
<i>- Thermal</i>	<i>821</i>	<i>12,483</i>
Manpower	518	7,867
Catering & Camp Services	132	1,999
Maintenance	358	5,443
Transport	181	2,756
OPERATIONAL CASH COSTS	3,718	56,506
INDIRECT COSTS		
General & Administration	146	2,220
INDIRECT COSTS SUBTOTAL	146	2,220
TOTAL PRODUCTION COSTS	3,864	58,726

As indicated in Table 21-9, energy costs -electrical and thermal- are the major operating cost of the project, closely followed by chemical reagents. Fuel consumed by the Salt Removal Plant is the major component of energy costs. Over 90% of the chemical reagents costs correspond to soda ash and hydrochloric acid. Over 35,000 tonnes of soda ash are required to produce an average of 15,200 tonnes of Li_2CO_3 . Other important expense items are manpower, maintenance, and salt harvesting.

21.2.2 REAGENTS COSTS

Table 21-10 Reagents Costs⁵

Description	Formula	US\$ / yr	US\$ / Tonne Li ₂ CO ₃
Soda ash	Na ₂ CO ₃	11,602,282	763
Sodium hydroxide	NaOH (50%)	429,400	28
Hydrochloric acid	HCl	3,996,749	263
Sodium sulphite	Na ₂ SO ₃	111,366	7
Flocculant	Polyelectrolito	54,720	4
Calcium oxide	CaO	312,816	21
SX Reactants: Diluent	Exxsol D80 o Escaid 110	76,033	5
SX Reactants: Extractant	Exxal 8	120,384	8
CHEMICAL CONSUMPTION TOTAL		16,703,750	1,099

21.2.3 ENERGY COST

Diesel fuel consumption in the Salt Removal Plant is by far the major component of energy expenses; these amount to over US\$ 13 million per year. In this plant, Diesel fuel is used for boilers to produce steam required by the process. The same type of fuel is used by salt harvesting equipment, but this cost is considered under item 21.2.5.

Other major energy items are the electricity required by the wells, the ponds, and the process plants. Electrical transmission tolls are also significant. However, the project is planning to use an existing line, built by another mining company, and which would be shared by both companies. MSB has had discussions with the line owner in this respect, but power line sharing is a well-regulated matter in Chile. At the PEA stage it was thought that there was enough capacity on the line to allow both companies to operate, but revised estimates of the Project power consumption indicate that it will be necessary to build a new substation and reinforced the line. The cost of this item has been included in the project's CAPEX. Transmission tolls have been estimated according to the prevailing methodology in Chile.

⁵ It is to note that Table 21-10 includes all reactants used regularly in the process, as well as other reactants that are required occasionally for equipment cleaning purposes, or for process control.

Table 21-11 Energy Cost

Electrical Energy Consumption	Installed Power Load, kW	Average Load Connected, kW	Consumed Energy, MWh/yr	Electric Energy Cost, US\$/MWh	Consumed Energy, US\$/yr	Cost US\$/Tonne Li ₂ CO ₃
Wells	437	341	2,898	59.05	171,147	
Transfer Ponds	983	785	6,683	59.05	394,618	
Evaporation Ponds	907	725	6,167	59.05	364,158	
Salt removal - Phase 1	7,475	6,466	47,176	59.05	2,785,739	
Lithium carbonate Plant - Phase 2	3,087	2,402	17,522	59.05	1,034,678	
Camp	902	690	2,937	59.05	173,459	
Truck Shop	379	271	1,153	59.05	68,107	
Transmission Losses	556	425	3,618	59.05	213,619	
Process Services	1,894	1,383	10,092	59.05	595,922	
Power and lighting	366	301	1,279	59.05	75,521	
TOTAL ELECTRICAL ENERGY	16,984	13,788	88,155	59.05	5,205,525	342
*Transmission toll included on electrical energy cost.						
Thermal energy consumption		Plant Steam Consumption, kg/h	Diesel Consumption, m3/h	Annual diesel consumption, m3/year	Steam energy cost, US\$	Cost US\$/Tonne Li ₂ CO ₃
Phase 1		26,911				
Phase 2		1,933				
Dryer		500				
ITC Ceniza de soda		1,245				
TOTAL THERMAL ENERGY		30,589	2.40	17,528.25	12,483,122	821
TOTAL ENERGY COST					17,688,647	1,164

21.2.4 MAINTENANCE COST

Maintenance costs have been estimated by applying experience-based factors to capital outlays for the different budget items. It is to be noted that maintenance of the salt harvesting equipment, which is a significant amount, is included in the Salt Harvesting cost sub section.

Table 21-12 Maintenance Cost

Description	Projected Budget US\$ 000	Avg. Maintenance US\$ 000 / yr	US\$ / Tonne Li ₂ CO ₃
Brine Extraction Wells	33,235	922	61
Evaporation Ponds	89,878	416	27
Salt Removal Plant	110,322	1,531	101
Lithium Carbonate Plant	55,754	774	51
General Services	83,953	1,165	77
Infrastructure	45,814	636	42
Total	418,957	5,443	358

21.2.5 SALT HARVEST AND TRANSPORT

This item corresponds to the costs incurred from harvesting the ponds and transporting discarded salts to their established dumping places, within MSB's surface property, and according to the EIA, expected to be approved. Material to be transported is approximately 1.7 million Tonnes/year. It should be noted that, generally, material transport of this type is usually subcontracted to third party operators, which provide the required equipment and personnel necessary for this operation, for an agreed fee. Thus, in order to make this cost comparable to third party rates, in this item we have included all costs related to this operation.

In spite of the above, to maintain the full project basis for economic evaluation purposes, all equipment required in the operation, as well as the personnel involved, have been assumed to be owned or employed directly for MSB.

Table 21-13 Salt Harvest and Transport Cost

Description	US\$ 000	US\$ / Tonne Li_2CO_3
Operators Salt Harvest	1,554	102
Maintenance Personnel	680	45
Fuel & lubricants	1,046	69
Tires	399	26
Maintenance and spare parts	371	24
Total	4,049	266

21.2.6 MANPOWER, CATERING AND CAMP SERVICES COST

Headcount for the plant was estimated based on experience in similar facilities, while personnel salaries and benefits were projected using data from actual costs for mining operations in the north of Chile, adjusted by relevant factors. Headcount increased substantially from that estimated at the PEA stage mainly due to a stricter interpretation of Chilean regulations concerning admissible personnel shifts.

Table 21-14 Manpower, Catering and Camp Services Cost

Description	Number of people	Cost US\$ 000 / Y	Cost US\$ / Tonne Li ₂ CO ₃
Plant Operations	152	7,867	518
Catering and Camp Services		1,999	132
Total	152	9,866	649
Memo items:			
Ponds Harvesting (1)	36	1,554	102
Truck Workshop (1)	20	680	45
Management (2)	15	1,488	98
Soda Ash and Product Drivers (3)	16	747	49
Total	239	14,335	943

Notes:

(1) Costs included in Salt Harvesting expenses

(2) Costs included in G & A expenses

(3) Costs included in Transport

21.2.7 PRODUCT TRANSPORTATION COSTS

Costs of all production supply items, except soda ash, have been considered at the Maricunga plant, thus there are no transport costs to add from the supply side, except for that corresponding to the above mentioned reactant, whose cost has been considered on a CIF Mejillones (Chile) port basis. Thus land transport costs for soda ash need to be considered. For this purpose, a fleet comprising nine trucks has been included in the CAPEX. Furthermore, since it takes approximately 2.35 tonnes of soda ash to produce one tonne of Li₂CO₃, it has been assumed that the trucks that bring soda ash from the port, will take the lithium carbonate product to that destination, at no extra cost, given that the haulage will be done by a MSB owned fleet.

In addition, since prices for lithium carbonate shown in Section 19, and considered in the economic evaluation, correspond to CIF China prices, we need to include all cost items necessary to transport produced lithium carbonate to China. These costs include trucking the lithium carbonate to Antofagasta, or nearby Mejillones, both in Chile, and which are the usual export locations for this product. Additional costs to be considered correspond to port warehousing and handling fees, as well as ocean freight and insurance to a destination port in China. These costs are shown in Table 21-15.

Table 21-15 Soda Ash and Lithium Carbonate Transportation Costs

Description	Costs US\$	Rate US\$/Ton
Road transportation cost for soda ash and lithium carbonate (1)	1,564,825	103
Port Storage Fees - per container	588	24
Port Receiving and Dispatching Fees - per container	278	11
Ocean Freight & Insurance - per container	1,093	44
Total		181

(1) Fuel consumption for soda ash+final product transport+manpower+ truck maintenance+ tires

21.2.8 INDIRECT COSTS

Indirect costs include management compensation, office space rental, plant insurance, communications and other expenses.

Costs exclude Board of Directors compensation and expenses, and any other expenses above those corresponding to the company's local General Manager. These costs are shown in Table 21-16.

Table 21-16 General & Administration

Description	000 US\$	US\$ / Tonne Li ₂ CO ₃
Management	1,488	98
Office Rental	130	9
Insurance	168	11
Personnel Transportation	374	25
Communications, office supplies & sundries	60	4
LOCAL G & A TOTAL COSTS	2,220	146

22. ECONOMIC ANALYSIS

This section analyses the economic feasibility of the MSB Stage One Project, which aims to produce an average 15,200 TPY of lithium carbonate.

To carry out the project's economic evaluation, MSB developed a pre-tax and after-tax cash flow model. Inputs for this model were the capital and operating cost estimates presented in the previous sections, as well as a production program developed by the hydrogeological and process consultants, and the pricing forecast included in Section 19.

Model results include the project's NPVs at different rates, IRR and payback period. These parameters were calculated for different scenarios; in addition, a sensitivity analysis on the most important revenue/cost variables was performed.

22.1 EVALUATION CRITERIA

- Pricing has been obtained from Company calculations based on the Roskill Lithium Carbonate market study report prepared for MSB in October 2021 and updated in December 2021, as indicated in Section 19.
- Long term lithium carbonate production rate has been assumed as approximately 15,200 TPY, of which 90% will be produced as battery grade material and the remaining 10% will be technical grade product. The long-term lithium carbonate production level is reached in the third year of operations. Production ramp up rates for technical grade lithium carbonate are higher than those assumed for battery grade lithium carbonate since the latter is a more technically demanding operation. Production ramp up rates and yearly output tonnages are shown in Table 22-2 and Table 22-3.
- Project horizon: Time allowed for engineering, final permits and construction is 3 years, with commercial production starting in the fourth year. Projected operating period is 20 years. Project life is currently controlled by mineral reserves. It is important to note that this Feasibility Study corresponds only to the development of MSB's "old code concessions"⁶ or "grand fathered" mining properties, which may be developed without a special government authorization, or CEOL⁷. If this authorization is granted to MSB, it may choose to extend project life, and/or increase the annual production rate of lithium carbonate.

⁶ Código de Minería de 1932.

⁷ Contrato Especial de Operación para Exploración y Explotación de Litio.

- It is noted that, even though the ramp-up period (production period) will start during the third quarter of 2025, the cash flow projection assumes that no revenues will be recognized during that year, and that this period will be used as an additional control interval of the production facilities. Therefore, the financial model assumes that Commercial operation will start in 2026.
- Equity basis: For economic evaluation purposes, it has been assumed that 100 % of capital expenditures, including pre-production expenses and working capital are financed solely with owner's equity. Given the level of rates of return obtained, considering leverage would further improve these rates of return. This is done later as part of the sensitivity analysis.

22.2 INCOME TAX AND ROYALTIES

The following tax assumptions and criteria have been considered in the project's evaluation:

22.2.1 INCOME TAXES

Chilean Income Tax Law (Ley N° 20.899) sets income tax rate for corporations such as MSB at 27 %. Said law allows for rapidly accelerated depreciation of capital goods. This provision results in losses, for tax purposes, in the early operating phase of project, losses which can be carried forward indefinitely. It has also been assumed that MSB projected total exploration and other capitalized project expenditures before construction, estimated by the company as approximately US\$ 40.8 million, can be used as amortization, once the project starts operations. However, this assumption has not been ratified by legal or tax advisors.

22.2.2 VALUE ADDED TAX (19 % FLAT ON ALL ITEMS)

In the case of long lead projects, such as MSB's, Chilean VAT law allows for direct recovery from the government of VAT paid during the construction period. Additionally, in the case of companies that export all or nearly all their production, they can recover directly from the government VAT paid on all supplies. Considering that there are natural delays involved in this draw back system, the model considers that VAT payments are recovered six months after their payment.

22.2.3 GOVERNMENT ROYALTIES

Given that this project is based on developing exclusively MSB's lithium mining properties registered under the Chilean old mining law, it is MSB's interpretation of the relevant legislation that they are

exempt from any special royalties on lithium carbonate production. In this case, production from these properties would be only subject to royalties under the general mining regime, in which royalties to be paid depend on both the facility's revenue level, and on the relation between lithium carbonate and copper prices. Royalties would amount to approximately US\$ 4.6 million per year⁸. This is equivalent to about 1.2 % of yearly sales.

It should also be mentioned that a project to increase general mining royalties is under discussion in the Chilean Congress. Even though, as of today, nothing has been decided, two ideas are being put forward. The first one is to set a flat 3% royalty on net sales and the second proposition is to set a 5% royalty on Mining Margin⁹. In the case of MSB, using the realizations that result from its production plan and Roskill's projected prices, the second alternative is equivalent to a 2.7% royalty on net sales. In both instances royalties to be paid by MSB would increase substantially. However, as it will be shown in the Project Sensitivity sub section, the impact on the project's profitability, as measured by NPV and IRR, is very minor.

22.2.4 OTHER PAYMENTS

Project expenditures include agreed compensations and contributions to communities in the general vicinity of the project. Also included are the regular payments for the project's mining licenses and permits, as well as water usage fees.

22.3 CAPITAL EXPENDITURES

As indicated in Section 21 and in Table 21-1, capital investment for the MSB project, including equipment, materials, indirect costs and contingencies, during the construction period is estimated to be US\$ 626 million. As also indicated in the same section, working capital requirements are estimated to be US\$ 15.8 million and sustaining capital expenditures total US\$ 42 million, over the horizon of the project. Expected timing of investments is as indicated in Table 22-1.

⁸ Royalties payable have been calculated at the project's expected lithium carbonate prices, and at the World Bank's long term projected real copper price of US\$/lb 3,07.

⁹ Basically, the Mining Margin corresponds to net profit after taxes, excluding interest expense, and calculated with linear depreciation and amortization.

Table 22-1 Capex Schedule

Description	Capex Schedule			
	US\$ 000			
	2023	2024	2025	Total
Brine Wells	12,422	32,298	4,969	49,689
Evaporation Ponds	33,594	87,343	13,437	134,374
Salt Removal	8,247	82,470	74,223	164,940
Lithium Carbonate Plant	4,168	41,678	37,511	83,357
Plant Services	3,765	43,931	77,820	125,516
Infrastructure	3,425	23,974	41,097	68,496
Total	65,621	311,694	249,057	626,372

22.4 LITHIUM CARBONATE PRODUCTION AND RAMP UP

The project's annual production rate is controlled by hydrogeological considerations. These determine a relatively variable annual production rate, in the range of 14,000 TPA to 16,500 TPA, with an average of 15,200 TPA, over the project's expected 20-year life. The economic evaluation considers that 90% of the production is expected to be battery grade lithium carbonate and 10% technical grade lithium carbonate.

Since it is known that the ramp up of lithium carbonate production is a difficult process, it has been assumed that full design capacity production is achieved during the third year of operations. Ramp up of technical grade product is somewhat faster, given its less strict specifications.

Table 22-2 Production Ramp Up (%)

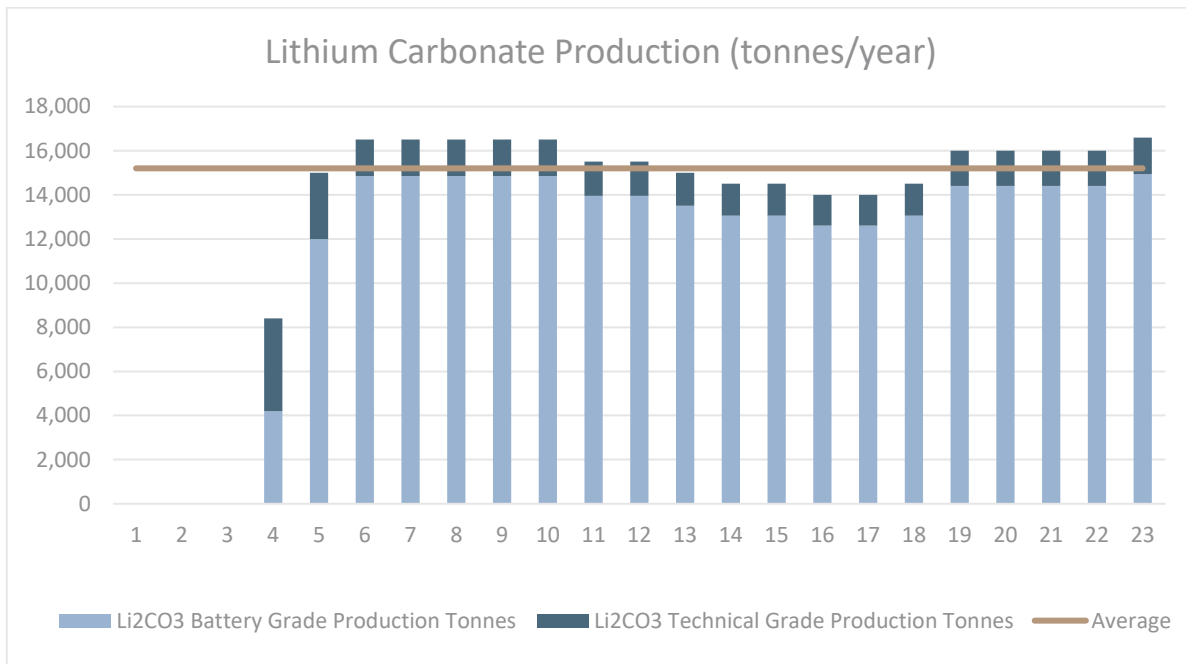
Production Ramp Up % of Average Capacity (15,200 TPA)			
Year	2026	2027	2028
	4	5	6
Battery Grade Ramp Up	50%	80%	90%
Technical Grade Ramp Up	50%	20%	10%

Given the above presented production ramp up table, expected quantities of battery grade and technical grade lithium carbonate to be produced are as follows:

Table 22-3 Li₂CO₃ Production

Selected Years	2026	2027	2028	2032	2036	2037	2042	2045	Total	Average
	4	5	6	10	14	15	20	23		
Li ₂ CO ₃ Battery Grade Production Tonnes	4,200	12,000	14,850	14,850	13,050	13,050	14,400	14,940	268,740	13,437
Li ₂ CO ₃ Technical Grade Production Tonnes	4,200	3,000	1,650	1,650	1,450	1,450	1,600	1,660	35,260	1,763
Total Production	8,400	15,000	16,500	16,500	14,500	14,500	16,000	16,600	304,000	15,200

Figure 22-1 Li₂CO₃ Production



22.5 OPERATING COSTS

As shown in section 21.2.1, Table 21-9, direct operating costs per tonne of lithium carbonate are estimated to be US\$ 3,718. Indirect operating costs are estimated to be US\$ 146 per tonne of lithium carbonate; thus, the total estimated operating cost is US\$ 3,864 per tonne of lithium carbonate.

Table 22-4 Operating Costs

Average Operating Costs	US\$ / Tonne Li ₂ CO ₃	Total 000 US\$
DIRECT COSTS		
Chemical Reactives and Reagents	1,099	16,704
Salt Harvesting	266	4,049
Energy	1,164	17,689
<i>Memo: - Electrical</i>	342	5,206
<i>- Thermal</i>	821	12,483
Manpower	518	7,867
Catering & Camp Services	132	1,999
Maintenance	358	5,443
Transport	181	2,756
OPERATIONAL CASH COSTS	3,718	56,506
INDIRECT COSTS		
General & Administration	146	2,220
INDIRECT COSTS SUBTOTAL	146	2,220
TOTAL PRODUCTION COSTS	3,864	58,726

22.6 PRODUCTION REVENUES

Production revenues result from projected product prices, shown in Figure 19-10, and production quantities, shown in Table 22-3. The production revenues are shown in Table 22-5. It should be mentioned that since Roskill's price projection ends in 2036, MSB assumed that lithium carbonate prices remained constant from that year, until the end of project life in 2045.

Table 22-5 Production Revenues (Selected Years)

Revenues	2026 4	2027 5	2028 6	2032 10	2036 14	2037 15	2042 20	2045 23	Total 000 US\$	Average
Li ₂ CO ₃ Battery Grade	100,218	275,427	347,010	375,201	342,207	342,207	377,608	391,768	6,828,137	341,407
Li ₂ CO ₃ Technical Grade	95,302	69,387	37,843	38,919	35,560	35,560	39,238	40,710	837,799	41,890
Total	195,521	344,814	384,853	414,120	377,767	377,767	416,846	432,478	7,665,936	383,297

22.7 CASH FLOW PROJECTION

The combination of assumptions on investments, revenues, costs, income taxes, royalties, amortization, depreciation, working capital, etc, produces the cash flow projection shown in Table 22-6.

It should be mentioned that the cash flow projection, shown in the above referred table, corresponds to the evaluation base case which, as mentioned, assumes full equity project funding.



Table 22-6 Project Summary Cash Flow Projection

Year	2023	2024	2025	2026	2027	2028	2029	2030	2031	2032	2037	2042	2044	2045	Totals
Period	1	2	3	4	5	6	7	8	9	10	15	20	22	23	
Revenues	-	-	-	195,521	344,814	384,853	389,906	395,987	407,734	414,120	377,767	416,846	416,846	432,478	7,665,936
Li2CO3 Battery Grade	-	-	-	100,218	275,427	347,010	352,806	358,241	369,383	375,201	342,207	377,608	377,608	391,768	6,828,137
Li2CO3 Technical Grade	-	-	-	95,302	69,387	37,843	37,100	37,745	38,351	38,919	35,560	39,238	39,238	40,710	837,799
Cost of Goods Sold	-	-	-	(34,903)	(53,147)	(58,430)	(63,112)	(63,112)	(63,112)	(63,112)	(57,640)	(61,744)	(61,744)	(63,386)	(1,174,520)
OPEX Li2CO3	-	-	-	(34,903)	(53,147)	(58,430)	(63,112)	(63,112)	(63,112)	(63,112)	(57,640)	(61,744)	(61,744)	(63,386)	(1,174,520)
Gross Margin	-	-	-	160,617	291,667	326,423	326,794	332,874	344,622	351,008	320,126	355,102	355,102	369,092	6,491,416
Gross Margin%				82%	85%	85%	84%	84%	85%	85%	85%	85%	85%	85%	85%
Other cash expenses				(2,545)	(7,411)	(8,488)	(7,268)	(7,467)	(7,861)	(8,211)	(7,070)	(8,265)	(8,174)	(30,949)	(170,006)
Current Royalties		-	-	(906)	(4,877)	(5,713)	(4,462)	(4,625)	(4,948)	(5,260)	(4,337)	(5,298)	(5,207)	(5,085)	(91,887)
Eventual Royalties (3% of Sales)		-	-	-	-	-	-	-	-	-	-	-	-	-	-
Communities		-	-	(1,173)	(2,069)	(2,309)	(2,339)	(2,376)	(2,446)	(2,485)	(2,267)	(2,501)	(2,501)	(2,595)	(45,996)
Mining Licenses & Water Rights		-	-	(352)	(352)	(352)	(352)	(352)	(352)	(352)	(352)	(352)	(352)	(352)	(7,040)
Insurance Policy for Rem Allowance - 0,5 %		-	-	(114)	(114)	(114)	(114)	(114)	(114)	(114)	(114)	(114)	(114)	(114)	(2,280)
Remediation		-	-	-	-	-	-	-	-	-	-	-	-	(22,803)	(22,803)
EBITDA	-	-	-	158,072	284,256	317,935	319,526	325,407	336,761	342,797	313,057	346,837	346,928	338,143	6,321,410
- Depreciation	-	-	-	(225,494)	(200,439)	(200,439)	(4,512)	(4,011)	(4,011)	(76)	(1,494)	(3,815)	(4,659)	(4,929)	(671,183)
- Amortization	-	-	-	(40,803)	-	-	-	-	-	-	-	-	-	-	(40,803)
Profit Before Taxes	-	-	-	(108,225)	83,816	117,495	315,014	321,396	332,750	342,721	311,563	343,021	342,269	333,214	5,609,424
Income Taxes (27%)	-	-	-	-	-	(25,133)	(85,054)	(86,777)	(89,843)	(92,535)	(84,122)	(92,616)	(92,413)	(89,968)	(1,514,545)
Profit After Taxes	-	-	-	(108,225)	83,816	92,362	229,960	234,619	242,908	250,186	227,441	250,406	249,856	243,246	4,094,880
+ Depreciation & Amortization	-	-	-	266,297	200,439	200,439	4,512	4,011	4,011	76	1,494	3,815	4,659	4,929	711,986
Operating After Tax Cash Flow	-	-	-	158,072	284,256	292,801	234,472	238,630	246,919	250,262	228,935	254,221	254,515	248,176	4,806,866
Non Operating Cash Flow	(71,855)	(335,071)	(243,107)	10,901	(7,024)	(1,988)	(15,340)	1,191	-	(231)	(1,939)	(4,260)	(5,104)	17,795	(676,526)
Initial Investment and Sustaining Capital	(65,621)	(311,694)	(249,057)	-	-	-	(12,534)	-	-	(211)	(1,899)	(4,220)	(5,064)	(5,064)	(676,045)
VAT on CAPEX and OPEX, net of refunds	(6,234)	(23,377)	5,950	19,627	(2,463)	(668)	(1,636)	1,191	-	(20)	(40)	(40)	(40)	7,424	(481)
Working Capital Variation	-	-	-	(8,726)	(4,561)	(1,321)	(1,171)	-	-	-	-	-	-	15,436	-
Cash Flow Before Interest and Tax	(71,855)	(335,071)	(243,107)	168,973	277,232	315,946	304,186	326,598	336,761	342,566	311,117	342,576	341,824	355,939	5,644,884
Accumulated Cash Flow (Before Interest and Tax)	(71,855)	(406,926)	(650,033)	(481,060)	(203,828)	112,118	416,304	742,902	1,079,663	1,422,229	3,013,042	4,604,934	5,288,945	5,644,884	
Financing cash flow	-	-	-	-	-	-	-	-	-	-	-	-	-	-	-
Before Tax Cash Flow	(71,855)	(335,071)	(243,107)	168,973	277,232	315,946	304,186	326,598	336,761	342,566	311,117	342,576	341,824	355,939	5,644,884
After Tax Cash Flow	(71,855)	(335,071)	(243,107)	168,973	277,232	290,813	219,132	239,821	246,919	250,031	226,996	249,960	249,411	265,971	4,130,340

22.8 ECONOMIC EVALUATION RESULTS

The cash flow projection shown in Table 22-7 results in the following project economic metrics:

Table 22-7 Base Case Economic Results (full equity project funding)

ECONOMIC RESULTS		BEFORE TAXES	AFTER TAXES
NPV 6%	MM US\$	2,529	1,827
NPV 8%	MM US\$	1,971	1,412
NPV 10%	MM US\$	1,545	1,095
IRR	%	33.4%	29.3%
PAYOUT	Time	2 Y, 8 M	2 Y, 8 M

After tax cash flow results from the model can also be visualized in the graphs presented on the following page. These graphs indicate that the project generates substantial positive cash flow from the third year of operations onwards, and cumulative cash flow turns positive before three years have elapsed after the start of operations.

Figure 22-2 Yearly Cash Flow

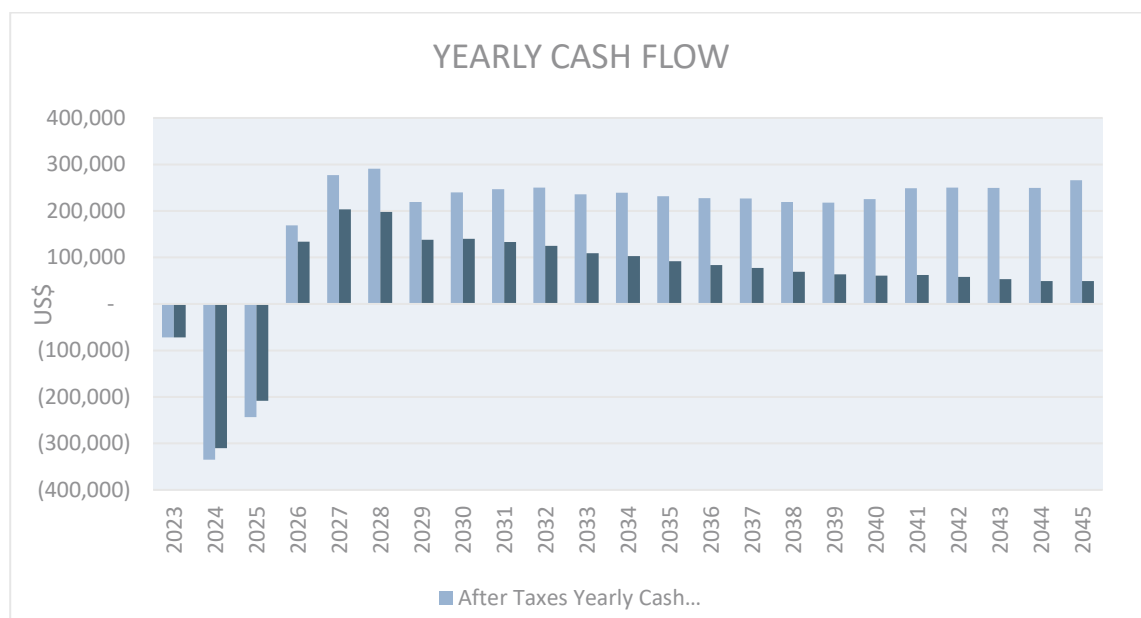
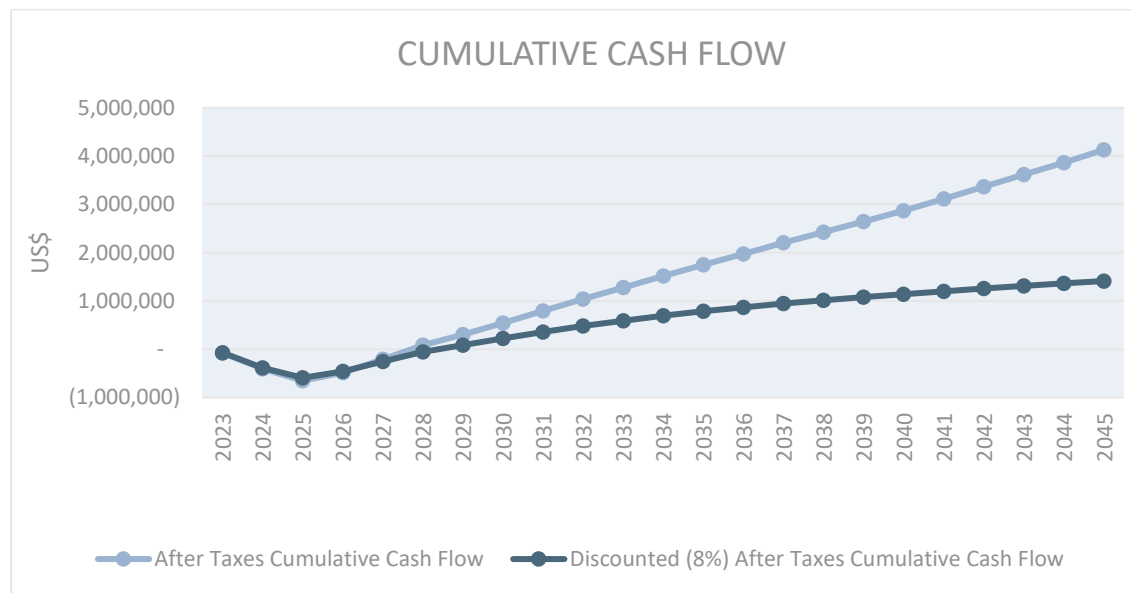


Figure 22-3 Cumulative Cash Flow



22.8.1 PROJECT LIFE

Project life, for evaluation purposes, as well as for environmental and other permit purposes, has been assumed as 20 years. If the authorization to bring into production MSB's additional mining properties¹⁰ is granted then project life might be extended.

22.8.2 SENSITIVITY ANALYSIS

22.8.2.1 IMPACT OF FINANCING ON PROJECT'S OWNER RETURNS

Since in practice, a clear majority of large investment projects, such as MSB's, are financed with a variable mixture of debt and equity. It is very relevant to consider the impact on project owner's return when assuming the project is financed partly on credit.

For this purpose, we have assumed the project receives a loan amounting to slightly less than 50% of its total expenditures during the first three years of construction (US\$ 300 million). This is approximately equivalent to a 50/50 debt to equity ratio, when including capitalized interest during construction and without considering MSB's pre-construction expenditures. Other assumed

¹⁰ We refer to MSB's current law or not grandfathered mining concessions, whose resources are approximately equal to the old law properties.

conditions for the loan include a 6% real annual rate¹¹, loan disbursements roughly equal to MSB's contribution during construction, with repayment over a 10-year period, in equal yearly instalments. While we believe these financial conditions to be realistic for a mining project in Chile, there are no assurances that these conditions will be available in the market for MSB's project.

Table 22-8 Loan Disbursement and Repayment

Description	2023	2024	2025	2026	2027	2028	2029
	1	2	3	4	5	6	7
Beginning of Year Debt	-	20,600	170,236	328,850	303,901	277,455	249,422
Debt Drawdown	20,000	140,000	140,000	-	-	-	-
Yearly Payment	-	-	-	44,680	44,680	44,680	44,680
Amortization (YE)	-	-	-	24,949	26,446	28,033	29,715
Interest	600	9,636	18,614	19,731	18,234	16,647	14,965
Year End Debt	20,600	170,236	328,850	303,901	277,455	249,422	219,707
Financing Cash Flow	20,000	140,000	140,000	(44,680)	(44,680)	(44,680)	(44,680)

Description	2030	2031	2032	2033	2034	2035	Totals
	8	9	10	11	12	13	
Beginning of Year Debt	219,707	188,209	154,822	119,431	81,916	42,151	
Debt Drawdown	-	-	-	-	-	-	300,000
Yearly Payment	44,680	44,680	44,680	44,680	44,680	44,680	446,802
Amortization (YE)	31,498	33,388	35,391	37,514	39,765	42,151	328,850
Interest	13,182	11,293	9,289	7,166	4,915	2,529	117,952
Year End Debt	188,209	154,822	119,431	81,916	42,151	-	
Financing Cash Flow	(44,680)	(44,680)	(44,680)	(44,680)	(44,680)	(44,680)	(146,802)

Considering the above financing conditions, project owner returns are as follows:

Table 22-9 Economic Results (50/50 debt / equity project funding)

ECONOMIC RESULTS		BEFORE TAXES	AFTER TAXES
NPV 6%	MM US\$	2,513	1,811
NPV 8%	MM US\$	1,984	1,425
NPV 10%	MM US\$	1,582	1,131
IRR	%	44.5%	39.6%
PAYOUT	Time	2 Y, 0 M	2 Y, 0 M

As expected, leveraged project returns improve substantially over the unleveraged case.

¹¹ Given that all values in the project are in real terms -this is excluding inflation- assumption of a 6% real interest rate in the evaluation, is equivalent to assuming a 6% plus inflation rate, in nominal terms.

22.8.2.2 SENSITIVITY ANALYSIS - MAIN DRIVERS

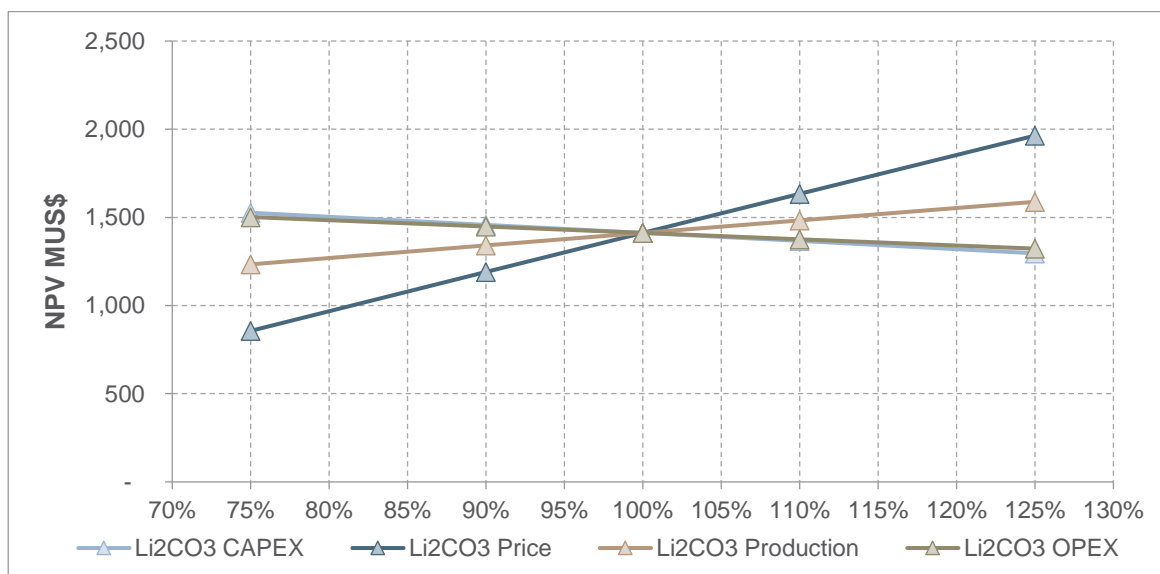
To further investigate the impact on the project's economic results – NPV and IRR – for changes in key variables, a post-tax sensitivity analysis was carried out. This analysis considers separate variations in four project driver variables, these being project CAPEX, Lithium Carbonate prices, production level and project OPEX.

Results of this analysis are presented in the following tables and figures. These show the changes that the project's NPV (8%) and its IRR undergo, when the driver variable -Project CAPEX, lithium carbonate price, project production rate and project OPEX- assumes values equivalent to 75%, 90%, 110% and 125% of their bases case values.

Table 22-10 Project After Taxes – NPV 8% Sensitivity

Driver Variable	Base Case Values		Project NPV (MUS\$)				
			75%	90%	100%	110%	125%
CAPEX	MUS\$	626	1,526	1,458	1,412	1,366	1,296
Price	US\$/tonne	25,217	856	1,191	1,412	1,633	1,964
Production	Tonne/yr	15,200	1,234	1,341	1,412	1,483	1,588
OPEX	US\$/tonne	3,864	1,502	1,448	1,412	1,377	1,323

Figure 22-4 Project After Taxes NPV 8% Sensitivity



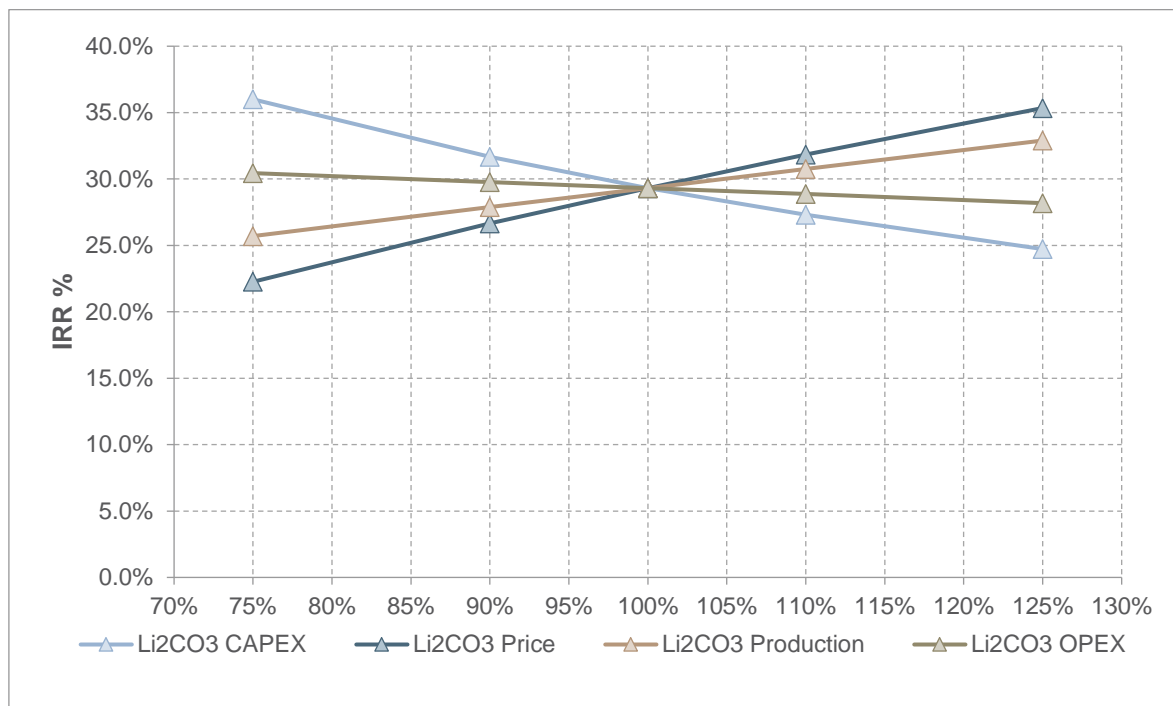
Conclusions that can be drawn from the above table and graph are that -as expected- the project's NPV results are quite sensitive to the price level of lithium carbonate, since a 25% variation in this parameter causes a 39% variation in NPV. The project is less sensitive to variations in the production level, since a 25% variation in this second parameter causes only a 12% variation in NPV.

Maybe contrary to expectations, the project's NPV is very slightly sensitive to variations in CAPEX or OPEX, given that a 25% variation in each of these two parameters translates into, respectively, an 8% and a 6% variation in it.

Table 22-11 Project After Taxes – IRR Sensitivity

Driver Variable	Base Case Values		IRR				
			75%	90%	100%	110%	125%
CAPEX	MUS\$	626	36.0%	31.7%	29.3%	27.3%	24.7%
Price	US\$/tonne	25,217	22.3%	26.7%	29.3%	31.8%	35.3%
Production	Tonne/yr	15,200	25.7%	27.9%	29.3%	30.8%	32.9%
OPEX	US\$/tonne	3,864	30.4%	29.8%	29.3%	28.9%	28.2%

Figure 22-5 Project After Taxes IRR Sensitivity



Conclusions to be drawn from the above table and graph differ somewhat from those mentioned in the case of NPV sensitivity. Thus, while the project's IRR results, again, are very sensitive to the price level of lithium carbonate, they are also quite sensitive to the CAPEX level. Also, the IRR is slightly less sensitive to variations in the production level and quite insensitive to the OPEX level.

The reason why both the NPV and the IRR are relatively insensitive to the OPEX level is that the project's gross margin is so high -it averages 85% over LOM- that relatively high variations in the OPEX (the other 15% in this measure) translate into quite small variations in the gross margin. Thus there is little impact on the project's profitability.

22.8.2.3 SENSITIVITY TO ROYALTY RATE

Since in Section 22.2.3 it is stated that there is some uncertainty in the royalty rate that the project will face in the future, at this point we investigate the project's economic results sensitivity to changes in the royalty rate. In particular MSB estimate the impact on project economic results of two royalty alternatives that have been discussed. Results are presented in the following table:

Table 22-12 Sensitivity to Royalty Rate

PROJECT SENSITIVITY TO ROYALTY RATE				
AFTER TAX RESULTS				
Assumed Royalty Regime	LOM Royalties		NPV 8%	IRR
	as % of Sales	MMUS\$	MMUS\$	%
Base Case - Current Regime	1.20%	91.9	1,412	29.3%
Proposals:				
a) 5 % of Mining Margin	2.61%	200.1	1,378	28.9%
b) 3% of Net Sales	3.00%	230.0	1,371	28.8%

Table 22-12 shows that the project is quite insensitive to the royalty rate. More than doubling the royalty rate, increasing it from 1,20% of sales to 3% of sales, reduces the project's NPV (8%) by 2,9% and the IRR by less than 0,5%.

The overall conclusion of the sensitivity analysis is that the project is quite robust in the face of important changes in its main cost and output parameters. As it may be expected, the only variable that produces significant variations in the project's economic results, is the lithium carbonate price. However, all projections indicate a strong and growing future demand for lithium carbonate.

23. ADJACENT PROPERTIES

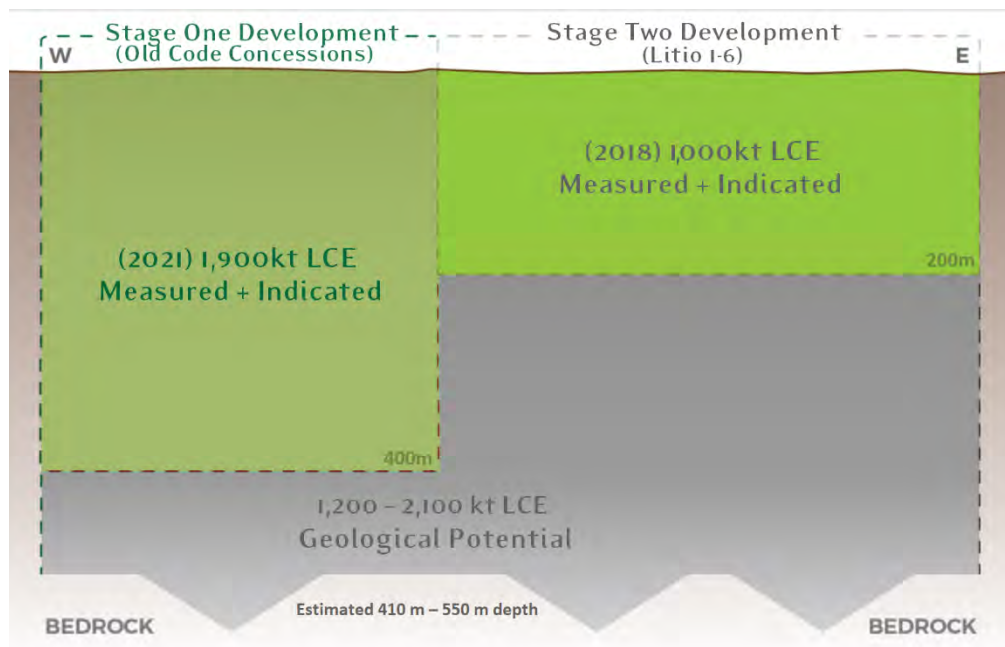
MSB mining concessions (*Litio 1-6, Cocina 19-27, San Francisco, Despreciada and Salamina*) are located in the northern part of Salar de Maricunga. Other adjacent mining concessions in the Salar are held by SQM, Cominor and Codelco. SQM is a major lithium carbonate producer with operations at Salar de Atacama. Codelco is a Chilean government-owned copper producer. Codelco and SQM have not undertaken any significant exploration work on their properties in the Salar. To date no lithium production is taking place from the Salar and the Stage One Project is at the most advanced stage of project evaluation.

24. OTHER RELEVANT INFORMATION

24.1 EXPLORATION POTENTIAL

Measured and Indicated resource have been defined to 400 m depth in the OCC and to 200 m depth in the Litio 1-6 concessions. The geological model for the Project suggests that the same geological units that host the lower brine aquifer below the OCC between 200 and 400 m depth continue below the Litio 1-6 concessions. Geophysical data suggest that the lower aquifer hosted in the Volcanoclastic units and Volcanic breccia continues to the bedrock contact at a variable depth of up to 550 m as shown in Figure 7.11 above. An exploration target is therefore defined below the base of the current M+I Resources in the OCC and Litio 1- 6 concessions to the bedrock contact as shown in Figure 24-1.

Figure 24-1 Schematic of the lithium exploration target



The exploration target is where, based on the available geological evidence, there is the possibility of defining a mineral resource. The timing of any drilling with the objective of defining resources in the exploration target area has not been decided at this stage. In keeping with Clause 18 of the JORC Code and CIM requirements the exploration target defined for the Project is:

- Not to be considered a resource or reserve; and
- Based on information summarized below.

It is a requirement of stating an exploration target that it is based on a range of values, which represent the potential geological conditions. Values have been selected to present an upper and a lower exploration target size. It is likely that the lithium and potassium contained in the exploration target lies somewhere between the Upper and Lower Cases.

The following parameters have been used to estimate an Upper Assumption and Lower Assumption case for lithium:

- The exploration target covers 25.63 km² (2,563 ha) and is limited by the boundaries of the OCC and the Litio 1-6 concessions.
- The depth to the bedrock is interpreted from geophysical data and for the calculation of the exploration target the average thickness of the salar sediments ranges from 410 m in the lower case to 550 m for the upper case.
- An average specific yield of 0.08 has been assigned to the exploration target based on the results of the drainable porosity test work in the same adjacent and overlying hydrogeological units.
- The average lithium concentration is assumed to be 877 mg/l, identical to the average lithium concentration in the OCC between 200 and 400 m depth.

Table 24-1 shows the upper and lower ranges of the resource estimate of the exploration target.

It must be stressed that an exploration target is not a mineral resource. The potential quantity and grade of the exploration target is conceptual in nature, and there has been insufficient exploration to define a Mineral Resource in the volume where the Exploration Target is outlined. It is uncertain if further exploration drilling will result in the determination of a Mineral Resource in this volume.

Table 24-1 Project exploration target estimate

	OLD CODE (400 m to Basement)	LITIO 1-6 (200 m to Basement)	OLD CODE + LITIO 1-6 (Total Potential)
	Li	Li	Li
Upper range			
Area (Km2)	11.25	14.38	25.63
Aquifer volume (km ³)	0.36	5.05	5.41
Mean specific yield (Sy)	13%	8%	8%
Brine volume (km ³)	0.05	0.41	0.45
Concentration (mg/L)	877	877	877
Resource (tonnes)	41,000	357,000	398,000
Lower Range			
Area (Km2)	11.25	14.38	25.63
Aquifer volume (km ³)	0.11	3.02	3.13

Mean specific yield (Sy)	13%	8%	8%
Brine volume (km ³)	0.015	0.24	0.25
Concentration (mg/L)	877	877	877
Resource (tonnes)	13,000	212,000	225,000

Note: Numbers may not add due to rounding

24.2 FUTURE EXPANSION

A future expansion is under evaluation based on the brine coming from the Litio 1-6 mining concessions owned by MSB. Additional drilling as previously recommended in this FS will be required to further increase the existing M+I Resource from 200m depth, to 400m depth, to defined the potential size of a new development (refer to Table 24-1 included in previous point).

The evaluation will also consider the potential use of new technology (Direct Lithium Extraction – DLE) and will benefit from the existing infrastructure that will be part of the Stage One, thus reducing the construction costs and capital needs. Further engineering activities will be required in order to properly test and evaluate the use of new technologies.

Even though the final output of a new project will depend entirely on the resources contained, the technology used and the environmental restrictions that might be applied, based on the Stage One economics, there is a significant value on a subsequent development within the Litio 1-6 mining concessions.

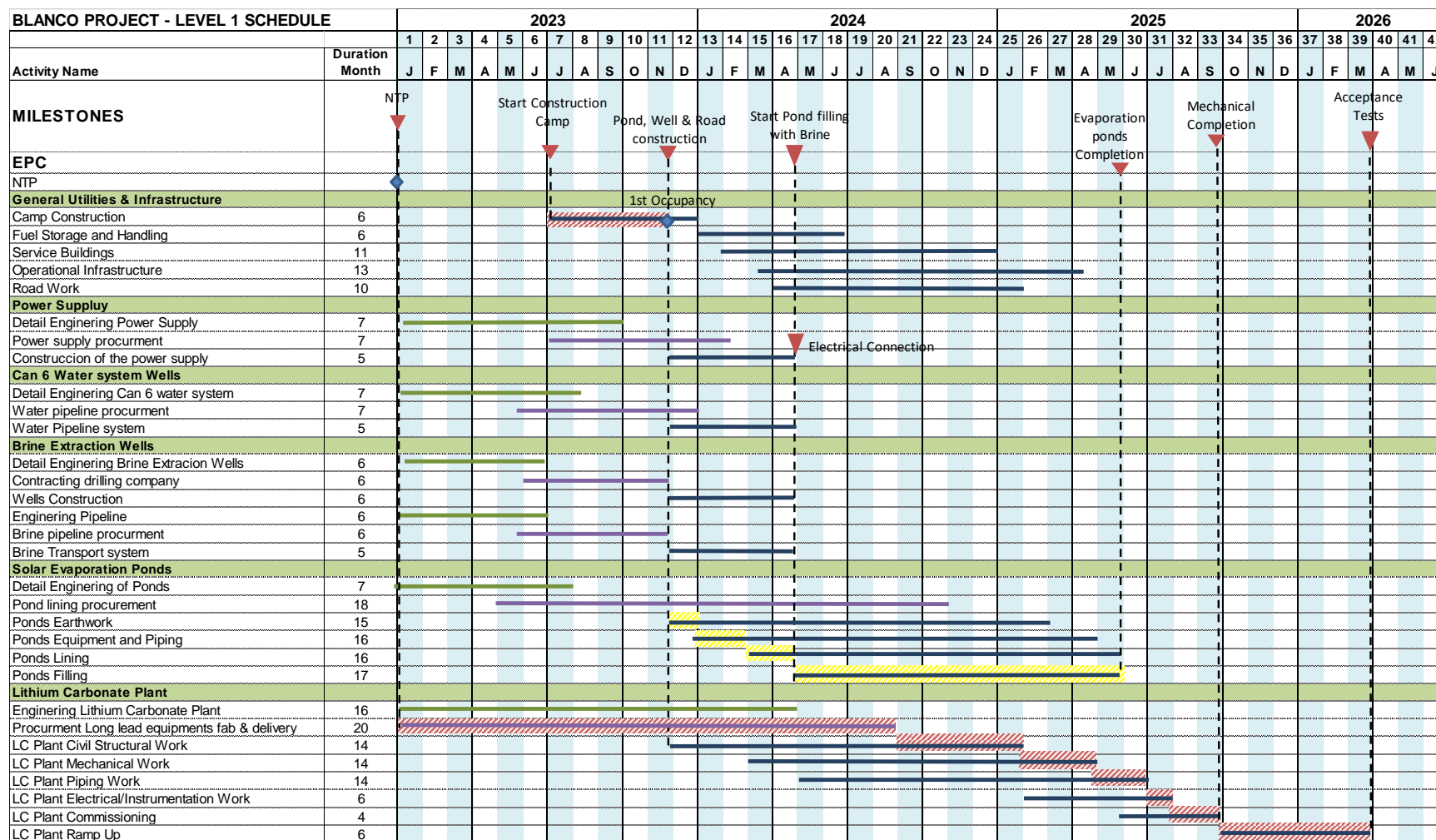
It is noted that a new environmental permit, as well as a new Chilean Nuclear Energy Commission (CCHEN) permit, will be required based on the design, technology used and size of the development. Additionally, a special license (Contrato Especial de Operacion de Litio – CEOL) would be required for the production and sale of lithium from these concessions.

24.3 PROJECT SCHEDULE

Figure 24-2 shows the schedule of the project.



Figure 24-2 Project Execution Schedule



25. INTERPRETATION AND CONCLUSIONS

25.1 HYDROLOGY, RESOURCES AND RESERVE ESTIMATE

Based on the analyses and interpretation of the results of the exploration work carried out for the Stage One Project in Salar de Maricunga between 2011 and 2021, the following concluding statements are prepared:

- The entire Project area has been covered by exploratory drilling between 2011 and 2021 at an approximate borehole density of one exploration borehole per 1.5 km²; it is the opinion of the author that such borehole density is appropriate for the mineral resource estimate described herein.
- The results of drilling 17 sonic and HQ coreholes and 8 rotary/HWT boreholes (all concessions) and the analysis of 718 primary brine samples identify distinct brine composition and grade at specific depth intervals, showing a relatively uniform distribution of lithium bearing brines throughout the OCC to a depth of 400 m. The brine composition for the Project is summarized in Table 25-1.

Table 25-1 Summary of the average brine composition (g/l) and ratios

K g/l	Li g/l	Mg g/l	Ca g/l	SO ₄ g/l	B g/l	Mg/Li	Ca/Li	K/Li
8.14	1.12	7.33	12.85	0.71	0.57	6.53	11.45	7.26

- The lithium bearing brine contains sufficient levels of lithium and potassium to be potentially economic for development.
- The geology in the Project consists of a permeable upper halite brine aquifer with a thickness of up to 34 m in the central part of the Project area. This upper aquifer is underlain for most parts by low permeable lacustrine sediments. Below the lacustrine deposits occurs a lower brine aquifer hosted in relatively permeable sediments consisting of Lower Alluvial sediments, volcanoclastics, a lower sand unit and volcanic breccia. Permeable alluvial fans surround the Salar; these fan deposits at depth grade into the Lower Alluvial deposits that are underlain by the volcanoclastics and lower sand and volcanic breccia.
- The results of four (4) pumping tests and 561 drainable porosity analyses indicate that the specific yield (or drainable porosity) for the Upper Halite unit averages 0.06; sediments of the lower brine aquifer have a drainable porosity between 0.06 to 0.13; and the lacustrine deposits 0.02.
- It is the opinion of the author that the Salar geometry, brine chemistry composition and the specific yield of the Salar sediments have been adequately defined to a depth of 400 m on the OCC to support the Measured and Indicated Resource Estimate described in Table 25-2.

- An exploration target has been identified below the base of the current M+I Resources in the OCC and Litio 1-6 concessions to the bedrock contact with an estimated 1,2 Mt – 2,1 Mt LCE.

Table 25-2 Measured and Indicated Lithium and Potassium Resources of the Stage One Project – ‘Old Code’ Concessions – Dated September 20, 2021

	Measured (M)		Indicated (I)		M+I	
	Li	K	Li	K	Li	K
Area (Km ²)	4.5		6.76		11.25	
Aquifer volume (km ³)	1.8		1.8		3.6	
Mean specific yield (Sy)	0.09		0.12		0.1	
Brine volume (km ³)	0.162		0.216		0.378	
Mean grade (g/m ³)	87	641	111	794	99	708
Concentration (mg/l)	968	7,125	939	6,746	953	6,933
Resource (tonnes)	154,500	1,140,000	203,500	1,460,000	358,000	2,600,000

Notes to the resource estimate:

1. CIM definitions were followed for Mineral Resources.
2. The Qualified Person for this Mineral Resource estimate is Frits Reidel, CPG.
3. No cut-off values have been applied to the resource estimate.
4. Numbers may not add due to rounding.
5. The effective date is September 20, 2021.

Table 25-3 OCC resources expressed LCE and potash

	M+I Resources	
	LCE	KCL
Tonnes	1,905,000	4,950,000

1. Lithium is converted to lithium carbonate (Li₂CO₃) with a conversion factor of 5.32.
2. Potassium is converted to potash with a conversion factor of 1.9
3. Numbers may not add due to rounding

It should be noted that the OCC M+I Resources described in Table 25-2 and 25-3 are in addition to the M+I Resources (2018) of 184 Kt Lithium (979 Kt LCE) in the Litio 1-6 concessions to a depth of 200 m.

A three-dimensional finite element groundwater flow and transport model (FEFLOW code) was constructed and successfully calibrated to steady state pre-mining conditions and to transient pumping test responses. The calibrated model was used to simulate brine production scenarios from the Stage One concessions over a 20-year project life. These simulations form the basis for the Stage One Lithium Mineral Reserve Estimate.

The reserve estimate for the Stage One Project was prepared in accordance with the guidelines of National Instrument 43-101 and uses the best practices methods specific to brine resources. The lithium reserves are summarized in Table 25-4 and Table 25-5.

Table 25-4. Stage One Brine Mining Reserve for pumping to ponds

Category	Year	Brine Vol (Mm3)	Ave Li conc (mg/l)	Li metal (tonnes)	LCE (tonnes)
Proven	1-7	19	1,024	14,000	75,000
Probable	1-7	13		19,000	102,000
Probable	8-20	60	950	57,000	302,000
All	1-20	92	976	90,000	479,000

Table 25-5. Stage One Brine Production Reserve for Lithium Carbonate production (assuming 65% lithium process recovery efficiency)

Category	Year	Brine Vol (Mm3)	Ave Li conc (mg/l)	Li metal (tonnes)	LCE (tonnes)
Proven	1-7	19	1,024	9,000	49,000
Probable	1-7	13		12,000	66,000
Probable	8-20	60	950	37,000	196,000
All	1-20	92	976	58,000	311,000

Notes to the Reserve Estimate:

1. The Stage One Reserve Estimate includes an optimized wellfield configuration and pumping schedule to comply with environmental constraints and water level decline restrictions as part of the environmental approval document (RCA) issued by the Chilean Environmental Agency.
2. Lithium is converted to lithium carbonate (Li_2CO_3) with a conversion factor of 5.32

3. The qualified Person for the Mineral Reserve estimate Frits Reidel, CPG
4. The effective date for the Reserve Estimate is December 22, 2021.
5. Numbers may not add due to rounding effects.
6. Approximately 25 percent of the Measured and Indicated Resources are converted to Proven and Probable Reserves as brine feed from the production wellfield to the evaporation ponds without accounting for the lithium process recovery efficiency. The overall conversion from M+I Resources to Total Reserves including lithium process recovery efficiency of 65% is approximately 16 percent.

25.2 PERMITS

25.2.1 CHILEAN NUCLEAR ENERGY COMMISSION (CCHEN)

MSB was awarded a key regulatory license by the Chilean Nuclear Energy Commission (CChEN) to produce, market and export lithium products from Salar de Maricunga on March 9th, 2018. The CChEN license is for the production of an initial 88,885 t lithium metal or 472,868 t of LCE over a 30year term.

- The permit is limited to the MSB's grandfathered mining concessions This permit allows MSB to request an increase on the initial quota under any of the following conditions:
- The current Indicated and Measured Mineral Resources are increased in grandfathered mining concessions
- The process recovery efficiency exceeds 40%.
- If MSB is awarded Special Operation Contract (CEOL) for the exploitation of lithium from the Litio 1-6 (new code) mining concessions. MSB is currently negotiating this contract with Chilean Government covering these mining concessions, i.e. those registered after 1979.

25.2.2 ENVIRONMENTAL IMPACT ASSESSMENT

MSB received the environmental approval for its Maricunga project on February 4, 2020, by Resolution N°94 considering the construction and operation of both, a 58,000 ton/year Potassium Chloride (KCL) Plant and a 20,000 ton/year Lithium Carbonate plant over a period of 20 years (the KCL plant has not been included in this DFS). The EIA approved a brine extraction of 209 l/s, freshwater extraction of 35 l/s and all associated industrial facilities, including evaporation pond areas, brine pipelines and the campsite. The Environmental Impact Assessment (EIA), prepared by international consulting company Stantec (previously MWH), was submitted to the Chilean

Environmental Assessment Service (SEA¹²) in September 2018 and was the culmination of more than two years of field and desk work.

25.2.3 WATER RIGHTS

MSB has secured the water supply during the construction and operation of the project through a long-term lease agreement for the use of Can-6 water well, that has all the water rights in place. Also, that the use of this water well has been environmentally approved in the EIA.

25.3 ECONOMICS

Based on the engineering and economic analysis of the project the following conclusions are presented:

- The CAPEX for the 15,200 TPY lithium carbonate Stage One Project is US\$ 626 million. This total is higher than for other similar size lithium carbonate projects due to the consideration of a Salt Removal Plant. This is required due to the high calcium content in the brine and with the objective to maintain a consistent and continuous feed to the Lithium Carbonate plant, thus decreasing the operational risk and increasing the overall efficiency. It also must be mentioned that the Salt Removal Plant has the following advantages:
 - It allows ending the solar pond evaporation stage with a comparatively low lithium concentration brine (0.8% to 0.9%), given that in addition to Ca removal, substantial evaporation and concentration takes place at this plant. Thus, if the Salt Removal Plant was not necessary, additional pond area would be required to obtain a concentrated brine suitable for the Lithium Carbonate Plant.
 - It allows recovery of part of the water contained in the brine, thus reducing the total water consumption.
 - It allows extracting impurities (mainly calcium) contained in the brine without the use of chemical reagents.
 - It allows obtaining battery-grade lithium carbonate without adding a CO₂ purification stage.
- Total average unit operating cash cost for the Project is US\$ 3,718 per tonne of lithium carbonate. Again, this is relatively higher than some comparably sized lithium brine projects,

¹² "Servicio de Evaluación Ambiental".

the main reason being the energy cost associated with the Salt Removal Plant, but which has the advantages pointed out in the previous commentary.

- The project's economic results are very positive, with a full equity, after-tax base case that generates, an NPV (8%) of US\$ MM 1,412, an IRR of 29,3 % and pay-out period of 2 years and 8 months. On a pre-tax basis, the NPV (8%) is US\$ MM 1,971, resulting in a 33,4 % IRR. On a levered basis (50:50 debt/equity), after-tax NPV (8%) is US\$ MM 1,425, resulting in a 39.6 % IRR.
- The main reasons for the above results are the favourable outlook for lithium prices, as developed in Section 19, relatively low -27 %- corporate income tax rate in Chile, as well as an expected low royalty rate regime for MSB, due mostly to the special "grandfathered" conditions affecting the OCC mining properties included in the Stage One Project.
- The project's sensitivity analysis carried out in sub section 22.8.2, which examines its results when base case assumptions can deviate from expected values. The outcome of this analysis indicates that the project is sensitive to the expected price of lithium carbonate. In this way, if lithium prices were to be permanently only 75 % of the base case projection, the project's NPV after-tax (8%) declines to US\$ MM 856 and IRR drops to 22,3 %. Conversely, the project's results improve very substantially - NPV after-tax (8%) US\$ MM 1,964 and IRR 35,3 % if lithium prices were to be permanently 125 % of the base case projection.
- The project is less sensitive to variations in the production level, since a 25% variation in this second parameter causes only a 12% variation in NPV. Maybe contrary to expectations, the project's NPV is very slightly sensitive to variations in CAPEX or OPEX, given that a 25% variation in each of these two parameters translates into, respectively, an 8% and a 6% change. This indicates project resilience in the face of possible negative CAPEX or OPEX scenarios.

26. RECOMMENDATIONS

MSB has obtained the main environmental permit that is needed to start the construction and operation of the project. Only several minor permits must be processed before construction.

- Secure the financing of the project for the execution phase. And continue to work on the minor permits for the start of the construction of the project.
- It is recommended that for the project's next stage, a cost reimbursable type EPC (Engineering, Procurement and Construction) contract, with the support of an Owner's Engineer, be considered. Another possible alternative would be an EPCM (Engineering, Procurement and Construction Management) contract. In either case, experience in lithium projects of the engineer/contractor is recommended.
- Continue to work with GEA on a fixed price contract with process warranties, for production of Battery Grade Lithium Carbonate, for the procurement of the equipment.
- Explore if it is feasible to procure from GEA only the Salt Removal plant, while maintaining the associated process guarantee. In this case, arrange the supply of the equipment and construction of the Lithium Carbonate Plant with a local EPC/EPCM contractor since the Lithium Carbonate Plant is a better-known process. This could lead to savings in the CAPEX, but MSB should not under any circumstances jeopardize the quality of the final product, Battery Grade Lithium.
- Continue immediately, after this basic engineering, with the detail engineering of the evaporation ponds. This does not represent a significant cost but can reduce the time to have concentrated brine for forced evaporation plant while it is developing a detail engineering for plants.
- Prioritise obtaining permits to modify the course of Highway C-13, given that solar evaporation pond construction is the most critical element in the project's construction plan and whose current routing runs through the project's pond farm.
- Given the very large pond surfaces that need to be covered with plastic liner, enter as soon as possible into a production contract with a reputable supplier of this critical material. Considering that it may be possible that one, or more, additional lithium brine projects might be under construction at the same time, straining plastic liner production capacity.
- Carry out a Detail Engineering Optimization in the project plant layout to minimize construction cost.
- In keeping with the PEA study recommendation, postpone the investment in a KCl plant for a few years, reconsidering the decision to build it, if there is a clear improvement in the expected long-term pricing outlook.

- The Maricunga Salar is a mid-size salar and the mineral property in the salar is divided among four large holders (MSB being the one of the largest) and many other small holders. There will, therefore, be a material advantage to the party that is able to progress its project faster, because the resource of the Salar might not support another competitively sized lithium carbonate plant. Thus, if MSB can proceed quickly with this project, it may become “dominant” in the salar and might be in a position to acquire additional resources at favourable conditions.
- Explore the replacement of thermal energy by electrical renewable energy supply.
- To evaluate the increase of the power line capacity for the use of electrical boilers in the Salt Removal Plant.

26.1 ENERGY EXPENSES AND COGENERATION

The project’s energy expenses total approximately US\$ 17.2 million per year. Out of this total, US\$ 12.5million corresponds to Diesel fuel used to generate steam required at the Salt Removal Plant. This represents over 20 % of the project’s cash operating costs. For this reason, it is very important to try to reduce this cost. In theory, the simplest way to achieve this purpose may be to switch the boilers to residual fuel oil, which is more complicated to handle than Diesel, and would surely require heating at Maricunga, but considerable savings could still be possible. However, given the additional emissions that this solution entails, the proposed change in the type of fuel would require an amendment to the project’s approved EIA. Thus, the latter may not be advisable to present to the authorities, at this time.

As recommended in the project’s PEA, MSB carried out an economical evaluation into cogeneration. In this process, electricity and steam are produced jointly. This study concluded that the cogeneration alternative was not profitable. This, mainly due to the need of high energy steam in the salt removal plant, which requires that additional fuel be used in the boiler, over and above that required to produce electricity, thus partially negating the cogeneration advantage. Prices of electrical energy in the north of Chile have dropped substantially due to the plentiful availability of solar power, a situation that is not expected change in the short and medium term, making cogeneration difficult to justify.

Finally, given the project’s location, solar steam generation could be an attractive new technology to be investigated, in the future.

27. REFERENCES

- Brüggen, J. 1950. Fundamentos de la Geología de Chile. Instituto Geográfico Militar (Chile), 378 p.
- CORFO (1982): Informe Prospección Preliminar salar de Maricunga; Comité de Salas Mixtas CORFO, Santiago, Chile.
- Cornejo, P., Mpodozis, C., Ramírez, C., y Tomlinson, A., 1993a. Estudio geológico de la región de Potrerillos y El Salvador (26°–27° lat. S): Santiago, Reporte registrado, IR-93–01, 2 volúmenes, 12 mapas escala 1:50000, Servicio Nacional de Geología y Minería.
- Cornejo, P., y Mpodozis, C., 1996. Geología de la región de Sierra Exploradora (25°–26° Lat. S): Santiago, Chile, Reporte registrado, IR-96–09, 2 volúmenes, 8 Mapas, escala 1:50000, Servicio Nacional de Geología y Minería.
- Cornejo, P., Mpodozis, C., y Tomlinson, A., 1998. Hoja Salar de Maricunga: Santiago, Servicio Nacional de Geología Minería, Mapa Geológico N°7, escala 1:100000.
- Dirección General de Aguas, (DGA) 1987. Balance Hídrico de Chile.
- DGA, 2006, Análisis de la Situación Hidrológica e Hidrogeológica de la Cuenca del Salar de Maricunga, III Región. DGA, Departamento de Estudios y Planificación (2006). S.D.T. N° 255.
- DGA, 2009, Levantamiento hidrogeológico para el Desarrollo de Nuevas Fuentes de Agua en Areas Prioritarias de la Zone Norte de Chile, Regiones XV, I, II, y III. Etapa 2 Sistema Piloto III Region Salares de Maricunga y Pedernales. Realizado por Departamento de Ingenieria Hidraulica y Ambiental Pontificia Universidad Catolica de Chile (PUC). SIT No. 195, Noviembre 2009.
- EDRA, 1999, Hidrogeología Sector Quebrada Piedra Pómez- Placer Dome
- Ehren-Gonzalez Limitada, 2015: Salar de Maricunga Desktop Study, Update of May, 2014 report, prepared for Minera Salar Blanco SPA, October, 2015
- Atacama Water, 2015a: Proyecto Blanco, Programa 2015, Presentación de resultados, Septiembre 16, 2015
- Atacama Water, 2015b: Proyecto Blanco, Informe Técnico: Programa de Pruebas de Bombeo 2015, Análisis y Resultados
- Gabalda G., Nalpas T. y Bonvalot S., 2005. Base of the Atacama Gravels Formation (26°S, Northern Chile): first results from gravity data. ISAG YI, Barcelona.
- García, F. 1967. Geología del Norte Grde de Chile. In Symposium sobre el Geosinclinal Yino No. 3, Sociedad Geológica de Chile: 138 p.

Gardeweg, M., Mpodozis, C., Clavero, J., y Cuitiño, L., 1997. Mapa Geológico de la Hoja Nevado Ojos de Salado, Región de Atacama, escala 1:100000: Santiago, Servicio Nacional de Geología y Minería.

Golder Associates, 2011, Línea Base Hidrogeológica y Hidrológica Marte Lobo y Modelo Hidrogeológico Ciénaga Redonda – Kinross Gold Corporation.

González-Ferrán, O., Baker, P.E., y Rex, D.C., 1985. Tectonic-volcanic discontinuity at latitude 27° south, Yean Range, associated with Nazca plate subduction: *Tectonophysics*, v. 112, p. 423–441.

Hartley, A.J., May, G., 1998. Miocene Gypcretes from the Calama Basin, northern Chile. *Sedimentology* 45, 351–364.

Houston, J., 2006. Evaporation in the Atacama desert: An empirical study of spatio-temporal variations and their causes. *Journal of Hydrology*, 330:402–412.

Houston, J., Butcher, A., Ehren, P., Evans, K., Godfrey, L. 2011. The Evaluation of Brine Prospects y the Requirement for Modifications to Filing Styrads. *Economic Geology*, v. 106, pp. 1225–1239.

Isacks, B.L. 1988. Uplift of the Central Yean plateau y bending of the Bolivian orocline. *Journal Geophysical Research*, Vol. 93: 3211–3231.

Iriarte D., Sergio., 1999, Mapa hidrogeológico de la cuenca Salar de Maricunga: sector Salar de Maricunga, Escala 1:100.000, Región de Atacama. Nº Mapa: M62. SERNAGEOMIN, 1999.

Iriarte, S, Santibáñez, I y Aravena, 2001. Evaluation of the Hydrogeological Interconnection between the Salar de Maricunga and the Piedra Pomez Basins, Atacama Region, Chile; An Isotope and Geochemical Approach

Kay, S.M., Coira, B., y Viramonte, J., 1994. Young mafic back-arc volcanic rocks as indicators of continental lithospheric delamination beneath the Argentine Puna plateau, central Andes: *Journal of Geophysical Research*, v. 99, p. 24,323–24,339.

Kay, S.M., y Mpodozis, C., 2002. Magmatism as a probe to the Neogene shallowing of the Nazca plate beneath the modern Chilean fl at-slab: *Journal of South American Earth Sciences*, v. 15, p. 39–59.

Kay, S.M., y Copely, P., 2006. Early to middle Miocene back-arc magmas of the Neuquén Basin of the southern Andes: Geochemical consequences of slab shallowing y the westward drift of South America, en Kay, S.M. y Ramos, V.A., eds., *Evolution of an Yean margin: A tectonic y magmatic perspective from the Andes to the Neuquén Basin (35°–39°S lat.)*: Geological Society of America Special Paper 407, p. 185–213.

Lara L, Godoy E, 1998. Hoja Chañaral-Diego de Almagro, III Región de Atacama: Santiago, Chile. Servicio Nacional de Geología y Minería, Mapas Geológicos, escala 1:100000.

Mercado, M., 1982. Hoja Laguna del Negro Francisco, Región de Atacama: Servicio Nacional de Geología y Minería, Carta Geológica de Chile, N° 56, p. 73.

Mortimer, c., 1980. Drainage evolution of the Atacama Desert of northernmost Chile. *Revista Geológica de Chile*, no. II, p. 3-28

Moscoso, R., Maksaev, V., Cuitiño, L., y Díaz, F., Koeppen, R., Tosdal, R., Cunningham, C., McKee, E., y Rytuba, J., 1993. El complejo volcánico Cerro Bravos, región de Maricunga, Chile: Geología, alteración hidrotermal y mineralización, in *Investigaciones de Metales Preciosos en el complejo volcánico neógeno-cuaternario de los Andes Centrales: Bolivia*, Servicio Geológico, Banco Interamericano de Desarrollo, p. 131–165.

Mpodozis, C., Cornejo, P., Kay, S.M., y Tittler, A., 1995. La Franja de Maricunga: Síntesis de la evolución del frente volcánico oligoceno-mioceno de la zona sur de los Andes Centrales: *Revista Geológica de Chile*, v. 22, p. 273–314.

Mpodozis, C., y Clavero, J., 2002. Tertiary tectonic evolution of the southwestern edge of the Puna Plateau: Cordillera Claudio Gay (26°–27°S): Toulouse, *Proceedings of Fifth International Symposium on Yean Geodynamics*, p. 445–448.

Muntean, J.L., y Einaudi, M.T., 2001. Porphyry-epithermal transition: Maricunga belt, northern Chile: *Economic Geology y the Bulletin of the Society of Economic Geologists*, v. 96, p. 743–772.

Nalpas, T.; Dabard, M-P.; Ruffet, G.; Vernon, A.; Mpodo-zis, C.; Loi, A.; Hérail, G. 2008. Sedimentation y preservation of the Miocene Atacama Gravels in the Pedernales-Chañaral Area, Northern Chile: *Climatic or tectonic control? Tectonophysics* 459: 161-173.

Risacher, Alonso y Salazar, *Geoquímica de Aguas en Cuencas Cerradas: I, II y III Regiones de Chile, Volumen I, Síntesis. S.I.T N° 51, Convenio de Cooperación DGA – UCN – IRD*, 1999.

Risacher, F., Alonso, H. and Salazar, C. 2003. The origin of brines and salts in Chilean Salars: a hydrochemical review. *Earth Science Reviews*, 63: 249-293.

Riquelme, R., 2003. Evolution geomorphologique neogene de Andes Centrales du Desert d'Atacama (Chili): interaction tectonique-climat, Ph.D. Thesis, Université Paul Sabatier (Toulouse, France) y Universidad de Chile (Santiago, Chile), 258 p.

SRK Consulting, 2011, Hidrogeología Campo de Pozos Piedra - Compania Minera Casale.

Sillitoe, R.H., Mortimer, C; y Clark, A.H., 1968. A chronology of lyform evolution y supergene mineral alteration, southern Atacama Desert, Chile. *Institute of Mining y Metallurgy Transactions*, v. 77, p.

Sillitoe, R.H., McKee, E.H., y Vila, T., 1991. Reconnaissance K-Ar geochronology of the Maricunga gold-silver belt, northern Chile: *Economic Geology y the Bulletin of the Society of Economic Geologists*, v. 86, p. 1261–1270.

Tassara, A. 1997. Geología del Salar de Maricunga, Región de Atacama. Servicio Nacional de Geología y Minería (SERNAGEOMIN). Informe Registrado IR-97-10.

Tomlinson, A., Mpodozis, C., Cornejo, P., Ramirez, C.F., y Dimitru, T., 1994, El sistema de Fallas Sierra Castillo-Agua Amarga: Transpresión sinistral Eocena en la Precordillera de Potrerillos-El Salvador: Congreso Geológico Chileno VII, Actas, v. 2, p. 1459–1463.

Tomlinson, A., Cornejo, P., y Mpodozis, C., 1999, Hoja Potrerillos, Región de Atacama: Santiago, Servicio Nacional de Geología y Minería, Mapa Geológico no. 14, escala 1:100000.

Venegas, M.; Iriarte, S. y Aguirre, I., 2000, Mapa hidrogeológico de la Cuenca Salar de Maricunga: sector Ciénaga Redonda, escala 1:100.000, Región de Atacama. N° Mapa: M65. SERNAGEOMIN, 2000.

Vila, T., y Sillitoe, R.H., 1991, Gold-rich porphyry systems in the Maricunga belt, northern Chile: *Economic Geology y the Bulletin of the Society of Economic Geologists*, v. 86, p. 1238–1260.

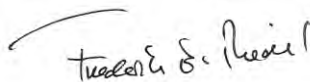
Zentilli, M., 1974, Geological evolution y metallogenetic relationships in the andes of northern Chile between 26° y 29° south. Kingston, Ontario, Queen's University.

Qualified person Frederik Reidel

I, Frederik Reidel, CPG, as author of this report entitled "NI 43-101 Technical Report: Definitive Feasibility Study Update Minera Salar Blanco Lithium Project Stage One, Atacama Region Chile", prepared for Minera Salar Blanco S.A., dated January 07, 2022 do hereby certify that:

1. I am employed as Principal Hydrogeologist and General Manager by Atacama Water-Chile, residing at Badajoz 45, OF 1701, Las Condes, Santiago, Chile.
2. I am a graduate of New Mexico Institute of Mining and Technology with a Bachelors of Science Degree in Geophysics, 1986
3. I am registered a Certified Professional Geologist (#11454) with the American Institute of Professional Geologists
4. I have worked as hydrogeologist for more than 30 years since my graduation. My relevant experience for the purpose of the Technical Report is:
 - Qualified Person for the Sal de los Angeles Project, Salta Argentina for LiX Energy Corp 2016 – to date).
 - Qualified Person and Member of the technical committees of Li3 Energy Ltd and Minera Salar Blanco for the development of the Maricunga Lithium Project in Chile (2011 – to date).
 - Co-author of the NI 43-101 Technical Report on the lithium and potash resources in Salar de Maricunga for Li3 Energy Ltd (2012).
 - Evaluation of lithium and potash resources in Salar de Olaroz for Orocobre Ltd. in support of the project's DFS and NI 43-101 Technical Report (2010-2011).
 - Evaluation of lithium and potash resources in Salar de Cauchari for Lithium Americas Corporation; NI 43-101 Technical Report preparation; member of the company's Technical Advisory Panel (2009-2010).
 - Evaluation of brine resources in Salar de Hombre Muerto for FMC (1992-1993)
 - Consulting hydrogeologist in the evaluation and development of groundwater resources for international mining companies in North- and South America (1989-2012).
5. I have read the definition of "qualified person" set out in National Instrument 43-101 (NI 43-101) and certify that by reason of my education, affiliation with a professional association (as defined in NI 43-101) and past relevant work experience, I fulfil the requirements to be a "qualified person" for the purposes of NI 43-101.
6. I have visited the Salar de Maricunga and the Project area numerous times between August 2011 and to date. I was present on site on a regular basis during the 2011 - 2021 drilling and testing programs.
7. I have been involved as a QP with the property since 2011.
8. I am responsible for the overall preparation of this report.
9. I am independent of the Issuer applying the test set out in Section 1.4 of NI 43-101.
10. I have read NI 43-101, and the Technical Report has been prepared in compliance with NI 43-101 and Form 43-101F1.
11. To the best of my knowledge, information, and belief, the Technical Report contains all scientific and technical information that is required to be disclosed to make the technical report not misleading.

Dated this 7th of January of 2022.



Frederik Reidel, CP

Qualified person Marek Dworzanowski

I, Marek Dworzanowski, CEng, as author of this report entitled “NI 43-101 Technical Report: Definitive Feasibility Study Update Minera Salar Blanco Lithium Project Stage One, Atacama Region Chile” and dated the 07th January 2022 (the “**Technical Report**”), do hereby certify that:

1. I am employed as an independent consulting metallurgical engineer, residing at Les Chenes, Lieu dit Langlade, 82110, Trejoux, France
2. I am a graduate of the University of Leeds with a Bachelors of Science Degree with honours in Mineral Processing, 1980
3. I am registered as a Chartered Engineer (CEng) with the Engineering Council of the United Kingdom, registration number 357983
4. I am an Honorary Fellow of the Southern African Institute of Mining and Metallurgy (HonFSAIMM), membership number 19594
5. I am a Fellow of the Institute of Materials, Minerals and Mining (FIMMM), membership number 485805
6. I have worked as a metallurgical engineer for more than 40 years since my graduation. My relevant experience for the purpose of the Technical Report is:
 - QP for the Minera Salar Blanco PEA for Proyecto Blanco in Chile in 2017;
 - QP for Millennial Lithium PEA for the Pastos Grandes Project in Argentina in 2018;
 - QP for Advantage Lithium PEA for the Cauchari Project in Argentina in 2018;
 - QP for the Minera Salar Blanco FS for Proyecto Blanco in Chile in 2018;
 - QP for Millennial Lithium FS for the Pastos Grandes Project in Argentina in 2019;
 - QP for Advantage Lithium PFS for the Cauchari Project in Argentina in 2019;
 - QP for Standard Lithium PEA for the Lanxess Smackover Project in the USA in 2019;
 - QP for Centaur Resources PEA for Proyecto Pacha in Argentina in 2019;
 - QP for Lithium Americas FS for the Cauchari-Olaroz Project in Argentina in 2020;
 - QP for NeoLithium FS for the Tres Quebradas Project in Argentina in 2021
7. I have read the definition of "qualified person" set out in National Instrument 43-101 (NI 43-101) and certify that by reason of my education, affiliation with a professional association (as defined in NI 43-101) and past relevant work experience, I fulfill the requirements to be a "qualified person" for the purposes of NI 43-101.
8. I have visited the Salar de Maricunga and the Project area in August 2017.
9. I have been involved as a QP with the project since 2017.
10. I am responsible for the preparation of Chapters 1, 2, 3, 18, 19, 20, 21, 22, 24, 25 and 26 of this report.
11. I am independent of the Issuer applying the test set out in Section 1.4 of NI 43-101.
12. I have read NI 43-101, and the Technical Report has been prepared in compliance with NI 43-101 and Form 43-101F1.
13. To the best of my knowledge, information, and belief, the Technical Report contains all scientific and technical information that is required to be disclosed to make the technical report not misleading.

Dated this 7th day of January 2022.



Marek Dworzanowski QP
CEng, BSc(Hons), HonFSAIMM, FIMMM

Qualified person Peter Ehren

I, Peter Ehren, MSc., AusIMM (CP = Chartered Professional), as author of chapter 13 “Mineral Processing and Metallurgical Testing and chapter 17 “Recovery Methods” of this report entitled “NI 43-101 Technical Report: Lithium Resources Update, Blanco Project- ‘Old Code’ Concessions, III Region Chile, prepared for Minera Salar Blanco S.A., dated January 7th, 2022, do hereby certify that:

1. I am an independent consultant and owner of Ehren-González Limitada at Alberto Arenas 4005 112, La Serena, Chile
2. I graduated with a Master of Science Degree in Mining and Petroleum Engineering, with a specialization in Raw Materials Technology and Processing Variant at the Technical University of Delft, The Netherlands in the year 1997
3. I am an independent consultant, a Member of the Australasian Institute of Mining (AusIMM) and metallurgy and a Chartered Professional of the AusIMM.
4. I have practiced my profession for 25 years.
5. I have read the definition of “qualified person” set out in National Instrument 43-101 (“NI 43-101”) and certify that by reason of my education and past relevant work experience, I fulfill the requirements to be a “qualified person” for the purposes of NI 43-101. This report is based on my personal review of information provided by the Issuer and on discussions with the Issuer’s representatives. My relevant experience for the purpose of this report is:
 - 1997 Final Thesis of MSc.degree: “Recovery of Lithium from Geothermal Brine, Salton Sea”, BHP Minerals, Reno Nevada.
 - 1998-2001 Process Engineer, Salar de Atacama, SQM
 - 2001-2006 R&D Manager, Lithium and Brine Technology, SQM.
 - 2006 Process Project Manager, SQM
 - 2007 till date Independent Lithium and Salt Processing Consultant, Ehren-González Limitada

I have previously been involved in the several brine resource projects, where under:

- Salar de Olaroz for Orocobre, Argentina (2009-2019)
 - Salar de Cauchari for Advantage and Orocobre, Argentina (2010-2019)
 - Salar Salinas Grandes for Orocobre, Argentina (2010-2013)
 - Salar de Maricunga for Li3 Energy and Minera Salar Blanco, Chile (2011-2019)
 - Salar de Atacama and Silver Peak for Albermarle, Chile (2014 - 2016)
 - Rann of Kutch, Archean Group, India (2015)
 - Lake Mackay, Agrimin, Australia (2014-2016)
 - Salar Pastos Grandes, Argentina (2018-2019)
7. The latest site visit was for the duration of 2 days in the September, 2019.
 8. I am independent of Lithium Power International and Lithium Bearing.
 9. I have not had prior involvement with the properties that are the subject of the Technical Report.
 10. As of the date of this certificate, to the best of my knowledge, information and belief, the technical report contains all scientific and technical information that is required to be disclosed to make the technical report not misleading.
 11. I am independent of the issuer applying all of the tests in section 1.5 of National Instrument 43-101.
 12. I have read National Instrument 43-101 and Form 43-101F1, and the Technical Report has been prepared in compliance with that instrument and form.
 13. I consent to the filing of the Technical Report with any stock exchange or other regulatory

authority and any publication by them for regulatory purposes, including electronic publication in the public company files on their websites accessible by the public, of the Technical Report.

Dated 7th of January 2022



Peter Ehren, AusIMM (CP)

APPENDIX 1

Philippi
Prietocarizosa
Ferrero DU
&Uría

Santiago, Chile, September 2021

Minera Salar Blanco S.A.

ATT: Mr. Cristóbal García-Huidobro
(the "Recipient")

Dear Sirs,

This opinion (the "Opinion") is delivered to Minera Salar Blanco S.A. ("MSB" or the "Company") in connection with the Maricunga project (the "Maricunga Project") in Chile.

We have acted as counsel to MSB in connection with the negotiation, execution and delivery of several agreements and instruments related thereto, as well as the proceedings for granting of new mining properties.

It is noted that the Mining Exploration Concessions (*Concesiones de Exploración*), Mining Exploitation Concessions (*Pertenencias*), whether fully granted or still under procedure (*pedimentos* or *manifestaciones*) are indistinctly and collectively referred to herein as the "Mining Concessions". The Mining Exploitation Concessions subject to the Old Mining Chilean Legislation of 1932 are referred hereinbelow as the "Old Legislation Concessions" and the Mining Exploitation Concessions subject to the Current Mining Chilean Legislation of 1983 as the "1983 Exploitation Concessions".

To deliver the present Opinion we have examined originals, certified copies or otherwise of the documents and/or have reviewed the relevant registrations in the corresponding Registries, relating to the Mining Concessions applied for by, granted to, and transferred to MSB, as applicable.

Where our Opinion relates to our knowledge, that knowledge is based solely upon our examination of the records, documents, instruments, and certificates listed or described above and the actual contemporaneous knowledge of attorneys in this firm who are currently involved in legal representation of MSB in connection with the Maricunga Project.

Subject to the foregoing, we are of the Opinion that:

1. MSB has been duly incorporated and is a validly existing company under the laws of Chile and is in good standing.
2. The statutory capital of the Company is CH\$ 52,568,795,484 divided into 4,431,705,749 nominatives shares (the "Shares"), all of the same class and value.
3. The Shares have been fully subscribed as follows:

Philippi
Prietocarizosa
Ferrero DU
&Uría

Shareholder	Shares and Stake
Lithium Power Inversiones Chile SpA	2,284,535,868 equivalent to 51.55%
Minera Salar Blanco SpA	1,387,726,646 equivalent to 31.31%
Li 3 Energy Inc.	759,443,235 equivalent to 17.14%
Total	4,431,705,749 – 100.00%

4. MSB has all necessary corporate faculties and authority to carry on its business as now conducted by it and to own its properties and assets.
5. MSB is duly licensed to carry on its business in Chile.
6. The Company currently has a portfolio of 35 Mining Exploitation Concessions, as follows:
 - 4 Old Legislation Concessions (*pertenencias*)
 - 31 1983 Exploitation Concessions (*pertenencias*)
7. All titles of the Mining Concessions set out on **Schedule A** are in good standing.
8. Pursuant to the Old Mining Chilean Legislation, MSB is entitled to explore and exploit lithium in the Old Legislation Concessions, fulfilling all legal requirements provided by the Chilean legislation.

The 1983 Exploitation Concessions do not allow to explore nor exploit lithium, unless a Special Operation Contract for Lithium (*Contrato Especial de Operación del Litio* “CEOL”) is obtained, but do permit the exploration and exploitation of any other mining substances, whether metallic or non-metallic, for example potassium, where lithium may be a sub product. In other words, the 1983 Exploitation Concessions, do not entitle to appropriate the extracted lithium, but only other concessible substances.
9. According to the legal documentation reviewed, the Mining Concessions are valid and in force.
10. The Mining Concessions have no marginal records evidencing mortgages, encumbrances, prohibitions, interdictions or litigations.
11. The Mining Concessions have all their mining licenses duly paid.
12. Except for the Blanco I 31 1/60; Blanco I 32 1/60; Blanco I 33 1/60; Blanco I 34, 1/60; and Blanco I 35 1/60 Mining Concessions; all the Mining Concessions have preferential rights over the relevant area comprised by them and there is no mining concession nor

Philippi
Prietocarrizosa
Ferrero DU
& Uria

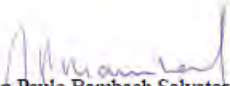
mining rights held or filed by third parties challenging the rights and preference of the Mining Concessions.

Third parties' rights over the aforementioned Blanco properties are shown (hatched areas) in the mining cadaster prepared by Landman Services and attached to this Opinion as **Schedule B**.

The foregoing opinions are subject to the following additional qualifications:

1. This Opinion does not refer to nor comprise any information or conclusion on the geologic potentiality of the Mining Concessions, technical matter which is beyond the scope of our review.
2. We are attorneys duly qualified to practice law in Chile and we express no opinion herein as to any laws other than the laws of Chile as in effect on the date hereof and thereof any references to applicable law and approvals are limited to the applicable laws of Chile and approvals by Governmental Agencies of Chile.
3. This Opinion is solely for the benefit of MSB and may not be relied upon or used by, circulated, quoted or referred to, nor may copies be delivered to any other person, without our prior written approval.
4. This Opinion is effective only as of the date hereof. We expressly disclaim any responsibility to advise you of any development or circumstance of any kind, including any change of law or fact that may occur after the date of this letter even though such development, circumstance or change may affect the legal analysis, a legal conclusion or any other matter set forth in or relating to this letter. Accordingly, any person relying on this letter at any time after the date hereof should seek advice of its counsel as to the proper application of this letter at such time.

Very truly yours,



Juan Paulo Bambach Salvatore
Philippi Prietocarrizosa Ferrero DU & Uria

Schedule A Mining Concessions

1. MSB is the sole and exclusive owner of the following mining concessions:

a. Old Legislation Concessions:

Exploitation Concessions	Holder	Granting Registration					Property Registration				
		Folio	N°	Year	Registrar		Folio	N°	Year	Registrar	Surface
1 COCINA 10/27 (19/27)	MSB	392	150	1937	Copiapó		2070	575	2016	Copiapó	450
2 SAN FRANCISCO 1/10	MSB	72	56	1945	Copiapó		331 ov.	91	2017	Copiapó	425
3 DESPRECIADA 6/7	MSB	22 ov.	12	1950	Copiapó		329	89	2017	Copiapó	100
4 SALAMINA	MSB	66	32	1954	Copiapó		330 ov.	90	2017	Copiapó	150

2. MSB is also the owner of the following 1983 Exploitation Concessions:

Exploitation Concessions	Holder	Granting Registration					Property Registration				
		Folio	N°	Year	Registrar		Folio	N°	Year	Registrar	Surface
1 LITIO 1/1/29	MSB	478 ov.	158	2004	Copiapó		1234 ov	332	2019	Copiapó	131
2 LITIO 2 1/30	MSB	485 ov.	159	2004	Copiapó		1244 ov	333	2019	Copiapó	143
3 LITIO 3 1/58	MSB	491 ov.	160	2004	Copiapó		1246	334	2019	Copiapó	286
4 LITIO 4 1/60	MSB	498	161	2004	Copiapó		1247	335	2019	Copiapó	297
5 LITIO 5 1/60	MSB	504	162	2004	Copiapó		1248 ov	336	2019	Copiapó	297
6 LITIO 6 1/60	MSB	511	163	2004	Copiapó		1249 ov	337	2019	Copiapó	282
7 BLANCO 1, 1/60	MSB	84	19	2019	Copiapó						300
8 BLANCO 2, 1/60	MSB	228	56	2019	Copiapó						300
9 BLANCO 3, 1/60	MSB	234	57	2019	Copiapó						300
10 BLANCO 4, 1/50	MSB	1044	257	2019	Copiapó						250
11 BLANCO 5, 1/60	MSB	21	5	2019	Copiapó						300
12 BLANCO 6, 1/60	MSB	164	31	2019	Copiapó						300
13 BLANCO 15, 1/60	MSB	963	241	2019	Copiapó						300
14 BLANCO 16, 1/50	MSB	824	210	2019	Copiapó						250
15 BLANCO 17, 1/40	MSB	1014	252	2019	Copiapó						200
16 BLANCO I 18, 1/60	MSB	3805	2442	2019	Copiapó						300
17 BLANCO 19, 1/60	MSB	3795	2438	2019	Copiapó						300
18 BLANCO I 20, 1/60	MSB	3797	2439	2019	Copiapó						300
19 BLANCO I 29, 1/40	MSB	734	0442	2019	Copiapó						200
20 BLANCO I 30, 1/60	MSB	736	0443	2019	Copiapó						300
21 BLANCO I 31, 1/60	MSB	739	0444	2019	Copiapó						300
22 BLANCO I 32, 1/60	MSB	741	0445	2019	Copiapó						300
23 BLANCO I 33, 1/60	MSB	744	0446	2019	Copiapó						300
24 BLANCO I 34, 1/60	MSB	746	0447	2019	Copiapó						300
25 BLANCO I 35, 1/80	MSB	749	0448	2019	Copiapó						300
26 BLANCO I 36, 1/60	MSB	751	0449	2019	Copiapó						300
27 BLANCO I 37, 1/60	MSB	754	0450	2019	Copiapó						300
28 BLANCO I 38, 1/60	MSB	756	0451	2019	Copiapó						300
29 BLANCO I 39, 1/60	MSB	759	452	2019	Copiapó						300

Philippi
Prieto Carizosa
Ferrero DU
& Uria

30	BLANCO I 40, 1/60	MSB	761	453	2019	Copiapó					300
31	BLANCO I 41, 1/60	MSB	764	454	2019	Copiapó					300

Philippi
Prietocarizosa
Ferrero DU
&Uria

